GEOLOGY AND GEOCHEMISTRY OF THE MINERALIZATION AND ALTERATION IN THE STEEPLE ROCK DISTRICT, GRANT COUNTY, NEW MEXICO AND GREENLEE COUNTY, ARIZONA

by
Virginia T. McLemore

New Mexico Bureau of Mines and Mineral Resources

Open-file Report 397

December 1993

GEOLOGY AND GEOCHEMISTRY OF THE MINERALIZATION AND ALTERATION IN THE STEEPLE ROCK DISTRICT, GRANT COUNTY, NEW MEXICO AND GREENLEE COUNTY, ARIZONA

VIRGINIA T. MCLEMORE

Department of Geological Sciences

APPROVED:

Kenneth F. Clark, Chair

Roy Arrowood

Charles E. Chapin

Jerry M. Hoffer

Frances E. Julian

Nicholas E. Pingitore

Associate Vice President for Research
and Graduate Studies

GEOLOGY AND GEOCHEMISTRY OF THE MINERALIZATION AND ALTERATION IN THE STEEPLE ROCK DISTRICT, GRANT COUNTY, NEW MEXICO AND GREENLEE COUNTY, ARIZONA

by

VIRGINIA T. MCLEMORE, B.S., B.S., M.S.

DISSERTATION

Presented to the Faculty of the Graduate School of

The University of Texas at El Paso

in Partial Fulfillment

of the Requirements

for the Degree of

DOCTOR OF PHILOSOPHY

Department of Geological Sciences

THE UNIVERSITY OF TEXAS AT EL PASO

December 1993

ACKNOWLEDGMENTS

This dissertation is dedicated to my family: my grandfather, Howard P. Somers (1909-1981); my two daughters, Jennifer and Christine McLemore; my husband, James McLemore; and my grandparents Gordon Filbey (1908–1993) and Elizabeth Somers Filbey. Without their patience, encouragement, financial support, and enthusiasm this project would never have been completed. I especially owe gratitude to my daughters and husband who not only did not have much of a mother or wife for three and a half years, but fed me, washed my clothes, carried my rocks, and kept me company at home and in the field during that time. Thanks to Jim for repairing my equipment and providing me with support, money, and equipment throughout this project. Although my grandfather, H. P. Somers, was not alive to actively take part in this project, he and my grandmother taught me the skills and the attitude to finish and succeed.

This project was supported financially by the New Mexico Bureau of Mines and Mineral Resources (NMBMMR), Frank E. Kottlowski, former Director, and Charles E. Chapin, current Director and State Geologist. Their assistance and encouragement throughout are greatly appreciated. Scholarships provided by the Department of Geological Sciences, University of Texas at El Paso (UTEP) and the International Mining Days Scholarship enabled me to attend UTEP. A grant provided by Mount Royal Mining Co., John Ewing, president, provided additional financial support for this project. Financial support was also provided by my grandmother, Elizabeth Somers Filbey, and room and board was provided by Mr. and Mrs. Ed Carrier while I attended UTEP.

Many people assisted me with this project over the years. Steve Redd, Dewayne Johnston, and Bill Nielson of R&B Mining Co., current operators of the Center mine, allowed access to their mine as well as taught me about mining and grade control at this deposit. Leonard J. Taylor, president of Biron Bay Resources, Ltd., allowed access to the records and drill core of Biron Bay's Summit project. Discussions with Mr. Taylor and geologists Alexander Poe and Scott Klundt were extremely beneficial. Thomas Quigley, vice

president of Great Lakes Exploration, Inc. provided data and drill core on the Alabama mine. Queenstake Minerals, Ltd. allowed access to data and drill core from the Jim Crow-Imperial mines. George Ryberg provided data and drill cuttings from the Carlisle mine. Douglas Hanson allowed access to his mines and data from the Carlisle and East Camp Group. Discussions with Paul Eimon concerning alteration and potential at Telephone Ridge were enlightening. Robert Appelt and William McIntosh provided paleomagnetic analyses that were vital to stratigraphic correlations.

The Smithsonian Institute, Washington, D.C. (Division of Petrology and Volcanology, Department of Mineral Sciences), allowed access to samples collected by Waldemer Lindgren in the early 1900s (NMNH 87905.0400-0404). Five samples were examined and thin sections made and are on file at the Smithsonian. The U.S. Geological Survey (USGS) Core Library, William Linenberger, provided working space and samples of the U.S. Bureau of Mines (USBM) drill core from the 1940s exploratory drilling project. Thin sections and data from that core are on file at the USGS Core Library in Denver, Colorado. I would also like to thank Roderick A. Hutchinson and several park rangers at Yellowstone National Park for discussions and tours of various hot springs and geysers at the Park.

Several people assisted me in the field at various times and their help and company were appreciated: Coralie Carrier, Jennifer and Christine McLemore, James McLemore, Lia Walker, Ron Lowery (Phelps Dodge, Inc.), Lynn Brandvold (NMBMMR), Douglas Jones, Robert Appelt, William McIntosh (NMBMMR), Thomas Quigley (Great Lakes Exploration, Inc.), Dave Hedlund (USGS), Jim Ratté (USGS), Philip Goodell (UTEP), Kenneth Clark (UTEP), Frances Julian (UTEP), Mark Ouimette, Randy Ruff, Daren Dresser, and Paul Eimon. Daren Dresser, David Bright and Douglas Jones assisted with sample preparation and computer applications. Chris McKee and Jacques Renault (NMBMMR) assisted with x-ray diffraction and fluorescence analyses. Lynn Brandvold and associates (NMBMMR) analyzed numerous samples for precious- and base-metals and mercury. Discussions with various individuals were helpful throughout the project, including Mike Pawlowski, Robert North,

Sterling Cook and Ron Lowery (Phelps Dodge, Inc.), David Wahl, Bill Tipton (USBLM), Russell Schreiner (USBM), Pat Freeman (St. Cloud, Inc.), George Ryberg, Patrick Browne (University of Aukland, New Zealand), Donald White, Andrew Campbell (New Mexico Institute of Mining and Technology, NMIMT), George Austin (NMBMMR), Robert Eveleth (NMBMMR), Marc Wilson (NMBMMR), and Paul Eimon.

All or portions of this manuscript were reviewed by members of my committee, James McLemore, Douglas Hanson, Chris Beck, Robert Appelt, William McIntosh, Paul Eimon, Abe Gundelier, amd John Ewing.

Finally, a few special people have aided me and given of their time and deserve special recognition. I would like to thank my committee for their support and what they have taught me: Kenneth Clark, Nicolas Pingitore, Jerry Hoffer, Frances Julian, Roy Arrowood, and Charles Chapin. Coralie Carrier not only assisted me in the field but provided a home while I attended UTEP and has my gratitude. Discussions with George Ryberg were enlightening, however I especially enjoyed flying over the district and taking pictures from his airplane. Patrick Browne (Geothermal Institute, University of Auckland, New Zealand) was extremely helpful in discussing geothermal processes and alterations which aided my understanding of epithermal systems. I want to thank Ibrahim (Abe) Gundiler (NMBMMR) for his encouragement and advice, discussions on mineralogy, and providing SEM data on the ore minerals from the Center mine. Thanks also to Dr. Ruth Gross who taught me Spanish and enabled me to fulfill my language requirement. I also want to thank friends and classmates from UTEP and NMIMT (Mark Ouimette, Qingping Deng, Chris Beck, Lia Walker, Tanya Baker, Clara Podpora, Kevin Crain); together we got each other through! Thanks!

Lynne Hemenway typed this manuscript and Virginia McLemore, Kathryn Campbell, Rebecca Titus, and Michael Wooldridge drafted the figures and maps.

This dissertation was submitted to the committee on September 2, 1993.

ABSTRACT

The Steeple Rock district is one of several epithermal volcanic-hosted epithermal districts in southwestern New Mexico and southeastern Arizona. This area offers an excellent opportunity to examine the relationship between the distribution and timing of alteration and the formation of fissure veins in an epithermal environment. Five distinct types of vein deposits occur in the district: base with precious-metals, precious-metal, copper-silver, fluorite, and manganese. These veins are structurally controlled; hosted by Miocene to Oligocene volcanic, volcaniclastic, and intrusive rocks; and they appear to be spatially related to two types of alteration: alkali-chloride (propylitic to argillic to sericitic) and acid-sulfate (advance argillic). Mineralogic and chemical zonations, preserved textures, multiple horizons, stratigraphic relationships, and limited sulfur isotopic data are consistent with the acid-sulfate alteration being produced by acidic magmatic-hydrothermal fluids at temperatures less than 340°C in a relatively shallow environment (< 1.5 km) such as a hot springs system. The acidic fluids are produced by disproportionation of sulfate in magmatic fluids with decreasing temperature as the fluids rose toward the surface. The epithermal fissure veins are younger than the acid-sulfate alteration as evidenced by cross-cutting, stratigraphic, and textural relationships, and age determinations. The epithermal veins were formed by low salinity (< 5 eq wt% NaCl), slightly acidic to neutral pH fluids at temperatures between 240 and 320°C at relatively shallow depths (360–1300 m) and pressures (< 150 bars) as evidenced by preserved textures, fluid inclusion data, mineralogy, and chemical composition. The alteration and mineralization in the Steeple Rock district occurred in response to cyclic volcanic activity and subsequent development of local hydrothermal systems in structurally-controlled areas of high heat flow. While the exact timing and duration of these events is unknown there is no evidence to support that these events were continuous; rather the alteration and mineralization were episodic, waning, and migrating from one locality to another. Economic potential for additional low-sulfidation, fissure vein deposits in the Steeple Rock district is excellent and potential also exists for the discovery of high-sulfidation, disseminated gold deposits.

associated with the acid-sulfate alteration.

SUMMARY

The Steeple Rock mining district is located in the Summit Mountains in southwestern New Mexico and southeastern Arizona. An estimated $10 million worth of gold, silver, copper, lead, and zinc have been produced from the district since 1880. In addition, minor quantities of fluorite, manganese, and decorative stone were produced. Most of the metal production was from the Carlisle (inactive) and Center (active) mines along the west-northwest-trending Carlisle fault and the inactive mines along the East Camp-Summit fault. But more recently, Biron Bay Resources Ltd. (Toronto, Canada) has announced a discovery along the northwest-trending East Camp-Summit fault of 1.45 million tons of ore grading 0.18 oz/ton (6 ppm) Au and 10.3 oz/ton (353 ppm) Ag (press release, May 1992). Additional mineralized zones have been encountered in drill holes.

The district occurs in a tectonically complex region. It lies on the southern edge of the Mogollon-Datil volcanic field (late Eocene-Oligocene), on the northern edge of the Burro uplift, and near the intersection of the northwest-trending Texas and northeast-trending Morenci lineaments. Volcanic activity in the district occurred during mid-Tertiary extensional tectonics, but many of the regional faults have similar trends as older Laramide structures formed as a result of compressional tectonics. This suggests that reactivation of older crustal features may have occurred and may have controlled volcanic and geothermal activity. Rocks exposed in the Steeple Rock district consist of a complex sequence of Oligocene to Miocene (34 to 27 Ma) andesitic, basaltic andesitic, and dacitic lavas interbedded with andesitic to dacitic tuffs, sandstones, volcanic breccias, and rhyolite ash-flow tuffs which were subsequently intruded by rhyolite plugs, dikes, and domes (33 and 28–17 Ma).

Two distinct types of alteration occur in the district: (1) alkali-chloride (propylitic to argillic to sericitic to silicic) and (2) acid-sulfate (advanced argillic). At least three stages of alkali-chloride alteration affected the rocks: (1) regional premineralization, (2) localized synmineralization, and (3) regional post-mineralization. Alkali-chloride alteration is the most pervasive alteration type and is characterized by quartz, chlorite, and pyrite and a variety of

additional minerals depending upon host rock composition, permeability, composition of the fluids, temperature, and duration of the alteration process. Some of these additional minerals are temperature dependent: high-temperature assemblages (>200°C: epidote, illite, titanite, anhydrite), low-temperature assemblages (<200°C: smectite, illite/ smectite, dolomite, kaolinite, and mordenite), and low- to intermediate-temperature assemblages (chlorite, pyrite, calcite, adularia, illite, quartz).

Several areas of acid-sulfate alteration which are superimposed and surrounded by alkali-chloride alteration have been mapped in the district. Three of these altered areas occur near epithermal veins, whereas the others are in the vicinity of mineralized faults. The acid-sulfate altered areas are mineralogically, texturally, and probably temperature zoned and grouped into three types: (1) clay zone (outermost zone, lowest temperatures), (2) silicified zone (intermediate zone), and (3) massive silica/chert zone (innermost zone, highest temperatures). The clay zone is characterized by fine-grained, sugary, and vuggy to soft and friable textures. The silicified zone is characterized by fine- to medium-grained, massive to brecciated to vuggy textures. The clay and silicified zones are gradational and consist of kaolinite, quartz, hematite, pyrite, and locally alunite, pyrophyllite, anatase, diaspore, illite/smectite, illite, jarosite, and iron and manganese oxides. The quartz content increases from the clay zone to the silicified to the massive silica/chert zones. The massive silica/chert zone is characterized by massive, locally brecciated, quartz and/or chert, but no relict textures are preserved. Hydrothermal brecciation and hydrofracturing are common and suggestive of hydrothermal eruptions. The massive silica/chert zone consists of quartz with minor amounts of kaolinite, hematite, alunite, pyrophyllite, pyrite, and anatase. Some areas contain high gold anomalies. Examination of drill core reveals that these acid-sulfate altered zones are repeated at different intervals and are separated by areas of alkali-chloride alteration.

Five types of mineral deposits occur in the district: (1) base-metals veins with considerable gold and silver (5–20% base-metal sulfides), (2) precious-metals veins (<1% base-metals sulfides), (3) copper-silver veins (low gold), (4) fluorite veins, and (5) manganese

veins. A sixth type of deposit may also occur in the district: disseminated gold deposits associated with the acid-sulfate alteration. District wide zonation of epithermal veins is present. The base-metals veins occur along the west-northwest-trending Carlisle fault and may represent the center of the district. Fluid inclusion temperatures are highest in this area (240–325°C). Outward from the Carlisle fault, precious-metals veins occur along the northwest-trending faults. These veins grade into copper-silver veins locally. The veins in the eastern portion of the district along the East Camp-Summit fault are associated with calcite and fluorite, whereas the veins in the western portion of the district are associated with rhyolite intrusives. On the fringes or outer margins of the district, fluorite and manganese veins occur. Two or more centers of fluorite mineralization may exist on the basis of fluid inclusion temperatures. The epithermal deposits in the district are (1) low-sulfidation vein deposits, (2) structurally controlled, (3) younger than acid-sulfate alteration, and (4) deposited by low salinity (<5 eq. wt.% NaCl), slightly acidic to neutral pH fluids at temperatures between 240° and 325°C and at relatively shallow depths (360–1300 m). Faulting probably occurred throughout mineralization.

The alkali-chloride and acid-sulfate alteration probably represents a hot springs geothermal system, such as that at the Norris Geyser Basin in Yellowstone National Park. Some of the acid-sulfate altered areas were faulted and perhaps covered by younger volcanic rocks (34–27 Ma). Epithermal vein mineralization, along with associated synmineralization alteration and rhyolite intrusives, formed along the faults (28–18 Ma) after the acid-sulfate alteration. Locally, epithermal veins cut the acid-sulfate alteration, but elsewhere in the district, acid-sulfate alteration caps epithermal veins. Acid-sulfate alteration and epithermal mineralization were subsequently affected by post-mineralization alkali-chloride alteration.

The alteration and mineralization in the Steeple Rock district occurred in response to cyclic volcanic activity and subsequent development of local hydrothermal systems in areas of high heat flow. Timing and duration of these events is only speculative and based on a few age determinations and field relationships. There is no evidence to support that these events

were continuous; instead the alteration and mineralization were probably episodic, waning and migrating from one locality to another. Similar complex trends are observed in modern geothermal systems and other epithermal vein districts. The Steeple Rock district, other epithermal deposits, and modern geothermal systems have three similar controlling factors: (1) most occur in areas containing deep-seated intrusives that provide heat for convective hydrothermal systems consisting of meteoric and locally other fluids; (2) all are formed at shallow crustal levels; and (3) all are located along regional structures. Many ancient epithermal deposits occur in areas of modern geothermal systems. However, the Steeple Rock district is one example of the early development of a geothermal system with both alkali-chloride and acid waters followed by younger epithermal mineralization.

TABLE OF CONTENTS

13. Figures

1. INTRODUCTION

1.1 Purpose

Epithermal mineral deposits have been recognized as an important class of mineral deposits for many years. Some of the largest gold and silver deposits in the world are epithermal deposits, including the "bonanza" gold deposits of the Comstock Lode and Sleeper deposit, Nevada; Creede, Colorado; and El Indio, Chile. There are many studies of epithermal deposits in the geologic literature, and several genetic models have been proposed (Buchanan, 1981; White, 1981; Hayba et al., 1985; Berger and Henley, 1989; White and Hedenquist, 1990). However, despite the large number of published reports, one of the current controversies in economic geology involves the relationship, classification, and genesis of precious-metal deposits, base-metal deposits, and associated alteration that occur in some fissure-vein, epithermal districts (Beane, 1991; Mango et al., 1991; Albino and Margolis, 1991; Margolis et al., 1991; Rye et al., 1992).

The main objective of this study is to determine how the distribution and timing of the alteration assemblage are related to the formation of precious- and base-metal veins in an epithermal environment. The Steeple Rock district in southwestern New Mexico and southeastern Arizona provides an opportunity to examine this relationship, because five distinct types of ore deposits occur in the district and they appear to be related spatially to two types of alteration assemblages (1) acid-sulfate (advanced argillic) and (2) alkali-chloride (propylitic to argillic to sericitic to silicic). Furthermore, district-wide variations in both alteration and mineralization also can be studied at Steeple Rock. The Steeple Rock district is also ideal for this study because of the three-dimensional (topographic relief as well as subsurface drilling data) and historical production data available.

In anticipation of identification of the contrasting but overlapping characteristics of these mineral assemblages, these data can be used to (1) provide geologic criteria in the Steeple Rock district to enhance successful exploration and development currently in progress, (2) determine the district zonation and genesis of the mineralization and alteration of the

district, (3) provide an exploration model for epithermal deposits with similar characteristics to the Steeple Rock district, and (4) enhance current understanding of the processes involved in forming epithermal mineral deposits. A secondary objective of this study is to evaluate the economic resources of the Steeple Rock district.

1.2 Epithermal mineral deposits

Lindgren (1922, 1933) defined the term "epithermal" to include a broad range of deposits that formed by ascending waters at shallow to moderate depths (< 1500 m), low to moderate temperatures (50°–200°C), and which are typically associated with intrusive and/or volcanic rocks. From fluid inclusion and isotopic data, it is now generally accepted that epithermal deposits were formed at slightly higher temperatures (50°–300°C) and relatively low pressures (few hundred bars). In addition, not all epithermal deposits occur in igneous rocks; for example, the Carlin-type deposits which are found in sedimentary rocks (Bagby and Berger, 1985; Berger and Henley, 1989). Work by White (1955, 1981) established the now-recognized association between epithermal mineral deposits and active geothermal (or hot springs) systems. Subsequent work by Henley (1985) and associates (Henley and Brown, 1985) in New Zealand confirmed this association.

Epithermal mineral deposits occur in structurally complex tectonic settings that provide an excellent plumbing system for circulation of hydrothermal fluids. Numerous volcanic-hosted epithermal deposits occur along the margins of calderas (Rytuba, 1981), although other structurally complex volcanic settings, such as silicic domes and andesitic stratovolcanoes, are not uncommon for these deposits. It is important to note that not all calderas are mineralized (Rytuba, 1981). Only a few calderas in New Mexico contain epithermal mineral deposits (Fig. 1.1; North and McLemore, 1986, 1988).

Typical epithermal deposits occur as siliceous vein fillings, breccia pipes, disseminations, and replacement deposits in intermediate to silicic volcanic and volcaniclastic rocks. Common ore textures characteristic of epithermal deposits include: open-space and

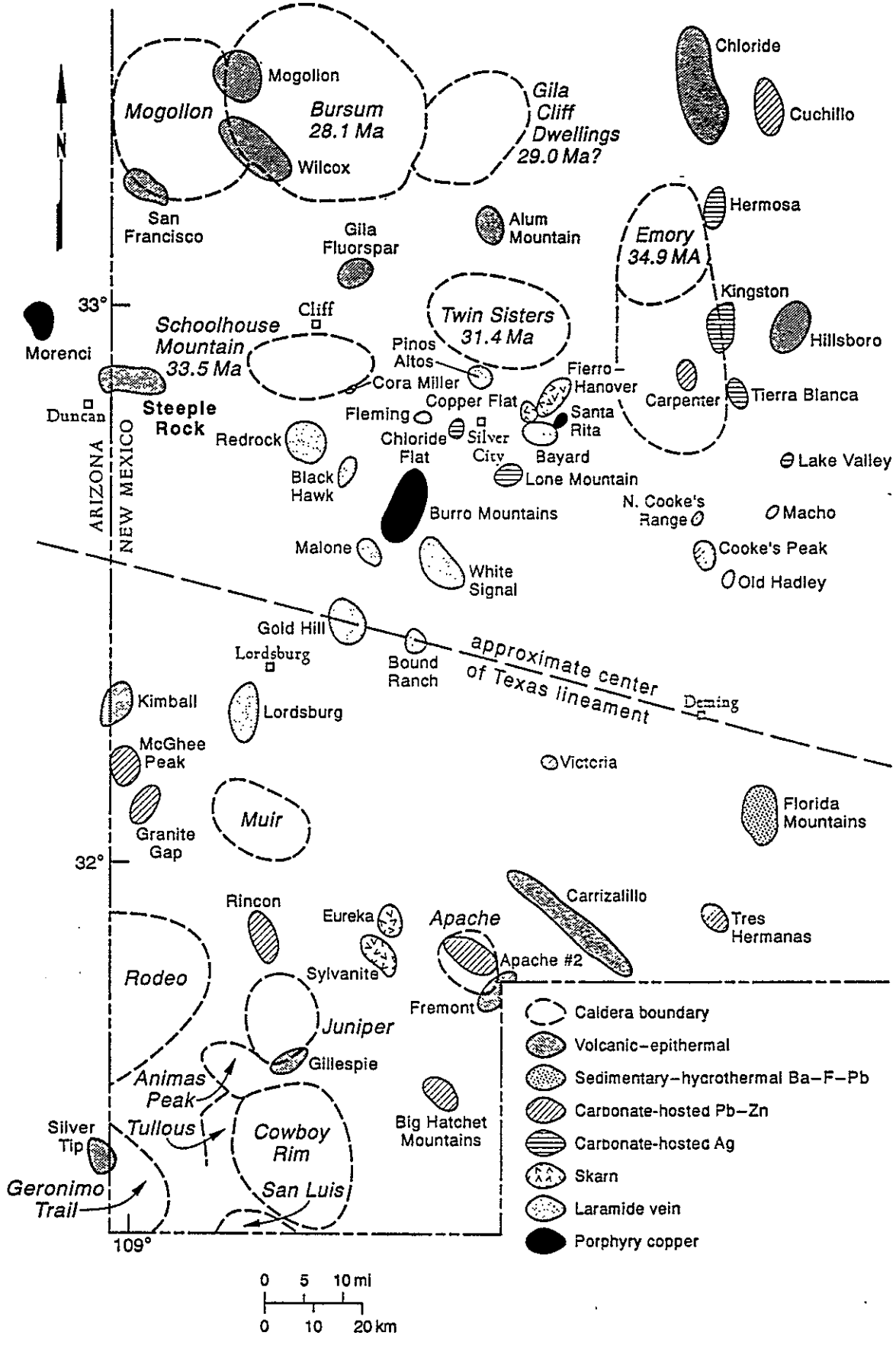

Figure 1.1 Location of Steeple Rock district in relation to other metal districts in southwestern New Mexico (modified from North and McLemore, 1986; McIntosh et al., 1992 a, b; NMGS, 1982)

cavity filling, drusy cavities, comb structures, crustification, colloform banding, brecciation (typically multi-stage), replacement, lattice (quartz pseudomorphs after bladed calcite), and irregular sheeting (Buchanan, 1981; Dowling and Morrison, 1989). The mineralogy and metal associations of these deposits are diverse and typically vary from one deposit to another. Both gold and silver are usually produced from these deposits with variable base-metal production. District zoning is also diverse, and in many districts precious metals occur in the upper levels of the epithermal system and grade into base metals at depth (Buchanan, 1981).

Hydrothermal systems undergo constant and, sometimes, abrupt physical and chemical changes. Equilibrium may never be achieved in these systems. This occurs as a result of (1) change from lithostatic to hydrostatic pressure (resulting in boiling), (2) changes in permeability, and (3) interaction of fluids derived at depth with near-surface, meteoric waters and host rocks of different lithologies. Consequently, fluid temperature, composition, and pressure are constantly changing.

The alteration mineral assemblage varies with changes in temperature, pressure, permeability, fluid composition, original host rock composition, and duration of activity (Silberman and Berger, 1985; Browne, 1978; P. R. L. Browne, written commun., 1992). Alteration assemblages include silicification, propylitic, argillic, advanced argillic, potassic, sericitic, illitic, and chloritic. This terminology is used to describe alteration that is associated with vein deposits in this study. Alteration assemblages reflect the composition of the prevailing fluid type and may also be referred to by the type of fluid as alkali-chloride, acid-sulfate, bicarbonate, or mixed fluids. This terminology is used to describe the regional alteration in this report. A clay alteration halo typically surrounds the deposits and in some areas the alteration is capped by a silicified zone or a sinter deposit, similar to deposits formed by active hot springs (Buchanan, 1981). Detailed clay analyses in some districts have defined the temperature of formation as well as general characterization and zonation of the mineralization and alteration. Studies by Hemley et al. (1980) suggest that the occurrence of pyrophyllite indicates alteration temperatures above 280°C. On occasion gold and silver are

closely associated with zonation of clay minerals (i.e. Golden Cross, New Zealand, DeRonde and Blattner, 1988; Pueblo Viejo, Dominican Republic, Vennemann et al., 1991). Studies by Yau et al. (1988) indicate a zonation of illite-muscovite (115–220°C) to chlorite (220–300°C) to biotite (310°C) with increasing depth in the Salton Sea geothermal field. Identification and recognition of this association of gold and alteration is important in identifying potential exploration targets.

Fluid inclusion analyses provide data on temperature of formation, salinity, and composition of the mineralizing fluids and may indicate a district-wide zonation of heat sources (Bodnar et al., 1985). Fluid inclusions sometimes show evidence of boiling (i.e. the presence of vapor-rich and vapor-poor inclusions). Boiling is one of the more popular mechanisms that have been invoked to explain the precipitation of gold from mineralized fluids. Precipitation of the metals could also occur by mixing of fluids and/or cooling. Most epithermal deposits formed at temperatures ranging from 50 to 300°C.

An important advance in the knowledge of epithermal mineral deposits occurred when Hayba et al. (1985) provided a two-fold classification of volcanic-hosted epithermal deposits based on mineralogy and associated alteration: adularia-sericite and acid-sulfate. In order to be consistent in terminology by defining both classes according to mineralogy, Berger and Henley (1989) refined this classification to adularia-sericite (illite) and alunite-kaolinite ($\pm$ pyrophyllite). Earlier models referred to these deposits as quartz-adularia and quartz-alunite (Cox and Singer, 1986, model #25). One problem with applying this classification in the field is that some of the minerals, such as alunite, diaspore, adularia, etc., are too fine-grained to be identified easily (Berger and Henley, 1989). Thus White and Hedenquist (1990) refined this classification even further to low sulfidation and high sulfidation. The characteristics of each type are summarized in Table 1.1.

Hayba et al. (1985), Heald et al. (1987), Berger and Henley (1989), and White and Hedenquist (1990) provide convincing evidence that low-sulfidation (alkalie-chloride; adularia-sericite) and high-sulfidation (acid-sulfate; alunite-kaolinite) deposits occur in separate and

TABLE 1.1—Characteristics distinguishing the low-sulfidation (adularia-sericite) and high-sulfidation (acid sulfate) epithermal deposits (from Hayba et al., 1985; Cox and Singer, 1986; Heald et al., 1987; Berger a Henley, 1989; White and Hedenquist, 1990).

	HIGH SULFIDATION (Alunite-kaolinite; quartz-alunite; acid-sulfate)	LOW SULFIDATION (Adularia-sericite; quartz-adularia)
Structural Setting	intrusive centers	structurally complex
Host rocks	rhyodacite common, acid to intermediate	various acid to intermediate fluids
Timing of ore and host	similar ages of the host and ore	ages of the host and ore distinct
Mineralogy	enargite, pyrite, gold, electrum, base-metal sulfides including covellite chlorite rare no selenides Mn minerals rare Bismuthinite Higher sulfide mineral assemblage Chalcedony and adularia absent unless overprinting, abundant alunite and pyrophyllite	argentite, tetrahedrite, tennantite, silver, gold, base-metal sulfides chlorite present selenides Mn minerals common No bismuthinite Lower sulfide mineral assemblage Chalcedony common, adularia, minc alunite and pyrophyllite
Production	Gold, silver, and copper	Gold, silver, variable base metals
Alteration	Extensive propylitic with advanced argillic to argillic with hypogene alunite and kaolinite, but no adularia	Extensive propylitic with sericitic to argillic with supergene alunite and kaolinite and abundant adularia
Localizing controls	any faults or fracture zones related to volcanic centers	major regional faults or subvolcanic
General character of fluids	low to high salinity meteoric with magmatic waters pH acid from magmatic HCl and H_2S oxidized to reduced Total S typically high Base-metal content low to high	low salinity meteoric waters pH near neutral reduced Total S low Base metal content low

distinct geochemical environments that rarely overlap. However, there are a few districts with characteristics of both low-sulfidation and high-sulfidation deposits (Heald et al., 1987; Beane, 1991), but these districts are rare and not well studied. The Steeple Rock district in southwestern New Mexico and southeastern Arizona (Fig. 1.1) appears to be an example of a district with characteristics of both low-sulfidation and high-sulfidation deposits, even though Berger and Henley (1989) classified the Steeple Rock district as a low-sulfidation (adularia-sericite) epithermal deposit based on limited published geologic data.

1.3 Location, production, and exploration activity in the Steeple Rock district

The Steeple Rock mining district is in the Summit Mountains in Grant County, New Mexico and Greenlee County, Arizona (Fig. 1.1). The district derives its name from a prominent mountain peak, Steeple Rock (Fig. 1.2), in the southern part of the area. For the purposes of this report the Steeple Rock mining district refers to the entire area covered by Maps 1 and 2 (Figure 1.3) as well as some mines and prospects north and west of Maps 1 and 2. Other reports refer to various mining districts and subdistricts in the area; including Twin Peaks in the northern part of the mapped area (Biggerstaff, 1974; Keith et al., 1983), Bitter Creek district along Bitter Creek (Hedlund, 1990b), Duncan fluorspar district in the western part of the area (Hedlund, 1990b), and Goat Camp district west of Vanderbilt Peak (Keith et al., 1983). Some reports separate the Carlisle and East Camp into separate districts. It is appropriate to describe the area as one district because the geology is similar throughout the area and the various types of deposits are similar and possibly related to each other.

Exploration began about 1860, but production was not reported until 1880. An estimated $10 million worth of metals were produced from the district between 1880 and 1991, which includes approximately 151,000 ounces of gold, 3.4 million ounces of silver, 1.2 million pounds of copper, 5 million pounds of lead, and 4 million pounds of zinc (Table 1.2). In addition, approximately 11,000 tons of fluorspar have been produced from the Mohawk, Powell, Leta Lynn, and other mines (McAnulty, 1978; Richter and Lawrence, 1983;

Table 1.2: Production from the Steeple Rock district, Grant County, New Mexico and Greenlee County, Arizona. (NMBMMR files; USGS and USBM Mineral Yearbooks; Anderson, 1957; Griggs and Wagner, 1966; Keith et al., 1983.) e - estimated

Year	Ore (short tons)	Copper (lbs)	Gold (oz)	Silver (oz)	Lead (lbs)	Zinc (lbs)	Total value ($
GRANT COUNTY, NEW MEXICO							
e1880-1897	112,000	---	e102,000	e1,618,000	---	---	e4,000,
1904	4	---	?	?	---	---	
1905-1906	Production not reported						
1907	1,000	---	750	15,150	---	---	e25,
1908	750	---	375	17,000	---	---	e16,
1909	65	770	17	1,410	9,140	---	e1,
1910	Production not reported						
1911	224	---	143	5,902	---	---	e6,
1912	269	3,706	402	5,157	950	---	e12,
1913	381	7,602	417	1,453	7,914	---	e11,
1914	41	1,342	42	88	---	---	e1,
1915	295	7,276	229	11,031	3,000	---	e12,
1916	165	17,500	124	3,491	6,753	---	e9,
1917	5,202	68,502	88	10,642	617,989	139,490	e96,
1918	82	10,677	39	999	6,775	---	e4,
1919	228	11,027	27	3,817	157,812	---	e14,
1920	2,111	5,837	642	3,566	36,937	---	e21,
1921	91	---	45	2,363	1,000	---	e3,
1922	Production not reported						
1923	36	---	23	1,685	286	---	e1,
1924-1927	Production not reported						
1928	23	1,132	---	130	---	---	e
1929	Production not reported						
1930	50	121	15	891	23	---	e
1931	Production not reported						
1932	19	21	13	780	152	---	
1933	5	31	2	94	216	---	
1934	1,617	1,700	421	21,141	500	---	28,
1935	1,377	2,200	407	19,470	---	---	28,
1936	3,777	5,600	850	54,173	300	---	72,
1937	16,147	57,550	5,552	200,863	68,175	55,000	364,
1938	14,740	33,300	5,687	239,119	38,500	---	358,
1939	12,772	13,000	4,487	237,030	19,000	---	320,
1940	22,915	20,900	5,414	216,374	74,000	---	349,
1941	39,018	53,200	6,685	252,509	226,000	---	432,
1942	9,426	29,000	1,390	60,220	86,700	---	100,
1943	11,645	202,800	250	20,870	683,000	703,500	177,
1944	15,460	210,800	295	21,181	838,500	944,000	228,
1945	19,366	232,200	963	25,494	1,079,500	1,156,400	309,
1946	9,535	87,800	408	8,797	405,200	328,800	119,
1947	1,348	10,500	61	1,010	42,800	40,800	16,
1948	428	2,000	149	1,735	3,000	2,000	8,

Table 1.2 continued

Year	Ore (short tons)	Copper (lbs)	Gold (oz)	Silver (oz)	Lead (lbs)	Zinc (lbs)	Total value ($)
1949	347	2,000	101	1,409	3,000	3,000	6,050
1950	855	1,300	259	11,004	1,700	---	19,523
1951	2,288	19,700	271	11,259	36,400	36,700	37,418
1954	104	500	8	52	1,400	---	667
1955	2,619	2,900	376	28,410	---	300	39,990
1956	1,979	1,644	186	11,345	5	---	17,476
1957	115	169	10	680	239	---	e1,000
1960	?	?	?	?	?	?	8,383
TOTAL 1907-1957	198,919	1,126,307	37,623	1,529,794	3,409,990	3,285,402	3,544,287
TOTAL 1974-1991	e55,000	e40,000	e12,000	e226,000	e90,000	---	---
TWIN PEAKS SUBDISTRICT, GREENLEE COUNTY, ARIZONA							
1906-1970	2,000	15,000	500	10,500	17,000	---	---
GRAND TOTAL 1880-1991	e365,000	e1,200,000	e151,000	e3,400,000	e5,000,000	e4,000,000	e10,000,000

Hedlund, 1990b). In the Goat Camp Springs area, 2,000 tons of ore containing 74,500 lbs of manganese was produced, probably in the 1940s. Two rock quarries were opened and mined for decorative or building stone.

In the 1970s, 1980s and 1990s, exploration for gold and silver intensified and resulted in additional exploration drilling and some production, mainly for silica flux. Only one mine is operating in the district in 1993, the Center mine owned by Mount Royal Mining Co. However, at least three different exploration programs are under way. Great Lakes Exploration Co. drilled at the Alabama mine during July and August 1991 and Biron Bay Resources Ltd. is drilling along the Summit vein as part of their joint venture agreement with Nova Gold Resources Ltd. Weaco Exploration Ltd. drilled in the fall of 1991 at the Carlisle mine and is evaluating the mineral-resource potential of land adjacent to the Carlisle mine.

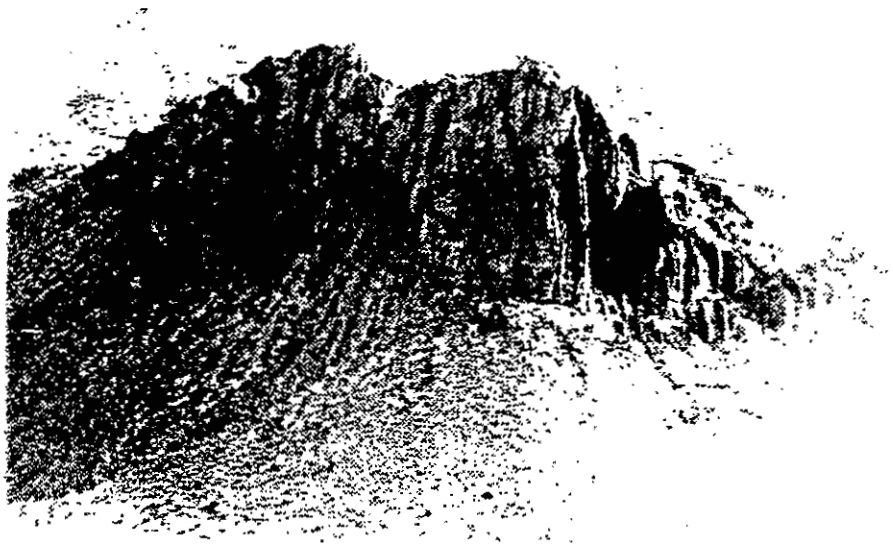

Figure 1.2—Steeple Rock, looking northeast. Note the spiral configuration giving its name that is formed by the rhyolite of Steeple Rock (age 33.1 Ma).

Despite this significant production and exploration activity, relatively minor detailed mineralogic and geochemical studies have been published on the Steeple Rock district.

1.4 Previous Work

The ore deposits were first described by Lindgren et al. (1910) who recognized that these deposits are epithermal. During World War II (early 1940s), the USGS and USBM examined the ore deposits along the Carlisle fault and conducted surface and underground mapping, drilling, and sampling as part of the national strategic minerals evaluation (Johnson, 1943; Russell, 1947; Griggs and Wagner, 1966). This investigation failed to locate any additional base-metal orebodies based on the economics at that time (Russell, 1947). The fluorspar deposits were described by Trace (1947), Wilson (1950), Williams (1966), Rothrock et al. (1946), and McAnulty (1978).

Geologic mapping of the area has been accomplished only in the last 30 years. Elston (1960) published a reconnaissance geologic map at a scale of 1:126,720 as part of the state geologic map compilation. The volcanic units were thought to be Cretaceous in age (Elston, 1956, 1961), but regional correlations and recent age determinations have confirmed a Mid-Tertiary age (Hedlund, 1990a,c, 1993; McIntosh et al., 1990a,b). Griggs and Wagner (1966) mapped the Carlisle-Center area.

More recent mapping includes several dissertations and theses which were completed as exploration for porphyry copper deposits intensified in southwestern New Mexico (Fig. 1.3; Wargo, 1959; Biggerstaff, 1974; Powers, 1976; Wahl, 1980). Of these theses, Biggerstaff (1974) presented the most detailed descriptions of the geology and mineralization of the district. Wahl (1980; 1983) also described the geology and mineralization in the Steeple Rock district and a few additional districts in western Grant County. Powers (1976) concentrated on the alteration within the district. In the late 1970s and early 1980s, regional reconnaissance geologic mapping of six quadrangles, including the Steeple Rock area, was completed as part of the Silver City CUSMAP project (Fig. 1.3; Tillie Hall Peak, Crookson

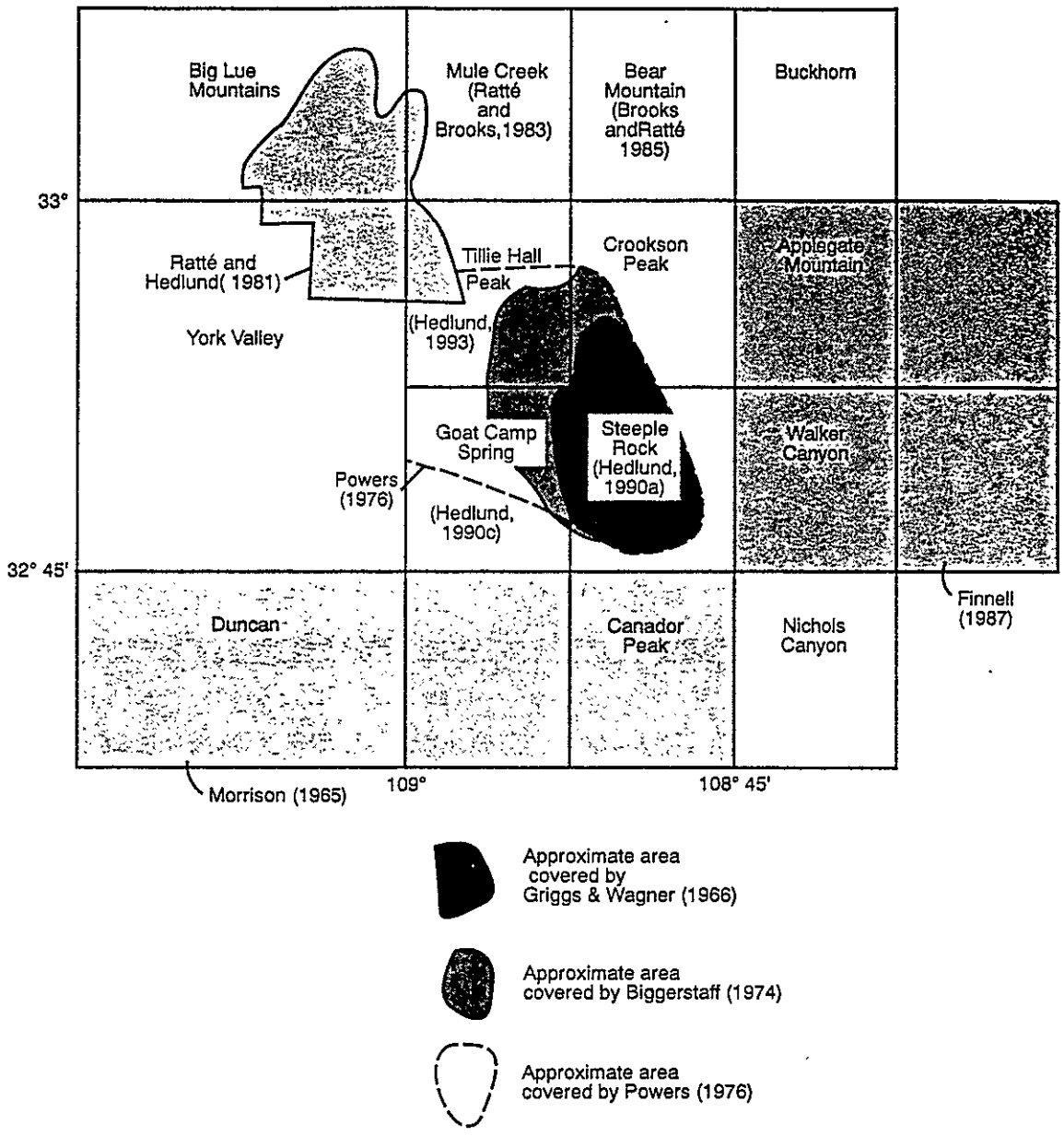

Figure 1.3 Index to geologic mapping prior to this study. This area was mapped regionally by Elston (1960), Wahl (1980), Wargo (1959), and Drewes et al.(1985). The area covered on Maps 1 and 2 for this study is approximately the same area covered by Powers (1976).

Peak, Applegate Mountain, Goat Camp Spring, Steeple Rock, Walker Canyon, and parts of Canador Peak and Nichols Canyon); these maps were available to the author for this study (Hedlund, 1990a,c; 1993).

Areas surrounding the Steeple Rock district also have been mapped (Fig. 1.3). The geology of the Hells Hole RARE II planning area, north of the Steeple Rock district, was mapped by Ratté and Hedlund (1981). Several quadrangles adjacent to the district also have been mapped including the Mule Creek (Ratté and Brooks, 1983), Bear Mountain (Brooks and Ratté, 1985), and Cliff quadrangles (Finnell, 1987). Additional regional geologic mapping is by Morrison (1965) and Drewes et al. (1985).

Six abstracts have been published describing the mineral deposits and associated alteration of the district. Robinson (1984) and Eimon and Bazrafshan (1989) briefly describe the alteration and mineralization potential at Telephone Ridge, north of the Carlisle mine in the Steeple Rock district. Ruff and Norman (1991) present preliminary results of gas analyses of fluid inclusions from quartz samples from throughout the district: CO_2 and H_2S occur with some of the ore deposits in Steeple Rock. A thesis by Ruff (1993) updates these results. McLemore (1991) briefly described the mineralization and alteration of the district. McLemore and Quigley (1992) briefly described the mineralization at the Alabama mine, a low-sulfidation epithermal deposit. McLemore and Clark (1993) describe in more detail the mineralization and alteration of the district.

The mineral resources of the Hells Hole area were studied by Hassemer et al. (1983), Briggs (1981, 1982), and Ratté et al. (1982). Hedlund (1990b) briefly summarizes the geology of the mineral deposits in the Steeple Rock district. Sharp (1991) presents geochemical analyses of some igneous rocks in the district. Additional mineral resource reports briefly describe some of the mineral deposits in the Steeple Rock district and adjacent areas (Anderson, 1957; Gillerman, 1964; Hall, 1978; Richter and Lawrence, 1983; Wahl, 1983; Keith et al., 1983; North and McLemore, 1986, 1988; Richter et al., 1986; Tooker and Vercoutere, 1986; Raines, 1984; Watts and Hassemer, 1988).

At least two remote sensing studies of the Steeple Rock district have been released. Raines (1984) identifies two limonitic areas in the district (Goat Camp Springs and Saddleback Mountain areas) on the basis of landsat color-ratio composite images. Magee et al. (1986) identify six areas of alteration (Saddleback Mountain, Goat Camp Springs, Telephone Ridge, Raeburn Hills, Laura-Alabama area, and East Camp area) using landsat thematic mapper imagery techniques. However, Magee et al. (1986) were unable to distinguish between acid-sulfate alteration and silicification.

Numerous unpublished mine and exploration reports were obtained concerning the various mines and exploration projects in the Steeple Rock mining district. Many of these reports include geochemical data, production data, and mine maps. This information was synthesized and utilized whenever pertinent. Individual reports and maps are referenced in this study as unpubl. report with the author and date noted. The reports are on file at NMBMMR.

1.5 Methods of Study

1.5.1 Geologic mapping and structural analysis

Detailed geologic mapping of altered areas and veins is necessary to determine the spatial relationships and timing of these events. Approximately 171 sq km were mapped in detail at a scale of about 1:12,000 and transferred to a map scale of 1:24,000. Standard U.S. Geological Survey 7½-minute topographic quadrangle maps (Goat Camp Springs, Steeple Rock, Crookson Peak, and Tillie Hall Peak; Fig. 1.3) were used as base maps. In addition, the eastern portion of the area was mapped at a scale of 1:4,800, using topographic base maps provided by Nova Gold Resources, Ltd. Outcrop mapping techniques were employed by locating actual outcrops on the geologic outcrop map (Map 1). Locations of mines and samples are on Map 2 and geologic cross sections are on Map 3.

Numerous mine adits and declines were mapped using a Brunton compass and measuring tape. The Center mine was mapped in more detail (Map 4); engineering surveys were available for some levels which provided better control.

Structural analysis of geologic data is important to determine the orientation of applied stress fields during deformation of the country rocks and to evaluate the possible relationship between structural style and timing of mineralization. Orientations of faults (281 measurements) and foliation and bedding planes (350 measurements) of various lithologic units were measured during the course of the field work. Locally, orientations of fault slickensides, joints, and fractures were also measured. These data were entered into QUATTRO PRO (Borland International, Inc., 1991). Stereonet plots were then constructed using the computer program STEREO (RockWare, Inc., 1992b). Unfortunately, many orientations could not be utilized in the structural analysis because only the strike could be measured in the field. The dip was not measured because of lack of exposure of the fault or foliation planes.

1.5.2 Drill core examination

Subsurface data provide the third dimension to this study. Diamond drill core from Jim Crow-Imperial mines (Queenstake Resources, Ltd.), Alabama mine (Great Lakes Exploration, Inc.), Carlisle-Center mines (USBM and R&B Mining Co. Inc.), Bitter Creek (Kennecott), and Summit project (Biron Bay Resources, Ltd.) were examined and logged (over 3600 m). Cuttings from reverse circulation drilling at the Carlisle mine (Weaco Ltd.) were also examined and logged. A binocular microscope and hand lens were used in examining the drill core. Samples were obtained for thin section preparation and geochemical analyses. A summary of pertinent drill core data is in Appendix 11.1.

1.5.3 Petrography and mineralogy

Petrographic analysis and mineral identification are important in differentiating various rock units, determining rank and intensity of alteration, determining chemistry of alteration fluids, and determination of paragenesis of mineralization. Alteration rank is based upon the mineral assemblages which infers temperature, pressure, and permeability conditions at the

time of formation (section 5.1). Samples were cut and chips were sent to Spectrum Petrographics, Inc. for preparation of thin sections and polished thin sections. Petrography was performed using standard petrographic and reflected ore microscopy techniques. Mineral concentrations were estimated using standard charts (Swanson, 1981) and data are summarized in Appendix 11.2. Estimates of both primary and alteration minerals were determined and the alteration intensity was determined by the concentration of alteration minerals.

Altered, unaltered, and mineralized samples were powdered and analyzed by x-ray diffraction (XRD) at NMBMMR using pressed powder slides (Appendix 11.3). Some minerals with small sample volume were analyzed using a turbine drive sample spinner (Renault, 1984). Heavy mineral separates of high-grade gold-silver samples were obtained using a magnetic separator and gravity concentration. Clay minerals of many samples were determined separately using sedimented slide techniques of the <2-μm size fraction (to eliminate or reduce non-clay minerals). All XRD analyses were determined using a Rigaku Geigerflex D/MAX series XRD unit with CuKα at 50 kV and 25 mA. Specific clay minerals were identified on randomly oriented powder packed into 2-mm-deep, side-loaded sample holders and examined using a Norelco XRD unit with CuKα at 40 kV and 25 mA. XRD results are summarized in Appendix 11.3.

Polished sections of heavy mineral concentrates from the Center mine were examined using a scanning electron microscope (SEM) by Ibrahim Gundiler (NMBMMR, metallurgist). Heavy metal concentrates were obtained by flotation methods described in Wilson et al. (1993; I. Gundiler and M. Brueggemann, written communication, May 25, 1990) and set in epoxy and polished. Samples were carbon-coated, degassed, and examined with a Hithachi hi-scan HHS-2R model with an energy-dispersive x-ray spectrometer (EDS) at 20 Kv. All work was performed by Dr. Gundiler under the guidance of a technician at NMIMT and the results were made available for this study.

1.5.4 Geochemical and statistical analyses

Geochemical analyses of veins and rocks from the Steeple Rock district are important to (1) determine the composition of the magmatic systems and compare and contrast with known mineralized, magmatic systems, (2) determine the metal enrichment in the buried magma systems, (3) identify chemical zonations throughout the district, (4) characterize chemical composition of alteration and mineralization, and (5) determine potential for economic mineral resources. Samples of veins and country rock were collected in the field and submitted for geochemical analyses (Appendices 11.4, 11.5, 11.6). Locations of samples are on Map 2. Most field samples were grab samples, although some chip samples were also collected. Samples of drill core and drill cuttings were also collected, washed, and submitted. Samples were air dried, if necessary, crushed in a rock crusher to sand-size fragments and then powdered in a shatterbox. Powdered samples were split using standard splitting techniques (Obenauf and Bostwick, 1988).

Samples of veins and mineralized or altered country rocks were submitted to the NMBMMR Chemistry Laboratory (Lynn Brandvold, manager). Gold and silver were determined by fire assay techniques using one-half assay ton sample size (Hafty et al., 1977). Copper, lead, zinc, manganese, and iron were determined using aqua regia dissolution followed by analysis using atomic absorption spectrometry (American Public Health Association, 1992). Mercury was determined by cold vapor atomic absorption spectrometry using EPA method #245 (EPA, 1979). Fluorine was determined by sodium carbonate fusion followed by ion chromatography. Some duplicate samples as well as internal standards were included in the analyses. Commercial atomic absorption standards were obtained from Fisher Scientific and VWR Scientific and used in the analyses. AA analyses were performed on an instrumentation Laboratory Inc. AA (Model 857, Date 7/85) and instrument conditions were according to manufacturer's specifications using air-acetylene flame (Allied Analytical Systems, 1985, Methods manuel for flame operation). For example, Cu was determined using a wavelength of 324.7 nm, Pb a wavelength of 217.0 nm, and Zn a wavelength of 213.9 nm. Summary of trace elements and detection limits are in Table 1.3.

Table 1.3. Trace elements, method of analyses, and detection limits. (a) - % precision in fire assay of gold and silver is variable because of the nugget effect. (b) XRF is not the best method to analyze for Mo. Mo was analyzed to determine only if it occurred in large concentrations (> 100 ppm). 1 - From Lynn Brandvold (pers. commun. 9/23/93) and J. Renault and C. McKee (written commun. 5/11/93). Note that samples with analyses at or near the detection limits may have higher errors due to accuracy and precision—in some cases as much as 50%.

Element	Method	Lower limit of detection (ppm)	% Accuracy	% Precision
Ba	XRF	10	4	5
V	XRF	5	7	5
Cr	XRF	3	6	5
Pb	XRF	9	29	20
	AA	5	5	5
Th	XRF	9	21	20
Rb	XRF	3	6	5
U	XRF	3	7	10
Sr	XRF	3	2	5
Y	XRF	3	3	5
Zr	XRF	3	4	5
Nb	XRF	3	14	15
Mo	XRF	5	(b)	(b)
Ga	XRF	3	12	15
Zn	XRF	6	2	5
	AA	1	4	5
Cu	XRF	5	11	10
	AA	5	5	5
Ni	XRF	2	3	5
Au	fire assay (gravimetric)	0.02 oz/ton	1	(a)
Ag	fire assay (gravimetric)	0.01 oz/ton	3	(a)
Hg	AA	0.02	3	5

Samples of some veins, mineralized or altered country rock, and unaltered country rock were submitted to the NMBMMR x-ray facility (Jacques Renault and Chris McKee, managers). Major element oxides were determined by x-ray fluorescent spectrometry (XRF) on a Rigaku SYN 3064 model at standard operating conditions (Rigaku Manuel no. ME 300 BM) and using fused glass discs following the method of Norrish and Hutton (1969). USGS

rock standards were used to calculate the concentrations. Some major element oxides were determined by XRF using the fundamental parameters program of Criss Software (Criss, 1980). Trace elements were determined by XRF using pressed powder briquets (Obenauf and Bostwick, 1988).

Estimates of accuracy and precision are in Table 1.3. Errors due to accuracy were determined by multiple analyses of commerical standards for which acccepted values are known. XRF analyses utilized commercial standards consisting of BR (basalt) and GA (granite). AA analyses utilized SY-2 and SY-3 (Abbey, 1979). Errors due to precision were determined by multiple analyses of selected sample splits as well as multiple analyses of standard samples. In addition, Cu, Pb, and Zn were determined by both AA and XRF and the values were typically within 10% (Appendices 11.5 and 11.6).

Statistical analyses of chemical analyses determined for this study and of data sets provided by various companies are important in summarizing the data and ultimately in interpreting the significance of each data set. Each data set was statistically analyzed separately using RockStat (Rockware, 1991), MSTAT (Rockware, 1992a), and SPSS (Nie et al., 1975). Means, standard deviations, and correlation coefficients were determined where appropriate and factor analyses and discriminate analyses were employed. Petrologic calculations of major element analyses of unaltered and altered rock samples were obtained by using PETCAL (Bingler et al., 1976).

1.5.5 Paleomagnetic analyses

Paleomagnetic analysis of ash-flow tuffs (ignimbrites) is an acceptable, inexpensive, and rapid means of correlating compositionally similar ash-flow tuffs of different ages (McIntosh, 1991). A paleomagnetic study of ash-flow tuffs in the Steeple Rock area was undertaken by Robert Appelt in 1992. For this study, 236 oriented samples were field drilled from 37 sites. Sample locations are on Map 2. These data also include sites located by W. I. McIntosh from previous work.

Samples were drilled in the field in situ using portable rock drills. Samples were then oriented by sun and magnetic compasses. The orientation of the paleo-horizontal was determined at each site using attitudes of pumice foliations, welding zones, and bedding contacts. Remnant magnetizations were measured using spinner and cryogenic magnetizations according to standard techniques described by McIntosh (1991). Demagnetization paths were analyzed using Zijderveld plots and principal component analyses to determine paths of univectoral decay and then processed using Fisher statistics to arrive at mean directions and alpha-95 confidence circles (Fisher, 1953; Kirschvink, 1980; Zijderveld, 1967). Acceptable alpha-95 data were set at $\leq 10\%$ confidence level. Robert Appelt performed all laboratory measurements and data reduction according to standard techniques described by McIntosh (1991). A paper is planned describing the results and significance of this study.

1.5.6 Fluid inclusion analyses

Fluid inclusion analyses provide data on temperature of formation and chemistry of mineralizing fluids. Double-polished thin sections of 0.1 to 0.2 mm thickness were prepared by a commercial laboratory according to standard procedures. Homogenization temperatures (T_H) and last ice melting temperatures (T_M) of the fluid inclusions were determined by using a Fluid Inc. adapted USGS heating/freezing system assembled on a Leitz microscope. Duplicate measurements were run on all temperature analyses. The instrument was calibrated by fluid inclusion standards of pure water (T_M = 0.0°C) and CO_2 + H_2O (T_M = -56.6°C) provided by Fluid Inc. Periodic experimental runs were made using fluorite from the Hansonburg district with known T_H and T_M. The difference between temperature readings of repeated measurements in the same inclusion typically is less than 0.5°C. Fluid inclusion data are summarized in Appendix 11.7.

1.6 Units used in this report

For the most part, standard international or metric units are used in this report, with

one exception. All production and reserve figures are reported in English units of short tons and ounces per ton (oz/ton). The equivalent metric units are listed in parentheses adjacent to the English units. English units for production and reserve figures were used because the original data were reported in these units and the data may be incorrectly calculated when converting back from metric to English units. In addition, many American miners and some explorationists are more familiar with the English system. In order to be consistent, all chemical analyses were reported in a similar manner. Conversion factors are as follows:

1 short ton x 0.9 = 1 metric ton

1 troy ounce/ton (oz/ton) = 34.286 ppm

3.281 ft = 1 meter (m)

0.61 mile = 1 kilometer (km)

Data in the appendices and Map 2 are reported in English units in order to conserve space.

2. GEOLOGIC SETTING

2.1 General Statement

The Steeple Rock mining district lies in a tectonically active and structurally complex area of the southwestern United States that is known for numerous types of mineral deposits (Fig. 1.1). It lies in the Summit Mountains which are on the southwestern edge of the Mogollon-Datil volcanic field. The Mogollon-Datil volcanic field is part of a regional late Eocene-Oligocene volcanic province that extends from west-central New Mexico southward into Chihuahua, Mexico (McDowell and Claubaugh, 1979; McIntosh et al., 1990a, b). In southwestern North America, volcanic activity began about 40-36 Ma with the eruption of andesitic volcanism and, subsequently, episodic bimodal silicic and basaltic andesite volcanism followed from 36 to 24 Ma (Cather et al., 1987; Marvin et al., 1988; McIntosh et al., 1990a, b). About 25 high- and low-silica rhyolite ignimbrites (ash-flow tuffs) were erupted and emplaced throughout the Mogollon-Datil volcanic field during this event; source calderas have been identified for many of the ignimbrites (McIntosh et al., 1990a, b, 1992a). At least six of the ignimbrites crop out in the Steeple Rock mining district as outflow sheets. There is no structural or lithologic evidence to support the presence of a caldera in the Steeple Rock district, contrary to earlier interpretations (Biggerstaff, 1974; Elston, 1978). Subsequent faulting and volcanism have offset and covered portions of the ignimbrites making regional correlations difficult. Paleomagnetic analyses and radiometric age dating have aided in correlating the ignimbrites. Generalized stratigraphy of the Summit Mountains is shown in Fig. 2.1.

The Summit Mountains are situated within a transition zone between the Colorado Plateau to the north and the Basin and Range province to the south and west (Fig. 2.2). The prominent structural trend in the Summit Mountains is northwest, which subparallels the west-northwest-trending Texas lineament of Wertz (1970a,b), Lowell (1974), Chapin et al. (1978), and Muehlberger (1980). The Summit Mountains lie on the northern edge of the Texas lineament. The northeast-trending Morenci lineament of Chapin et al. (1978) lies north of the

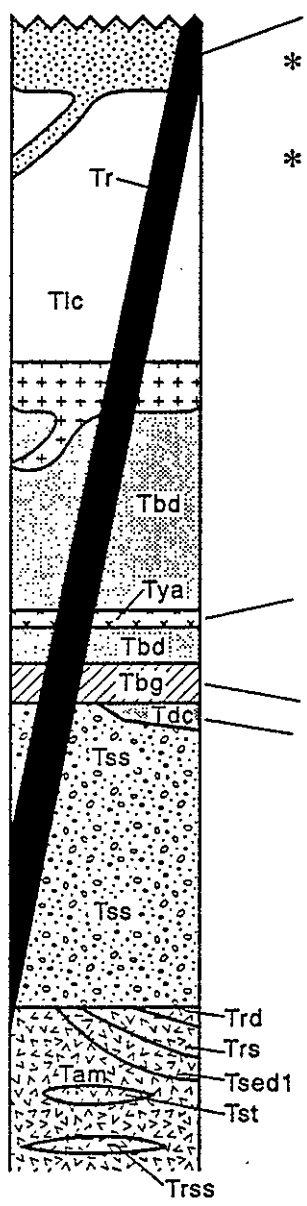

Intrusive rhyolite dikes, plugs, and domes

* Rhyolite of Mule Mountains (17.7 Ma)

* Bearwallow Mountain andesite (23, 25 Ma)

Lava flows of Crookson Peak (27.6 Ma)

* Rhyolite of Hells Hole (26–28 Ma)

Dark Thunder Canyon formation (amygdaloidal andesitic basalt of Griggs and Wagner, 1966; basaltic and andesitic rocks of Dark Thunder Canyon of Hedlund, 1990 a, c, 1993)

Younger ash-flow tuffs

Dark Thunder Canyon formation

Bloodgood Canyon Tuff (28.05 Ma)

Davis Canyon Tuff (29.01 Ma)

Summit Mountains formation

Summit Mountains formation (31, 32 Ma) (purple andesite porphyry of Griggs and Wagner, 1966; dacite of Summit Mountains of Hedlund, 1990 a, c)

OLDER VOLCANIC ROCKS

Rhyodacite of Mt. Royal (Trd), rhyolite of Steeple Rock (Trs; 33, 34 Ma)

Misc. ash flow tuffs (Tst, Trss) & undifferentiated sedimentary rocks (Tsed1)

Andesite of Mt. Royal (Tam; 34.3 Ma older volcanic series of Griggs and Wagner, 1966, and Biggerstaff, 1976)

* Rocks not exposed in Steeple Rock district

Figure 2.1 Generalized stratigraphy of the Summit Mountains (modified after Hedlund, 1990 a, b, c, 1993). See Table 2.1 for compilation of age dates.

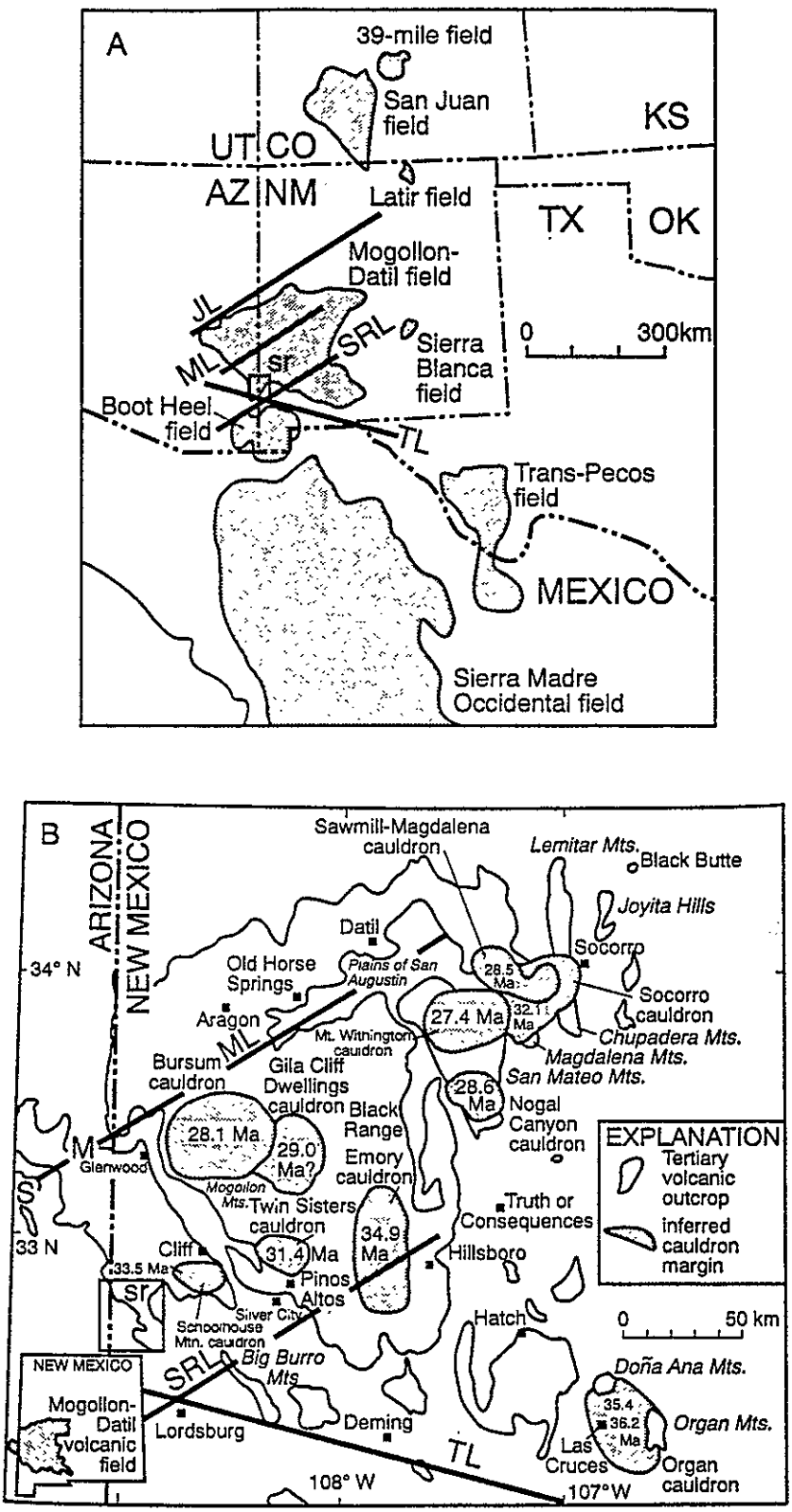

Figure 2.2 Regional structural features in southwestern United States. a) Regional map, b) Map of the Mogollon-Datil volcanic field. JL - Jemez lineament, ML - Morenci lineament, SRL - Santa Rita lineament, TL - Texas lineament, M - Morenci copper porphyry deposit, S - Safford copper porphyry deposit. Small box (sr) represents approximate location of the Steeple Rock mining district. Modified from McIntosh et al. (1990a, b) and Chapin et al. (1978).

Steeple Rock district. The Summit Mountains also lie on the northwestern edge of the Burro uplift.

The Steeple Rock mining district is one of several epithermal vein deposits found in southwestern New Mexico (North and McLemore, 1986, 1988) and southeastern Arizona (Keith et al., 1983) and is one of the few major epithermal districts not associated with any caldera (Fig. 1.1). Several porphyry copper deposits of Laramide age (>50 Ma) occur in southwestern New Mexico and southeastern Arizona, such as the Morenci deposit located about 48 km northwest of the Steeple Rock district (Figs. 1.1, 2.2).

2.2 Stratigraphy

2.2.1 Introduction and nomenclature

Although the Steeple Rock district is highly fractured and faulted, stratigraphic relationships are partially preserved. The oldest volcanic rocks (33-34 Ma) crop out in the southernmost portion of the area and the volcanic rocks decrease in age to the north and northeast (Maps 1, 2; Hedlund, 1990a, b, c, 1993; Ratté and Hedlund, 1981; Biggerstaff, 1974). The volcanic rocks in the mapped area range in age from 34 to younger than 27 Ma (Table 2.1). However, on an outcrop scale, the stratigraphic relationships in the Steeple Rock area are complex and are difficult to correlate in some areas. The andesites and dacites, especially where altered or weathered, are similar in appearance and difficult to differentiate. Likewise, the ash-flow tuffs are difficult to distinguish locally. Field relationships, petrography, whole rock geochemistry, and paleomagnetic analyses were utilized to decipher the local stratigraphy.

In simple terms, the volcanic activity in this area consists of successive periods of basaltic andesitic to andesitic to dacitic volcanism (about 2000-3000 m thick) that was periodically interrupted by the intrusion of rhyolites (Fig. 2.1; Table 2.1). At least four ash-flow tuffs (or ignimbrites) were erupted from distal calderas and the outflow sheets extended as far as the Steeple Rock area. These ash-flow tuffs provide excellent stratigraphic markers

Table 2.1—Compilation of age dates of rocks within the Summit Mountains area.

Map No. (Map 2)	Location (sec, township, range)	Unit	Age (Ma)	Method	Reference
Samples within mapped area					
	unknown	rhyolite dike	18 Ma	K-Ar	Wahl (1983; pers. comm. April 1992)
	25.17S.20W	quartz monzonite dike	21.4 ± 1.6	Fission track on zircon	Hedlund (1990a)
	30.16S.21W	vitrophyre, rhyolite dome (#955A, Map 2)	25.3 ± 0.10	$^{40}Ar/^{39}Ar$	W. McIntosh and R. Appelt (unpublished data, Aug. 1993)
	24.16S.21W	Lava flows of Crookson Peak	27.6 ± 2	Fission track on zircon	Hedlund (1990c)
	10.6S.32E	Bloodgood Canyon Tuff	24.0 ± 2.2*	Fission track on zircon	Wahl (1980, TF2)
	27.17S.21W	Bloodgood Canyon Tuff	30.3 ± 1.9*	Fission track on zircon	Ratté et al. (1984, #21); Marvin et al. (1987, #173a)
	15.17S.21W	Bloodgood Canyon Tuff	31.0 ± 2.1*	Fission track on zircon	Ratté et al. (1984, #21); Marvin et al. (1987, #173b)
	21.17S.20W	Bloodgood Canyon Tuff	27.4 ± 1.2*	Fission track on zircon	Ratté et al. (1984, #21); Marvin et al. (1987, #173c)
	21.17S.20W	Bloodgood Canyon Tuff	30.0 ± 1.4*	Fission track on zircon	Ratté et al. (1984, #21); Marvin et al. (1987, #173d)
	28.17S.20W	Bloodgood Canyon Tuff	31.0 ± 1.5*	Fission track on zircon	Ratté et al. (1984, #21); Marvin et al. (1987, #173e)
	27.17S.21W	andesite, Summit Mountain formation	22.6 ± 0.8	K-Ar, whole rock	Marvin et al. (1988, #66); Hedlund (1990b)
	17.16S.21W	andesite, Summit Mountain formation	31.3 ± 2.2	K-Ar, hornblende	Hedlund (1993)
	29.16S.21W	altered andesite, Summit Mountain formation	31.3 ± 1.1	K-Ar, quartz-alunite	Marvin et al. (1987, #175); Hedlund (1993)
	29.17S.20W	rhyolite of Steeple Rock	33.1 ± 1.1	K-Ar, biotite (NOTE: sanidine gives an age date of 20.3 ± 0.7 Ma)	Marvin et al. (1988, #67); Hedlund (1990b)
	25.17S.21W	andesite of Mount Royal	34.3 ± 0.09	$^{40}Ar/^{39}Ar$	D. C. Hedlund (unpubl. report, 1990)
Selected samples adjacent to mapped area					
	3.14S.20W	rhyolite of Mule Mountains	17.7 ± 1.0	Fission track, zircon	Ratté and Brooks (1983)
	18.16S.18W	rhyolite flow	21.3 ± 0.7	K-Ar, biotite	Finnell (1987); Marvin et al. (1988, #65)
	24.15S.21W	Bearwallow Mountain Andesite	23.7 ± 0.5	K-Ar, whole rock	Strangway et al. (1976, IIRB, RB9B); Marvin et al. (1987, #174)
		(andesite of Brushy Mountain)	25.6 ± 0.5	K-Ar, whole rock	Ratté and Brooks (1983)
	7.15S.21W	Rhyolite of Hells Hole	26.7 ± 2	Fission track, zircon	Ratté and Brooks (1983)
	33.4S.3W	Rhyolite of Hells Hole	27.1 ± 1	K-Ar	Ratté and Hedlund (1981)
			28.7 ± 3.7	Fission track, zircon	
	33.17S.20W	Fall Canyon Tuff(?)	32.42 ± 0.14	$^{40}Ar/^{39}Ar$, biotite	Marvin et al. (1987, #172)
			32.5 ± 1.2	K-Ar, biotite	
	22.17S.19W	ash-flow tuff of Redrock Basin	33.3 ± 1.1	K-Ar, biotite	Marvin et al. (1988, #69)
	11.18S.20W	ash-flow tuff	33.8 ± 1.1	K-Ar, biotite	Marvin et al. (1988, #68)

*NOTE: The fission track data show large variations. The accepted age of the Bloodgood Canyon Tuff is 28.05 ± 0.01 and the accepted age of the Davis Canyon Tuff is 29.01 ± 0.11 based on $^{40}Ar/^{39}Ar$ on sanidines from throughout the Mogollon-Datil volcanic province (McIntosh et al., 1990a, b).

in the mapped area. The local volcanic stratigraphy is summarized in Figure 2.1, and Figure 2.3 is a simplified geologic map of the area. Some age determinations of rocks within and adjacent to the mapped area are reported in the literature and are summarized in Table 2.1.

Wherever practical, the stratigraphic nomenclature used in this study is the same as that established by reconnaissance regional mapping by Hedlund (1990a, b, c, 1993). He refers to two units as the dacite porphyry (or dacitic and andesitic rocks) of Summit Mountain and the basaltic and andesitic rocks of Dark Thunder Canyon. For the purposes of this study, these two units have been simplified to the Summit Mountain formation and the Dark Thunder Canyon formation. It is hoped that these two units will be formalized as formations in the future because they are the two major units that host economic mineralization. But, it must be emphasized that the usage in this study does not conform to standard U.S. Geological Survey nomenclature. The older literature refers to these units (and other units) in very informal terminology. Wherever possible, both Hedlund's nomenclature and the terminology in the older literature are correlated in this study (Fig. 2.1). Map symbols for each unit used on the map are in parentheses.

The classification of igneous rocks used in this study is that recommended by the International Union of Geological Sciences (LeMaitre, 1989). However, most rocks in the Steeple Rock area are altered and in some areas rock terminology was defined on the basis of both petrography and chemical analyses. Wherever possible, the precursor rock-type was defined. Terminology describing the grain size, crystallinity, crystal shapes, and textures of igneous rocks follows that described by MacKenzie et al. (1991). Terminology and classification of the sedimentary rocks follows Scholle (1979). Alteration is briefly mentioned in the following section, but more precisely described in section 5. A summary of petrographic descriptions is in Appendix 11.2.

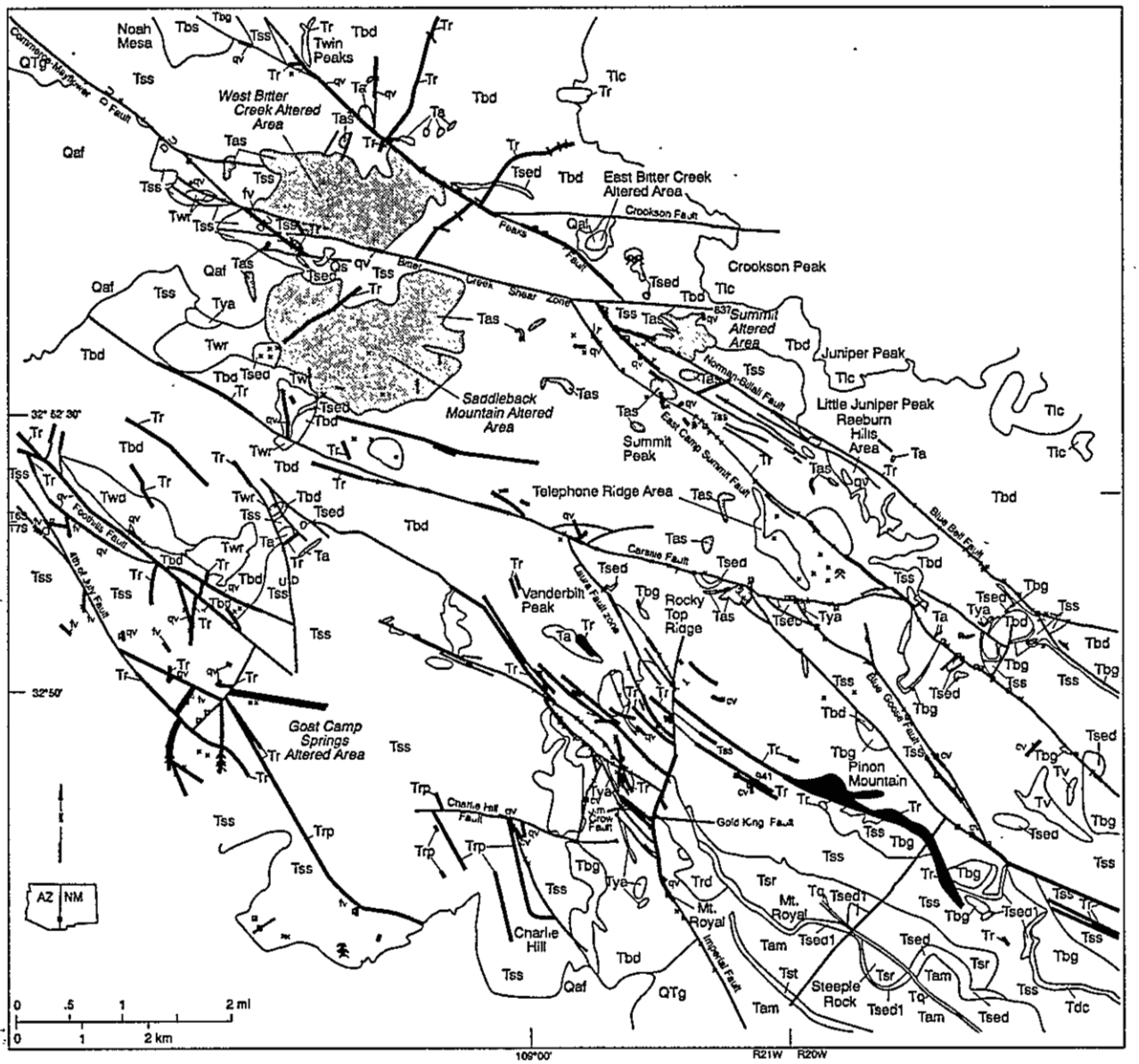

Quaternary-Pliocene rocks

- Qaf - Alluvial fan deposits
- Qs - Spring deposit
- Qtg - Gila Group

Oligocene-Miocene rocks

- Tr, Trp - Intrusive rhyolite dikes, plugs and sills
- Tq - Quartz Monzonite dike
- Td - Diabase dike
- Twr - Rhyolite flows and/or domes
- Twd - Rhyodacite of Willow Creek
- Tlc - Lava flows of Crookson Creek
- Tbd - Dark Thunder Canyon Formation
- Ta, Tya - Younger ash-flow tuffs
- Tbg - Bloodgood Canyon Tuff
- Tas - Altered rocks
- Tss - Summit Mountain formation
- Tsed - Undifferentiated sedimentary rocks
- Trd - Rhyodacite of Mt.Royal
- Tam - Andesite of Mt. Royal

Figure 2.3 Generalized geologic map of the Steeple Rock district. Geologic symbols described in Figure 2.1 and in text.

TABLE 2.2—Paleomagnetic data from Steeple Rock area ash-flow tuffs. Units are listed in order of decreasing age. Explanation: inc, dec and int are site-mean inclination, declination, and intensity; k is Fisher (1953) precision parameter; α_{95} is radius of cone of 95% confidence.

Field No.	Lab No.	No. of samples	Inc.	Dec	Int	K	α_{95}	Formation
	NM513	2	-63.0	162.0	1.86 E-02	7576.9	2.87	Trss
	NM512	8	50.8	26.7	7.87 E-03	140.5	4.69	Tst
	NM267	8	-53.9	166.2	1.84 E-01	104.3	5.45	Tdc
	NM691	7	-60.9	151.0	3.13 E-01	994.9	1.91	Tdc
1101	NM988	4	-54.8	10.8	4.55 E+00	123.6	8.3	Tdc?
	NM692	8	-51.4	167.5	1.66 E-01	227.6	3.68	Tdc
	NM690	8	-52.0	189.4	1.20 E-00	1416.3	1.47	Tbg
1031	NM976	5	-33.6	170.1	3.96 E+00	95.4	7.88	Tbg
1031	NM977	5	-43.2	177.2	5.62 E+00	132.7	6.67	Tbg
1100	NM987	8	-15.7	185.5	6.37 E-01	26.2	11.03	Tbg?
	NM266	6	-28.5	180.2	1.16 E-01	283.5	3.99	Tbg
1036	NM979	6	-11.8	168.1	6.67 E-01	70.6	8.03	Tbg?
1039	NM980	6	-21.7	164.4	2.45 E+00	501.8	2.99	Tbg
529	NM685	9	-24.3	169.6	9.30 E-02	522.3	2.25	Tbg
725	NM856	8	-25.3	169.9	3.01 E+01	237.1	3.6	Tbg
	NM689	8	-51.2	168.7	2.54 E-02	192.8	4.0	Tbg
739	NM868	8	-39.8	164.5	3.19 E+01	2231.7	1.17	Tbg
	NM514	5	-36.0	172.0	2.64 E-01	151.6	6.23	Tbg
1035	NM978	3	-11.3	152.3	2.80 E+00	303.3	7.09	Tbg?
732	NM864	8	32.4	148.0	5.47 E+00	88.1	5.93	Tbg?
738	NM867	8	-8.8	161.2	2.26 E+01	621.1	2.22	Tbg?
	NM990C	8	64.6	61.9	0.00 E+00	39.1	8.97	Tya
520	NM686	6	62.3	350.6	3.38 E-03	65.1	8.37	Tya
1102	NM992	4	16.0	131.0	6.12 E+00	91.3	9.67	Tsed
731	NM863	5	59.3	350.5	6.96 E+00	72.5	9.05	Tya1
733	NM865	8	57.4	335.0	3.62 E+00	171.2	4.25	Tya1
727	NM858	8	51.3	342.1	1.01 E+00	293.2	3.24	Tya1
1088	NM984	7	58.1	329.0	1.90 E+00	28.3	11.54	Tya1
	NM989	8	66.7	307.8	5.00 E-01	51.2	7.81	Tya1
726	NM857	6	74.4	356.9	1.47 E+00	503.5	2.99	Tya2
729	NM861	5	50.7	16.7	5.76 E+00	112.4	7.25	Tya3
730	NM862	8	62.2	26.9	4.92 E+00	49.5	7.95	Tya3
728	NM859	3	76.2	259.4	1.63 E+00	124.0	11.12	Tya?
	NM990A	8	48.1	140.6	3.30 E+00	79.4	6.25	Tya
	NM990B	5	47.8	3.4	0.00 E+00	43.4	11.75	Tya
740	NM869	9	44.6	16.9	9.30 E+00	116.8	5.61	Tya3
955A	NM985	3	8.7	338.5	3.30 E+00	139.5	10.48	Twr
1084	NM982	5	16.9	7.0	3.04 E+00	71.1	9.13	Ta
*	Mean	6	-53.9	159.6		81	7.5	Tdc
*	Mean	22	-27.1	165.3		100	3.1	Tbg

mean remanence data for each site are in Figures 2.4. Paleomagnetic data for each site are summarized in Table 2.2. For more details concerning potential problems utilizing paleomagnetic data, the reader is referred to McIntosh (1991).

From this study at least six different ash-flow tuffs are distinguishable in the Steeple

2.2.2 Paleomagnetic studies

Ash-flow tuffs (ignimbrites) provide excellent time-stratigraphic markers throughout the Mogollon-Datil volcanic field (McIntosh, 1991). Some of these flows extend as far as 140 km from their source caldera and provide stratigraphic markers within otherwise indistinguishable andesite flow sequences. However, regional correlations of many ash-flow tuffs are difficult at best because of disruption by regional faulting during Basin and Range extensional deformation. In addition, lithologic and geochemical similarities between different ash-flow tuffs and within the same ash-flow sequence hamper regional correlations (Hildreth and Mahood, 1985; Bornhorst, 1980, 1986, 1988). High precision $^{40}Ar/^{39}Ar$ geochronology of ash-flow tuffs have yielded precise age dates of ash-flow tuffs within the Mogollon-Datil volcanic field enabling correlation of various tuffs (McIntosh et al., 1990a, b, 1992a, b). However, there are problems with $^{40}Ar/^{39}Ar$ dating of ash-flow tuffs. Some tuffs do not contain useable, unaltered sanidines suitable for dating. Furthermore, $^{40}Ar/^{39}Ar$ dating is too expensive and time-consuming to be used on an outcrop to outcrop scale (McIntosh, 1991). However, paleomagnetic studies, especially where used in conjunction with detailed mapping and regional $^{40}Ar/^{39}Ar$ dating is an acceptable, inexpensive method for correlating ash-flow tuffs because of known magnetic reversals and secular variations of the magnetic field.

In the Steeple Rock area, numerous outcrops of ash-flow tuffs occur innerbedded throughout the Summit Mountain and Dark Thunder Canyon formations. These ash-flow tuffs typically occur near the contact of the Summit Mountain and Dark Thunder Canyon formations, are similar in appearance and composition, and difficult to correlate. Stratigraphic relationships are ambiguous in many areas. Preliminary paleomagnetic analyses by W. C. McIntosh (pers. commun. 1990) indicated the presence of three or four tuffs in the mapped area. Therefore, a paleomagnetic study of ash-flow tuffs in the Steeple Rock area was undertaken by R. Appelt in 1993.

Combined data from both McIntosh's and Appelt's studies were utilized to correlate various outcrops of ash-flow tuffs in the Steeple Rock area. Stereographic projections of site-

Rock area (Fig. 2.5). The oldest tuffs are two units within the older volcanic rocks of Steeple Rock (Tst, Trss, both known as the ash flow tuff of Steeple Rock; Hedlund, 1990b). Only one of these tuffs (Tst) occurs in the mapped area. The other tuff is to the south (Trss; Hedlund, 1990b). The Davis Canyon Tuff (Tdc) is the next oldest and has been dated elsewhere in the Mogollon-Datil volcanic field at 29 Ma (Table 2.1; McIntosh et al., 1990a, b). These three tuffs occur only in the southern portion of the mapped area. The Bloodgood Canyon Tuff (Tbg; Fig. 2.1) lies unconformably on the Davis Canyon Tuff in the southern area and lies unconformably on the andesites of the Summit Mountain formation elsewhere. It has been dated as 28 Ma (McIntosh et al., 1990a, b). The Bloodgood and Davis Canyon tuffs have different paleomagnetic characteristics, which distinguish them from a group of one or more overlying ash-flow tuffs, called younger ash-flow tuffs (Tya; Fig. 2.1) for the purposes of this study. The younger ash-flow tuffs typically occur at or near the base of the Dark Thunder Canyon formation and have a normal paleomagnetic polarity. The Davis Canyon and Bloodgood Canyon Tuffs have a reversed paleomagnetic polarity (Table 2.2, Fig. 2.4). The younger ash-flow tuffs are tentatively correlated with one or more tuffs in the Boot Heel field in southern New Mexico that have an age of about 27 Ma. Correlations of these younger ash-flow tuffs are currently under study (W. C. McIntosh, pers. comm. 1993). There may also be ash-flow tuffs associated with the rhyolite domes and plugs; these tuffs are designated Tya3 in Figure 2.4. Any outcrops of ash-flow tuffs of questionable origin are designated Ta. A summary of the correlation of the ash-flow tuffs in the Steeple Rock area is in Figure 2.5.

2.2.3 Pre-Oligocene rocks

The oldest rocks in the immediate vicinity of the Summit Mountains area are Proterozoic in age. Small outcrops of coarse-grained, equigranular, locally porphyritic granite occur in the Riley Peaks area of the Canador Peak 15-minute quadrangle, south of Steeple Rock (Morrison, 1965). The granite is weathered and consists of feldspar, quartz, biotite, and accessory minerals. It is similar in appearance and composition to the Proterozoic granite

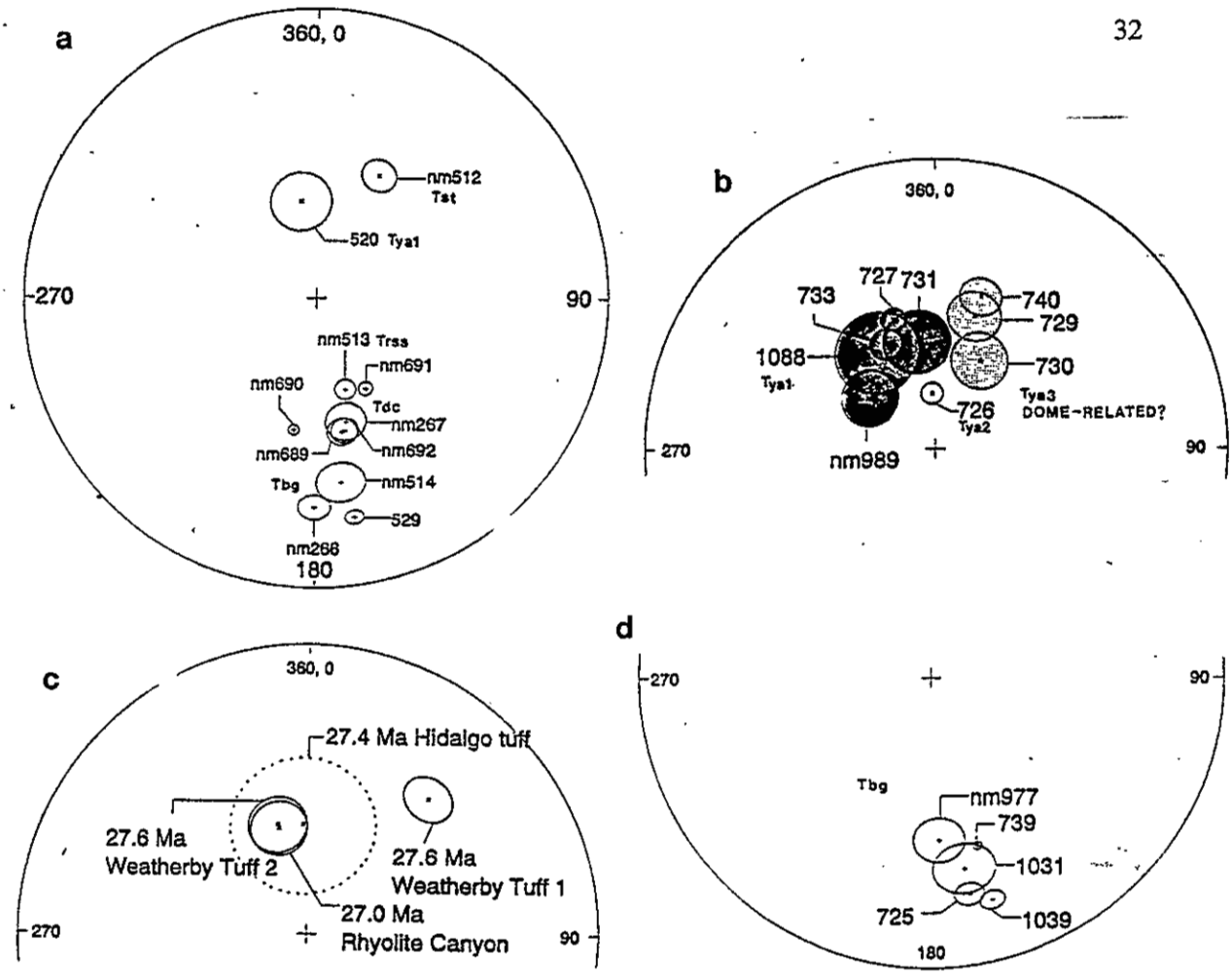

FIGURE 2.4—Stereographic projections of paleomagnetic data from the Steeple Rock area. Sample numbers refer to Table 2.2 and Map 2.

a) Samples from McIntosh et al. (1990a, b). Trss, Tst (NM513, NM512) – ash-flow tuff of Steeple Rock, Tdc (NM267, NM692, NM689) – Davis Canyon Tuff, Tbg (NM514, 529, NM266) – Bloodgood Canyon Tuff, Tya (520) – younger ash-flow tuffs.

b) Samples of younger ash-flow tuffs from R. M. Appelt, unpublished data. Note that there are three separate tuffs Tya1, Tya2, and Tya3.

c) Plots of ash-flow tuffs from the Boot Heel field in southern New Mexico (Fig. 2.2). Data from W. C. McIntosh, unpublished data. Note the similarity with younger ash-flow tuffs from Steeple Rock (Fig. 2.4b), suggesting possible correlations.

d) Samples of Bloodgood Canyon Tuff (Tbg) from R. M. Appelt, unpublished data.

e) Average plots of Bloodgood Canyon Tuff and Davis Canyon Tuff from McIntosh et al. (1990a, b) for comparison.

f) Plots of samples from unidentified tuffs from the Steeple Rock district, R. M. Appelt, unpublished data. Samples 1100, 1136, 738, 732, and 1038 are probably altered and/or remagnetized Bloodgood Canyon Tuff.

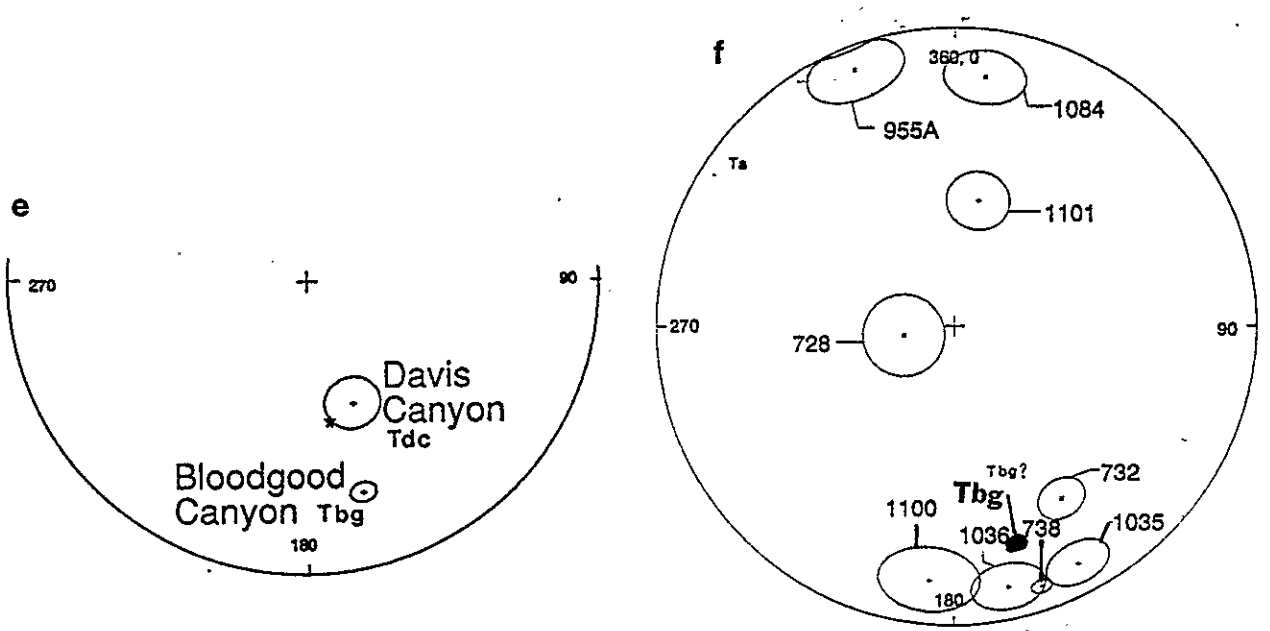

Figure 24 – continued

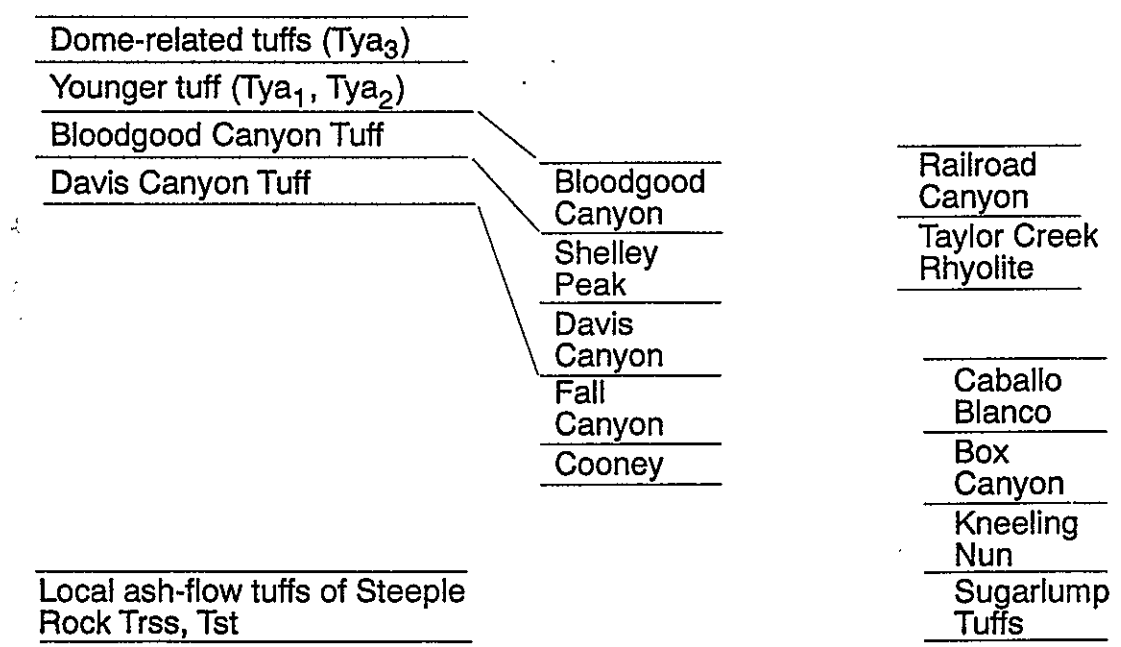

FIGURE 2.5—Stratigraphic correlations of ash-flow tuffs in the Steeple Rock district with Mogollon Mountains and Black Range (Appelt, 1993; McIntosh et al., 1990a, b).

granite exposed in the Burro Mountains and at Redrock (Morrison, 1965; Drewes et al., 1985; McLemore and McKee, 1988a, b). The granite in the Burro Mountains has been dated as 1445-1600 Ma (Stacey and Hedlund, 1983) and a similar age is envisioned for the granite at the Riley Peaks area, which most likely underlies the Summit Mountains at depth.

Cretaceous sedimentary rocks unconformably overlie the Proterozoic granite in the Riley Peaks area. The oldest unit is the Beartooth Quartzite and consists of sandstone and orthoquartzite (Morrison, 1965). The Colorado Formation conformably overlies the Beartooth Quartzite and consists of shallow marine shales, siltstones, sandstones, and minor limestones and conglomerates (Hedlund, 1990b; Morrison, 1965). The Virden Formation (Paleocene and Upper Cretaceous; Elston, 1960; Hedlund, 1990b) also crops out near Riley Peaks and consists of nonmarine fluvial sandstones, conglomerates, and siltstones (Morrison, 1965). The entire exposed Cretaceous-Paleocene section is probably less than 300 m thick in the Riley Peaks area (Morrison, 1965; Hedlund, 1990b).

Thicker Mesozoic and Paleozoic sections occur in southeastern Arizona which suggests a possibility that pre-Cretaceous rocks may occur beneath the volcanic rocks exposed in the Summit Mountains (Ross, 1973; Hayes, 1978; Hayes and Drewes, 1978; Schumacher, 1978). Up to 1500 m of Paleozoic marine sedimentary rocks (middle Cambrian to late early Permian) occurs in southeastern Arizona (Hayes and Drewes, 1978). Unconformably overlying the Paleozoic rocks, are as much as 12,000 m of Mesozoic sedimentary, volcaniclastic, and volcanic rocks (Hayes and Drewes, 1978). Up to 500 m of Paleozoic and Mesozoic rocks are exposed at Morenci (Moolick and Durek, 1966). However, it is unlikely that the Paleozoic and Mesozoic rocks are more than 500 m thick in the area of study because the Steeple Rock area was probably part of the Burro uplift throughout most of this time (Ross and Ross, 1986; Drewes, 1991). Without extensive subsurface drilling the presence and extent of Paleozoic and Mesozoic rocks beneath the Summit Mountains is only speculative.

2.2.4 Volcanic rocks of Steeple Rock and Mt. Royal

The oldest rocks exposed in the mapped area are the volcanic rocks of Steeple Rock and Mt. Royal in the southern part of the area (Fig. 2.3; Maps 1, 2). These rocks were not studied in thin section for this study because they are not significantly mineralized. Descriptions are based on Hedlund (1990a), Biggerstaff (1974), and field observations. Biggerstaff (1974) calls these rocks the Steeple Rock group, whereas Hedlund (1990a) refers to them as a series of andesites, rhyolites, and tuffs with specific names or designations. They range in age from 34 to 33 Ma (Table 2.1). This sequence of units certainly deserves more study in the future.

2.2.4.1 Andesite of Mt. Royal (Tam) (Hedlund, 1990a)—A sequence of andesite flows forms much of these older rocks. The flows vary in thickness but appear uniform in composition. They are reddish-brown to purplish-gray, highly jointed or fractured, and locally porphyritic. This andesite is difficult to impossible to distinguish from younger andesites of Summit Mountain and Dark Thunder Canyon formations. Total thickness is probably 125-900 m (Biggerstaff, 1974; Hedlund, 1990a).

The andesite is microcrystalline to locally porphyritic, holocrystalline and typically has a trachytic texture. It consists of plagioclase (andesine, Hedlund, 1990a) and biotite with accessory apatite and possibly hornblende. Alteration minerals include sericite, quartz, and hematite (Biggerstaff, 1974). An $^{40}Ar/^{39}Ar$ age of 34.3 Ma is reported by Hedlund (unpubl. report, 1990; see Table 2.1).

2.2.4.2 Ash-flow tuff of Steeple Rock (Tst)—A series of ash-flow tuffs crop out south of Steeple Rock and are interlayered with andesites of Mt. Royal and the older Mud Springs (Hedlund, 1990a), but only one is exposed in the mapped area. It is thin (less than 50 m), gray to orange-gray, poorly to moderately welded, devitrified, lithic-rich and crystal-poor tuff. It is poorly sorted and consists of 1-2% biotite and 1-2% quartz phenocrysts in a fine-grained groundmass of quartz and feldspar. Lithic fragments consist of andesite and andesite porphyry. Paleomagnetic data (Table 2.2) is inconclusive in correlating these tuffs with any

other known major ignimbrites in the area (McIntosh, 1991). This may suggest that these tuffs are locally derived, perhaps from rhyolite doming such as at Steeple Rock.

2.2.4.3 Older sedimentary rocks (Tsed1)—At the base of the rhyolite of Steeple Rock and the rhyodacite of Mt. Royal, a sandstone unit crops out. In both areas, the sandstone units are similar in appearance and composition, and it is unknown if they are the same stratigraphic unit or separate units. The sandstone is light brown to brown to gray, thin to medium bedded, and locally laminated. It is medium to coarse grained, poorly sorted, and consists of lithic fragments, quartz, feldspar, hematite, and a variety of accessory minerals. It is typically less than 5 m thick. These rocks unconformably overlie the andesite of Mt. Royal.

2.2.4.4 Rhyolite of Steeple Rock (Trs) (Hedlund, 1990a)—The rhyolite of Steeple Rock (Steeple Rock flow of Biggerstaff, 1974) is a prominent, massive rhyolite flow or dome that forms much of Mt. Royal and Steeple Rock (Fig. 2.3; Maps 1, 2). It unconformably overlies the older sedimentary rocks (Tsed1) and the andesite of Mt. Royal. It is brecciated toward the top of the unit suggesting a dome-like emplacement. It is light gray to pale red, flow-banded, locally spherulitic, devitrified, and locally, slightly porphyritic lava flow or dome. It ranges in thickness from less than a meter to 200 m. It has been dated as 33.1 ± 1.1 Ma (Table 2.1; Marvin et al., 1988; Hedlund, 1990b). Hedlund (1990a) suggests a vent may occur near the Old Man Hext windmill.

The rhyolite consists of 2% sanidine, 1-2% biotite, and 1-2% quartz phenocrysts in a groundmass of quartz, feldspar, and volcanic glass. Accessory minerals include magnetite, hornblende, and iron oxides. Alteration consists of iron oxides, sericite, and minor silicification. This unit is unconformably overlain by the Summit Mountain formation or the rhyodacite of Mt. Royal (Maps 1, 3).

2.2.4.5 Rhyodacite of Mt. Royal (Trd)—A rhyodacite crops out on the north end of Mt. Royal. Hedlund (1990a) calls this unit the rhyodacite of Carlisle Canyon. This unit is brown-gray to pale-red, foliated, devitrified, and spherulitic rhyodacite dome or intrusive. It is highly fractured and jointed. The joints and fractures do not correspond to foliation; they

may be cooling features. It consists of 25% plagioclase (oligoclase, Hedlund, 1990a), 1% sanidine, 2% quartz, and 3-5% biotite in a fine-grained groundmass of feldspar, volcanic glass, and hornblende or biotite. Accessory minerals include magnetite and apatite. Alteration minerals include chlorite, calcite, quartz, and possibly epidote near the Imperial fault which cuts the unit. This unit has a maximum thickness of 125 m (Hedlund, 1990a) and is unconformably overlain by the Summit Mountain formation.

2.2.5 Summit Mountain formation (Tss)

The Summit Mountain formation (Tss) is the most economically important unit in the Steeple Rock district because it is the predominant host of epithermal mineralization and alteration. Alteration of this unit is extensive and fresh, unaltered outcrops are rare. In addition, this unit is highly faulted and nowhere is there a complete unfaulted section exposed. Age dates of this unit range from 31 to 32 Ma (Table 2.1).

The Summit Mountain formation consists of lava flows, breccias, and volcaniclastic sedimentary rocks. An intrusive andesite also crops out near New Seep windmill. The unit unconformably overlies the rhyodacite of Mt. Royal and the rhyolite of Steeple Rock. It is unconformably overlain by Bloodgood Canyon Tuff, younger ash-flow tuffs, or Dark Thunder Canyon formation.

Total thickness of this unit is uncertain because of faulting. Griggs and Wagner (1966) report a minimum thickness of 457 m. Biggerstaff (1974) reports a minimum thickness of 700 m based on drilling east of Twin Peaks, whereas Hedlund (1990a) reports a possible thickness of 610 m. Drill holes along the East Camp-Summit and Norman King-Billali faults are as much as 518 m deep and remain within the Summit Mountain formation. The Bitter Creek #1 drill hole is 762 m deep and remains in andesite, presumably of the Summit Mountain formation, although the bottom of the hole may actually be in older andesites of Mt. Royal or Mud Springs, which are similar in appearance and composition. The thickness of the Summit Mountain formation is unknown, but probably exceeds 760 m in some areas.

This unit was referred to as the purple andesite porphyry by Griggs and Wagner (1966) and Biggerstaff (1974). Hedlund (1990a, b, c, 1993) designated this unit as the dacite (or dacite porphyry) of Summit Mountain.

2.2.5.1 Andesite and dacite lava flows (Tss)—Lava flows within the Summit Mountain formation are predominantly andesites, andesite porphyries, and less common dacites. Quartz is rarely present as a primary mineral, however, visual examination of many flows will show the presence of small "phenocrysts" of quartz (up to 5 mm in diameter). In thin section, these quartz "phenocrysts" are actually infilling of vugs or amygdules. Some flows do contain primary quartz phenocrysts and are true dacites.

The flows vary somewhat in color from purple to gray to red to brown to black. They are typically porphyritic, thin bedded to massive and locally contain small vesicles or amygdules (Fig. 2.6). The flows vary in appearance and composition; this heterogeneity is characteristic of the entire formation and enables it to be differentiated from the older andesite of Mt. Royal and the younger Dark Thunder Canyon formation. The flows also vary in composition (Appendix 11.4) but typically contain as much as 20% (up to 60% locally) phenocrysts of plagioclase (oligoclase to andesine, Hedlund, 1990a, 1993), hornblende, biotite, pyroxene, and magnetite. Accessory minerals include apatite, titanite, zircon, quartz, and perhaps olivine. Alteration is pervasive and discussed elsewhere. Trachytic textures are common. Some flows are aphanitic.

2.2.5.2 Volcaniclastic sedimentary rocks (Tsed)—Numerous outcrops of volcaniclastic sedimentary rocks occur throughout the Summit Mountain formation. Correlation is difficult because of discontinuity, pinchouts, faulting, and lack of distinguishing characteristics. These units vary from volcanic breccias to andesitic-dacitic tuffs to sandstones to siltstones to rare mudstones. Where altered, they are difficult to distinguish from altered rhyolite ash-flow tuffs. In general, these units are variable in color ranging from various shades of purple, red, gray, green, white to brown, are thin- to medium-bedded, locally laminated or crossbedded, poorly sorted, and consist of angular to subangular fragments of

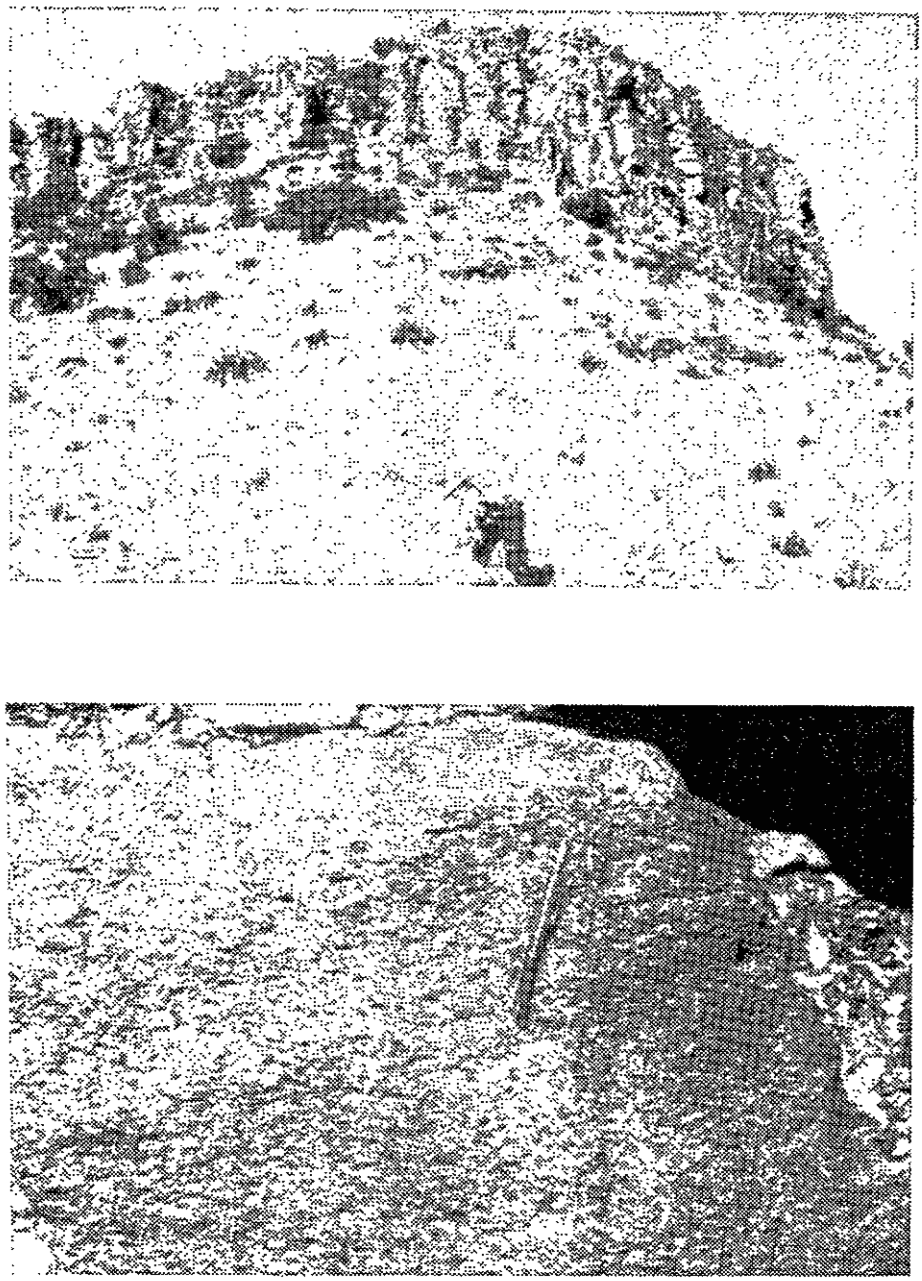

Figure 2.6—View of andesite flow in Summit Mountain formation at Summit Mountain.

lithic fragments of andesite, andesite porphyry, rhyolite, and breccia. Material from silicified veins and breccia zones is absent, indicating deposition prior to epithermal mineralization. Sand and silt size grains consist of lithic fragments, quartz, plagioclase, magnetite and K-feldspar cemented by clay, silica, manganese, or hematite. Tuffs consist of volcanic glass as well as quartz, feldspar, and lithic fragments. Alteration is common and many areas have been intensely altered to clays and other minerals indicative of acid-sulfate alteration (Appendix 11.2). These breccias are poorly sorted, consist of angular fragments in a mudstone matrix, and were probably deposited as mudflows and volcanic lahars. The sandstones and siltstones were deposited as river or stream deposits between periods of lava eruption. They are more common near the top of the Summit Mountain formation and locally occur at depth in the drill holes. The most extensive outcrops of volcaniclastic sediments are at the Carlisle-Center area and east of Telephone Ridge in the Raeburn Hills area (Maps 1, 2; Fig. 2.3). Total thickness rarely exceeds 30 m, however drilling by FMC Gold Co. at Raeburn Hills indicates total thickness of 213 m (E. M. Crist, unpubl. report, October 1988).

2.2.5.3 Intrusive andesite (Tv)—Intrusive andesite intrudes the Summit Mountain andesite flows just east of the New Seep Windmill. This unit is a red to brown, porphyritic plug or dome. Hedlund (1990a) refers to it as porphyritic dacite. Near the top of the unit are several outcrops of volcanic breccia. The contacts with the andesite lava flows are not well exposed, but appear irregular and intrusive. Fine-grained margins occur locally in the intrusive andesite near contacts with andesite flows. It consists of 35% plagioclase (andesine, Hedlund, 1990a), 5-10% hornblende, and 2-5% biotite in a fine-grained spherulitic groundmass of feldspar, volcanic glass, and hornblende or biotite.

2.2.5.4 Altered tuff, sediments and andesite undifferentiated (Tas)—Near the top of the Summit Mountain formation are local zones of intensely acid-sulfate altered rocks, up to 500 m thick locally. These rocks are silicified and altered to clay. They are typically white to maroon to variegated gray, purple, brown, and red. The original lithology of these rocks is obscured by the intense alteration, but they appear to be andesites, sedimentary rocks, and

ash-flow tuffs on the basis of stratigraphic position and relict textures and mineralogy. These rocks are described in more detail in section 5.3.

2.2.6 Davis Canyon Tuff (Tdc?)

A tuff crops out in the southern portion of the study area, east of Steeple Rock (Maps 1, 2) and is tentatively correlated with the Davis Canyon Tuff (Tdc?) on the basis of stratigraphic position. The tuff is light gray to tan to white, locally welded, devitrified, ash-flow tuff that is crystal poor, but characterized by coarse stringy white to gray to brown pumice, several millimeters long, which is characteristic of the Davis Canyon Tuff (Ratté et al., 1984; Hedlund, 1990a). The tuff contains less than 15% phenocrysts (up to 3 mm long) of sanidine, plagioclase, quartz, and biotite with accessory titanite. Lithic fragments of andesite are common (up to several centimeters in diameter; #649, NM960, Appendix 11.2). The tuff is poorly sorted and consists of angular to subangular, broken crystals. It is unconformably overlain by the Bloodgood Canyon Tuff and it unconformably overlies volcaniclastic sandstones or andesites of the Summit Mountain formation. Locally the tuff consists of large boulders of andesite, rhyolite, and tuff (1 m diameter).

The Davis Canyon Tuff is a distinctive outflow sheet derived from the Bursum caldera in the Mogollon Mountains, northeast of the study area (Figs. 2.2, 2.5; Ratté et al., 1984). The Steeple Rock district is the southwestern extent of the Davis Canyon Tuff (McIntosh et al., 1990b). The age of the tuff has been determined by $^{40}Ar/^{39}Ar$ dating as 29.01 ± 0.11 Ma (McIntosh et al., 1990a, b). The tuff has a distinctive paleomagnetic character which enables differentiation from other tuffs in the area (Table 2.2, Fig. 2.4).

2.2.7 Bloodgood Canyon Tuff (Tbg)

The Bloodgood Canyon Tuff (Tbg) crops out throughout the mapped area (Fig. 2.3; Maps 1, 2). The tuff is a light-gray to white, typically welded, devitrified ash-flow tuff that is crystal rich and is characterized by round "eyes" of sanidine and bipyramidal quartz (Ratté et

al., 1984; Hedlund, 1990a, b, c, 1993). The tuff is poorly sorted, angular to subangular and consists of 10-20% phenocrysts, up to 3-5 mm across, of sanidine, quartz, and accessory titanite, biotite, hornblende, and iron oxides (Appendix 11.2). This unit was mapped as Noah Mesa tuff by Wahl (1980), however not all of Wahl's Noah Mesa tuff is Bloodgood Canyon Tuff. Hedlund (1990a, b, c, 1993) also mapped some outcrops of ash-flow tuff as Bloodgood Canyon Tuff which are actually younger ash-flow tuffs. The Bloodgood is easily confused with the younger ash-flow tuffs, especially where weathered or altered and locally only paleomagnetic analysis can distinguish between the tuffs. The Bloodgood Canyon Tuff has a distinctive reversed-polarity paleomagnetic signature that distinguishes it from the younger ash-flow tuffs which have normal polarity (Table 2.2, Fig. 2.4). The Bloodgood Canyon Tuff also contains variable amounts of volcanic lithic fragments, typically andesite or basaltic andesite.

In the Steeple Rock district, the Bloodgood Canyon Tuff unconformably overlies either volcaniclastic sedimentary rocks, andesites and dacites of Summit Mountain formation or the Davis Canyon Tuff (Fig. 2.3; Maps 1, 2). The Bloodgood Canyon Tuff is unconformably overlain by the basaltic andesites of the Dark Thunder Canyon formation. In the Steeple Rock district the Bloodgood Canyon Tuff ranges in thickness from less than a meter to approximately 75 m locally.

The Bloodgood Canyon Tuff is one of the most widespread ash-flow tuffs in the Mogollon-Datil volcanic field. It extends from its source, the Bursum caldera in the Mogollon Mountains (Fig. 2.5), northward to Aragon and as far south as a few kilometers south of Steeple Rock. It extends as far west as Clifton and as far east as Beaverhead (McIntosh et al., 1990a, b). The age of the unit has been determined by $^{40}Ar/^{39}Ar$ dating as 28.05 ± 0.01 Ma (McIntosh et al., 1990a, b).

2.2.8 Dark Thunder Canyon formation (Tbd)

The Dark Thunder Canyon formation (Tbd) consists of multiple gray to brown to

purple to red porphyritic amygdaloidal andesitic to basaltic andesite lava flows with interbedded younger ash-flow tuffs and volcaniclastic sandstones. Griggs and Wagner (1966) called this unit the amygdaloidal andesitic basalt whereas Biggerstaff (1974) called it andesitic basalt. Hedlund (1990a, c; 1993) called the unit basaltic and andesitic rocks of Dark Thunder Canyon. Individual lava flows are typically uniform in composition (Fig. 2.7) and range up to 15 m thick. The unit is characterized by abundant vesicles or amygdules, typically filled with quartz, calcite, and thomsonite (Biggerstaff, 1974). The unit is unconformably overlain by lava flows of Crookson Peak and it unconformably overlies younger ash-flow tuffs, Bloodgood Canyon Tuff or Summit Mountain formation. The younger ash-flow tuffs (Tya, Ta) are also interbedded with the lavas near the base of the unit.

In thin section, the lavas are fine- to medium-grained, hypocrystalline (original glass content probably as much as 15%), trachytic, porphyritic, and locally seriate. The flows typically consist of plagioclase (andesine; Hedlund, 1990a, c, 1993), magnetite, hornblende, pyroxene, and biotite. Alteration minerals include chlorite, calcite, clay, quartz, hematite, and leucoxene. Local accessory minerals include apatite, zircon, and titanite. Olivine was not seen in this study but has been reported by previous workers (Biggerstaff, 1976; Griggs and Wagner, 1966).

The Dark Thunder Canyon formation is as much as 800 m thick (Hedlund, 1990a, c, 1993). Near the base of the unit, the lava flows are interbedded with younger ash-flow tuffs (Ta or Tya) or poorly sorted, poorly rounded, volcaniclastic sandstones, conglomerates, and locally, volcanic breccias (Tsed). These rocks were probably deposited between periods of lava eruption.

2.2.9 Younger ash-flow tuffs

A series of outcrops of ash-flow tuffs (Tya, Ta) occur at or near the base of the Dark Thunder Canyon formation (Maps 1, 2). These tuffs can be distinguished from one another and from the Bloodgood Canyon Tuff primarily by paleomagnetic analyses (Table 2.2). These

tuffs typically have a normal paleomagnetic polarity as opposed to the reverse paleomagnetic polarity characteristic of the Bloodgood Canyon Tuff. The younger ash-flow tuffs have different declinations which suggest two or three closely erupted ash-flow tuffs were emplaced in the Steeple Rock area (Fig. 2.5). Where paleomagnetic or other data are lacking, the tuffs are designated as undifferentiated on Maps 1 and 2 (Ta).

D. C. Hedlund (pers. comm. June 1990) recognized the difficulty in correlating these tuffs because of their similarity in appearance and composition, especially where altered. They vary in color from various shades of yellow, gray, brown to white. Some are lithic rich and crystal poor and locally vary within both a vertical section and laterally. Thicknesses vary from 0 to 30 m. Welding varies from nonwelded to welded.

The tuffs are lighter in color than the andesites and contain essential quartz, sanidine, and biotite phenocrysts in a groundmass of pumice, quartz, and feldspar. Lithic fragments, typically andesite and andesite porphyry, are common and range in size from microscopic to 0.8 m in diameter.

The tuffs are interbedded within the lower portion of the andesite of Dark Thunder Canyon formation (Fig. 2.8), although locally they may also lie unconformably on Summit Mountain formation. In places, they commonly form ridges and hill tops.

2.2.10 Lava flows of Crookson Peak (Tlc)

The lava flows of Crookson Peak (Tlc) consist of predominantly red-brown to grayish-red dacitic to andesitic lava flows that lie unconformably on the Dark Thunder Canyon formtaion. These lava flows form prominent southwest-facing cliffs along the eastern border of the mapped area from Apache Box (north of the mapped area) southward to Crookson Peak and Juniper Peak (Fig. 2.3; Maps 1, 2). This is the same unit as the brown andesite porphyry unit of Biggerstaff (1974) and Griggs and Wagner (1966). Maximum thickness is approximately 460 m (Hedlund, 1990b, c). No thin sections of this unit were examined for

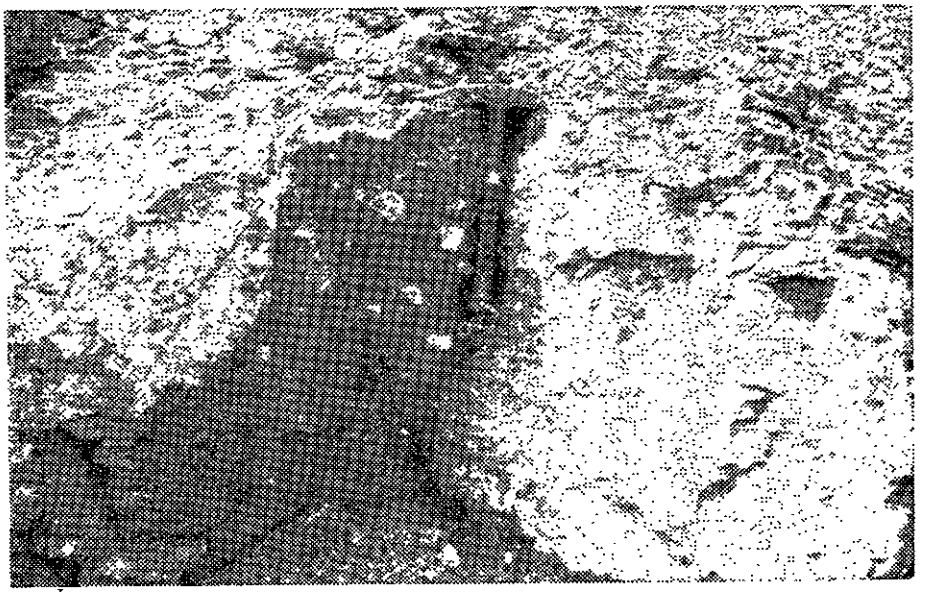

Figure 2.7—View of andesite of Dark Thunder Canyon, near Alabama Ridge.

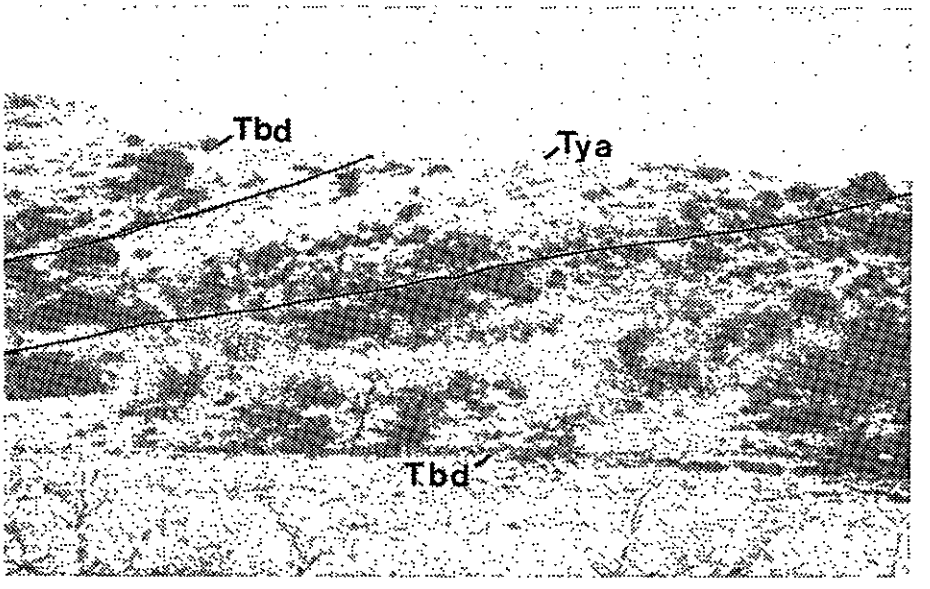

Figure 2.8—View of younger ash-flow tuff (Tya) interbedded within andesite of Dark Thunder Canyon (Tbd). Located in Carlisle Canyon, south of Mt. Royal mine (#726, Map 2).

this study. However, Hedlund (1990a) describes the unit as containing 10-20% oligoclase andesine (An_{28-33}) phenocrysts, locally glomeroporphyrtic, in a felted to pilotaxitic groundmass with disseminated iron oxides and clinopyroxene granules. Griggs and Wagner (1966) also report the presence of augite, magnetite, biotite, and rare quartz and K-feldspar. Less altered portions of the lava flows also contain volcanic glass.

2.2.11 Rhyodacite of Willow Creek (Twd)

The rhyodacite of Willow Creek (Twd) crops out north of the Foothills fault in the northwestern portion of the mapped area (Fig. 2.3; Maps 1, 2). It corresponds to the rhyodacite porphyry of Willow Creek of Hedlund (1990c). It is light brown to gray to gray-red, porphyritic to glomeroporphyritic, foliated rhyodacite flow and lies unconformably on the Summit Mountain formation. This unit grades into a rhyolite flow or dome. Thin sections of this unit were not examined for this study, however, Hedlund (1990c) describes it as a porphyritic flow with a pilotaxitic groundmass. It consists of 5% quartz, 2-3% sanidine, 10% plagioclase (andesine; Hedlund, 1990c) phenocrysts in a groundmass of volcanic glass, feldspar and hornblende or biotite. Accessory minerals include biotite, hornblende, and possibly magnetite. Alteration minerals include iron oxides, sericite, calcite, chlorite, and quartz.

2.2.12 Rhyolite flows and/or domes (Twr)

Rhyolite flows and/or domes (Twr) occur in four areas west of Saddleback Mountain in the northwestern portion of the map area (Maps 1, 2). These units are pink to red to white to gray, foliated to flow-banded, aphanitic to slightly porphyritic rhyolite flows or domes. Locally, they are associated with ash-flow tuffs and/or small zones of pyroclastic fall deposits. Brecciation is locally common. The complex due west of Saddleback Mountain also is associated with black, discontinuous bands of vitrophyre that contain small phenocrysts of sanidine. A sample of the vitrophyre has an $^{40}Ar/^{39}Ar$ date of 25.3 $\pm$ 0.10 Ma (W. C.

McIntosh and R. Appelt, unpublished data, Aug. 1993). Local ash-flow tuffs may also be derived from these domes and rhyolite plugs.

The rhyolites consist of quartz, plagioclase, sanidine, biotite, and volcanic glass. The groundmass is spherulitic to cryptocrystalline (Appendix 11.2). Alteration minerals include iron oxides and sericite and silicification is common locally. Thicknesses probably do not exceed 250 m except at the vents. They are younger than the Summit Mountain and Dark Thunder Canyon formations and may be erupted from a similar source at depth.

2.2.13 Intrusive rocks

Numerous dikes, plugs, and domes occur throughout the study area (Maps 1, 2). Compositions include diabase dikes, quartz monzonite dikes, and rhyolite and rhyodacite dikes, which also include the Apache Box complex, Vanderbilt Peak complex, Piñon Mountains rhyolite, and Twin Peaks rhyolite. Most of the intrusive rocks appear to be fault controlled. Although their age is uncertain, most are younger than 27 Ma because they intrude rocks of that age. Many of the intrusives in the Steeple Rock area have not been dated because they are too silicified and altered. However, a rhyolite dome and two rhyolite dikes in the Steeple Rock district and a number of rhyolite intrusives elsewhere in the vicinity of the study area have been dated (Table 2.1) and these age dates suggest that multiple periods of rhyolitic intrusion occurred between 17 and 28 Ma (Hells Hole; Ratté and Brooks, 1983). The intrusive rocks in the Steeple Rock area possibly represent similar successive periods of emplacement. Some rhyolite dikes intrude older rhyolites. Brecciation is common. Some rhyolites are cut by faults and younger rhyolites, whereas other rhyolites are emplaced along faults. The age of the Steeple Rock rhyolites is probably between 17-28 Ma.

2.2.13.1 Diabase dikes (Td)—Small dikes of altered diabase are found sporadically throughout the Steeple Rock area; some of the larger dikes are shown on Maps 1 and 2. One or more dikes occur in the vicinity of Twin Peaks (Biggerstaff, 1974), near Summit Peak, near the Rattlesnake mines (west of Charlie Hill), north of the Carlisle mine (Powers, 1976),

and at East Camp. Powers (1976) called these microdiorite porphyry, Biggerstaff (1974) calls these basalt or microdiabase, and Griggs and Wagner (1966) called these diorite or diorite porphyry. These dikes are green to gray-green, less than a meter wide, and characterized by a trachytic texture of white plagioclase needles in a fine-grained, chloritized matrix. In thin-section, the diabase is fine- to medium-grained, with a seriate, holocrystalline, and porphyritic to glomeroporphyritic texture. It consists of essential plagioclase and hornblende, pyroxene, or biotite (now completely altered to chlorite) and accessory magnetite, biotite and titanite. Alteration minerals include chlorite, sericite, quartz, hematite, leucoxene, pyrite, epidote, and adularia (#169,187, Appendix 11.4).

2.2.13.2 Quartz monzonite dike (Tq)—A dike of quartz monzonite which is up to 30 m wide and almost 8 km long cuts the rhyolite of Steeple Rock in the southern portion of the mapped area (Fig. 2.3; Maps 1, 2; Hedlund, 1990a). Hedlund (1990a) reports an age date of 21.4 $\pm$ 1.6 Ma from this dike. Powers (1976) refers to the dike as granite porphyry whereas Hedlund (1990a) called it quartz monzonite porphyry. According to the classification of LeMaitre (1989) the dike is a quartz monzonite.

The dike is medium- to coarse-grained, porphyritic to glomerophyritic, and holocrystalline. It is sinuous and pinches and swells along strike. It consists of plagioclase (oligoclase; Hedlund, 1990a), K-feldspar, quartz, and accessory biotite, magnetite, titanite, hornblende, and zircon (#651, Appendix 11.4). Alteration minerals (probably originally hornblende, biotite, titanite, and feldspar) consist of sericite and hematite.

2.2.13.3 Rhyolite and rhyodacite dikes (Tr, Trp)—Numerous rhyolite and rhyodacite dikes cut the volcanic rocks of the Steeple Rock area (Fig. 2.3; Maps 1, 2). Hedlund (1990b) reports a fission track age on zircon from a rhyolite dike as 21 Ma, however the exact sample location is unknown. Wahl (1983) also reports an age from a rhyolite dike of 18 Ma, but the location is unknown. R. Applet (unpublished data, 1993) reports an age determination from a rhyolite dome west of Saddle Back Mountain as 25.3 $\pm$ 0.10 Ma (Table 2.1). Many are undoubtedly related to intrusive plugs and necks and some may be

indicative of larger intrusions at depth. Many occur in discrete belts or swarms that commonly trend northwest and northeast. Most previous workers have identified them as rhyolite or rhyodacite composition. However, Powers (1976) also refers to them as intrusive breccia, banded rhyolite, and granite porphyry. Terminology defined by LeMaitre (1989) is used here.

The intrusive rocks range in color, depending on alteration and composition, from white to gray to pink to red to purplish gray. The dikes range in size from less than 6 m wide and up to several 100s of meters long. They are sinuous and pinch and swell along strike. Textures are variable. They are aphanitic or microcrystalline to porphyritic to glomeroporphyritic (Fig. 2.9). Near vertical flow-banding is common. Spherulitic textures are locally preserved. Autobrecciation is also locally common. The rhyolites are typically phenocryst poor (less than 15%) and consist of quartz, k-feldspar, and accessory biotite, hornblende, titanite, and zircon. Alteration is common, especially silicification (Appendix 11.4).

2.2.13.4 Apache Box rhyolite complex—Although the Apache Box rhyolite complex lies just north of the mapped area, it is described here because it is similar in age and appearance to other rhyolite intrusives within the mapped area. This complex consists of a series of rhyolite plugs and dikes, some of which are vertically flow-banded, that have intruded Dark Thunder Canyon formation and the lava flows of Crookson Peak (Hedlund, 1990c; Ratté and Hedlund, 1981).

The rhyolite is pink to red to light brown-gray, fine-grained, crystal-poor to porphyritic to glomerophyritic and holocrystalline. It consists of plagioclase (oligoclase; Ratté and Hedlund, 1981), sanidine, quartz and accessory biotite, zircon, and magnetite (#1048, Appendix 11.4). Alteration minerals include sericite and hematite and silicification is common.

2.2.13.5 Vanderbilt Peak rhyolite complex (Tr)—Rhyolite plugs intrude the Dark Thunder Canyon formation on the southern end of Vanderbilt Peak and south of the peak (Fig. 2.3; Maps 1, 2). Numerous rhyolite dikes extend southward from the peak and also

Figure 2.9—Flow-banded rhyolite dike, Alabama Ridge.

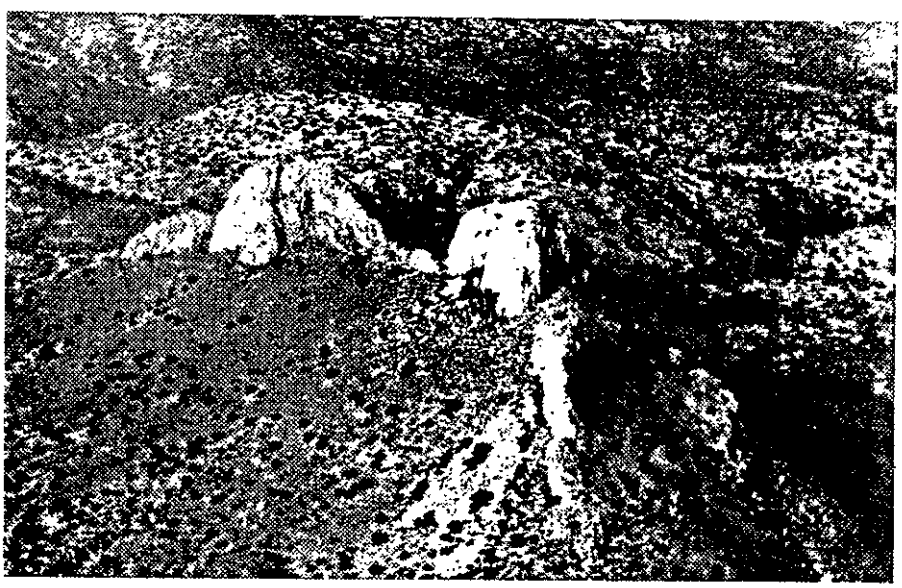

Figure 2.10—View of Twin Peaks rhyolite (northern part of map area). View from the air looking southwest.

form dike swarms around Vanderbilt Peak. Most of the plugs and dikes appear to be fault controlled, although some have been offset by younger faulting. The dikes continue southward, where they become part of the Piñon Mountains rhyolite plug. The dikes and plugs are similar in appearance, mineralogy, and chemistry and probably were emplaced at the same time from the same source (Biggerstaff, 1974). Ash-flow tuffs and volcanic breccia deposits surround some of the plugs, suggesting the plug breached the surface and produced pyroclastic deposits.

The rhyolite is fine- to medium-grained, flow-banded, and varies in color from various shades of red, brown to gray. It is crystal-poor to porphyritic to glomerophyritic and holocrystalline. The rhyolite consists of quartz, sanidine and accessory biotite, hornblende, zircon, and magnetite. Accessory minerals include sericite, hematite, and silicification is common (Appendix 11.2).

2.2.13.6 Piñon Mountains rhyolite (Tr)—A large rhyolite plug forms much of the Piñon Mountains. This rhyolite intrudes Summit Mountain formation and Bloodgood Canyon Tuff. Paleomagnetic data confirms this tuff as Bloodgood Canyon Tuff (#1039, Table 2.2); however, it is possible that some outcrops of tuff may actually be related to emplacement of the Piñon Mountains rhyolite. Rhyolite dikes extend northwest and southeast which are probably related to this intrusion.

This rhyolite is fine-grained, locally flow-banded, and varies in color from various shades of red to gray. It is typically crystal-poor, although locally it is porphyritic. It is holocrystalline and consists of quartz, plagioclase, sanidine, and accessory biotite, magnetite, zircon, and possibly hornblende. This rhyolite is less altered than at Vanderbilt Peak, however locally it is altered to hematite and sericite and silicification is also locally common (Appendix 11.4).

2.2.13.7 Twin Peaks rhyolite (Tr)—The Twin Peaks rhyolite dike or plug forms the prominent Twin Peaks (Fig. 2.10). The intrusive is gray to red to orange, fine-grained, porphyritic, and holocrystalline to hypocrystalline (less than 5% glass; Biggerstaff, 1974). It

is up to 100 m wide and 600 m long and forms prominent cliffs. The rhyolite consists of K-feldspar, biotite, magnetite, and titanite (#1028, Appendix 11.4). Biggerstaff (1974) also reports primary hornblende. Alteration minerals consist of sericite, hematite, leucoxene, kaolinite, pyrite and malachite. Some quartz is probably also hydrothermal or secondary. Nearby dikes may also be genetically related to the Twin Peaks rhyolite.

2.2.14 Quaternary rocks

It is beyond the scope of this report to examine the Quaternary units in any detail; however, four units are designated on the geologic maps (Maps 1, 2; Hedlund, 1990a, b, 1993). The oldest unit, the Gila Group, is Pleistocene to Miocene in age (QTg; Maps 1, 2). This unit consists of poorly bedded, moderately indurated, poorly-sorted fanglomerate with some sand, silt and gravel deposits. This unit is as much as 300 m thick (Hedlund, 1993). The next unit (Qaf) consists of alluvial-fan deposits which contain floodplain deposits of unconsolidated, poorly sorted, subangular to angular fragments of Tertiary volcanic rocks. Locally these fan deposits are as thick as 85 m (Hedlund, 1990a, b, c). The youngest unit (Qal), alluvial gravels, consists of unconsolidated, poorly-sorted gravel, sand, and silt and also contains fragments, including boulders, of Tertiary volcanic rocks. This unit occurs within arroyos and streams and is probably less than 3-4 m thick.

A sinter or spring deposit (Qs), presumably of Quaternary age, crops out in Bitter Creek (sec. 20, T16S, R21W). The material is soft, friable, unconsolidated, white to tan, and varies in texture from spongy to poorly indurated. It consists of gypsum, silica (amorphous), and calcareous clay (SINTER, Appendix 11.3). The maximum thickness is probably less than 8 m.

2.3 Structural Geology

2.3.1 Regional

The regional structural evolution of the southwestern United States and northern

Mexico has been dominated by a succession of dynamic and sometimes rapidly changing plate tectonic settings from the Proterozoic to the Recent (Coney, 1978; Karlstrom and Bowring, 1988; Karlstrom et al., 1990). This prolonged history of complex continental tectonics can be divided into eight phases: (1) Mazatzal orogeny, 1650-1600 Ma (Karlstrom and Bowring, 1988; Karlstrom et al., 1990), (2) Late Proterozoic granitic plutonism, 1450-1400 Ma (Karlstrom and Bowring, 1988; Stacey and Hedlund, 1983), (3) Paleozoic period of basin formation and uplift (Florida uplift, Pedregosa Basin, southern extension of Ancestral Rocky Mountains, Ross and Ross, 1986), (4) late Triassic to late Jurassic magmatic arc activity in western Arizona, northern Mexico, and California (which did not extend into New Mexico; Drewes, 1991), (5) Cretaceous back-arc, shallow marine deposition, (6) Laramide compressional deformation and magmatic arc volcanism and plutonism (Late Cretaceous to early Tertiary), (7) mid-Tertiary calc-alkaline volcanism to bimodal volcanism with caldera formation, and (8) late Tertiary-Quaternary Basin and Range extensional deformation (Coney, 1978). Each of these tectonic periods left remnant structural trends that were either reactivated or crosscut by younger tectonic events and together have resulted in a structurally complex, relatively thin, brittle crust; a perfect setting for epithermal deposits.

Although each tectonic event had lasting effects, the most important tectonic events affecting the Steeple Rock area are the more recent events. Since Late Cretaceous times, southwestern New Mexico, and most of the southwestern United States and northern Mexico, have undergone episodic tectonic activity. This tectonic activity was related to complex motions of lithospheric plates off the coast of California. Laramide compressional deformation from Late Cretaceous to early Tertiary formed a series of north- to northwest-trending uplifts and broad shallow basins (Seager et al., 1986; Drewes, 1991). This Laramide compressional event resulted from the rapid subduction of the Farallon plate beneath the North American plate (Coney and Reynolds, 1977; Keith, 1978; Dickinson, 1981). Most of the Laramide event in New Mexico was amagmatic, however, arc magmatism migrated eastward as subduction continued, producing several Laramide intrusions in eastern Arizona and

southwestern New Mexico. The copper porphyry intrusives at Safford, Morenci, Santa Rita, and Tyrone are products of this event (Figs. 1.1, 2.2; Coney and Reynolds, 1977; Titley, 1982; Davies, 1989). Although rocks of Laramide age are not exposed in the mapped area of the Steeple Rock district, Laramide faults have exposed portions of the Proterozoic and Paleozoic crust south of Steeple Rock at Riley Peaks (Hedlund, 1990a; Drewes et al., 1985).

Starting at 50-40 Ma, extensive intermediate to silicic calc-alkaline volcanism and associated plutonism occurred throughout southwestern New Mexico and adjacent Mexico and resulted in major andesitic volcanic centers and numerous calderas (Table 2.3). Then at about 40–50 Ma, several large volcanic fields developed in the area from Colorado southward into Mexico and Texas (Table 2.3, Fig. 2.2) and temporally coincided with the change in tectonic style from Laramide compressional to Tertiary extensional deformation. This change in tectonic style also coincided with a change in magmatism from calc-alkaline to bimodal compositions.

The tectonic style during this period is controversial and varies from place to place. Individual rhyolite ash-flow sheets (ignimbrites) spread across thousands of square kilometers in southern New Mexico and Arizona (Ratté et al., 1984; Ratté and Gaskill, 1975; Morgan et al., 1986; Drewes et al., 1985; McIntosh et al., 1990a, b, 1992a) and suggest to some investigators that neither active extension nor active compression was dominant. Many of the volcanic rocks in the Steeple Rock district were emplaced during this period.

Some geologists believe that mid-Tertiary arc magmatism was accompanied by back-arc or arc extension during this time (Elston, 1984; Engebretson et al., 1984). Cather (1990) suggests incipient extension in central New Mexico began about 36 Ma. Others believe that Laramide compression continued until about 32 Ma (Henry and Price, 1986; Price and Henry, 1984). It is apparent from the literature that the transition between Laramide compressional and mid-Tertiary extensional deformation varied from place to place and is difficult to date in most areas.

Thus the orientation of the stress fields and resultant structural styles of deformation

Table 2.3—Volcanism in eastern Arizona, New Mexico, Texas and northern Mexico (from Elston, 1989; Henry et al., 1989; Henry and Price, 1984; 1986; Goff et al., 1989; Lipman and Reed, 1989; Lipman, 1989; de Cserna, 1989; McIntosh et al., 1992a).

Field	Type of Volcanism	Age	Area
San Juan field	intermediate composition then shifts to bimodal at 26 Ma	35-26 Ma	25,000 sq km
Jemez-Questa	Questa-bimodal, peralkaline; Valles-bimodal, subalkaline	26-15 Ma 13-0.13 Ma	
Mogollon-Datil	calc-alkaline to bimodal volcanism with calderas	40-20 Ma	40,000 sq km
Trans-Pecos Texas	alkaline volcanism with calderas, change from bimodal to alkaline–intermediate at 28 Ma	48-17 Ma	4,000 sq km
Sierra Madre-Occidental	calc-alkaline to intermediate volcanism with some mafic flows (bimodal) associated with calderas	100-45 Ma, 34-23 Ma	450,000 sq km

during this transition period are uncertain. However, by 30-25 Ma, the changing patterns of sedimentation, magmatism, and deformation throughout New Mexico and eastern Arizona indicate that extensional deformation was the dominant tectonic style. The prominent structural features resulting from this extensional tectonic period were half-grabens bounded by near-surface high-angle normal faults which produced the valleys and mountains so characteristic of the Basin and Range province. These high-angle faults may flatten at depth forming listric faults. Most of the rocks in the Steeple Rock mining district were erupted and emplaced at the end of this transition period, 34 to 17 Ma.

Many of the intrusives and volcanic centers in southwestern United States and Mexico

appear to be controlled by regional lineaments (Mayo, 1958; Wertz, 1970a, b; Lowell, 1974; Chapin et al., 1978). For the purposes of this study, a lineament is defined as a broad, linear zone of topographic, structural, and magmatic features, including faults, alignment of volcanic and plutonic centers, uplifts and basins (Bates and Jackson, 1980; Heyl, 1983). Current theories on the evolution of continental lineaments suggest that they are deep-seated, reactivated zones of crustal weakness that have been active sporadically since Proterozoic times (Heyl, 1983; Favorstiaya and Vinogradov, 1991).

At least three lineaments occur in the vicinity of the Steeple Rock area (Fig. 2.2). The Texas lineament extends from Trans-Pecos Texas west-northwestward into southeastern Arizona where it probably joins the Arizona transitional zone (Muehlberger, 1980; Wertz, 1970a, b). It is a prominent 80-150 km wide zone that is defined by basins, ranges, and structural features (Lowell, 1974; Wertz, 1970a, b; Turner, 1962; Schmitt, 1966; Drewes, 1991). Dip-slip (normal, steep reverse or thrust) movements are common throughout this zone and locally strike-slip movement has been documented (Turner, 1962; Wertz, 1970a, b; Muehlberger, 1980). The Steeple Rock mining district lies on the northeastern edge of the Texas lineament.

North of the Steeple Rock area is the prominent northeast-trending Morenci lineament (Fig. 2.2). The Morenci lineament can be traced from Safford, Arizona, northeast to Reserve, New Mexico, and includes the Safford and Morenci porphyry copper deposits. The epithermal silver-gold deposits of the Mogollon district lie on the southern edge of the lineament (Lowell, 1974; Chapin et al., 1978). It also includes the Morenci uplift of Cather and Johnson (1986).

A third potential, but not as well accepted, lineament is positioned south of the Steeple Rock district and is known as the New Mexico mineral belt (Lowell, 1974) or the Santa Rita lineament (Chapin et al., 1978). This lineament extends from Cananea, Sonora, Mexico, northeastward to Santa Rita, New Mexico, and includes the Cananea, Bisbee, Santa Rita, and Tyrone porphyry copper deposits and numerous smaller epithermal districts (Lowell, 1974). It may continue to the northeast through the Kingston and Hillsboro districts

in Sierra County, New Mexico (Fig. 1.1; Rose and Baltosser, 1966). This lineament is defined by Laramide intrusives and northeast-trending faults (Rose and Baltosser, 1966).

2.3.2 Local structure

Faulting and tilting of the volcanic rocks in the Steeple Rock district produced a series of half-grabens and horsts (Map 3) with a district-wide, regional northwest strike of foliation and bedding planes that dip northeast (10-35°; Fig. 2.11). Foliation, for the purposes of this report, is defined as flow foliation formed by flattening of vesicles or pumice fragments and alignment of phenocrysts. Rhyolite dikes, plugs, and domes were emplaced along some of the faults and then subsequently cut by other faults (Table 2.4). Overall, orientations of rhyolite dikes exhibit a random pattern (Fig. 2.12).

Most faults in the Steeple Rock district are high-angle and well exposed because they are filled with quartz veins and/or silicified, brecciated country rock. The faults can be classified by orientation as (1) northwest-trending faults, (2) north-trending faults, (3) west-northwest-trending faults and shear zones, and (4) northeast-trending faults (Fig. 2.13, Table 2.4). Relative ages of these faults are difficult to interpret because of conflicting field relationships and multiple periods of movement. The term "shear zone" is used in this report to describe a zone of parallel to subparallel anastomosing faults or brittlely shattered or pulverized rock (Marshak and Mitra, 1988). All faults and shear zones in the Steeple Rock district are indicative of brittle deformation; no ductile or brittle-ductile shear zones are recognized in this area.

2.3.3 Northwest-trending faults

The northwest-trending faults are the most prominent and most numerous structural features in the Steeple Rock area (Map 1, Figs. 2.3, 2.13, 2.14). This same northwest trend is observed in both the aeromagnetic and Bouguer gravity data (Wynn, 1981; Klein, 1987), suggesting that deep-seated, regional northwest-trending structural features exist. This

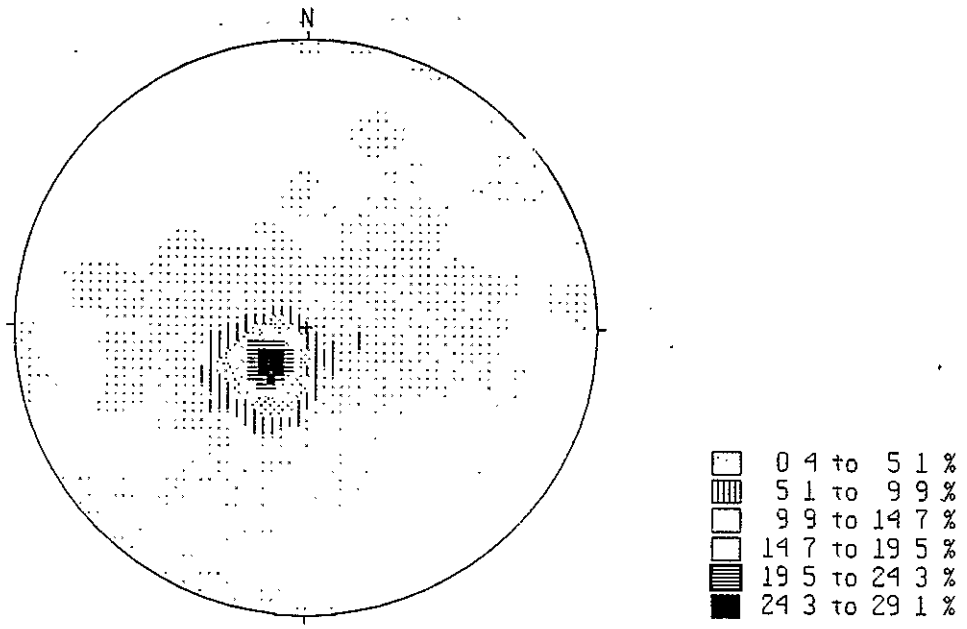

Figure 2.11—Stereonet of orientations of foliation and bedding planes of extrusive volcanic units in the Steeple Rock district (step function grid, n = 282).

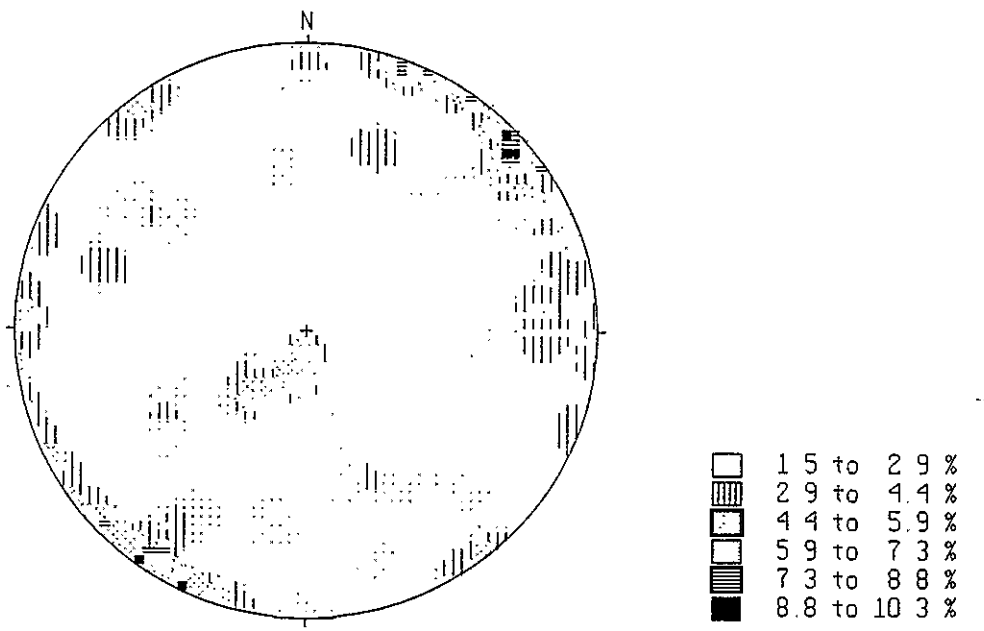

Figure 2.12—Stereonet of orientations of foliation and attitude of rhyolite intrusives in the Steeple Rock district (step function grid, n = 68). Note the orientations have a random pattern.

TABLE 2.4—Summary of faults in the Steeple Rock district. Faults are mid-Tertiary in age although movement occurred along some faults as early as Miocene to Pleistocene as evidenced by offset of the Gila Group (Quaternary-Tertiary). *Faults truncated by the Carlisle fault.

Fault	Fault segments	Average strike	Average dip	Displacement (m)	Downthrown	Known mineralization	Hosts rhyolite dikes, plugs	Other comments
Bluebell	--	N50 - 60°W	Steep NE	60?	NE	yes	yes	Bloodgood Canyon Tuff and Summit Mountain formation against Dark Thunder Canyon formation.
	west	N65 - 80°W						
	east	N45°W						
East Camp-Twin Peaks	--	N50-55°W	Steep NE to SW	90-427	NE	yes	yes	Summit Mountain formation against Dark Thunder Canyon. Also offsets acid-sulfate altered rocks.
	East Camp-Summit							
	Norman King-Billali							
	Twin Peaks							
*Blue Goose	--	N30-55°W	65-80°SW	<30	SW	yes	yes	Younger ash flow tuff (Tya3) against sedimentary rocks. Merges with Apache fault.
	east	N10°W						
	Center	N30°W						
*Apache	--	N40-50°W	50-70°SW	150-240	SW	?	yes	
*Laura fault zone	multiple segments	N30-50°W	80-85°SW	250-300	SW	yes	yes	Summit Mountain formation against Dark Thunder Canyon formation.
Jim Crow-Gold King-New Years Gift	3 or more parallel to subparallel segments	N45-65°W	75-86°SW	30-50	SW	yes	no	Offsets rhyolite dike at Alabama Ridge.
				?	N			
Commerce-Mayflower	--	N60°W	70-80°SW	≥100	SW	yes	no	Gila Group against Summit Mountain formation. Merges into Bitter Creek shear zone.
Foothills	2 or more subparallel faults	N50°W	70-85°SW	≥100	SW	yes	no	Gila Group against Summit Mountain formation. Offsets rhyolite dome or lava.
Fourth of July	--	N30-40°W	55-60°S	small	SW	yes	no	Offsets fluorite and quartz veins.
Alabama	--	N10°W	80°W	40-50 M	W	yes	yes	Offsets younger ash flow tuff (Tyal).
Alabama crossfault	--	N70°W	70°N			?	no	Offsets gold-silver veins.
Imperial	--	N10W to N20°E	70-85°W	920 m	W	yes	no	Rhyodacite of Mt. Royal against Dark Thunder Canyon formation. Largest displacement in area. Offsets rhyolite dikes and Gila Group.
Carlisle	--	N75°W-N85°E	60-70°S	varies from 180 to 610 m	S	yes	yes	Oblique movement to SW.
Bank shear zone	--	?	?	?	?	no	no	Obscured by acid-sulfate alteration.
	north	N10°W to N20°W	steep	?	?	yes	no	
Bitter Creek shear zone	several subparallel segments	W to NW	steep?	?	N	yes	no	Offsets rhyolite dikes and fluorite veins and East Camp-Twin peaks fault.
Crookson	--	N85°E	?	small	S	no	no	Offsets lava flows of Crookson Peak.
Charlie Hill	--	N70°W to N80°E	80°S to 80°N	50-60 m	N	no	no	Offsets rhyolite dike.

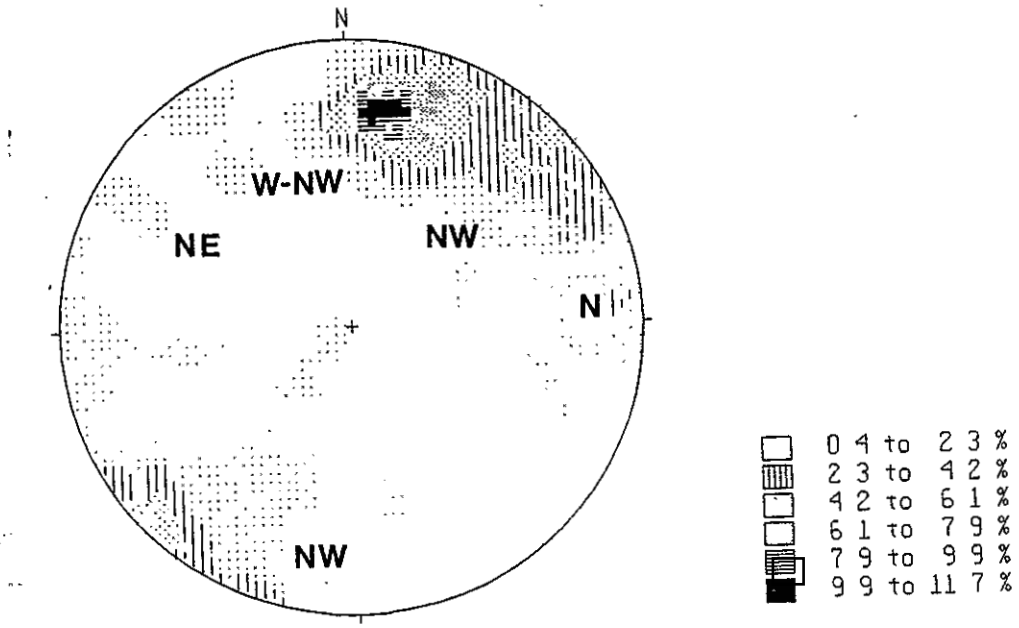

Figure 2.13—Stereonet of orientations of fault planes in the Steeple Rock district (step function grid, n = 281).

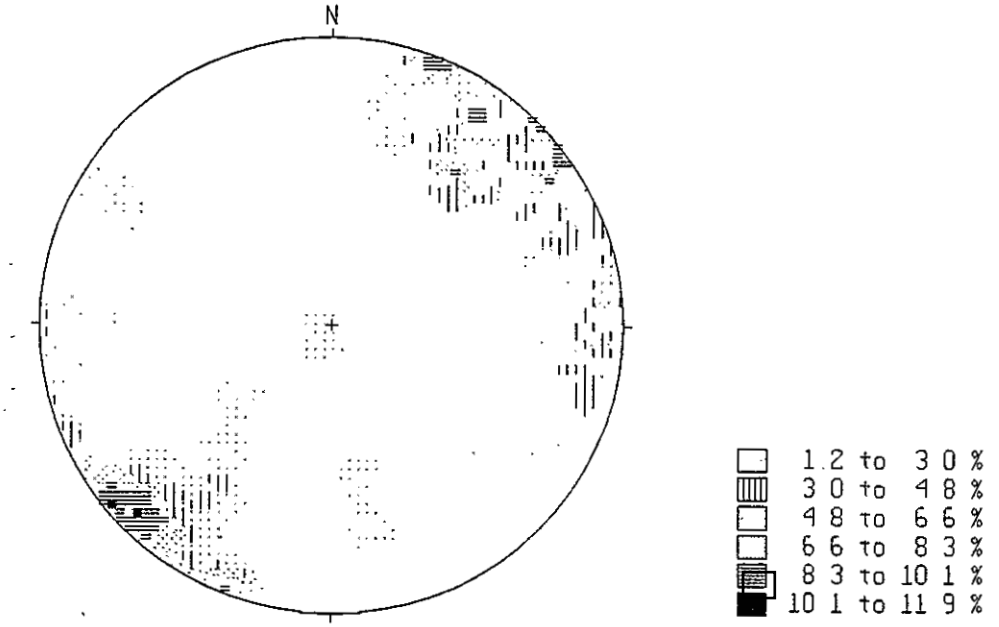

Figure 2.14—Stereonet of orientations of northwest-trending fault planes in the Steeple Rock district (step function grid, n = 84). West-trending orientations represent bends along the fault surface.

northwest trend subparallels the west-northwest-trending Texas lineament of Wertz (1970a, b), Chapin et al. (1978) and others. Some of these faults may be a continuation of similar trending faults in the Burro Mountains (Drewes et al., 1985). The Laramide Burro uplift also has a similar northwest trend (Mack and Clemons, 1988; Drewes, 1991). Some of the rhyolite dikes and plugs also have a similar northwest trend, especially south of the Carlisle fault (Maps 1, 2; Fig. 2.12). Some rhyolite intrusives follow discrete fault zones; whereas others occur along northwest-trending fractures or joints. The quartz monzonite dike cutting Steeple Rock also has a northwest trend (Fig. 2.3; Maps 1, 2).

Most of the northwest-trending faults are characterized by quartz veins, silicified wall rock, and/or rhyolite dikes that form prominent outcrops. These faults rarely follow arroyos or current drainage features, although some arroyos will follow northwest-trending faults for short distances. The age and displacements along these faults vary and are the subject of controversy.

South of the Carlisle fault (Fig. 2.3; Maps 1,2), the northwest-trending faults dip to the southwest 55-80° and are downthrown to the southwest. However, the major northwest-trending faults north and east of the Carlisle fault are steeply dipping (> 80°) to vertical and are typically downthrown to the northeast (Griggs and Wagner, 1966). Some faults also show reverse movement (Bluebell and East Camp-Summit faults). Displacements also vary along strike of many faults. Faults will be discussed from northeast to southwest.

2.3.3.1 Blue Bell fault—The Blue Bell (Bluebird) fault lies northeast of and subparallel to the East Camp fault. The strike ranges from N50 to 60°W, although local variations are common. The fault consists of either massive quartz veins, quartz-calcite veins or silicified, closely fractured host rock and is up to 8 m wide. South of the Raeburn Hills area, the fault dips steeply to the northeast and is downthrown to the northeast. South of the Blue Bell shaft, the fault splits into two segments (Maps 1, 2; Griggs and Wagner, 1966), which die out southeast of the mapped area (Drewes et al., 1985). The southwestern segment is northwest-trending (N45°W) and offsets a younger ash-flow tuff. The northeastern segment

strikes N65-80°W and is roughly aligned with the Carlisle fault. However, the eastern segment is downthrown to the northeast unlike the Carlisle fault which is downthrown to the south.

North of the Raeburn Hills area, the Blue Bell fault dips to the southwest, but is downthrown to the northeast. The Blue Bell fault splits into a 150-m wide zone consisting of a series of multiple, bifurcating subparallel quartz veins. Some of the thin (< 1 m wide) quartz veins intersect the East Camp-Summit fault near the Summit and Bank mines. This zone is probably the continuation of the Blue Bell fault which continues trending northwest, although poorly exposed northwest of Juniper Peak. This zone finally intersects the Norman King-Billali fault near the Mohawk mine. The total length of the Blue Bell fault is approximately 13 km.

Displacement along and age of the Blue Bell fault zone are uncertain. It is unlikely that more than 60 m of displacement have occurred along the Blue Bell fault, based on displacement of the Bloodgood Canyon Tuff (Map 3). The fault cuts the Dark Thunder Canyon formation and the Bloodgood Canyon Tuff. An undeformed rhyolite dike has also been intruded along the fault at Raeburn Hills. Therefore the last movement along the Blue Bell fault must have occurred before emplacement of the rhyolite intrusive and quartz veins.

Production along the Blue Bell fault has occurred only at the Blue Bell mine (copper, gold, silver; Table 3.2), although the fault is silicified and stained with malachite, chrysocolla, and azurite along much of its length. The Blue Bell fault south of Raeburn Hills consists of massive to bladed, white quartz (locally pseudomorphed after bladed calcite) and bladed, white to clear calcite. North of Raeburn Hills only quartz is present. Shallow drilling by FMC at Raeburn Hills and by Nova Gold Resources, Ltd. (probably less than 200 m) south of Raeburn Hills failed to delineate any economic potential.

2.3.3.2. East Camp-Twin Peaks fault system—The East Camp-Twin Peaks fault system is one of the most prominent fault systems in the district (Fig. 2.3; Maps 1, 2). The fault begins near Blue Creek, southeast of the mapped area (Drewes et al., 1985) and can be

traced as one or more parallel to subparallel faults for approximately 30 km to the northwest, where it joins the Twin Peaks fault of Hedlund (1990a). It is finally cut off by a northeast-trending fault and covered by alluvium northwest of the mapped area.

The fault system strikes N50-55°W, but has numerous local variations, and typically dips steeply to the northeast but locally to the southwest as well (Fig. 2.15). It is downthrown to the northeast (Map 3). Throughout most of its length, the fault is silicified and mineralized and forms prominent outcrops. Rhyolite dikes intrude along the fault at the junction with the Carlisle fault, east and north of Telephone Ridge, and possibly at the Bank mine. Intense acid-sulfate alteration has obscured the lithologies at the Bank mine. Numerous mines occur along the fault system (Table 3.2). The fault typically exceeds 9 m in width and at the Summit mine the fault is 45 m wide at the surface (Fig. 2.16).

Displacement along and age of the East Camp-Twin Peaks fault system are uncertain. The fault cuts the Dark Thunder Canyon formation, the Summit Mountain formation, and a younger ash-flow tuff. In addition, the fault places acid-sulfate altered rocks adjacent to relatively unaltered Dark Thunder Canyon andesites north of Bitter Creek. This suggests a large displacement has occurred along the fault (>100 m). Hedlund (1990a) suggests total displacement is approximately 420 m but provides no evidence. The East Camp-Twin Peaks fault system also is intruded by rhyolite dikes and offsets other rhyolite dikes. Right-lateral strike separation of about 150-200 m is suggested north of Bitter Creek where the fault offsets a rhyolite dike (Maps 1, 2; Powers, 1976). Therefore, the East Camp-Twin Peaks fault system is probably of a similar age as the Blue Bell fault, i.e. older than the youngest rhyolite intrusives and quartz veins.

The East Camp-Twin Peaks fault system is cut by two shear zones in the mapped area: a shear zone near the Bank mine (Bank shear zone) and the Bitter Creek shear zone. Both shear zones are poorly exposed at the surface. The Bitter Creek shear zone is west-northwest-trending. The Bank shear zone is concealed and has either an east or north trend. Both shear zones, described further in this section, have greatly influenced the distribution of

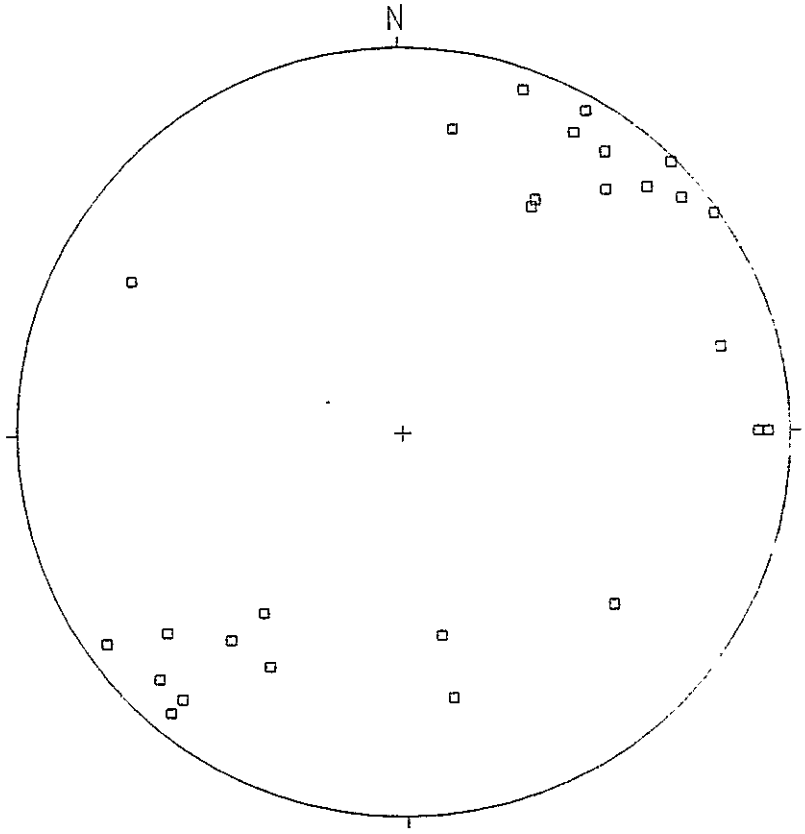

Figure 2.15—Stereonet of orientations of fault planes along the East Camp-Twin Peaks fault system (Schmidt projection, n = 30).

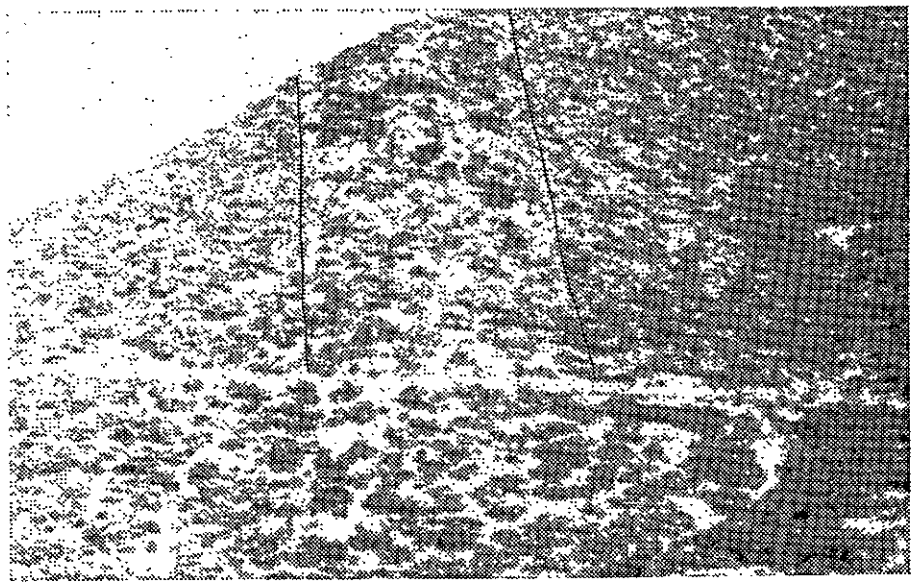

Figure 2.16—Photo looking at the East Camp-Summit fault which is up to 45 m wide. Located in roadcut just southeast of Bank mine (note head frame in lower right corner). Looking southeast.

mineralization along the East Camp-Twin Peaks fault system. Because of these shear zones and their effects on mineralization, it is convenient to divide the East Camp-Twin Peaks fault system into three segments (southwest to northeast): East Camp-Summit fault, Norman King-Billali fault, and Twin Peaks fault (Maps 1, 2). The Blue Bell fault merges with the East Camp-Twin Peaks fault near the Norman King mine.

The East Camp-Summit fault is the southeasternmost segment and is represented by numerous mines with significant production including the Thanksgiving, Davenport, McDonald, East Camp, Gold Nugget, Summit, and Bank mines. The fault extends northwestward past the Bank mine, where it is cut by the Bank shear zone. It is mineralized along most of the strike length in the mapped area (Map 2).

The middle segment is the Norman King-Billali fault which is a prominent, quartz-filled zone. This segment is mineralized along its entire length, from the Bank shear zone to the Bitter Creek shear zone and consists of numerous mines including the Billali, Hover Tunnel, Norman King, and Mohawk mines. North of the Mohawk mine, the Norman King-Billali fault is offset by the Bitter Creek shear zone.

North of the Bitter Creek shear zone, only one major fault of the East Camp-Twin Peaks system is exposed, the Twin Peaks fault. Much of this fault segment is also silicified and mineralized along strike, but rarely exceeds 6 m in width. Production has not been as significant along the Twin Peaks fault as from mines south of Bitter Creek. The Fraser and Black Willow mines occur along this fault segment.

South of the Bank shear zone, the East Camp-Twin Peaks fault system consists of the prominent East Camp-Summit fault on the southwest side of the Blue Bell zone of multiple, bifurcating quartz veins. All of the past production, except the Blue Bell mine, has come from mines along the East Camp-Summit fault. The Blue Bell mine is a copper-gold-silver mine with relatively minor production (Table 3.2).

North of the Bank shear zone, the East Camp-Twin Peaks fault system consists of a wide zone with three major faults. The northeastern fault is narrow and poorly exposed along

much of its strike length and may be the extension of the Blue Bell fault. It intersects the Norman King-Billali fault at the Mohawk mine. The middle and most prominent fault is the Norman King-Billali fault. The southwestern fault is poorly exposed, less than 1 m wide, and is only locally silicified and filled with quartz. All of the past production from mines between the Bank and Bitter Creek shear zones has been from mines that occur along the Norman King-Billali fault.

Several crossfaults have either caused minor bends or offsets to the faults of the East Camp-Twin Peaks fault system or are truncated by the fault system. Two minor east-west to northeast-trending faults southwest of the East Camp mine are truncated by the East Camp-Summit fault. A third fault northwest of the mines also is truncated by the East Camp-Summit fault. The west-northwest-trending Carlisle fault appears to be truncated by the East Camp-Summit fault, however the Carlisle fault did produce a small offset (less than 5 m) or bend in the East Camp-Summit fault. The Carlisle fault could not be found northeast of the East Camp-Summit fault. The Twin Peaks fault offsets two rhyolite dikes and the Twin Peaks plug.

2.3.3.3 Blue Goose fault—The Blue Goose fault, named for the Blue Goose mine, strikes N30-55°W and dips 65-80° southwest. It is downthrown to the southwest and is about 4-5 km long. To the south, the fault is not well exposed, although the fracture probably intersects the Apache fault near the Hext mine. Near the Goldenrod adit, the fault splits into two segments. The eastern segment strikes N10°W with a steep dip and an altered, silicified rhyolite dike has intruded along the fault. The western segment strikes northwest and splits; the western segment is the Center fault. Both segments intersect the Carlisle fault. The Blue Goose fault intersects the Carlisle fault near the Pennsylvania mine where the Bloodgood Canyon Tuff is brought down against clastic sedimentary rocks (Maps 3, 5). The displacement along the Blue Goose fault is probably less than 30 m, based on offset of the Bloodgood Canyon Tuff. The Blue Goose fault is older than the Carlisle fault and the rhyolite intrusive.

2.3.3.4 Apache fault—The Apache fault is south of the Carlisle fault and southwest

of the Blue Goose fault. It strikes N40-50°W and dips 60-70° southwest. It is downthrown to the southwest. The Apache fault begins near Blue Creek, southeast of the mapped area (Drewes et al., 1985), and trends northwest until it intersects the Carlisle fault at the Carlisle mine. The Apache fault produced a northwest-trending bend or offset in the Carlisle fault at the mine that localized mineralization (Map 5). The Apache fault cannot be traced north of the Carlisle fault, even though Hedlund (1990a) shows some faulting in that area. The Apache fault is approximately 12 km long along strike and, unlike most faults in the district, it is marked by several arroyos, including Possum Hollow. The fault is mineralized and silicified along portions of the strike length, however the only mine along the fault is the Hext mine (copper, gold, silver).

Displacement and age of the Apache fault are uncertain. Powers (1976) suggests displacement near the Hext mine is 450 m but provides no conclusive evidence. About one kilometer northwest of the Hext mine, a downthrown block of Dark Thunder Canyon formation overlying the Bloodgood Canyon Tuff is exposed on the southwest side of the fault. The Bloodgood Canyon Tuff is exposed to the east on a hill northeast of the Blue Goose fault. This suggests a total displacement produced by the two faults of only 150-200 m (Map 3). Rhyolite dikes intrude along the Apache fault south of the Hext mine, yet the Apache fault cuts a rhyolite intrusive northwest of the Hext mine. Therefore it is likely that the last movement along the Apache fault occurred during or after the rhyolite intrusive event.

2.3.2.5 Laura fault zone—The Laura fault zone lies east of Vanderbilt Peak and is approximately 3 km long. This fault zone strikes N30-50°W (Fig. 2.17) and merges with the Imperial fault (Steeple Rock fault of Hedlund, 1990a and Gillerman, 1964; Laura fault of Powers, 1976) to the east. The southern portion of the fault consists of several subparallel fault strands. Brecciated and fractured andesite occur between the various strands forming a zone up to 800 m wide. The Laura fault zone then converges to the northwest into one or two faults at the Laura mine (Fig. 2.18). The Laura fault continues to trend northwest until truncated by the Carlisle fault. The faults dip steeply, 80-85° southwest and are downthrown

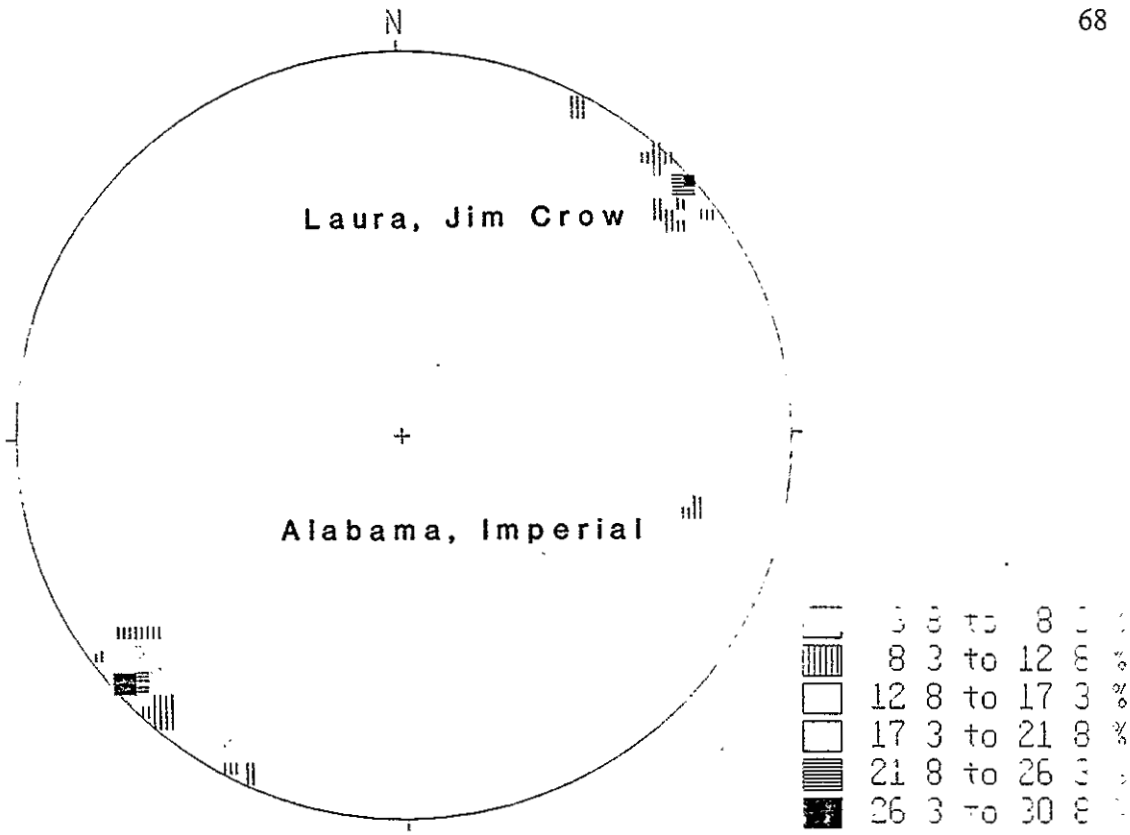

Figure 2.17—Stereonet of orientations of fault planes in the Laura-Jim Crow-Vanderbilt Peak area (step function, n = 26). Note the predominant northwest trend.

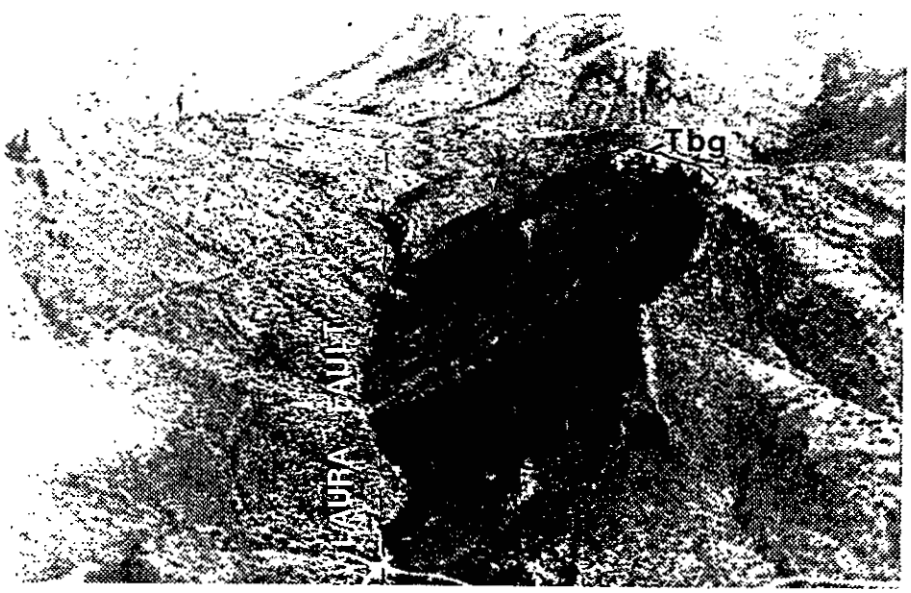

Figure 2.18—View of Laura Canyon from the air looking north. Note cap of Bloodgood Canyon Tuff (Tbg) on Rocky Top Ridge (to the right).

to the southwest. Rhyolite dikes and quartz veins commonly fill the various fault segments south of the Laura mine. The Laura, Big Horseshoe, and Smuggler mines occur along the fault zone. Assays along the faults suggest some mineral potential; one sample, #287, contained 0.18 oz/ton (6 ppm) Au and 3.5 oz/ton (120 ppm) Ag (Map 2; Appendix 11.6). A rhyolite dike and quartz vein southeast of the Smuggler mine may be the continuation of the Laura fault zone southeast of the Imperial fault, in which case there appears tobe some lateral displacement.

The fault zone places Dark Thunder Canyon formation adjacent to Summit Mountain formation. On Rocky Top Ridge, east of Laura Canyon, an ash-flow tuff, presumably Bloodgood Canyon Tuff, crops out (Fig. 2.18). This suggests that displacement along the Laura fault zone could be as much as 250-300 m. The fault is older than the rhyolite intrusives, quartz veins, and the Imperial fault.

2.3.3.6 Jim Crow-Gold King-New Years Gift fault zone—In the area of the Alabama, Jim Crow, and Imperial mines, south of Vanderbilt Peak, numerous northwest-trending faults of varying displacements and ages cut Dark Thunder Canyon formation, younger ash-flow tuff, and Summit Mountain formation. Rhyolite dikes and plugs are intruded along many of these faults and then subsequently offset by others (Maps 1, 2; Fig 2.19). Economically, the most important of these faults are the Jim Crow, Gold King, and New Years Gift faults. The Jim Crow and Gold King faults lie south of Alabama Ridge and merge with or are truncated by the Imperial fault. The Jim Crow fault is the southwestern fault, whereas the Gold King fault lies to the northeast and parallels the Jim Crow fault. The faults trend northwest and merge with the New Years Gift fault which continues northwestward to the Mulberry Springs area (Maps 1, 2). This entire area is highly fractured and faulted and structural interpretations are difficult at best.

In this area, these faults typically trend northwest with a strike of N45-65°W and a southwesterly dip of 75-85° to near vertical (Fig. 2.17). The faults are downthrown to the southwest and displacements are typically less than 30-50 m, based on displacement of the

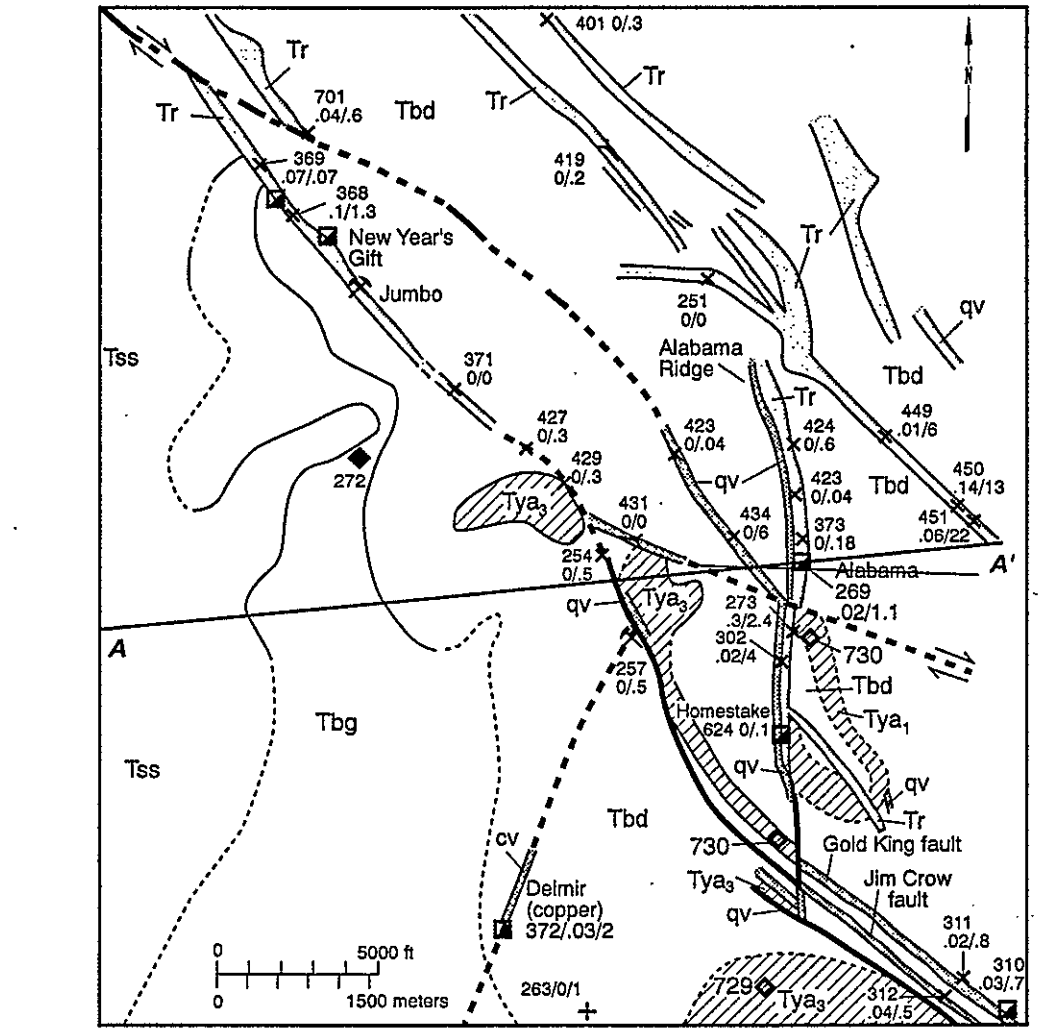

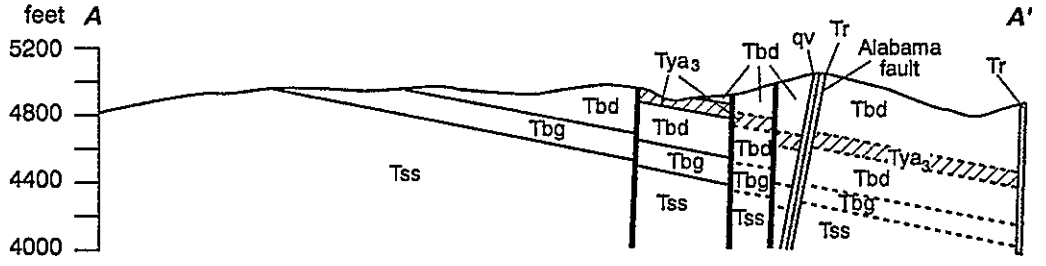

- shaft
- × prospect pit, no production
- open pit with production
- ◆ location of whole rock analyses
- adit
- 253 0/1 sample number with gold(oz.ton)/silver(oz/ton)
- ◇ location of sample for paleomagnetic sample (Table 2.2)

- qv - quartz vein
- cu - copper vein
- Tr - rhyolite dike
- Tya_1 - younger ash flow tuff
- Tya_3 - younger ash flow tuff (dome related)
- Tbd - Dark Thunder Canyon Tuff
- Tbg - Bloodgood Canyon Tuff
- Tss - Summit Mountain formation

Figure 2.19 Geologic map of the Alabama Ridge and surrounding area

younger ash-flow tuff. Minor right lateral offset of about 30 m or less is suggested by offset of some quartz veins, indicating strike-slip or oblique-slip movement along some of the faults. The faults are typically filled by quartz and/or quartz-hematite breccia and are locally gold bearing (Map 2, Appendix 11.6).

2.3.3.7 Commerce-Mayflower fault—The Commerce-Mayflower fault is a prominent, curvilinear northwest-trending fault southwest of Noah Mesa in the northwestern part of the district. Powers (1976) called it the Mayflower fault, whereas Hedlund (1990a; Ratté and Hedlund, 1981) called it the Commerce fault. The fault strikes N60°W and dips 70-80° southwest. It is downthrown to the southwest. It can be traced from south of Cottonwood Creek, northwest of the mapped area, southeastward to north of Bitter Creek where the fault curves and subparallels the Bitter Creek shear zone. The fault may actually become part of the Bitter Creek shear zone, and is about 7 km long.

The fault throws Quaternary-Tertiary Gila Group clastic rocks adjacent to Summit Mountain formation northwest of the mapped area (Hedlund, 1993). In the mapped area, the fault cuts Summit Mountain formation, the Wampoo fluorite vein, and a rhyolite dike. Displacement along the Commerce-Mayflower fault is unknown, but presumed to be large ($\geq$100 m). Movement along this fault has been relatively recent as indicated by the Gila Group rocks.

Portions of the Commerce-Mayflower fault are silicified and filled with quartz and fluorite. Production from the Commerce-Mayflower mines has been insignificant.

2.3.3.8 Foothills fault zone—The Foothills fault zone of Powers (1976) occurs in the western portion of the mapped area, northwest of Goat Camp Springs area. It is a series of two or more faults with an average strike of N50°W with steep southwesterly dips (70-85°). The fault is interpreted to be downthrown to the northeast in order to bring younger rocks adjacent to older rocks (Map 3; Powers, 1976). The best exposures of the fault zone are along the western portion where thick quartz veins filled the fault segments and form prominent outcrops (Fig. 2.20). The fault zone is not as well exposed to the east (Map 1) and

is inferred in most places (Map 2). The fault zone is covered by alluvium to the northwest of the mapped area (Hedlund, 1993) and is most likely truncated by a north-trending fault to the southeast. The fault zone is approximately 7 km long. It places Quaternary-Tertiary Gila Group adjacent to the Summit Mountain formation, northwest of the mapped area. Therefore the displacement along the fault is large ($\geq$100 m) and movement along the fault is recent.

2.3.3.9 Fourth of July fault—The Fourth of July fault (Powers, 1976) is a minor, northwest-trending fault that probably intersects the Foothills fault zone northwest of the mapped area (Fig. 2.20). The fault cuts acid-sulfate altered rocks to the southeast. The Fourth of July fault is southwest of the Foothills fault zone and is filled by quartz, fluorite, and fault-breccia. It strikes N30-40°W and dips to the southwest 55-60°. It is downthrown to the southwest (Map 3) and is about 7 km long. Displacement along the Fourth of July fault is probably small.

2.3.4 North-trending faults

Very few faults in the Steeple Rock district have a northerly trend (Fig. 2.12; Table 2.4). Economically, the most important north-trending faults are the Imperial (Mt. Royal, Imperial, Smuggler mines) and the Alabama fault (Alabama, Homestake mines). A number of short, north-trending faults occur in the Goat Camp Spring, Willow Creek, Daniels Camp, and western Bitter Creek areas that localized rhyolite dikes and/or fluorite veins. A north-trending quartz-copper vein occurs east of Twin Peaks and is truncated by the Twin Peaks fault. The rhyolite plug at Twin Peaks is elongated in a northerly direction. Rhyolite dikes cutting Charlie Hill and near the Fraser mine also trend northward. Most of the north-trending faults are not long in strike length and many are truncated or offset by northwest-trending faults.

Griggs and Wagner (1966) and subsequently Biggerstaff (1974) and Powers (1976), map a north- to northeast-trending fault west of Telephone Ridge which they called the Summit fault. They offer no evidence for the fault, although Griggs and Wagner (1966) did

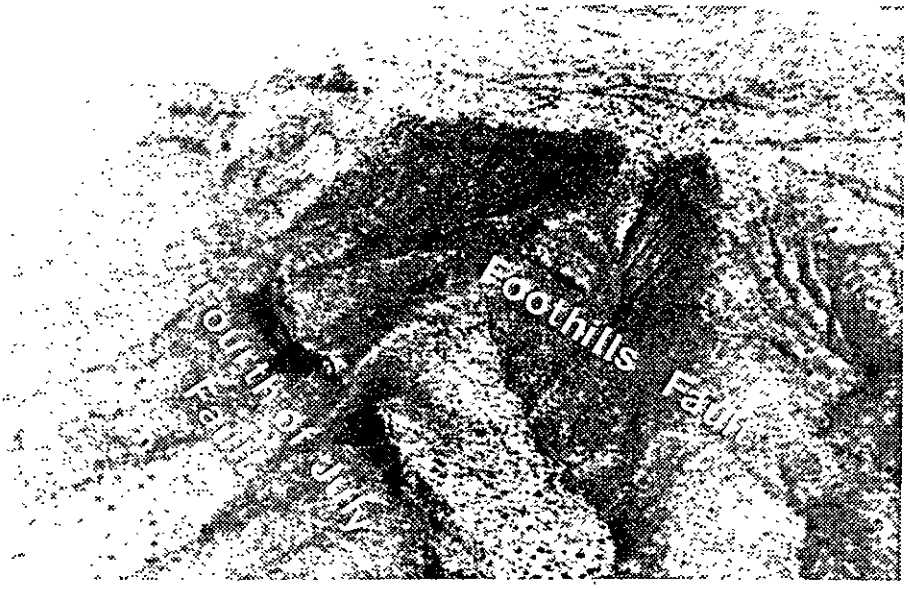

Figure 2.20—Aerial view of Foothills fault zone, looking toward the northwest.

only infer its location. The only evidence for faulting in this area is the presence of acid-sulfate altered rocks of the Summit Mountain formation. Hedlund (1990a) places an intrusive rhyolite in this region. Because of lack of field evidence supporting a fault, there are no faults mapped in this area on Maps 1 and 2.

2.3.4.1 Alabama fault—The north-trending fault at the Alabama mine strikes N10°W and dips 80° west (Fig. 2.17) and is one of numerous faults in the area (Fig. 2.19). The Alabama fault is about 450 m long and merges with northwest-trending faults at both ends. The fault cuts Dark Thunder Canyon formation and a younger ash-flow tuff. Rhyolite dikes and plugs have been intruded along much of the fault and are probably related to the rhyolite plug at Vanderbilt Peak. The rhyolite was subsequently silicified and locally mineralized. Displacement along the Alabama fault is approximately 40-50 m based on displacement of the younger ash-flow tuff (Fig. 2.19). The age of the fault is older than the rhyolite and mineralized quartz veins.

A northwest-trending crossfault offsets the Alabama fault 3 m south of the Alabama shaft (Fig 2.19). The crossfault strikes N70°W and dips 70° north. Subsurface mine maps indicate that this fault offsets the mineralized zone (Fig. 3.8; F. W. Smith, unpubl. report, 8/5/1910) and therefore must be younger than mineralization.

2.3.4.2 Imperial fault—The Imperial fault is a curvilinear, north-trending fault that lies east of Alabama Ridge and northwest of Mt. Royal. Hedlund (1990a) and Gillerman (1964) call this fault the Steeple Rock fault and Powers (1976) calls it the Laura fault. Elston (1960) labels a fault south of Mt. Royal and Steeple Rock the Steeple Rock fault. Therefore, to avoid further confusion, the fault in this report is called the Imperial fault after the Imperial mine, which is located in the southern part. The fault includes the Imperial, Mt. Royal, and Smuggler mines. The fault can be traced south-southwest of Mt. Royal where it is covered by alluvium and only inferred (Hedlund, 1990a). The fault trends north, partially following Carlisle Canyon, to south of Pennsylvania Canyon where it dies out. The fault truncates the northwest-trending Laura fault zone and Jim Crow and Gold King faults.

The Imperial fault ranges in strike from N10°W to N20°E and dips to the west 70-85° (Fig. 2.17). The fault is downthrown to the west. It places the older rhyodacite of Mt. Royal and andesite of Mt. Royal on the east, adjacent to the Dark Thunder Canyon formation and a younger ash-flow tuff. The Imperial fault also offsets and truncates rhyolite dikes and quartz veins. The Imperial fault is filled locally with quartz, forming prominent outcrops; however, in many places the fault is poorly exposed. Displacement along the fault is uncertain but could be as much as 900 m, based on the displacement between the Dark Thunder Canyon formation and the andesite of Mt. Royal. Numerous splays and fault segments split off the main fault and in some places are too numerous to map at the scale employed. There are also numerous faults visible underground which are not exposed at the surface, causing locally wet, unstable ground conditions (Queenstake Resources Lt., unpubl. report, April 1982).

2.3.5 West-northwest-trending faults and shear zones

Several west-northwest-trending faults and shear zones occur in the Steeple Rock mining area (Figs. 2.12, 2.21; Table 2.4). At least three are important in the distribution of mineralization: Carlisle fault, Bank shear zone, and Bitter Creek shear zone. The Bank and Bitter Creek structures are called shear zones because they are not well exposed and actual displacement and fault surfaces are not well documented. However, these two areas are altered and sheared, indicating tectonic movement, and both zones substantially affect the distribution of mineralization, as previously discussed. The Carlisle fault is perhaps the most important fault economically in that most of the production from the Steeple Rock district has come from mines along it. Two additional west-northwest-trending faults are worth describing, the Crookson fault north of Bitter Creek and the Charlie Hill fault (part of the Foothills fault of Powers, 1976) in the southern part of the mapped area. A few rhyolite dikes in the Goat Camp Spring area and east of Charlie Hill also have a west-northwest trend.

2.3.5.1 Carlisle fault—The Carlisle fault is the major west-northwest-trending fault in the Steeple Rock district. The strike ranges from N75°W to N85°E with numerous local

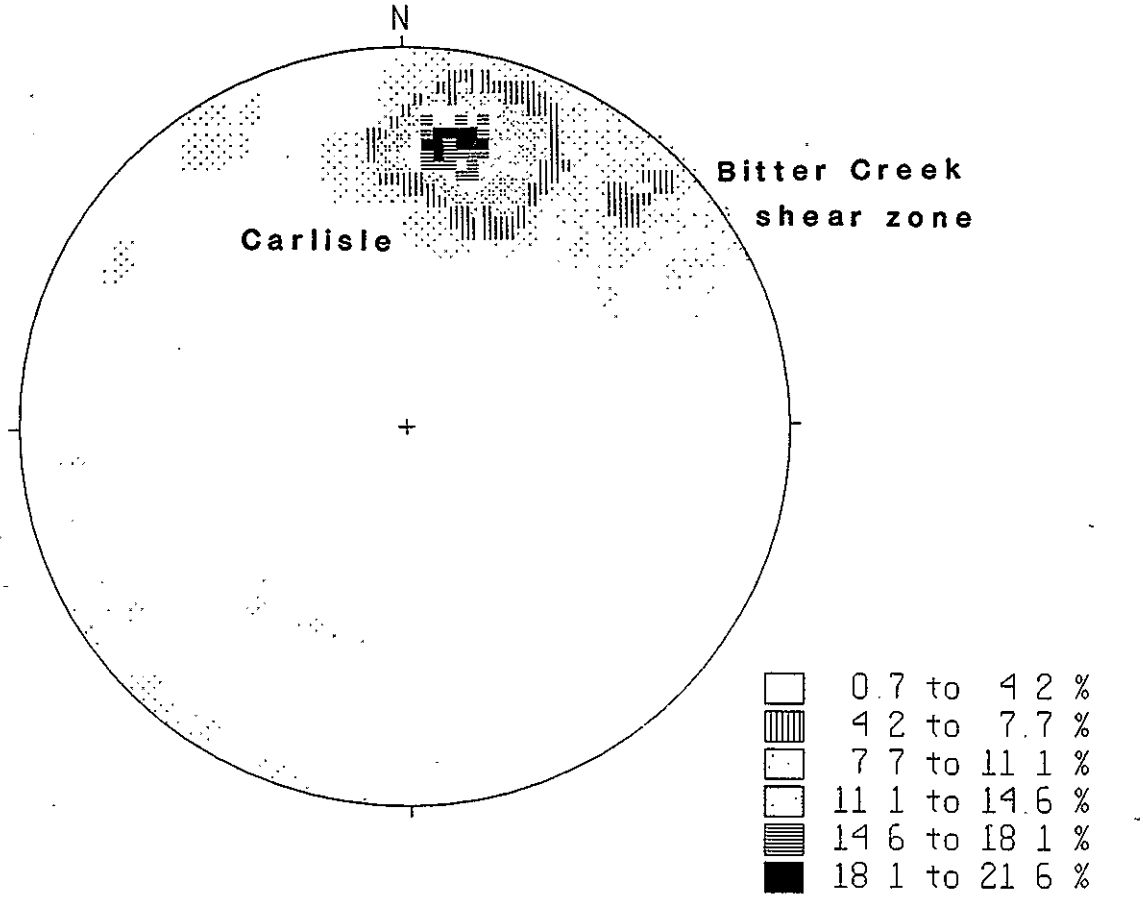

Figure 2.21—Stereonet of orientations of fault planes along the west-northwest trending faults (step function grid, n = 148).

variations and it dips 60-70° to the south (Fig. 2.21). The fault can be traced from the East Camp-Summit fault westward past Laura Canyon, where it curves northwest. The fault eventually is covered by alluvium west of the mapped area (Hedlund, 1993). Hedlund (1990a, c) calls the western portion of the fault the Whiskey Creek fault. For the purposes of this study, the entire fault is called Carlisle after previous workers and it is suggested that the term Whiskey Creek fault be discontinued.

The Carlisle fault is a prominent quartz-breccia vein or silicified zone along much of its strike, however it appears to be mineralized only from the Carlisle mine eastward to the Ontario mine (Map 5). Additional mineralized zones also occur in section 2, west of the Carlisle mine. The fault is downthrown to the south and has variable displacement. It varies in width from less than one to 30 m. Locally, two parallel or subparallel fractures are present; both constitute the Carlisle fault.

West of the Pennsylvania mine, near the intersection with the Blue Goose fault, the displacement is approximately 210 m; west of the Apache fault the displacement is approximately 270 m (Map 3; Griggs and Wagner, 1966). The Carlisle fault has a displacement of as much as 610 m west of the Laura fault where Dark Thunder Canyon formation to the south is adjacent to Summit Mountain formation to the north. Further to the west where the Carlisle fault cuts a rhyolite dome west of Saddleback Mountain, the displacement is only 140-180 m. The difference in displacement is the result of northwest-trending faults, downthrown to the south that are truncated by the Carlisle fault. Oblique movement is also indicated by fault slickensides plunging 45-60°SW. The Blue Goose and Apache faults do not offset the Carlisle fault, but produce bends in the Carlisle fault, suggesting that movement along these northwest faults occurred after formation of the Carlisle fault. These bends localized mineralization and are evidence of different periods of oblique-slip movement.

2.3.5.2 Bank shear zone—A poorly exposed shear zone north of the Bank mine has affected the distribution of mineralization along the East Camp-Twin Peaks fault zone.

Alteration of the area in the vicinity of the Bank mine, which is either related to the shear zone or to early acid-sulfate alteration, has obscured lithologies and any traces of faults. This shear zone exists primarily because of the change in character of mineralization along the East Camp-Twin Peaks shear zone (previously discussed). The zone is characterized by gouge zones, brecciated and fractured country rocks, and acid-sulfate alteration. This zone continues at depth as an unaltered, poorly consolidated shear zone. Geologists of Biron Bay Resources Ltd. believe that the zone trends east-west based on subsurface data. Mapping for this project revealed a north-south fault (N10°W to N20°W), filled with quartz that cuts the East Camp-Summit fault, however this fault could not be traced along strike for any distance. Therefore the Bank shear zone cannot be plotted on Maps 1, 2 with any certainty.

Displacement, if any, and age of the zone are unknown. More will be discussed about this zone under alteration (section 5).

2.3.5.3 Bitter Creek shear zone—The Bitter Creek shear zone, first recognized by Powers (1976), occurs along Bitter Creek north of Saddleback Mountain. This zone strikes west to northwest (Fig. 2.21) and is characterized by parallel to subparallel fault segments, fractured and brecciated country rock, gouge zones, and offsets of rhyolite dikes and the East Camp-Twin Peaks fault system.

In the western Bitter Creek area, the Bitter Creek shear zone consists of two or more west-northwest-trending faults. These faults are locally filled with quartz veins with local pyrite and fluorite. The Commerce-Mayflower fault curves north of Bitter Creek and may be part of the shear zone. Although dips cannot be measured, the zone probably dips steeply to the north because of displacement of the altered rocks north and south of the zone (Map 3). A drill hole near the Recent spring deposit (Bitter Creek #1 drill hole) intersects several quartz-fluorite veins at depth which could represent part of this shear zone. The Recent spring deposit overlies one segment of the fault and it has not been faulted.

The Bitter Creek shear zone changes character to the east, where discrete fault zones are not exposed. Areas of fractured and brecciated country rock and gouge zones are typical

of the fault trace. The shear zone has also laterally offset a rhyolite dike and the East Camp-Twin Peaks fault system approximately 300-600 m. Vertical displacement is unknown.

The Bitter Creek shear zone is not mineralized except for a few local areas along the western portion and in the Bitter Creek #1 drill hole (Appendix 11.1). However, the zone offsets the Powell and Leta Lynn fluorite veins as well as the East Camp-Twin Peaks fault system. Most of the production along the East Camp-Twin Peaks fault system has come from mines south of the shear zone. Only the Fraser and Black Willow mines occur along the Twin Peaks fault north of the Bitter Creek shear zone.

2.3.5.4 Crookson fault—The Crookson fault of Biggerstaff (1976) is north of Bitter Creek, averages N85°E in strike, and parallels the Bitter Creek shear zone. The fault is approximately 7 km long and extends to the east beyond the mapped area (Hedlund, 1993). The fault is truncated by or merges with the Twin Peaks fault at mine #1002 (Map 2) and trends easterly to Cherry Creek and beyond. The fault is poorly exposed along most of its strike in the mapped area and is characterized by local zones of closely spaced west-trending joints and minor brecciation. Apparently the fault is better exposed to the east (Biggerstaff, 1974; Powers, 1976).

The fault offsets several outcrops of altered sandstones of Dark Thunder Canyon formation. At mine #1002, fractures and thin quartz veins strike east-west for several meters east of the mine. Mine #1002 is actually part of the Twin Peaks fault. Hedlund (1993) suggests that the fault is downthrown to the south (Map 3), but dips could not be measured because of poor exposure. The fault cuts Dark Thunder Canyon formation and lava flows of Crookson Peak and thus is younger than the lava flows of Crookson Peak (27.6 $\pm$ 2 Ma, fission track age on zircon, D. E. Hedlund, unpubl. report, 1990). Displacement along the fault is probably small. The fault appears to have no effects on mineralization, except perhaps at depth at mine #1002. This needs to be tested at depth by drilling.

2.3.5.5 Charlie Hill fault—The Charlie Hill fault is a poorly exposed west-northwest-trending fault that lies north of Charlie Hill in the southern portion of the mapped

area (Maps 1, 2). The fault is probably less than 3 km in length and strikes N70°W to N80°E with a steep dip (80°S to 80°N). The fault offsets Bloodgood Canyon Tuff east of Charlie Hill. Displacement along the fault is approximately 50-60 m, where it cuts the Bloodgood Canyon Tuff. The fault is downthrown to the north. Right-lateral offset is indicated along the western edge of the Charlie Hill fault where a rhyolite dike is offset along strike approximately 90-100 m, suggesting strike-slip or oblique-slip movement. Parts of the fault are filled with quartz and/or clay, however it is relatively unmineralized along most of its strike length.

2.3.6 Northeast-trending faults

Northeast-trending faults are extremely rare in the Steeple Rock district (Maps 1, 2; Fig. 2.12; Table 2.4). A few rhyolite dikes north of Twin Peaks fault trend N30-40°E to north-south (Fig. 2.11). Several minor faults in the Goat Camp Spring area also trend north-northeast and are filled with quartz, quartz-fluorite, and/or rhyolite dikes. These typically are downthrown to the northwest with minor displacement. The Delmir fault, containing the Delmir copper mine, strikes northeast and is cut off by the Charlie Hill fault to the southwest and the Jim Crow fault to the northeast (Fig. 2.19). It is downthrown to the northwest and displacement is small.

Southwest of the Imperial fault, Hedlund (1990a, c) maps a curvilinear, east-northeast-trending fracture he called the Carlisle Canyon fault. He further suggests that the supposed Carlisle Canyon fault is a ring fault, but provides no conclusive evidence. This fault is not located on Maps 1 or 2 because of lack of field evidence in the mapped area to support the occurrence of a fault. However, this area should be re-examined in greater detail to determine if Hedlund's fault exists to the south.

2.4 Petrochemistry

Samples of various volcanic, volcaniclastic, and intrusive rocks from throughout the

Steeple Rock district were analyzed for major and trace elements. Geochemical data, including selected published data, are in Appendix 11.4 and sample locations are on Map 2. The samples are grouped according to lithology and mineralogy as rhyolite/rhyodacite intrusives, ash-flow tuffs, andesites and related volcaniclastic rocks, and acid-sulfate altered rocks. Methods of analyses, detection limits and estimates of error are discussed in section 1.5.4 and Table 1.3.

Despite variable intense alteration, the Steeple Rock samples are grossly similar in chemical composition to similar lithologies elsewhere in the Mogollon-Datil volcanic field (Bornhorst, 1980, 1986, 1988; Sharp, 1991). The Steeple Rock samples are predominantly peraluminous (i.e. $Al_2O_3/(CaO + K_2O + Na_2O) > 1.0$), high K, silica-saturated, calc-alkaline basaltic andesite to rhyolite. Most of the Steeple Rock samples are subalkaline and form trends typical of calc-alkaline igneous rocks, according to the definition of Irvine and Baragar (1971). However, a few andesites plot in the alkaline field, probably as a result of alteration (Fig. 2.22).

Igneous petrologists commonly compare geochemical data to various studies that relate chemical compositions of igneous rocks from throughout the world to plate tectonic settings. A study by Pearce et al. (1984) establishes that igneous rocks formed in various tectonic settings have different chemical signatures. Pearce et al. (1984) refers to these settings as ocean ridge, volcanic arc, syn-collision (formed by collision of two plates), and within-plate fields. Rocks formed in these tectonic settings are characterized by well defined fields on chemical variation plots. Most Steeple Rock andesites plot within the volcanic arc or syn-collision fields. Most of the Steeple Rock rhyolites and ash-fow tuffs plot near the tectonic fields of volclanic arc, syn-collision, and within-plate (Figs. 2.23, 2.24). The similarity in chemical composition of rocks in the Steeple Rock district to the composition of rocks formed in volcanic arc, syn-collision, and within-plate tectonic settings infers that the Steeple Rock rocks were formed in complex tectonic settings related to the subduction of lithospheric crust. These chemical trends are consistent with current theories of the tectonic

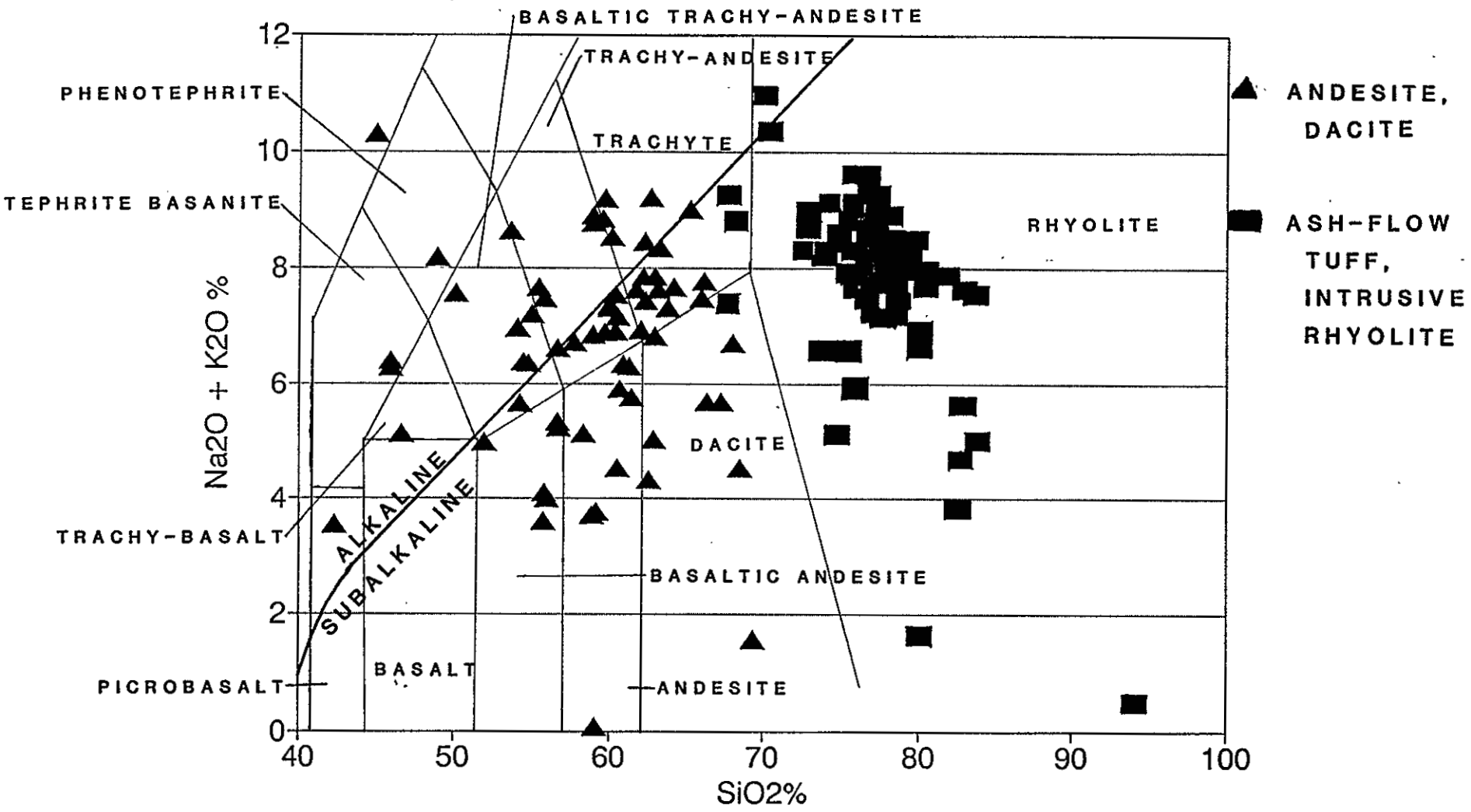

FIGURE 2.22 TAS (Total alkali-silica) diagram of samples from the Steeple Rock district. Analyses are in Appendix 11.4. Lithologic fields from Le Bas et al. (1986). Alkaline-subalkaline fields from Irvine and Baragar (1971).

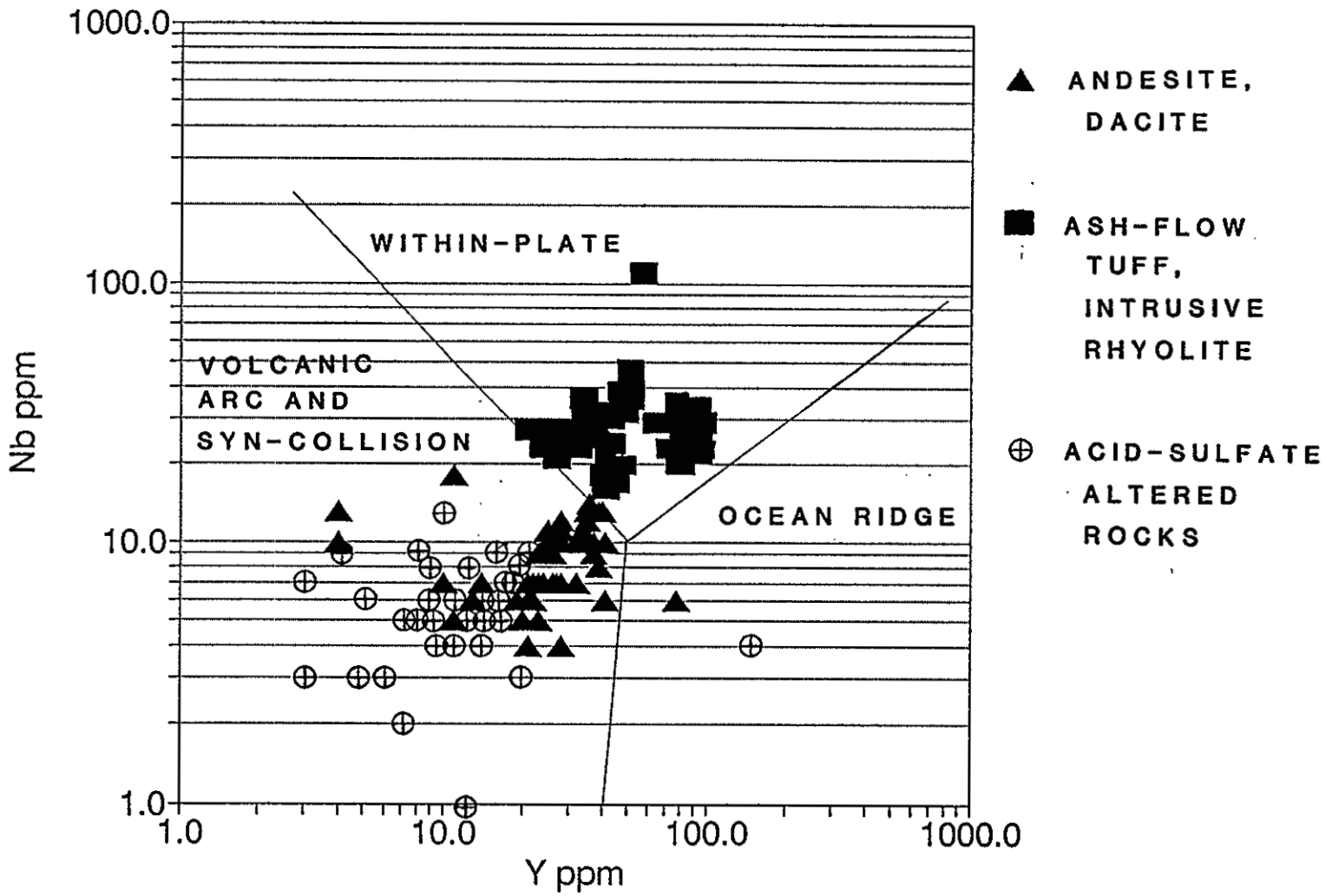

FIGURE 2.23 Nb vs. Y diagram of samples from the Steeple Rock district. Tectonic fields from Pearce et al. (1984).

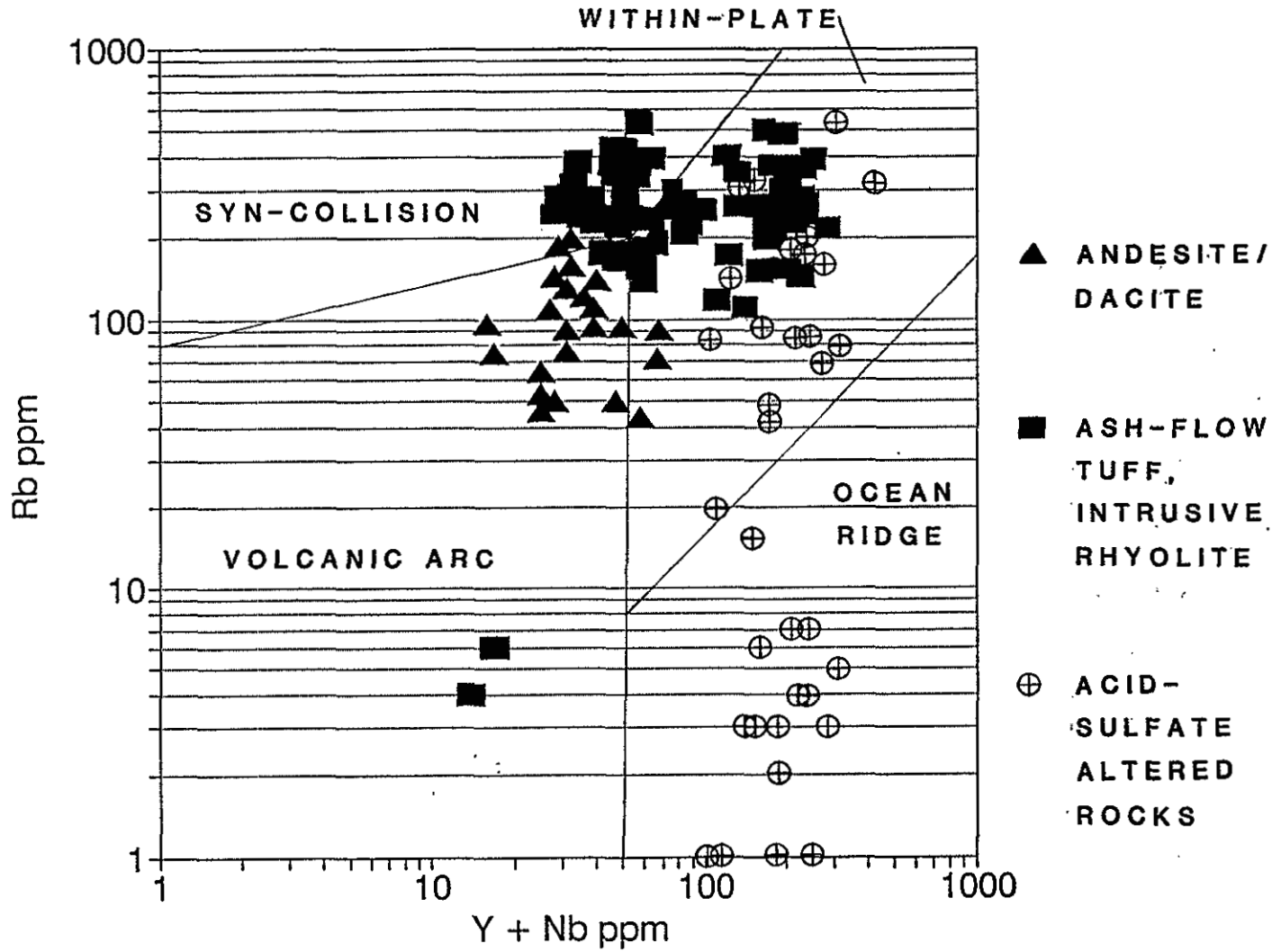

FIGURE 2.24 Rb vs. Y+Nb diagram of samples from the Steeple Rock district. Tectonic fields from Pearce et. al. (1984).

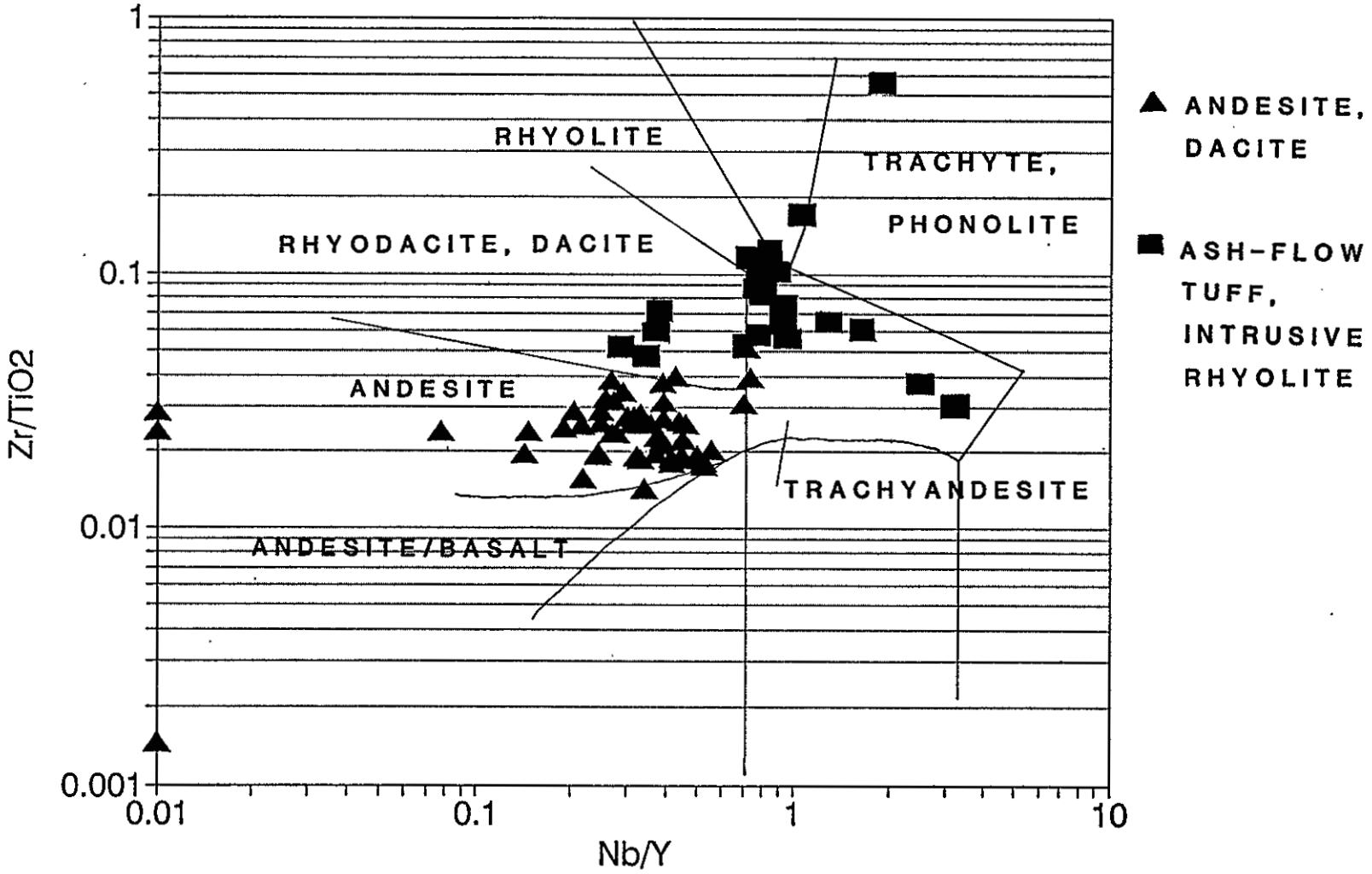

FIGURE 2.25 Zr/TiO2 vs. Nb/Y diagram of samples from the Steeple Rock district. Fields from Winchester and Floyd (1977).

evolution of the Steeple Rock area as discussed in section 2.3.

Geochemistry is also utilized in classifying volcanic rocks. However, geochemical classifications are not adequate to describe the Steeple Rock samples because of the variable intensity of alteration. The TAS (total alkali-silica) diagram is widely used in classifying volcanic rocks (Le Bas et al., 1986). However, only the rhyolites and ash-flow tuffs from the Steeple Rock area plot in the correct field (Fig. 2.22). The andesites are scattered throughout the diagram because of addition of silica and remobilization of alkalis. A similar scatter is observed in the popular R_1–R_2 classification scheme by De La Roche (1980). Winchester and Floyd (1977) developed a classification scheme on the basis of Zr/TiO_2 and Nb/Y, because these elements are typically immobile during alteration. Most Steeple Rock samples plot in or near their respective lithologic fields (Fig. 2.25): rhyolites as rhyolites or rhyodacites and andesites as andesites or rhyodacites/dacites.

Geochemical data indicate that the andesites are more altered than the rhyolites or ash-flow tuffs. The ash-flow tuffs and rhyolites have similar chemical compositions. Interpretation of magmatic differentiation trends on the basis of chemistry is not possible, because the rocks in the Steeple Rock district are too altered. Finally, petrochemical theories pertaining to the origin and genesis of the Steeple Rock samples cannot be established with these data because of the variable intensity of alteration.

2.5 Water Resources

Water resources in the Steeple Rock district are not abundant except locally along faults. The streams and few springs in the area are ephemeral and depend upon local precipitation. Annual precipitation is typically less than 40 cm/yr, although wet years with higher rates do occur (Trauger, 1972). The Steeple Rock district, as part of the Summit Mountains, is one of many recharge areas for the Gila valley. The ephemeral streams enter the Gila River.

There are no major aquifers in the district. Water occurs along fractures, bedding

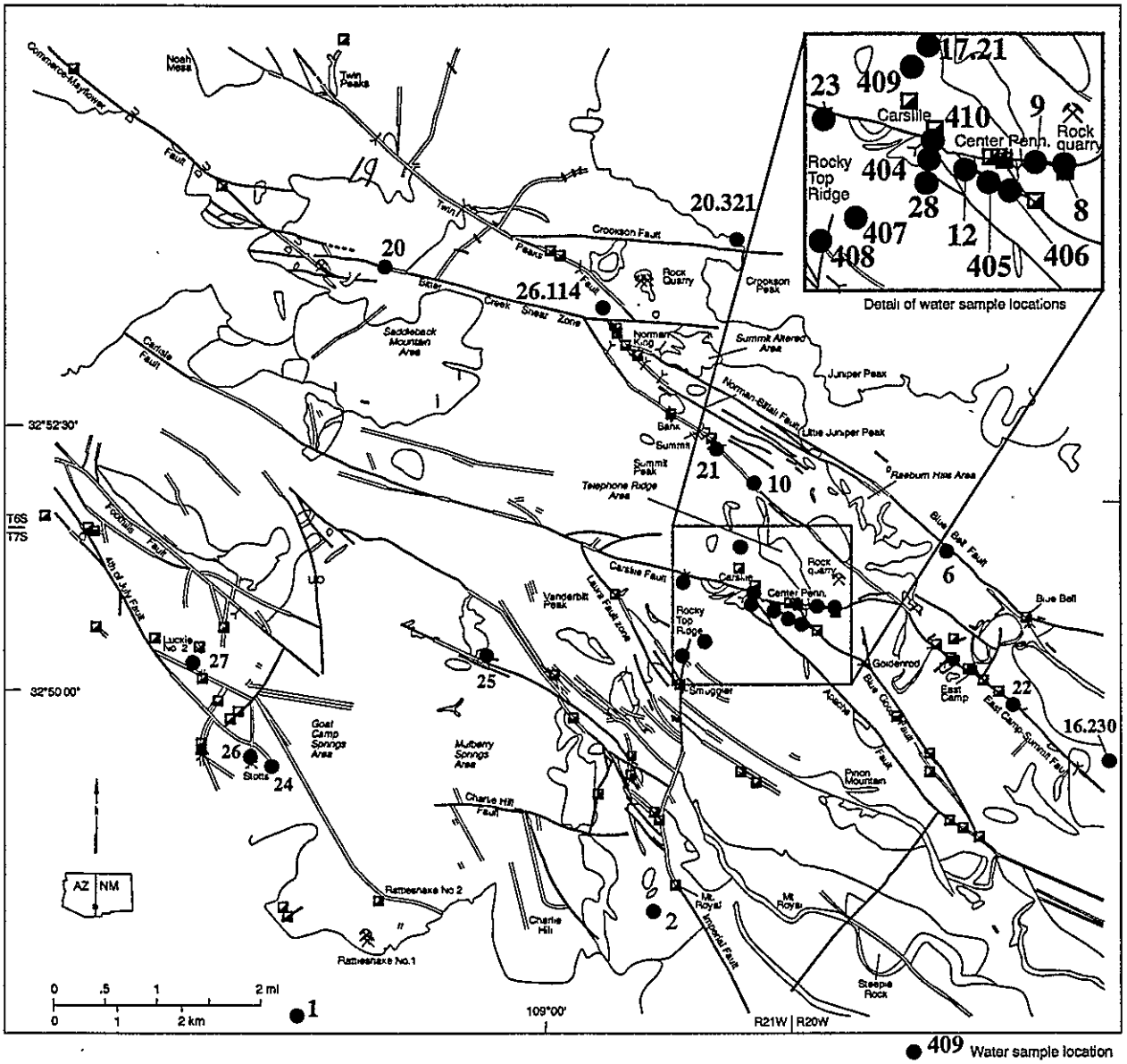

Figure 2.26 - Location of water samples. Numbers refer to Table 2.5.

Table 2.5—Chemical analyses of water samples from mines, wells, and arroyos from the Steeple Rock district, New Mexico and Arizona. Analyses by Lynn Brandvold and associates, NMBMMR Chemistry Laboratory. Samples are surface water samples, unless otherwise indicated. * denotes mine water sample. # denotes sample from windmill. @ denotes data from Trauger (1972). Analyses are in ppm (parts per million) unless otherwise specified. epm - equivalents per million. Locations of samples in Figure 2.26. bd - Below detection.

Sample no.	Collection date	pH	TDS	Conductivity (mhos)	Hardness	CO_3	HCO_3	Cl	SO_4	NO_3	PO_4	F	Na	K	Mg	Ca	Hg ppb	Total cations (epm)	Total anions (epm)	% Error	Cu ppb	Comments
409	2/28/92	8.45	909	700	314	1.9	324	11.0	109	1.3	0	0.4	36	4	29	78	<1.0	7.95	8.00	-0.62	--	Carlisle Creek, upstream from mine
410*	2/28/92	3.05	5321	3500	1808	1.9	324	7.4	2460	0.7	0	16.0	56	17	145	485	<1.0	55.40	57.67	-4.02	--	standing water in Carlisle adit
404	2/28/92	4.75	3741	2700	1378	0	0	3.1	1780	32.0	0	10.0	33	17	98	390	<1.0	37.39	38.20	-2.14	--	Carlisle lower pond
404	6/93	2.3	--	3300	--	--	--	--	--	--	--	--	55	9.4	48.5	--	--	--	--	--	1.8	standing water in Carlisle pit
405	2/28/92	7.90	1617	1300	597	0	220	7.4	91	26.0	0	3.0	58	6	48	160	<1.0	14.61	14.62	-0.06	--	dewatering pond at the Center mine
405	6/93	7.4	73	1300	--	--	--	1.6	--	--	--	--	59	2.8	--	38.6	--	--	--	--	bd	dewatering pond at the Center mine
406	2/28/92	8.20	1443	1150	543	0	258	21.0	375	3.7	0	0.8	48	8	50	135	<1.0	13.14	12.73	3.18	--	Center Creek, below outfall from pond
407	2/28/92	8.10	1209	1000	448	0	228	9.3	314	1.4	0	2.0	40	6	30	130	<1.0	10.85	10.67	1.69	--	Carlisle Creek, below mines (S7)
408	2/28/92	8.20	1112	850	407	0	224	10.0	280	1.9	0	1.0	37	6	28	117	<1.0	9.90	9.87	0.38	--	Carlisle Creek, below mines (S10)
1#	10/14/92	7.51	1200	1150	873	--	--	--	--	--	--	--	--	--	--	--	--	--	--	--	--	Rim Rock windmill
2#	10/14/92	7.50	920	870	365	--	--	--	--	--	--	--	--	--	--	--	--	--	--	--	--	Mt. Royal windmill (depth 2.4 m)
6#	10/14/92	6.90	3640	460	468	--	--	--	--	--	--	--	--	--	--	--	--	--	--	--	--	Raeburn windmill (depth 9.1 m)
6#	8/6/55	7.60	1740	1970	1100	0	287	39.0	964	9.6	--	1.1	15000	92	111	260	--	--	--	--	--	(Thygerson windmill)
8*	10/15/92	6.50	870	410	37	--	--	--	--	--	--	--	--	--	--	--	--	--	--	--	--	standing water in Ontario shaft
8*	6/93	6.3	68.3	70.9	--	--	--	1.5	--	--	--	--	39	3.6	--	45.7	--	--	--	--	bd	standing water in Ontario shaft
9	10/15/92	7.38	910	1300	567	--	--	--	--	--	--	--	--	--	--	--	--	--	--	--	--	Ontario Pond
10#	10/15/92	7.10	1520	1000	374	--	--	--	--	--	--	--	--	--	--	--	--	--	--	--	--	Angello windmill
12*	10/15/92	7.10	1380	1500	1030	--	--	--	--	--	--	--	--	--	--	--	--	--	--	--	--	Center mine
12*	6/93	7.2	74	1500	--	--	--	0.3	--	--	--	--	56	3.1	--	31.4	--	--	--	--	bd	Center mine
20.321a@	9/20/41	--	2290	2550	1610	0	164	21.0	1519	0.8	--	1.1	62	--	67	536	--	--	--	--	--	Bitter Creek spring (16s.21w)
26.114@	3/8/56	7.20	1170	1420	808	0	289	17.0	589	0.0	--	0.2	8000	30	71	207	--	--	--	--	--	Lon Moore windmill (depth 34.4 m,16s.21w)
16.230@	10/5/41	--	--	703	341	23	333	27.0	61	0.4	--	1.5	35	--	35	79	--	--	--	--	--	Thanksgiving spring
17.21@	9/6/55	6.90	--	1040	490	0	336	18.0	--	--	--	--	--	--	--	--	--	--	--	--	--	USFS windmill (depth 18.3+ m)
20#	6/93	8.5	--	610	--	--	--	--	--	--	--	--	--	--	--	--	--	--	--	--	--	Croookson windmill
21*	6/93	8	75	500	136	--	--	1.3	--	--	--	--	35	2	--	28.2	--	--	--	--	bd	Lower Apex adit
22*	6/93	7.9	70.5	690	400	--	--	1.7	--	--	--	--	57	2	--	44.3	--	--	--	--	bd	Lower McDonald adit
28*	6/93	2.5	58	2300	--	--	--	--	--	--	--	--	55	9.4	--	48.5	--	--	--	--	6.6	Carlisle lower adit
23*	6/93	6.7	--	510	--	--	--	0.8	--	--	--	--	28	0.8	--	23.5	--	--	--	--	bd	standing water in Section 2 adit
24	6/93	6.1	70.6	2100	--	--	--	3.5	--	--	--	--	140	5.2	--	33.6	--	--	--	--	bd	Goat Camp Springs
25#	6/93	8.9	--	70	--	--	--	--	--	--	--	--	--	--	--	--	--	--	--	--	--	Mulberry Spring windmill
26*	6/93	5.5	51.5	500	--	--	--	6.5	--	--	--	--	410	1.5	--	24.5	--	--	--	--	0.22	Ellis mine at 510
27#	6/93	8	62.6	1100	--	--	--	3.7	--	--	--	--	49	2.1	--	13.5	--	--	--	--	bd	Luckie windmill at Luckie No. 2 mine

planes, and faults. Most windmills in the district are situated along faults, with a few exceptions (Fig. 2.26). The sedimentary rocks in the area are relatively thin and may provide local but small quantities of water. Most mines contain substantial quantities of water and must be pumped. A few mines and windmills can sustain pumping rates of 1.6 liters per second (25 gallons per minute), but most pumping rates are less (Trauger, 1972). The Center mine pumps 5 liters per second (80 gallons per minute) for 3½ hrs/day. The depth to water in the mines and along faults varies from 2 to 73 m according to elevation and annual precipitation. The Carlisle mine is flooded below 25 m. Silicification along most faults restricts migration of groundwater, especially away from the faults into the country rocks.

Chemical analyses of water samples typically exceeds EPA guidelines or standards for drinking water (Table 2.5; Fig. 2.26); most of the water in the district is of suitable quality for livestock, irrigation, and some industrial uses. Some water is used for domestic purposes without any ill-effects. Most of the water from mines, except for the Carlisle mine, is also suitable for these purposes. The water at the Carlisle mine is acidic and contains elevated levels of iron, copper, lead, and zinc (Table 2.5). The quality of water deeper in the Carlisle mine is unknown and must be tested prior to dewatering.

3. MINING HISTORY AND DESCRIPTION OF MINES

3.1 General mining history and production

The earliest mention of mining activity in the Steeple Rock district was a report of a military dispatch of troops from Ft. Thomas (near Duncan, Arizona) in 1860 to assist miners in the area from interference by Apache Indians (Russell, 1947). The earliest production reported from the district occurred in 1880 when a 20-stamp amalgamating mill was erected at the Carlisle mine. By 1886, the mill was enlarged to 60 stamps. The first mining claims were filed in January 1881, and included the Carlisle, Star of the West, Center, and Pennsylvania (Table 3.1; Griggs and Wagner, 1966). Prior to 1904, accurate production records were not kept by any government agency, therefore production is only estimated from old mining records. In addition, many early records were lost in the San Francisco earthquake in 1906 (NMBMMR file data). The Carlisle mine was the largest producer and most of the estimated production prior to 1904, amounting to about 112,000 tons, is attributed to the Carlisle mine.

By 1897, most of the mines in the district were located and operated by several different companies (Table 3.1, 3.2; Fig. 3.1). Open stope mining was employed in most mines, although shrinkage stope methods were used locally. Square-set mining was also used in some of the East Camp mines. Small shipments, some high grade in gold and silver, were made from many of the mines but total production was small. Herbert Hoover worked in the district in the late 1890s as a mining engineer before becoming President of the United States (Gillerman, 1964).

In 1933, the price of gold rose from $20.67 to $35 per ounce and many of the mines in the district were re-examined for gold potential. Several mines operated over the next few years (Table 3.2). From 1934 to 1942, total production from the district amounted to about 30,000 ounces of gold and over 1 million ounces of silver (Table 1.2; Griggs and Wagner, 1966); most of this production came from the East Camp mines.

In 1942, the federal government closed all gold-silver mines as a result of World War II. Men were needed elsewhere and only base-metal mines were allowed to operate. The

TABLE 3.1—Patented mining claims in the Steeple Rock district, Grant County, New Mexico.

Patented Claim	Mineral Survey No.	Acres	Month/Year	Location
Summit Group				
Alta	1010A	14.1		35,36 T16S R21W
Surprise	1010B	10.9		
Summit	1010D	9.5		
Summit Tunnel	1010E	9.4		
Apex	1010F	11.0		
Irish Jew	1010G	18.3		
Puzzle	1010H	10.4		
Black Spar	1010I	7.2		
Jack Pot	1010J	17.5		
Surprise Tunnel	1010C	9.4		
Billali	1021			26 T17S R21W
Mohawk (Bitter Creek)				26 T16S R21W
Carlisle	279	20.7	1/1881	
Homestake	283	17.9		
Columbia	284	19.5		
Carlisle Mill Site	280	5.0		
New Years Gift	1013A	9.7		
Jumbo	1013B	17.9		
Geronimo	1013C	20.1		
Star of the West			1/1881	
Laura-Clara	1067			2,3,11 T17S R21W
East Camp Group				5,7,8,9,16,17 T12S R20W
Gold Pick	1011A	18.6		
Gold Note	1011B	10.7		
Sunset	1011C	13.0		
Nugget	1011D	17.4		
Great Eastern	1011E	7.8		
McDonald	1011F	16.5		
Davenport	1011G	17.6		
Gold Bug	1011H	16.3		
Jim Crow-Imperial-Gold Bug Group				
Imperial	1012A	15.5	9/1889	23 T17S R21W
Jim Crow	1012B	14.8	7/1889	23 T17S R21W
Gold King	1012C	16.6	4/1888	14, 12 T17S R21W
Tunnel	1012D	20.0	11/1890	14,23 T17S R21W
Gold Bug	1012E	14.1	4/1893	23 T17S R21W
Red Prince	1012C	17.0	1/1889	14,23 T17S R21W
Three Brothers	1012G	13.5	11/1889	14 T17S R21W
Contention	1012H	11.6	1/1896	14 T17S R21W
Mt. Royal Group				
Golden Fleece 1, 2, 3	1712		10/10/22	23 T17S R21W
Imperial Extension	1712		10/10/22	23 T12S R21W
South Jim Crow	1712		10/10/22	23 T12S R21W

Table 3.2. List of mines in the Steeple Rock mining district and adjacent area, New Mexico and Arizona. From Griggs and Wagner (1966), Hedlund (1990a,b), McAnulty (1978), McLemore (field mapping) and unpublished reports (NMBMMR files).

Name	Location	Years of Production	Development	Metals (minor)	Production
Alabama Group[2]	14.17S.21W	1936-38, 1950-51	113 m shaft, pits	Au,Ag (Cu,Pb)	4000 tons of 0.3 oz/ton Au, 13 oz/ton Ag, 2.03% Cu
Apache Box Canyon[2,6]	2,3,10,11,16S.21W	---	3 adits, 12 m shaft	Au, Ag, Cu	none
Big Horse Shoe[2]	11.17S.21W	1904	pits, shallow shafts	Au (Ag)	<10 tons
Billali[2]	26.16S.21W	1935-36, 1940	shaft, adit	Au,Ag (Cu)	0.19 oz/ton Au, 12.2 oz/ton Ag
Black Cat[5]	33.6S.32E	1953-55	2 shafts, 15, 13 m deep	Mn, fluorite	86 tons of 43.2% Mn
Black Widow[2,4]	22.16S.21W	1920s	20 m shaft	Au,Ag, fluorite	none
Blue Bell (Shamrock, Bluebird)[3]	8.17S.20W 8.17S.20W	late 1800s, 1909, 1916, 1918	61 m shaft	Au,Ag,Cu	<500 tons of 0.6-0.9 oz/t Au, 10-12 oz/t Ag, 6-11% Cu
Blue Goose[2]	7.17S.20W	none	shaft	Au,Ag	none
Carlisle[1]	1.17S.21W	1880-1897, 1904, 1913, 1916-20, 1928, 1936-54, 1960	218 m shaft with 6 levels	Au,Ag,Cu,Pb,Zn	about $5 mill worth of metals, 0.2 oz/t Au, 3 oz/t Ag, 1% Cu, 4-5% Pb, 4-5% Zn
Carnation[2]	6.17S.20W	---	shaft, pits	Au,Ag	none
Center, Penns.[1]	1,12.17S.21W	1944-46, 1984-86	116 m	Au,Ag,Cu,Pb,Zn	0.4 oz/ton Au, 4 oz/ton Ag, 2% Pb, 0.4% Cu, 2.8% Zn
Center decline[1]	1.17S.21W	1987-present	158 m	Au,Ag,Cu,Pb,Zn	active
Commerce-Mayflower[3]	8,9.6S.32E	---	shaft, pits	Cu, Ag (Au)	some
Copper Basin[3,6]	10.6S.32E	---	shaft, pits	Cu, Ag (Au)	some
Daniels Camp[4,6]	5.7S.32E	---	shaft	fluorite	some
Davenport[2]	8.17S.20W	1981-82	decline	Au,Ag (Cu,Pb,Zn)	some
Dean[4]	15.7S.32E	---	shaft	fluorite	some
Delmir mine[3] (Delamar)	36.17S.21W	1915, 1917	shafts	Au,Ag,Cu,Pb	<200 tons
East Camp Group[2]	8.17S.20W	1932, 1934-42, 1951, 1955-57, 1981-82	shafts	Au, Ag (Cu,Pb,Zn)	0.22 oz/ton Au, 15 oz/ton Ag
Forbis[4]	4,9.7S.32E	---	55 m shaft	fluorite	some
Fourth of July[4] (Ellis)	4.7S.32E	1936-42, 1960	46 m shaft	fluorite (Au,Ag,Cu)	3,190 tons of 64% CaF_2
Fraser[2] (Fraser-Martin)	17.16S.21E	1880-1958	4 shafts (deepest is 200 m)	Au, Ag, Cu	some
Golden Nugget[2]	8.17S.20W	---	shaft	Au,Ag	some
Goldenrod[2]	7.17S.20W	---	44 m adit	Au,Ag	none
Hext[5]	20.17S.20W	---	shafts, adit, trenches	Cu, Au, Ag	unknown
Homestake[2]	14.17S.21W	1936, 1938-39, 1941	40 m shaft, adits	Au,Ag (Cu)	<500 tons of 0.23 oz/ton Au, 6 oz/ton Ag
Hoover[2]	26.16S.21W	---	adit	Au,Ag	some (with Norman King)
Jim Crow-Imperial-Gold King[2]	23.17S.21W	Intermittently 1897-1985	several shafts	Au,Ag (Cu,Pb)	6,806 tons of 0.17 oz/t Au and 7.6 oz/t Ag
Jumbo[2]	15.7S.20W	none	shaft	Au, Ag	---
Laura[2]	2.17S.21W	1860s, 1907-09, 1938-42, 1982	196 m shaft	Au,Ag (Cu,Pb)	11,800 tons of 0.29 oz/ton Au, 9.6 oz/t Ag
Leta Lynn[4]	19.16S.21W	1971-72	shaft, trench	fluorite	3 tons 65% CaF2
Luckie[4]	3,10.7S.32E	1914-1944	open pit, shaft	fluorite	2,200 tons 65-70% CaF2
Mohawk[4]	26.16S.21W	1942-44, 1972	4 shafts	fluorite, Au, Ag	6,500 tons 50-75% CaF2
Mount Royal[2] (Golden Fleece)	23.17S.21W	1939-41, 1970-71, 1981	91 m shaft	Au,Ag (Cu,Zn)	2,542 tons of 0.12 oz/ton Au, 3.0 oz/t Ag
National Bank #1[2] (Bank)	35.16S.21W	1936-37	shaft	Au,Ag (Cu)	0.2 oz/t Au, 17 oz/t Ag
New Years Gift[2]	10.17S.21W	1915, 1919, 1940-41	76 m shaft	Au,Ag (Cu,Pb)	0.2 oz/t Au, 8-9 oz/t Ag
Norman King[2]	26.16S.21W	1919, 1921, 1923, 1930, 1932-33, 1935-42	152 m shaft	Au,Ag (Cu,Pb)	0.63 oz/ton Au, 43 oz/t Ag, 1919-1921; 0.18 oz/ton Au, 11 oz/ton Ag, 1936-40
Ontario[1]	7.17S.20W	1941, 1942, 1945, 1949	49 m shaft, 27 m adit	Au,Ag,Cu,Pb,Zn	<1,500 tons of 0.24 oz/t Au, 13.6 oz/t Ag
Powell[4]	20.16S.21W	1942-43	trench, pits	fluorite	127 tons 65% CaF2
Rattlesnake[4]	20,29.18S.20W	1970s	pits	fluorite	120-150 tons of CaF_2
Section 2 adit[2]	2.17S.20W	---	adit	Au,Ag	none
Smuggler[2]	11.17S.21W	prior to 1925	61 m adit	Au,Ag	some ($150,000)
Stotts-Ontario[4] (Phillips)	15.7S.32E		shafts, trenches, pits	fluorite	unknown
Summit Group[2] (Apex, Inspiration)	36.16S.21W	1936-40, 1979-83	shaft, 61 m adit	Au,Ag (Cu,Pb)	73,550 tons of 0.13 oz/ton Au, 5.54 oz/ton Ag
Thanksgiving[2] (Alberto)	8,16.17S.20W	1934-35, 1939	shaft	Au,Ag	<100 tons ore
Twin Peaks[2,6] (Fraser, FreeGold, Rival, New Strike)	8.16S.21W	1912-14, 1916, 1935, 1937, 1939, 1946	5 shafts (up to 282 m deep)	Au,Ag (Cu)	<1,000 tons ore
Yellow Jacket[3,6]	28.15S.21W	---	adit, shaft	Cu	none
Wampoo[3]	15.6S.32E		trench, shaft	Cu, Au, Ag	some

Type of deposit: [1] Base-metal veins [2] Silver-gold veins [3] Copper veins [4] Fluorite [5] Manganese [6] Not in mapped area

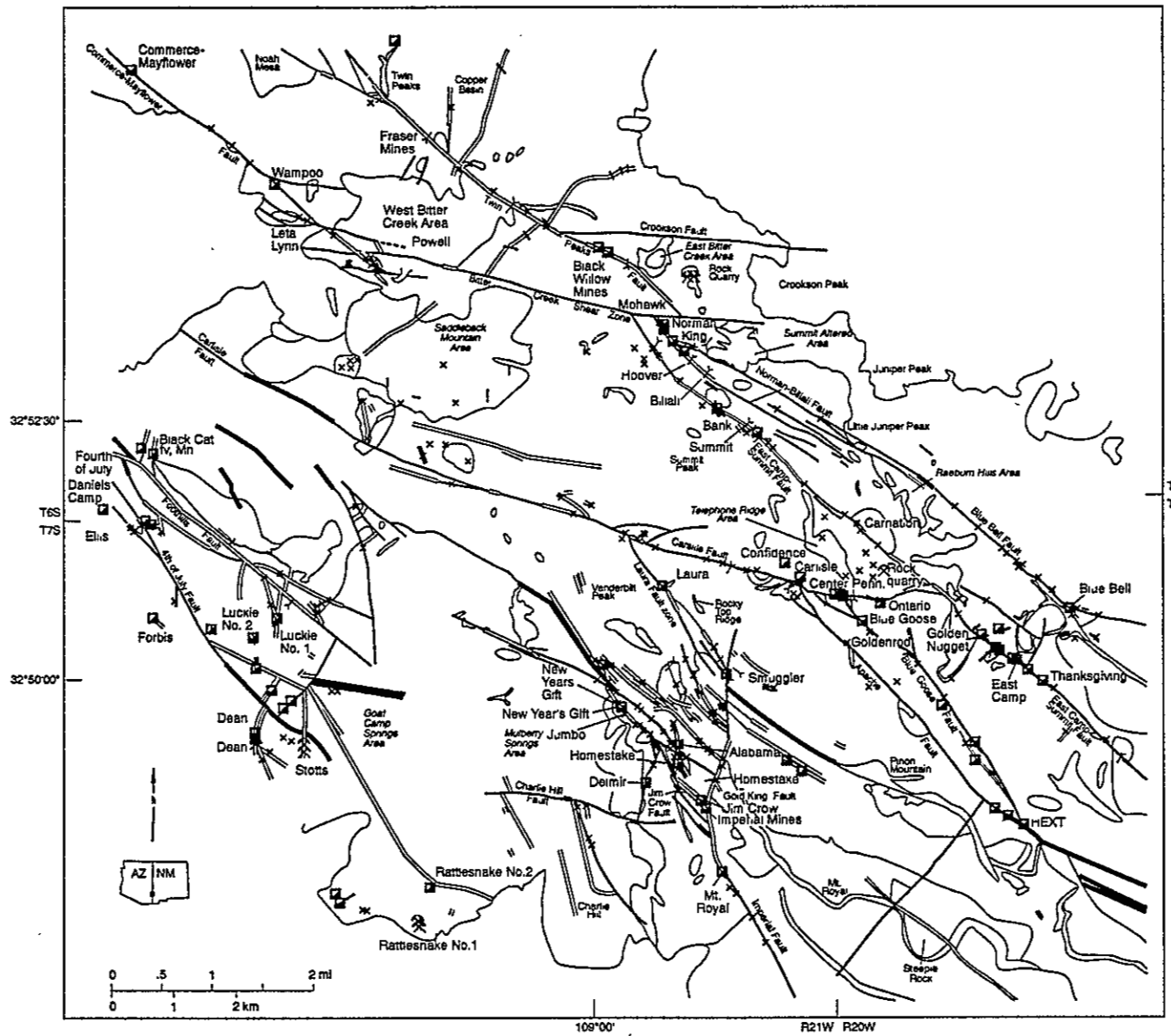

Figure 3.1-Mines in the Steeple Rock mining district.

USBM evaluated the Carlisle, Center, and Pennsylvania mines, including sampling of the underground workings and drilling, to determine the potential for base metals (Russell, 1947; Griggs and Wagner, 1966). Drill core from this project is stored at the USGS core facility in Denver, Colorado. From 1942 to 1946, total production from these mines amounted to more than 8 million pounds of copper, lead, and zinc (Table 3.2). These ores were first processed in Duncan and then, in 1944, the ores were processed at the rehabilitated East Camp mill. Processing of ore from the Carlisle mine at the East Camp mill resulted in some confusion in production records and assays of mine dumps. Contamination of East Camp dumps occurred and some of the ore attributed to East Camp mines may have actually come from the Carlisle mine.

Some of the fluorite mines in the western part of the district operated in the 1930s and 1940s and again in the 1970s (Table 3.2). About 11,000 tons of fluorite were produced (Hedlund, 1990a). Manganese from the western part of the district was also produced (Keith et al., 1983). Most of this production was minor.

Production and exploration between 1947 and 1980 were minor (Table 3.2, 1.2). In 1954, Kennecott Co., presumably looking for porphyry copper deposits, drilled a hole in the Bitter Creek altered area (Bitter Creek #1, sec. 20 T16S R21W, Appendix 11.1) to a depth of 762 m (Hedlund, 1990b; Powers, 1976; W. M. Sheperd, pers. comm. April 1993). Exploration drilling occurred periodically throughout the district from 1950 to 1980 (Hedlund, 1990b; unpublished company reports). Drilling occurred at the Carnation mine in 1959-60 and at East Camp in 1965 (Banner Mining Co.) and again in 1973 (Mt. Royal Mining Co.). Dresser Industries Inc. drilled at the Center mine in 1977-79 (Appendix 11.1). Douglas Hansen rehabilitated and intermittently shipped ore from the Summit, Center, Bank, Laura, Carlisle, and East Camp mines in 1975-90. In 1980, Queenstake Resources Ltd. (Canada) examined the Jim Crow, Gold King, and Imperial mines and holes were drilled in 1985 and 1987 (Appendix 11.1). Calculated reserves were reported as 155,535 tons of ore averaging 0.11 oz/ton (4 ppm) Au and 3.45 oz/ton (118 ppm) Ag (Queenstake Resources Ltd., press

release, 4/2/87).

Exploration intensified in the 1980s and into the 1990s but not much production has occurred (Table 3.2). Superior Mining Division drilled in the Bitter Creek altered area (sec 27 T16S R21W) to 274 m. FMC drilled an altered area along the Blue Bell fault at Raeburn Hills east of Telephone Ridge in 1987 (Appendix 11.1). Impala Resources Ltd. (Canada) drilled at East Camp in 1986. Inspiration Mining Co., Phelps Dodge Inc., Hecla Mining Co., St. Cloud Mining Co., Noranda Exploration, Inc., and Pioneer Nuclear Corp. also had exploration projects in the district in the 1980s. Pioneer Nuclear Corp. drilled at Telephone Ridge in 1984-86. Results of these programs are largely unknown but did not result in any mining or announcement of major discoveries. Dresser Industries, Inc. drilled at the Center and East Camp mines; results are unknown except at the Center mine where production began in 1987.

In 1987, R and B Mining Co. obtained a lease from Mt. Royal Mining Co. (Houston, Texas) and began mining at the Center via a decline. The mine has produced silica flux with significant gold and silver since 1987. In 1988, Nova Gold Ltd. (Canada) initiated exploration of the Summit vein. A joint venture with Biron Bay Resources Ltd. (Canada) was formed in 1990 and drilling continued with proving of ore reserves. Biron Bay announced the discovery of a deposit containing 1,450,000 tons of ore grading 0.179 oz/ton (6 ppm) Au and 10.26 oz/ton (398 ppm) Ag for a width of 4 m (Petroleum and Mining Review, May 1992, p. 2). Additional exploration drilling is planned for 1993.

In July 1991, Great Lakes Exploration Co. (Minnesota) drilled at the Alabama (Appendix 11.1). This drill core is stored at NMBMMR, Socorro, New Mexico. Douglas Hansen shipped ore from the East Camp. A Canadian firm drilled at the Carlisle mine in August 1991 (Appendix 11.1). Cuttings are stored at NMBMMR. Mining for gold-silver flux continues at the Center mine; some ore shipments assay as much as 0.8 oz/ton (27 ppm) Au and 5 oz/ton (171 ppm) Ag.

Numerous abandoned shafts, pits, trenches, and adits occur throughout the Steeple Rock district (Maps 1, 2). Some are accessible, but many are dangerous and should be

avoided. Only adits and shallow shafts with competent ground were examined during this study using proper equipment and accompanied by additional trained personnel. The district is dry most of the year. Groundwater is found only along major faults.

The mines can be grouped according to predominant mineralogy as base-metal mines, gold-silver mines, copper-silver mines, fluorite mines, and manganese mines. In addition, the district may contain alunite (Hall, 1978) and clay resources. These commodities have not been exploited in the Steeple Rock district, but are described under economic potential. At least two quarries in sec. 23, T16S, R21W and sec. 6, T17S, R20W were mined for decorative stone, but no production figures are available. The district also has been examined for molybdenum, porphyry copper, and uranium (see economic potential). The following descriptions of the more important deposits are from field observations and published and unpublished reports, as cited. Lack of proper exposure of some deposits hampered field descriptions locally. Not all mines could be properly described because of poor exposure and dangerous, abandoned workings.

3.2 General description of vein deposits

In the Steeple Rock district, the vein deposits occur exclusively along faults and fractures within fault zones. Some vein deposits occur along, and cut across, rhyolite dikes and plugs which are intruded along faults. In some places, later faults offset the vein deposits and rhyolite dikes (Maps 1.2). The veins typically form prominent outcrops and are bifurcating, sinuous, and pinch and swell along strike. Complex vein textures, especially brecciation and rhythmic layering, are typically associated with high metal concentrations, although many complexly-textured veins are barren of any mineralization. At least four stages of mineralization separated by periods of brecciation occurred: stage 1, stage 2, stage 3, and late stage mineralization. Additional information concerning paragenesis will be discussed in section 6.4.

Five types of vein deposits are distinguished on the basis of mineralogy and metal

content: base-metal (silver-±gold), gold-silver (±base metals), copper-silver, fluorite, and manganese veins. A sixth type of deposit, high-sulfidation disseminated gold deposits, may also occur in areas of acid-sulfate alteration.

The age of the vein deposits in the Steeple Rock district is problematical. Wahl (1983) reports a K-Ar age on adularia from the East Camp vein as 18 Ma. Veins cut the Bloodgood Canyon Tuff and younger ash-flow tuffs and therefore must be younger than 27 Ma. The age of the vein deposits will be discussed in more detail later in this report.

3.2.1 Base-metal veins

The base-metal veins in the Steeple Rock district occur exclusively along the Carlisle fault, from the Carlisle mine eastward to the Ontario mine (Maps 1, 2). These veins consist of 5–20% sulfides as galena, sphalerite, and chalcopyrite with considerable silver and gold and local secondary sulfide and carbonate minerals in a gangue of quartz, pyrite, chlorite, illite/sericite, rare adularia, and a few additional accessory minerals. Sulfide minerals vary in concentration throughout the fault zone, as they occur in two or three ore shoots and appear to increase with depth, then decrease near the base of the mineralization. Early reports indicate that gold and silver with only trace amounts of base metals occurred near the surface of the Center and Pennsylvania mines and graded with depth to base-metal veins. Base metals occur at the surface at the Carlisle mine, however, early reports show gold and silver were also concentrated in a separate ore shoot (Griggs and Wagner, 1966).

The ore occurs as 1) coarse-grained, massive sulfides (up to 20% base metals total), locally with little quartz, and 2) medium- to fine-grained sulfides disseminated throughout the brecciated quartz veins and fault gouge. Sulfides in the massive zone occur as streaks, irregular masses, and veinlets in zones up to 4 m across. Banded, rhythmic layering, and brecciated textures are characteristic. At least three periods of brecciation and cementation by silica have occurred. Sulfides occur in stage 2 mineralization and locally in stage 3. Lenses or zones of chlorite locally occur between bands of sulfides. Alteration is variable but typically

silicification, chloritization, and clay alteration is well developed along and between the veins. Acid-sulfate alteration occurs at the surface at the Carlisle and Ontario mines.

3.2.2 Gold-silver veins

The precious metal veins in the Steeple Rock district consist of gold and silver with local but minor sulfides (less than 1%) as pyrite, galena, sphalerite, and chalcopyrite disseminated in a gangue of quartz, calcite, chlorite, illite/smectite, rare adularia, epidote, and additional accessory minerals. These veins are predominantly quartz and quartz breccias and occur along the northwest-trending faults, but they may occur along any fault trace. They grade along strike locally with the Carlisle base-metal veins, fluorite veins, and copper-silver veins. Base-metal sulfides occur at depth in many of these deposits, but total base metals rarely exceed 1-3%. In two deep drill holes near the Mohawk mine, zones of disseminated galena, sphalerite, chalcopyrite, and pyrite occur in silicified porphyritic andesite. Up to 5% sulfides have replaced feldspar phenocrysts and the groundmass.

The best gold-silver values occur in complex veins that are banded, rhythmically layered, and brecciated. At least three periods of brecciation and cementation by silica has occurred in many areas. Gold and silver occur in stage 2 and locally in stage 3. Lattice textures are locally common. A yellow to yellow-green staining of mottramite $(Cu,Zn)Pb(VO_4)(OH)$ or mimetite $Pb_5(AsO_4,PO_4)_3Cl$ is characteristic of higher values of gold and silver. Sulfides tend to occur in streaks or thin zones of disseminated sulfides and give the quartz a bluish or black tint. Distinction between mineralized veins and barren veins is difficult and confirmed only by fire assays.

3.2.3 Copper-silver veins

The copper-silver veins are characterized by secondary copper minerals, predominantly malachite and pseudomalachite, with detectable silver concentrations and rare gold concentrations. These veins are sporadically distributed throughout the district and

locally grade laterally and vertically with gold-silver or fluorite veins (Map 2). The copper-silver veins have not been major producers of ore, although some deposits have yielded minor quantities of ore in the past (Table 3.2).

The copper-silver veins are typically short, rarely exceeding a few tens of meters in length. Malachite, pseudomalachite, azurite, chalcanthite, chalcocite, chrysocolla, and other secondary copper minerals are prevalent along fractures and cracks within fault zones. The faults typically trend north to northwest to northeast. Gangue minerals include quartz, calcite, and clay minerals and locally iron and manganese oxides. In contrast to the base-metal and gold-silver veins, the copper-silver veins are simple fissure-filling or fracture-coating deposits. Locally the veins may be zoned with quartz forming the outer portions and quartz, calcite, and copper minerals forming the cores of the veins. Either one period of or no brecciation occurred. Silicification is not as extensive as in the base-metal and gold-silver veins. Pyrite, malachite, and chalcopyrite may occur disseminated through the silicified host rock for several meters distal from the veins.

3.2.4 Fluorite veins

The fluorite veins in the Steeple Rock district occur predominantly along the western edge of the district and along Bitter Creek. These veins are typically simple fissure-filling or fracture-coating of fluorite with minor quartz and calcite. In general, they occur along splays of major faults and along minor faults (Maps 1, 2).

3.2.5 Manganese veins

Manganese oxides, typically psilomelane, occur as late-stage coatings along with other vein minerals throughout the Steeple Rock district. Locally manganese oxides form thin veins and fracture-fillings up to 10 cm thick. The Black Cat deposit in the Foothills fault area is the single locality where manganese was mined and produced in the 1950s. This zone is up to 3-5 m wide. Fluorite is an accessory mineral and silicification is common.

3.2.6 Disseminated gold deposits(?)

Disseminated gold deposits (high sulfidation) are associated with acid-sulfate altered rocks in several mining districts in the world, such as Round Mountain, Nevada (Tingley and Berger, 1985), Pueblo Viejo, Dominican Republic (Kesler et al., 1981; Muntean et al., 1990; Vennemann et al., 1991, 1993), Summitville, Colorado (Perkins and Nieman, 1983; Stoffregen, 1987; Rye et al., 1992) and El Indio, Chile (Walthier et al., 1982). These deposits are characterized by gold, pyrite, and enargite in vuggy silica, veinlets, stockworks, and breccias in zones of acid-sulfate altered rocks. Bonanza veins are common, but deposits of fine-grained gold disseminated in the host rock are also common (Cox and Singer, 1986; Heald et al., 1987; White and Hedenquist, 1990).

The intense acid-sulfate alteration cropping out locally in the Steeple Rock area indicates a potential for similar gold deposits. Although no disseminated gold deposits yet have been found in the Steeple Rock area, at least two companies (Pioneer Nuclear and FMC) have drilled in altered areas, presumably exploring for similar deposits (Appendix 11.1). Although drilling is inconclusive, a few assays of the drill core are indicative of the presence of gold. Furthermore, surface samples collected for this study also contain gold locally and are indicative of disseminated gold deposits (Appendix 11.5, 11.6). Further discussions of this type of deposit are in section 5 of this report.

3.3 Description of base-metal mines

3.3.1 Carlisle mine

The principal mine in the Steeple Rock district is the Carlisle mine and much of the production from the district is attributed to this mine. The Carlisle mine is located on the Carlisle fault at the junction with the Apache fault in sec. 1, T17S, R21W (Maps 1, 2, 5).

Although there was reported production from the mine prior to 1880, the first mining claims were not filed until 1881. In January 1881, Daniel Remington, James Mounts, William Johns, and A. G. P. George from Carlisle, Pennsylvania, filed four claims: Carlisle, Star of

the West, Center, and Pennsylvania. In 1883, the Carlisle group of claims was sold to a group of Chicago merchants who formed the Carlisle Mining Co. In January 1887, the Carlisle Mining Co. was sold, reportedly for $1 million, to a group of London investors. From 1880 to 1890 total production is reported as $4 million of gold and silver (R. Blanchard, unpubl. report, 8/20/28). The new company developed the Carlisle mine to 183 m depth, via a winze on the 152-m level and enlarged the mill from 20 stamps to 60 stamps. Ore from throughout the district was processed at the Carlisle mill. In 1887, a smelter was built and attempted unsuccessfully to recover lead and zinc from the mine.

The mine closed in 1890 when the easily recoverable gold and silver orebodies were exhausted. Although gold and silver were found in the lead-zinc sulfide orebodies, the sulfide ore could not be processed at this time. Attempts at recovering the sulfides and gold and silver were unsuccessful until the 1900s. By 1892, only 10 stamps remained operating at the mill. The Steeple Rock Development Co. was organized in 1896 and assumed the assets of the Carlisle Mining Co. The mine was reopened in the 1890s and again in 1904 and 1913, but only minor production occurred. Figures 3.2 and 3.3 are photographs of the Carlisle mine area in the early 1900s.

From 1876 to 1914, the Steeple Rock Development Co. consolidated numerous claims throughout the district and milled much of the ore at the Carlisle mill. However, as silver prices dropped, the company was forced to sell off portions of the properties. In 1914, George H. Utter bought the remaining assets, including the Carlisle and began processing mill tailings at the Carlisle until 1920. Utter may have produced from the Carlisle mine during 1914-1920 as well. In 1927, United Metals Corp. dewatered the Carlisle and continued development. By 1928, total development consisted of approximately 3000 m of drifts, crosscuts, winzes, raises, and the 158-m shaft (R. Blanchard, unpubl. report, 8/20/28). The ultimate depth reached in the mine is 219 m.

The mine closed again in 1930. In 1936-1941, Veta Mines, Inc. and other lessors operated the mine. Minor production occurred. In 1941-1942, Southwest Minerals Co.

Figure 3.2—Photo of mill at the Carlisle mine in 1903 looking north (from Douglas Hanson collection).

Figure 3.3—Photo of the town of Carlisle in the early 1890s. Telephone Ridge is in the background and the headframe is to the right (from Douglas Hanson collection).

produced from the Carlisle (Gillerman, 1964). The U.S. Bureau of Mines examined the mine and other operating mines from 1942 to 1944 in response to government directives as a result of World War II. Description of drill core data is in Appendix 11.1. The East Camp Syndicate, Inc. (later the Exploration Syndicate, Inc.) leased and operated the Carlisle mine from 1943 to 1946. The mine closed again in 1951 and was allowed to fill with water to the 61-m level. Some production occurred from the open pit in 1954, 1960, 1970s, 1982, and 1989-1990.

The Carlisle mine, now flooded, consists of a three-compartment shaft (157 m deep) with a winze on the 152-m level to 219 m total depth. Levels are reported at 12, 49, 61, 76, 91, 102, 122, 137, 152, 183, and 213 m. Mine maps are in Griggs and Wagner (1966) and a longitudinal section is on Map 5. An open pit with a decline connects to the 12-m level. A second short adit occurs on the west side of the pit (Fig. 3.4).

The Carlisle orebodies occur at the junction of the normally west-northwest-trending Carlisle fault and the northwest-trending Apache fault. The Apache fault has caused the Carlisle fault to strike locally N45°W with a 65-80°S dip (Fig. 3.5). The Carlisle fault resumes a more westerly strike about 30 m east of the shaft and 243 m west of the shaft (Map 1, 2; Gillerman, 1964). The Carlisle orebodies are within the northwest-trending segment.

The host rock is altered andesite and andesite porphyry of the Summit Mountain formation. Rhyolite ash-flow tuffs are probably present but the alteration is too intense to be certain. The orebodies occur in one to three major breccia veins consisting of rock fragments, quartz, pyrite, illite, kaolinite, chlorite, and adularia (Fig 3.6). The surface ore minerals include oxidized copper and lead minerals, whereas galena, sphalerite, chalcopyrite, bornite, and chalcocite are found in the mine. Ore shoots are pods, stringers, and irregular masses within the breccia veins. Some shoots were up to 2.4 m wide and 61 m long (Gillerman, 1964). Base metal concentrations increased with depth (Gillerman, 1964; Griggs and Wagner, 1966). Drilling by the U.S. Bureau of Mines on the 213-m level did not indicate reserves at depth (Griggs and Wagner, 1966), however, early descriptions suggest not all reserves were

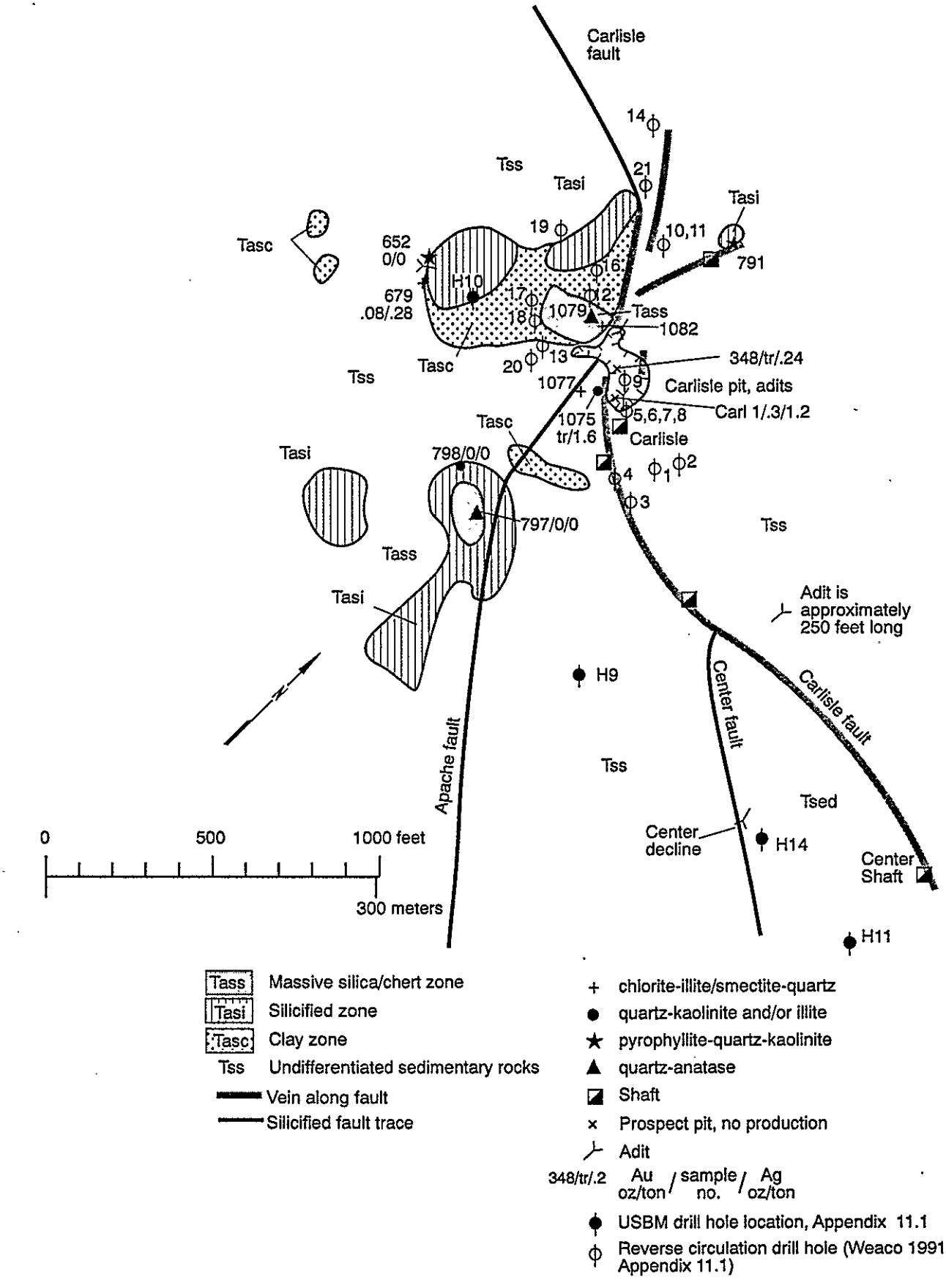

Figure 3.4 Geologic and alteration map of the Carlisle mine.

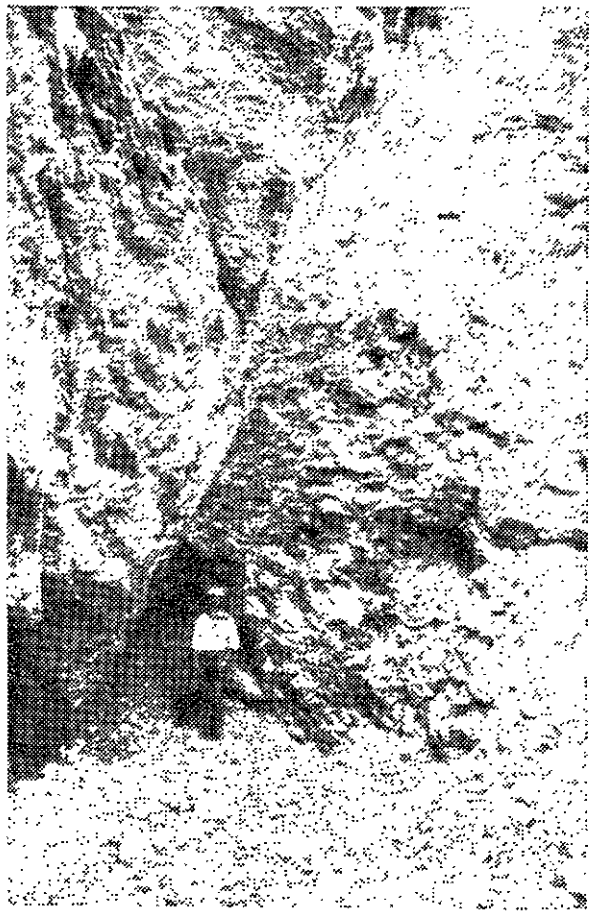

Figure 3.5—View of fault zone on west side of Carlisle pit where the Apache fault merges with the Carlisle fault.

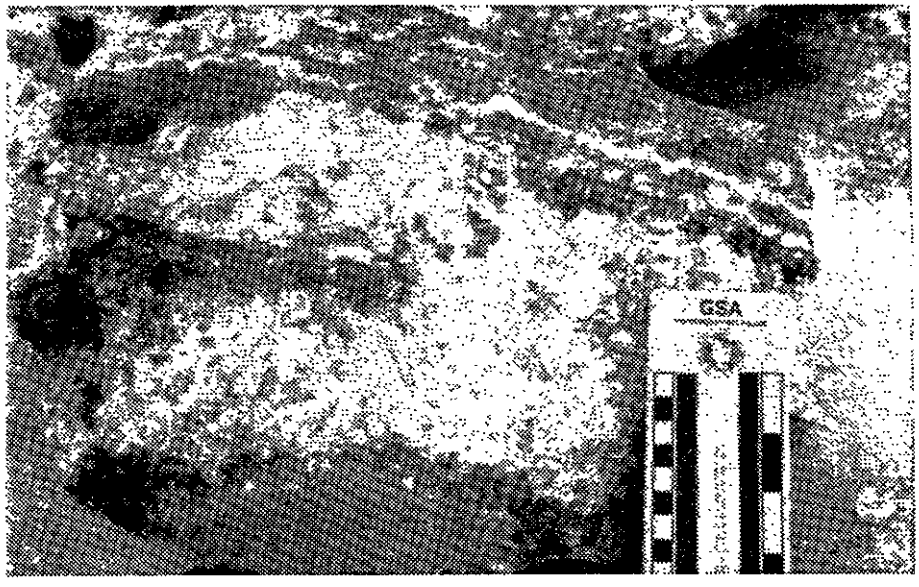

Figure 3.6—Photo of ore from the Carlisle mine consisting of alternating zones of chlorite-quartz, sulfides (galena, chalcopyrite, sphalerite), and quartz.

mined. Mineralized zones west of the pit were encountered in drill holes by Weaco Exploration Ltd. in 1991 (Appendix 11.1). Chemical assays of recent production from the open pit are given in Table 3.3. Assays of drill hole samples from holes drilled by the U.S. Bureau of Mines are in Table 3.4. The geochemistry of the deposit is discussed in section 4.4.2.

3.3.2 Center mine

The Center mine occurs along the Carlisle fault in sec. 1, 12, T2S, R21W at an elevation of 1642 m (collar of shaft). The mine consists of a shaft and a decline (Map 4).

As ore shoots were not exposed at the surface, production did not occur until 1937. The Center mine was found when miners drifted from the adjacent Pennsylvania mine on the 37-m level. In 1941, a raise was driven to the surface which subsequently became the Center shaft. From 1944 to 1946, the Carlisle Development Co. sank the shaft to 91 m and developed about 914 m of drifts. Four levels were developed at 37, 46, 76, and 91 m. Production during this period is summarized in Table 3.5.

Various operators controlled the Center mine from 1942 to 1975, but little development occurred. In 1975, Dresser Industries Corp. began minor production, development, and core drilling (Hedlund, 1990b). In 1985, Mt. Royal Mining and Exploration Co. acquired the Center mine and in 1987 leased it to R and B Mining Co., who drove a decline below the old Center shaft and began production (Fig. 3.7). R and B Mining Co. is currently producing and shipping the ore to ASARCO, El Paso, Texas. R and B Mining Co. drilled underground and descriptions of drill core are in Appendix 11.1. The Center decline is at an elevation of 1615 m and extends to about 122 m below the surface.

The Center deposit consists of a breccia zone up to 24 m wide along the Carlisle fault. The host rocks consist of altered purple to green andesite porphyry flows of the Summit Mountain formation and purple to green to white tuffs, sandstones and volcanic breccias. Ore consists of gold, electrum, silver minerals, sphalerite, galena, and chalcopyrite in a gangue of

TABLE 3.3—Chemical analyses of some recent ore shipments from the Carlisle mine. From ASARCO smelter return receipts. Max - maximum value, Min – minimum value; Avg – mean value; Stds –standard deviation.

Date	Lot	Au (oz/ton)	Ag (oz/ton)	Cu%	Zn%	As%	Bi%	Fe%	SiO_2%	Al_2O_3%
10/17/90	1522	0.305	2.7	0.15	0.6	0.008	0.035	2.75	78.83	7.3
04/26/90	605	0.2	0.2	0.37	2.0	0.006	0.01	2.9	78.75	6.0
11/13/89	1405	0.115	1.0	0.76	2.1	0.01	0.01	4.2	74.1	6.4
06/19/90	654	0.212	0.6	0.31	1.43	0.004	0.034	2.78	80.26	5.5
04/10/90	255	0.327	0.775	0.33	1.1	0.006	0.006	2.775	79.515	6.275
07/31/90	712	0.305	0.8	0.31	1.43	0.006	0.016	2.5	80.3	5.4
09/12/90	1039	0.19	1.2	0.24	0.95	0.006	0.01	2.8	80.6	6.2
09/12/90	858	0.206	7.05	0.21	1.12	0.006	0.016	2.6	82.32	4.7
08/26/82	1040	0.11	1.1	0.11	2.9	--	--	--	80.0	8.0
Max	--	0.327	7.05	0.76	2.1	0.01	0.035	4.2	82.32	7.3
Min	--	0.115	0.2	0.15	0.6	0.004	0.006	2.5	74.1	4.7
Avg	--	0.233	1.791	0.34	1.34	0.007	0.017	2.913	79.334	4.972
Stds	--	0.073	2.25	0.19	0.51	0.002	0.011	0.535	2.4	0.78

Table 3.4—Assays of drill core samples at the Carlisle mine by the USBM at the 213.3 m level (Appendix 11.1; Russell, 1947).

Hole no.	Sample intercept (m)	Au oz/ton	Ag oz/ton	Cu%	Pb%	Zn%
USBM H-1	176.9-179.6	tr	0.64	0.5	5.4	3.7
	182.8-185.3	tr	0.56	1	0.9	1.5
USBM H-2	246-247.3	0.02	3	1.2	1.7	2
USBM H-3	232.2-237.5	tr	0.24	0.6	3	0.5
USBM H-4	120.5-124.1	0.02	2.78	1.24	3.3	6
	124.1-140.3	tr	0.52	0.64	0.6	0.5
	140.3-141.4	0.01	1.48	1.24	2.5	3.6
	141.1-143.3	0	0.56	0.9	1.3	2.2
	143.3-144.1	0	0.16	0.17	0.2	0.5
	144.1-145.9	tr	0.6	0.33	1.2	1.8
USBM H-5	166.6-170	0	0	0.2	1.4	2.1
	168.2-170	0.02	1.22	1	4.1	7.8
	188.9-189.9	tr	0.52	1.4	--	--
USBM H-6	212.5-215	tr	0.56	0.31	1.2	1.5
USBM H-7	129.1-130	tr	0.2	0.04	0.15	0.38
USBM H-8	189.2-190.7	0.01	0.8	0.35	1.2	1.9
	199.7-200.8	0.04	3.68	1.1	3.15	3

TABLE 3.5—Ore production from the Center mine 1937-1946, Steeple Rock district (K. C. Richmond, unpublished report, 10/24/46).

Years	Ore tons	Grade Au oz/t	Grade Ag oz/t	
1937-1939	12,000	0.6	3.0	120 level
1939-1942*	15,000	0.4	2.0	probably 120, 250 level
1944-1946	1,474	0.55	2.0	probably 250,300 level
TOTAL 1937-1946	28,474	0.49	2.4	

* 0.3% Cu, 2% Pb, 3% Zn reported

TABLE 3.6—Assays of drill core samples from holes drilled by U.S. Bureau of Mines at the Center mine (Russell, 1947).

Drill hole	Depth (ft)	Au oz/t	Ag oz/t	Cu%	Pb%	Zn%
11	310.4-311.5	0.02	0.48	0.31	1.14	2.00
	311.5-314.5	0.04	0.16	0.12	0.36	0.30
	319.6-322.8	nil	0.04	tr	0.06	0.25
14	344.0-345.8	tr	0.80	0.25	1.7	2.2
	345.8-348.8	0.01	0.28	0.26	0.53	0.89
	348.8-352.2	nil	0.20	0.07	tr	0.40

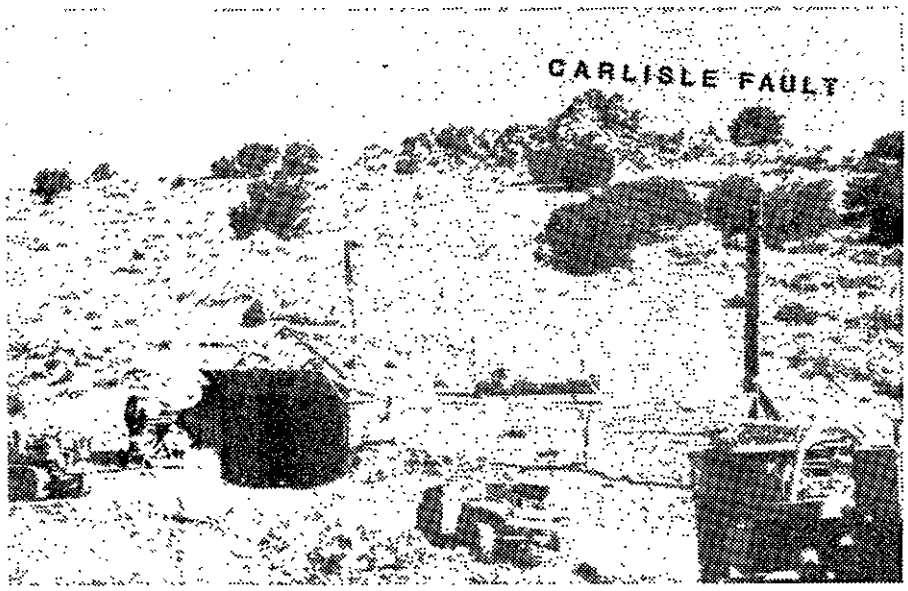

Figure 3.7—View of Center decline in 1990.

quartz, pyrite, chlorite, iron oxides, adularia, gypsum, calcite, illite, siderite, dolomite, and clay minerals. Ore shoots are 0.3-1.8 m thick and occur in bends and splays of the Carlisle fault. Fault and vein orientations of each level were plotted on stereonets, however no structural trends with depth were observed. All orientations are shown in Figure 2.21. Two holes were drilled by the U.S. Bureau of Mines in 1941; assays are in Table 3.6 (Griggs and Wagner, 1966; Russell, 1947). Dresser Minerals also drilled at the Center mine (Appendix 11.1; Maps 5, 6). The chemistry of ore shipments is discussed in section 4.4.1.

3.3.3 Pennsylvania mine

The Pennsylvania mine was one of the first claims filed in the district in 1881. It is located east of the Carlisle and Center mines on the west-northwest-trending Carlisle fault in sec. 1, 12, T17S, R20W (elevation 1640 m). Development consists of three inclined shafts to approximately 37 m depth with 70° dip south. A short adit and several cuts also occur at the surface. The mine connects with the Center mine on the 37-m level, but the underground workings are extremely hazardous (Map 4).

The Pennsylvania mine consists of a breccia zone up to 24 m wide. The host rocks consist of andesite and sandstones of the Summit Mountain formation and younger ash-flow tuff. The Blue Goose fault intersects the Carlisle fault at the Pennsylvania mine (Map 1, 2). Ore is concentrated at inflections within the Carlisle fault zone produced by the Blue Goose fault. Ore consists of gold, silver minerals, sphalerite, galena and chalcopyrite and is similar to ore at the Center and Carlisle mines. Two drill holes were driven at the Pennsylvania by the U.S. Bureau of Mines which did not indicate any additional ore (Appendix 11.1; Griggs and Wagner, 1966). A series of samples were collected and assayed, probably in the early 1900s (Table 3.7). Two samples were collected for this study and assayed, but did not contain gold or silver (P1, P2, Appendix 11.6).

Table 3.7—Chemical analyses of samples from the Pennsylvania adit and shaft. From NMBMMR map files (no date). Samples 7-17 from upper adit and samples 18-21 from shaft.

Sample no.	Au oz/ton	Ag oz/ton	Cu%	Pb%	Zn%	Comments
7	tr	0.88				
8	0.04	1.14	0.74	2	0	1.2 m channel
9	nil	0.42	0.18	3.3	9.2	2 m channel
10	nil	0.2	tr	0.5	0	2 m channel
11	0.06	0.28	--	--	--	1.7 m channel
12	nil	0.08	--	--	--	5.5 m channel in waste rock
13	1.2	1.5	0.74	0.8	6.1	1.7 m channel
14	1	1.26	0.23	5.1	5.1	1.4 m channel
15	nil	0.14	--	--	--	2.7 m channel
16	0.96	1.88	tr	7	0	1.2 m channel
17	nil	0.12	tr	0.3	0	0.5 m channel
18	0.04	1.52	tr	0.8	4.8	1.2 m channel
19	0.98	1.02	0.23	2.2	4.3	1.2 m channel
20	0.14	1.06	tr	2.7	4	1.4 m channel
21	0.88	1.96	--	4.5	4.3	1.4 m channel

3.3.4 Ontario mine

The Ontario mine is located along the Carlisle fault east of the Pennsylvania shaft in sec. 7, T17S, R20W (elevation 1600 m) and consists of an inclined shaft (70°S dip) and one short adit (27 m long) intersecting the 12-m level. The shaft is 49 m deep with levels at 12, 30, and 43 m. R and B Mining Co. drove a second adit (9 m long) west of the shaft in 1988 in hope of intersecting the Pennsylvania workings (Map 5). Although sulfide ore was found, it was too high in fluorine and too low in gold to be economical. Several pits and shallow shafts also expose the vein along strike.

Production from the Ontario mine is minor and amounts to less than 1500 tons of ore averaging 0.24 oz/ton (8 ppm) Au and 13.6 oz/ton (466 ppm) Ag. The mine produced in 1941, 1942, 1945, and 1949.

The Carlisle fault strikes east-west and dips 70°S at the Ontario mine (Map 1, 2). The host rocks consist of sandstones and andesite porphyry of the Summit Mountain formation. The vein is about 0.3 m wide on the 12-m level, but widens to about 1.5 m in the R and B Mining Co. adit to the west. Sampling of the 30- and 43-m levels by J. D. Lowell in 1971 ranged from 0.003 to 0.485 oz/ton (0.1-17 ppm) Au, 0.54 to 23.94 oz/ton (18-820 ppm) Ag, and 0.19 to 0.46% Cu, but mineralized zones were small and spotty (J. D. Lowell, unpubl. report, 5/28/71). A sample from the ore zone collected in 1966 assayed 0.01 oz/ton (0.3 ppm) Au, trace Ag, 0.10% Cu, 0.10% Pb, and 0.20% Zn (Shattuck Denn Mining Corp., unpubl. report, 3/10/66). Sampling for this report detected no significant gold or silver, although one sample assayed 0.3 oz/ton (10 ppm) Ag (#ONTARIO, Appendix 11.6). Copper values ranged from 40 to 12,700 pm; lead values ranged from 30 to 29,200 ppm; and zinc values ranged from 18 to 46,800 ppm (#328a, b, c; 340a, b, c, O-1, ONTARIO, Appendix 11.6). All of the samples contained quartz and illite. Adularia, calcite, and sphalerite are common in some samples. Samples enriched in base metals contained galena, chalcopyrite, and sphalerite and sample #ONTARIO (dump sample) contained nantokite (CuCl). Acid-sulfate alteration occurs at the Ontario shaft and is discussed in section 5.

3.4 Description of gold-silver mines

3.4.1 Alabama and Homestake mines

The Alabama and Homestake mines occur along the north-trending Alabama fault in sec. 14, T17S, R21W. The Alabama mine is at an elevation of 1580 m (collar of shaft). The Homestake mine is at an elevation of approximately 1603 m (Map 1, 2).

The Alabama group of claims consist of nine patented claims which were patented on October 2, 1915 by the Torreroca Mining Co. (mineral survey #1624). The Homestake No. 1 was patented on October 18, 1904 (patent #39753, mineral survey #1448) by the Dixie Gold Mining and Reduction Co.

Several shallow pits and shafts comprise the Alabama-Homestake groups. The Alabama mine consists of a 1½ compartment shaft with eight levels at depths of 11, 24, 34, 46, 61, 76, 91, and 107 m below the shaft collar (Fig. 3.8). The 46- and 61-m levels are the most extensive and are 61-91 m long. The shaft dips 80°W and is 113 m deep. The underground workings are flooded to the 11-m level and are currently inaccessible. Two holes were drilled in 1991 by Great lakes Exploration Inc.; a summary of the drill data is in Appendix 11.1. Locations and summary of geochemical analyses are in Figure 4.27.

The Homestake mine consists of several shallow pits, a few short adits and a 40-m shaft. The shaft consists of two levels at depths of 20 and 35 m. Early production occurred from the Alabama in the late 1800s (Engineering Mining Journal, 3/30/1895, p. 302), but total production prior to 1908 is unknown. In 1908, less than 1000 tons of ore was shipped by the Torreroca Mining Co. (NMBMMR files). By 1910, the Alabama shaft was at a depth of 113 m and development began on all levels (F. W. Smith, unpubl. report, 8/5/1910). In the 1930s, development of the mines resumed and the mine produced from 1936 to 1938. In June 1938, George Utter produced 1038 tons of ore averaging 0.32 oz/ton (11 ppm) Au and 14 oz/ton (480 ppm) Ag (H. Schmidt, unpubl. report, 7/18/53). The mine closed in 1939 and remained idle until 1950 when L. H. Foster mined 1526 tons of ore averaging 0.31 oz/ton (11 ppm) Au and 14.3 oz/ton (487 ppm) Ag (Table 3.8; ASARCO, El Paso smelter return

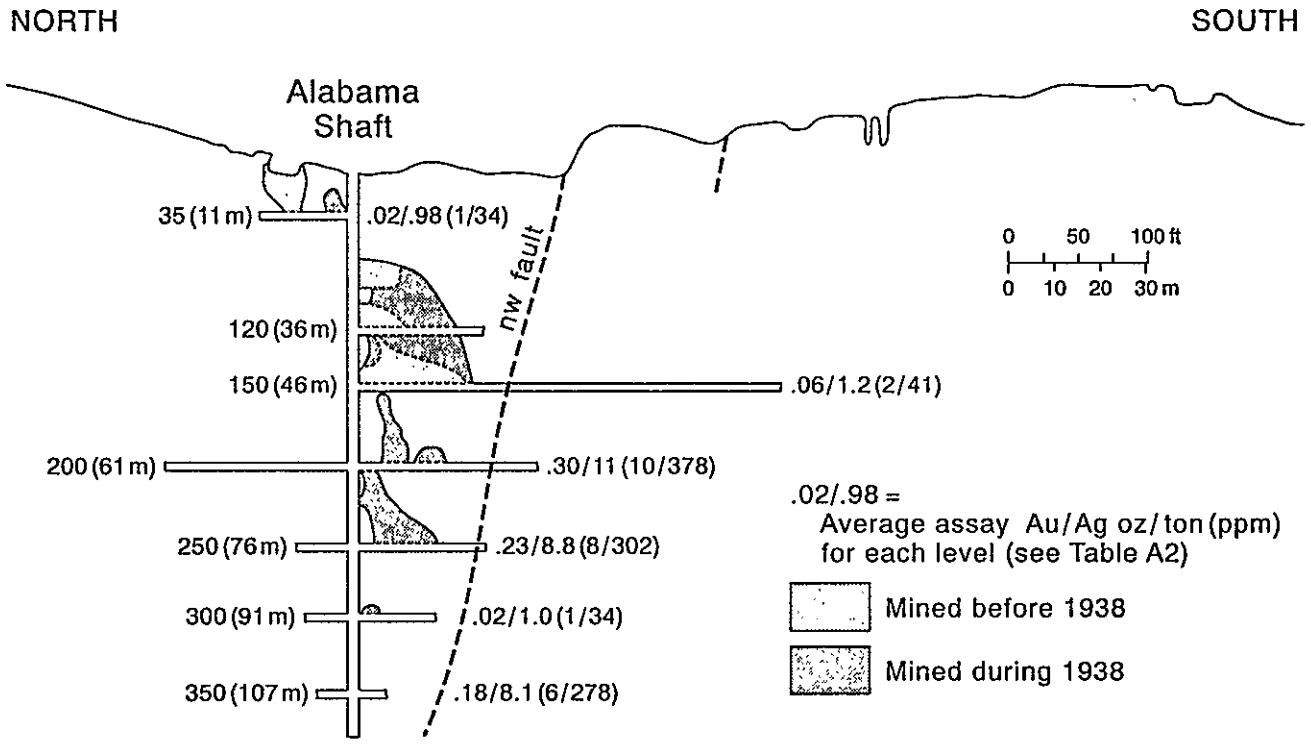

Figure 3.8 Longitudinal section of the Alabama mine (F.W. Smith, written communication, August 5, 1910). Does not show mining in 1950 and 1951.

TABLE 3.8—Chemical analyses of ore shipments from the Alabama mine. Not all ore shipments are listed. From ASARCO, El Paso smelter return receipts (1950-1951).

Date	Lot	Tons	Au		Ag		Cu%	SiO_2%
			oz\ton	(ppm)	oz\ton	(ppm)		
1950	--	47.8	0.138	5	5.69	195	--	82.2
1950	--	60.72	0.23	8	9.73	334	--	84.1
1950	--	60.96	0.22	8	9.7	333	--	86.7
1950	--	56.7	0.495	17	19.93	683	--	--
1950	--	58.9	0.27	9	9.89	339	--	84.3
1950	--	60.9	0.325	11	13.89	476	--	83.8
1950	--	61.5	0.28	10	11.94	409	--	82.6
1950	--	47.8	0.43	15	22.01	755	--	82.7
1950	--	62.6	0.265	9	18.06	619	--	87.2
1950	--	62.7	0.2	7	9.6	329	--	83.4
1950	--	57.7	0.08	3	3.84	132	--	80.7
1950	--	58.5	0.29	10	17.15	588	--	83.2
1950	--	63.6	0.465	16	28.53	978	--	86.2
1950	--	46.7	0.21	7	9.8	336	--	--
1950	--	60.0	0.23	8	9.25	317	--	--
1950	--	65.1	0.54	19	22.75	780	--	--
1950	--	62.3	0.25	9	11.2	384	--	--
08/15/50	2104	66.9	0.515	18	21.9	751	0.1	--
09/20/50	4397	58.5	0.29	10	17.15	588	0.15	83.2
01/02/51	4754	60.7	0.23	8	9.73	334	--	84.1
02/06/51	4892	61.0	0.22	8	9.7	333	--	86.7
03/06/51	5004	56.7	0.495	17	19.93	683	--	--
04/09/91	5116	58.9	0.27	9	9.89	339	--	84.3
04/23/51	5154	60.9	0.325	11	13.89	476	--	83.8
05/07/51	5195	61.5	0.28	10	11.94	409	--	82.6
06/11/51	5318	47.8	0.43	15	22.01	755	--	82.6
TOTAL	--	1527.38	0.29	10	14.2	488	--	--

TABLE 3.9—Average and range of assays for each level in the Alabama mine (F. W. Smith, written communication, 8/5/10).

Level (m)	No. of samples	Avg Au oz/t (ppm)	Range Au oz/t (ppm)	Avg Ag oz/t (ppm)	Range Ag oz/t (ppm)
35 and 80	4	0.02 (1)	0.01-0.06 (0.3-2)	0.98 (34)	0.6-1.8 (21-62)
150 (46)	5	0.06 (2)	0.02-0.19 (1-6)	1.2 (41)	1.2-6.2 (41-213)
200 (61)	13	0.30 (10)	0.04-1.12 (1-38)	11.0 (378)	1.5-61.1 (51-2095)
250 (76)	15	0.23 (8)	0.01-0.81 (0.3-28)	8.8 (302)	0.7-28 (24-960)
300 (91)	4	0.02 (1)	0.01-0.05 (0.3-2)	1.0 (34)	0.6-1.3 (21-45)
350 (107)	2	0.18 (6)	0.11-0.25 (4-8)	8.1 (278)	6.9-9.3 (237-319)

receipts, 1950-1951). Total production is estimated at about 4000 tons of ore averaging 0.3 oz/ton (10 ppm) Au, 13 oz/ton (446 ppm) Ag, and 0.03% Cu. In July 1991, Great Lakes Exploration Co. began a surface sampling and drilling program at the Alabama to evaluate the economic potential. Additional drilling is recommended by this author. Ore was produced from the Homestake mine in 1936, 1938, 1939, and 1941; however, less than 500 tons of ore averaging 0.23 oz/ton (8 ppm) Au and 5.8 oz/ton (199 ppm) Ag was shipped (NMBMMR files).

The Alabama orebody occurs along the north-trending Alabama fault in a silicified hematite-rhyolite breccia. Fragments of andesite, rhyolite, and vein quartz are cemented by silicified hematite. The breccia zone occurs along the fault with a strike of N10°E and dips 80°W. The zone is about 2-3 m wide at the Alabama shaft and varies along strike between 1.2 and 6.1 m in width. The ore zone averages 1-2 m wide but varies from 1.2 to 1.8 m in width. Some ore shoots were up to 18 m long (H. Schmidt, unpubl. report, 8/18/53). Early reports state that ore averaged 1 oz/ton (34 ppm) Au and 20 oz/ton (186 ppm) Ag (Engineering Mining Journal, 3/16/1895, p. 302).

The host rocks consist of the younger ash-flow tuff overlain by the porphyritic andesite of the Dark Thunder Canyon formation. Rhyolite dikes and plugs have intruded along the Alabama fault (Fig. 2.18; McLemore and Quigley, 1992).

The ore at the Alabama and Homestake mines consists of gold and silver, with trace amounts of galena, sphalerite, and chalcopyrite in a gangue of quartz, hematite, pyrite, sericite, and mixed-layer chlorite/smectite. Visible gold or electrum is locally found (T. Quigley, pers. comm. August 1991). Seams of calcite, 1 mm or less wide, cut the ore and altered rocks and were reported to be associated with zones assaying low gold values (George Utter, unpubl. report, 1938). Averages of gold and silver assays from each level of the Alabama mine suggest an increase in gold and silver with increase in depth (Table 3.9; Fig. 3.8).

A northwest crossfault (strike N70°W, dip 70°N; Fig. 2.18) offsets the Alabama fault

south of the Alabama shaft. Subsurface mine maps indicate that this fault also offsets the orebody (F. W. Smith, unpubl. report, 8/5/10). Additional faults occur in the vicinity (Map 2, Figs. 2.18, 3.8) but the offset in mineralization is unknown.

3.4.2 Jim Crow–Imperial–Gold King mines

The Jim Crow, Imperial, and Gold King mines occur along various north and northwest-trending faults in sec. 14, T17S, R21W. Eight patented claims make up this group (Imperial, Jim Crow, Gold King, Tunnel, Gold Bug, Red Prince, Three Brothers, and Contention) which were patented on July 11, 1899 by the Steeple Rock Development Co. (mineral survey #1012A-H, patent #31323).

Most of the development work was completed prior to patenting in 1899. However, early records of the mining claims were lost during the San Francisco earthquake in 1906, so very little concerning the early history is known. In 1914, George Utter purchased the group of claims. He continued development and production. Two diamond drill holes were drilled prior to 1936. Sludge samples had assays ranging from 0.03 to 0.04 oz/ton (1 ppm) Au and 4.05 to 7.08 oz/ton (139-243 ppm) Ag. By 1941, development consisted of two 61-m shafts (Jim Crow and Imperial), four 30-m shafts, and at least ten additional shafts ranging in depths from 3 to 18 m. Several adits, crosscuts, trenches, and pits also expose the veins. In 1967, McFarland and Hullinger conducted a percussion drilling program near the Imperial shaft, but results are unknown. In 1969, Grant County Mining Co. leased the property and made one ore shipment. In 1977, Oak Creek Contracting, Inc. obtained the property and in 1981 entered a joint venture agreement with Queenstake Resources, Ltd. (Fig. 3.9).

Production prior to 1912 is largely unknown due to loss of most of the early records, but at least 429.9 tons of ore averaging 0.82 oz/ton (28 ppm) Au and 38.3 oz/ton (1310 ppm) Ag were produced (L. Utter, unpubl. report, 6/19/36). Production from 1912 to 1969 was sporadic (1915-1917, 1920, 1932, 1936-1938, 1940, 1969) and amounted to 1341 tons of ore averaging 0.31 oz/ton (11 ppm) Au and 13.9 oz/ton (477 ppm) Ag. Most of this production

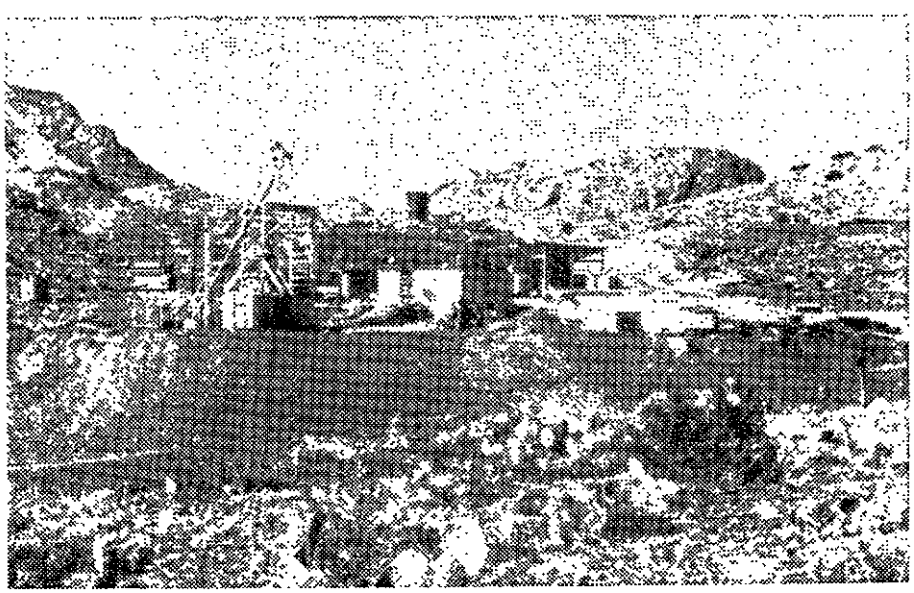

Figure 3.9—View of Imperial mine in 1984.

(1915-1938) was by George Utter. Oak Creek Contracting, Inc. produced 5035.1 tons of ore averaging 0.074 oz/ton (3 ppm) Au and 3.33 oz/ton (114 ppm) Ag from 1980 to 1984 (Queenstake Resources Ltd., unpubl. report, 1987). Total production is estimated as 6806 tons of ore averaging 0.17 oz/ton (6 ppm) Au and 7.6 oz/ton (261 ppm) Ag (Table 3.10). Copper, if present, rarely exceeded 0.4% Cu. Chemical analyses of some ore shipments are listed in Table 3.11. A summary of drill data is in Appendix 11.1.

Ore from this group of claims occurs along several northwest-trending faults (Maps 1, 2). The host rocks consist of younger ash-flow tuff interbedded within the porphyritic andesite of the Dark Thunder Canyon formation (Fig. 2.7). Several minor faults split off of the main fault and many are mineralized. Underground, several post-mineralization faults cut and offset the orebodies (Queenstake Resources Ltd., unpubl. report, April 1982). The ore occurs in silicified hematite breccia, similar to ore at the Alabama and Homestake mines. Veins vary in width from 0.6 m to 12 m and dip steeply to the west or southwest 60-80°. The breccia zone consists of fragments of rhyolite, andesite, and vein quartz all cemented by silica and iron oxides. Locally small breccia fragments of high grade ore (1 m diameter) occur in the veins. Ore minerals include native gold, native silver, galena, sphalerite, chalcopyrite, covellite, and bornite in a gangue of quartz, sericite, pyrite, chlorite, calcite, feldspar, and hematite (personal examination of drill core and Queenstake Resources Ltd., unpubl. report, April 1982). Sulfide minerals, except for pyrite, are extremely small ($<$100 microns). Mottramite ($(Cu,Zn)Pb(VO_4)(OH)$) is a common alteration product associated with the sulfides. It is reported that the upper portions of the Imperial orebody contained more gold than silver (Lindgren et al., 1910) grading at depth to more silver than gold. Base-metal sulfides appear to increase with depth. Hedlund (1990a) reports a chemical analysis of a sample from the Jim Crow mine that contained 100 ppm Mo. Queenstake Resources Ltd. reports reserves of 155,535 tons of ore averaging 0.11 oz/ton (4 ppm) Au and 3.45 oz/ton (118 ppm) Ag from the property (Queenstake Resources Ltd., unpubl. report, 1987).

TABLE 3.10—Summary of production from the Jim Crow-Imperial-Gold King mines (L. Utter, unpub. report, 6/19/36; Phelps Dodge smelter return receipts, 1980-1981; Queenstake Resources Ltd., unpub. report, 1987).

Years of Production	Tons	Au oz/ton (ppm)	Ag oz/ton (ppm)
1897-1912	429.9	0.82 (28)	38.3 (1310)
1912-1969	1341.0	0.31 (11)	13.9 (477)
1980-1984	5035.1	0.074 (3)	3.33 (114)
TOTAL	6806.0	0.17 (6)	7.6 (261)

Table 3.11 - Chemical analyses of ore shipments from the Jim Crow-Imperial mines. Not all ore shipments are listed. From G. Utter (unpubl. report, 6/19/36; Phelps Dodge Smelter return receipts).

DATE	LOT	TONS	Au		Ag		Cu%	Zn%	Pb%	SiO_2%	Al_2O_3%
			oz/ton	(ppm)	oz/ton	(ppm)					
10/04/1897	12.7	1.93	66.17	122.0	4182.9	--	--	--	--	--	--
12/17/1897	16.8	2.45	84.0	195.0	6685.8	--	--	--	--	--	--
05/07/15	986.0	40.2	0.93	31.89	54.6	1872.0	--	--	--	--	--
05/11/15	775.0	25.0	0.92	31.54	56.7	1944.0	0.36	1.2	--	81	4.5
05/17/15	846.0	37.8	0.89	30.51	54.3	1861.7	0.41	1.7	--	79.4	4.9
04/14/15	503.0	26.7	1.02	34.97	63.4	2173.7	0.32	1.0	--	82.5	3.9
05/30/15	981.0	40.9	0.74	25.37	38.4	1316.6	0.35	--	--	--	--
06/14/15	1011.0	32.0	0.7	24	42.8	1467.4	0.38	--	--	--	--
11/19/16	1813.0	3.7	9.0	308.57	550.0	18857.3	2.02	--	--	--	--
11/24/20	3125.0	28.3	0.79	27.09	42.7	1464.0	0.5	--	--	--	--
12/29/20	3309.0	24.6	0.33	11.31	17.8	610.3	--	--	--	--	--
02/02/37	206.0	102.0	1.24	42.51	91.5	3137.2	0.04	--	--	--	--
10/14/81	1907.0	38.7	0.071	2.43	2.52	86.4	0.17	0.08	0.07	84.9	3.6
10/14/81	1904.0	237.1	0.055	1.89	2.04	69.9	0.12	0.08	0.07	82.1	4.7
07/04/81	1384.0	271.4	0.068	2.33	2.54	87.1	0.11	0.12	0.11	84.5	4.0
02/26/80	1261.0	302.6	0.04	1.37	1.65	56.6	0.16	0.0	0	81.5	3.7
11/26/80	1123.0	220.3	0.087	2.98	2.69	92.2	0.08	0.0	0	88.1	3.0
11/18/80	1076.0	92.9	0.088	3.02	2.85	97.7	0.09	0.0	0	88.8	2.1
11/26/80	1100.0	91.4	0.09	3.09	3.17	108.7	0.22	0.0	0	87.3	2.9
06/24/80	837.0	183.3	0.055	1.89	2.26	77.5	0.09	--	--	--	--
06/10/80	796.0	379.9	0.055	1.89	2.87	98.4	0.09	--	--	--	--
05/23/80	727.0	127.7	0.06	2.06	2.84	97.4	0.22	--	--	--	--
05/07/80	636.0	177.0	0.08	2.74	2.93	100.5	0.14	--	--	--	--
04/09/80	444.0	156.2	0.051	1.75	2.79	95.7	0.09	--	--	--	--
TOTAL	--	2664.1	0.31	10.8	20.2	694.0	--	--	--	--	--

3.4.3 Mt. Royal mine

The Mt. Royal mine lies on the Imperial fault in sec. 23, T17S, R21W at an approximate elevation of 1463 m. The eight claims which make up this group are the Golden Fleece Nos. 1, 2, and 3, Ruby Quartz, Imperial Extension, South Jim Crow, Prince Imperial, and Prince Imperial Extension, which were patented on October 10, 1922 (mineral survey #1712, patent #881743). The mine consists of a 99-m shaft with levels at 30, 61, and 99 m. The shaft is inclined with a dip of 85°W (Fig. 3.10).

The Mt. Royal mine was first developed in the early 1900s, but early production, if any, is unknown. The first known reported production was in 1939-1941 by E. T. Richards. George Utter acquired the mine in 1941 and also shipped ore. In 1970-71 and 1981, Charles and Douglas Hanson produced additional ore. Total known production amounts to 2452 tons of ore averaging 0.12 oz/ton (4 ppm) Au and 3 oz/ton (103 ppm) Ag. Chemical analyses of some partial ore shipments are in Table 3.12.

The Mt. Royal deposit is an extension of the Jim Crow-Imperial deposit and is fault controlled. Early reports describe narrow streaks of gold within a hematite breccia that were mined out. Two subparallel veins occur at the mine (Fig. 3.10), the Mt. Royal and Jim Crow-Imperial veins. A zone of chloritic-altered porphyritic andesite separates the two veins (H. W. Evans, unpubl. report, 1/20/17). No samples were collected for this report.

3.4.4 Laura mine

The Laura mine is located in Laura Canyon, east of Vanderbilt Peak (Laura Mountain on some maps) in sec. 2, T17S, R21W. The main shaft is at an approximation elevation of 1707 m. In the late 1880s, a Chinese cook discovered the Laura deposit and sank a 20-m shaft. Two claims, the Laura and Clara, were subsequently patented on May 14, 1901 by Jesse Wasserman (mineral survey #1067). The two patented claims comprise 35.92 acres.

The main shaft is 196 m deep (Richter and Lawrence, 1983) and dips 80-85°W. Two additional shafts access the lower workings which consists of six levels and several sublevels.

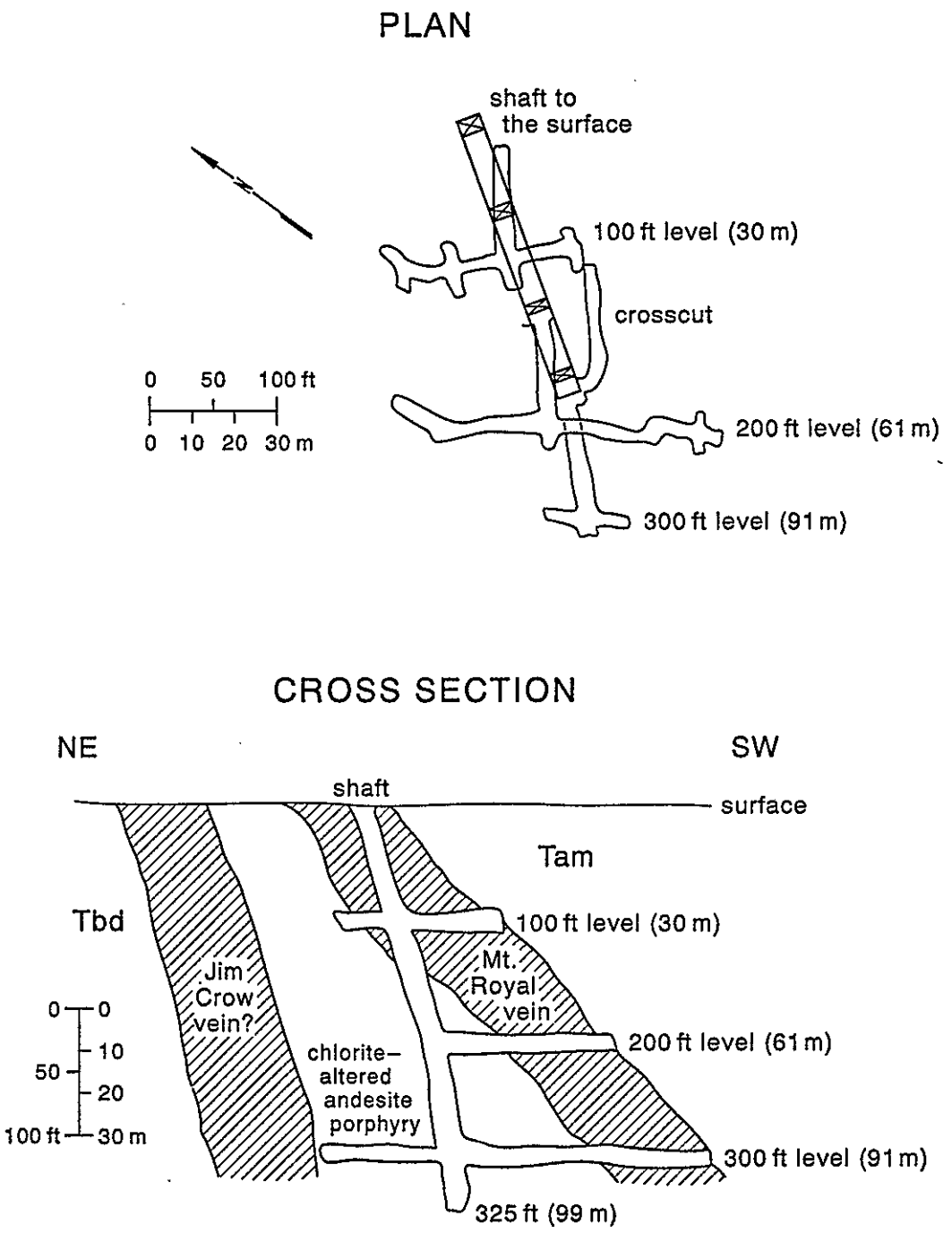

Figure 3.10 Cross section and plan of Mt. Royal mine (H.W. Evans, written communication, January, 20, 1917).
Tbd—andesite porphyry of Dark Thunder Canyon

Table 3.12—Chemical analyses of some ore shipments from the Mt. Royal mine. Not all shipments are listed. From ASARCO, El Paso smelter return receipts.

Date	Lot No.	Tons	Au oz/ton	(ppm)	Ag oz/ton	(ppm)	Cu %	SiO_2 %
04/14/39	918	59.5	0.248	9	4.88	167	0.05	57.4
12/16/40	4057	59.2	0.23	8	4.9	168	0.02	88
01/24/41	166	61.8	0.255	9	4.2	144	0.03	88.2
01/31/41	3266	56.8	0.207	7	3.72	128	--	88.9
01/21/41	3612	65.4	0.155	5	3.27	112	--	--
05/30/51	3640	65.9	0.205	7	3.35	115	--	87
06/05/41	3663	65.5	0.155	5	3.15	108	--	85
06/10/41	3682	66.7	0.133	5	2.97	102	--	--
06/14/41	3711	67.6	0.31	11	7.45	255	--	89.1
06/19/41	3682	66.7	0.15	5	3.15	108	--	--
06/19/41	3718	64.1	0.11	4	2.59	89	--	85.9
06/26/41	3752	57.6	0.155	5	3.88	133	--	88.4
07/02/41	3761	61.5	0.15	5	3.92	134	--	89.1
08/12/41	3868	65.3	0.175	6	3.27	112	--	--
08/13/41	3880	66.0	0.165	6	3.24	111	--	--
08/22/41	3897	59.6	0.125	4	3.33	114	--	--
08/22/41	3905	57.0	0.23	8	6.21	213	--	--
08/26/41	3922	60.4	0.125	4	2.8	96	--	87
03/26/70	644	120.9	0.16	5	3.4	117	0.1	84.9
07/02/71	2366	158.7	0.3	10	11.9	408	0.1	--
TOTAL	--	1406.2	0.2	7	4.8	165	--	--

The five upper levels are at depths of 15, 41, 59, 87, and 113 m. The second and third levels are the most extensive and are about 122-152 m long (Fig. 3.11). Several pits and open-cuts expose the vein at the surface.

The Laura mine was first worked in the late 1860s when approximately 1800 tons of ore averaging 1.2 oz/ton (58 ppm) Au and 15 oz/ton (514 ppm) Ag were produced (C. M. Autremict, unpubl. report, 3/10/39). The Twin Peaks Mining and Milling Co. produced approximately 3600 tons of ore grading 1.07 oz/ton (37 ppm) Au and 14.21 oz/ton (487 ppm) Ag from the first and second levels from 1907 to 1909. The Laura mine closed in 1909 but was reopened in 1937 by W. O. Wills, Jr. After sinking the shaft to 70 m, Wills produced 2,229 tons of ore with a grade of 0.4 oz/ton (14 ppm) Au and 13 oz/ton (446 ppm) Ag in 1938. The Wilmont Mining Co. acquired the mine and developed the shaft to at least 152 m. From 1939 to 1942, Wilmont Mining Co. produced 5000-6000 tons of ore averaging less than 0.2 oz/ton (7 ppm) Au and 12 oz/ton (411 ppm) Ag. Some copper and lead were also produced. The mine closed again in 1942. In July 1977, Charles and Douglas Hanson acquired the lease to the Laura mine. In 1982, the Hansons produced about 1000 tons of ore averaging 0.06-0.09 oz/ton (2-3 ppm) Au and 3-6 oz/ton (103-206 ppm) Ag (Douglas Hanson, pers. comm. December 1991). Some copper (0.03-0.05%) and lead (0.06%) were also produced. Production is summarized in Table 3.13.

The Laura mine occurs near the junction of several converging northwest-trending faults that make up the Laura fault, and the west-northwest-trending Carlisle fault (Map 1, 2). A rhyolite dike, 6-15 m wide, has been intruded within the Laura fault zone south of the shaft. The Laura fault zone separates andesite porphyry of the Summit Mountain formation to the northeast from basaltic andesite of the Dark Thunder formation (Map 1). Brecciated andesite, basaltic andesite, and rhyolite fragments comprise the fault zone and are cemented by at least two generations of quartz.

The vein is about 3 m wide near the shaft and dips 62°SW. Unpublished reports describe the presence of two veins in the inaccessible workings. The "pay ore shoot" is west

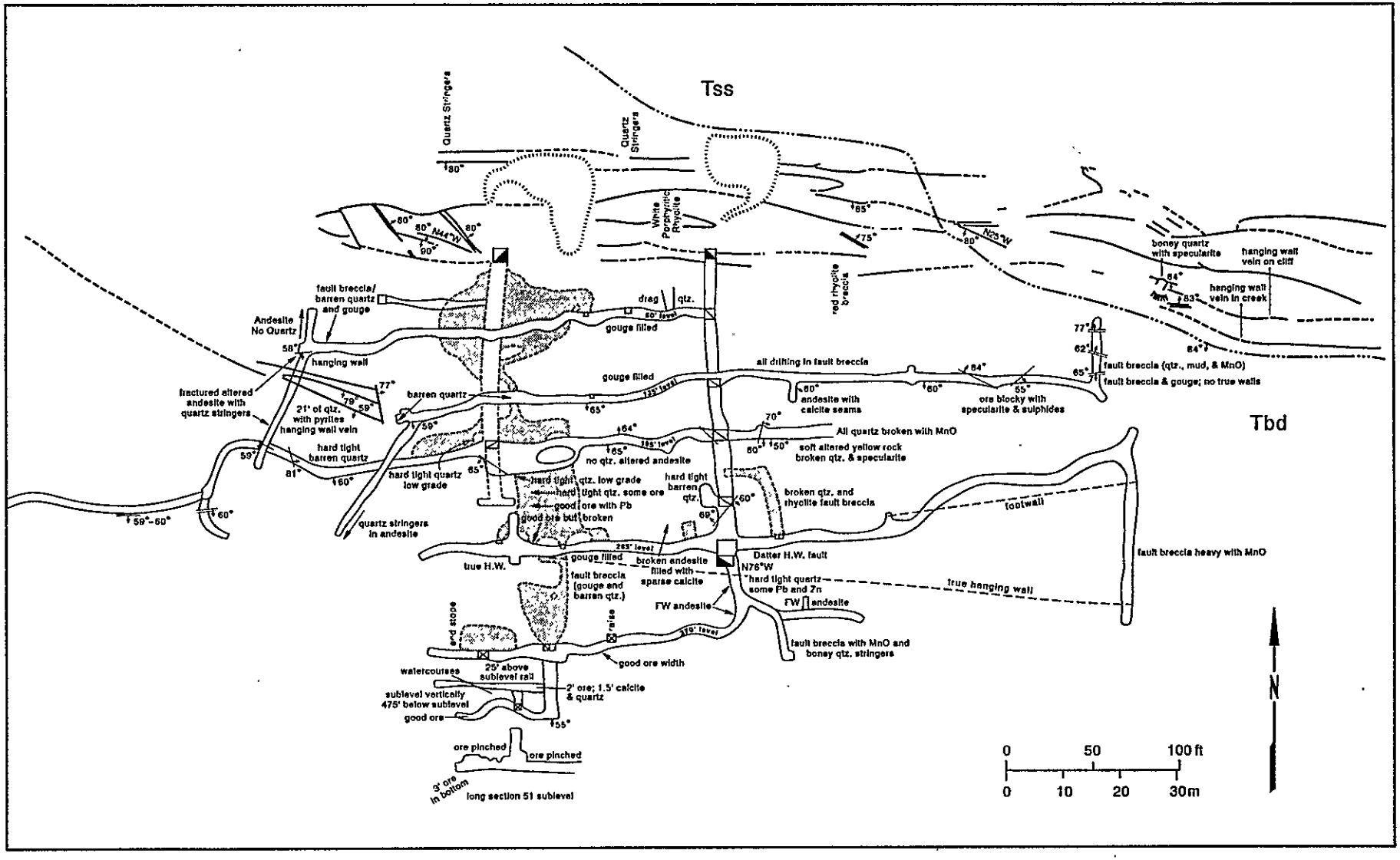

Figure 3.11 Plan of Laura mine (T.F.S., unpubl. report, July 20, 1940)
Tss—Summit Mountain formation, Tbd—Dark Thunder Canyon formation

TABLE 3.13—Summary of production from the Laura mine (from unpubl. report, NMBMMR files and smelter return receipts).

Year	Ore (tons)	Au oz/ton	(ppm)	Ag oz/ton	(ppm)
1860	1800	1.7	(58)	15	(514)
1907-1909	1800	1.07	(37)	14.21	(487)
1938	2229	0.4	(14)	13	(446)
1939-1940	5000	0.2	(7)	12	(411)
1982	1000	0.06-0.09	(2-3)	3-6	(103-206)
TOTAL	11,829	0.58	(20)	12.2	(419)

TABLE 3.14—Summary of assay data from each level in the Laura mine (unpublished assay map, Phelps Dodge Corp., Doug Hanson files, August 1982).

Level	Au		Ag		No. of Samples
	Average oz/ton (ppm)	Range oz/ton (ppm)	Average oz/ton (ppm)	Range oz/ton (ppm)	
1	0.1 (3)	0.01-0.6 (0.3-21)	2.79 (96)	0.74-6.4 (24-219)	
2	0.06 (2)	0.01-0.23 (0.3-8)	1.05 (36)	0.008-3.2 (0.3-110)	9
3	0.06 (2)	0.005-0.27 (0.2-9)	1.97 (66)	0.04-6.2 (1-212)	7
4	0.01 (0.3)	<0.005-0.07 (<0.2-2)	0.41 (14)	<0.1-0.71 (<3-24)	10

TABLE 3.15—Chemical analyses of ore shipments from the Laura mine (ASARCO, El Paso smelter return receipts). Not all shipments are listed.

Date	Lot No.	Ore	Au oz/t (ppm)	Ag oz/t (ppm)	Cu%	SiO_2%	Fe%	CaO%	Al_2O_3%	F%
07/12/82	630	100.4	0.07 (2)	4.1 (140)	0.03	74.9	3.6	4.2	4.9	0.34
10/07/82	1299	80.4	0.06 (2)	3.1 (106)	0.03	78.7	3.4	--	7.1	0.17

of the shaft and has been mined to at least the fifth level. This shoot is 0.3-6 m wide and intersects the larger vein (6-8 m wide) at slightly below the sixth level east of the shaft. Both veins consist of gold and silver with some fine-grained galena and chalcopyrite with a gangue of quartz and pyrite. Early reports state that the ore consisted of argentite, cerargyrite, pyrargyrite, and gold (Engineering Mining Journal, 10/26/1907, p. 805).

Sampling of surface outcrops for this report indicated sporadic assays; however, one sample assayed 0.12 oz/ton (4 ppm) Au and 11.2 oz/ton (384 ppm) Ag (#246; Map 2; Appendix 11.6). The sample consisted predominantly of quartz with minor amounts of feldspar, anatase, and illite. Sampling of underground exposures in 1982 by Phelps Dodge Corp. yielded assay results similar to production values from the various levels (Table 3.14). These assay data suggest that silver and gold assays decrease with depth, but this observation should be tested further by drilling. Chemical analyses of ore shipments are in Table 3.15.

3.4.5 Blue Goose and Goldenrod mines

The Blue Goose and Goldenrod mines lie along the northwest-trending Blue Goose fault in sec. 7, T17S, R20W. No production has been reported from either mine. The Blue Goose mine consists of a caved shaft surrounded by a mine waste dump and is probably less than 30 m deep. The Goldenrod mine consists of a 44-m adit, trending S56°E. Numerous prospect pits and shallow shafts expose the vein along strike between the Blue Goose mine (south of the Center shaft) and the Goldenrod mine (south of the Blue Goose mine; Maps 1, 2). The host rocks are sandstone and andesite porphyry of the Summit Mountain formation and the mineralization is fault controlled.

At the Blue Goose mine, dump samples contain quartz, clay minerals, and pyrite. A sample southeast of the mine consisted of quartz, chlorite, and pyrite and assays did not contain any gold, but did assay 0.54 oz/ton (19 ppm) Ag, 734 ppm Cu, 54 ppm Pb, and 482 ppm Zn (#148, Appendix 11.6). The vein is well exposed in the pit and strikes N52°W with a dip of 74°SW, but is less than a meter wide.

A 3-m chip sample collected across the back at the portal of the Goldenrod adit revealed no gold or silver and low values of copper, lead, and zinc (#60, Appendix 11.6). However, a 0.6-m chip sample across the face at the end of the adit, while it showed no gold, it did assay 0.22 oz/ton (8 ppm) Ag, 1200 ppm Cu, 5600 ppm Pb, and 5300 ppm Zn (#GOLDENROD, Appendix 11.6). The sample consisted of quartz, feldspar, chlorite, pyrite, titanite (sphene), and hedenbergite (Appendix 11.3). The vein exposed at the face is a silicified breccia cut by white quartz veins. The host rock (andesite porphyry) has been silicified and altered to chlorite.

Three additional samples were collected south of the Goldenrod adit and assayed. Only one sample contained detectable gold: 0.001 oz/ton (0.03 ppm) Au (#922; Appendix 11.6). Assays of samples ranged from 1.94 to 3.18 oz/ton (67-109 ppm) Ag, 2800 to 14,900 ppm Cu, 894 to 45,000 ppm Pb, and 235 to 1600 ppm Zn (#911, 923, 927; Appendix 11.6). The samples consisted of quartz, feldspar, kaolinite, and chlorite; one sample (#922) also consisted of trace amounts of cerusite, anhydrite, and brookite (Appendix 11.3).

3.4.6 East Camp group of mines

For the purpose of this study, the East Camp group of mines includes mines and prospects along the southeastern portion of the East Camp-Summit fault in sections 3, 6, 7, 8, 9, and 16, T17S, R20W. It includes eight patented claims (Table 3.1), numerous unpatented claims, and state land. Larger mines include Nugget, East Camp, McDonald (Fig. 3.12), Davenport, and Thanksgiving.

Development along the East Camp vein began in the late 1800s. Greatest production occurred from 1933 to 1942 when the East Camp mines were the largest producers. Development along the East Camp vein is the most extensive in the district (Fig. 3.13), but the entrances to most of the underground workings are caved and hazardous. The vein is mineralized for over 1372 m along strike from the Nugget southeastward to the Thanksgiving (Map 2). Numerous adits, stopes, drifts, and shafts (up to 193.5 m deep) are developed along

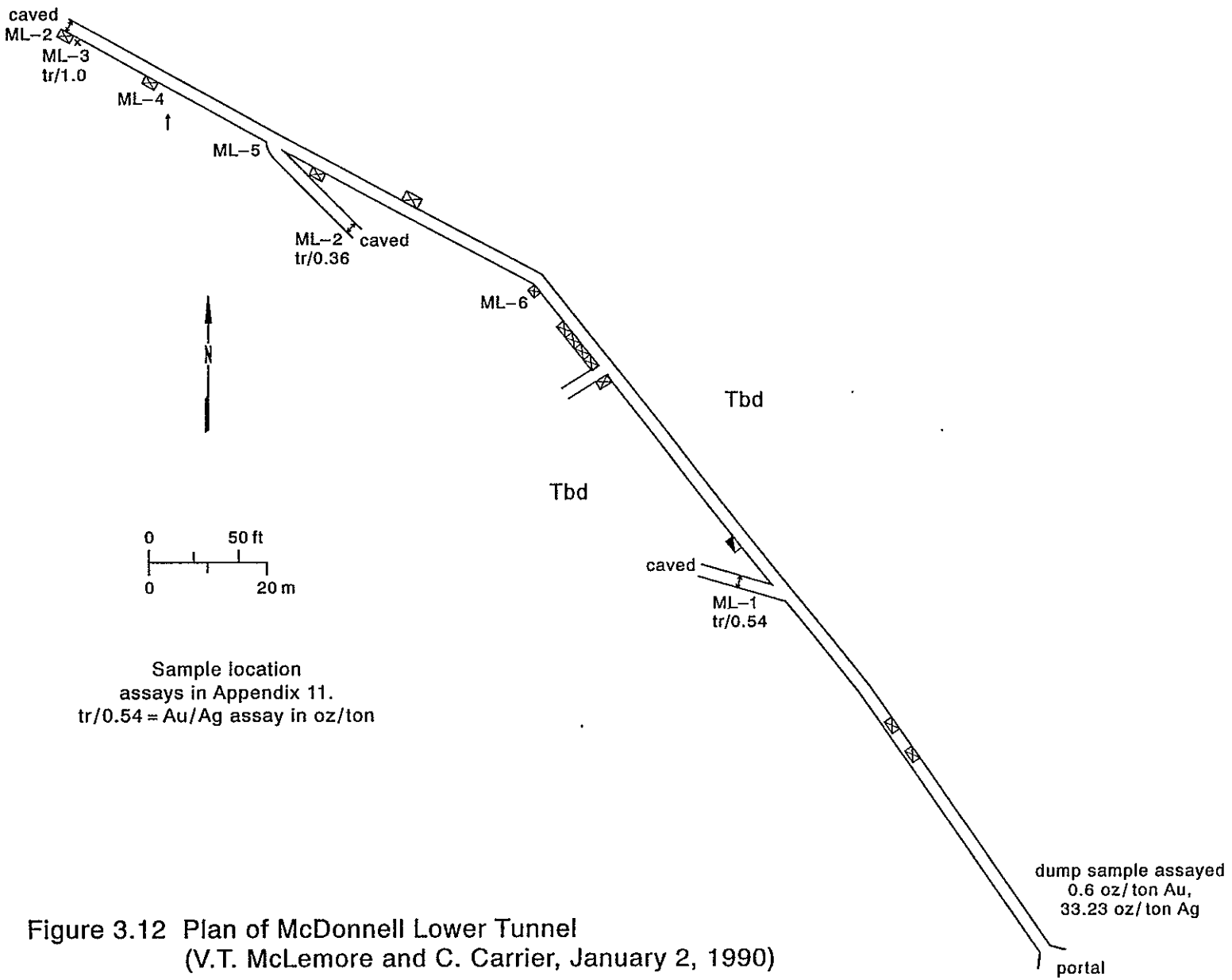

Figure 3.12 Plan of McDonnell Lower Tunnel
(V.T. McLemore and C. Carrier, January 2, 1990)

Table 3.16—Known production from the East Camp and Summit groups of mines (from various unpublished reports). These production statistics probably represent minimum production totals.

Mine	Years of production	Tons of ore	Au oz/ton	Ag oz/ton
		(ppm)	(ppm)	
East Camp	prior to 1987	88,115.5	0.293 (10.0)	21.89 (750)
Group	1936-1939	16,129	0.383 (13.1)	26.57 (911)
	1987	1500	0.05 (1.7)	1.16 (40)
Total East Camp	prior to 1988	105,744.5	0.303 (10.4)	22.3 (765)
Thanksgiving	1934-1940	68	0.29 (9.9)	11.90 (408)
Summit	prior to 1987	73,550	0.13 (4)	5.54 (190)
	1987	500	0.108 (4)	6.076 (208)
Total Summit	prior to 1988	74,050	0.13 (4)	5.54 (190)
National Bank	1936-1937	100	0.24 (8)	17.85 (612)

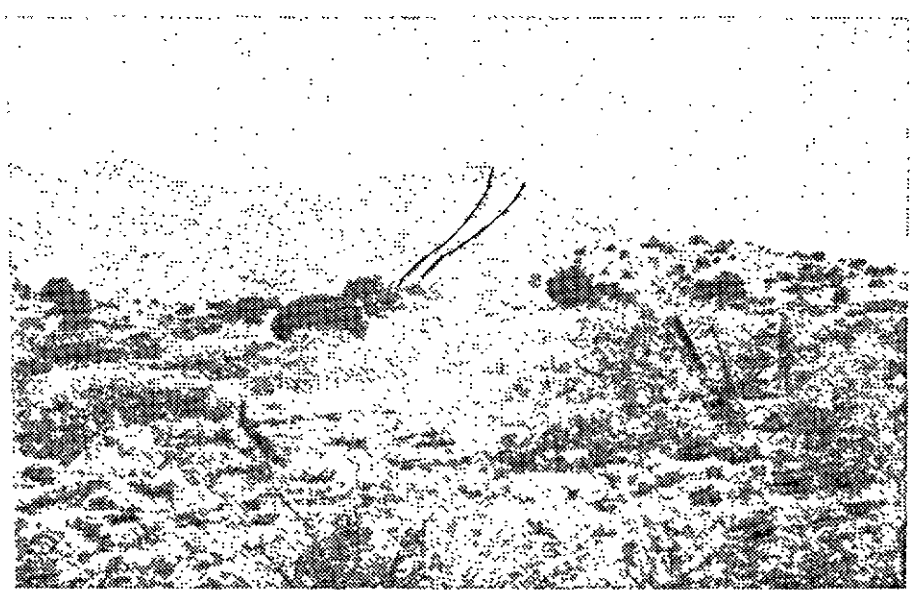

Figure 3.13—View of East Camp-Summit fault, looking northwest at the Summit Mountains.

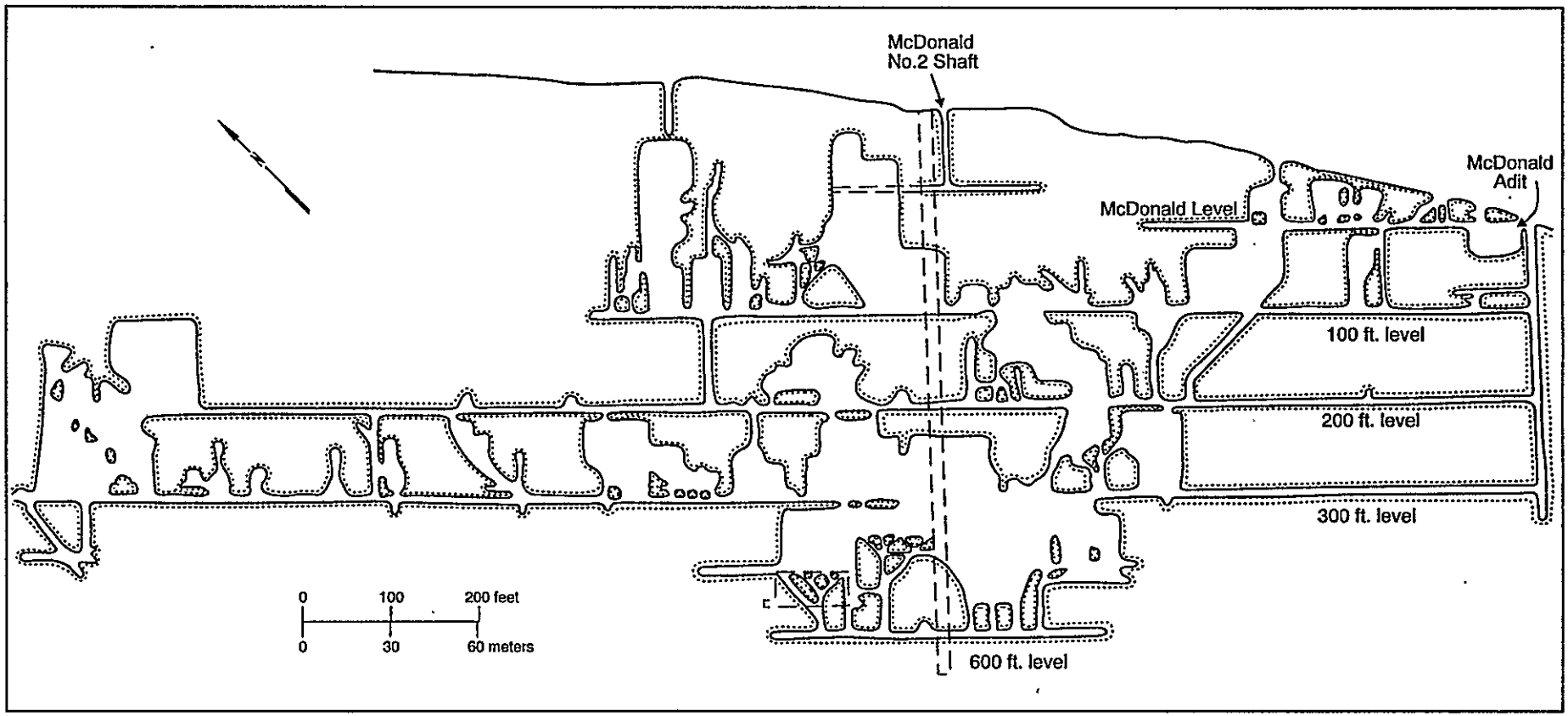

Figure 3.14 Longitudinal section through McDonald Mine, East Camp vein, Steeple Rock District (Gillerman, 1964).

the vein (Fig. 3.14). Known production amounts to 105,744.5 tons of ore averaging 0.303 oz/ton (10.4 ppm) Au and 22.3 oz/ton (765 ppm) Ag.

Little is known concerning the history and production of the various mines. Some records were lost in the San Francisco earthquake. Numerous companies have examined the property and a few companies drilled, but these data are unavailable.

The East Camp vein occurs along the East Camp fault which strikes N70°W and dips steeply to the northeast and locally to the southwest (Maps 1, 2). Host rocks are andesite and sedimentary rocks of the Dark Thunder Canyon and Summit Mountain formations. The vein varies in width but averages 2 m. Some ore shoots are 4.6-6.1 m wide. The veins are sinuous, pinch and swell along strike, and have complex textures, including comb, cockade, crustification, and drusy quartz. At least three periods of brecciation and recementation have occurred. Precious-metal values are low at the surface (Appendix 11.5, Map 2), but increase with depth. Some ore shoots may continue below the deepest level of workings. Small faults intersect the East Camp fault and appear to localize ore. Alteration includes argillic, propylitic, and silicification. Chemical analyses of some ore shipments from the East Camp mine are in Table 3.17.

3.4.7 Summit group of mines

For the purpose of this study, the Summit group of mines includes the mines and prospects along the Summit vein in sections 25 and 26, T16S, R21W, from the Angello windmill (north of Telephone Ridge) northwestward to, and including, the National Bank (Bank, Smith) mine (Maps 1, 2). This group consists of ten patented claims (Table 3.1) and numerous unpatented claims. Biron Bay Resources, Ltd. currently controls the property.

Little is known about the early history of the Summit mines. The patented claims were

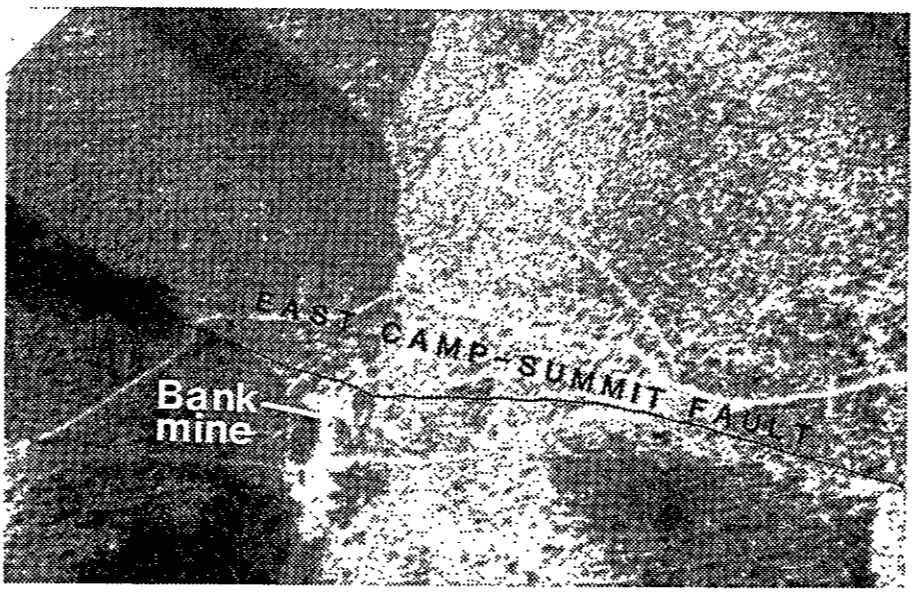

Figure 3.15—View, looking west, of Summit mines and drill roads (from the air).

Table 3.17—Chemical analyses of some ore shipments from the East Camp mine (D. Hanson, unpubl. report, 1992). MAX - maximum value, MIN - minimum value, AVG - mean value, STDS - standard deviation, VARS - variance.

DATE	Au oz/ton	Ag oz/ton	Pb%	Cu%	SiO_2%	Fe%	Al_2O_3%	F
10/7/82	0.06	2.7	0	0.02	83.1	2.2	5.2	0.03
9/21/82	0.08	4.3	0	0.02	86.6	2.3	5.2	0.04
9/21/82	0.035	2.9	0	0.03	78.1	2.6	8.1	0.04
9/21/82	0.05	2.9	0	0.03	79.5	2.5	7.7	0.06
10/7/82	0.02	2.8	0	0.02	79.8	2.6	5.8	0.04
10/21/82	0.05	2.2	0	0.01	78.2	3.3	6.3	0.11
10/21/82	0.03	1.5	0	0.01	76.1	3.4	8.2	0.09
10/21/82	0.04	1.8	0	0.01	79.3	3.1	7.4	0.08
10/7/82	0.07	2.9	0	0.01	82.3	2.4	5.7	0.04
MAX	0.08	4.3	0	0.03	86.6	3.4	8.2	0.11
MIN	0.02	1.5	0	0.01	76.1	2.2	5.2	0.03
AVG	0.05	2.67	0	0.02	80.33	2.71	6.62	0.06
STDS	0.02	0.8	0	0.01	3.17	0.44	1.23	0.03
VARS	0	0.65	0	0	10.04	0.2	1.51	0

most likely filed near the turn of the century. By 1920, the Summit adit was 148.4 m long and the Apex was 62.5 m long. Several shafts (up to 80 m deep) and prospect pits also developed the vein prior to 1920 (George H. Utter, unpubl. report, May 6, 1920). There was some production in 1895, but total figures are not known. At least $25,000 worth of gold and silver was produced from these mines from 1895-1920 (George H. Utter, unpubl. report, May 6, 1920).

The National Bank (Bank) mine operated in 1895 when the two Smith brothers sank the shaft to 61 m. A mill was built before 1900, but the mine and mill closed in 1900 and production is unknown. The Bank reopened in 1936-1937 when 100 tons of ore averaging 0.24 oz/ton (8 ppm) Au and 17.85 oz/ton (612 ppm) Ag were produced (Table 3.16). The Bank is now 60.8 m deep with levels of 22.9 m, 30.5 m, 45.7 m, and 61 m.

By 1964, the Apex adit was 91 m long and the Summit adit was 152 m long (Gillerman, 1964). In 1977, Summit Minerals, Inc. (Charles and Douglas Hanson) was formed and controlled the Summit group of mines. Several companies have examined the property over the years. The adits now connect (Fig. 3.16).

In 1982-1984, Inspiration Mines Inc. examined and drilled along the Summit vein (Fig. 3.16). Fifteen holes were drilled (Appendix 11.1). Reserves were calculated as 1,100,000 tons in three separate ore shoots above the 1615-m level (91.4 m below the Summit adit level) with combined grades of 0.062 oz/ton (2.1 ppm) Au and 4.57 oz/ton (157 ppm) Ag. Part of one orebody contained 207,400 tons of ore grading 0.076 oz/ton (2.6 ppm) Au and 7.76 oz/ton (266 ppm) Ag. Inspiration Minerals Inc. defined five additional ore shoots 121.9 m below the Summit adit level that contained 121,500 tons grading 0.079 oz/ton Ag. It is unknown how much, if any, of these reserves have been subsequently mined. These reserves occur over a strike length of over 480 m and averages 2 m thick with lower grades of ore surrounding the higher grade deposits. Two or more veins are locally present (Watts, Griffits, and McQuat, Inc., unpubl. report, February 12, 1988).

In 1988, Nova Gold Resources Inc. began exploration of the Summit mine area. Biron

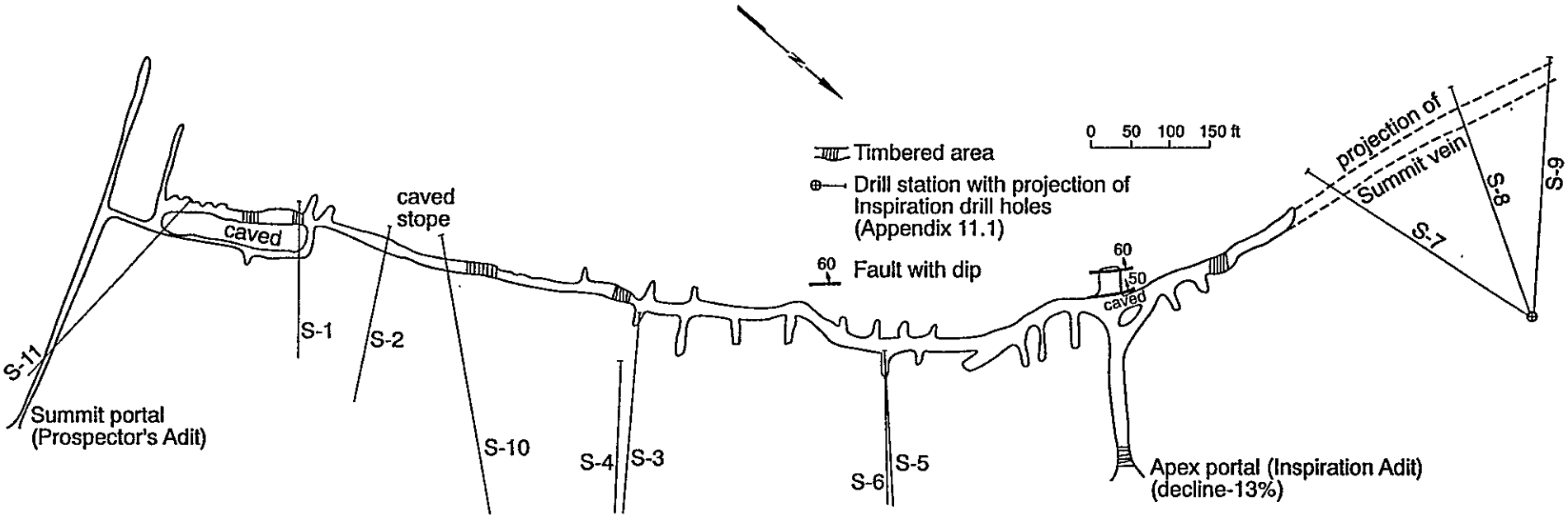

Figure 3.16. Map of Summit and Apex Mines, Summit vein. Modified from unpublished maps by V.T. McLemore and J.M. McLemore.

Bay Resources, Ltd. became a partner in 1989 and up to 120 drill holes have been drilled since 1988 (Appendix 11.1). Reserves are estimated as 1,450,000 tons of ore averaging 0.179 oz/ton (6.1 ppm) Au and 10.26 oz/ton (352 ppm) Ag (Petroleum and Mining Review, v. 14, 1992, p. 2). Total production from these mines is unknown, although known production is 74,050 tons of ore averaging 0.13 oz/ton (4 ppm) Au and 5.54 oz/ton (190 ppm) Ag (Table 3.16).

The Summit vein lies along the East Camp-Summit fault which strikes N40°W and dips 70-85° northeast. Host rocks are andesite and dacites of the Summit Mountain formation. Sericite and chlorite occur along the Summit vein with erratic but strong silicification. Acid-sulfate alteration occurs east of the Summit mine and at the Bank mine. The vein ranges in width from 6.0 to 30.5 m. Prominent quartz and quartz-calcite veins crop out (Fig. 2.15). Calcite is more abundant near the top and decreases with depth, but is still present at depth in drill cores (Appendix 11.1). Trace base-metal sulfides occur at depth. The vein consists predominantly of quartz which is generally brecciated and recemented. Comb, cockade, lattice, and drusy quartz are common. Large blocks of sericitized and silicified country rock are common in the vein. Manganese and iron oxides are locally abundant. Other gangue minerals include illite/sericite, chlorite, adularia, pyrite, kaolinite, and smectite (Appendix 11.3). Gold occurs as native gold, electrum, and is also associated with pyrite. Silver occurs as electrum, argentojarosite, tetrahedrite and similar sulfosalts, and is associated with iron and manganese oxides, and native silver (W. Baum, unpubl. report, March 31, 1988). Acanthite is probably also present. High gold and silver assays are locally associated with motramite or mimettite.

In 1921, sampling of the Summit and Apex mines occurred. Assays of 28 samples from the Summit adit averaged 0.0755 oz/ton (2.6 ppm) Au and 4.03 oz/ton (138 ppm) Ag. An average of 24 samples from the Apex adit was 0.0525 oz/ton (1.8 ppm) Au and 3.33 oz/ton (114 ppm) Ag (J. Daniell, unpubl. report, February 18, 1934). The higher values are in the center of the vein. Assays at the surface taken for this study are typically low (Map 2,

Appendix 11.5). However, one sample from the Bank mine contained 0.04 oz/ton Au, 0.44 oz/ton Ag, 1.51 ppm Hg, and 160 ppm Mo (#BA, Appendix 11.5). Ore shipments in the 1980s were rejected by the smelters because they contained too much calcium carbonate.

3.4.8 Norman King, Billali, and Hoover mines

The Norman King, Billali, and Hoover mines occur along the Norman King-Billali fault in sec. 26 T16S R21 W. The area consists of numerous pits, adits, and shafts (Map 2). The deepest is the Norman King mine, 152 m deep. A plan of the Hoover and Billali adits is in Figure 3.17. Total production from these mines since 1919 amounts to 4,120 tons grading 0.19 oz/ton (6.5 ppm) Au and 12 oz/ton (411 ppm) Ag (Table 3.18). Production, if any, prior to 1919 is unknown. Gillerman (1964) reports much higher production figures because he reported the figures in tons when actually his figures should be in pounds of ore produced (confirmed by this author from two separate unpublished sources). Another common mistake in the literature is the mislocation of the Billali mine. The Billali mine is south of the Norman King, even though some maps place it to the north where the Mohawk mine is. Also, different spellings of Billali occur; the most common in unpublished sources is used here.

The Norman King mine was originally located as the Norman mine in 1883 by B. V. Steed and F. L. Heft. A patent plat was prepared in 1885 (mineral survey #515), but the patent application was never completed. Not much development occurred until the late 1800s when Herbert Hoover worked in the area as a mining engineer. The Hoover Tunnel (also known as the Knutson adit) is named for him. The Norman claim was relocated as the Norman King mine in 1900 by O. V. Ward. The Billali claim was also staked in the 1880s.

The Norman King-Billali fault strikes northwest, dips 70°NE, and consists of a series of quartz veins that bifurcate and pinch and swell along strike. The entire zone is several tens of meters thick and consists of silicified country rock, quartz, some calcite, rare fluorite, pyrite, and traces of thin streaks of microscopic sulfides (galena, sphalerite, chalcopyrite). Bladed calcite (lattice texture) is present locally but in concentrations much less than found at

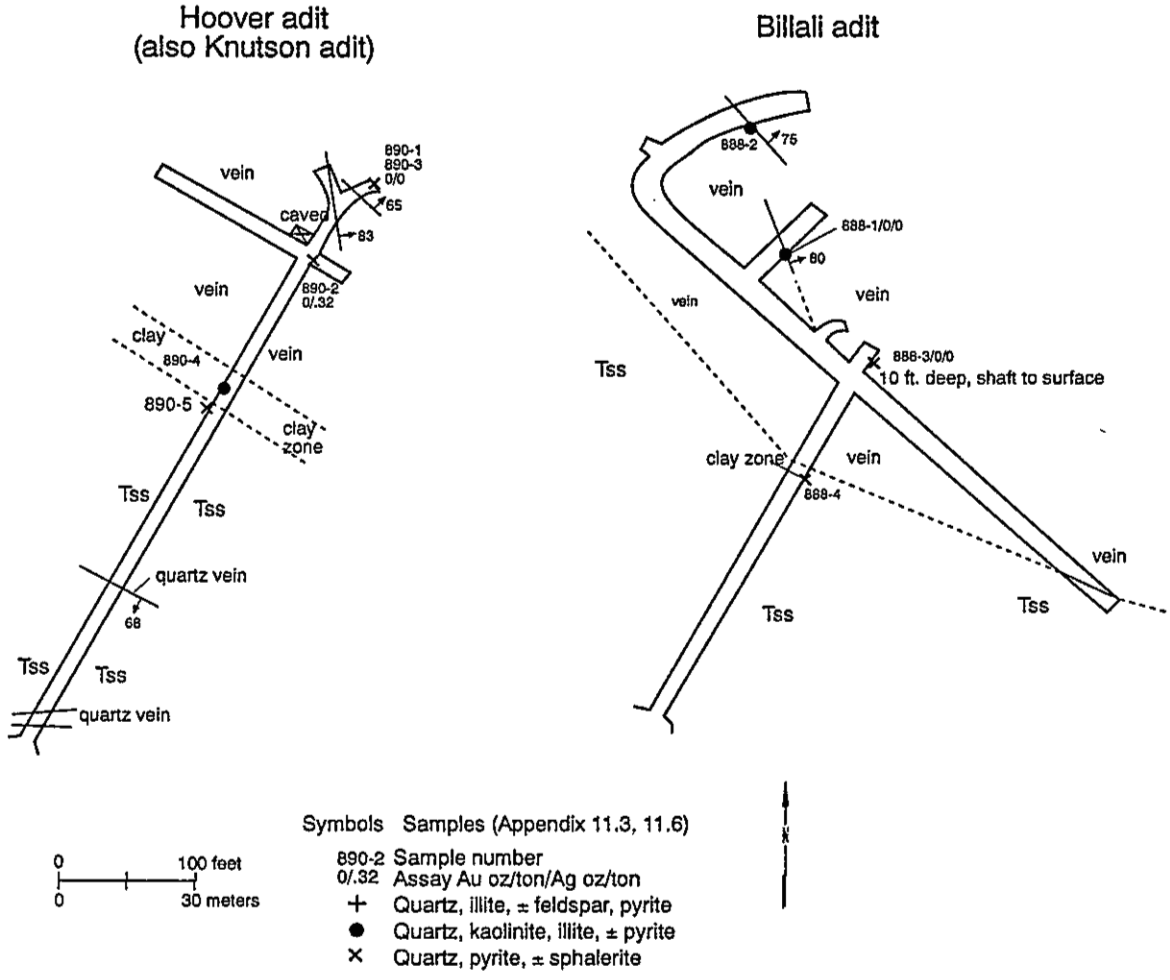

Figure 3.17 Plan maps of Hoover and Billali adits (V.T. McLemore and J.M. McLemore, brunton, pace and surveys, 6/8/92).

Table 3.18—Production from the Norman King and Billali mines (from unpublished reports).

Date	Tons	Au oz/ton	Ag oz/ton	Cu%	Pb%	Si%	Value
Norman King mine							
1919	120.4	1.08	74.4	--	--	--	--
1920	189.3	0.4	27.8	--	--	--	--
1921	33.3	0.26	18.1	--	0.005	--	--
1923	35.7	0.65	47.2	--	0.004	--	--
1930	50	0.02	17.8	0.001	--	--	--
1932	18	0.5	32.3	--	0.004	--	--
1933	5	0.4	18.6	0.003	--	--	--
1935	240	0.18	9.3	0.06	--	--	--
1936	1319.7	0.18	11	0.1	--	76.7	--
1937	724.5	0.15	9	0.1	--	83.4	--
1938	41.1	0.2	10.7	0.15	--	83.3	--
1939	143.4	0.15	10.9	0.06	--	80.2	--
1940	737.6	0.18	9.9	0.1	--	79.7	--
1941	46	8.4	0.001	--	--	--	--
1942	6	0.2	3.5	--	--	--	--
TOTAL	3710	0.19	11.7	0.06	0.004	80	$80,000
Billali mine							
1935	136	0.18	11.3	0.001	--	--	--
1936	211	0.22	15.1	0.002	--	--	--
1940	63	0.11	4.8	--	--	--	--
TOTAL	410	0.19	12.2	0.002	--	--	$20,000

the Summit mine. Fluorite veins are prevalent at the Mohawk but fluorite concentrations decrease southeastward, and only trace amounts of fluorite are found at the Billali mine. Fluorite is absent in drill core of holes beneath these zones. Two deep drill holes (M91-3, M91-4; Appendix 11.1) consist of deep intervals below the veins of silicified porphyritic andesite containing disseminated galena, sphalerite, chalcopyrite, and pyrite. The sulfides have replaced feldspar phenocrysts. Host rocks are andesites of the Summit Mountain formation. Alteration includes sericitic, chloritic, and silicification.

Very few data are available on the chemistry of the Norman King-Billali fault. Gold and silver assays are sporadic, production grades range from 0 to 8.4 oz/ton (0-288 ppm) Au and 3 to 433 oz/ton (103-14,846 ppm) Ag. The higher grade shipments were most likely hand-sorted ore. Copper content rarely exceeds 0.3% and lead content is also low (less than 0.005%). Silica is typically high (76-87% SiO_2). Hedlund (1990b) reports a semiquantitative spectrographic analyses of a sample from the Norman King that contained 100 ppm Ag, 100 ppm Ba, 150 ppm Cd, 5,000 ppm Cu, 20,000 ppm Pb, and 50,000 ppm Zn. Samples collected for this report (888, 889, and 890, Appendix 11.6) are low: no gold, 0-0.57 oz/ton (0-20 ppm) Ag, and up to 373 ppm Pb. Drilling by Biron Bay Resources, Ltd. has detected mineralized zones, and an ore shoot has been discovered with inferred reserves of 219,000 tons averaging 0.244 oz/ton (8.4 ppm) Au and 12.8 oz/ton (439 ppm) Ag (Petroleum and Mining Review, v. 14, 1992, p. 2). A second mineralized zone was also discovered, but reserves have not been announced.

3.4.9 Twin Peaks mines

The Twin Peaks mines lie north of the map area, north of Twin Peaks in sec. 8, T16S, R21W (Fig. 2.7). The deposit was discovered in the late 1880s. Development consists of five caved and inaccessible shafts: Discovery (87 m deep), Free Gold (282 m deep), Ethel (46 m deep with levels at 17 and 30 m), New Strike and Rival (probably less than 15 m or so). In 1973, Minerals Economic Corp. and Fraser-Martin Mines, Inc. core drilled about 610

m, however the results are unknown.

Production statistics are ambiguous. Briggs (1982) reports total production from the Mayflower-Commerce, Copper Basin, Twin Peaks, and possibly Fraser mines as 1000 tons of ore yielding 1,115 oz Au, 3,640 Ag, and 1,965 lbs Cu. However, Keith et al. (1983) reports total production from a Twin Peaks district in Arizona (which may include part of New Mexico) as 2000 tons of ore yielding 500 oz Au, 10,500 oz Ag, 15,000 lbs Cu, and 17,000 lbs Pb. Very few, if any, mines in the Arizona portion of the Steeple Rock district could yield such production as reported by Keith et al. (1983). Most likely, much of the production reported by Keith et al. (1983) includes production from Twin Peaks and possibly the Fraser mines, but the actual breakdown of production is unknown.

The Twin Peaks mines occur along a north- to northeast-trending fault in andesite of Dark Thunder Canyon. The fault is poorly exposed at the surface, but unpublished reports state that it strikes N46°E and dips 80-85°northeast. Numerous bends and splays of the fault act as ore-concentrators. The fault, where exposed in shallow pits and trenches at the surface, is 2-3 m wide and reportedly widens at depth to 6-15 m. The oxidized zone occurs above the 79-m level and sulfides below 79 m (J. F. Fraser, unpubl. report, 9/24/59). The vein consists of quartz, illite, feldspar, pyrite, chlorite, and iron oxides. Wahl (1980) reports that native wire gold occurs in hematite stringers at the Twin Peaks mines. Assay of a sample from the Discovery mine reportedly contained 6 oz/ton (206 ppm) Au and 60 oz/ton (2,057 ppm) Ag (Carl Boderick, pers. comm. 9/5/92). A chip sample across the vein (1 m wide) collected and assayed for this study contained 0.1 oz/ton (3 ppm) Au, 2.28 oz/ton (78 ppm) Ag, 110 ppm Cu, 110 ppm Pb, and 95 ppm Zn (#1086A, Appendix 11.6). Briggs (1982) reports two assays of tr—0.03 oz/ton (1 ppm) Au and 0.8 oz/ton (27 ppm) Ag with low copper, lead, and zinc values (less than 100 ppm).

Alteration at the Twin Peaks mines is weak and poorly exposed except in shallow pits. Examination of dump material and exposures suggest that acid-sulfate alteration is present along the fault. Silicification and chloritization are found but are minor.

3.4.10 Fraser mines

The Fraser mines, also known as the Fraser-Martin and Fraser Brothers mines, lie along the Twin Peaks fault in sec. 8, 9, 16, 17, 18, T16S, R21W. Development consists of four shafts, 4-9 m deep, and several trenches, and seven adits, 2-18 m long (Fig. 3.18). Production is unknown, but Briggs (1982) reports a total production for mines in the northern part of the district (Twin Peaks, Commerce-Mayflower, etc.) as 1,000 tons yielding 1,115 oz Au, 3,640 oz Ag, and 1,965 lbs Cu (see discussion on Twin Peaks mine, this report). The mine was worked in 1958.

The deposit consists of quartz veins and silicified breccia along the Twin Peaks fault. The fault has a strike of N40°-50°W but the dip could not be measured. The fault throws andesite of Dark Thunder Canyon formation and younger ash-flow tuff against andesite of Summit Mountain. The fault zone consists of quartz, calcite, iron oxides, malachite, and manganese oxides. Silicification, hematization, and clay alteration are common. Briggs (1982) reports assays that range from 0-0.01 oz/ton (0.3 ppm) Au, 0-1.0 oz/ton (34 ppm) Ag, and as much as 0.7% Cu, 0.02% Pb, and 0.02% Zn (Fig. 3.18).

3.5 Description of copper-silver mines

3.5.1 Blue Bell mine

The Blue Bell mine, also known as the Shamrock or Blue Bird mine, is located in Cottonwood Canyon along the northwest-trending Blue Bell fault in sec. 8, T17S, R20W. The claims are unpatented and the main shaft is at an approximate elevation of 1646 m.

The principle development work has been at the Blue Bell shaft which is approximately 61 m deep (Fig. 3.19). Two levels occur at 15 m and 30 m depths. A 41-m long adit intersects the 30-m level, and a second adit, about 40 m long, intersects the 15-m level. The underground workings are caved and inaccessible in 1993. A water well, supplying the nearby Croom ranch, intersects the shaft at a depth of 37 m (Gillerman, 1964). Numerous trenches and pits expose the vein along strike. In 1990, Nova Gold Resources Ltd. drilled

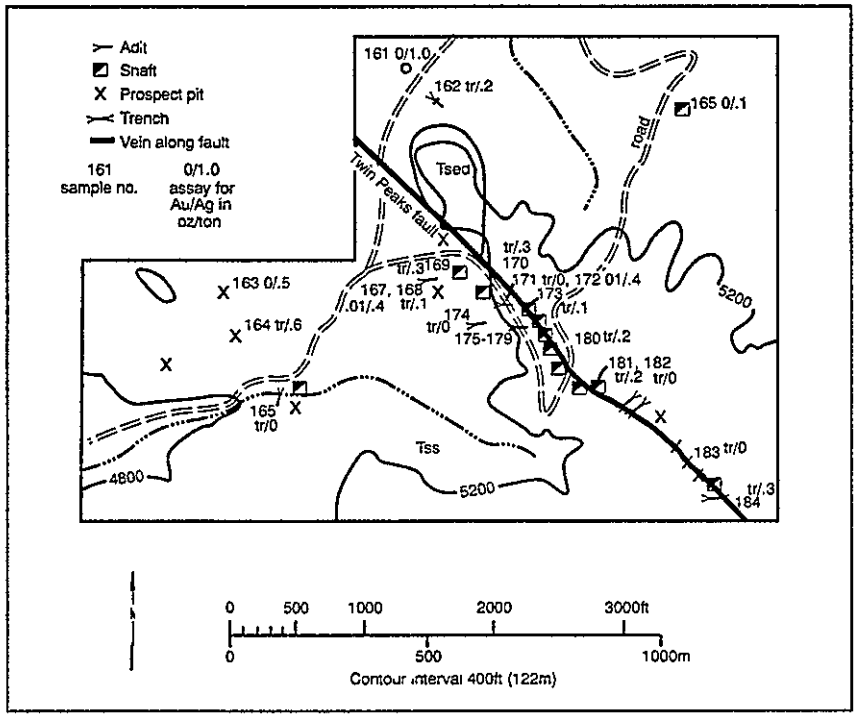

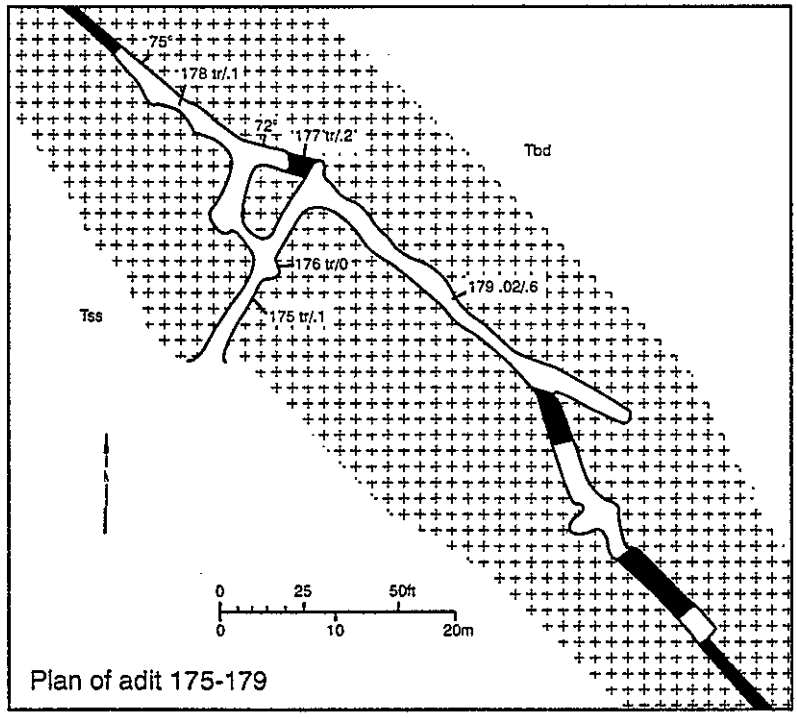

Fig. 3.18 - Map of Fraser Mines area (modified from Briggs, 1982; geology modified from V.T. McLemore mapping and Hedlund, 1993).Tss-Summit Mountains formation, Tbd-Dark Thunder Canyon formation, Tsed-undifferentiated sedimentary rocks (maps 1,2).

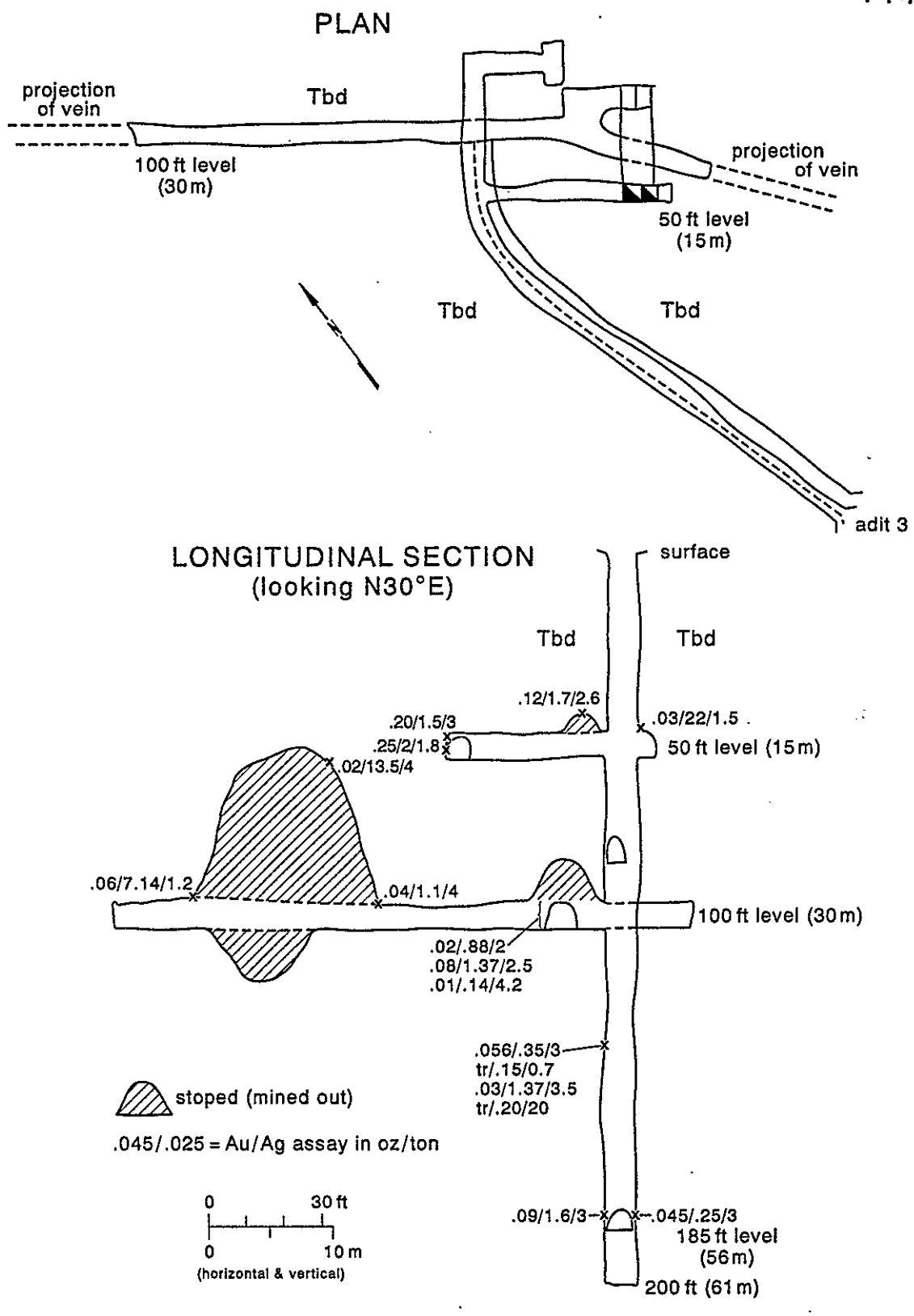

Figure 3.19 Longitudinal section and plan of the Blue Bell mine (modified from H. Schmidt, unpubl. report, January 28, 1938). Tbd—andesite of Dark Thunder Canyon formation

several diamond drill holes northwest of the shaft along the Blue Bell fault, but no economic intercepts were reported.

Early mine reports indicate a high-grade pocket of ore was found and mined prior to 1904. Production from this ore pocket is reported as 254 tons of ore averaging 0.96 oz/ton (33 ppm) Au, 4.5 oz/ton (394 ppm) Ag, and 11% Cu (C. W. Davis, unpubl. report, 6/14/37). The mine also yielded a few hundred tons of ore in 1909, 1916, and 1918. One smelter lot of 33.4 tons of ore assayed 0.87 oz/ton (30 ppm) Au, 11.8 oz/ton (404 ppm) Ag, and 4.9% Cu (C. E. Morgan, unpubl. report, 10/14/21). However, total production is probably less than 500 tons of ore averaging between 0.6-0.9 oz/ton (20-31 ppm) Au, 10-12 oz/ton (340-411 ppm) Ag, and 6-11% Cu (NMBMMR files).

Two veins occur at the Blue Bell mine, although typically only one vein is exposed at the surface. The No. 1 vein averages 1 m wide and rarely exceeds 1.5 m in width. The No. 2 vein is up to 15 m wide. The veins dip nearly vertical to about 80°E to 80°W and strike N45-60°W. On the 30 m-level, the vein is reported to be 3 m wide (G. A. Kalor, unpubl. report, 4/6/14). Host rocks are silicified porphyritic andesite to basaltic andesite of the Dark Thunder Canyon formation. Ore minerals include malachite, azurite, chrysocolla, chalcopyrite, bornite, and chalcocite in a gangue of quartz, calcite, pyrite, hematite, and minor feldspar, chlorite, and titanium oxides (Appendix 11.3). The center of the veins is commonly formed by bladed calcite, locally replaced by quartz (lattice texture). It is reported that copper carbonate minerals are found only above the 15-m level (C. E. Morgan, unpubl. report, 10/14/21). The copper-silver vein grades to gold-silver at depth.

Early mine reports also describe fine-grained streaks of bornite, about 1.2 m wide, that assayed 0.03 oz/ton (1 ppm) Au, 27.3 oz/ton (936 ppm) Ag, and 27.8% Cu (W. H. Seaman, unpubl. report, 5/21/22). Underground sampling by H. Schmidt (283 samples) averaged 0.34 oz/ton (12 ppm) Au and 4.65 oz/ton (159 ppm) Ag; average assays decreased with increase in depth (Map B; H. Schmidt, unpubl. report, 2/1/38).

Surface sampling for this report detected no significant gold or silver values except for

one sample that assayed 1 oz/ton (34 ppm) Ag (#31, Appendix 11.6). Copper values ranged from 8 to 26,700 ppm; lead and zinc values are low (#31, 32, 296, Appendix 11.6).

3.5.2 Delmir Mine

Very little is known about the Delmir mine. Various spellings of the name occur in the literature: Delmire, Delamar, Delmar, and Delmare, and it is also known as the Copper Hill mine. The mine occurs on the Delmir fault, which trends north-northeast, N20°E and dips 70° west (Fig. 2.18). The mine is located west of Alabama Ridge in sec. 36, T17S, R21W. Development consists of several shallow shafts and pits and trenches (at least 6 m deep). The mine was worked in the early 1900s but production in 1915 and 1917 amounts to less than 200 tons of ore which averaged 0.02 oz/ton (0.7 ppm) Au, 2.66 oz/ton (91 ppm) Ag, 0.07% Cu, and 0.15% Pb.

The ore at the Delmir occurs in andesite of Dark Thunder Canyon formation and Bloodgood Canyon Tuff. Copper carbonates (malachite, azurite) and chrysocolla occur with calcite, feldspar, and minor quartz and clay or disseminations within the andesite and tuff, thin veinlets, and fracture coatings. The andesite and tuff are not extensively altered and silicification is minor. Two samples were collected and assayed and contained 0-0.03 oz/ton (1 ppm) Au, 1.42-2.29 oz/ton (49-79 ppm) Ag, 0.81-0.58% Cu, 60-239 ppm Pb, and 240-1190 ppm Zn (#263,372; Appendix 11.2, 11.6).

3.5.3 Hext mine

The Hext mine lies along the Apache fault near the projected intersection of the Blue Goose fault in sec. 20, T17S, R20W. Development consists of trenches, pits, caved shafts, and a caved adit. Very little is known about the history of this mine, and production is unknown.

The fault strikes N60°W but the dip is unknown. The deposit consists of a silicified breccia zone with quartz, malachite, azurite, chryscolla, and traces of calcite. The andesite is

silicified and locally altered to clay. Three samples were collected and assayed for this report and contained 0.014-0.017 oz/ton (0.5-0.6 ppm) Au, 0.6-5.2 oz/ton (20-178 ppm) Ag, 0.2-3.7% Cu, 72-280 ppm Pb, and 25-57 ppm Zn (#639, 640, 641; Appendix 11.6).

3.5.4 Wampoo mine

The Wampoo mine lies on the Commerce-Mayflower fault, southeast of the Commerce-Mayflower mine, in sec. 15, T6S, R32E. Development consists of three inclined shafts (probably less than 20 m deep), short adit, trenches, pits and drill holes. Production is unknown but probably includes part of the production reported by Keith et al. (1983; see discussion of Twin Peaks mines, this report).

The deposit consists of silicified and brecciated andesite cut and cemented by quartz, calcite, azurite, malachite, fluorite, feldspar, illite/smectite, iron oxides (including goethite), chrysocolla, pyrite, and possibly chalcopyrite (#1068a, b; Appendix 11.3). Veins of white, massive calcite 5-8 cm wide cut across the breccia and quartz veins. The Commerce-Mayflower fault strikes N35°W at the Wampoo and dips 68° west. Some calcite veins strike N45°W and dip 52° west. Splays and branches along the fault are common. Two samples collected for this study contained no gold, 0-0.36 oz/ton (12 ppm) Ag, 0.11–0.31% Cu, 0.66-1.6% Pb, 0.72-1.1% Zn, and 0.08-0.04% CaF_2 (#1068a, b; Appendix 11.6).

3.5.5 Commerce-Mayflower mines

The Commerce-Mayflower group of mines lie on the Commerce-Mayflower fault in sec. 9, 10. 15, 16, T6S, R32E in Greenlee County, Arizona. Development consists of four shafts, 3-30 m deep, prospect pits, and trenches (Fig 3.20; Briggs, 1982). Production is unknown but probably includes part of the production reported by Keith et al. (1983; see discussion of Twin Peaks mines, this report).

The deposit consists of malachite, azurite, chrysocolla, pyrite, quartz, calcite, iron oxides, clay, and fluorite along the fault and fracture surfaces and as veins. Briggs (1982)

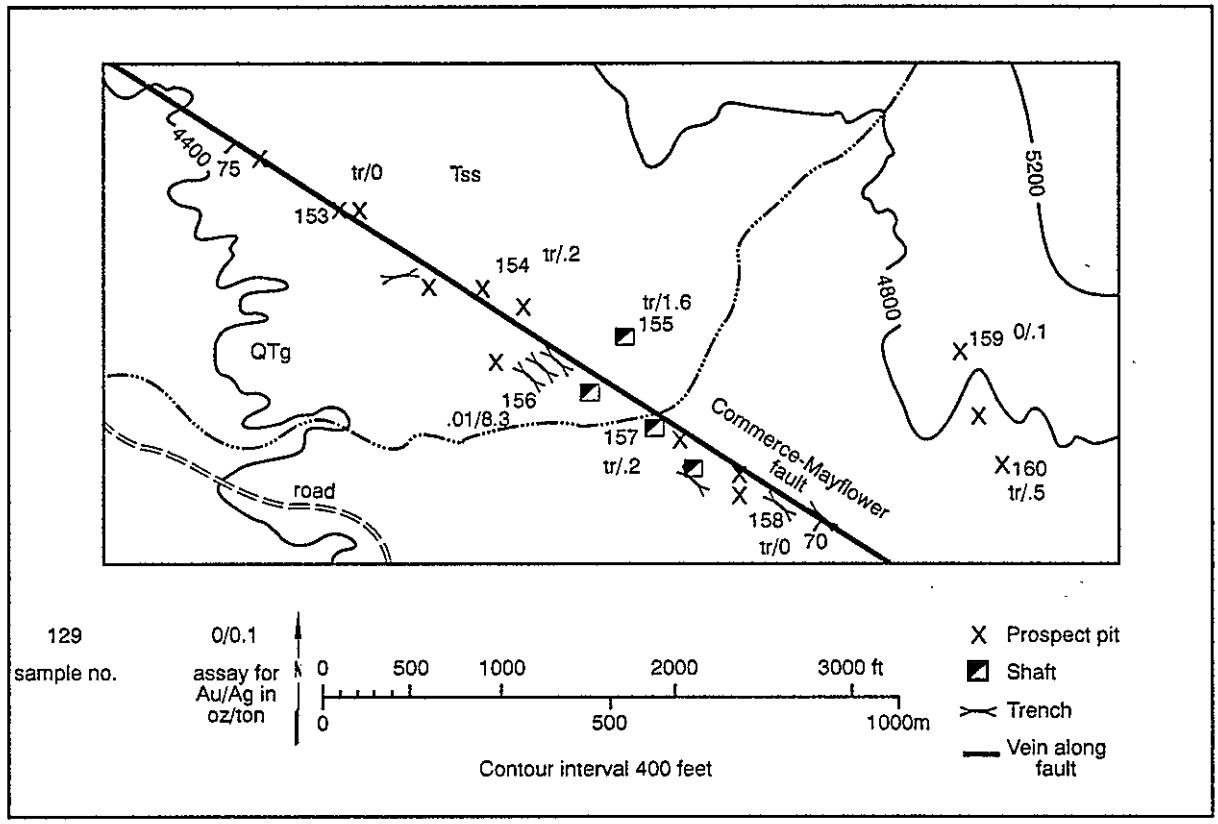

Fig. 3.20 - Map of Commerce-Mayflower Mine area (modified from Briggs, 1982; assays from Briggs, 1982; geology modified from V.T. McLemore mapping and Hedlund, 1993). Tss- Summit Mountain formation, QTg-Gila Group

reports the presence of native copper, chalcopyrite, covellite, and chalcocite. The andesite is silicified and contains chlorite. Clay alteration occurs along parts of the fault for 2-3 m. The fault has a strike of N55-60°W and dips 75° west. Assays reported by Briggs (1982) range from 0-0.01 oz/ton (0.3 ppm) Au, 0-8.3 oz/ton (34 ppm) Ag, 0.17-15.4% Cu and as much as 0.01% Pb and 0.01% Zn (Fig. 3.20).

3.5.6 Copper Basin

The Copper Basin prospects, also known as the Lotty-Independence prospect, lies west of Twin Peaks in sec. 10, T6S, R32E in Greenlee County, Arizona. Development in the vicinity consists of prospect pits, six adits (4-30 m long), seven shafts (3-9 m deep), and several trenches (Fig. 3.21; Briggs, 1982). Production is unknown but probably includes part of production reported by Keith et al. (1983; see discussion of Twin Peaks mines, this report).

The deposit consists of malachite, azurite, quartz, pyrite, and calcite in veins and along fracture coatings. The andesite is silicified and contains epidote and chlorite. The rhyolite is also silicified. The faults strike N35°W with a near vertical dip. Briggs (1982) reports assays of samples collected that contain 0.1-1.3 oz/ton (3-44 ppm) Ag, 0-0.03 oz/ton (1 ppm) Au, and <0.01-3.2% Cu (Fig. 3.21). A sample collected and assayed for this study contained no gold, 1.25 oz/t (43 ppm) Ag, 6.7% Cu, <20 ppm Pb, and 24 ppm Zn (#1085, Appendix 11.6).

3.6 Description of fluorite mines

3.6.1 Mohawk mine

The Mohawk mine occurs south of Bitter Creek at the northwestern end of the Bilalli-Norman King fault near the intersection with the Bitter Creek shear zone (Map 1, 2). It lies northwest of the Norman King mine in sec. 26, T16S, R21W. Formerly it was called the Bitter Creek mine and on some maps it is mislabeled as the Bilalli mine. Biron Bay Resources

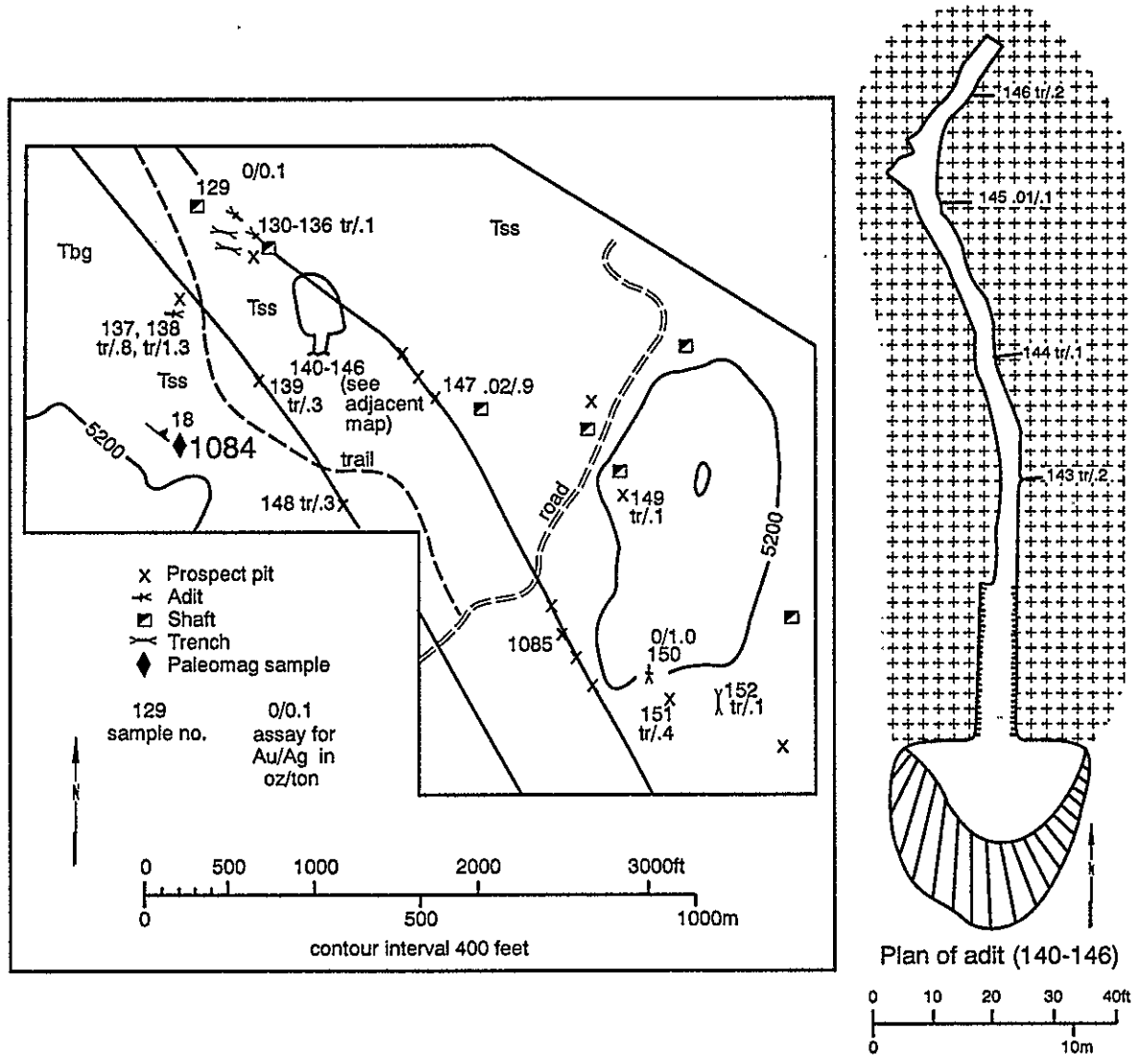

Fig. 3.21- Map of mines in Copper Basin mines area, west of Twin Peaks. (modified from Briggs, 1982; assays from Briggs, 1982; geology from V. T. McLemore mapping and Hedlund, 1993) #1085 collected for this study (appendix 11.6). Tss-Summit Mountain formation, Tbg-Bloodgood Canyon Tuff

Ltd. currently holds the lease.

Development consists of four shafts (15, 15, 24, and 61 m deep), drifts, trenches, and prospect pits (Gillerman, 1964; McAnulty, 1978). One shaft, 24 m deep, connects to a drift which is 91 m long (Rothrock et al., 1946). Most of the workings are caved, flooded, and inaccessible.

The mine first yielded production in the 1940s when Southwestern Minerals Co. operated it (Williams, 1966). Total production from 1940 to 1941 was 6,463 tons of ore averaging 60-70% CaF_2 and 30-35% SiO_2 (McAnulty, 1978). One ore shoot was 1.8 m wide, 30 m long, and was mined to a depth of 24 m. In 1972, Jim McBee operated the mine and shipped 40-50 tons of ore to Deming, New Mexico (McAnulty, 1978). Total production is estimated to be about 6,500 tons of ore averaging 50-70% CaF_2.

The Mohawk deposit is fault controlled. The main vein strikes N10-15°W and dips 80°E to vertical. Ore minerals consist of green to purple to colorless fluorite in a gangue of quartz, pyrite, hematite, calcite, barite, and manganese oxides. The fluorite is massive to fine-grained. Bladed quartz after calcite is common and fluorite typically occurs within the blades. Fluorite grades to the south into quartz veins with local pods of fluorite. Fluorite is found along the Bilalli-Norman King fault as far southeastward as the Hoover Tunnel. The andesites hosting the veins are silicified. No gold, silver, copper, lead, or zinc values were detected in a sample collected for this report (A#1012, Appendix 11.6). Fluorite reserves are probably minimal.

3.6.2 Black Willow prospects

The Black Willow prospects lie north of Bitter Creek along the Twin Peaks fault in sec. 22, T16S, R21 W (Map 2). This group of prospects consists of several pits, four shafts (up to 24 m deep) and about 61 m of drifts (N. Walcott, unpubl. report, 12/15/39). The prospects were developed in the 1920s (Gillerman, 1964; Biggerstaff, 1974), but there is no reported production.

The vein consists of brecciated and silicified andesite cut by veins of clear to white to green fluorite, quartz, calcite, pyrite, illite, feldspar, iron oxides, pyrolusite and other manganese oxides, and traces of barite. Manganese oxides typically coat the fluorite. Locally, yellow staining of mottramite can be found. Gillerman (1964) reports gold and silver with pyrite were found. Fluorite grades to quartz veins to the northwest. The vein strikes N45°W with a variable dip of 70° to the northeast to vertical and is 7-15 m wide. Changes in dip and strike along the fault appear to concentrate mineralization (McAnulty, 1978; Biggerstaff, 1974). The fault brings Dark Thunder Canyon formation in contact with Summit Mountain formation. Fluorite is found sporadically along the entire length of the vein (at least 900 m), but decreases in concentration to the northwest. Fluorite occurs as massive pods and veinlets within quartz veins and as disseminations and veinlets along the face of fractures and faults. Locally, quartz after bladed calcite and bladed calcite occur. Five samples were assayed and found to contain no gold, 0-0.42 oz/ton (ppm) Ag, 14-290 ppm Cu, 16-250 ppm Pb, and 17-370 ppm Zn (#1011, 1106, 1130, 1131, 1131g, 1131f; Appendix 11.3, 11.6). Sample #1131f contained 32.4% CaF_2. Samples collected by Biggerstaff (1974) reportedly averaged 16.7% CaF_2 and 83% SiO_2. Alteration is minor in the Dark Thunder Canyon formation and consists of silicification and minor clay alteration. Acid-sulfate alteration occurs in the Summit Mountain formation; the relationship of this alteration to mineralization will be discussed separately.

3.6.3 Powell mine

The Powell mine, also known as the Fork mine, lies south of Bitter Creek in sec. 18, T16S, R21W (Map 2). Development consists of a bulldozer trench and several prospect pits. Production from March 1942, to January 1943 amounts to 127 tons of ore averaging 0.59% CaF_2 and 41% SiO_2 (Rothrock et al., 1946; Williams, 1966; Biggerstaff, 1974; McAnulty, 1978). Eugene Belcher conducted a percussion drilling program in 1973 and drilled four holes to 27 m. Belcher reported one ore intercept of 2 m at 27 m depth (Biggerstaff, 1974).

The Powell mine occurs along a northwest-trending fault that is cut by two east-west-trending faults of the Bitter Creek shear zone (Map 1, 2). Typically, fluorite occurs as thin veins, stringers, and fracture coatings along porphyritic andesite of the Summit Mountain formation in zones as wide as 15 m. At the mine, fluorite occurs as veins up to 1 m wide in a 10-m-wide zone. The vein at the surface is less than 200 m long. The main vein along the fault strikes N80-85°W and dips steeply to the west. Ore consists of coarse- and fine-grained, green to blue to purple to colorless fluorite in a gangue of quartz, calcite, iron oxides, manganese oxides, clays and barite. One sample from a pit above the mine assayed no gold or silver, 223 ppm Cu, 162 ppm Pb, and <100 ppm Zn and consisted of quartz, fluorite, calcite, jarosite, pyrite, and goethite (A#984, Appendices 11.3, 11.6).

3.6.4 Leta Lynn mine

The Leta Lynn mine is located north of Bitter Creek, northwest of the Powell mine in sec. 7, T16S, R21W (Map 2). Development consists of several bulldozer trenches and prospect pits. Eugene Belcher discovered the deposit in 1971 and in 1972 produced 3 tons of fluorspar ore. Belcher also drilled three percussion drill holes in 1972 which showed that the width of the zone varies but averages 2 m in these holes (Biggerstaff, 1978).

The Leta Lynn mine occurs along a northwest-trending fault, probably the same fault system as the Powell mine. The Leta Lynn fault is offset to the south by an east-west-trending fault that is part of the Bitter Creek shear zone. To the northwest, the Leta Lynn fault is overlain by alluvium, but most likely continues into section 25, T6S, R32E where prospects have exposed portions of the fault (Maps 1, 2). Fluorite occurs as thin veins, stringers, and fracture coatings along porphyritic andesite of the Summit Mountain formation. The main vein strikes N80-85°W and dips 80-85°W and is up to 6 m wide and 300 m long. Ore consists of coarse- and fine-grained fluorite (green to blue to colorless) in a gangue of quartz, calcite, barite, clay, pyrite, iron, and manganese oxides. Some calcite is bladed; locally quartz replaces bladed calcite. Fluorite is intergrown with bladed quartz and calcite and also occurs

between the bladed quartz.

3.6.5 Fourth of July mine

The Fourth of July mine is in the Daniels Camp area in sec. 33, T6S, R32E and sec. 4, T7S, R32E in Greenlee County, Arizona. Development consists of several trenches and an inclined shaft 45 m deep with drifts at depths of 17, 31, and 45 m (Fig. 3.22; Trace, 1947; Meeves, 1966; Richter and Lawrence, 1983). Production in 1936-1942 and 1960 by Southwestern Minerals Co. and D. R. T. Ellis Mining Co. amounted to about 3,190 tons of 64% CaF_2 (Richter and Lawrence, 1983).

The Fourth of July and adjacent deposits consist of brecciated and silicified veins. Fluorite occurs as breccia cement, veins, disseminations, and pods within faults and fractures. The Fourth of July fault trends N35-45°W with a 60° dip to the southwest. A cross fault with a strike of N65°W and a 60° dip to the south cuts or merges with the northwest-trending Fourth of July fault, and the mine occurs near the junction of the two faults. North-trending faults in the immediate area host quartz veins with some fluorite locally.

The deposits consist of green to colorless fluorite, quartz, calcite, feldspar, kaolinite, rutile and other titanium oxides, and manganosite and other manganese oxides (Appendix 11.3). The silicified breccia at the Ellis shaft, east of the Fourth of July mine (Map 2), consists of quartz, fluorite, malachite, azurite, chrysocolla, calcite, and manganese oxides. Clay is common along the footwall. Silicification of the andesite of Dark Thunder Canyon is minor. Several stages of quartz deposition occurred: some quartz is overgrown with fluorite and calcite, whereas other quartz replaces or overgrows calcite. Fluorite occurs on quartz, as cubes within vugs, and crosscutting veinlets and is coated by manganese oxides.

Chemical analyses of these fluorite veins are variable. Trace (1947) reports assays containing up to 1-2% WO_3 locally with manganese oxides. Meeves (1966) reports analyses, using a radioactive beryllium detector, containing as much as 100 ppm Be in some veins, but spectrographic analyses by Hedlund (1990a) failed to detect any beryllium. The beryllium is

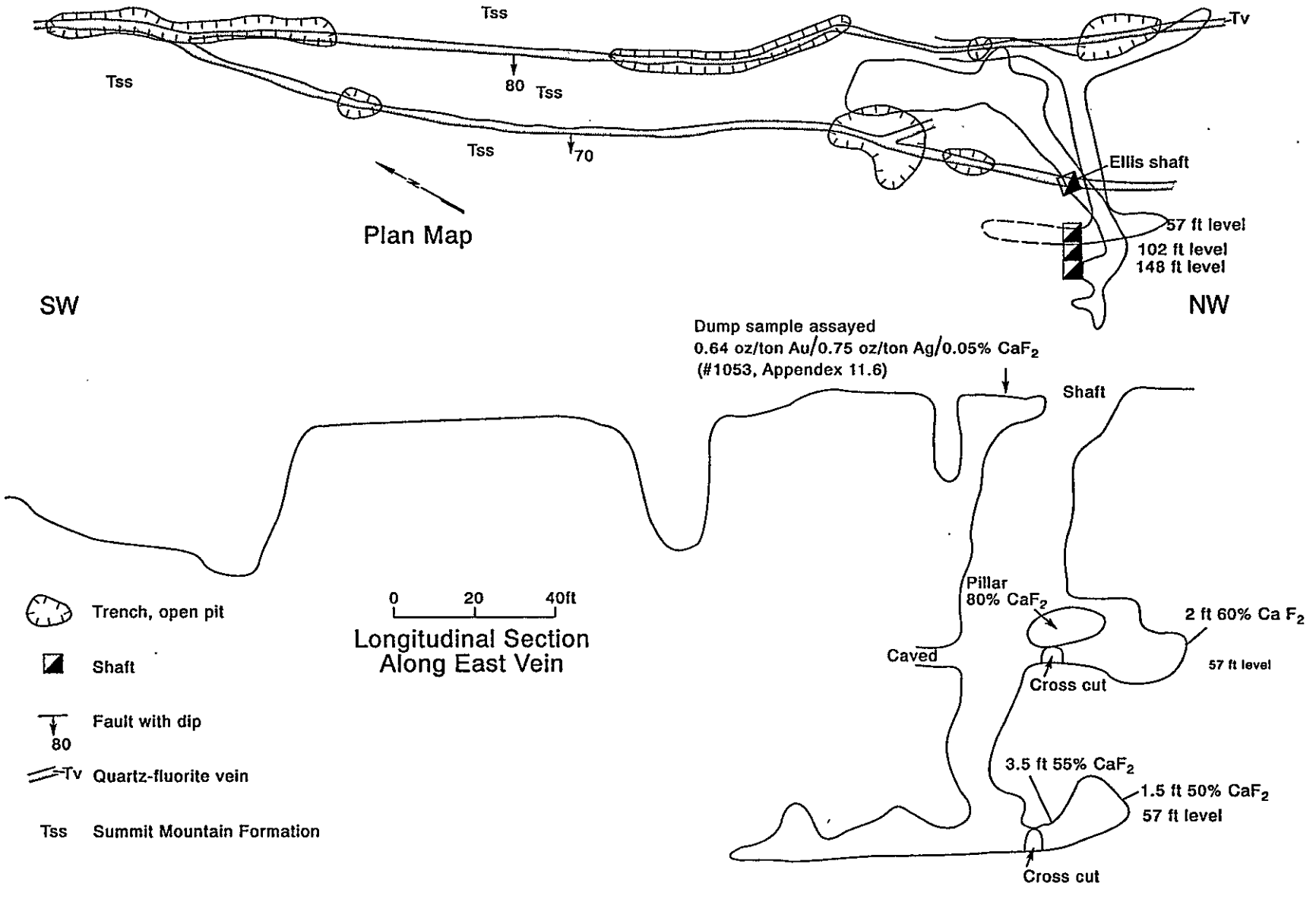

Figure 3.22- Plan and section along Fourth of July fluorspar mine (modified from Trace, 1944).

attributed to be bertrandite or helvite (Powers, 1976), but this identification is speculative and needs to be confirmed. Neither tungsten nor beryllium were analyzed for in this study. Two samples of veins in the Fourth of July mine area collected and assayed for this study contained 0-0.64 oz/ton (0-22 ppm) Au, 0-0.75 oz/ton (0-26 ppm) Ag, 46-16,000 ppm Cu, 27-62 ppm Pb, 30-50 ppm Zn, and 0.05-0.3% CaF_2 (#1042, 1053; Appendix 11.6).

3.6.6 Daniels Camp mines

The Daniels Camp mine lies just west of the mapped area in sec. 5, T7S, R32E in Greenlee County, Arizona. Development consists of several trenches, pits, and a shallow shaft (probably less than 10 m). The property was worked during the 1940s (Biggerstaff, 1974), but production, if any, is unknown.

Fluorite occurs as veins, pods, disseminations, thin veinlets, and fracture coatings along faults and fractures trending N10-15°E and N5°W and dipping near vertical (Biggerstaff, 1974; Richter and Lawrence, 1983). The mineralized zone rarely exceeds 2 m width at the surface. The veins consist of green to colorless fluorite, calcite, quartz, local pyrite, manganese oxides, iron oxides, clay, and traces of barite. Alteration of andesites of the Summit Mountain formation is mild to weak and consists of a zone 1-2 m wide of silicified or clay altered rock. Brecciation is common. Biggerstaff (1974) estimates the fluorite content as approximately 30-35% CaF_2.

3.6.7 Forbis mine

The Forbis mine, also known as the Polly Ann, occurs in sec. 4, 9, T7S, R32E in Greenlee County, Arizona. Development consists of three shafts, up to 57 m deep, with drifts and trenches. Some fluorite was produced, probably in the 1940s and again in 1982, but total production is unknown. The shaft has two compartments and is filled with water.

The Forbis deposit occurs along a minor, poorly exposed fault trending N15°-45°W and dipping 65° southwest. At the surface the deposit is about 2 m wide and less than 300 m

long. Fluorite is green to yellow to colorless and occurs as pods, veins, irregular masses, disseminations and thin veinlets with andesite and along fracture surfaces. A sample collected and assayed for this study contained no gold or silver, 86 ppm Cu, 52 ppm Pb, 20 ppm Zn, and 7.47% CaF_2 (#1041, Appendix 11.6). Minor silicification of the andesite (Summit Mountain formation) occurred along the fault. Some clay alteration also has occurred along the footwall.

3.6.8 Luckie mines

The Luckie No. 1 and Luckie No. 2 shafts are in sec. 3, 10, T7S, R32 E in Greenlee County, Arizona. Development consists of two inclined shafts (both 27 m deep), pits, and trenches (Figs. 3.23, 3.24; Trace, 1947). More than 2,200 tons of 65-70% CaF_2 were produced intermittently from 1914 to 1944 by Quien Sabe Mining Co. (Richter and Lawrence, 1983; Hedlund, 1990a).

Deposits at the Luckie mines consist of fluorite (green to blue to colorless), quartz, calcite, and manganese oxides with trace pyrite, chalcopyrite, and chrysocolla. The fluorite occurs as breccia cement, pods and irregular masses, and veins within the quartz along the margins of a rhyolite dike. Quartz is intergrown with fluorite and manganese coats both quartz and fluorite. The veins vary in width from 3-6 m and are less than 100 m long, although fluorite occurs along the Luckie No. 1 fault sporadically for 300 m or so. The veins occur in acid-sulfate altered andesites of Summit Mountain formation. The Luckie deposits occur along separate faults. The Luckie No. 1 fault has a strike of N15°E with a west dip of 75°. The Luckie No. 2 fault has a strike of N35°W with a near vertical dip. A sample collected for this study contained no gold or silver, 43 ppm Cu, 80 ppm Pb, and 60 ppm Zn (#559, Appendix 11.6). Hedlund (1990a) reports an analysis of a sample from the Luckie No. 2 mine that contained 0.03 oz/ton (1 ppm) Ag, 150 ppm Ba, 15 ppm Cu, 20 ppm Zn, and 15 ppm Pb. Meeves (1966) reports an assay, using a radioactive beryllium detector, containing as much as 100 ppm Be from the Luckie mines. The beryllium is attributed to bertrandite or

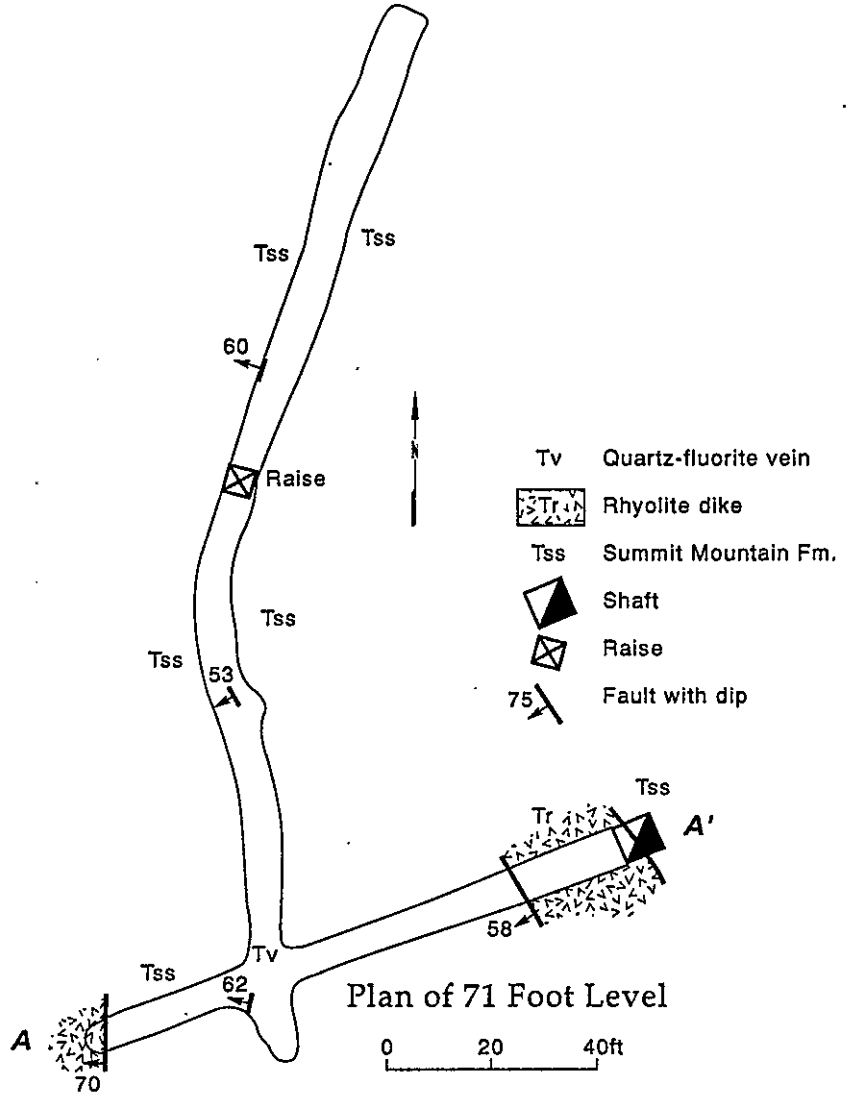

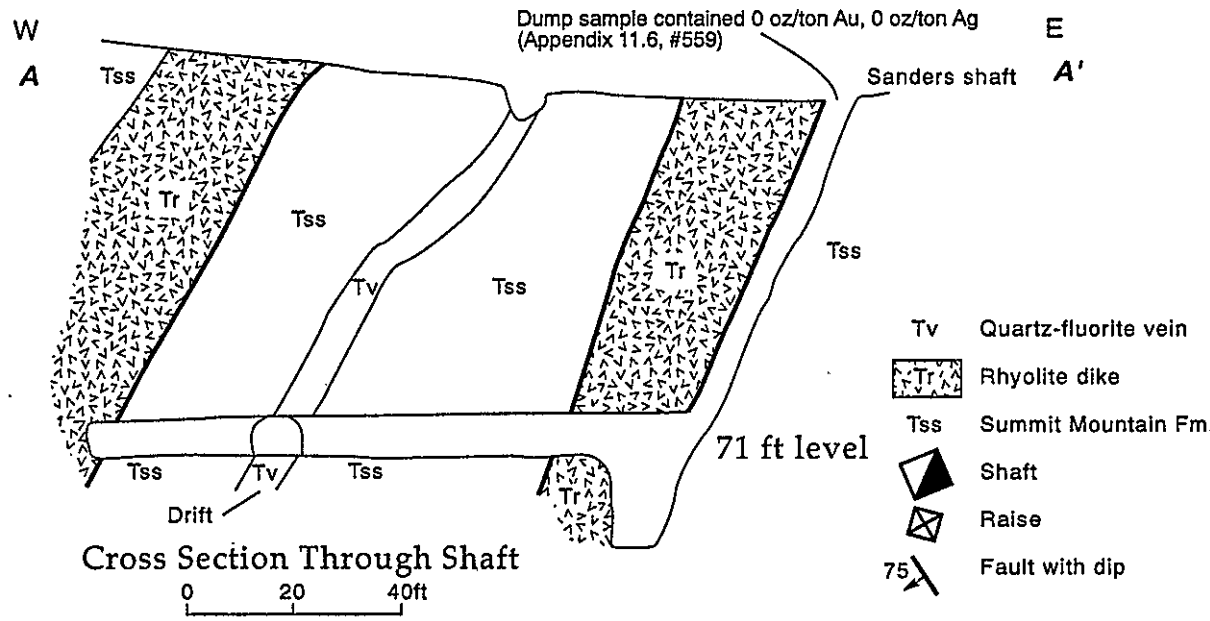

Figure 3.23- Plan and section of Luckie No. 1 fluorspar mine (modified from Trace, 1944).

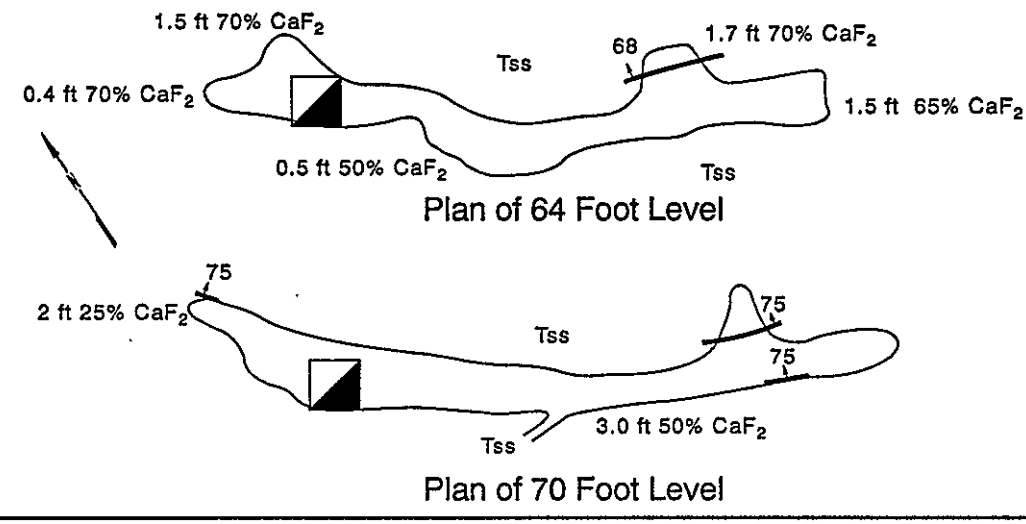

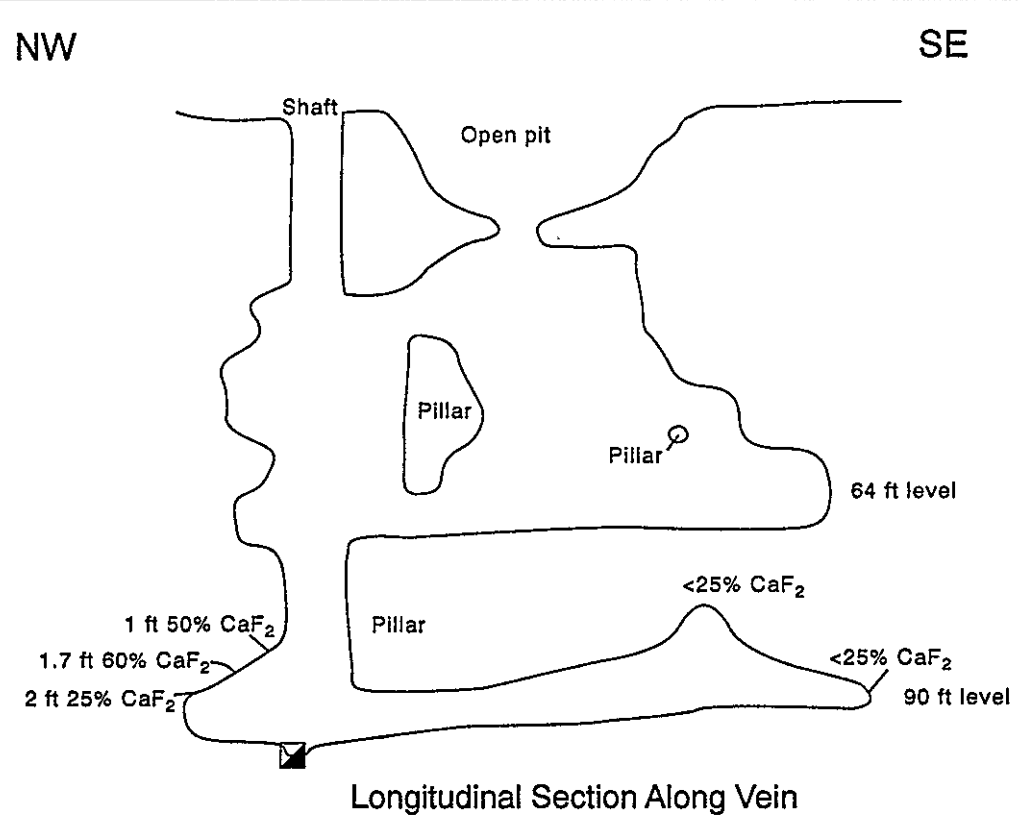

Figure 3.24- Plan and section of Luckie No. 2 fluorspar mine (modified from Trace, 1944)

helvite (Powers, 1976), but the identification is speculative and needs to be confirmed.

3.6.9 Goat Camp Springs mines

Several fluorite mines occur in the Goat Camp Springs area west of Vanderbilt Peak (Dean, Stotts, Ontario, Rattlesnake No. 1, Rattlesnake No. 2) (Maps 1, 2). These occur along faults of varying strikes, typically N10°W to N10°E, but some veins occur along northwest-trending faults as well. Development consists of shafts, trenches and pits. Total production is unknown but presumed minor. Between 120 and 150 tons of fluorite was produced from the Rattlesnake mines in the 1970s by R. Hill (Hedlund, 1990b).

The veins occur along faults and fractures in altered andesite of Summit Mountain formation. Fluorite and quartz with varying amounts of iron oxides, clay, calcite, and barite occur within the veins. Some veins occur along rhyolite dikes, whereas other veins change from quartz and fluorite to quartz and pyrite along strike. Assays are variable but typically low (Appendix 11.6, Map 2).

3.7 Description of manganese mine

Manganese oxides are common throughout the Steeple Rock district, but only one mine was developed specifically for manganese, the Black Cat mine. The Black Cat mine lies in sec. 33, T6S, R32E north of the Goat Camp Springs area in Arizona. The claims were first located in 1952 by L. A. Billingsley and Lewis Dean. In 1953-55, 86 tons of ore averaging 43.2% Mn (74,500 lbs Mn) were shipped to Deming, New Mexico (Farnham et al., 1961). Development consists of prospect pits, trenches, and two shafts, 15 and 13 m deep. Psilomelane and other manganese oxides occur in two narrow veins up to 1 m wide and along fractures and joints several meters into the country rock adjacent to the veins. Calcite, fluorite, quartz, and iron oxides are also present. One sample collected for this study did not contain any gold or silver, but assayed 21.8% Mn (Black Cat, Appendix 11.6).

4. MINERALIZATION

4.1 Mineralogy

In this section, the distribution, textures, and description of the major minerals of the vein deposits are presented. Techniques used include literature search, field observations, petrography, XRD, SEM, and chemical analyses (see section 1.5.3 for specific methods used).

4.1.1 Ore mineralogy

4.1.1.1 Gold, Au—Gold and silver are the most economically important minerals in the Steeple Rock district. Native gold is reported from numerous base-metal and gold-silver veins from throughout the district (Lindgren et al., 1910; Griggs and Wagner, 1966; Gillerman, 1964; unpublished reports). Most of the gold may actually be electrum, the natural occurring alloy of gold and silver which, by definition, contains more than 20% Ag.

Gold occurs as submicroscopic to rare visible flakes disseminated in complex quartz breccias. Typically gold is difficult to detect except by fire assay. Some wire gold is reported to occur at the Carlisle, Center, and other mines (D. Hanson, pers. comm. 1991). Native gold or electrum was found disseminated with fine-grained sulfides and disseminated in "blue" quartz in drill hole J87-3 at the Jim Crow-Imperial mines (Appendix 11.3; Queenstake Resources Ltd., unpubl. report, April 1982). It is associated with high gold assays (up to 2.2 oz/ton Au), however that section of the drill core is missing and no longer available for study. A sample from the Alabama vein contained a small flake of gold or electrum in a vug within quartz-hematite breccia. At the Summit vein, gold occurs in two associations: (1) electrum (with as much as 37% Ag content) occurs with silver sulfides and (2) native gold (with low silver) occurs with pyrite or iron oxides and in quartz-carbonate veins (W. Baum, unpubl. report, March 31, 1988).

Mineral concentrates from the Center mine were also examined. Only three grains of electrum were found by SEM, despite hours of examination (Wilson et al., 1993). The grains

were small (<200 μm), free grains and not intergrown with sulfides. EDS x-ray patterns indicate that these grains are electrum (Fig. 4.1). Figure 4.2 shows a back-scattered image (SEM) of an electrum grain adjacent to a grain of chalcopyrite. The x-ray scan maps show the concentration and distribution of copper, gold, and silver (Fig. 4.2). Note the purity of the grains. Metallurgical tests indicate that most of the gold and silver can be recovered from Pb-Cu flotation and only minor gold and silver occurs with the zinc and pyrite concentrates (Wilson et al., 1993; I. Gundiler and M. Brueggemann, unpubl. report, May 25, 1990).

In general, gold in the Steeple Rock district is rarely visible and the only sure detection is by fire assay. As previously stated, the gold most likely occurs as electrum or as native gold, and is associated with pyrite. It is found in complexly brecciated quartz veins. Gold and silver are strongly correlated in most deposits (Fig. 4.3), but not with other elements. Gold may be sporadically distributed within individual veins making grade control challenging.

4.1.1.2 Silver, Ag—Silver is typically more abundant than gold in the vein deposits of the Steeple Rock district (Appendix 11.6, Table 3.2), but identification of silver minerals is difficult because of their small size. Silver also occurs in electrum, in concentrations much less than gold; silver must occur in other minerals besides electrum because silver concentrations are typically greater than gold concentrations. Native silver is reported to occur at the Ontario mine (Griggs and Wagner, 1966). Numerous reports indicate that silver occurs as argentite, Ag_2S (Lindgren et al., 1910; Gillerman, 1964; unpublished reports), but argentite is not stable at room temperature and inverts to acanthite Ag_2S (Anthony et al., 1990). Therefore, most argentite is probably acanthite, although it was likely to have been deposited as argentite, if formed at greater than 176°C.

Cerargyrite (chlorargyrite), AgCl, is reported in the district (Gillerman, 1964), and occurs as an alteration product at the Carlisle mine (SEM study by W. Baum, unpubl. report, March 31, 1988), where it occurs as intergrowths with chalcopyrite, secondary copper minerals, and acanthite. Ultra-fine (<5 μm) native silver was found with iron and manganese

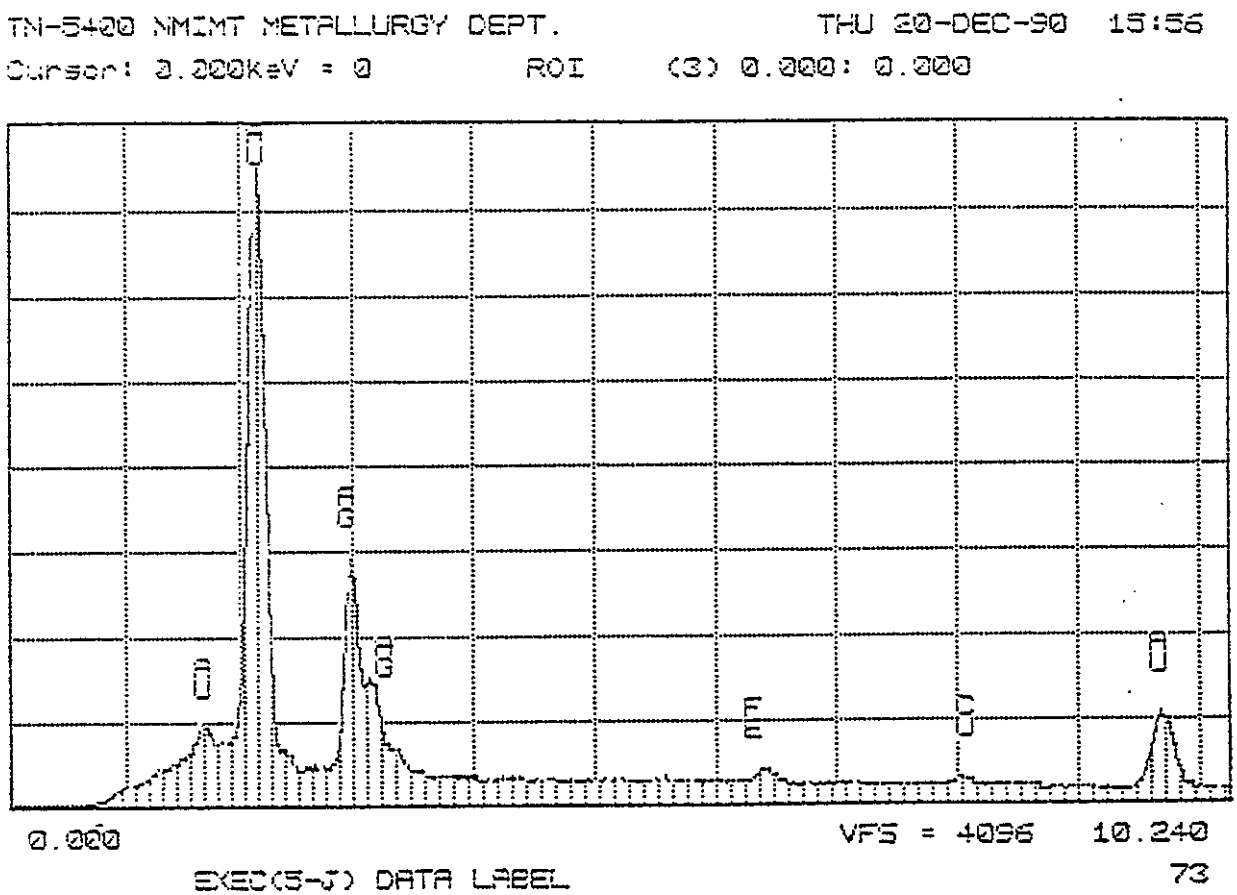

Figure 4.1—EDS X-ray spectrum of electrum, Center mine (20 kv).

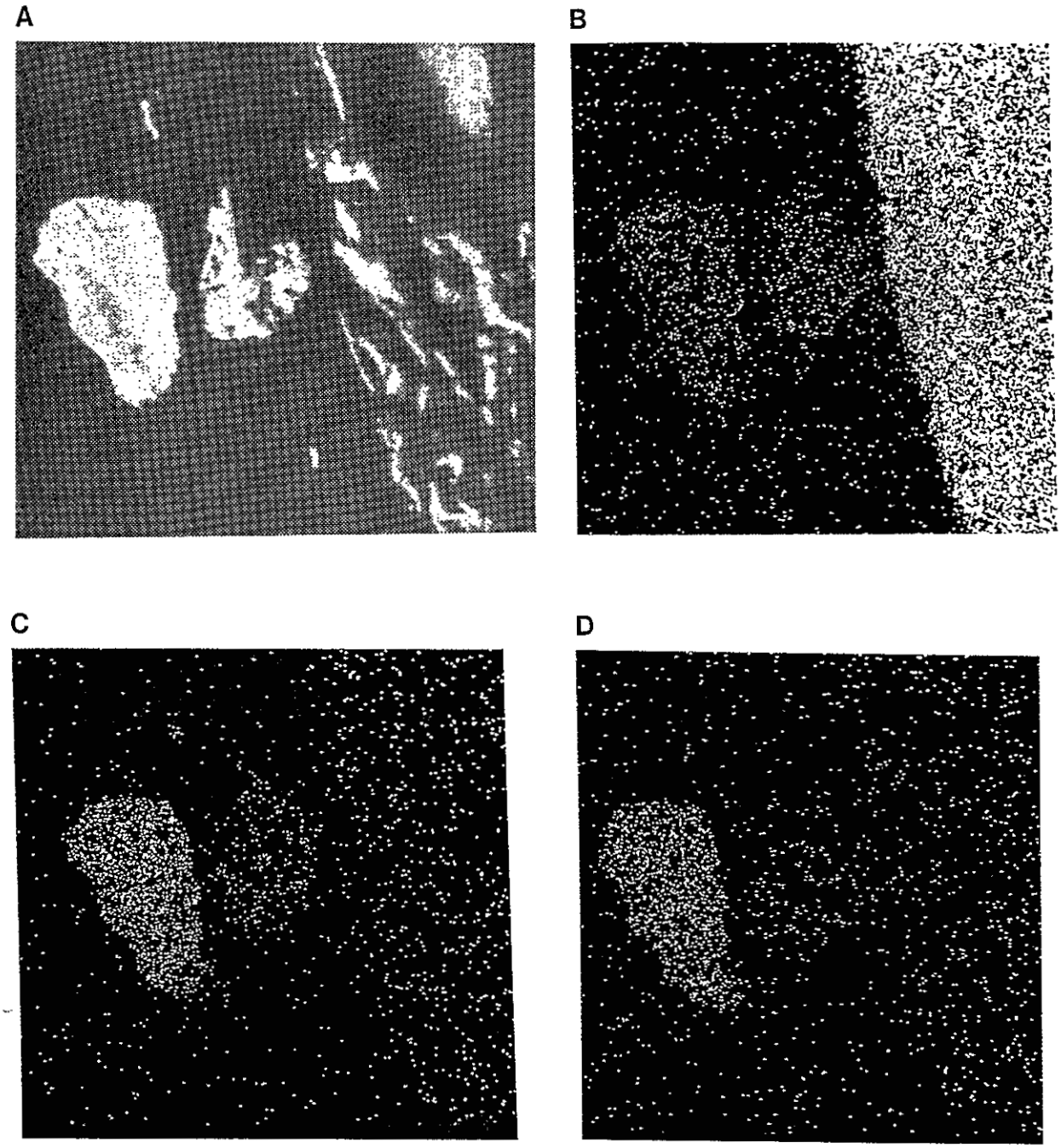

Figure 4.2—A. Back-scattered image (SEM at 20 kv) of an electrum grain (0.18 mm long) adjacent to a larger chalcopyrite grain. B. X-ray area scan map for copper. C. X-ray area scan map for gold. D. X-ray area scan map for silver. Sample from a polished grain mount from the Center mine. (From I. Gundiler in Wilson et al., 1993).

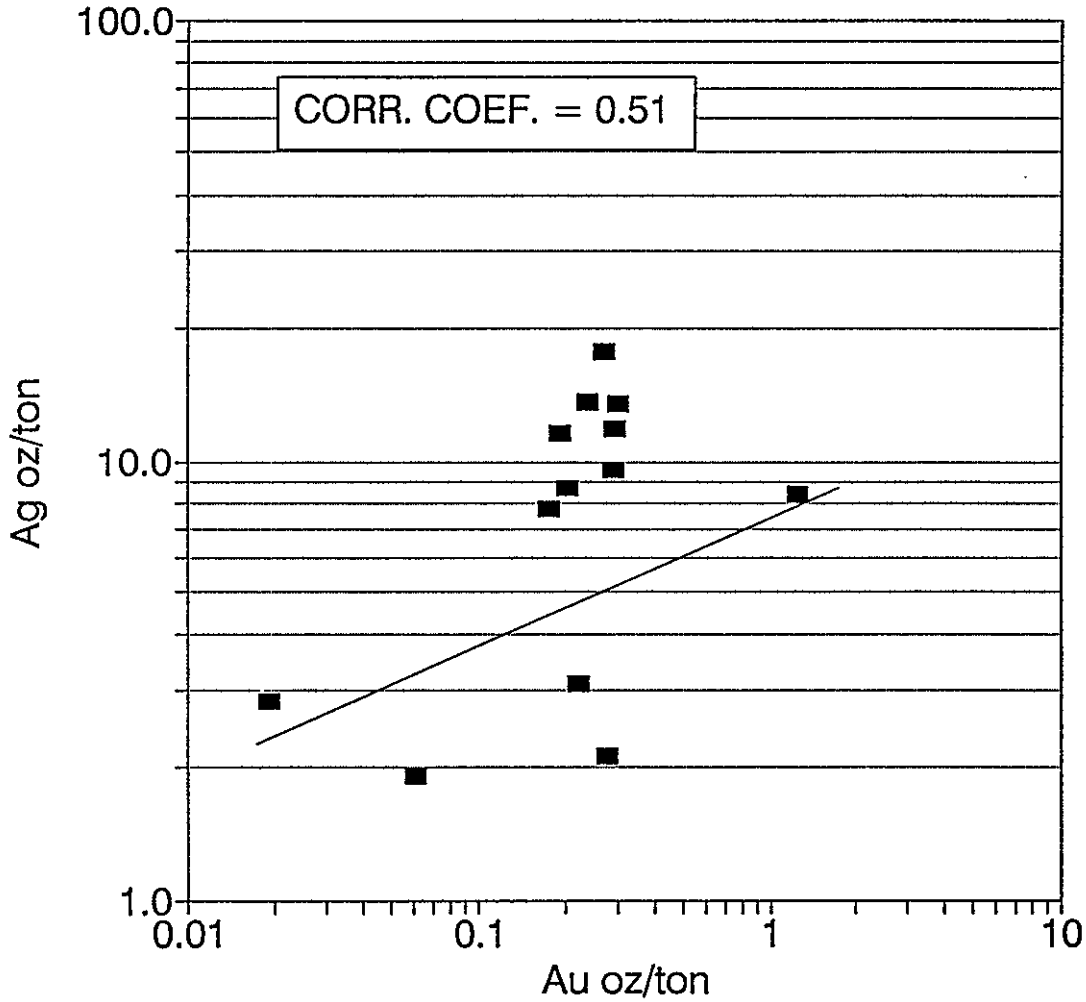

Figure 4.3 - Correlation of gold and silver from production totals of all mines in the Steeple Rock district.

oxides and as argentojarosite, Ag Fe_3 $(SO_4)_2$ $(OH)_6$, at the Summit vein (W. Baum, unpubl. report, 1988). W. Baum also reports silver occurring with tetrahedrite or other sulfosalts in the Carlisle and East Camp veins.

High silver values typically occur in complexly brecciated quartz veins, probably as fine disseminations or thin streaks of sulfides. Many samples coated or stained with mottramite or mimetite contain high values of gold and silver. Locally, silver concentrations correlate well with lead concentrations, suggesting that argentiferous galena may be present. In general, the only sure detection of silver is by fire assay.

4.1.1.3 Sphalerite, (Zn, Fe)S—Sphalerite is common as massive aggregates and intergrowths with galena, chalcopyrite, and pyrite (up to several centimeters long) only in the base-metal vein deposits along the Carlisle fault, specifically the Carlisle, Center, Pennsylvania, and Ontario mines. Up to 10% sphalerite can be found locally in these deposits. Sphalerite is also present as small, disseminated flakes or aggregates, typically microscopic (less than 0.5 mm) in samples from underground workings or drill core from gold-silver veins, specifically the Section 2, Alabama, Jim Crow, Imperial, McDonald, Summit, Bank, and Mohawk deposits. Zinc, most likely as sphalerite, was produced from the Carlisle, Center, Pennsylvania, Ontario, East Camp, Mt. Royal, and Summit mines. XRD patterns confirm the presence of sphalerite in most of these deposits (Appendix 11.3). Some deposits along the Foothills fault may also contain sphalerite; however, the XRD patterns are inconclusive because of interferences from other more abundant minerals (Appendix 11.3). Furthermore, zinc in excess of several hundred ppm occurs in samples from throughout the district and probably occurs as sphalerite (Appendix 11.5, 11.6). Sphalerite rarely exceeds 1% in any deposit other than those along the Carlisle fault.

In polished thin section, sphalerite occurs as massive aggregates intergrown with

galena, chalcopyrite, and/or pyrite or as small monomineralic aggregates. Sphalerite is commonly optically anisotropic, even though it has a cubic crystal structure. This anisotropy is a result of impurities (Deer et al., 1975). The crystals are anhedral and irregular and twinning and growth bands are rare, as are skeletal textures. In reflected light, sphalerite is gray, locally with a brown tint, and internal reflections are common. In transmitted light, sphalerite ranges in color from honey yellow to various shades of brown, including reddish brown. Brown colors in sphalerite are typically attributed to the presence of Fe; red to Sn, In, Ag, and Mo; and yellow to Ge, Ca, Cu, Hg, and Cd (Deer et al., 1975). An EDS x-ray spectrum (SEM) of yellow sphalerite from the Center mine indicates that Cd and Fe are present in small concentrations (Fig. 4.4; from I. Gundiler in Wilson et al., 1993).

Most sphalerite from all types of samples from the Steeple Rock district displays various intergrowth textures with chalcopyrite (Fig. 4.5, 4.6) and, to a lesser extent, galena and pyrite. These sphalerites contain randomly dispersed and/or crystallographically oriented rows of rods and blebs of chalcopyrite, and rarely galena, each typically less than 30 μm long. Some chalcopyrite replaces fluid inclusions in the sphalerite. This texture is similar to the myrmekitic and symplectitic textures of igneous rocks (MacKenzie et al., 1991) and is commonly referred to as "chalcopyrite disease" (Craig and Vaughn, 1981). Chalcopyrite, galena, and pyrite locally occurs along the rims of sphalerite as well as suturing fractures. Chalcopyrite disease has been commonly attributed to exsolution of dissolved copper on cooling of the sphalerite (Ramdohr, 1969). However, subsequent experimental studies (Wiggins and Craig, 1980; Hutchison and Scott, 1981) have demonstrated that sphalerite can not contain sufficient dissolved copper to produce the abundance of these chalcopyrite rods and blebs unless the temperatures of formation exceed 500°C. In the Steeple Rock samples (formed at less than 500°C), up to 30% chalcopyrite rods and blebs are visually estimated to

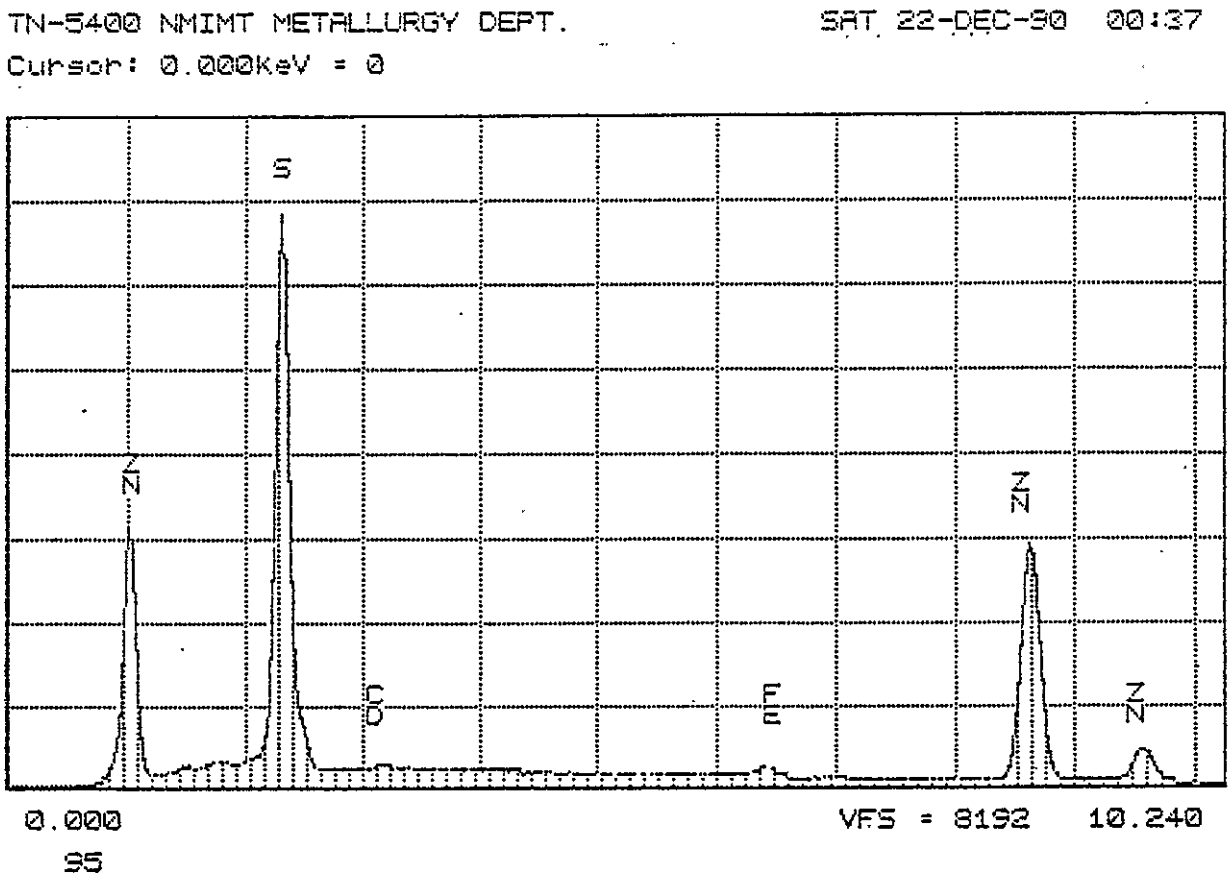

Figure 4.4—EDS x-ray spectrum of sphalerite from the Center mine (20 kv).

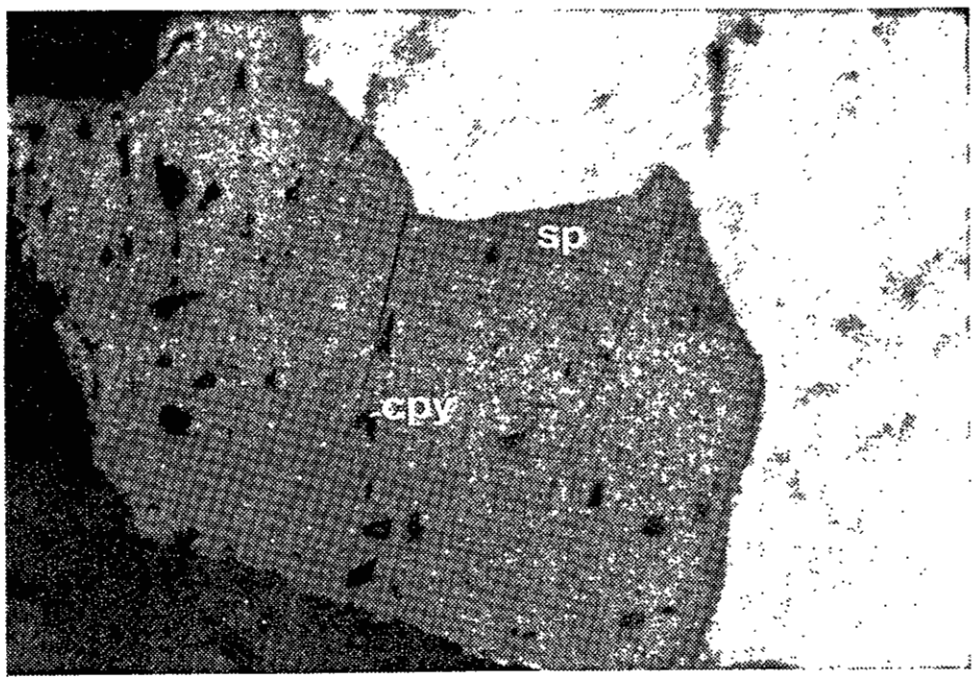

Figure 4.5—Photomicrograph of chalcopyrite disease in sphalerite, Carlisle mine. The chalcopyrite occurs as bright blebs within the sphalerite (sp). From drill hole H5 (depth of 52.1 m). Field of view is 0.325 mm.

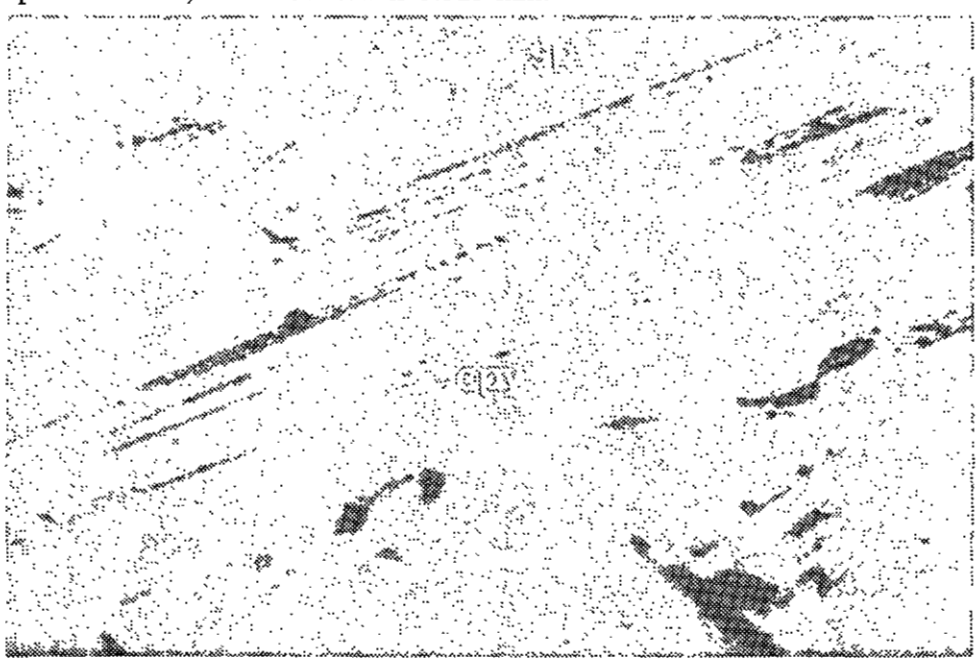

Figure 4.6—Photomicrograph of chalcopyrite disease in sphalerite. From drill hole H13 (depth of 30 m). Field of view is 0.325 mm.

estimated to occur in some sphalerites. Chalcopyrite disease is common in epithermal vein deposits and additional studies suggest that this disease is a result either of replacement as copper-rich fluids react with sphalerite after formation or of epitaxial growth during formation with sphalerite (Craig and Vaughn, 1981; Eldridge et al., 1988; Barton and Bethke, 1987; Bortnikov et al., 1991). Pattrick et al. (1993) suggest that this texture is a result of preferential adsorption (irreversible) of copper in response to repetitive changes in fluid pH and temperature. Barton and Bethke (1987) have also suggested that the rods and blebs of galena may result from similar processes.

In other samples from Steeple Rock, sphalerite is intergrown with chalcopyrite, galena, and pyrite (Fig. 4.7), suggesting coprecipitation locally occurred (Bortnikov et al., 1991; Kojima, 1992).

4.1.1.4 Chalcopyrite, $CuFeS_2$—Chalcopyrite is common as massive aggregates and intergrowths with galena, sphalerite, and pyrite only in the base-metal veins along the Carlisle fault. Up to 10% chalcopyrite is locally present. Chalcopyrite also is found in lesser amounts (typically less than 5%) in gold-silver and copper-silver veins. It occurs as small disseminations or aggregates, typically microscopic, in the silver-gold veins and as small disseminations commonly surrounded by secondary copper minerals in the copper-silver veins. The presence of chalcopyrite is confirmed by XRD (Appendix 11.3) and chemical assays (Appendix 11.5, 11.6).

Chalcopyrite is included in sphalerite (Figs. 4.5, 4.6) and rarely galena. It locally fills fractures in pyrite, galena, and sphalerite. An EDS x-ray spectrum of chalcopyrite from the Center mine shows no impurities (Fig. 4.8; Wilson et al., 1993). Locally, some zones of only chalcopyrite and pyrite occur in both base-metal and gold-silver veins. Elsewhere, chalcopyrite occurs with other sulfides. Copper was produced from many gold-silver and copper-silver deposits and probably occurred as chalcopyrite (Table 3.2). Some chalcopyrite is altered to or coated by secondary copper minerals and iron oxides.

4.1.1.5 Galena, PbS—Galena is common as massive aggregates and intergrowths

Figure 4.7—Photomicrograph of intergrown sphalerite (sp), chalcopyrite (cpy), and galena (ga), Center mine. Field of view is 0.325 mm.

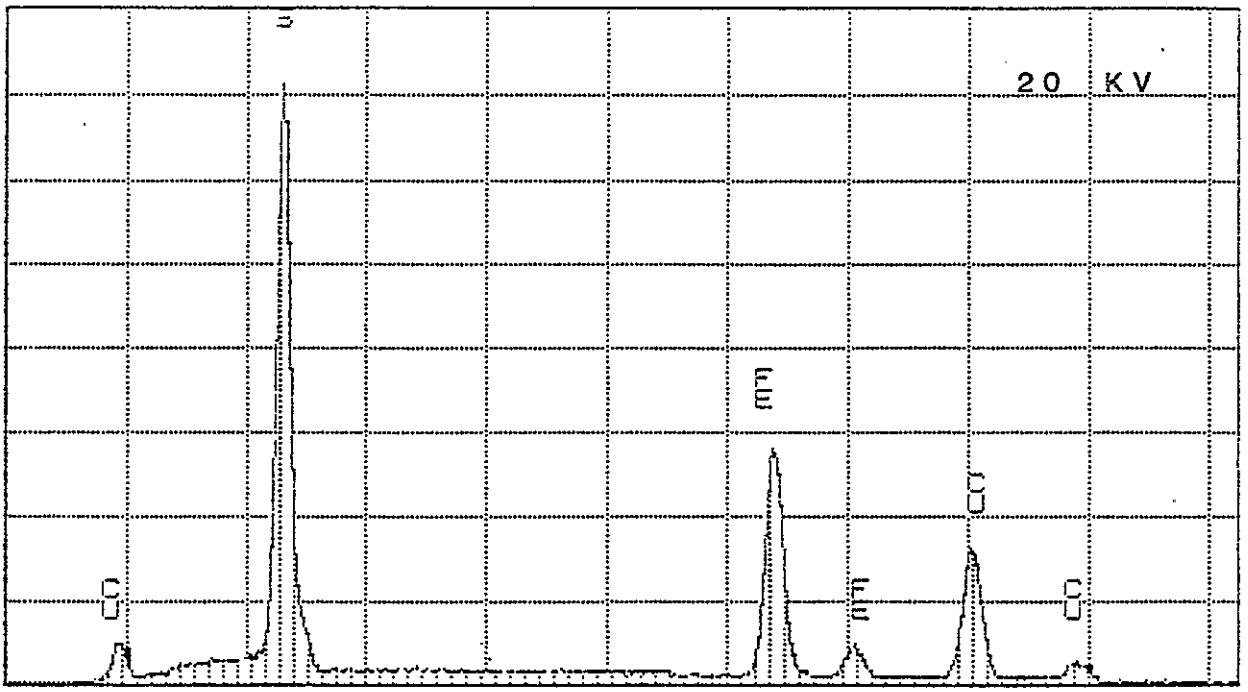

Figure 4.8—EDS x-ray spectrum of chalcopyrite from the Center mine.

with sphalerite, chalcopyrite, and pyrite only in the base-metal vein deposits along the Carlisle fault. It is rare in gold-silver veins where it occurs as fine-grained disseminations or thin black streaks in the quartz breccias. Galena also occurs in thin black streaks and as small disseminated aggregates in silicified and bleached andesite in drill hole M91-4 (Fig. 4.9). As much as 10% galena occurs in some ore shoots in base-metal veins, whereas galena rarely exceeds 1% in gold-silver veins. XRD patterns and chemical assays confirm the presence of galena in many deposits (Appendix 11.3, 11.5, 11.6). Despite the low concentrations, lead was produced as a byproduct from some gold-silver veins and probably occurred as galena (Table 3.2).

Galena is locally included in pyrite and sphalerite and locally fills fractures in pyrite (Fig. 4.10; Wilson et al., 1993). Some galena is cut by thin veinlets of chalcopyrite and sphalerite. Galena in gold-silver veins typically occurs as small monominerallic grains or intergrowths with sphalerite or pyrite.

An EDS x-ray spectrum of galena from the Center mine indicates that the galena contains few impurities of iron and silver (Fig. 4.11). However, assay data indicate a strong to moderate correlation locally between silver and lead, suggesting that argentiferous galena may be locally common.

4.1.1.6 Fluorite, CaF_2—Fluorite occurs as an ore mineral in fluorite veins in several areas of the Steeple Rock district; specifically the Rattlesnake, Goat Camp Springs, Foothills fault (Daniels Camp), West Bitter Creek (Mohawk-Black Willow), and East Bitter Creek (Powell-Leta Lynn) areas (Map 2). Numerous fluorite veins and breccia zones are found throughout the entire depth of drill hole BCl (at least nine zones to a depth of 670.2 m, Appendix 11.1).

Fluorite occurs in veins, pods, breccia cement, and cubes and octahedrons in vugs and other open-spaces. Some zones are up to 2 m wide. Fluorite is typically colorless to white to yellow to green to blue and is locally stained black (manganese oxides) or red to brown (iron oxides). Fluorite also occurs in amygdules in the lava flows of Crookson Peak in the

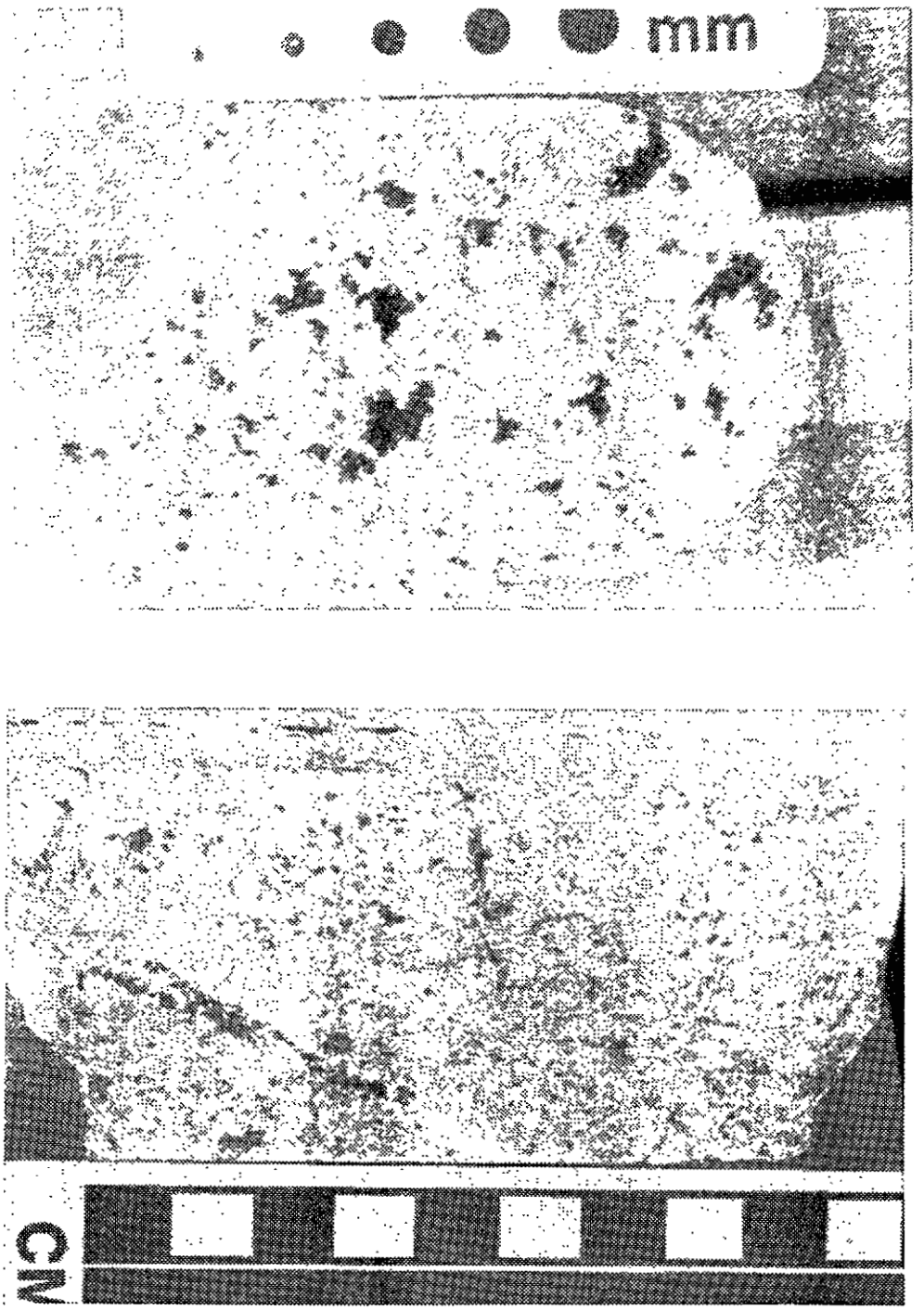

Figure 4.9—Galena disseminations and thin black veinlets within silicified and bleached andesite in drill core M91-4 (depth is 467 m), Summit vein. Drill core is 5 cm in diameter.

Figure 4.10—Photomicrograph (reflected light) of galena (ga) in pyrite (py). Grain is 0.2 mm in diameter. A polished grain mount from the Center mine (photographed by Marc Wilson).

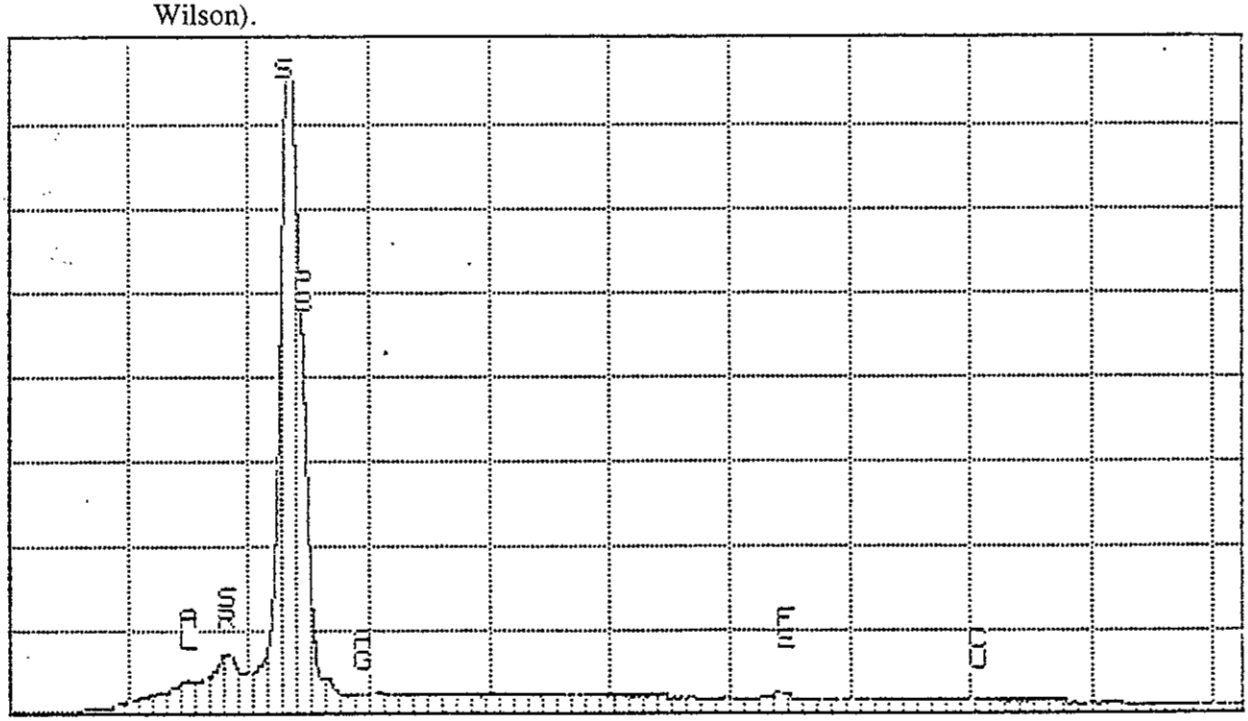

Figure 4.11—EDS x-ray spectrum of galena, Center mine.

northeastern portion of the area (Biggerstaff, 1974). It occurs as fine- to coarse-grained masses, disseminations in host rock and within bladed quartz and calcite. Brecciated, ribbon textures, and crustiform textures are common. Other minerals associated with these veins include pyrite, barite, calcite, and clay minerals.

Whereas Meeves (1966) reports the occurrence of as much as 100 ppm Be in some veins, and Trace (1947) reports the occurrence of as much as 1.97% WO_3 in some veins; these elements were not analyzed in this study. However, manganese and iron oxides are common and some veins contain minor amounts of mercury, up to 0.2 ppm (Appendix 11.5).

4.1.1.7 Other minor ore minerals and secondary minerals—This section contains a short description of other minor ore minerals and secondary ore minerals that occur in the Steeple Rock district. The minerals are arranged in alphabetical order and some minerals (designated by *) are suspect in their identification. Additional mineralogical work is needed because only field, petrographic and XRD studies were completed.

Anglesite, $PbSO_4$—Anglesite occurs as rare secondary coating or alteration of galena in base-metal veins. It forms a white to gray coating on galena. It is a secondary mineral in the Steeple Rock district that occurs in the near-surface, oxidized portions of base-metal veins.

Azurite, $Cu_3(OH)_2\ (CO_3)_2$—Azurite occurs as secondary, blue coatings and poorly developed crystals on quartz and other minerals in base-metal, gold-silver, and copper-silver veins in the Steeple Rock district. It typically occurs with malachite, chalcopyrite, and other copper minerals (Appendix 11.3). It occurs in the oxidized, near-surface portions of the veins, although some drill-core samples from the Carlisle and Center mines do locally contain azurite coating chalcopyrite.

Bornite, Cu_5FeS_4—Bornite is found in the base-metal and some copper-silver veins in the Steeple Rock district. It occurs as iridescent blue-purplish coatings on and alteration of chalcopyrite or chalcocite. It is a secondary mineral in the Steeple Rock district that occurs in the near-surface, oxidized portions of the base-metal and copper-silver veins.

Cerussite, $PbCO_3$—Cerussite is a common secondary, gray to black coating on galena

in the base-metal veins and some gold-silver veins (Appendix 11.3). It even occurs in some samples from the USBM drill core (#H10-279-279.8, Appendix 11.3). It occurs in the oxidized, typically near-surface portions of veins in the Steeple Rock district and indicates the presence of galena.

Chalcanthite, $CuSO_4 \cdot 5H_2O$—Crusts and fibers of blue to blue-green to green chalcanthite occur along the walls of many underground workings in the Steeple Rock district. The most abundant occurrence is in the Carlisle adit where chalcanthite forms crusts on the walls up to 10 centimeters thick. Crystals are fibrous and fragile. Chalcanthite is a recent, secondary mineral in the Steeple Rock district that indicates recent movement of acidic, copper-bearing waters. Water in the Carlisle mine has a pH of 2.5–3.5 (J. McLemore, unpubl. report, March, 1993).

Chalcocite, Cu_2S—Chalcocite occurs locally in base-metal and copper-silver veins in the Steeple Rock district (Griggs and Wagner, 1966; Gillerman, 1964). Thin bluish-black coatings of chalcocite occur on chalcopyrite in the Carlisle and Center mines. No crystals or aggregates have been found. Chalcocite in the Steeple Rock district is a secondary mineral that occurs in the oxidized portions of base-metal and copper-silver veins.

Chrysocolla, $(Cu,Al)_2H_2Si_2O_5(OH)_4 \cdot nH_2O$—Chrysocolla is a rare mineral in copper-silver and base-metal veins in the Steeple Rock district. It is green to bluish-green, translucent to opaque, vitreous to dull luster, and occurs as coatings, incrustations, and rare botryoidal aggregates up to 1-2 cm across. Locally, it may have been mined for use as turquoise. It typically occurs on quartz, malachite, or other copper minerals, although it also occurs alone as thin, fracture coatings. It occurs in the near-surface portions of veins in the Steeple Rock district. Identification by XRD is confirmed in some samples (#708, 963, Appendix 11.3).

Covellite, CuS—Covellite occurs as an alteration or coating of chalcopyrite and chalcocite in the base-metal and some gold-silver veins. It is indigo-blue to black and iridescent. It is a secondary mineral in the Steeple Rock district that occurs in the oxidized, near-surface portions of the veins.

Cuprite, Cu_2O—Cuprite occurs as thin, secondary, red to red-brown coating on chalcopyrite in base-metal veins. It is bluish-white in reflected light in polished sections and is an alteration of chalcopyrite. Only one sample that was x-rayed (XRD) contained cuprite (#H9.367.6; Appendix 11.3). Cuprite is a rare, oxidized mineral in the Steeple Rock district.

Malachite, $Cu_2(OH)_2(CO_3)$—Malachite is common in many base-metal, copper-silver, fluorite, and gold-silver veins in the Steeple Rock district. It occurs as green coating and prismatic or fibrous crystals on quartz or fracture surfaces. Some coatings are up to 1-2 cm thick. Malachite is typically intergrown with and difficult to distinguish from pseudomalachite. Malachite in the Steeple Rock district locally is distinguished from pseudomalachite by a lighter green color and earthy appearance or no luster. Identification is confirmed by XRD (Appendix 11.3). Malachite occurs in all copper-silver veins. It also occurs as fracture coatings and amygdules in andesite in several areas of the district (Biggerstaff, 1974). Such occurrences found east of Twin Peaks led to core drilling of a 650-m-deep hole. The core contained pyrite but low gold, silver, and copper values (Biggerstaff, 1974). Malachite in the Steeple Rock district occurs in the near-surface, oxidized portions of the veins and as fracture coatings locally along faults in andesite throughout the district.

Manganese oxides—Manganese oxides are common throughout the Steeple Rock district as fracture coatings and thin veinlets. They typically coat other vein minerals, although locally they are intergrown with white to black calcite. Various manganese minerals are present; manganosite MnO and pyrolusite MnO_2 are identified by XRD (Appendix 11.3). Most of the manganese oxides are probably psilomelane (romanechite) $BaMnMn_8O_{16}(OH)_4$. Manganese oxides are typically black, opaque, massive, and hard to soft, depending on amount of silicification. Manganese was mined at the Black Cat mine.

Mimetite, $Pb_5(AsO_4,PO_4)_3Cl$—Mimetite is a common secondary yellow to brown coating on samples containing sulfides and detectable gold and silver assays. One sample from the Near Years Gift vein (#257a, Appendix 11.3) consisted of small (1-3 mm), yellow plates or tabular crystals on quartz breccia. Numerous samples contain mimetite detectable by XRD

(Appendix 11.3). It occurs in the oxidized, near-surface portions of the vein deposits in the Steeple Rock district and indicates a good possibility of detectable gold and silver values.

Mottramite, $(Cu,Zn)Pb(VO_4)(OH)$—Mottramite is common as a secondary, yellow-green coating on samples that contain detectable gold and silver concentrations. A sample from a vein south of Saddleback Mountain (#600, Appendix 11.3) contains mottramite on quartz breccia with illite, kaolinite, and pyrite. In the Steeple Rock district, mottramite occurs in the oxidized, near-surface portions of the veins.

Nantokite, CuCl—Nantokite occurs as a secondary coating or alteration of copper minerals in base-metal veins along the Carlisle fault. It typically occurs as thin white to whitish-blue coatings or granular aggregates on quartz and copper sulfides. It is identified primarily by XRD (Appendix 11.3). In the Steeple Rock district, it occurs as a secondary mineral in the oxidized, near-surface portions of base-metal veins.

Pseudomalachite, $Cu_5(PO_4)_2(OH)_4 \cdot H_2O$—Pseudomalachite is common in all types of vein deposits except the manganese veins in the Steeple Rock district. It occurs as green coatings or needle or radiating fibrous crystals and is typically associated with malachite. It occurs as fracture coatings, intergrown with malachite, and crystals and coatings on quartz and calcite. In the Steeple Rock district, identification of pseudomalachite is by XRD (Appendix 11.3), although locally it forms darker, brighter green, and more vitreous crystals than malachite. In the Steeple Rock district, pseudomalachite occurs in the oxidized, near-surface portions of the veins.

***Tennantite, $(Cu,Ag,Zn,Fe)_{12}(As,Sb)_4S_{13}$**—Tennantite may occur in two samples according to XRD patterns (#755, B91-17-534-535; Appendix 11.3). Typically tennantite is a less common mineral, but locally is abundant in hydrothermal vein deposits (Anthony et al., 1990). The XRD patterns are not conclusive, but it is possible that tennantite may occur in gold-silver veins in the Steeple Rock district.

***Tetrahedrite, $(Cu,Fe)_{12}Sb_4S_{13}$**—Tetrahedrite is reported in veins in the Steeple Rock district by Gillerman (1964) and W. Baum (unpubl. report, March 31, 1988). Its occurrence

in the district could not be confirmed in this study.

***Wulfenite, $PbMoO_4$**—While wulfenite is identified by XRD in several drill core samples (Appendix 11.3) from the Steeple Rock district, it was not found in petrographic studies. However, elemental analyses of a few samples indicate several hundred ppm of molybdenum, suggesting that wulfenite may indeed occur in the district. Wulfenite is typically a secondary, oxidized mineral.

4.1.2 Gangue mineralogy

4.1.2.1 Quartz, SiO_2—Quartz is the most common mineral in the Steeple Rock district (Appendix 11.2, 11.3) and is the only mineral phase deposited throughout all periods of alteration and mineralization. Multiple, complex combinations of various textures, as defined by Dowling and Morrison (1989), occur throughout the Steeple Rock district. White, coarse-grained, and barren quartz veins are referred to as buck or bull quartz and rarely contain any impurities. Buck quartz may overlie rich gold-silver deposits, such as along the East Camp fault. Comb quartz, consisting of large, euhedral white to colorless to purple (amethyst) quartz is typically barren of metal values in the Steeple Rock district. Spider quartz veinlets, also barren, commonly cut white to gray to green chalcedonic to microcrystalline quartz which is also barren of mineralization. Recrystallized chalcedony or amorphous silica occurs also as small turbid, spheroidal fragments interstitial to vein quartz and is locally associated with gold and silver assays. Locally these chalcedonic fragments form triple-point grain boundaries typical of recrystallized amorphous silica (Herrington and Wilkinson, 1992). Gold and silver in the Steeple Rock district is typically associated with banded (crustiform and coloform), rhythmically-layered, and breccia quartz, although quartz veins displaying these textures may on occasion be barren of gold and silver. Banded and rhythmically-layered quartz consists of hundreds of thin bands or layers of quartz interlayered with thin black bands or streaks of sulfides (pyrite, galena, chalcopyrite, and/or sphalerite; Fig. 3.6). Veins displaying this texture typically carry gold and silver. Multiple periods of brecciation,

cementation by quartz, and rebrecciation are characteristic of the gold, silver, and base-metal veins in the Steeple Rock district (Fig. 4.12). The best grades appear to occur in areas of greatest textural complexity where multiple generations of quartz, chalcedony, and other minerals were deposited.

In thin section, quartz typically occurs as clear, euhedral crystals containing numerous fluid inclusions and the crystals are locally fractured (Fig. 4.13). Sutured and overgrowth boundaries are common as is locally strained quartz with undulatory extinction, which may represent recrystallized chalcedony or amorphous silica (Fig. 4.13; Sander and Black, 1988; Herrington and Wilkinson, 1992). Quartz typically contains many fluid inclusions and some quartz contains larger concentrations of inclusions along the crystal edges than in the crystal cores (Fig. 4.13). Growth zones are rare.

Most quartz is white to colorless. Local staining and dissolution of impurities or large accumulations of fluid inclusions may alter colorless quartz to shades of brown and black. Amethyst quartz (purple) is locally common and is found in both barren and mineralized veins. Bladed quartz, pseudomorphed after bladed calcite, forming a lattice texture is also common locally, especially along the East Camp-Summit fault (Fig. 4.14).

All of these characteristics are consistent with an epithermal origin (Dowling and Morrison, 1989).

4.1.2.2 Calcite, $CaCO_3$—Calcite is variable in distribution in the Steeple Rock district. Large, white to colorless to tan, bladed calcite occurs along the East Camp-Summit, Bluebell, and Norman King-Billali faults. Bladed calcite is commonly replaced by quartz (Fig. 4.15) and both are found throughout the various drill holes along these faults (Fig. 4.14). Bladed calcite and bladed quartz after calcite are indicative of boiling zones within modern geothermal fields; this process is further described in section 6.2.1.

Calcite is vertically zoned at the Summit mine. At the surface south of the Inspiration

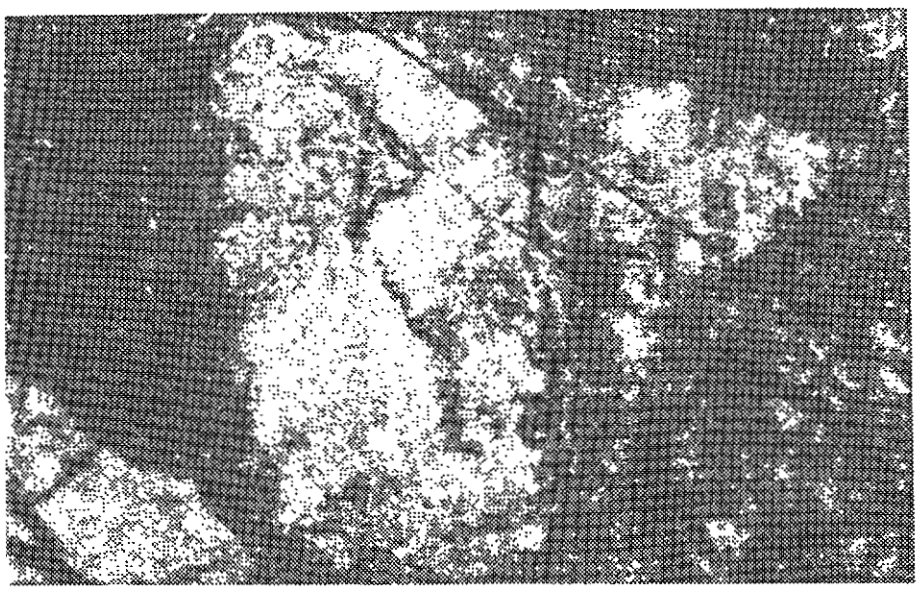

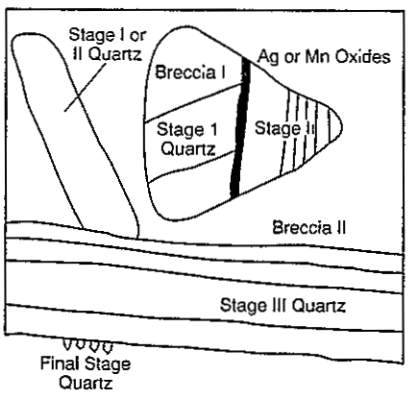

Figure 4.12—Photographs and sketch of brecciated quartz showing three periods of brecciation, from the East Camp vein.

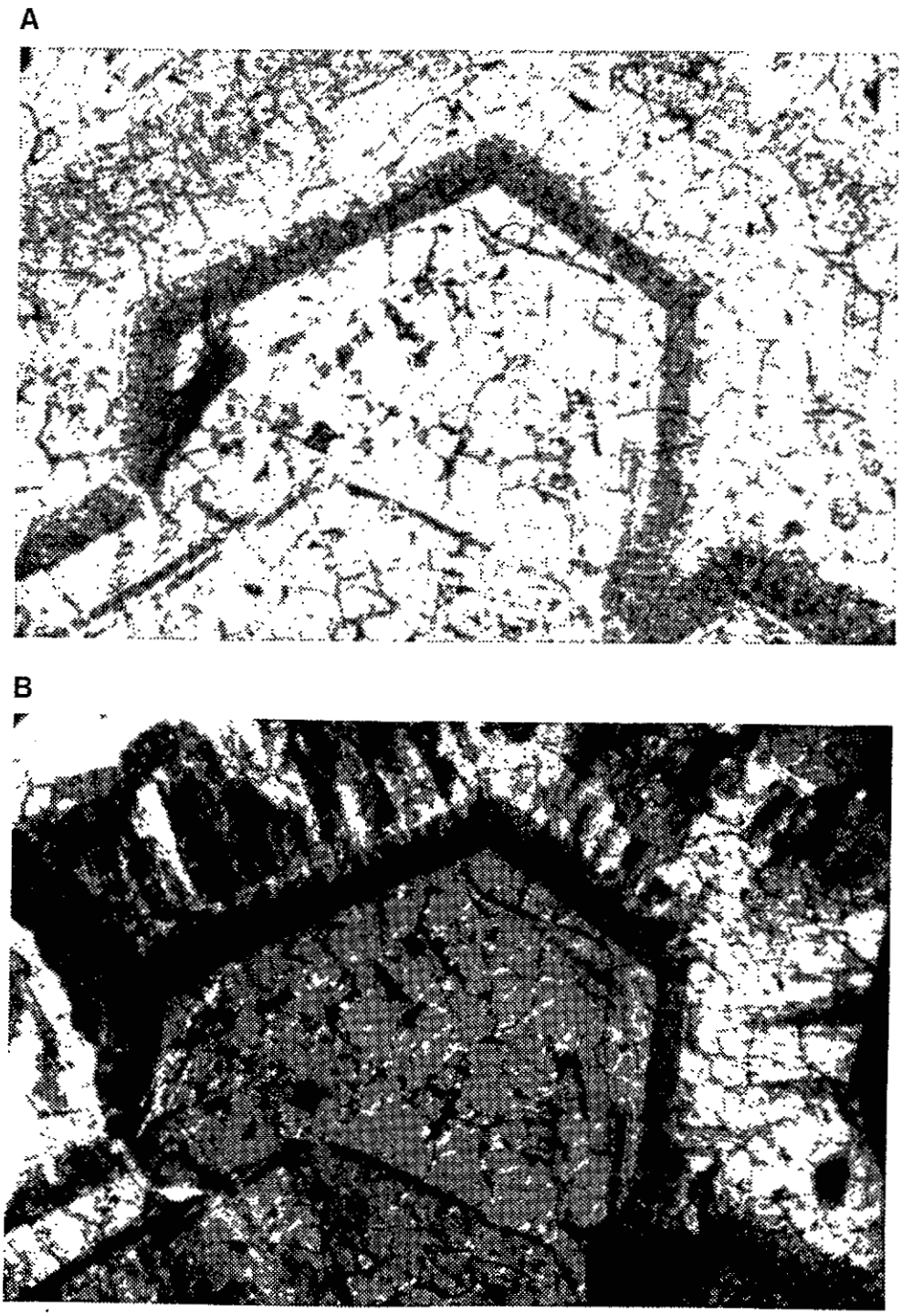

Figure 4.13—Photomicrographs of vein quartz with zones of small fluid and gas inclusions. Sample from the East Camp vein. Field of view is approximately 0.5 mm. A) Plane light. B) Crossed nicols. Note overgrowth of strained quartz with undulatory extinction.

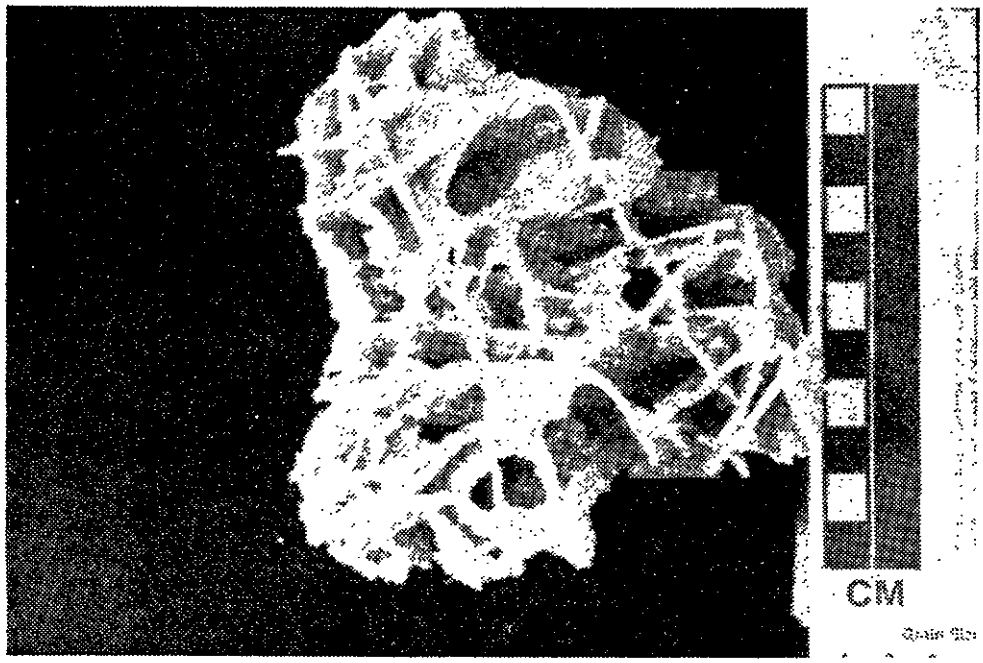

Figure 4.14—Bladed quartz after calcite. Sample from the Summit vein near the Bank mine.

Figure 4.15—Bladed calcite in drill core. Sample is approximately 6 cm across and from drill hole B91-17 (depth of 358 m).

and Apex adits, the vein consists of approximately 50% calcite, mostly forming the center of the vein. The outer edges are quartz. In the Inspiration and Apex adits, the vein consists of less than 25% calcite, whereas drill holes immediately beneath the workings failed to intersect any calcite. However, north of the adits, bladed calcite is found in veins at depths of 358 m in drill hole B91-17, but constitutes less than 10% of the vein. It appears that in the Summit vein calcite decreases with depth.

Black calcite is common in the Goat Camp Springs and Foothills fault areas and is associated with manganese oxides. Southeast of the Summit mine, a zone of black calcite and manganese oxides crops out along the East Camp-Summit fault. Some calcite is intergrown with manganese minerals, whereas other calcite is coated with manganese minerals.

Elsewhere in the district, clear to white calcite is locally present but rarely in large concentrations, typically less than a few percent. Distinct rhombohedrons of calcite crystals are rare and most calcite is massive.

4.1.2.3 Pyrite, FeS_2—Pyrite is the most abundant sulfide mineral in the Steeple Rock district. It occurs in all three stages of silicification and cementation of the vein deposits. It occurs in all five types of vein deposits and is disseminated throughout the host rocks. It is prevalent throughout most of the drill core and ranges in abundance from trace to 40% (Appendix 11.1). Pyrite grain size is variable from several microns to 1-2 cm, and typically occurs as euhedral to subhedral cubic crystals or irregular aggregates disseminated throughout the host rock. In the veins, pyrite occurs as (1) euhedral to subhedral cubic crystals or irregular aggregates disseminated throughout the vein quartz (Fig. 4.16); (2) streaks of aggregates of pyrite and other sulfides forming thin layers in the veins, or (3) irregular aggregates and intergrowths locally associated with other sulfides. An EDS x-ray spectrum of pyrite from the Center mine exhibits the purity of some pyrite (Fig. 4.17). In other sampled pyrite, solid inclusions and intergrowths of other minerals are present. Pyrite locally contains small inclusions of quartz, and fractures are locally healed by quartz, galena, sphalerite, and chalcopyrite. Pyrite also occurs intergrown with other sulfides and locally fills fractures in

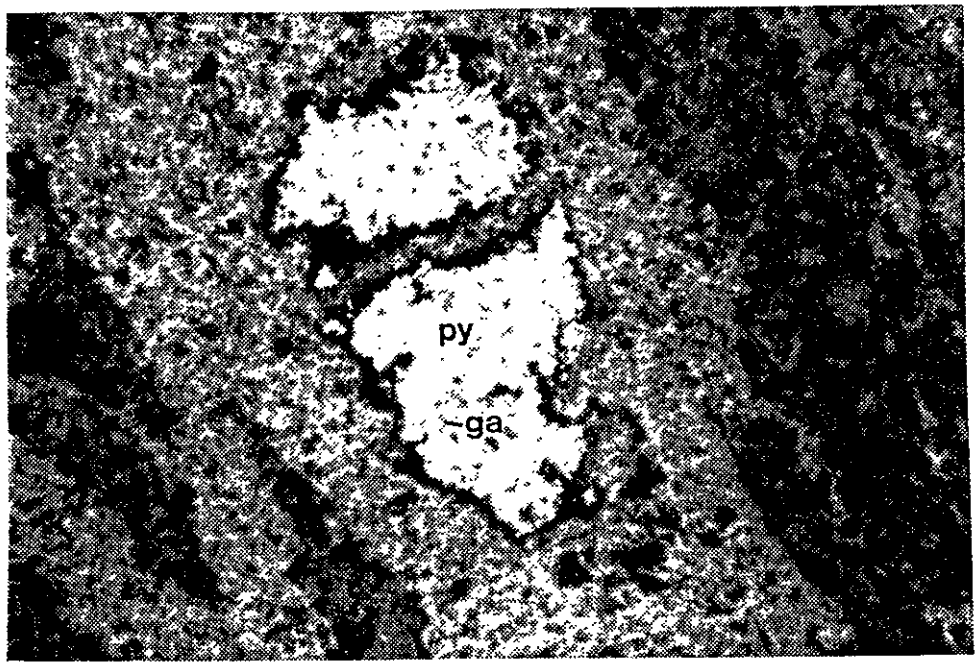

Figure 4.16—Irregular aggregate of pyrite within and cut by vein quartz. Note small inclusion of galena within pyrite grain. Field of view is approximately 0.5 mm. Sample is from the Alabama vein.

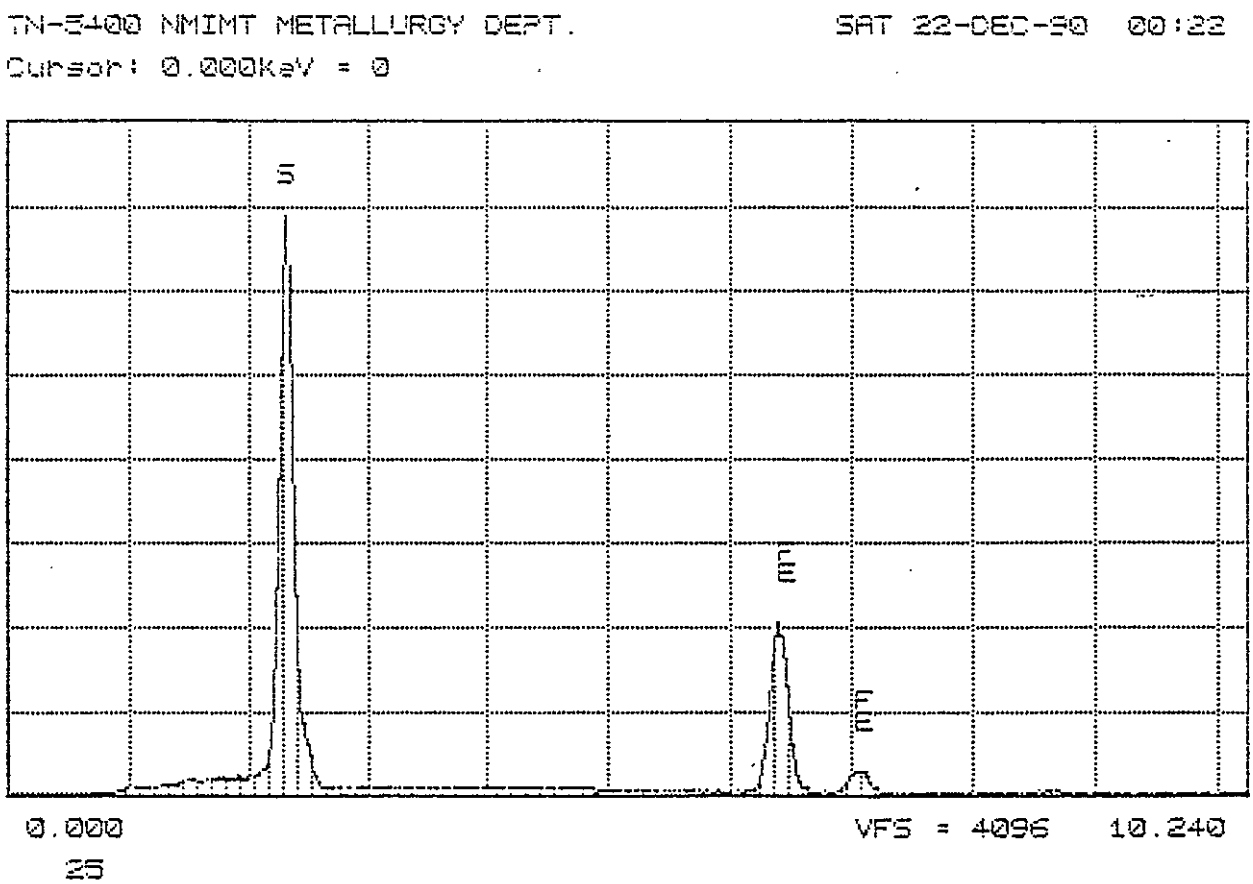

Figure 4.17—EDS x-ray spectrum of pyrite from the Center mine (20 kv).

chalcopyrite grains.

4.1.2.4 Adularia, $KAlSi_3O_8$—Adularia is a low-temperature variety of K-feldspar that is characteristic of epithermal deposits (Hayba et al., 1985). It is difficult to identify in vein deposits of the Steeple Rock district because it is small in size and intergrown with quartz. In thin section, it resembles quartz and can be distinguished from quartz only by its biaxial optical figure. Most adularia is clear, free of mineral or fluid inclusions, and may exhibit cleavage, whereas most quartz is clear to cloudy, contains numerous mineral and fluid inclusions, and does not exhibit cleavage. Adularia appears to occur in mineralization stages 2 and 3. Its presence is confirmed by XRD (Appendix 11.3). Locally small veinlets of adularia and quartz cut across early deposited quartz. Adularia content in the veins is low—less than 5%.

4.1.2.5 Clays—Clay alteration near and within veins is common. Typically kaolinite with illite and locally illite/smectite occurs near the surface. Illite is common in the deeper portions of the veins. Areas with two or more veins are typically altered to quartz and illite between the veins. Chlorite is also common in the host rock and in breccia fragments. In the Carlisle and Center mines, primary chlorite occurs within the veins and is a guide to ore zones. However, crosscutting relationships indicate that chlorite precipitated before or after the sulfides. Typically illite/smectite and smectite/chlorite forms zones or halos surrounding the veins. More data and details on alteration follow in Chapter 5.

4.1.2.6 Fluorite, CaF_2—Fluorite occurs as a gangue mineral in base-metal and gold-silver vein deposits along the Carlisle and Norman King-Billali faults. Small fluorite cubes and octahedrons, less than one millimeter across, occur in vugs and open spaces. The crystals are white to yellow to colorless and occur on quartz and sulfides. Locally, iron and/or manganese oxides coat the fluorite. Total fluorite concentrations rarely exceed 1-2% in these areas of the deposits.

Fluorite in the precious-metal veins is undesirable because the smelters in the area (Phelps Dodge and ASARCO) have very low limits on fluorine. Ores containing more than

0.5% may be rejected by the smelter. Fluorine is undesirable in the smelting process at local smelters and also is a pollutant to the atmosphere.

4.1.2.7 Manganese, titanium, and iron oxides—These oxides are relatively common throughout the vein deposits and altered rocks. They form alteration coatings and fracture fillings and locally form cement in the volcaniclastic sedimentary rocks. In thin sections, these oxides are typically prevalent and represent the oxidation of manganese, titanium, and iron-bearing minerals. Various manganese minerals are present: manganesite MnO, pyrolusite MnO_2, psilomelane (romanechite) $BaMnMn_8O_{16}(OH)_4$, and probably others. Titanium oxides present include rutile TiO_2, anatase TiO_2, leucoxene TiO_2, brookite TiO_2, pseudobrookite Fe_2TiO_5, and titanite (sphene) $CaTiSiO_5$ as determined by XRD (Appendix 11.3). Iron oxides include hematite Fe_2O_3, goethite FeO(OH), limonite $2Fe_2O_3 \cdot 3H_2O$, and ilmenite $(Fe,Mn)TiO_3$. Euhedral crystals are rare if even present. Irregular masses and aggregates of two or more oxides, locally with cores of the original mineral, are common.

4.1.2.8 Other gangue minerals—This section contains a short description of other minor gangue minerals that occur in the Steeple Rock district. They are arranged in alphabetical order and some minerals (designated by *) are suspect in their identification. Additional mineralogic work is needed.

Aragonite, $CaCO_3$—Aragonite occurs in some deeper level veins and is confirmed by XRD.

Dolomite, $CaMg(CO_3)_2$—Small (several millimeters) pink to tan to white rhombohedrons of dolomite occur in vugs and on quartz and other minerals. Its identification is confirmed by XRD. Rare veinlets of dolomite cut older veins. It is a late stage mineral.

Jarosite, $KFe_3(OH)_6(SO_4)_2$—Jarosite has been confirmed by XRD in some samples (Appendix 11.3). It is fine-grained and occurs with iron oxides. It is probably a result of oxidation of pyrite.

Marcasite, FeS_2—Some pyrite may be altered to marcasite. Marcasite has a strong anisotropy compared to pyrite, which is evident in some polished thin sections. Also some

XRD patterns suggest that marcasite may be present (Appendix 11.3).

***Pyrrhotite, $Fe_{1-x}S$**—Pyrrhotite may be present according to XRD data (Appendix 11.3). It is probably associated with pyrite and is not a major constituent.

Rhodochrosite, $MnCO_3$—Rhodochrosite is confirmed by XRD in some veins. It is probably late stage.

4.2 Fluid Inclusion Studies

4.2.1 Sample selection and measurements

Fluid inclusion studies provide data on the temperature, composition, and pressure of the mineralizing and later fluids and the variation of these properties in space and time. There are five major assumptions which must be considered when interpreting fluid inclusion data (Roedder and Bodner, 1980):

1) The fluid trapped was a single, homogeneous phase at the time of trapping.
2) The cavity in which the fluid resides has not changed volume.
3) The fluid has not changed composition.
4) The effects of pressure are insignificant or are known.
5) The origin of the inclusions is known.

These assumptions and various tests for their validity are discussed by Roedder and Bodner (1980), Roedder (1984), and Shepherd et al. (1985) and were applied in this study where appropriate.

Samples for fluid inclusion microthermometric measurements were selected from vein quartz, fluorite veins, and sphalerite disseminated in quartz veins. Surface samples, samples from underground workings, and samples of drill core were used. Doubly-polished thick sections of vein material plus cleavage fragments of fluorite were examined according to methods described in section 1.5.6.

Inclusions were identified as primary, pseudosecondary, and secondary according to the criteria of Roedder (1984). Primary and pseudosecondary inclusions are difficult to find in

many samples and any inclusions which did not adhere to the criteria of Roedder (1984) were assumed to be secondary. Microthermometric measurements were made on all three types of inclusions in order to better define the distribution of the measurements. Many inclusions, especially primary inclusions, are too small to measure last-ice melting temperatures; therefore salinities were not calculated for many inclusions.

Inclusions demonstrating evidence of leakage and necking down (Roedder, 1984; Shepherd et al., 1985) were not used in microthermometric measurements. Wherever possible, a statistically valid sample population of 30-40 inclusions was measured for each specific sample (Shepherd et al., 1985). However, the number varies because of lack of inclusions suitable for study or the variations in temperatures were small enough that a statistically valid sample population of fewer inclusions could be obtained. Many samples examined during the early stages of this study have a large number of measurements because of limited familiarity and expertise in the experimental procedures, and general trends of distributions of data for each type of inclusion which were required.

Fluid inclusions suitable for study are rare to absent in calcite, adularia, and malachite from Steeple Rock. The inclusions tend to be small (less than 3 μm), rod shaped, and show evidence of necking. Therefore these inclusions are unsuited for microthermometric measurements.

Fluid inclusions are also rare to absent in the altered rocks, even in quartz veinlets. Where formed, the inclusions tend to be small (less than 5 μm) and consist of either only liquid or liquid plus a small vapor bubble. These inclusions are difficult to impossible to obtain meaningful microthermometric measurements. Furthermore, studies have shown that fluid inclusions in silicified rocks within epithermal systems may not provide any meaningful data (Fournier, 1985a; Sander and Black, 1988). In the Steeple Rock district, it is sometimes difficult to determine the origin of the silica, much less determine the origin of the inclusions. Some of the quartz in the silica-altered zone may have been originally deposited as amorphous silica that was subsequently converted to chalcedony then to quartz. Much of the quartz in the

intermediate- and clay-altered zone is probably either silica residue or recrystallized quartz. It is impossible to determine what stage of fluids the fluid inclusions represent: (1) during original deposition, (2) after crystallization, (3) during the time of deposition of amorphous silica that was later remobilized during the transformation to quartz, or (4) much later fluids (Fournier, 1985a). Therefore microthermometric measurements of fluid inclusions in the altered rocks were not made.

4.2.2 Characteristics of fluid inclusions

Three types of fluid inclusions are found in quartz, fluorite, and sphalerite: liquid plus vapor, liquid, and vapor. No daughter minerals were found in any inclusions examined. The most-abundant type of inclusions found are two-phase inclusions: liquid plus vapor. The vapor phase accounts for 5 to 30% of the total inclusion volume, using the visual estimation charts of Roedder (1984). The inclusions are suboval to irregular to prism shaped and range in size from less than 3 μm to 100 μm (Fig. 4.18). Most inclusions are less than 15 μm. Many inclusions in fluorite retain a negative crystal shape (Fig. 4.19). The liquid and vapor inclusions are typically suboval to irregular in shape and less than 10 μm. Some vapor inclusions may actually be two-phase inclusions with a liquid phase of less than 15%. However, because of their small size, it is difficult to determine with any certainty if any liquid was present (Shepherd et al., 1985).

Primary inclusions occur as isolated inclusions, small clusters, or planes of hundreds of inclusions along growth zones. Typically inclusions along growth zones are less than 1 μm and not suited for microthermometric measurements (Fig. 4.13). Secondary inclusions occur as planes of tens to thousands of inclusions of all sizes along healed fractures. Pseudosecondary inclusions occur as tens to hundreds of inclusions along healed fractures that terminate within the crystal, typically at growth zone boundaries and represent fluid trapped within fractures during the crystal growth (Roedder, 1984).

Fluid inclusions are common in quartz from the Steeple Rock district, although not all

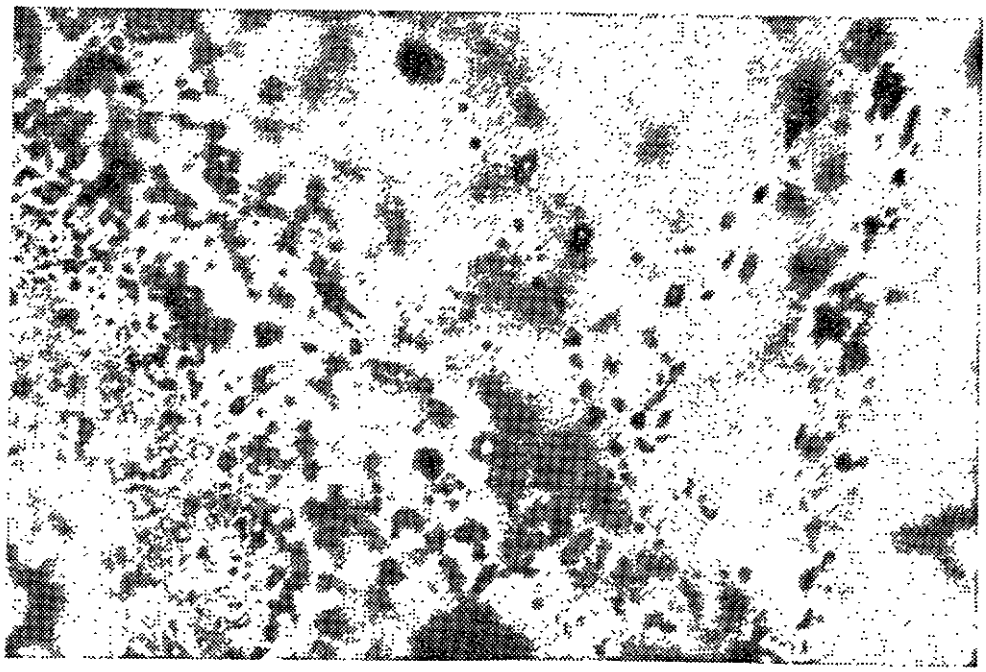

Figure 4.18—Photomicrograph of fluid inclusions in quartz. These inclusions are approximately 3 μm in diameter.

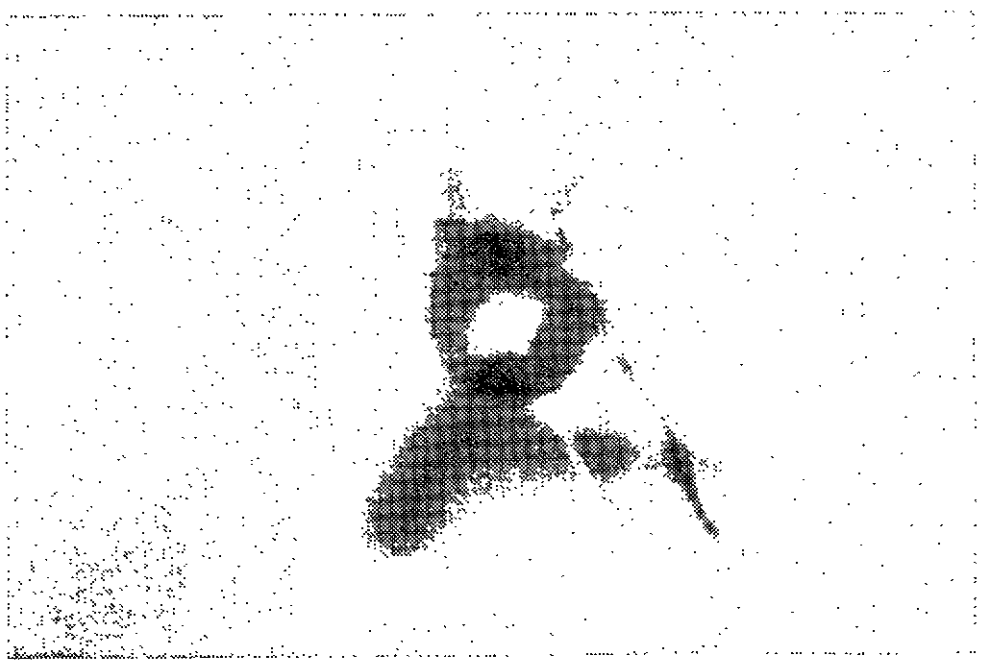

Figure 4.19—Photomicrograph of fluid inclusion retaining a negative crystal shape in fluorite. Fluid inclusion is approximately 15 μm across.

samples contain primary inclusions suitable for microthermometric measurements. Fluid inclusions are rare in sphalerite, especially where the sphalerite displays chalcopyrite disease (i.e. small solid mineral inclusions of chalcopyrite within larger sphalerite crystals). The sphalerites examined in this study typically are honey yellow to light brown in color. Dark brown to black sphalerite is too opaque to allow examination of fluid inclusions. Most fluorite contains numerous secondary inclusions and lesser numbers of primary inclusions.

Only a few samples contained coexisting liquid-rich and vapor-rich inclusions, but these inclusions were typically too small to be measured. Also it was difficult to determine if these inclusions were of the same fluids; most were secondary inclusions. If liquid-rich and vapor-rich inclusions from the same generation of fluids are present in a sample, this is interpreted as evidence of boiling (Roedder, 1984; Shepherd et al., 1985). Fluid inclusion evidence for boiling in the Steeple Rock samples examined is inconclusive.

Geochemical analyses of the gas and liquid composition of the inclusions are beyond the scope of this project. A Masters thesis by Randy Ruff (NMIMT Geoscience Department) indicates that gases indicative of magmatic fluids, such as H_2S, HS, CO_2, and He, are present in some veins in the district (Ruff, 1993; Ruff and Norman, 1991). These gases are found in other epithermal deposits (Ruff and Norman, 1991).

4.2.3 Microthermometric measurements

Temperatures of homogenization (Th) and last-ice melting temperatures (Tm) were measured on fluid inclusions from various parts of the district. Temperatures of homogenization are reported uncorrected for pressure and are assumed to represent temperature of entrapment, which is close to temperature of formation. Pressure corrections are assumed small to none because the minerals were deposited near the surface (see section 6.2.2). The salinity is reported in terms of equivalent weight % NaCl and is obtained by measuring the last-ice melting temperature and converting it to eq. wt.% NaCl by using the equation (Roedder, 1984):

$$W_S = 0.00 + 1.769580 - 4.2384 \times 10^{-2} O^2 + 5.2778 \times 10^{-4} O^3$$

where W_S = equivalent weight % NaCl (eq. wt.% NaCl), O = the freezing point depression (last-ice melting) in °C. The data are graphed for each group of mines in Appendix 11.7 and summarized in Tables 4.1, 4.2, and 4.3 and Figures 4.20, 4.21, and 4.22.

4.2.3.1 Quartz—Quartz is the most common mineral in the veins and was deposited continuously before, during, and after sulfide mineralization. Quartz is associated with the sulfide minerals and contains fluid inclusions, and therefore it is assumed that microthermometric measurements of quartz associated with sulfide minerals represents similar temperatures and chemistries as the sulfide minerals. Over 700 primary and secondary inclusions were measured for this study to determine (1) temperature of formation of the various mineral stages, (2) temperature zonations within the district (laterally, vertically, and with time), and (3) composition of the mineralizing fluids (salinity).

Most of the inclusions examined for this study were stage 2 mineralization— i.e. the sulfide deposition event. Samples of quartz deposited prior to the sulfide minerals (stage 1 mineralization) did not contain fluid inclusions large enough for microthermometric measurements. The inclusions, where present, were either too small (< 1 μm in diameter) or were necked inclusions and could not be measured. Some of the stage 1 quartz exhibits textures characteristic of original chalcedony or amorphous silica and fluid inclusion data is meaningless (Sander and Black, 1988).

Several samples of quartz from stage 3 mineralization contained some fluid inclusions suitable for measurements, but microthermometric measurements were similar to those of stage 2 mineralization (Table 4.1). Inclusions were found in one sample of quartz crosscutting acid-sulfate alteration (#341) and temperatures of homogenization were between 190 and 357°C. The origin of these inclusions is unknown but fluid inclusion data support a similar epithermal origin as the epithermal vein deposits.

Locally quartz occurs in the fluorite veins; however, samples of this late stage quartz did not contain any fluid inclusions that were suitable for measurements. Late stage quartz

Table 4.1—Summary of fluid inclusion analyses in quartz. Sample locations on Map 2. *Quartz veins in acid-sulfate altered rocks. †See paragenesis in section 6.5. prim - primary inclusion; sec - secondary inclusion.

Sample	No.	T_H avg	STD	No.	T_M ave	STD	T_H range	Type of inclusion	Ore deposition stage†
CARLISLE VEIN									
Ontario	14	253	50	16	1.7	0.7	150-310	prim, sec	stage 3
Ontario	8	283	21	7	1.9	1	255-310	prim	stage 2
182 (Sec. 2)	35	255	18	--	--	--	191-307	prim, sec	stage 3
400S (Carlisle)	4	262	27	4	0.8	1.5	237-288	prim, sec	stage 2
Center	22	282	29	21	2.1	1.0	227-327	prim, sec	stage 2
CARLISLE-CENTER DRILL CORE (USBM)									
H6-68.5A	24	265	19	24	1.9	0.4	238-306	prim, sec	stage 3
H6-76.8	4	250	5	7	1.7	0.8	245-257	prim, sec	stage 3
H6-196	68	283	21	51	1.9	0.5	244-344	prim, sec	stage 2
H11-34.2	9	242	13	--	--	--	255-270	prim, sec	stage 3
H11-331.2	87	270	17	76	2.6	0.7	234-315	prim, sec	stage 2
H9-497	3	232	13	2	2.3	0	218-243	prim, sec	stage 2
H9-501	27	266	16	21	2.4	0.6	241-313	prim, sec	stage 2
H14-259	44	269	25				237-331	prim, sec	stage 3
H14-315	42	267	26	15	1.4	0.4	234-324	prim, sec	stage 2
H14-344	42	247	18	8	0.9	0.6	197-288	prim, sec	stage 2
EAST CAMP-SUMMIT VEIN									
47 (East Camp)	16	239	9	--	--	--	223-254	prim, sec	stage 3
634 (Thanksgiving)	10	235	12	10	2.8	0.6	215-253	prim, sec	stage 2
McDon Upper	16	256	22	16	1.5	0.8	230-292	prim, sec	stage 2
SUMMIT DRILL CORE									
B91-17-992	1	214.9	--	1	1.4	--	--	sec	stage 2
ALABAMA-IMPERIAL									
231	18	249	10	--	--	--	229-264	prim, sec	stage 2
233	68	246	26	9	1	0.4	134-296	prim, sec	stage 2
310 (Imperial)	47	266	15	4	1.1	0.4	226-311	prim, sec	stage 2
434	3	235	0	--	--	--	235	prim, sec	stage 2
ALABAMA DRILL CORE									
Al-112.5	2	245	--	--	--	--	243-247	prim, sec	stage 2
A1-121	38	260	14	39	1.8	1.2	239.320	prim, sec	stage 2
Al-122	22	251	18	23	2.1	1.4	185-266	prim, sec	stage 2
OTHER									
148	58	244	17	--	--	--	194-321	prim, sec	stage 2,3
341*	3	275	83	--	--	--	190-357	prim, sec	alteration

Table 4.2—Summary of fluid inclusion analyses in sphalerite. All samples are stage 2 mineralization. Fluid inclusions in quartz were also measured (Table 4.1).

Sample	No.	T_H avg	STD	No.	T_M ave	STD	T_H range	Type of inclusion
Center	8	306	12	8	1.1	1.2	288-325	prim, sec
Al.112.5 (Alabama)	1	265.1	--	1	2.8	--	--	prim
B91.17-992	18	190	56	7	1.3	0.8	116-284	prim, sec
(Summit)	1	281	--	--	--	--	278-284	prim
AVG	27	227	71	16	1.3	1	116-325	prim, sec

Table 4.3—Summary of fluid inclusion analyses in fluorite. All samples are late stage mineralization.

Sample	No.	T_H avg	STD	No.	T_M avg	STD	T_H range	Type of inclusion
Mohawk	53	177	39	9	0.9	0.7	148-222	sec
472 (Rattlesnake No. 2)	18	171	5	17	0.6	0.2	163-179.5	sec
473 (Rattlesnake No. 1)	28	176	5	--	--	--	165-185	sec, prim
510 (Ontario)	42	189	15	18	0.8	0.2	171.7-215	sec, prim
516 (Dean)	47	196	15	23	0.8	0.4	103-207	sec
518 (Dean)	12	164	24	12	0.9	0.1	156-239	sec
536 (Dean)	12	194	12	12	0.9	0.5	168-210	prim, sec
538 (Dean)	34	177	20	34	0.6	0.3	150-234	prim, sec
545 (Goat Camp Springs)	18	193	9	18	0.8	0.2	174.7-215	prim, sec
	9	203	8	9	0.5	0.5	195-215	prim
559 (Luckie No. 1)	7	187	8	--	--	--	175-195	sec, prim
Luckie No. 2	15	19	34	--	--	--	188.3-202	prim
Center (6th level)	7	142	33	--	--	--	105-178	sec, prim
1043 (Forbis)	18	196	4	19	0.1	0.3	191.5-210	prim
1041 (Forbis)	11	195	3	10	0.1	0.2	190-198.4	prim
Fourth of July	18	161	9	12	0.5	0.6	141-176	prim
Daniels Camp	25	187	2	7	0.2	0.1	185-190.8	prim
1057 (Black Cat)	8	150	5	2	0.2	0.3	140-155	prim
1003 (Leta Lynn)	15	188	19	8	0.3	0.2	159-229	prim
BCI-271	9	159	33	6	0.6	0.5	102-190	prim
AVG prim	210	181	18	141	0.5	0.4	103-234	prim
AVG sec	188	184	19	103	0.8	0.4	102-239	sec
AVG (all)	398	183	19	227	0.6	0.4	103-239	prim, sec

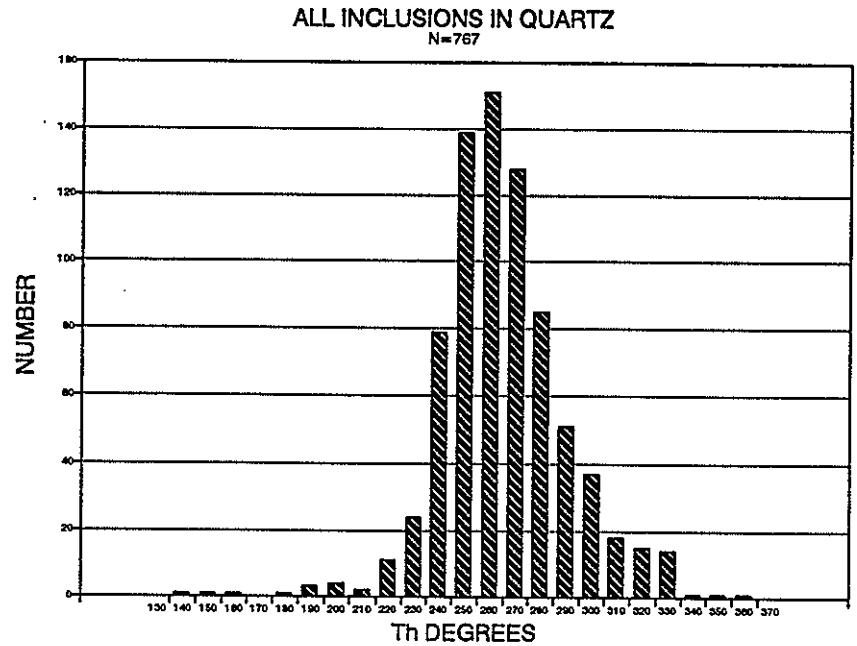

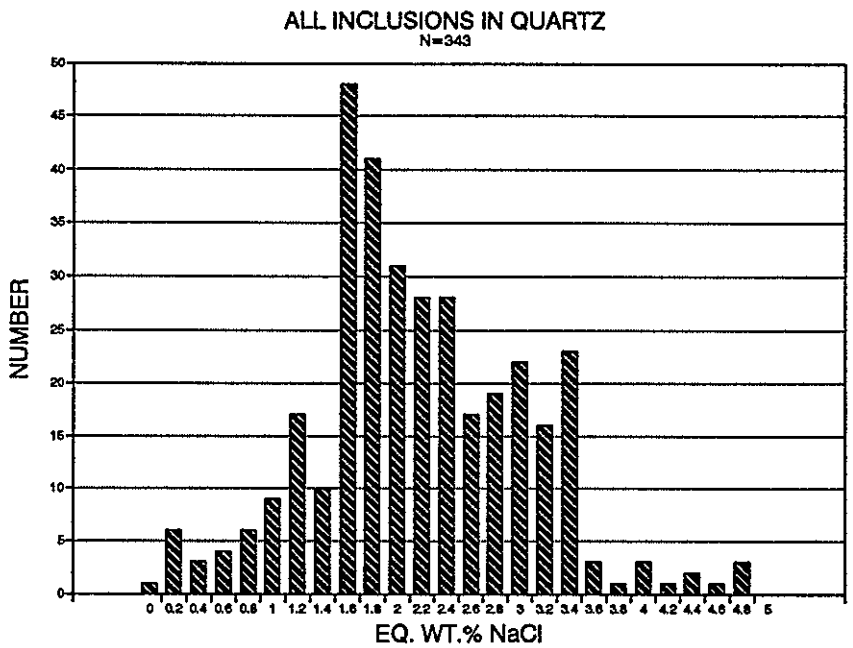

Figure 4.20—Histograms of temperature of homogenization (Th and salinities of fluid inclusions in quartz.

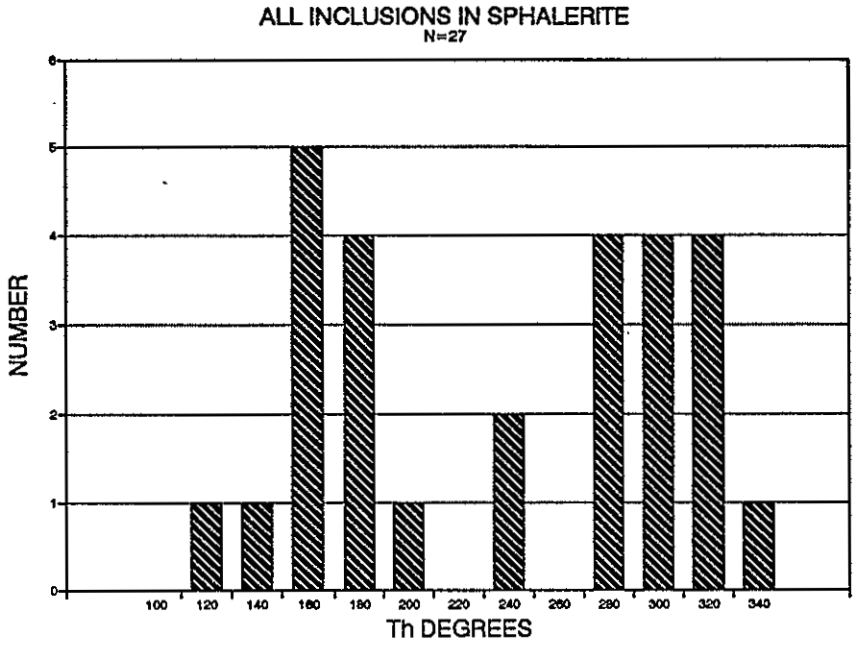

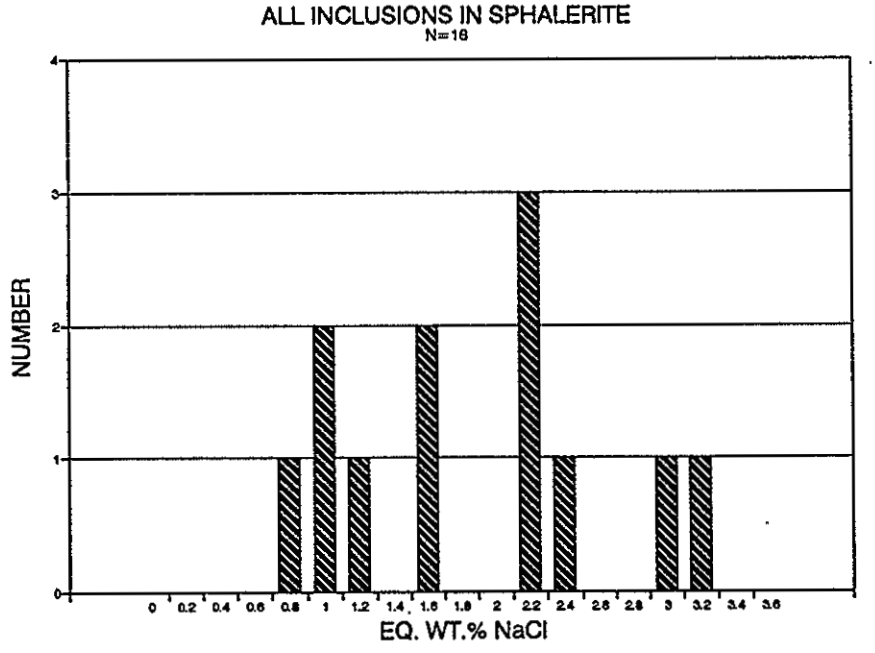

Figure 4.21—Histograms of temperatures of homogenization (Th) and salinities in sphalerite.

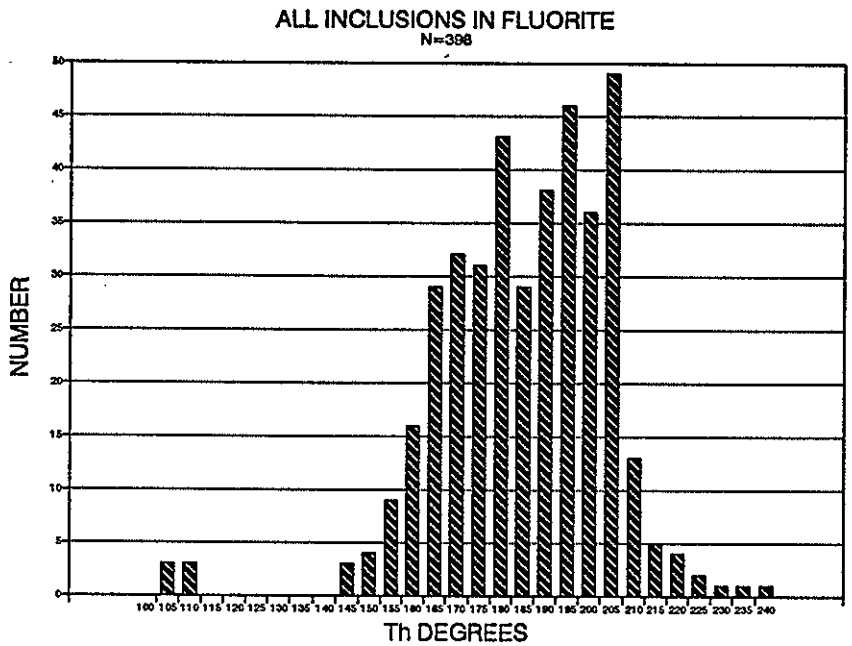

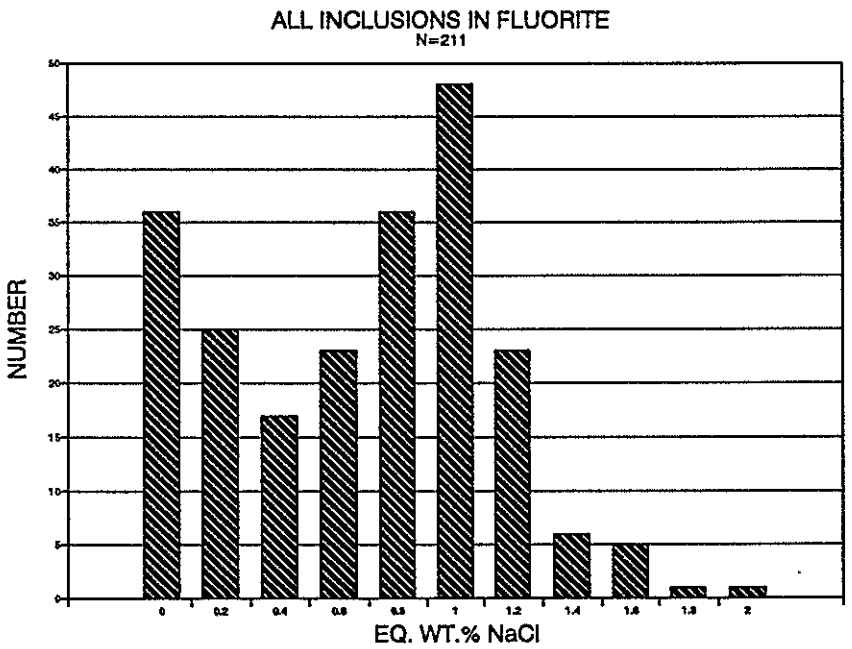

Figure 4.22—Histograms of temperatures of homogenization (Th) and salinities of fluid inclusions in fluorite.

crystals from the base- and precious-metal vein deposits were also examined, but no fluid inclusions were found.

Therefore this study is restricted to three types of quartz: (1) stage 2 mineralization, (2) stage 3 mineralization, and (3) one sample of vein quartz crosscutting the acid-sulfate alteration.

The highest temperatures of homogenization are in quartz samples from drill core at the Carlisle and Center mines. Temperature increases with depth (Appendix 11.7). The surface samples from the Carlisle fault area typically contained fluid inclusions with temperatures of homogenization higher than elsewhere in the district. The next-highest samples were from along the East Camp fault and in the Alabama-Imperial area.

Plots of primary and secondary inclusions in quartz are similar and probably represent similar fluids (Appendix 11.7); therefore, all data were combined. A normal distribution of temperature of homogenization of all samples exists (Fig. 4.20). Salinities of all quartz samples are less than 5 eq. wt.% NaCl (Fig. 4.20). The higher salinities are from samples at depth in the Carlisle-Center area.

4.2.3.2 Sphalerite, (Zn,Fe)S—Sphalerite is the only ore mineral which occurs in the base-metal and gold-silver veins that contains visible fluid inclusions. Fluid inclusions in sphalerite are probably most representative of the ore-bearing fluids. However, only 27 fluid inclusions in sphalerite from three sample sites were measured. More than 20 polished sections were examined and most sphalerites did not contain any primary fluid inclusions.

Two distinct populations of fluid inclusions are identified (Table 4.2, Fig. 4.21). The primary inclusions have an average temperature of homogenization of 285°C (range 231.8°-324.6°C) and an average salinity of 2.4 eq. wt.% NaCl (range 2.1-3.0%). Secondary inclusions have an average temperature of homogenization of 153.8°C (range 116.5°-184.8°C) and an average salinity of 1.1 eq. wt.% NaCl (range 0.7-1.4%). Two distinct populations are obvious on a temperature vs. salinity plot (Fig. 4.23). The fluid inclusions in the Center mine ore have the highest temperatures of homogenization (300–340°C; Appendix

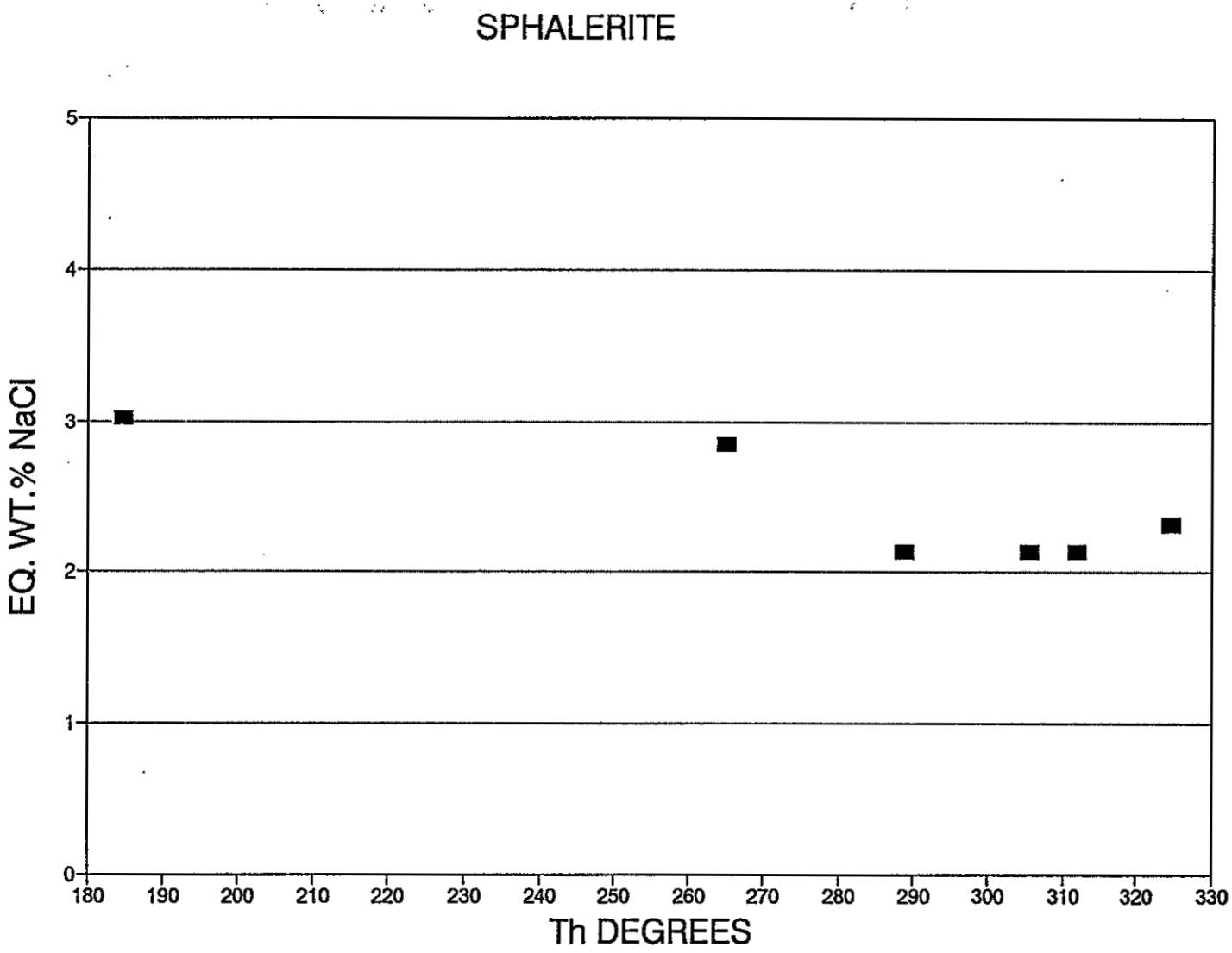

FIGURE 4-23 - Plot of temperature verses salinity of fluid inclusions in sphalerite.

11.7).

Fluid inclusions are rare in sphalerites that display chalcopyrite disease. The origin of chalcopyrite disease in epithermal deposits is best attributed to replacement by copper after formation of sphalerite or as epitaxial growth, as previously discussed in section 4.3.1.3. Fluid inclusions from both types of sphalerites (i.e. with and without chalcopyrite disease) were used in microthermometric measurements for this study, but only a few samples with chalcopyrite disease contained any usable fluid inclusions. No differentiation on the basis of presence or absence of chalcopyrite disease could be detected and, for the purposes of this study, it is suggested that chalcopyrite disease has no effect on fluid inclusion analyses. However, because of the small number of measurements, this hypothesis needs to be confirmed.

The highest temperatures of fluid inclusions come from samples from the Center mine. Samples from drill hole B91.17 (Summit-Bank properties, East Camp-Summit fault) contain numerous secondary inclusions of lower temperature and salinity. Temperatures of homogenization from all three sample sites are similar, therefore no temperature zonations or differences can be inferred.

4.2.3.3 Fluorite, CaF_2—Fluorite occurs in veins in the northern and western portions of the district and as late stage mineralization in the Center mine. Almost 400 fluid inclusions were examined in polished sections and cleavage fragments (Table 4.3). Two types of inclusions are identified in thin sections: primary and secondary inclusions (Table 4.3, Fig. 4.22). The primary inclusions have an average temperature of homogenization of 181°C (range 103–239°C) and salinity of 0.5 eq. wt.% NaCl. The secondary inclusions have an average temperature of homogenization of 184°C (range 102–239°C) and a salinity of 0.8 eq. wt.% NaCl. The difference in inclusion type does not account for the bimodal population. Both types of inclusions are treated in this report as one population of a similar fluid because the temperatures of homogenization and salinities overlap. As will be discussed later, this bimodal population is probably a result of either district zoning or two or more centers of

fluorite mineralization (see section 6.3).

The highest temperature of homogenization come from fluorite in the Goat Camp Springs, Luckie, and Forbis mines. The lowest temperatures are from the Center and Black Cat mines and drill hole BC1 (Table 4.3; Appendix 11.7).

4.3 Geochemistry and statistical analyses of vein deposits

Several companies provided geochemical analyses of production shipments, surface sampling programs, and drill core sampling (Table 4.4). Numerous unpublished reports on file at NMBMMR also contained similar data. Three data sets were chosen for statistical analyses in order to better characterize these deposits. The data include production data from the Center mine (R&B Mining Co.), surface geochemical sampling data from the Carlisle (Weaco Exploration, Ltd.) and Alabama mines (Great Lakes Exploration Co.). These three data sets were chosen because they include multi-element analyses of numerous samples and data on methods of sample collection and analyses were available.

The purposes of this study are (1) to characterize the geochemistry of the deposits, (2) identify any pathfinder elements to aid in exploration for precious- and base-metal deposits in the district, and (3) identify and characterize any possible metal zonations. The data sets cannot be combined because different elements were analyzed by different laboratories and the samples were collected for different purposes by different people.

Correlation coefficients and factor analysis of the chemical data were performed using MSTAT (Rockware, Inc., 1992a) and SPSS (Nie et al., 1975), using raw data and standard matrices. Correlation coefficients are measures of the linearity or correlation between two variables. Typically correlation coefficients greater than 0.4 are significant (dependent upon number of samples) and correlation coefficients greater than 0.8 exhibit strong correlation between the two variables. Factor analysis is a statistical method that reduces a set of numerous variables to a lesser number of mutually uncorrelated factors which may be related to similar origins or sources. Factor analysis also identifies the minimum number of

Table 4.4—Summary of different geochemical data sets used for this study.

Area	Source	Laboratory	Purpose of data	Elements
Center mine	ASARCO	ASARCO	smelter assays of production shipments	Au, Ag, Cu, Pb, Zn, SiO_2, F, As, Sb, Bi, Ni, Cd, Fe, CaO, Al_2O_3
Carlisle mine	Weaco, Ltd.	Acme Analytical Laboratory, Ltd.	exploration for Au and Ag in 1991	Au, Ag, As, Sb, Hg, F
Alabama mine	Great Lakes Expl., Inc.	Skyline, Tucson	exploration for Au and Ag in 1991	Au, Ag, As, Sb, Hg, F, plus additional major and trace elements on 20 samples by XRF (NMBMMR)
Entire district	V. T. McLemore	NMBMMR	characterize geochemistry of veins	Au, Ag, Cu, Pb, Zn, Hg plus additional major and trace elements (XRF, NMBMMR)
Entire district	Phelps Dodge Corp.	unknown	exploration geochemical sampling	Au, Ag, Hg, rarely Cu, Pb, Zn

variables necessary to account for the variation (% variance) in a data set.

4.3.1 Center mine

Chemical assay data of ore shipments from the Center mine were combined and the data are summarized in Table 4.5. The assays are from splits of ore shipments from the Center mine which were collected and analyzed by ASARCO laboratories. Periodically additional gold and silver assays were performed on some shipments by other laboratories and the duplicate analyses typically agreed. Correlation coefficients and factor analysis are in Tables 4.6 and 4.7.

Unfortunately, these data cannot be utilized in determining possible metal zonation because most shipments from the Center mine represent mixtures of different orebodies from throughout the mine. The miners were forced to mix high-grade with low-grade ore to maintain a constant shipment. Also the miners mixed high-fluorine with low-fluorine ore to keep fluorine concentrations below maximum standards set by ASARCO.

Statistical analyses of these data confirm a significant correlation between gold and silver and a strong correlation between lead and zinc (Fig. 4.24). Factor analysis confirms this correlation. Also factor analysis provides additional information. Factor group 1 indicates correlation between copper, zinc, lead, iron and a negative correlation with silica. This association is confirmed by field observations; copper, lead, and zinc minerals are associated with a decrease in quartz. Factor group 2 indicates a correlation between calcium and fluorine which corresponds to the late stage fluorite mineralization. Factor group 3 indicates a correlation between gold, silver, alumina, and negative correlation with silica. This corresponds to the association of gold and silver with illite, chlorite, and perhaps adularia. Note that 56.4% of the variation in the data is attributed to factors 1, 2, and 3. Factor group 4 indicates a correlation between antimony and alumina, whereas factor group 5 indicates a correlation between arsenic and iron. This suggests that antimony, arsenic, and iron are either late stage and not associated with the precious and base metals or are remobilized by

Table 4.5—Statistical data of assays of ore shipments from the Center mine (1941, 1942, 1984, 1986, 1988-1992). From ASARCO assay certificates and H. Schmidt, written communication, 1950). Au and Ag in oz/ton, other values in percent.

	Mean	Standard deviation	Range	Number of shipments
Au	0.44	0.2	0.11-1.12	210
Ag	3.91	2.5	0.40-23.1	210
Cu	0.34	0.1	0.10-1.28	210
Pb	2.31	0.8	0.20-4.30	184
Zn	2.76	0.8	0.60-4.84	200
SiO_2	73.6	3.0	66.3-84.6	172
F	0.27	0.2	0.004-2.15	145
As	0.009	0.02	0-0.17	160
Sb	0.019	0.01	0-0.07	163
Bi	0.015	0.01	0-0.099	163
Ni	0.009	0.02	0-0.255	146
Cd	0.021	0.04	0-0.064	3
Fe	3.84	0.4	2.7-5.1	172
CaO	0.84	0.4	0-3	154
Al_2O_3	5.21	1.4	3-9.3	172

Table 4.6—Pearson Correlation coefficients for assays of ore shipments from the Center mine (1941, 1942, 1984, 1986, 1988-1992; from ASARCO smelter assay certificates and H. Schmidt, written communication, 1950). Number of shipments in parenthesis.

	Au	Ag	Cu	Pb	Zn	SiO_2	Fe	CaO	Al_2O_3	As	Sb	Bi	F
Au	1.00												
Ag	0.42 (210)	1.00											
Cu	0.11 (210)	0.02 (210)	1.00										
Pb	0.34 (184)	0.12 (184)	0.41 (184)	1.00									
Zn	0.27 (200)	0.04 (200)	0.46 (200)	0.88 (180)	1.00								
SiO_2	-0.43 (172)	-0.25 (172)	-0.31 (172)	-0.64 (146)	-0.60 (162)	1.00							
Fe	0.18 (172)	0.34 (172)	0.43 (172)	0.37 (172)	0.30 (172)	-0.44 (172)	1.00						
CaO	0.04 (154)	0.03 (154)	-0.11 (154)	0.14 (154)	0.19 (154)	-0.33 (154)	-0.07 (154)	1.00					
Al_2O_3	0.21 (172)	0.18 (172)	-0.21 (172)	-0.22 (172)	-0.27 (172)	-0.42 (172)	-0.08 (172)	0.03 (172)	1.00				
As	0.03 (142)	-0.08 (142)	0.05 (172)	0.00 (128)	0.00 (134)	0.05 (142)	0.01 (142)	-0.10 (142)	-0.01 (142)	1.00			
Sb	-0.04 (156)	-0.02 (156)	0.13 (156)	0.08 (139)	-0.02 (152)	-0.06 (156)	0.08 (156)	-0.15 (156)	0.11 (156)	0.06 (139)	1.00		
F	-0.13 (145)	-0.20 (145)	-0.15 (145)	-0.09 (145)	-0.03 (141)	-0.01 (145)	-0.04 (145)	0.53 (145)	0.00 (145)	-0.14 (127)	-0.05 (135)	-0.03 (135)	1.00 (135)

Table 4.7—Varimax rotated factor analyses (R-mode) of assays of ore shipments from the Center mine.

Factor	1	2	3	4	5
Au	0.25	-0.06	-0.75	-0.16	0.12
Ag	0.08	-0.25	-0.69	-0.15	-0.37
Pb	0.9	0.09	-0.14	0.00	0.11
Cu	0.66	-0.29	0.02	0.09	-0.27
Zn	0.91	0.16	-0.06	-0.08	0.13
SiO_2	-0.59	-0.32	0.59	-0.28	0.00
Fe	0.53	-0.19	-0.22	0.10	-0.45
CaO	0.12	0.83	-0.10	-0.11	-0.02
Al_2O_3	-0.37	0.20	-0.65	0.48	0.09
F	0.08	0.78	0.19	-0.05	-0.17
As	0.07	-0.25	-0.03	0.02	0.74
Sb	0.10	-0.19	0.11	0.86	-0.01
% Variance	27.6	14.9	13.9	9.0	8.3
Cumulative % variance	27.6	42.5	56.4	65.4	73.7

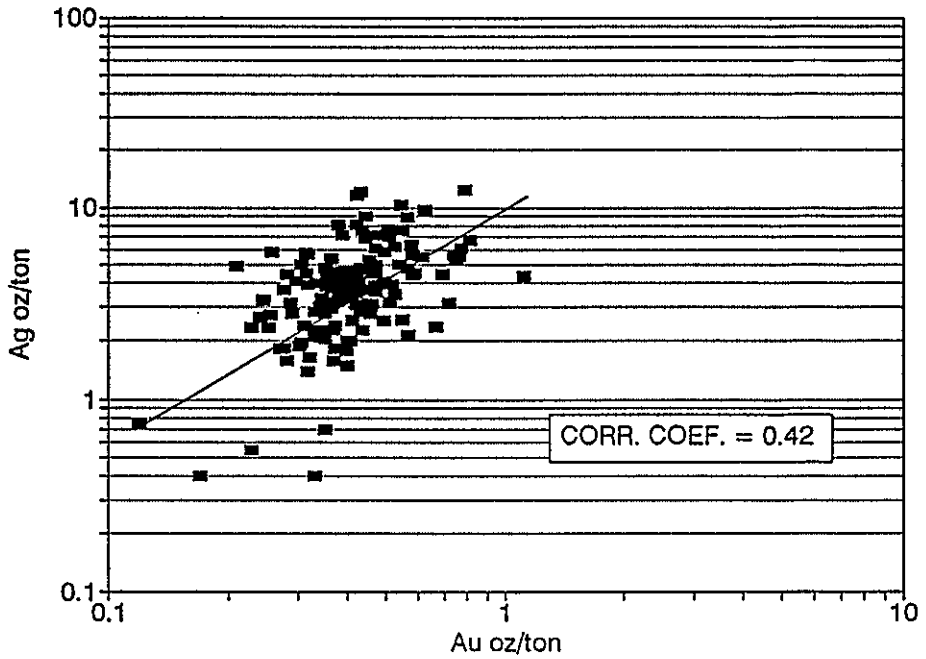

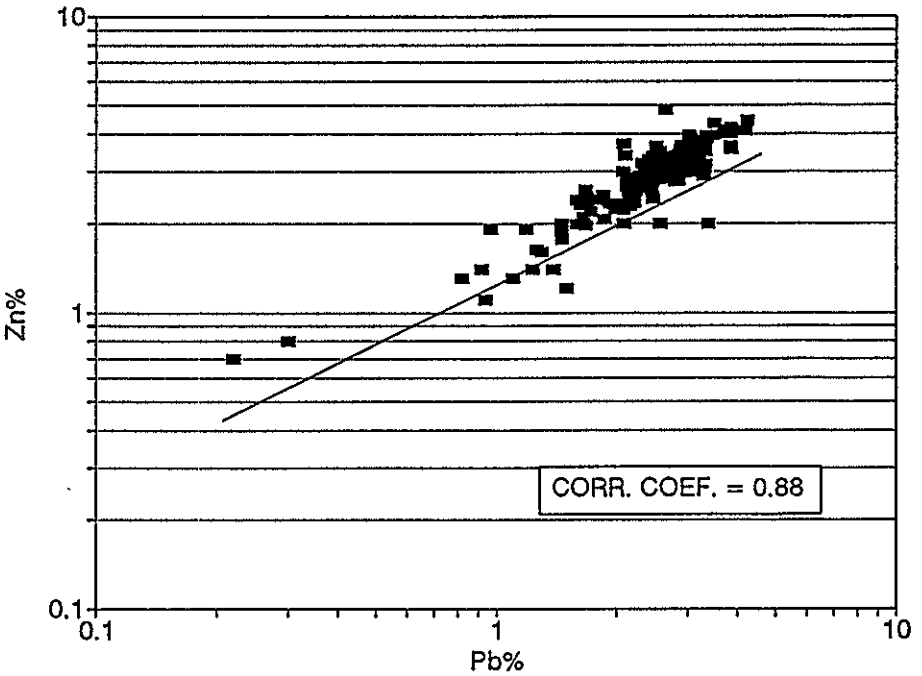

Figure 4.24 -Scatter plots of gold vs. silver and lead vs. zinc of assays from the Center mine.

subsequent supergene alteration and oxidation. This is supported by occurrence of iron oxides and mimetite coatings. Note that 73.7% of the variation in the data is attributed to Factors 1, 2, 3, 4, and 5.

4.3.2 Carlisle mine

Weaco Exploration Ltd. collected samples on a 100 m spaced grid at the Carlisle mine. Rock chip samples were collected at each location over approximately 0.5 m^2 and analyzed for a number of elements. Areas of mine tailings were not sampled. The data are summarized in Table 4.8. Correlation coefficients and factor analysis are summarized in Tables 4.9 and 4.10.

Statistical analyses confirm a strong correlation between gold and silver, lead and zinc, and bismuth, cadmium, zinc, and lead (Table 4.9; Fig. 4.25). These associations and other correlations are confirmed by factor analysis. Factor group 1 indicates a strong correlation between calcium, aluminum, nickel, cobalt, manganese, vanadium, phosphorus, lanthium, magnesium, titanium, sodium, and negative correlation with arsenic and molybdenum. This group most likely represents gangue and alteration mineralogy, because these elements are common to gangue and alteration minerals found at the Carlisle mine. Factor group 2 consists of lead, zinc, bismuth, and cadmium. Factor group 3 consists of gold, silver, manganese, and vanadium. Factor group 4 consists of arsenic, iron, and chromium. Factor group 6 consists of copper and calcium. The other factor groups are less important. The associations represented by factor groups 4 and 6 may be related to mobilization by supergene alteration and oxidation, because these elements are found in supergene minerals at the Carlisle. Iron and copper staining and chalcanthite are common along pit and adit walls and were deposited recently by acid mine water. The separate associations of gold-silver and lead-zinc represented by factor groups 2 and 3 are confirmed by field and production data. The veins in the upper levels of the Carlisle consist of a gold-silver (low base-metals) ore shoot and a parallel lead-zinc-copper (low gold and silver) ore shoot. The lack of a strong

Table 4.8—Statistical data of assays of surface samples from the Carlisle and Sec. 2 mines. Total sample population is 202 samples. Values in ppm unless otherwise specified.

	Mean	Standard deviation	Range of values
Au ppb	858	11198	1-159100
Ag	2.5	19	0.1-255.4
Cu	131.8	689	10-9030
Pb	216.5	863	2-9622
Zn	202.0	953	6.0-13148
As	9.0	8	2.0-52.0
Sb	2.2	1	2.0-19.0
Bi	2.3	2	2.0-22.0
Ni	18.9	10	1.0-60.0
Cd	1.4	4	0.2-39.8
Fe%	3.4	1	0.86-7.59
Ca%	0.4	0.3	0.02-2.87
Al%	1.2	0.6	0.05-3.23
Mo	7.6	11	1.0-95.0
Co	10.9	6	1.0-26.0
Mn	346.7	274	15.0-2384
Sr	48.8	39	8.0-447.0
V	43.3	27	3.0-297.0
P%	0.05	0.02	0.001-.117
La	14.1	8	2.0-47.0
Cr	19.3	11	1.0-117.0
Mg%	0.62	0.5	0.01-1.85
Ba	99.5	71	21.0-552.0
Ti%	0.08	0.1	0.01-0.26
B	3.7	5	2.0-36.0
Na%	0.03	0.03	0.01-0.17
K%	0.17	0.1	0.01-0.65
W	1.0	0.2	1.0-3.0

Table 4.9—Pearson correlation coefficients for chemical analyses of samples from the Carlisle and Sec. 2 mines.

	Au	Ag	Cu	Pb	Zn	As	Sb	Bi	Fe	Ca	Al	Mo	Ni	Co	Mn	Sr	Cd	V	P	La	Cr	Mg	Ba	Ti	B	Na	K	W
Au	1.00																											
Ag	0.96	1.00																										
Cu	0.05	0.13	1.00																									
Pb	0.22	0.40	0.33	1.00																								
Zn	0.10	0.23	0.37	0.85	1.00																							
As	0.25	0.27	0.14	0.11	0.07	1.00																						
Sb	0.05	0.09	0.07	0.09	0.05	-0.01	1.00																					
Bi	0.05	0.16	0.32	0.78	0.91	0.05	0.09	1.00																				
Fe	-0.11	-0.09	0.20	0.10	0.20	0.40	0.00	0.14	1.00																			
Ca	-0.06	-0.05	0.55	-0.02	0.09	-0.20	0.00	0.09	0.24	1.00																		
Al	-0.05	-0.07	0.05	-0.08	0.06	-0.29	0.03	0.01	0.41	0.62	1.00																	
Mo	-0.02	0.02	0.04	0.09	-0.01	0.39	-0.03	-0.03	-0.04	-0.36	-0.40	1.00																
Ni	-0.08	-0.08	0.26	-0.07	0.04	-0.18	0.16	0.02	0.37	0.60	0.73	-0.27	1.00															
Co	-0.07	-0.06	0.10	0.01	0.18	-0.25	0.06	0.15	0.39	0.65	0.82	-0.41	0.82	1.00														
Mn	0.52	0.54	0.19	0.19	0.23	-0.02	0.15	0.15	0.18	0.47	0.60	-0.31	0.54	0.66	1.00													
Sr	-0.07	-0.08	0.00	-0.06	-0.05	0.19	-0.09	-0.07	0.25	-0.01	-0.09	0.06	-0.16	-0.19	-0.21	1.00												
Cd	0.03	0.12	0.33	0.60	0.60	0.04	0.18	0.42	0.18	0.06	0.07	0.04	0.03	0.11	0.25	-0.06	1.00											
V	0.65	0.62	0.05	0.11	0.14	0.24	0.06	0.08	0.43	0.30	0.43	-0.24	0.32	0.45	0.68	-0.01	0.07	1.00										
P	-0.13	-0.13	0.00	-0.10	0.00	-0.10	0.11	-0.02	0.43	0.27	0.70	-0.25	0.67	0.71	0.42	0.10	0.02	0.27	1.00									
La	-0.11	-0.11	-0.05	-0.06	0.05	-0.24	0.07	0.03	0.22	0.29	0.64	-0.32	0.67	0.77	0.47	-0.17	0.04	0.29	0.71	1.00								
Cr	-0.01	-0.01	0.11	-0.03	0.03	0.27	0.22	0.01	0.52	0.47	0.33	-0.14	0.39	0.28	0.25	0.03	0.02	0.47	0.26	0.22	1.00							
Mg	-0.01	-0.02	0.01	-0.07	0.06	-0.33	0.04	0.04	0.28	0.44	0.92	-0.43	0.71	0.81	0.63	-0.16	0.03	0.44	0.67	0.63	0.32	1.00						
Ba	-0.06	-0.06	0.02	0.02	0.02	0.26	-0.04	0.04	0.15	0.01	-0.11	-0.01	-0.09	-0.06	-0.17	0.24	0.01	0.01	-0.02	-0.08	-0.11	-0.20	1.00					
Ti	-0.07	-0.09	-0.06	-0.07	0.04	-0.34	-0.12	0.06	0.08	0.36	0.56	-0.44	0.43	0.68	0.41	-0.01	-0.09	0.36	0.46	0.51	0.14	0.62	-0.01	1.00				
B	0.00	0.01	-0.04	-0.04	-0.02	0.14	-0.04	-0.04	0.04	0.06	0.11	0.07	0.12	0.14	0.12	-0.02	-0.03	0.06	0.16	0.19	0.02	0.11	0.09	0.11	1.00			
Na	-0.07	-0.09	-0.05	-0.08	0.01	-0.22	-0.11	0.03	0.29	0.28	0.46	-0.33	0.37	0.47	0.23	0.39	-0.11	0.28	0.49	0.36	0.18	0.48	0.03	0.68	0.08	1.00		
K	-0.12	-0.09	0.08	0.01	0.07	-0.14	0.01	0.00	0.25	-0.05	0.42	-0.12	0.49	0.44	0.27	0.10	0.12	-0.05	0.52	0.46	0.02	0.29	-0.10	0.03	0.06	0.21	1.00	
W	0.35	0.33	0.00	0.05	0.02	0.13	0.00	0.01	-0.02	0.24	-0.08	0.13	-0.07	-0.07	0.15	0.04	-0.01	0.24	-0.13	-0.09	0.02	-0.07	0.01	-0.07	-0.03	-0.08	-0.16	1.00

Table 4.10—Varimax rotated factor matrix (R-mode), samples from Carlisle and Sec. 2 mines.

	F1	F2	F3	F4	F5	F6	F7	F8
Au	-0.04	0.05	0.99	-0.06	-0.03	0.00	0.01	-0.02
Ag	-0.06	0.19	0.96	-0.06	-0.06	0.03	0.04	-0.01
Cu	-0.01	0.32	0.04	0.11	-0.02	0.86	0.07	-0.01
Pb	-0.08	0.89	0.19	-0.02	-0.02	0.05	0.02	-0.01
Zn	0.07	0.99	0.05	0.03	0.01	0.05	-0.02	0.02
As	-0.41	0.05	0.28	0.49	0.10	0.08	0.00	0.62
Sb	0.01	0.09	0.05	0.19	-0.20	0.03	0.10	-0.13
Bi	0.06	0.87	0.00	0.01	0.01	0.05	-0.10	0.01
Fe	0.24	0.16	-0.05	0.70	0.26	0.08	0.16	0.22
Ca	0.68	0.07	-0.02	0.03	0.08	0.65	-0.08	0.01
Al	0.85	-0.01	-0.01	0.21	-0.04	0.05	0.18	-0.05
Mo	-0.50	0.02	-0.02	0.04	-0.06	0.01	0.10	0.24
Ni	0.73	-0.02	-0.06	0.24	-0.16	0.24	0.29	0.05
Co	0.92	0.12	-0.03	0.13	-0.11	0.07	0.14	0.14
Mn	0.63	0.16	0.56	0.10	-0.20	0.12	0.15	0.00
Sr	-0.13	-0.06	-0.03	0.12	0.77	0.02	0.13	0.01
Cd	0.00	0.59	0.03	0.09	-0.10	0.12	0.15	-0.05
V	0.45	0.05	0.70	0.44	0.06	-0.03	-0.17	0.07
P	0.71	-0.04	-0.10	0.20	0.12	-0.01	0.38	0.17
La	0.75	0.01	-0.08	0.06	-0.14	-0.09	0.26	0.16
Cr	0.25	-0.02	0.05	0.74	-0.03	0.04	-0.08	-0.07
Mg	0.88	-0.01	0.03	0.16	-0.10	0.00	0.06	-0.10
Ba	-0.11	0.04	-0.05	0.02	0.25	0.03	-0.08	0.29
Ti	0.82	-0.01	-0.02	-0.15	0.22	-0.01	-0.36	0.07
B	0.13	-0.04	0.02	-0.02	-0.02	-0.03	0.04	0.33
Na	0.61	-0.03	-0.03	0.02	0.60	-0.04	-0.05	-0.04
K	0.34	0.06	-0.12	-0.06	0.07	0.03	0.73	0.01
W	-0.09	0.00	0.35	0.03	-0.01	0.00	-0.07	0.02
% variance	26.8	14.1	9.6	7.7	5.9	4.6	4.2	4.0
Cumulative % variance	26.8	40.9	50.5	58.1	64.0	68.6	72.8	76.8

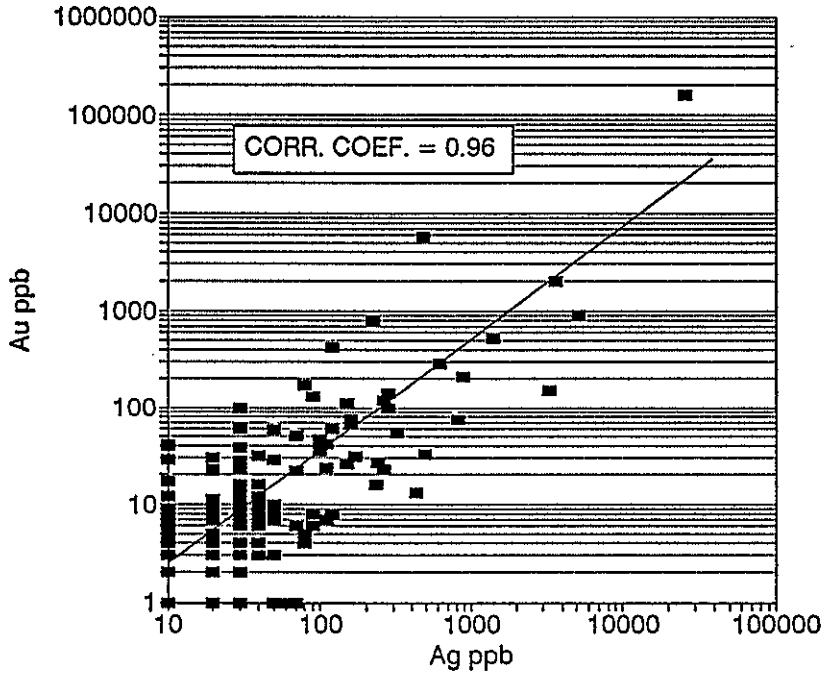

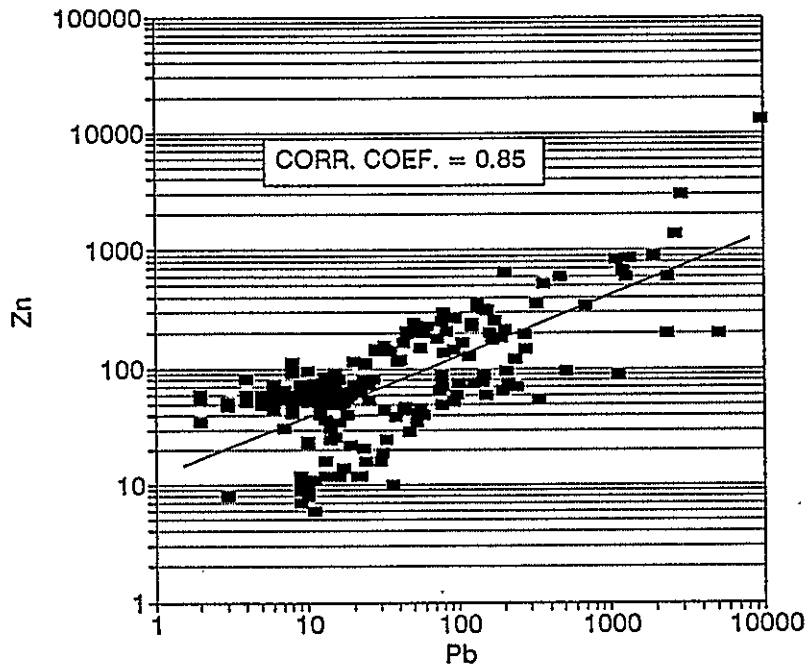

Figure 4.25 - Scatter plots of gold vs. silver and lead vs. zinc of assays from the Carlisle and sec. 2 mines.

correlation of copper in factor group 3 is also confirmed by field and geochemical evidence. In recent weathering, rainwater reacts with pyrite and other sulfides to form acidic water which accumulates and locally drains from the Carlisle mine. The acidic water tends to dissolve pyrite and chalcopyrite before galena and sphalerite. Thus the waters are more concentrated with iron and copper (J. McLemore, unpubl. report, March 1993).

Geochemical concentration maps of the various metals and pathfinder elements were prepared. These maps indicate that gold and silver anomalies occur along the Carlisle fault. A geochemical concentration map of arsenic values reported for each rock chip sample reveals a halo of slightly elevated arsenic concentrations over the Carlisle orebody (Fig. 4.26). This suggests that arsenic may act as a pathfinder element; this needs to be confirmed by additional studies. No other zonations of metals could be detected.

4.3.3 Alabama mine

Great Lakes Exploration Co. collected and assayed samples from the surface along the veins and faults in the Alabama mine area (Fig. 4.27). Channel samples comprised of rock chips from traverses 1 to 2 m long were collected at each location. The data are summarized in Table 4.11. All samples were analyzed for gold, silver, arsenic, antimony, mercury, and fluorine by Skyline Analytical Laboratory; 19–20 samples were also analyzed for major and trace elements by XRF by NMBMMR (Appendix 11.6). Correlation coefficients and factor analysis are in Tables 4.12 and 4.13.

Statistical analyses of these data confirm a strong correlation between gold and silver and copper, lead, and zinc (Fig. 4.28). Factor analysis confirms this correlation (Table 4.13). Factor 1 consists of SiO_2, F, As, Sb, Fe_2O_3, CaO, MgO, P_2O_5, Ba, and Zr which reflects original and alteration mineralogy, because these elements occur in the original host rock and altered minerals. Factor 2 consists of Au, Ag, Pb, F, and Hg. Factor 3 consists of Cu, Pb, Zn, Sb, and V. The remaining factors reflect original and alteration mineralogy. Note the lack of any arsenic halo over the Alabama mine in Figure 4.27.

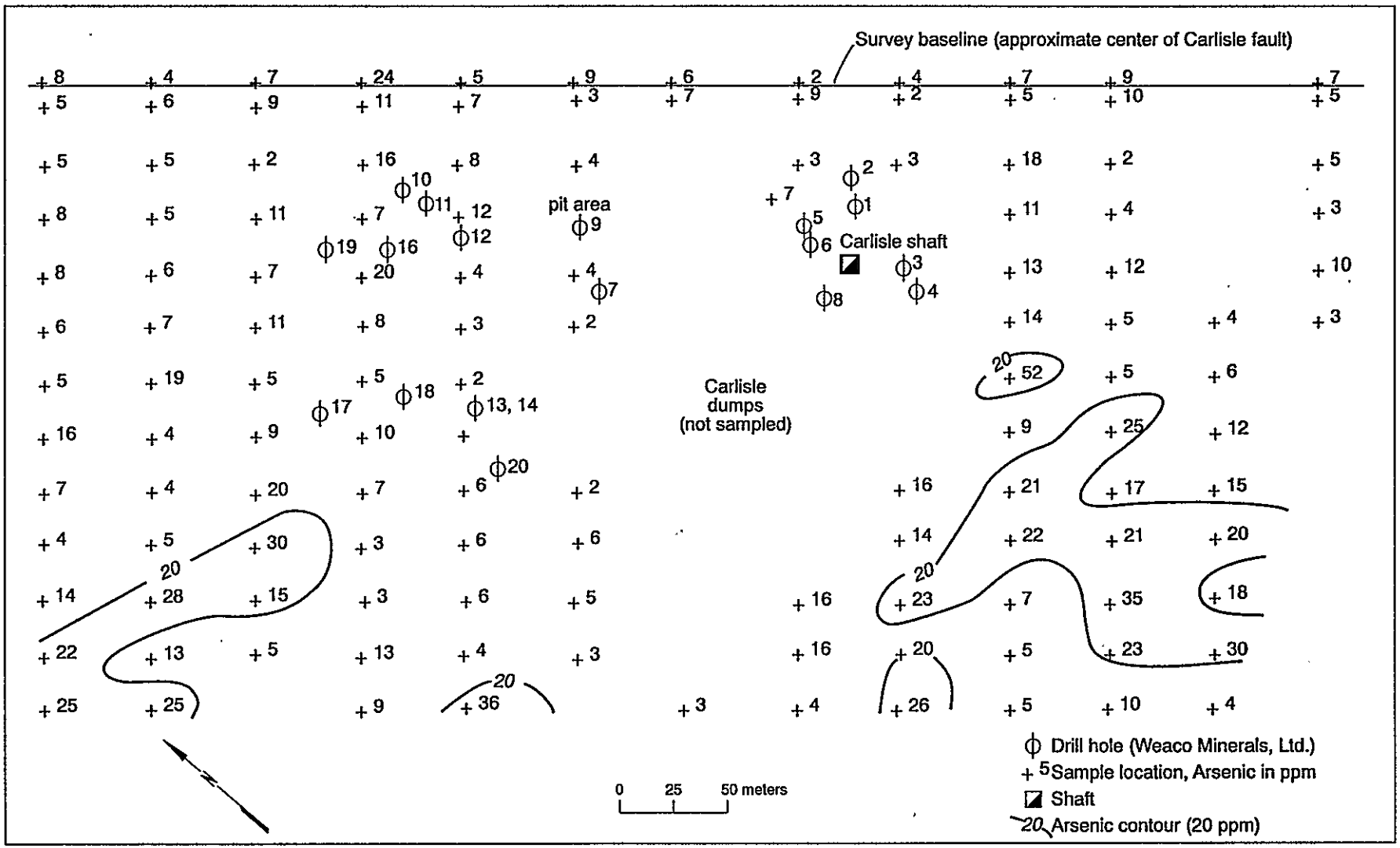

Figure 4.26 - Geochemical concentration map of arsenic at the Carlisle Mine. Weak arsenic anomalies (> 20 ppm As) overlie projected ore shoots.

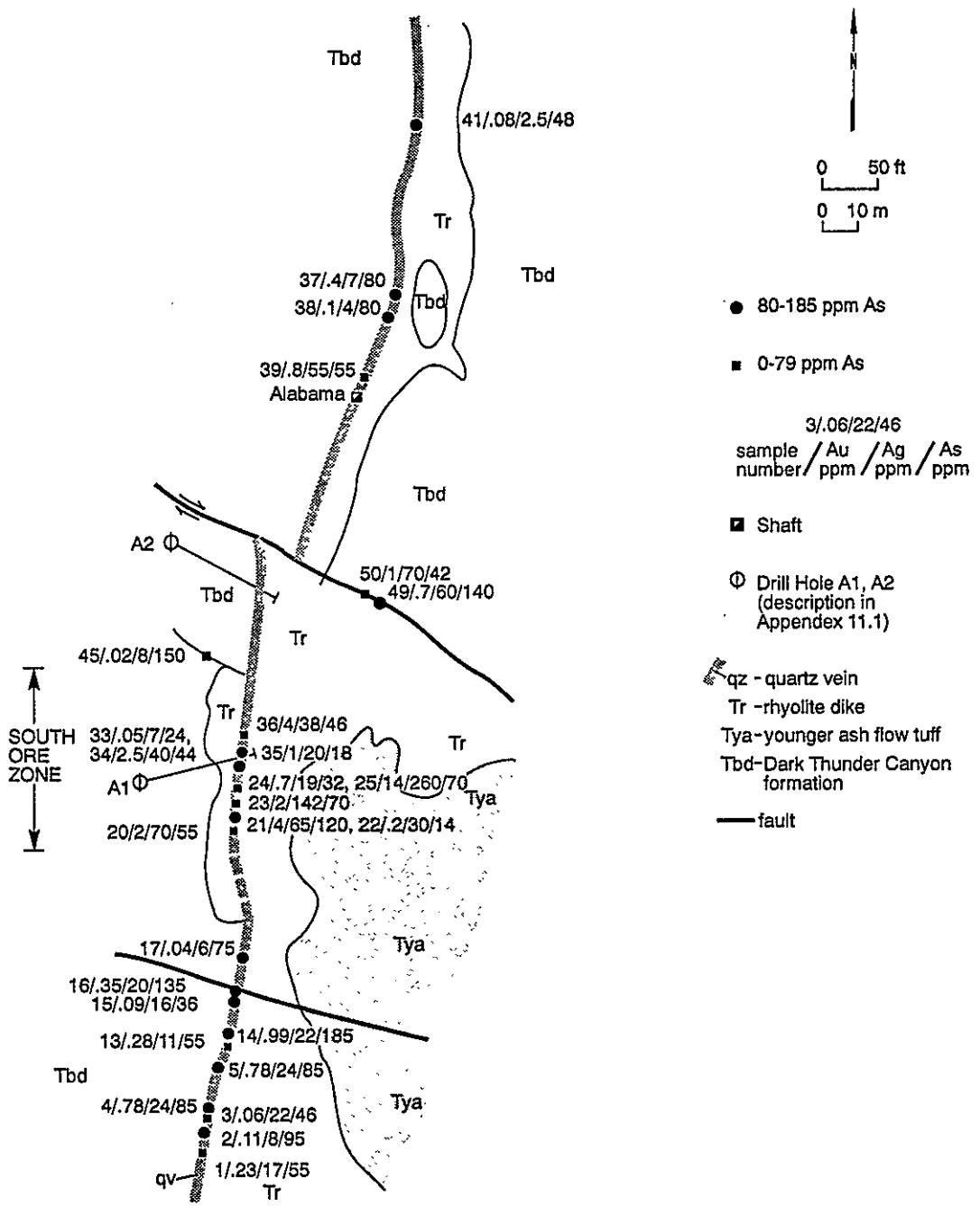

Figure 4.27- Geochemical concentration map of arsenic at the Alabama Mine area. Geology and samples by T. Quigley (1991). South ore zone defined by outcrop assays and limited subsurface data.

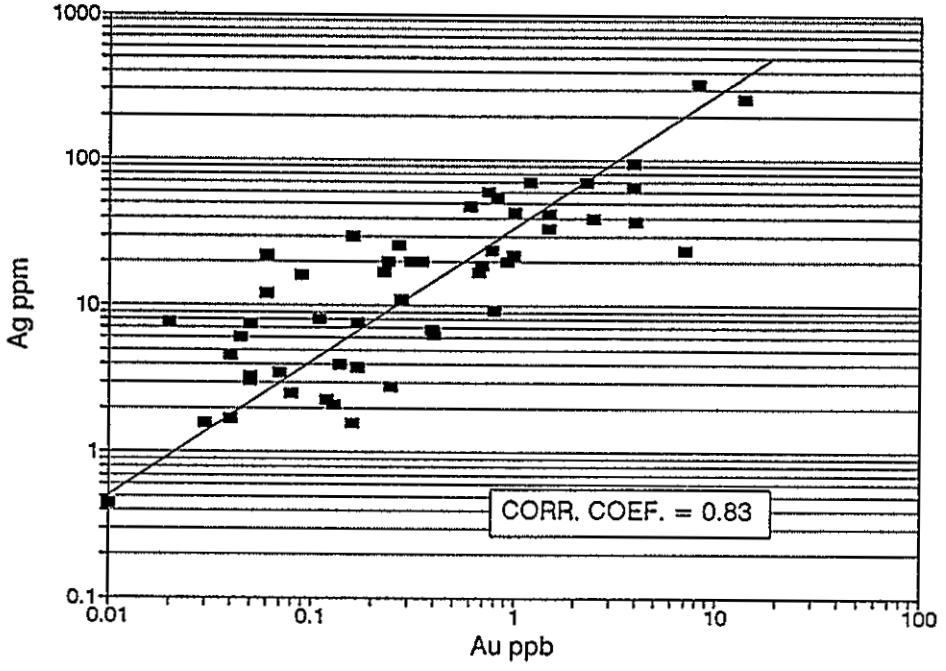

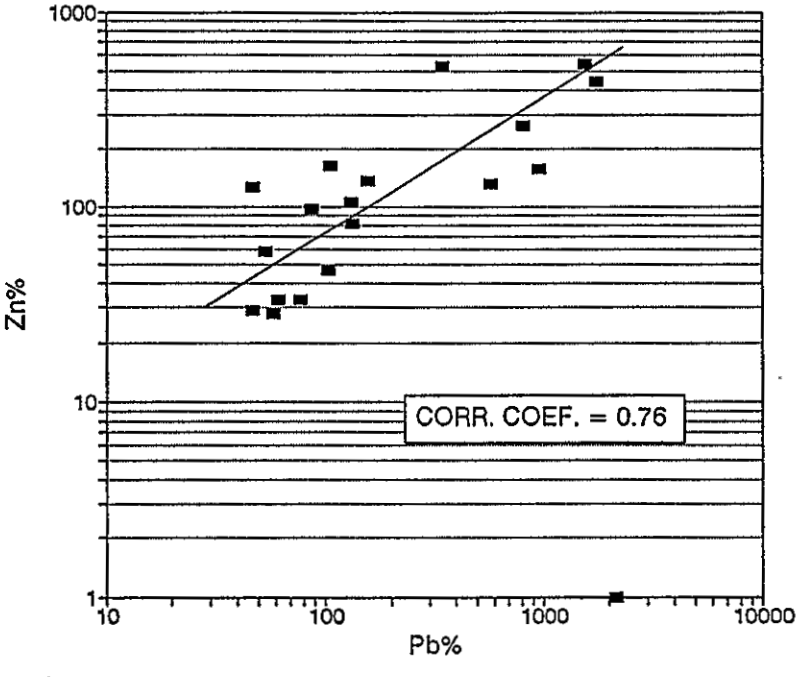

Figure 4.28 - Scatter plot of gold vs. silver and lead vs. zinc of assays from the Alabama mine area.

Table 4.11—Statistical data of assays of surface samples from the Alabama mine area. Values in ppm, unless otherwise noted. Au and Ag in oz/ton, value in parentheses is in ppm.

	Mean	Standard deviation	Range	Number of samples
Au	0.04 (1.21)	(2.5)	0-0.41 (0.01-14.0)	52
Ag	0.94 (32.1)	(57.8)	0.01-9.6 (0.42-330	52
Cu	86	106	8-328	18
Pb	486	660	47-2167	19
Zn	167	167	28-540	18
SiO_2%	87.4	5	78.2-92.2	20
F%	0.05	0.02	0.02-0.15	52
As	68.3	44	10-185	52
Sb	14.1	12	2-55	52
Fe_2O_3%	2.4	1	0.8-4.1	20
CaO%	0.26	0.1	0.05-0.49	20
Al_2O_3%	5.4	2	3.1-10.0	20
Hg	0.08	0.06	0.02-0.31	52
Ga	10.6	5	6-24	19

Table 4.12—Pearson correlation coefficients for assays of surface samples from the Alabama mine area. Number of samples in parentheses.

	Au	Ag	Cu	Pb	Zn	SiO_2	F	As	Sb	Fe_2O_3	CaO	Al_2O_3	Hg	MnO	MgO	K_2O	P_2O_5	Ba	V	Zr
Au	1.00																			
Ag	0.83 (52)	1.00																		
Cu	0.21 (18)	0.28 (18)	1.00																	
Pb	0.69 (19)	0.79 (18)	0.79 (18)	1.00																
Zn	0.19 (18)	0.45 (18)	0.98 (18)	0.76 (18)	1.00															
SiO_2	0.42 (20)	0.33 (20)	0.47 (18)	0.50 (19)	0.44 (18)	1.00														
F	-0.34 (52)	-0.36 (52)	-0.32 (18)	-0.41 (19)	-0.31 (18)	-0.48 (20)	1.00													
As	-0.05 (52)	-0.04 (52)	-0.34 (18)	-0.04 (19)	-0.34 (18)	-0.51 (20)	-0.33 (52)	1.00												
Sb	0.16 (52)	0.26 (52)	0.20 (52)	0.35 (19)	0.16 (18)	-0.35 (20)	0.00 (52)	0.42 (52)	1.00											
Fe_2O_3	-0.16 (20)	-0.03 (20)	-0.48 (18)	-0.28 (19)	-0.47 (18)	-0.74 (20)	0.57 (20)	0.77 (20)	0.52 (20)	1.00										
CaO	-0.36 (20)	-0.11 (20)	-0.43 (18)	-0.40 (18)	-0.37 (18)	-0.72 (20)	0.34 (20)	0.45 (20)	0.26 (20)	0.77 (20)	1.00									
Al_2O_3	0.43 (20)	-0.11 (20)	-0.35 (18)	-0.35 (19)	-0.40 (18)	-0.95 (20)	0.39 (20)	0.33 (20)	0.28 (20)	0.52 (20)	0.50 (20)	1.00								
Hg	0.48 (52)	0.37 (52)	0.33 (18)	0.56 (19)	0.23 (18)	0.06 (20)	-0.20 (52)	0.11 (52)	0.03 (52)	0.15 (20)	-0.03 (20)	-0.11 (20)	1.00							
MnO	-0.01 (19)	0.23 (19)	-0.02 (19)	0.12 (19)	0.03 (19)	0.01 (19)	-0.02 (19)	0.21 (19)	-0.16 (19)	0.16 (19)	0.13 (19)	-0.13 (19)	0.28 (19)	1.00 (19)						
MgO	-0.23 (19)	-0.11 (19)	-0.40 (19)	-0.27 (19)	-0.35 (19)	-0.48 (19)	0.18 (19)	0.5 (19)	0.27 (19)	0.57 (19)	0.61 (19)	0.32 (19)	0.10 (19)	0.26 (19)	1.00					
K_2O	-0.42 (19)	-0.43 (19)	-0.31 (19)	-0.49 (19)	-0.29 (19)	-0.94 (19)	0.43 (19)	0.35 (19)	0.32 (19)	0.52 (19)	0.51 (19)	0.99 (19)	-0.1 (19)	-0.21 (19)	0.31 (19)	1.00				
P_2O_5	-0.31 (19)	-0.15 (19)	-0.53 (19)	-0.50 (19)	-0.50 (19)	-0.65 (19)	0.51 (19)	0.68 (19)	0.24 (19)	0.89 (19)	0.85 (19)	0.41 (19)	0.02 (19)	0.27 (19)	0.52 (19)	0.41 (19)	1.00			
Ba	-0.20 (19)	-0.11 (19)	-0.31 (19)	-0.34 (19)	-0.29 (19)	-0.71 (19)	0.34 (19)	0.44 (19)	0.29 (19)	0.71 (19)	0.64 (19)	0.58 (19)	0.11 (19)	0.31 (19)	0.38 (19)	0.57 (19)	0.74 (19)	1.00		
V	-0.04 (19)	0.17 (19)	0.48 (19)	0.23 (19)	0.45 (19)	-0.14 (19)	-0.15 (19)	0.29 (19)	0.17 (19)	0.15 (19)	0.08 (19)	0.09 (19)	0.39 (19)	0.40 (19)	-0.01 (19)	0.05 (19)	0.11 (19)	0.23 (19)	1.00	
Zr	-0.42 (19)	-0.33 (19)	-0.49 (19)	-0.58 (19)	-0.46 (19)	-0.94 (19)	0.56 (19)	0.62 (19)	0.36 (19)	0.86 (19)	0.82 (19)	0.82 (19)	-0.66 (19)	-0.01 (19)	0.49 (19)	0.83 (19)	0.83 (19)	0.78 (19)	0.05 (19)	1.00

Table 4.13—Varimax rotated factor matrix (R-mode), samples from Alabama mine area.

	F1	F2	F3	F4	F5
Au	0.18	0.89	-0.19	-0.10	0.22
Ag	0.02	0.87	-0.16	0.18	0.23
Cu	0.34	0.01	0.91	0.01	0.17
Pb	0.15	0.78	0.43	-0.09	0.31
Zn	0.31	-0.06	0.90	0.04	0.18
SiO_2	0.53	0.19	0.09	0.00	0.81
F	-0.54	-0.49	-0.01	-0.24	-0.11
As	-0.80	0.27	-0.05	0.03	-0.22
Sb	-0.56	0.36	0.46	-0.46	0.22
Fe_2O_3	-0.91	0.02	-0.11	0.01	-0.34
CaO	-0.79	-0.15	-0.13	0.11	-0.32
Al_2O_3	0.25	-0.22	-0.07	-0.08	-0.92
Hg	-0.21	0.73	0.35	0.12	-0.02
MnO	-0.26	0.11	0.07	0.84	0.18
MgO	-0.66	-0.07	-0.17	0.14	-0.10
K_2O	-0.26	-0.22	-0.06	-0.16	-0.91
P_2O_5	-0.85	-0.18	-0.24	0.22	-0.22
Ba	-0.56	-0.03	-0.07	0.32	-0.55
V	-0.10	0.22	0.61	0.57	-0.24
Zr	-0.68	-0.24	-0.18	-0.01	-0.66
% variance	42.0	17.4	12.1	8.0	5.4
Cumulative % variance	42.0	59.4	71.5	79.5	84.9

4.3.4 Summary of geochemical and statistical analyses

The veins in the Steeple Rock district are enriched in silica (>75%) and provide excellent silica flux for local smelters. Although anomalously high concentrations of copper, lead, and zinc occur in most ore shoots (section 3, Tables 4.5, 4.8, 4.11), the base metals are higher in the base-metal veins (>2% Pb, >2% Zn, and 0.4–1.5% Cu) than in the gold-silver veins (<0.5% combined Cu, Pb, Zn). Impurities such as aluminum, antimony, arsenic, mercury, bismuth, and cadmium are typically below limits set by the local smelters. However, fluorine and calcium concentrations are variable in all types of deposits and may exceed local smelter limits. Some ore shipments from the Center, Laura, Carlisle, and Summit mines were rejected or penalized by local smelters because of high concentrations of calcium or fluorine. Locally, elevated levels of bismuth, especially at depth, have resulted in penalties by the smelters (i.e. Center mine).

The Steeple Rock vein deposits are characterized by a strong correlation between lead and zinc and, to a lesser extent, between gold and silver. These correlations exist in both base-metal and gold-silver veins and are apparent in additional assay and production data of most mines besides the three data sets presented here. Statistical analyses of various data sets from the Steeple Rock district indicate that gold and silver exhibit little or no correlation with copper, lead, and zinc. Furthermore, statistical analyses indicate that copper exhibits little or no correlation with lead and zinc. This is a result of complex, constantly evolving chemical and physical conditions described in section 6.

Although typical pathfinder elements for precious- and base-metal deposits, such as arsenic, antimony, mercury, and bismuth, locally have strong correlations with specific precious or base metals in the Steeple Rock district, no definite pattern exists district-wide except for arsenic. A pathfinder is a relatively mobile element that is associated with an element of economic interest, but the pathfinder is more easily found because it forms a broad halo surrounding the element of interest. Some studies suggest that a halo of elevated arsenic concentrations may occur over mineralized deposits, such as the Carlisle (Fig. 4.26) and

Summit (Don Burton, NovaGold Resources, Inc., pers. comm. April 1993) mines. However, arsenic halos were not observed at the Alabama mine (Fig. 4.27). These data suggest that locally pathfinder elements should be used but with caution. The best geochemical pathfinders for gold-silver deposits in the Steeple Rock district are gold and silver. It should also be noted that most samples containing anomalously high concentrations of gold and silver typically also contain elevated concentrations of copper, lead, and zinc (Appendix 11.6). However, not all samples containing elevated copper, lead, and zinc contain detectable gold or silver.

Analyses of the various geochemical data indicate that little or no chemical zonations exist laterally. Locally, in some mines, precious and base metals either decrease or increase in concentration with depth (see mine descriptions in Chapter 3: Laura, Alabama). Decrease in precious metals and increase in base metals with depth suggests the bottom of the ore shoot has occurred and either the mine is depleted in precious metals or parallel blind veins may occur, as at the Carlisle and Center mines. Increase in precious metal concentrations with depth also could suggest that additional ore may occur below the present level of mining (see section 3).

4.4 Economic Potential

A secondary objective of this study was to evaluate the district in terms of economic resource potential of all possible commodities. This section includes evaluations and brief discussions of various commodities that occur or were thought to occur in the Steeple Rock district.

4.4.1 Gold and silver

Known resources of gold and silver have been delineated by drilling along the Jim Crow-Imperial and East Camp-Summit faults (Queenstake and Biron Bay). Additional drilling along the Norman King-Billali fault indicates additional ore exists. These resources will become more attractive with an increase in the price of gold and silver.

The resource potential for epithermal gold-silver veins elsewhere in the Steeple Rock district is excellent but will require extensive drilling and assaying to locate such deposits. Much of the district remains unexplored at depth.

Drilling has occurred between the Carlisle and Center mines, along the East Camp, Summit, and Blue Bell veins, in the Jim Crow and Imperial mines area, at the Alabama mine, and locally one or two drill holes were placed elsewhere in the district. Many areas have not been adequately drilled, such as the Laura-Smuggler veins, New Year's Gift vein, Mt. Royal mine area, west of the Carlisle mine along the Carlisle fault, at the Ontario mine, along the Apache and Blue Goose faults, and in the Goat Camp Springs and Foothill fault areas (Map 2). Of over 60 mines in the district, only seven mines exceeded depths of 100 m (Alabama, Carlisle, Center, East Camp, Laura, Norman King, and Twin Peaks mines).

Blind ore shoots which do not crop out at the surface but are parallel to outcropping gold-silver veins are common and are similar to those found at the Carlisle mine. Many ore shoots in the district do not crop out at the surface (such as the Center vein).

Ore is commonly associated with inflections and changes in strike and dip of the faults. Some ore shoots, especially in the East Camp area, are indicated at the surface by pods of barren, white quartz, referred to as quartz blowouts by early miners (Griggs and Wagner, 1966; Gillerman, 1968).

Mineralogical and chemical zoning may be important and is discussed in more detail in section 6.3. Copper-silver veins locally grade into precious metal veins (i.e. Blue Bell mine) and may offer viable exploration targets. Fluorite veins may also grade with depth to gold-silver veins and should be examined by drilling (i.e. Goat Camp Springs area). Geochemical sampling at the Carlisle and Summit mines suggests that an arsenic halo may exist over some orebodies. Therefore surface geochemical sampling around outcropping structures may also provide drilling targets for blind veins. However, geochemical sampling at the Alabama did not show an arsenic halo; so such studies may not aid in exploration everywhere in the district.

The resource potential in the Steeple Rock district for undiscovered disseminated high-sulfidation gold deposits associated with the acid-sulfate alteration is also excellent, but unproven. Assays of some samples are indicative of disseminated gold deposits (Raeburn Hills; Telephone Ridge area; Saddleback Mountain; Appendix 11.6), but drilling in some of these areas failed to delineate any deposits.

Some potential may also exist for disseminated gold in brecciated and silicified rhyolite intrusions (Wahl, 1980). Areas within the Apache Box intrusion contain anomalously high concentrations of gold (Wahl, 1980; Briggs, 1982).

4.4.2 Base metals

The potential for base-metals vein deposits is excellent along the Carlisle fault; however, drilling is required to locate additional deposits. The base-metals concentration increases with depth in many precious-metals deposits (Summit, Jim Crow-Imperial, Alabama, Laura, Carlisle, Center veins) and may offer some potential by-product production as in the past.

The pervasive alteration and regional proximity to several major porphyry copper deposits (Fig. 1.1; Morenci, Tyrone, Chino, Safford) have enticed exploration geologists to the district for years. The known copper porphyries in the area are Laramide in age (56–73 Ma; Titley, 1982), but the Steeple Rock host rocks are younger than Laramide-age rocks. Some geologists have suggested the possibility of Tertiary porphyry deposits at depth on the basis of alteration and epithermal veins exposed at the present surface. But deep drill holes (Bitter Creek BC1 hole, 762 m and Biron Bay drilling; Appendix 11.1) have failed to penetrate any copper porphyry deposits or Laramide-age rocks. Although it is possible a copper porphyry may occur at depth, it is unlikely that it would have undergone supergene enrichment and is most likely uneconomic because of low grades and extreme depths.

4.4.3 Fluorite

Fluorite veins are common in the western and northern parts of the Steeple Rock district, especially near rhyolite intrusives. Fluorite also has been produced in the past. Fluorite is the principle source of fluorine, which is a vital raw material in the chemical and metallurgy industries. The United States imports a large amount of fluorite (McAnulty, 1978; U.S. Bureau of Mines, 1992).

The fluorite deposits in the Steeple Rock district are small and contain impurities such as quartz, calcite, and manganese. These deposits are uneconomic compared to foreign sources. However, should local fluorite deposits become desirable, the fluorite deposits in the Steeple Rock district should be re-examined by drilling and detailed mapping for potential use.

4.4.4 Manganese

Manganese veins and fracture coatings are common throughout the Steeple Rock district and one deposit produced some ore. However, the manganese veins in the Steeple Rock district are small and contain impurities such as country rock, quartz, fluorite, calcite, and iron oxides. These deposits are not economic under current economic conditions.

4.4.5 Alunite

Alunite is a potential source of aluminum and has been mined in several places in the world for its aluminum content (Hall, 1978). The alunite deposit at Saddleback Mountain contains the largest amount of alunite in New Mexico with an estimated resource of 6 million tons of potential resources of 30% alunite (Hall, 1978). However, the alunite deposits in the Steeple Rock district contain impurities such as quartz, pyrite, and clay. Currently, the alunite deposits in the Steeple Rock district, as in other localities in the United States, are uneconomic. Nevertheless, as the United States imports all of its required aluminum and if foreign supplies should be threatened or exhausted, the potential in Steeple Rock would

change.

4.4.6 Clay

Clay is an important industrial mineral used in a variety of industrial and chemical uses. Kaolinite is particularly important in manufacture of paper, ceramics, bricks, and other uses. The acid-sulfate altered areas in the Steeple Rock district have an unknown potential for clay, especially kaolinite. Although impurities such as quartz, alunite and pyrite occur in much of the altered areas, locally small areas of relatively pure clay occur. Exploration and testing is required to determine if the clay deposits in the Steeple Rock district are economic.

4.4.7 Decorative Stone

At least two quarries (near Telephone Ridge and Bitter Creek area) were operated for decorative or building stone. Production is unknown, but the quarries are small, and thus production was probably small. The leisegang-banded rocks are quite suitable for decorative stone. The potential markets would be Tucson, Phoenix, and El Paso. Transportation costs would be high and prohibit large-scale exploitation, although resources are probably extensive and quarrying is feasible.

4.4.8 Beryllium

Several fluorspar mines and prospects were examined for beryllium (Meeves, 1966). Concentrations were low. Beryllium was not analyzed for in this study. It is possible that local concentrations of beryllium could exist with fluorite veins or with the acid-sulfate alteration. However, tonnage is probably small and therefore the potential for beryllium is probably low.

4.4.9 Molybdenum

It has been suggested by some explorationists that a porphyry molybdenum deposit

could occur at depth in the Steeple Rock district. Certainly the regional alteration and epithermal mineralization is consistent with a deep porphyry molybdenum deposit. Many of the rhyolites from the district are similar in chemistry to granitic molybdenite source rocks (i.e. $\geq$74% SiO_2, $\geq$4.5% K_2O, $\leq$3.6% Na_2O; Bornhorst, 1986). In addition, stream-sediment samples from the area suggest elevated molybdenum values (Hassemer et al., 1983). Therefore, molybdenum was analyzed for on many samples throughout the Steeple Rock district (Appendix 11.4, 5, 6), but values are typically low. Porphyry molybdenum deposits are typically zoned and the sampling for this study was reconnaissance in nature and could easily miss a molybdenum anomaly. Therefore, the data available are inconclusive to determine the potential for a porphyry molybdenum deposit at depth. Additional drilling, geochemical and perhaps geophysical studies would be required, but are not viable under current economic conditions.

4.4.10 Uranium

The Steeple Rock district was first examined for the possibility of uranium resources in the 1950s, when the Carlisle mine was examined and determined not to be favorable for uranium deposits (R. B. Stroud, U.S. Atomic Energy Commission, PRR Report DEB-RRA-1169, January 11, 1954). During the 1970s volcanic rocks were of interest in uranium exploration and geologists once again examined the district with discouraging results.

The Steeple Rock district, part of the Silver City 1° x 2° quadrangle, was examined again during the NURE (National Uranium Resource Evaluation) program. Aerial radiometric reconnaissance survey of the Steeple Rock district delineated three minor uranium anomalies in and near the Steeple Rock district (Texas Instruments, Inc., 1978). These are best explained by uranium associated with intrusive rhyolites. Reanalysis of the aerial radiometric data indicates the area has low background levels of radioactivity ($<$2 ppm eU, Duval, 1988). Data from the stream-sediment sampling survey indicate average or below average values for uranium (less than 3 ppm; Sharp et al., 1978).

During the course of field work a gamma-ray scintillometer was used sporadically to locate areas of anomalous radioactivity. A few rhyolite intrusives were slightly above background (up to three times background radioactivity). Samples analyzed for uranium were low (less than 15 ppm, Appendix 11.4, 5, 6). It is therefore concluded that the potential for uranium resources in the Steeple Rock district is low.

4.4.11 Tungsten

Several fluorspar mines and prospects were examined for tungsten (Trace, 1947) where up to 1-2% WO_3 was found locally with manganese oxides. A few stream-sediment samples in the northern portion of the area have anomolously high tungsten values (>100 ppm; Hassemer et al., 1983). Tungsten was not analyzed for in this study. There are not enough data to adequately address the resource potential for tungsten and additional geochemical analyses would be necessary to confirm any tungsten potential.

5. ALTERATION

5.1 Introduction

Alteration is a general term describing the mineralogic, textural, and chemical changes of a rock as a result of a change in the physical, thermal, and chemical environment in the presence of water, steam, or gas (Bates and Jackson, 1980; Henley and Ellis, 1983). The nature of the alteration depends upon (a) temperature and pressure at the alteration site, (b) composition of the parent rock, (c) composition of the altering (invading) fluids, (d) permeability of the parent rock, and (e) duration of the alteration process (Browne, 1978; Henley and Ellis, 1983). Recognition and genesis of alteration are important in mineral exploration and understanding the formation of ore deposits, because specific alteration types are associated with specific ore deposits. Furthermore, alteration halos surrounding ore deposits are typically more widespread and easier to recognize than some of the orebodies themselves (Guilbert and Park, 1986).

Research by White (1955, 1981) established the now recognized association between epithermal mineral deposits and modern, active geothermal systems. Alteration assemblages associated with epithermal vein deposits are similar to alteration assemblages found in modern geothermal systems (Buchanan, 1981; Mitchell and Leach, 1991). Therefore analogies between modern geothermal systems and ancient epithermal deposits will aid in understanding the genesis of epithermal mineral deposits, such as those found in the Steeple Rock district.

Alteration can be classified and defined in many ways but most classifications are based upon mineral assemblages (Guilbert and Park, 1986). The term assemblage implies mutual equilibrium growth of mineral phases, whereas association implies that the mineral phases are only in physical contact. A number of terms are applied to various alteration assemblages. Deuteric alteration refers to the interaction between volcanic or magmatic rocks and magmatic-hydrothermal fluids during the cooling of the igneous rocks. A variety of alteration minerals may be produced. Propylitic alteration is the mineral assemblage consisting of epidote, chlorite, pyrite, quartz and carbonate minerals. Sericitic alteration is defined by

the dominance of illite, sericite, and/or muscovite. The major difference between these three K-micas is size: illite is a clay-size K-mica, whereas muscovite is larger. Sericite is of intermediate size. Some minor compositional differences also occur between the three minerals. Argillic alteration consists of kaolinite, smectite (montmorillonite clays), chlorite, and sericite. Advanced argillic alteration consists of kaolinite, quartz, alunite, pyrophyllite, and other aluminosilicate minerals. Silicic alteration is produced by the addition of silica, predominantly as quartz. Other terms are used for these and other alteration assemblages, but these are the classic alteration assemblages associated with epithermal vein deposits.

In modern geothermal systems, the alteration mineral assemblages reflect the composition of the prevailing fluid chemistry and it is common to describe the alteration assemblage according to fluid chemistry (Browne, 1978; Mitchell and Leach, 1991; Simmons et al., 1992; Reyes, 1990). There are three end member types of fluid compositions in modern geothermal systems: (1) alkali-chloride waters, (2) acid-sulfate waters, and (3) bicarbonate waters. Each type is characterized by specific mineral assemblages and other characteristics (Table 5.1). Mixing of these end member fluid types is common and more than one type of fluid can be present (Browne, 1978). Geothermal systems are dynamic, constantly changing, and rarely in equilibrium. Processes such as boiling, mixing, and condensation constantly occur in the geothermal system, producing a wide range of overlapping mineral assemblages and associations. For the purposes of this study, the alteration types are classified according to the type of fluids as indicated by the alteration mineralogy because it is typically difficult to distinguish between and map deuteric, propylitic, argillic, and advanced argillic alteration types in the epithermal deposits, especially in the Steeple Rock district.

Alteration of a parent rock occurs by several processes: (1) direct deposition, (2) replacement, (3) leaching, and (4) ejecta (Browne, 1978). All four processes are found in the Steeple Rock district. Direct deposition occurs by precipitation of new minerals in open spaces, such as vugs or fractures. Replacement occurs when one mineral is converted to a new mineral by fluids entering the rock. These two processes are common and depend upon

Table 5.1—Characteristics of geothermal fluids and associated alteration (modified from Simmons et al., 1992; Hedenquist, 1991; Henneberger and Browne, 1988; Henley and Ellis, 1983; Browne, 1978).

Fluid type	Alkali-chloride	Acid-sulfate	Bicarbonate
Source of fluid	deep circulation	surfaced steam-heated condensate, locally with magmatic gases	condensation of steam and CO_2 into shallow groundwater
Typical pH	6–7.5 (neutral)	<2.5 (acidic)	5–6
Surface discharge	boiling spring, geyser, silica sinter	mud pools, collapse craters, hot springs	hot springs
Typical alteration	propylitic, potassic	advanced argillic	argillic
Mineral assemblage	chalcedony, quartz, albite, adularia, illite/smectite, chlorite, zeolites, epidote, calcite, pyrite	opal, kaolinite, alunite, diaspore, pyrophyllite, quartz, pyrite, sulfur	chalcedony, kaolinite, illite/smectite, chlorite, carbonates, pyrite
Predominant fluid chemistry	chloride waters	sulfate waters	bicarbonate waters
Form of alteration	direct deposition and replacement, ejecta	leaching followed by direct deposition and replacement, ejecta	direct deposition and replacement
Modern example	Luzon, Philippines Broadlands and Wairakei, New Zealand	Norris Geyser Basin, USA Bacon-Manito, Philippines	Mammoth Springs, Yellowstone

permeability and duration of the process. Complete fluid/mineral equilibrium is rarely achieved because of these factors. Leaching and supergene enrichment occurs locally where steam condensate reacts to form acidic solutions by the oxidation of H_2S or CO_2 which then attacks the parent rock and dissolves primary or secondary minerals. Silica residue is a common result of leaching and is a spongy or vuggy altered rock consisting of predominantly quartz, iron and titanium oxides. Direct deposition or replacement may occur after leaching, thereby producing overlapping alteration types. Ejecta, hydrothermal brecciation, and hydrofracturing are another form of alteration where hot water and/or steam physically breaks the parent or even altered rock apart. If this forceful ejection of fluids occurs at or near the surface, hydrothermal eruptions of water, steam, and rock can occur. Silicification following the brecciation is common.

It is convenient to describe alteration in terms of intensity and rank. Intensity of alteration is a measure of how much alteration has occurred and can be estimated by determining the percentage of newly formed secondary minerals by visual estimation or more precisely by point counting (P. R. L. Browne, unpubl. report, Spring 1992). For example, a parent rock that has not been affected by any alteration would have zero intensity of alteration, whereas a parent rock in which all primary minerals have been replaced by secondary minerals would have an alteration intensity of 100%. In Appendix 11.2, each sample description includes a visual estimate of alteration intensity.

Alteration rank is based upon the identity of new secondary minerals and their significance in terms of alteration conditions such as temperature, pressure, and permeability. The intensity of alteration is independent of rank of alteration (Browne, 1978; Simmons et al., 1992). It is possible to have rocks with a high rank but low intensity (hot, impermeable zones) or other rocks of low rank, but high intensity (cooler, permeable zones; P. R. L. Browne, unpubl. report, Spring 1992).

Two types of alteration assemblages occur in the Steeple Rock district: (1) alkali-chloride (propylitic to argillic to sericitic to silicic) and (2) acid-sulfate (advanced argillic).

However, the intensity and rank of alteration varies and there appears to be at least three distinct stages of alteration based on crosscutting relationships in examination of outcrops, drill core samples, and thin sections: (1) regional pre-mineralization, (2) localized syn-mineralization, and (3) regional post-mineralization. Several areas of intense acid-sulfate alteration are superimposed on regional alkali-chloride alteration. Furthermore, the relationship between the alteration and vein mineralization is complex. The remainder of this chapter will describe the alteration assemblages in the Steeple Rock district.

5.2 Alkali-chloride alteration (propylitic-argillic-sericitic-silicic alteration)

5.2.1 Regional premineralization alkali-chloride alteration

The most extensive type of alteration in the Steeple Rock district is an early regional pre-mineralization alkali-chloride alteration. This type of alteration has been briefly described as deuteric to propylitic alteration by Powers (1976) and Wahl (1980) and as argillization and chloritization by Biggerstaff (1974). The intensity and rank of alteration are variable and dependent upon lithology, permeability, and temperature.

This early alteration phase is typically characterized by a green to green-gray color of the altered rocks. Most rocks in the mapped area (Maps 1, 2) have been affected by this alteration; very few areas contain unaltered rocks. The mineral assemblage consists of essential chlorite (producing the green color), quartz, and pyrite and a variety of additional minerals depending upon host rock lithology, temperature, and composition of the fluids, including calcite, epidote, zeolites, adularia, sericite/illite, smectite, etc. Hematitization producing a brown to red-brown color masking the green color, is also common. The groundmass is altered to quartz and chlorite and feldspar phenocrysts are replaced by quartz, chlorite, adularia, and calcite.

One of the most important analogies between modern geothermal systems and ancient epithermal systems is the relationship of temperature and mineral assemblages. Numerous studies of modern geothermal systems have shown that certain minerals form in specific

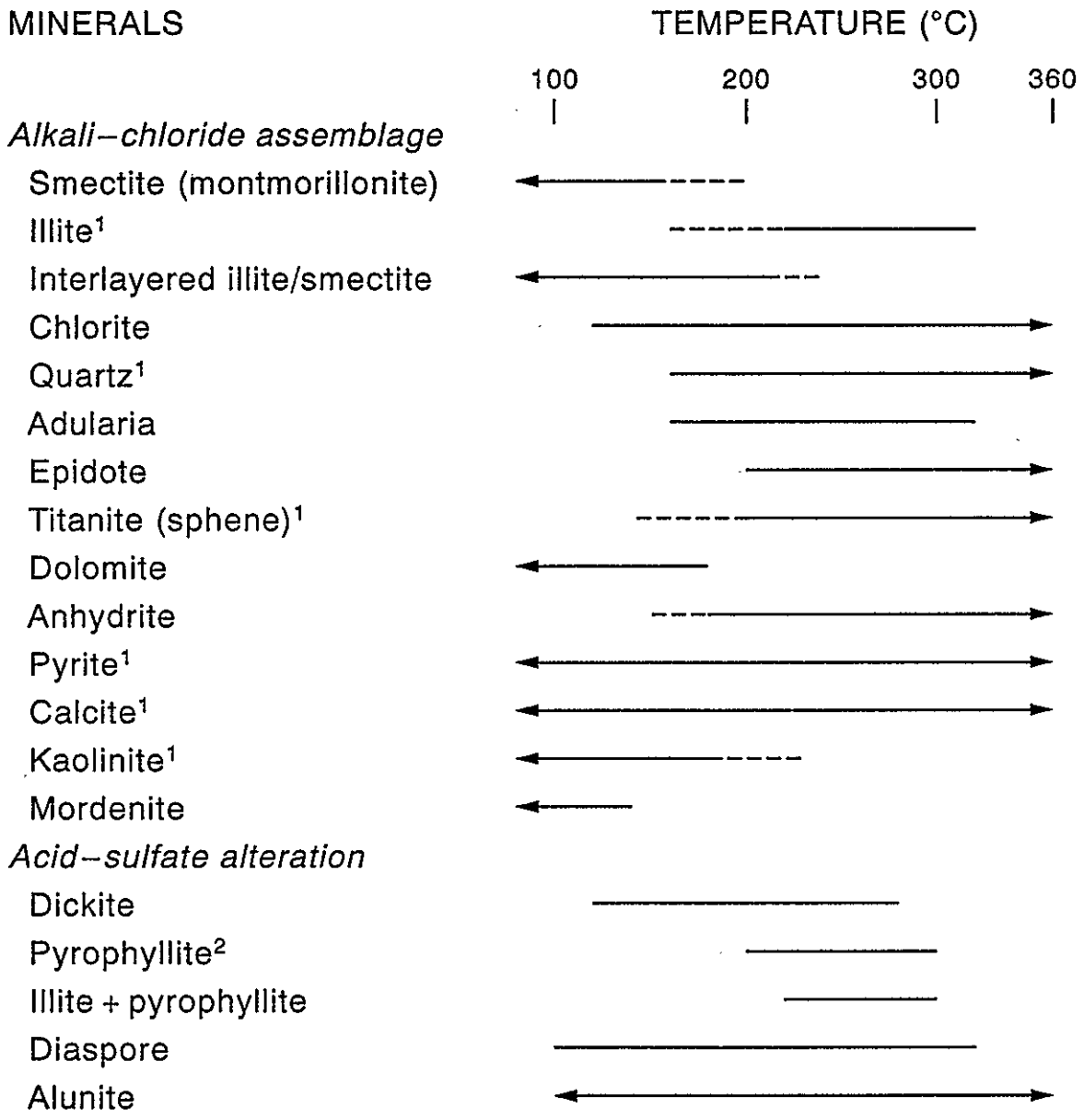

Figure 5.1–Temperature ranges of hydrothermal minerals in modern geothermal systems. Minerals listed are found in the Steeple Rock district. [1] These minerals occur in both alkali–chloride and acid–sulfate alteration assemblages. [2] Pyrophyllite may occur on the surface associated with hot springs and geysers at approximately 100°C; temperature range given is for subsurface precipitation. Arrows indicate direction in which mineral can still be precipitated. Data from Reyes (1990), Elders et al. (1981), and Simmons et al. (1992)

temperature ranges (Reyes, 1990; Beaufort et al., 1992; Arnorsson et al., 1983; Henley and Ellis, 1983; Elders et al., 1981; Simmons et al., 1992). If modern geothermal systems and ancient epithermal systems are indeed analogous, then these studies can be used to reconstruct temperature ranges and variations in epithermal systems. Figure 5.1 is a summary of temperature ranges for hydrothermal minerals that occur in the Steeple Rock district.

This early alteration can be divided into three zones on the basis of mineral assemblages and inferred temperatures: (1) high temperature (>200°C), (2) intermediate to low temperature, and (3) low temperature (<200°C). The high temperature zone is less common in the district and is found along some epithermal veins and at depth. It consists of chlorite, quartz, pyrite, epidote, titanite (sphene), and a variety of other minerals such as calcite, adularia, and anhydrite. The intermediate to low temperature zone is the most extensive and consists of chlorite, quartz, pyrite, illite or illite/smectite, and a variety of additional minerals. The low temperature zone occurs in areas distant from faults and typically in less permeable rocks. It consists of chlorite and variable quartz, zeolites, pyrite, illite/smectite, smectite, kaolinite, and locally calcite. The intensity of alteration is typically low in the low temperature zone reflecting lower permeabilities.

Episodic periods of alteration probably occurred. Thin veinlets of quartz-chlorite (± pyrite), less than a millimeter wide, cut across chloritized andesite, but are subsequently offset by younger veinlets (Fig. 5.2). Quartz-sulfide veinlets also cut across older quartz-chlorite veinlets. Locally hematite-quartz veins cut across older alteration (Fig. 5.3). These cross-cutting relationships are found throughout the drill core and locally at the surface and in the Center decline.

5.2.2 Localized syn-mineralization

The most extensive alteration adjacent to and along faults in the district is silicification. Silicified zones vary in width along strike and some zones reach widths of several hundred meters. Locally parallel or bifurcating faults or veins occur that are separated

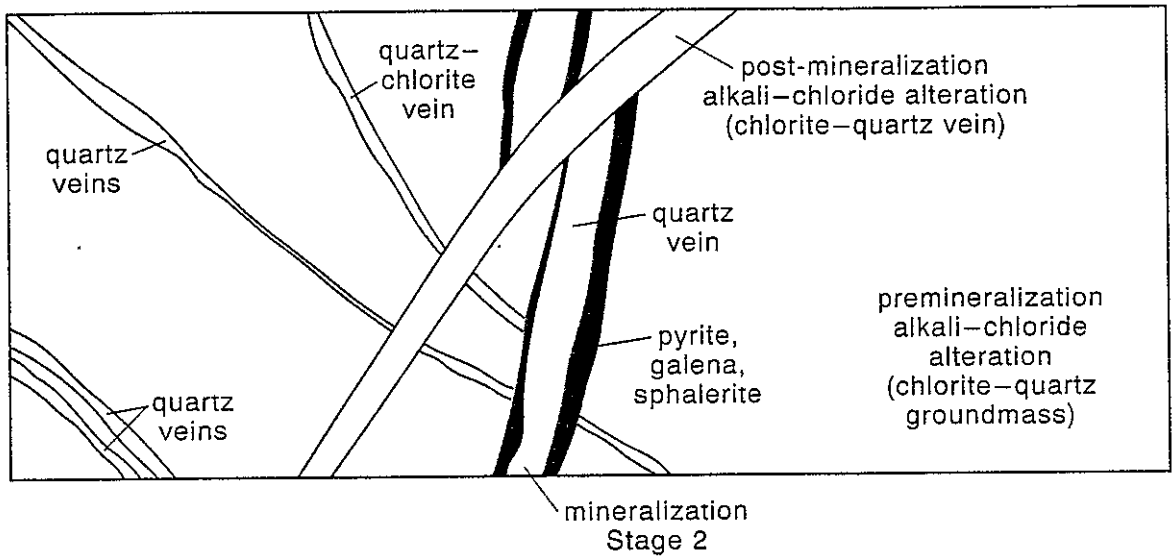

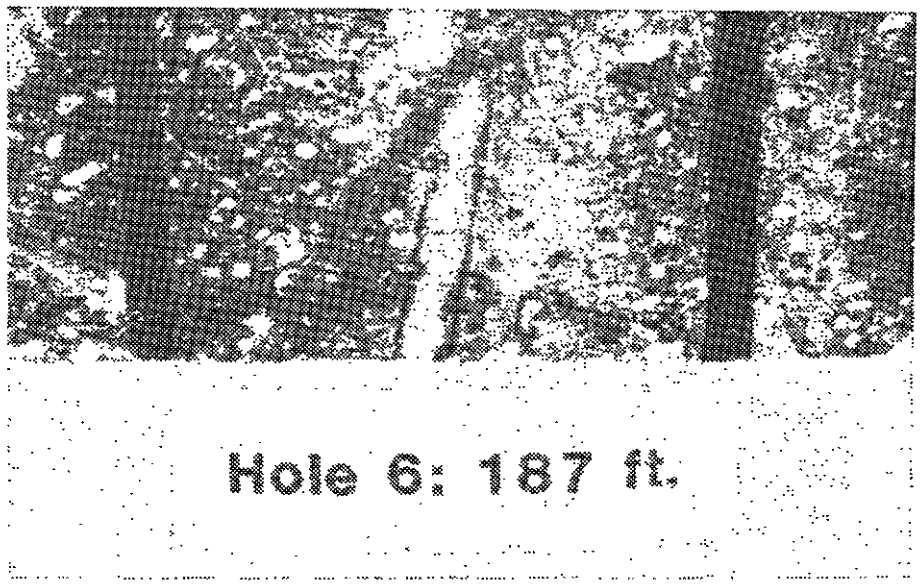

Figure 5.2—Photo and sketch of drill core showing complex alkali-chloride alteration. From USBM Drill Hole 6 at depth of 57 m (drilled at the 213 m level of the Carlisle mine). Distance between black ink lines is approximately 4 cm.

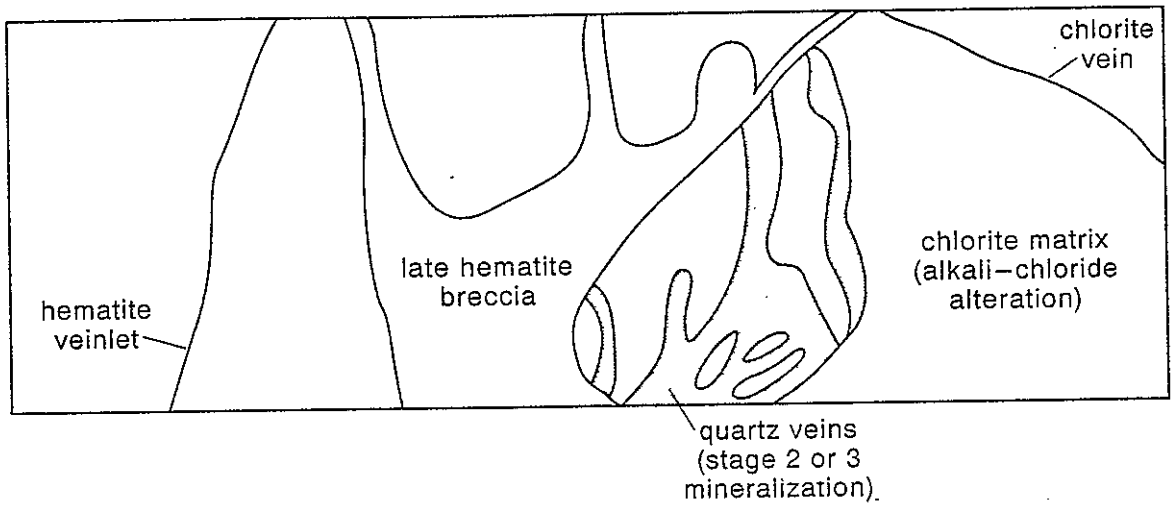

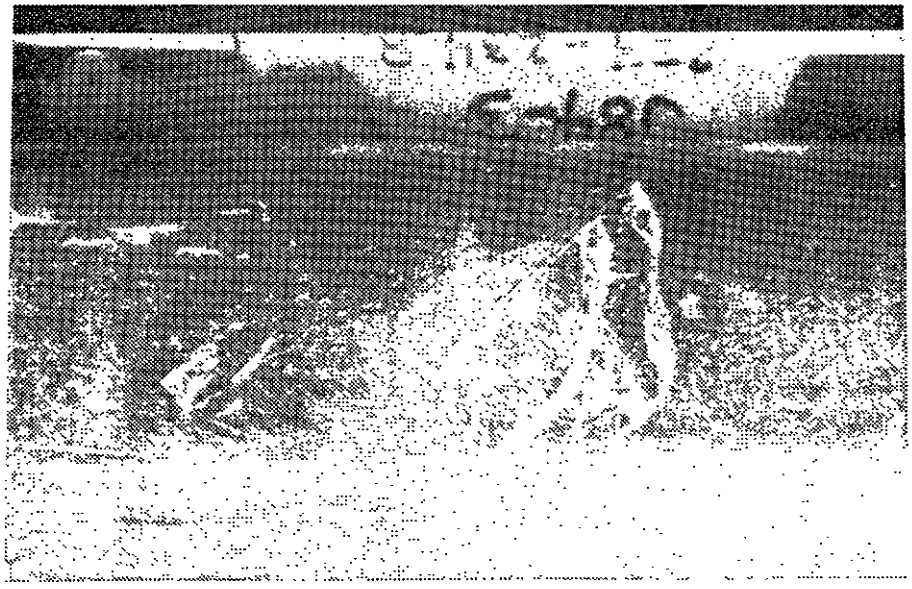

Figure 5.3—Photo and sketch of drill core showing hematite-quartz vein cutting older quartz-chlorite veins. From Jim Crow Drill Core J84–3 at depth of 71 m.

by silicified and locally brecciated host rock. Quartz occurs as amygdule-fillings, fracture coatings, thin quartz veins, breccia cements, and as replacements of primary minerals.

Locally, chloritization, argillization, and sericitization occur in a halo surrounding mineralized faults. Epidote locally occurs within this halo at depth and indicates temperatures of formation >200°C (Fig. 5.1). In the Center and Carlisle mines, altered zones occur between two subparallel veins. Near the surface, the altered zones consist of illite, kaolinite, chlorite, quartz, iron oxides, and lithic fragments. This assemblage grades with depth to predominantly illite and quartz zones within silicified andesite cut by stockwork veins of illite, quartz, and chlorite (Appendix 11.3; Maps 4, 5). This zone disappears with a dramatic decrease in metal concentrations in the footwall vein although metallic mineralization continues in the hanging wall vein (Map 4). Late primary calcite and hematite veins cut older alteration. Elsewhere in the district the halo consists of silicified and bleached rocks adjacent to the vein and grading into green rocks with chlorite and epidote away from the vein.

5.2.3 Regional post-mineralization alkali-chloride alteration

Superimposed on older alteration and mineralization is a regional post-mineralization alkali-chloride alteration. This late alteration is characterized by veinlets, typically less than a few millimeters wide, crosscutting older alteration and mineralization. These veinlets consist predominantly of quartz, chlorite, calcite, hematite, and locally zeolites (mordenite, thompsonite). Oxidation, supergene alteration, and weathering also occurred during this late alteration. Oxidation and remobilization of iron and manganese minerals have resulted in regional fracture coatings and staining by iron and manganese oxides. Some supergene alteration and oxidation are currently active at the Carlisle and Ontario mines where acidic waters are precipitating chalcanthite and other base-metal carbonates and oxides along the pit and adit walls.

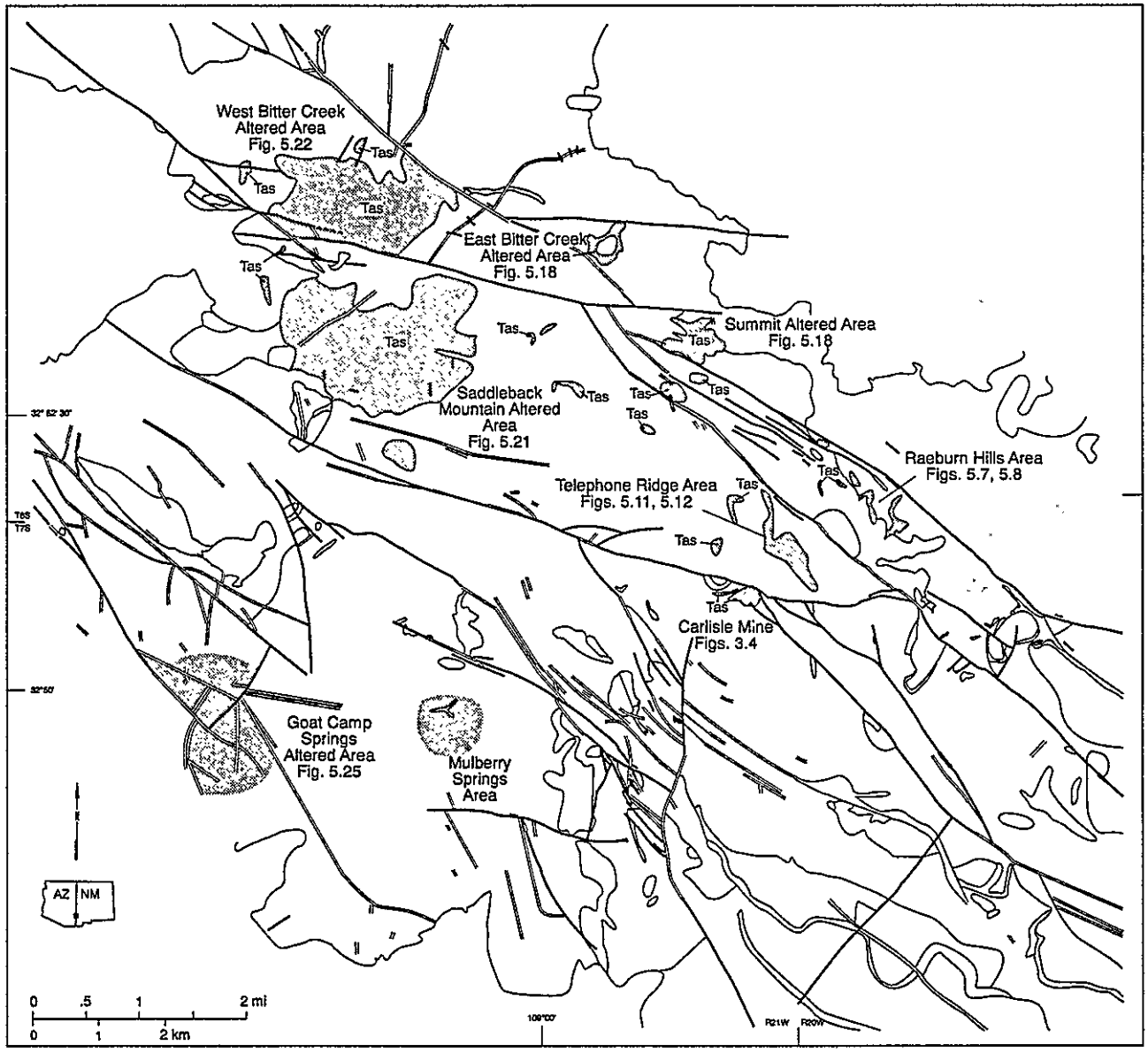

Figure 5.4 Areas of acid-sulfate alteration in the Steeple Rock mining district

5.3 Acid-sulfate alteration (advanced argillic)

5.3.1 Description

Several areas of intense acid-sulfate (advanded argillic) alteration superimposed on regional alkali-chloride alteration have been mapped in the district (Fig. 5.4; Maps 1, 2). Several of these areas are located near mineralized areas: Telephone Ridge north of the Carlisle and Center mines, a ridge east of the Summit mine, at the Bank mine, and at Goat Camp Springs. Other altered areas are in the vicinity of mineralized faults. Faults may occur in the altered areas; however, the alteration is typically too intense to accurately map them. Only a few faults are therefore mapped (Maps 1, 2). Original lithologies are typically observed and many areas are mapped as Tas on Maps 1 and 2; however, stratigraphic position and relict textures suggest that original lithologies were andesites and dacites (Summit Mountain and Dark Thunder Canyon formations), sedimentary rocks, and ash-flow tuffs.

The altered areas can be differentiated into three zones on the basis of mineralogy, texture, and inferred temperatures (Fig. 5.1) as (1) clay zone, (2) silicified zone, and (3) massive silica/chert zone. Boundaries between the zones are typically gradational and are characterized by quartz content and texture. Examination of drill core at the Carlisle, Center, and Summit mines indicates that two to three vertical zones of alteration occur separated by zones of alkali-chloride alteration.

The mineral assemblages are related to temperature similar to alkali-chloride alteration assemblages (Figure 5.1). Generally, the mineral assemblages suggest that the clay zone is typically the lowest temperature ($<200°C$), whereas the massive silica/chert zone is the highest temperature ($>200°C$). The mineralogy also confirms low pH fluids, as reflected by the phases present, specifically kaolinite, alunite, and pyrophyllite (White et al., 1988; Simmons et al., 1992; Mitchell and Leach, 1991).

5.3.2 Clay zone (Tasc)

The outermost altered zone in the acid-sulfate altered areas in the Steeple Rock district

is designated the clay zone, which is characterized by the alteration and replacement of the matrix and primary minerals in the host rock by kaolinite, illite, quartz, hematite, and locally illite/smectite, pyrite, anatase, tridymite, diaspore, alunite, despujolsite(?), and rare pyrophyllite. This mineral assemblage results in bleached and iron-stained rocks that occur in multiple shades of white, red, yellow, orange, purple, green, brown, and black. The intensity of alteration varies and locally some primary minerals such as quartz, titanite, zircon, and apatite are locally preserved (Appendix 11.2). Relict primary textures of original lithologies, such as trachytic and porphyritic, are also locally preserved. Some areas within the clay zone are soft and friable and consist only of clay minerals.

Commonly, the clay zone is also characterized by fine-grained, sugary, and vuggy texture, sometimes referred to as silica residue. Silica residue is formed in modern geothermal systems by leaching of the host rock by acid waters, which dissolve the alkali elements, leaving behind only silica, aluminum, iron, and titanium (P. R. L. Browne, unpubl. report, 1992). The porous residue allows additional fluids to pass through the rock which locally deposit secondary minerals in the void spaces.

5.3.3 Silicified zone (Tassi)

The silicified zone is typically the most extensive zone in most acid-sulfate altered areas in the district and is intermediate in composition and texture between the clay and massive silica/chert zones. This zone is characterized by alteration and replacement of primary minerals by quartz, kaolinite, illite, and locally pyrite, diaspore, pyrophyllite, alunite, jarosite, despujolsite(?), tridymite, anatase and other titanium oxides. The intensity of alteration varies, but is typically higher than in the clay zone and increases to 100% near the massive silica/chert zone (Appendix 11.2). Quartz content is typically high (>60%) and increases toward the massive silica/chert zone. Local areas of less intense altered rocks surrounded by intensely altered rocks are common. Relict primary textures are common.

These rocks are usually bleached and iron stained and occur in multiple shades of

white, red, yellow, orange, purple, green, brown, and black. Textures vary from fine- to medium-grained, massive to brecciated to vuggy to sugary. Silica residue, silica deposition and replacement are common. In some thin sections, thin quartz veins cut the altered rock. Quartz also locally replaces primary minerals such as feldspar, pyroxenes, and amphiboles.

Local areas of intense brecciation and hydrofracturing occur in this zone. Breccias of various lithologies with differing alteration types and intensities are cemented by silica (Fig. 5.5). These breccias are poorly sorted, randomly oriented, and consist of angular fragments. There are no chilled or altered zones surrounding the breccia fragments. Locally the breccias form a jigsaw pattern where the pieces could be put back together (hydrofracturing or hydrobrecciation). The rock fragments are rarely in contact with one another and they do not appear to have formed by grinding. Rock fragments are typically less than 1 m in diameter.

Hydrothermal explosions or eruptions are common in near-surface geothermal systems (Muffler et al., 1971; Phillips, 1972; Fournier et al., 1991; Sigvaldason, 1992). A hydrothermal explosion takes place when water flashes to steam and violently disrupts the confining rocks and expels water, steam, and solid material. A hydrothermal explosion or eruption is not a volcanic eruption because no magma is directly involved. One result of these explosions are geysers. Craters formed by hydrothermal explosions can range in size from very small (2–50 m) to as large as 1500 m or more (Muffler et al., 1971). The local areas of brecciation and hydrofracturing in the Steeple Rock district may have formed by hydrothermal explosions or eruptions and represent either the surface or subsurface remnants of these violent events. Some areas of acid-sulfate alteration in the Steeple Rock district have circular, elongate, or horseshoe shapes, which along with the texture, composition and appearance are suggestive of hydrothermal eruptions (i.e. east of the Summit vein; Fig. 5.19; Sigvaldason, 1992).

5.3.4 Massive silica/chert zone (Tass)

The innermost, central zone of the acid-sulfate alteration is designated the massive

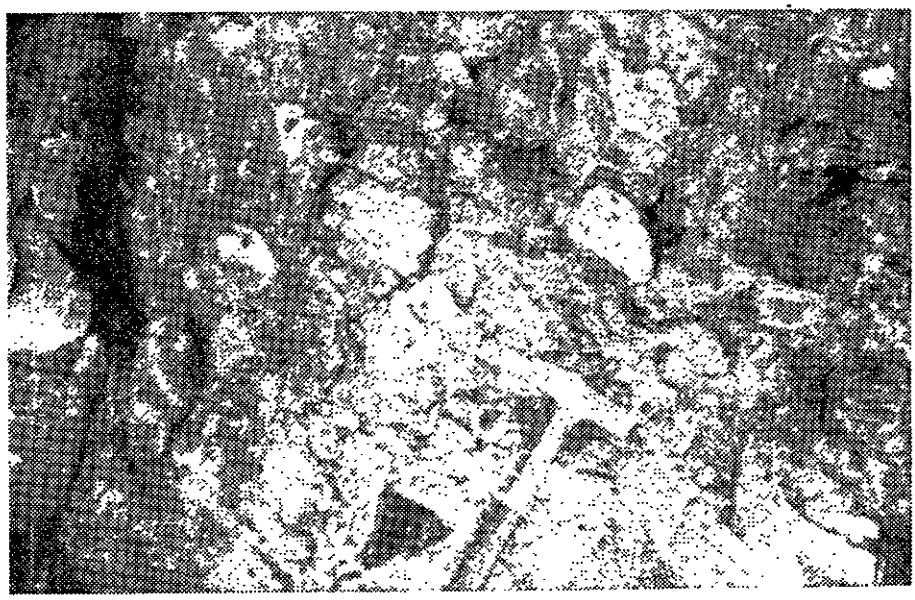

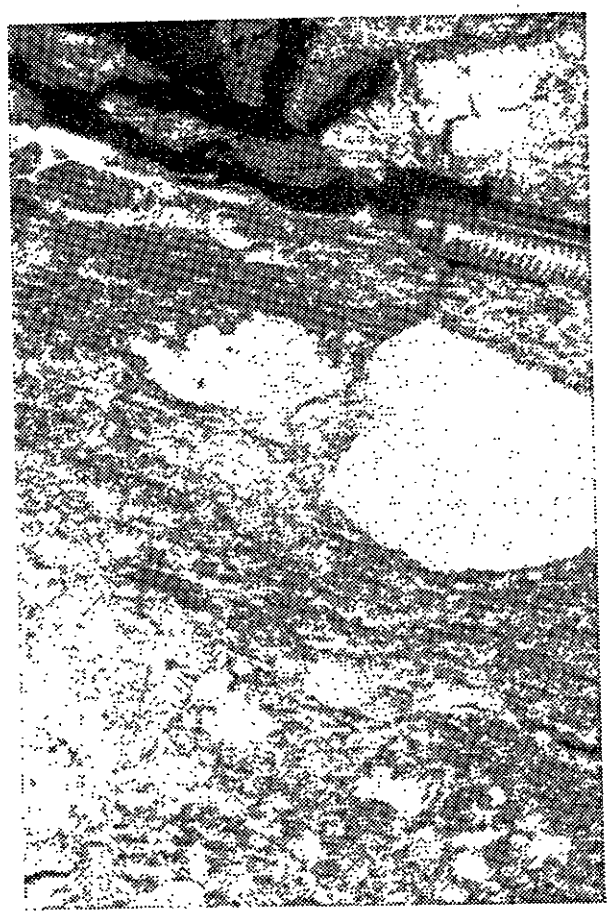

Figure 5.5—Hydrothermal breccias from the Raeburn Hills area.

silica/chert zone. This zone is referred to by Biggerstaff (1974) as quartz knobs, jasperoids, and silica replacement caps; and is characterized by >90% silica, typically as quartz and/or chert with minor amounts of kaolinite, anatase, alunite, pyrophyllite, hematite, and pyrite (Appendix 11.3). These rocks are typically white to light gray in color and extremely hard. The massive silica/chert zone has a fine- to medium-grained, massive to brecciated to locally vuggy texture. Intensity of alteration is typically 100% and relict textures are seldom preserved (Appendix 11.2). Locally areas of brecciation and hydrofracturing occur, similar to areas in the silicified zone. This zone formed by dissolution of most elements by the acid fluids and subsequent recrystallization and/or deposition by silica.

5.4 Description of areas

5.4.1 Raeburn Hills area

Raeburn Hills is located along the Bluebell fault in the east-central part of the district (Fig. 5.4, Maps 1, 2). The area is named after a windmill in the arroyo that cuts the alteration. FMC drilled 12 holes (reverse circulation) in the area, but only limited data were available for this study.

The altered rocks in the Raeburn Hills area were originally andesites of the Dark Thunder Canyon formation, an ash-flow tuff of unknown age, and volcaniclastic sedimentary rocks of the Summit Mountain formation. Intensity of alteration varies. All three advanced argillic alteration zones are present in the area (Figs. 5.6, 5.7, 5.8). There are three areas of massive silica/chert zones: two capping hills (Fig. 5.8) and a third forming the knob in the northern part of the area (Fig. 5.9). The acid-sulfate altered rocks overlie alkali-chloride altered andesites and sandstones. The total thickness of acid-sulfate alteration is probably less than 200 m based on surface exposure and limited drill data (Fig. 5.8).

Quartz, kaolinite, and iron and manganese oxides are common to all three zones. Locally, tridymite, diaspore, alunite, and illite occur in the clay zone and alunite, pyrophyllite, and illite occur in the silicified zone (Fig. 5.7; Appendix 11.3). Barite, calcite,

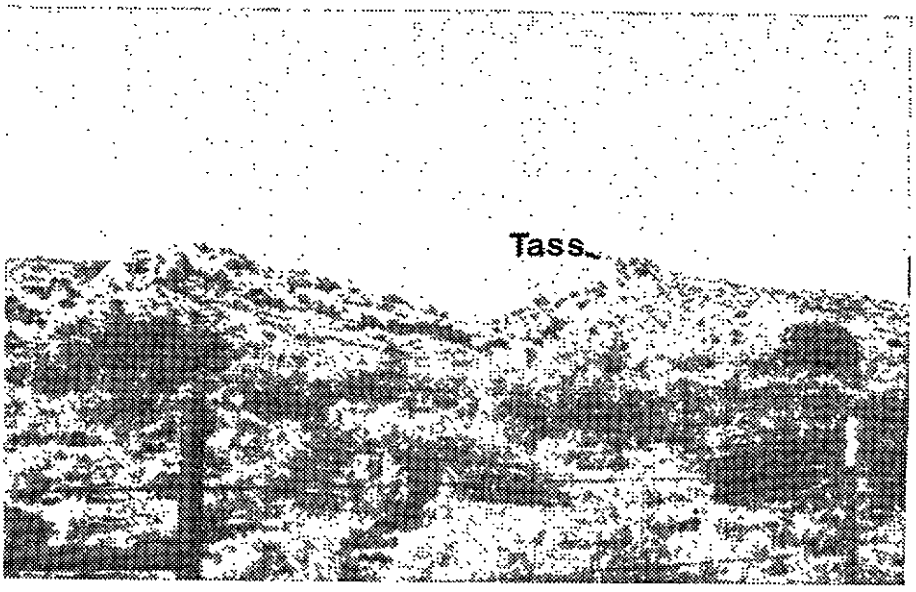

Figure 5.6. View of Raeburn Hills altered area, looking east, capped by massive silica/chert. See Figure 5.8 for cross section of this view.

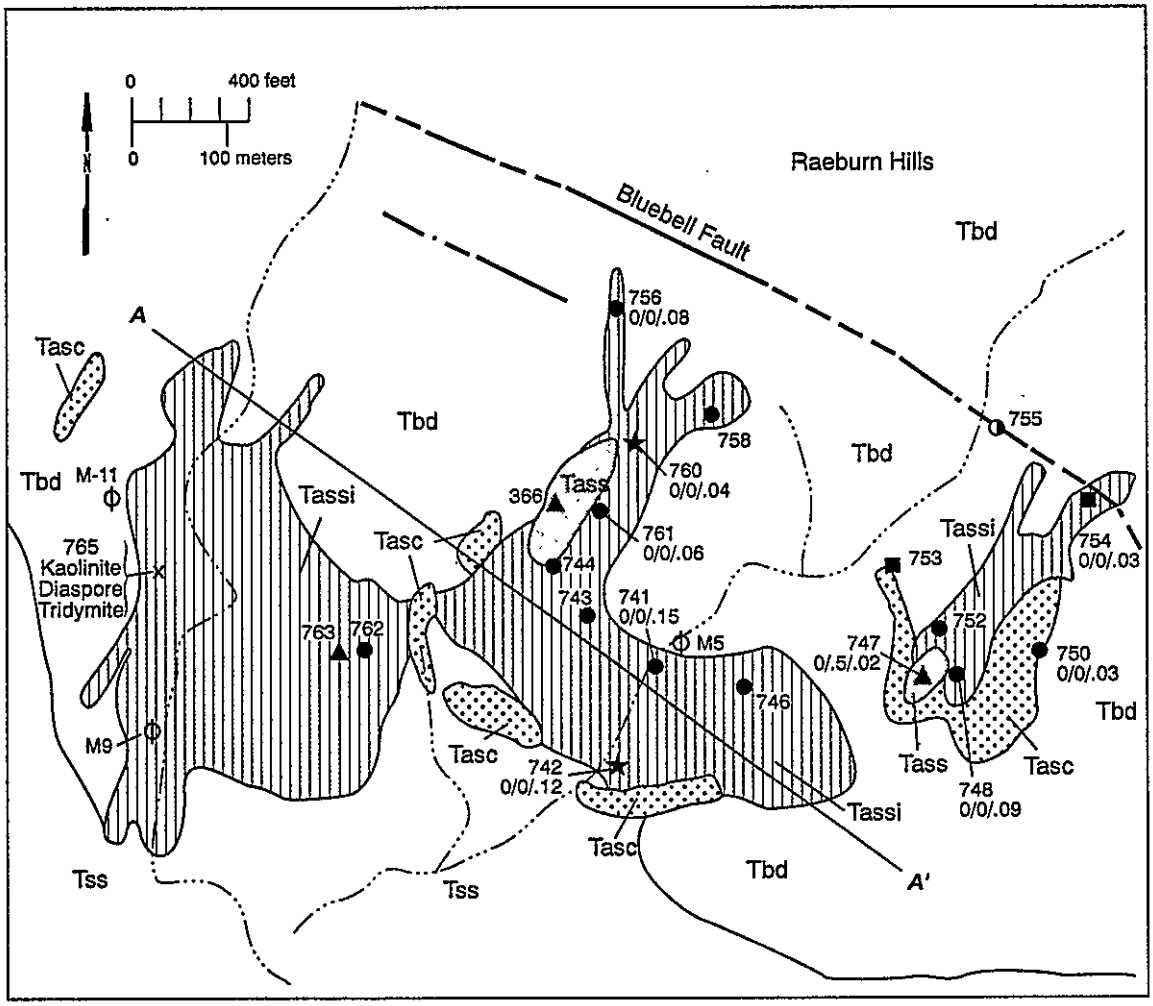

Tass Massive silica/chert zone
Tassi Silicified zone
Tasc Clay zone
Tbd - Dark Thunder Canyon formation
Tsed - Summit Mountain formation
Tss - Undifferentiated sedimentary rocks

- quartz-kaolinite and/or illite
- jarosite-quartz-kaolinite and/or illite
- alunite-quartz-kaolinite and/or illite
- ★ pyrophyllite-quartz-kaolinite
- ▲ quartz-anatase
- ϕ drillhole
- x prospect pit, no production

0/0/.12 - assay
Au oz./ton/Ag oz./ton/Hg ppm

Figure 5.7 Geology and alteration map of Raeburn Hills area.

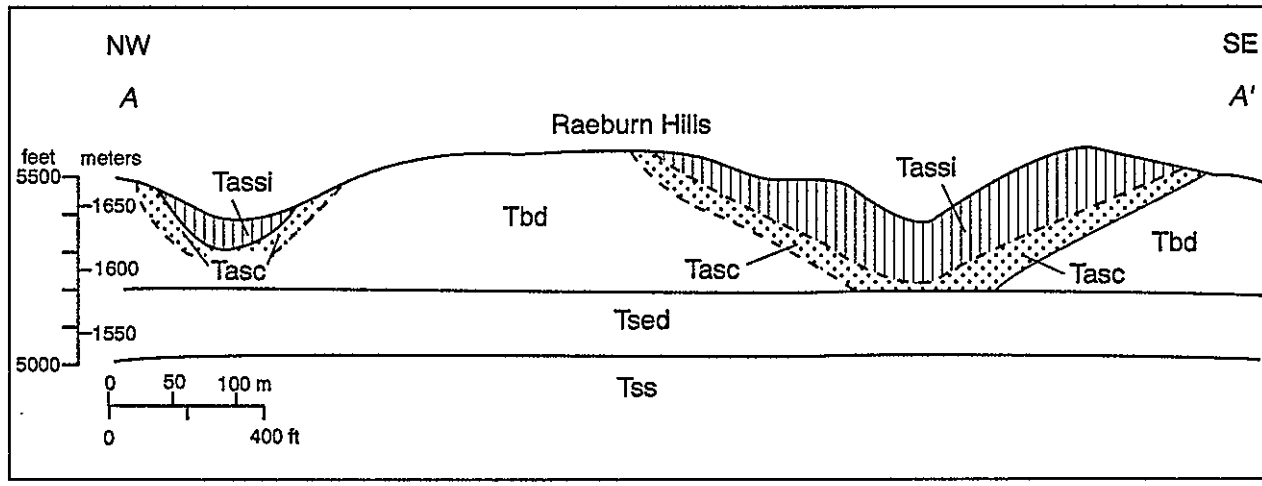

Tassi - Silicified zone

Tasc - Clay zone

Tbd - Dark Thunder Canyon formation

Tsed - Undiferentiated sedimentary rocks

Tss - Summit Mountain formation

Figure 5.8 Cross section through Raeburn Hills (modified from FMC drill data).

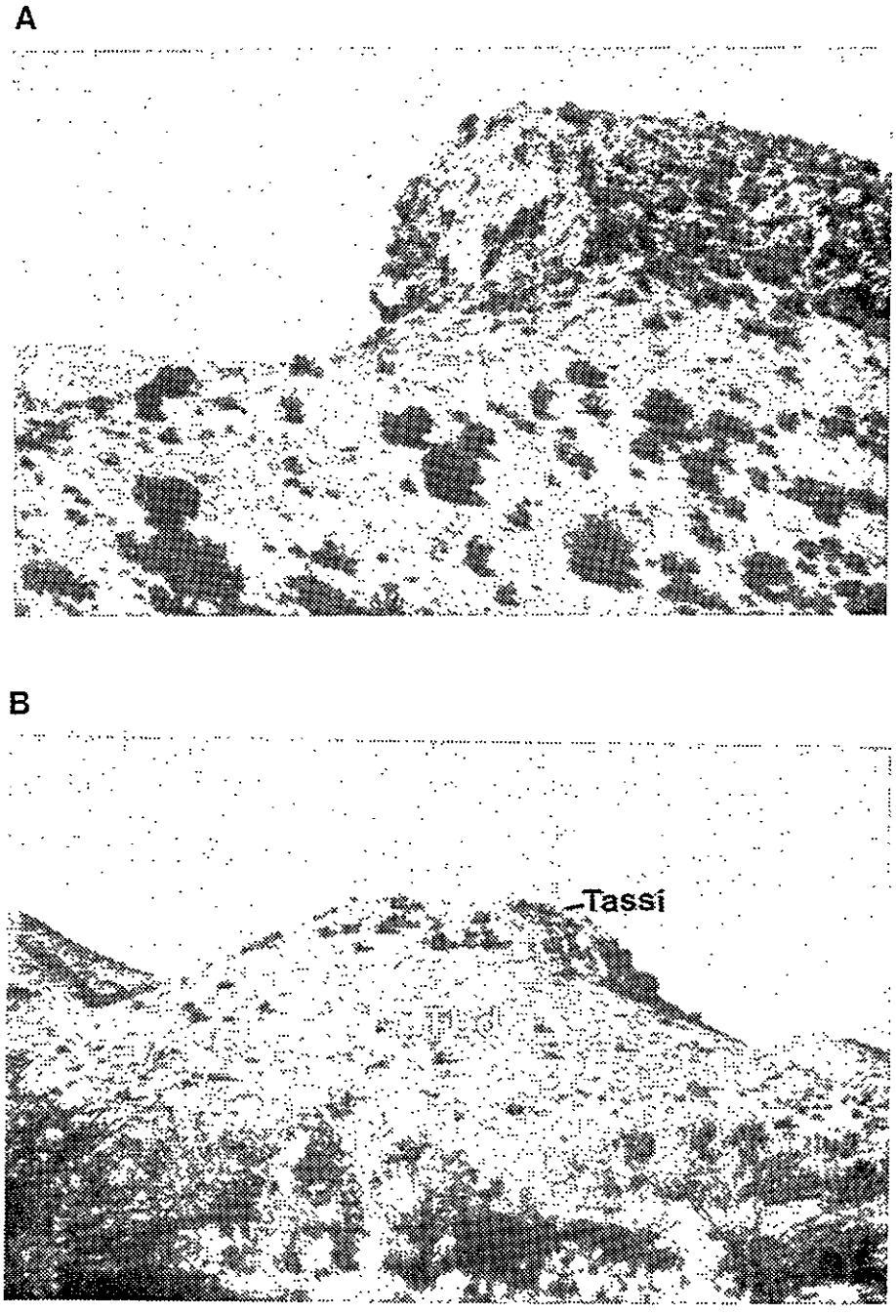

Figure 5.9—View of the Knob at Raeburn Hills overlying andesites of Dark Thunder Canyon formation. A) View looking north. B) View looking east.

and pyrite are locally present in the silicified and massive silica/chert zones. Relict porphyritic textures characteristic of the porphyritic andesite, sandstone, and tuff are locally preserved. Pyrite casts are common in the silicified zone. Hydrothermal brecciation and hydrofracturing are preserved in the silicified and massive silica/chert zone (Fig. 5.5).

A geochemical sampling program by FMC indicates that samples from this area are relatively low in gold, silver, and mercury, although local anomalies do occur (Table 5.2). A map showing location of FMC samples was not available; however, samples for this study confirm the low values (Fig. 5.7; Appendix 11.5). One sample contained 0.5 oz/ton (17.1 ppm) Ag (#747, Appendix 11.5).

Table 5.2—Summary of geochemical analyses of Raeburn Hills altered area reported by FMC (both surface and drill cuttings samples; E. M. Crist, pers. comm. October 1988) and reported in this study (Appendix 11.5). Average crustal abundances and in basalts from Krauskopf (1979).

Element	FMC data Range (ppm)	This study data Range (ppm)	Average crustal abundance (ppm)	Average basalt (ppm)
Au	<0.04–2.4	<0.7	0.003	0.004
Ag	5–40	0.7–17.1	0.07	0.1
Hg	0.5–5	0.02–0.15	0.02	0.01
As	50–>300	--	1.8	
Sb	10–>350	--	0.2	0.2
Mo	10–>250	--	1.5	1.0
Cu	<200	6–41	50	100
Pb	<200	4.8–63	12.5	3.5
Zn	<200	4.8–27	70	100

Epithermal veins along the Blue Bell fault cut and are younger than the acid-sulfate alteration (Fig. 5.7). Silicification and minor clay alteration occurs along the veins. Elsewhere, veins cut alkali-chloride altered andesites with only weak silicification. Locally jarosite is present in the wallrock.

5.4.2 Telephone Ridge area

Telephone Ridge lies north of the Carlisle and Center mines and west of Raeburn Hills (Fig. 5.4; Maps 1, 2). It is bounded on the south by the Carlisle fault and on the east by the East Camp fault. Pioneer Nuclear drilled four diamond drill holes; logs and chemical analyses are summarized in Appendix 11.1. The core has disappeared.

The rocks on Telephone Ridge are intensely altered and the original lithology is locally difficult to determine. Hedlund (1990a) mapped them as rhyolite intrusives. Biggerstaff (1974), Powers (1976), and Wahl (1980) mapped them as rhyolite ash-flow tuff. Drill data do not support an intrusive rhyolite; however, it is possible that an intrusive was missed by the large spacing of the drill holes. Hydrothermal breccias are common along the ridge and are similar in appearance to autobreccias observed in rhyolite plugs and domes. However, the breccias also could be attributed to hydrothermal eruptions. Outcrop examinations and petrographic studies suggest that the original rocks were ash-flow tuffs, sandstones, and hydrothermal breccias (Appendix 11.2). This area is mapped as altered tuff, sediments, and andesites undifferentiated (Tas) because of the intense alteration (Maps 1, 2).

All three alteration zones are present in the area (Figs. 5.10, 5.11, 5.12). The most impressive outcrops are the massive silica/chert zone (Figs. 5.10, 5.13), which forms some of the largest and best exposures of this zone in the district. Silicified and clay zones surround the massive silica/chert zone and together overlie slightly altered andesite flows and tuffs (Fig. 5.14). Some areas of alkali-chloride altered rocks are surrounded by acid-sulfate altered rocks. Some fractures within the alkali-chloride altered rocks are bleached and the alkali-chloride altered andesites are sandwiched between acid-sulfate altered rocks suggesting that permeability and lithology controlled fluid migration (Fig. 5.15). Fossil fumaroles occur in andesite beneath the massive silica/chert zone (Figs. 5.16, 5.17) and indicate migration of gases. Fossil fumaroles (or vesicle cylinders) may also indicate gases escaping during deuteric cooling of the flows. However, they are only found at Telephone Ridge beneath zones of acid-sulfate alteration and suggest a spatial relationship to the alteration.

Figure 5.10—Massive silica/chert zone at Telephone Ridge overlying silicified zone. Looking north.

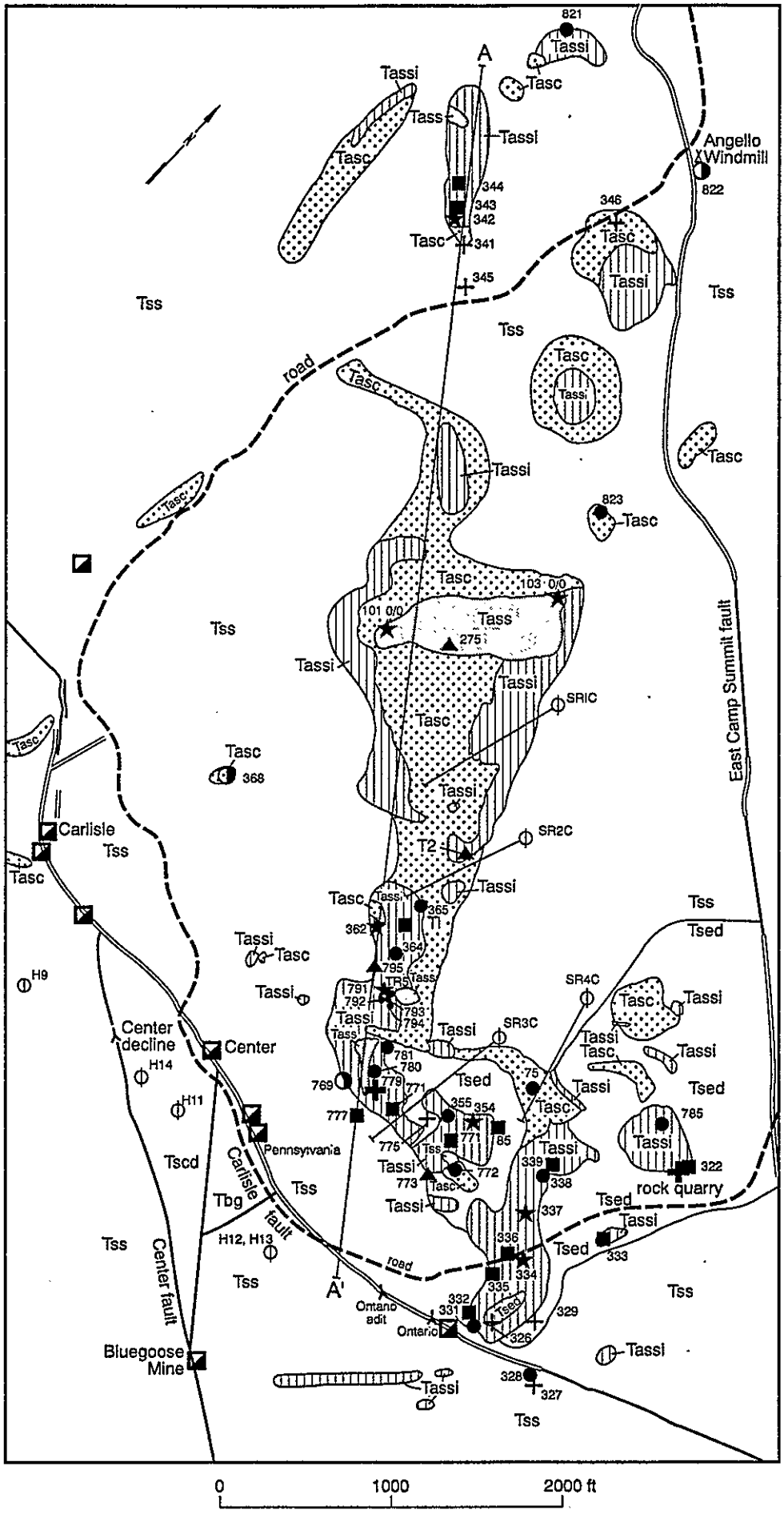

Figure 5.11. Geologic and alteration map of Telephone Ridge.
Legend on next page

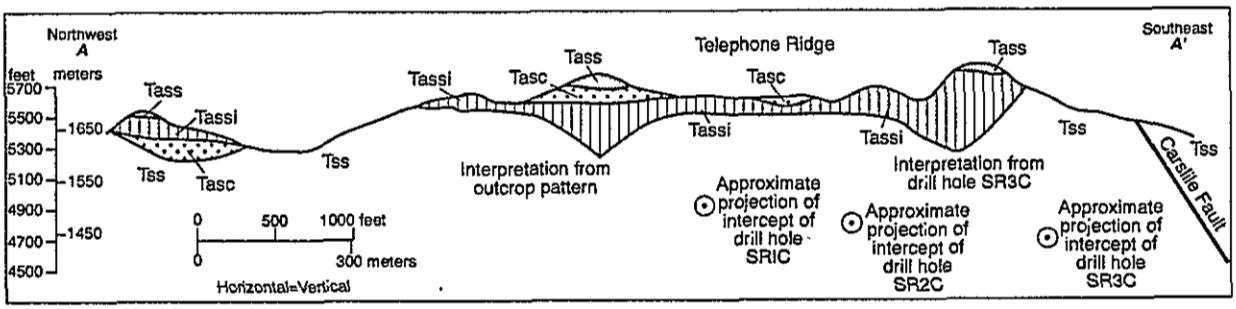

Tass Massive silica/chert zone

Tassi Silicified zone

Tasc Clay zone

Tss Summit Mountain formation

▲ quartz-anatase

\+ chlorite-illite/smectite-quartz

● quartz-kaolinite and/or illite

◑ jarosite-quartz-kaolinite and/or illite

■ alunite-quartz-kaolinite and/or illite

✚ illite-quartz-diaspore and/or kaolinite

★ pyrophyllite-quartz-kaolinite

0/0/.12 assay
Au oz/ton/Ag oz/ton/Hg ppm

shaft

× prospect pit, no production

893■ sample number

⚒ open pit with production

Figure 5.12 - Cross section through Telephone Ridge (modified from Pioneer Nuclear drill data).

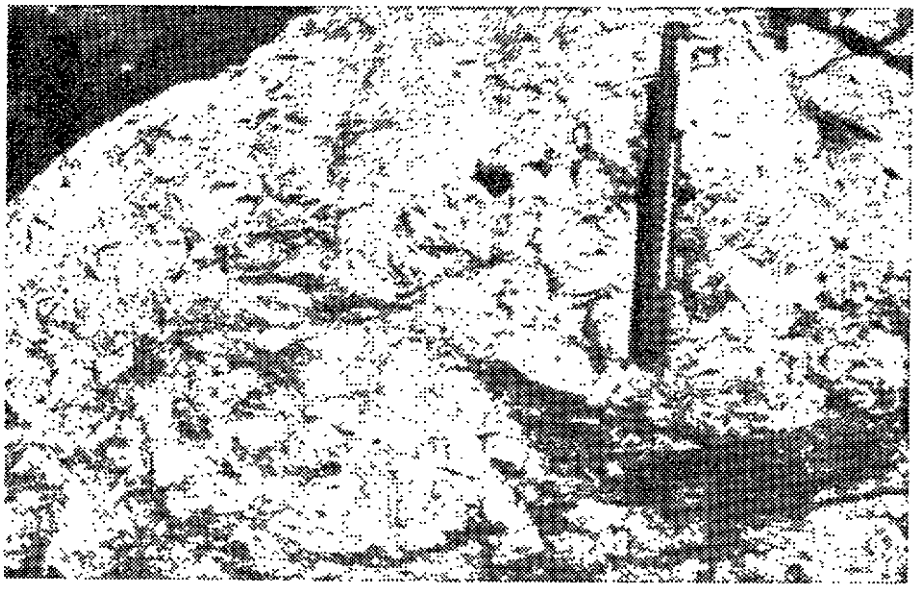

Figure 5.13—Closeup view of massive silica/chert zone at Telephone Ridge.

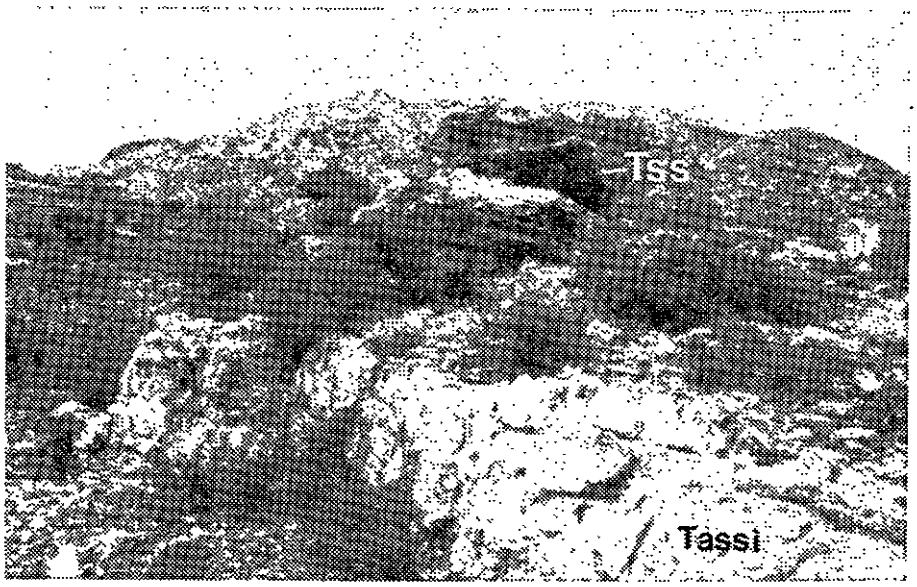

Figure 5.14—Silicified zone overlain by slightly altered andesite lava.

A variety of textures is preserved in outcrop and thin sections. Original phenocrysts are completely or nearly completely replaced by alunite, pyrophyllite, quartz, iron oxides, and kaolinite. Late post-mineralization alkali-chloride alteration is superimposed locally over acid-sulfate alteration; quartz-adularia veinlets cut acid-sulfate alteration locally. Quartz-pyrite veins are common. Ghosts of plagioclase phenocrysts similar to those found in porphyritic andesites are locally preserved. Liesegang-banded altered rocks are common.

The acid-sulfate alteration extends from Telephone Ridge southward to the hanging wall of the Carlisle fault at the Ontario mine (Fig. 5.11). The footwall of the Carlisle fault at the Ontario mine exhibits silicification and chloritization (i.e. alkali-chloride alteration). Acid-sulfate alteration is present at the Carlisle mine forming a partial cap to epithermal mineralization (Fig. 3.4), however, some veins do penetrate the acid-sulfate alteration and cut the earlier altered rock (Fig. 5.11). There is no acid-sulfate alteration at the Center or Pennsylvania mines. If present, acid-sulfate altered rocks could have been eroded away.

The mineralogy of samples from Telephone Ridge and near the Ontario mine is shown in Figure 5.11. Figure 3.4 illustrates the mineralogy at the Carlisle mine. In addition, fluorite, barite, calcite, and pyrite are locally disseminated throughout the altered rock in trace amounts. Quartz, kaolinite, and iron oxides are abundant.

Anomalously high gold, silver, and mercury concentrations are locally present at Telephone Ridge and are typically associated with the silicified and massive silica/chert zones (Fig. 5.11; Appendix 11.5). Surface sampling by Pioneer Nuclear Corp. indicates anomalous concentrations of gold (>0.02 ppm), silver (>0.2 ppm), mercury (>0.10 ppm), and arsenic (>30 ppm) occur in the vicinity of the massive silica/chert zone (Pioneer Nuclear, geochemical map).

A series of samples was collected vertically along a steep hillside west of Telephone Ridge (#341–346; Appendix 11.4, 11.5; Figs. 5.15, 5.18). The intensity and rank (temperature) of alteration increases from bottom to top, as indicated by the mineral assemblage. Mineralogy also changes (from bottom to top): illite/smectite to illite–kaolinite

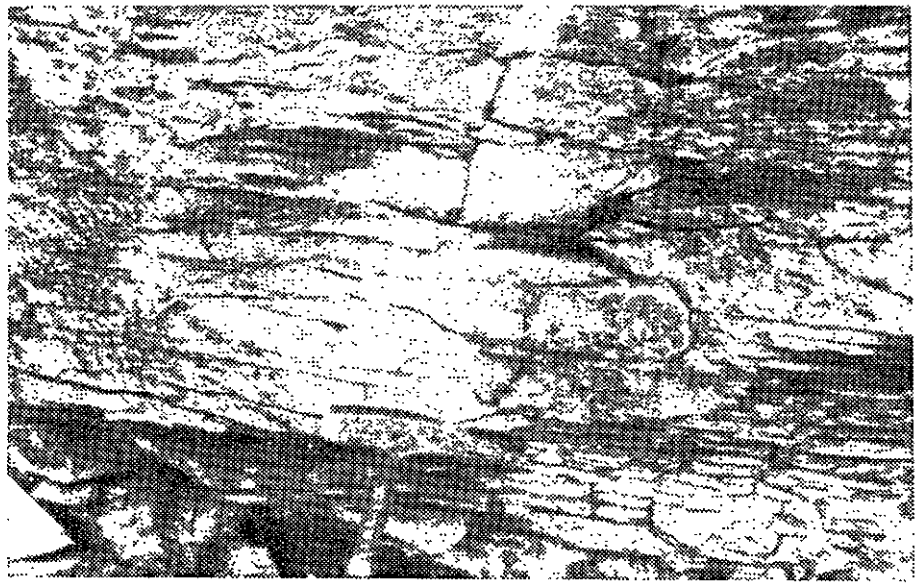

Figure 5.15—Bleached clay zone along fracture in slightly altered andesite lava. The lava is overlain by the silicified zone.

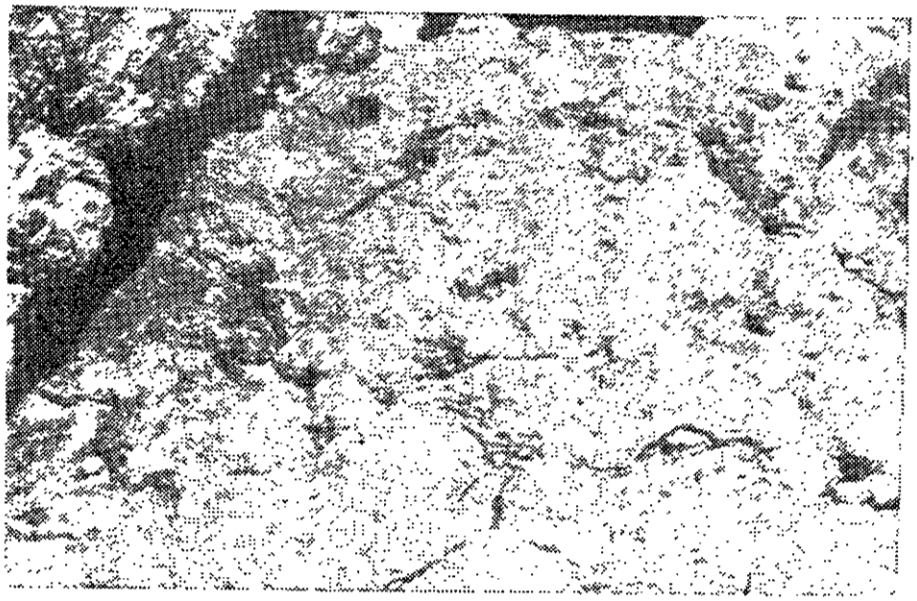

Figure 5.16—Fossil fumaroles in andesite lava at Telephone Ridge, underlying the massive silica/chert zone (Fig. 5.10). Circular features in the andesite are the top of fumaroles.

Figure 5.17—Cross section of fumaroles characterized by porous circular pipes or tubes in the andesite.

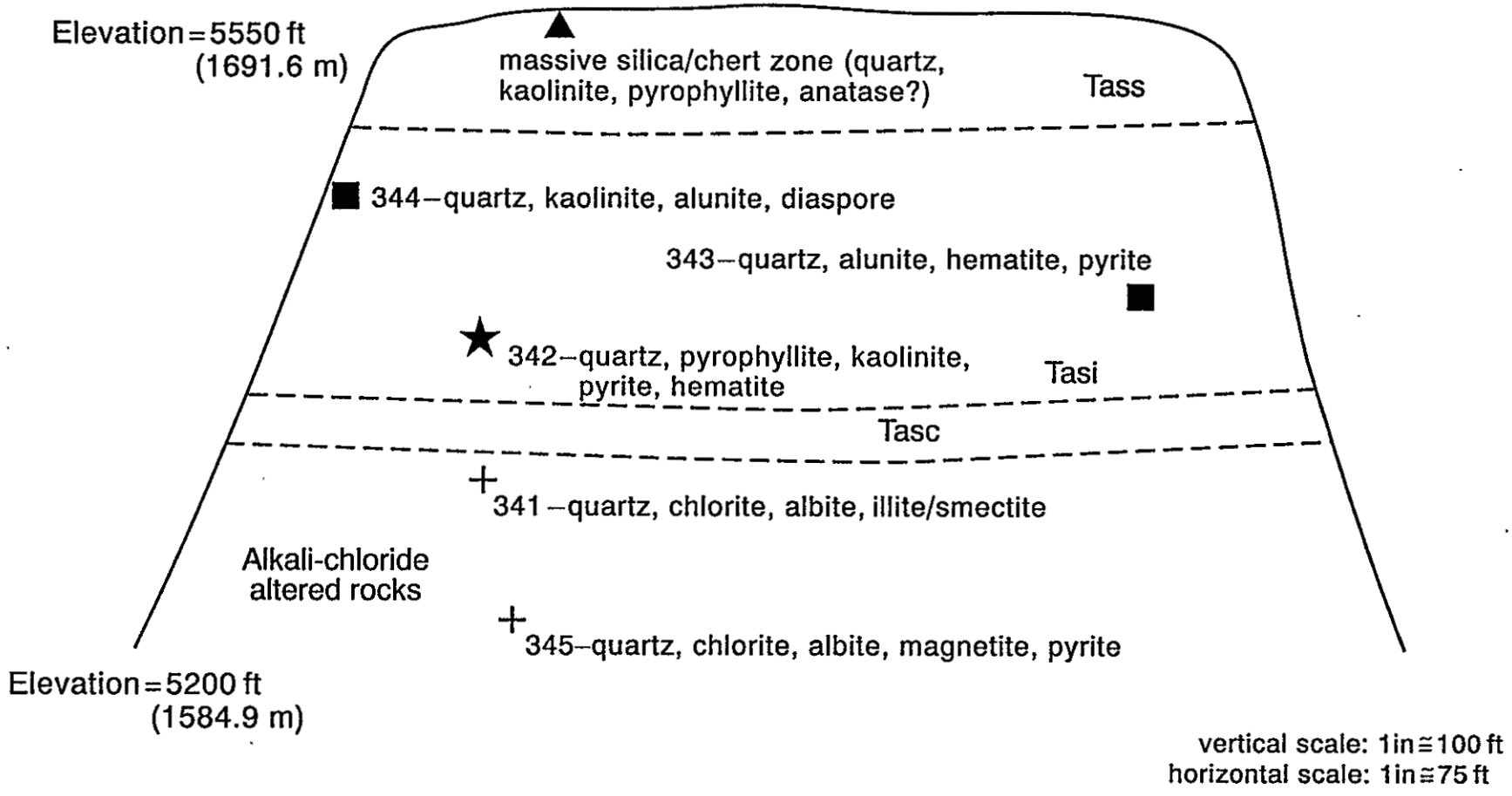

Figure 5.18– Sketch of vertical profile east of Telephone Ridge showing vertical zonation. Mineral identification from x-ray diffraction studies (Appendix 11.3). See Figure 5.11 for identification of symbols and location on map.

(clay zone) to kaolinite to pyrophyllite–diaspore–kaolinite (silicified zone) to alunite–kaolinite with local anatase and pyrophyllite (silicified zone). A discontinuous silica replacement body (massive silica/chert zone) occurs on top. Subsurface and surface data indicate that acid-sulfate altered rocks are probably less than 400 m thick and overlie alkali-chloride altered rocks (Appendix 11.1).

Examination of drill core along the Carlisle fault indicates that similar acid-sulfate zones are sandwiched between alkali-chloride altered rocks. Several acid-sulfate zones exist in the subsurface but none are extensive (Appendix 11.1).

5.4.3 Summit and East Bitter Creek altered zones

Acid-sulfate alteration occurs along some of the ridges west of the Summit mine and elsewhere along the East Camp-Summit and Twin Peaks faults (Fig. 5.10). Biron Bay Resources Inc. has drilled numerous diamond drill holes along the East Camp-Summit fault, some of which have penetrated the acid-sulfate alteration (Appendix 11.1).

The altered rocks were originally andesites and, perhaps, tuffs of the Summit Mountain formation. Intensity of alteration varies. All three zones of acid-sulfate alteration are locally present (Fig. 5.19). The massive silica/chert zone is rare, outcrops are typically small and form the caps of the ridges, and it is surrounded by the silicified and clay zones. Syn-mineralization alteration may be superimposed on acid-sulfate alteration at the Bank mine where the area is completely altered to clay and quartz. Total thickness of the acid-sulfate alteration is probably less than 200 m.

The mineralogy of samples collected is shown in Figure 5.18. Illite is predominant in the silicified and clay zones; kaolinite occurs in lesser amounts. Calcite, gypsum, pyrite, tridymite, and barite are locally common in trace amounts in the silicified and clay zones. Liesegang-banded altered rocks are common (Fig. 5.20). Hydrothermal brecciation and hydrofracturing are common in the silicified and massive silica/chert zones. Several areas have circular, elongate, or horseshoe-shaped outcrops that are perhaps indicative of

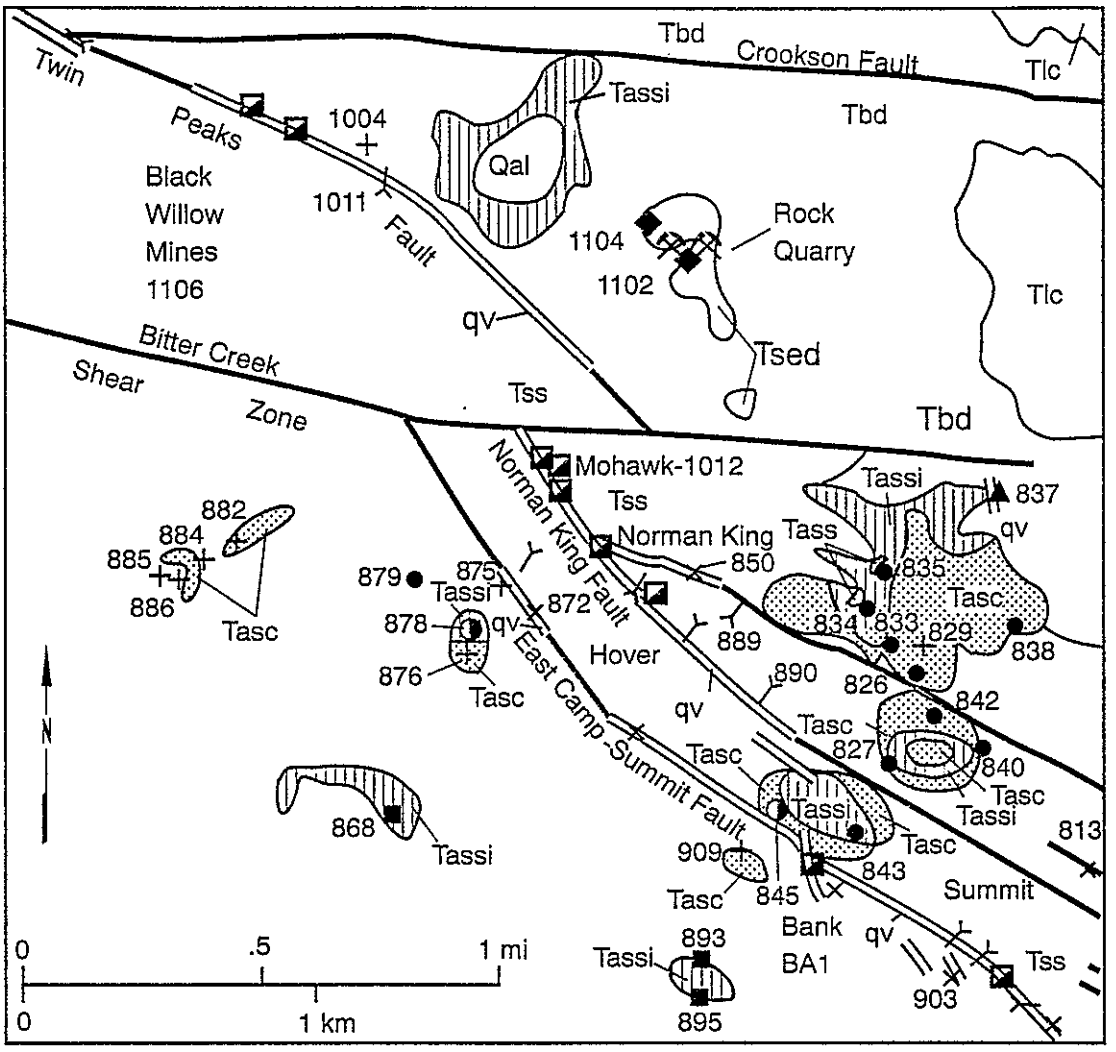

Tass Massive silica/chert zone
Tassi Silicified zone
Tasc Clay zone

Qal - Alluvium
Tlc - Lava flows of Crookson Peak
Tbd - Dark Thunder Canyon formation
Tsed - Undifferentiated sedimentary rocks
Tss - Summit Mountain formation
qv - Quartz vein

+ chlorite-illite/smectite-quartz
● quartz-kaolinite and/or illite
◑ jarosite-quartz-kaolinite and/or illite
■ alunite-quartz-kaolinite and/or illite
★ pyrophyllite-quartz-kaolinite
▲ quartz-anatase
0/0/.12 assay Au oz./ton/Ag oz./ton/Hg ppm
◪ shaft
× prospect pit, no production
⊁ adit
893■ sample number
◆ location of whole rock analyses
⚒ open pit with production

Figure 5.19 Geology and alteration of the Summit and East Bitter Creek altered areas

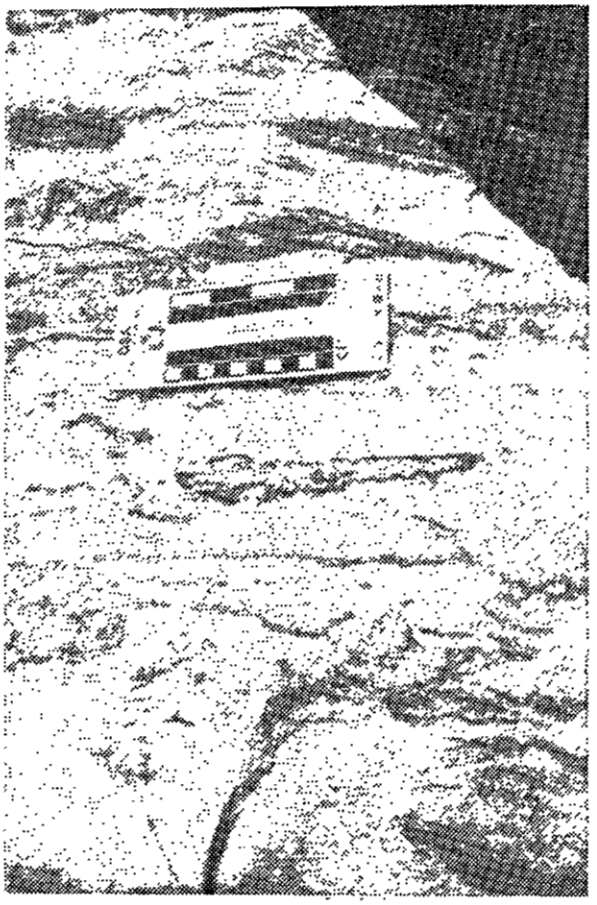

Figure 5.20—View of liesegang-banded altered rock.

hydrothermal vents or craters (Fig. 5.19). Several vertical zones are present in outcrop and in the drill core (Appendix 11.1).

5.4.4 Saddleback Mountain and West Bitter Creek areas

The largest and most extensively acid-sulfate altered areas are the Saddleback Mountain and West Bitter Creek areas (Fig. 5.10). The Bitter Creek fault zone separates the two areas and the West Bitter Creek area is bounded on the north by the Twin Peaks fault (Figs. 5.21, 5.22).

Saddleback Mountain is one of the most rugged and highest mountains in the mapped area and most of the mountain is altered (Figs. 5.23, 5.24). All three zones are present in both areas; the massive silica/chert zone caps the uppermost ridges. The silicified zone surrounds the massive silica/chert zone and is the most extensive zone at Saddleback Mountain. The clay zone forms the lower foothills and is more extensive at West Bitter Creek. Alteration is at least 500 m thick in places (Map 3).

The mineralogy is illustrated in Figures 5.21 and 5.22. Kaolinite, illite, and quartz with local pyrophyllite, pyrite, and jarosite occur in the clay zone. Quartz, kaolinite, illite, alunite, jarosite, pyrite, barite, and anatase occur in the silicified zone. The massive silica/chert zone consists of quartz, anatase, pyrite, and alunite (Appendix 11.3). Large veins (up to 1 m wide) of gray to gray-white alunite-quartz ($\pm$pyrite) and green-gray to gray kaolinite-quartz cut the silicified zone locally. Areas of alkali-chloride altered andesites are preserved throughout and are surrounded by acid-sulfate altered rocks. A rhyolite dike striking northeast cuts the acid-sulfate altered rocks. Vertical pipes of quartz-alunite are preserved in Wampoo Canyon and are capped by alkali-chloride altered andesites (Wahl, 1980).

The original rocks were probably andesites and volcaniclastic sediments of the Summit Mountain formation, although one or two rhyolite ash-flow tuffs may also be present. The intensity of alteration is high and much of the area was mapped as altered rocks

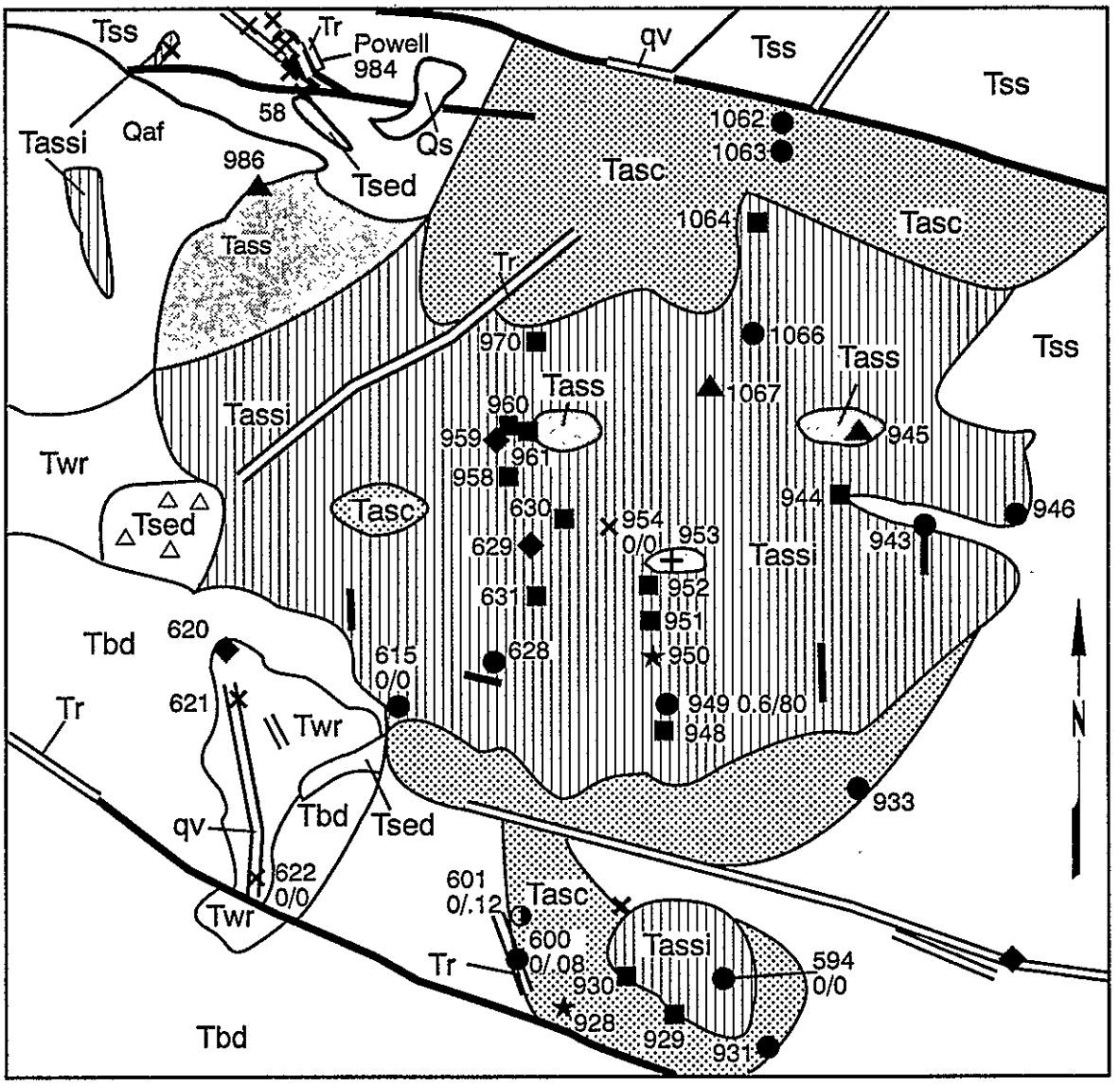

Figure 5.21 Geologic alteration map of Saddleback Mountain area

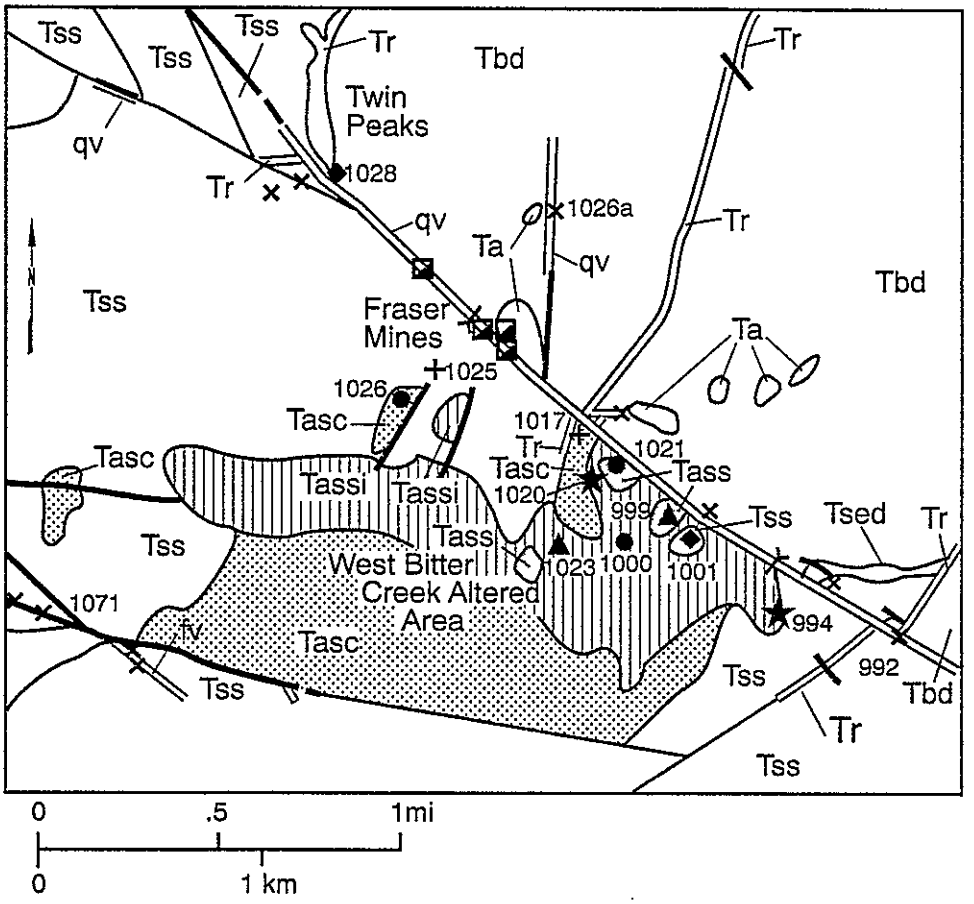

Tass Massive silica/chert zone
Tassi Silicified zone
Tasc Clay zone

Tbd - Dark Thunder Canyon formation
Tss - Summit Mountain formation
Tsed - Undifferentiated sedimentary rocks
Ta - Ash-flow tuff

\+ chlorite-smectite/iillite-quartz
● quartz-kaolinite and/or illite
★ pyrophyllite-quartz-kaolinite
▲ quartz-anatase
0/0/.12 assay
Au oz./ton/Ag oz./ton/Hg ppm
shaft
× prospect pit, no production
adit
893 sample number
◆ location of whole rock analyses

Figure 5.22 Geology and alteration map of the West Bitter Creek area

Figure 5.23—Aerial view of Saddleback Mountain, looking north.

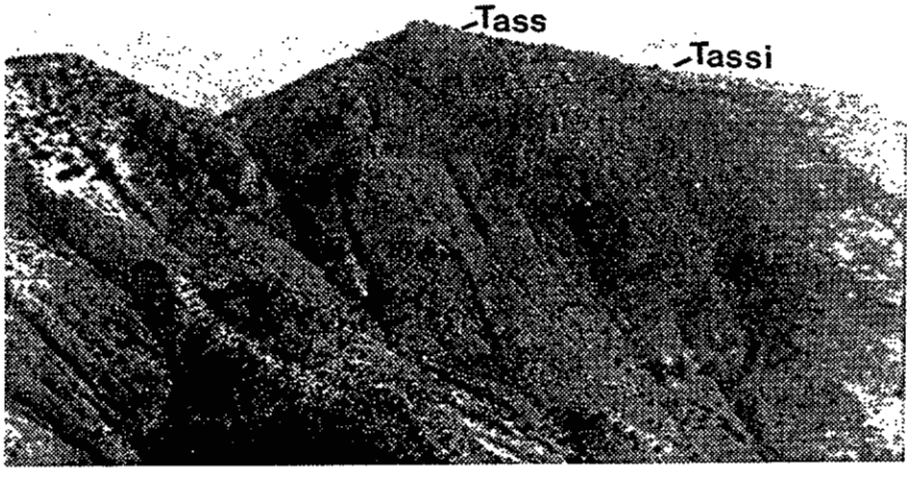

Figure 5.24—Closeup aerial view of massive silica/chert zone at Saddleback Mountain, looking north.

undifferentiated (Tas; Maps 1, 2). One age determination of quartz-alunite altered rock from Saddleback Mountain is reported as 31.3 Ma (Table 2.1; Hedlund, 1993), which is the reported age of the Summit Mountain formation (Table 2.1). Sulfur isotope data are also reported by Field (1966), which will be discussed in section 6.1.2.

5.4.5 Goat Camp Springs area

The Goat Camp Springs area lies west of Vanderbilt Peak (Fig. 5.10) in the vicinity of the Goat Camp Springs fluorite mines (Ontario, Stotts, Dean, Luckie mines; Maps 1, 2). Several mineralized faults and rhyolite/rhyodacite dikes cut the acid-sulfate alteration (Fig. 5.25). Some dikes have been silicified and sericitized, probably in response to quartz and fluorite mineralization, but the intrusives have not been affected by acid-sulfate alteration.

Intensity of alteration varies. Outcrops in this area are colorful, forming bleached and variegated, barren wasteland (Fig. 5.26), similar in appearance and composition to the hot springs, mud pots, and geysers at Norris Geyser Basin, Yellowstone National Park (Fig. 5.27). Hydrothermal breccias with iron and manganese oxides occur along some ridges forming a silicified zone (Fig. 5.25). The massive silica/chert zone is not exposed in this area. The clay zone is the most extensive zone. Some isolated patches of acid-sulfate altered rock are surrounded by alkali-chloride altered rock. Large areas of illite with little quartz occur in the clay zone. Kaolinite is locally present.

Mineralogy of samples from this area is shown in Figure 5.25. Barite, calcite, pyrite, and tridymite are locally present, especially in the hydrothermal breccias. Sampling for this study detected no gold or silver anomalies (Appendix 11.5); however, sampling by R. S. Powers (unpubl. report, 1968) indicates some local areas may contain anomalously high gold and silver (Table 5.3).

5.4.6 Mulberry Springs area

The Mulberry Springs area lies west of Vanderbilt Peak (Fig. 5.10). This area is less

Table 5.3—Summary of geochemical analyses of altered samples from the Goat Camp Springs area from R. S. Powers (written communication, 1968) and this study (Appendix 11.5). Total number of samples: Powers had 104 samples for Au, Ag, and Hg and 4 samples for Cu, Pb, Zn, and Mo. There were seven samples from this study. Average crustal abundances and average basalt from Krauskopf (1979).

	Powers data			Data, this study			Average crustal	Average
Element	Range (ppm)	Average (ppm)	Standard deviation	Range (ppm)	Average (ppm)	Standard deviation	abundance (ppm)	basalt (ppm)
Au	0.0–1.04	0.03	0.10	<0.7	–	–	0.003	0.004
Ag	0.6–2.4	0.67	0.24	<0.7	–	–	0.07	0.1
Hg	0.012–1.295	0.191	0.25	<0.1–0.8	0.3	0.3	0.02	0.01
Cu	92–1760	0.191	0.25	7.9–41	22	10	50	100
Pb	40–128	75	40	10–32	17	8	12.5	3.5
Zn	18–460	152	270	7.4–20	16	10	70	100
Mo	0–32	12.5	16	–	–	–	1.5	1.0

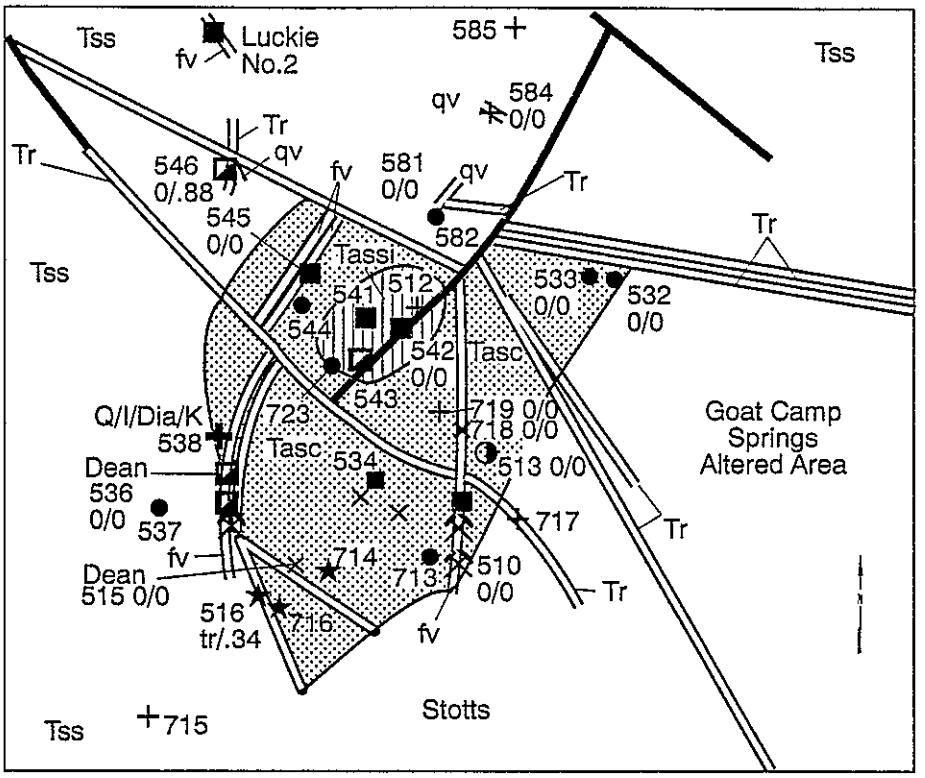

Tassi Silicified zone

Tasc Clay zone

qv - Quartz vein
fv - Fluorite vein
Tss - Summit Mountain formation
Tr - Rhyolite/rhyodacite dike

Stratigraphic symbols are defined in figure 2.2.

\+ chlorite-illite/smectite-quartz
● quartz-kaolinite and/or illite
◑ jarosite-quartz-kaolinite and/or illite
■ alunite-quartz-kaolinite and/or illite
✚ illite-quartz-diaspore and/or kaolinite
★ pyrophyllite-quartz-kaolinite
0/0/.12 assay
Au oz/ton/Ag oz/ton/Hg ppm
◪ shaft
× prospect pit, no production
893■ sample number
⚒ open pit with production

Figure 5.25 Geological alteration map of the Goat Camp Springs altered area

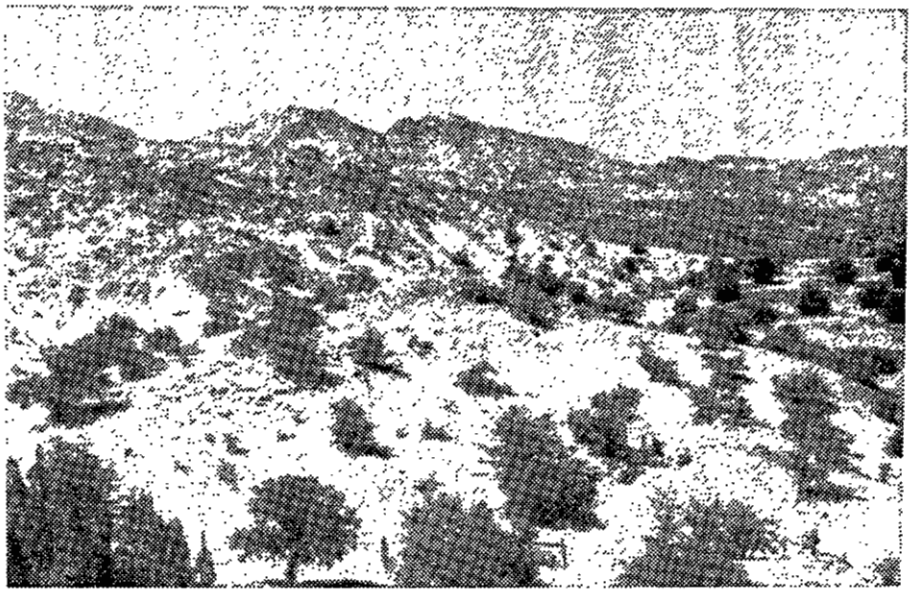

Figure 5.26—View of Goat Camp Springs, looking east. Saddleback Mountain forms the skyline.

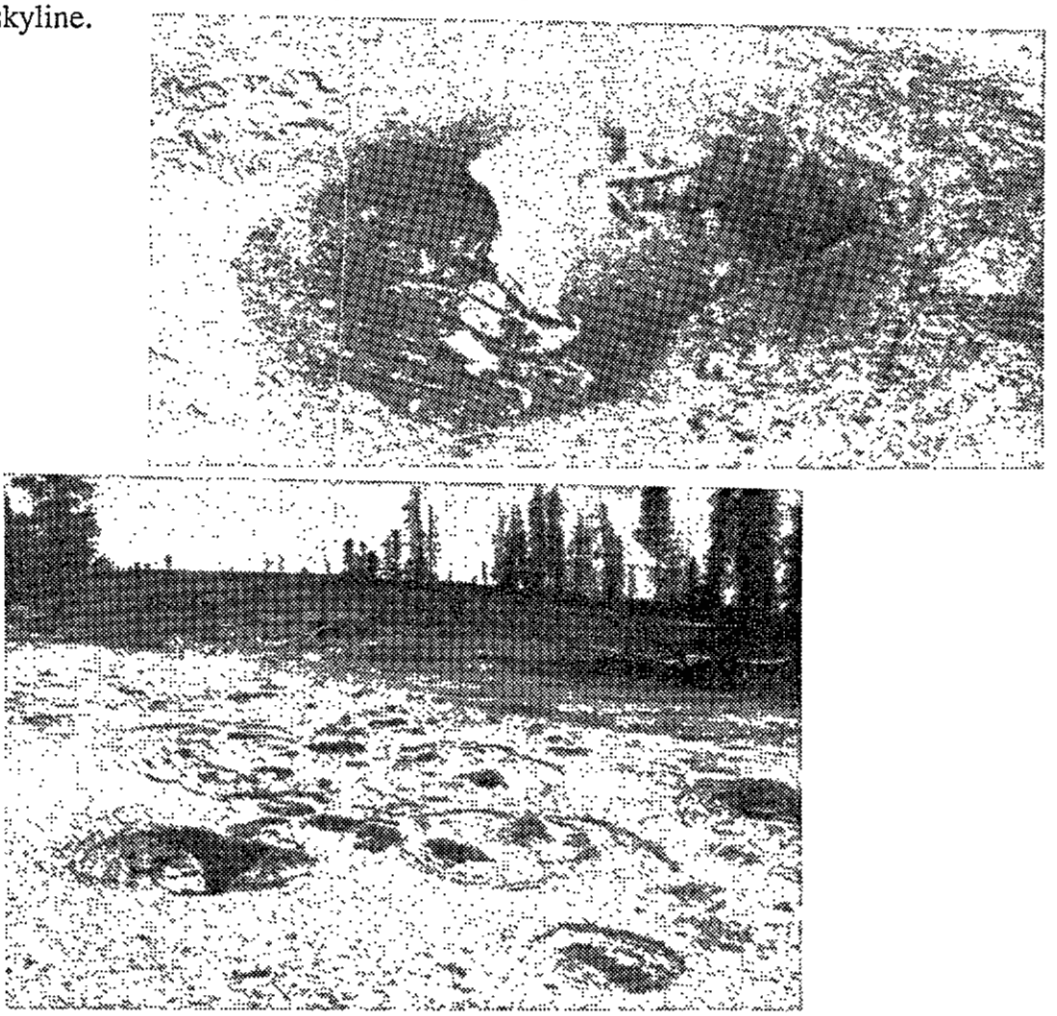

Figure 5.27—Mudpots at Norris Geyser Basin, Yellowstone National Park.

intensely altered and only the clay zone is exposed. Andesite and volcaniclastic sediments of the Summit Mountain formation have been altered to kaolinite and quartz. Iron oxide staining and fracture coatings are common. Original textures are preserved locally. Outcrops are rare (Map 1). No samples were collected in this area during the present study.

5.5 Mineralogy

In this section, the distribution, textures, and description of the major alteration minerals, both alkali-chloride and acid-sulfate, are presented. Techniques used include literature search, field observations, petrography, XRD, and chemical analyses.

5.5.1 Quartz, SiO_2

The predominant alteration mineral in the Steeple Rock district is quartz. Quartz is common to all types of alkali-chloride and acid-sulfate alteration. Quartz occurs as (1) replacement of primary minerals, especially feldspar; (2) vug and other open-space fillings; (3) breccia cement; and (4) veinlets. The massive silica/chert zone (acid-sulfate alteration) consists of $>90\%$ quartz. Some quartz may have originally been deposited as amorphous silica or other silica minerals (tridymite, cristobalite, chalcedony, chert) and subsequently converted to quartz. This quartz typically exhibits undulatory or wavy extinction in thin section (Sander and Black, 1988). Quartz is typically white to colorless to tan or gray. It generally occurs as clear, subeuhedral crystals to extremely fine-grained massive replacements. Rare euhedral, double terminated crystals occur in vugs. Amethyst quartz is present in epithermal veins and as vug-fillings near the epithermal veins.

5.5.2 Pyrite, FeS_2

Pyrite is an abundant alteration mineral in the district, including drill core samples. It

ranges in abundance from trace to 40% and is found in all types of alteration. Grain size varies from submicron to several millimeters. It typically occurs as euhedral to subhedral cubic crystals or aggregates that are disseminated throughout the host rock. Some pyrite replaces primary magnetite, ilmenite, pyroxenes, and amphiboles. It is easily altered to iron oxides in the near-surface environment.

5.5.3 Chlorite, $Mg_3(Si_4O_{10})(OH)_2 \cdot Mg_8(OH)_6$

Chlorite is restricted to alkali-chloride altered rocks; it is unstable and converts to other minerals or is dissolved by acidic waters in the acid-sulfate environment. Specific chlorite minerals have not been identified yet. Chlorite occurs as (1) replacement of original matrix, (2) replacement of iron and magnesium silicates, and (3) as thin veins and veinlets (Fig. 5.3). It results in a greenish-colored rock. In thin section, it occurs as minute crystals, aggregates, and foliated masses.

5.5.4 Adularia, $KAlSi_3O_8$

Adularia is a low-temperature variety of K-feldspar and is restricted to the alkali-chloride alteration. Locally, quartz-adularia veinlets cut the acid-sulfate alteration, but adularia is not stable under acidic conditions (Fig. 6.9). Adularia found in this environment represents superimposed, younger alkali-chloride alteration. Adularia occurs as small replacements of primary feldspar and vug fillings ($<0.05\mu$ in size). Adularia content rarely exceeds 1% in any altered rock. It is similar in appearance to quartz except adularia exhibits cleavage.

5.5.5 Clays

Clay mineralogy is important in determining the rank of alteration; many clays are

indicative of temperature (Fig. 5.1). Clays are common in all types of alteration in the district.

In the alkali-chloride altered rocks, the predominant clay mineral groups present are smectite, illite/smectite, illite, and less common kaolinite. Chlorite is abundant and has been previously described. Illitic clays are common in syn-mineralized altered zones and probably represent higher temperatures (Fig. 5.1). Smectite and illite/smectite are rare to absent immediately adjacent to and within veins. Pure smectite clays or predominantly smectite/illite clays are less abundant but are found locally away from veins. Chlorite/smectite clays are also abundant in some areas and locally form a halo surrounding vein deposits. Locally, kaolinite and kaolinite-illite form gray to green veins and veinlets in altered areas near the veins (3–4 cm).

In the acid-sulfate altered rocks, smectitic clays are absent except around the margins of such alteration. Kaolinite and illite are the predominant clay mineral groups in the acid-sulfate altered rocks and are indicative of deposition by low pH fluids. Clays are abundant in this zone and decrease in abundance toward the massive silica/chert zone. Kaolinite is typically finely disseminated throughout the rock, filling void spaces and replacing primary minerals. Kaolinite is typically white to green to gray and when intergrown with quartz becomes rather hard and difficult to identify except by XRD. XRD analyses of randomly packed powders indicated kaolinite and dickite are present locally. Some veins are several centimeters wide. Illite is also green to gray to white, and finely disseminated throughout the rock, but locally occurs as very small tabular, moderate to high birefringence crystals. Illite typically indicates temperatures of formation greater than 200°C, whereas mixed layered clays indicate lower temperatures (<200°C; Fig. 5.1). Veins of white to green illite and quartz are locally common.

5.5.6 Titanite (sphene), $CaTiSiO_5$

Titanite is common in both types of alteration in the district and is also a primary mineral in the volcanic rocks. It occurs as small anhedral crystals with high relief and high birefringence. It is semiopaque to opaque and is white in reflected light. Typically the crystals are absorbed or skeletal creating a spongy appearance. It is commonly identified only by XRD (Appendix 11.3).

5.5.7 Anatase/rutile/leucoxene, TiO_2

Anatase, rutile, and leucoxene are common alteration minerals in the district, especially in acid-sulfate altered rocks. These minerals may be complexly intergrown and occur as opaque, yellow to red to brown in thin section and white under reflected light microscopy. The crystals or aggregates are small (<0.05 μm) and are identified by XRD (Appendix 11.3).

5.5.8 Epidote, Ca-Mg-Mn $(Al,Fe)_3(OH)(SiO_4)_3$

Epidote is found locally in the district and is restricted to alkali-chloride altered rocks. It occurs as replacement of primary and alteration minerals, veinlets, aggregates with chlorite, and as distinct fibrous aggregates. It is typically colorless to green in thin section, pleochroic, and has moderate birefringence. Epidote is an important alteration mineral because it indicates deposition from fluids at $>200°C$ (Fig. 5.1; Reyes, 1990; Simmons et al., 1992).

5.5.9 Carbonates

Various carbonate minerals occur in the altered rocks; for example calcite, dolomite, anhydrite, and siderite. They typically occur as replacements of primary minerals, vug

fillings, and veinlets; locally they form small rhombhedron-shaped crystals. They are especially common in alkali-chloride altered rocks and rare in acid-sulfate altered rocks. Bladed calcite indicates boiling (White and Hedenquist, 1990). Dolomite is typically deposited by fluids at $<180°C$ and anhydrite is typically deposited by fluids at $>150°C$ (Fig. 5.1).

5.5.10 Zeolites

Zeolites are present in low-temperature alkali-chloride altered rocks. Mordenite $(Ca,Na_2,K_2)Al_2Si_{10}O_{24} \cdot 7H_2O$ and gismondine $CaAl_2Si_2O_8 \cdot 4H_2O$ are more common in the andesites, but thompsonite $NaCa_2Al_5Si_5O_{20} \cdot 6H_2O$ and other low-temperature zeolites are also found. They typically occur as vug or open-space fillings and replacement of groundmass. They are indicative of temperatures $<200°C$ (Fig. 5.1). Wairakite $CaAl_2Si_4O_{12} \cdot 2H_2O$ is a higher temperature zeolite (220–300°C; Reyes, 1990) and is found in one sample (#178, Appendix 11.3)

5.5.11 Alunite, $KAl_3(OH)_6(SO_4)_2$

Alunite is found in the acid-sulfate altered rocks; typically in all three zones in varying amounts. Alunite is difficult to identify visually in the district. Its identification is confirmed only by XRD and petrographic studies, because it is fine-grained (<0.05 mm) and disseminated. Alunite is one end member of a series of sulfates that occur in several geologic environments, all of which are low pH environments. Alunite-group minerals are common products of hydrothermal alteration (specifically acid-sulfate alteration) and weathering and are found in modern hot springs, sedimentary rocks, and low-grade metamorphic rocks (Stoffregen and Cygan, 1990). In the Steeple Rock district, alunite locally occurs with pyrite, which, along with additional data, suggests a hydrothermal origin.

Minerals of the alunite-group have the general composition $AB_3(SO_4)_2(OH)_6$ where A is typically K^+, Na^+, Pb^{++}, NH_4^+, or Ag^+ and B is typically Al^{+3} or Fe^{+3} (Brophy et al., 1962). The alunite-group consists of many mineral species, and nine of the more common minerals are (Brophy et al., 1962; Altaner et al., 1988):

Alunite – $KAl_3(SO_4)_2(OH)_6$

Natroalunite – $NaAl_3(SO_4)_2(OH)_6$

Ammonioalunite – $NH_4Al_3(SO_4)_2(OH)_6$

Jarosite – $KFe_3(SO_4)_2(OH)_6$

Natrojarosite – $NaFe_3(SO_4)_2(OH)_6$

Ammoniojarosite – $NH_4Fe_3(SO_4)_2(OH)_6$

Argentojarosite – $AgFe_3(SO_4)_2(OH)_6$

Beaverite – $Pb(Cu,Fe,Al)_3(SO_4)_2(OH)_6$

Plumbojarosite – $PbFe_6(SO_4)_2(OH)_6$

Solid-solution between the minerals is common (Brophy et al., 1962; Stoffregen and Cygan, 1990) but not well understood (Rye et al., 1992). Considerable solid-solution occurs between K^+ and Na^+ of the alunite (Al^{+3}) and jarosite (Fe^{+3}) series (Altaner et al., 1988; Stoffregen and Cygan, 1990), but solid-solution between the Al^{+3} and Fe^{+3} series appears to be minor in natural systems. In addition, PO_4^{-3} can substitute for SO_4^{-2} forming a series of aluminum phosphate minerals (Stoffregen and Alpers, 1987).

Only XRD and petrographic studies have been performed on the alunites from Steeple Rock; therefore the specific mineralogy is not well known. Chemical analyses and XRD patterns indicate that alunite, jarosite, natrojarosite, and natroalunite are present, but some of the other minerals may exist as well.

Alunite typically occurs as fillings of void spaces, thin veinlets (Fig. 5.28), and

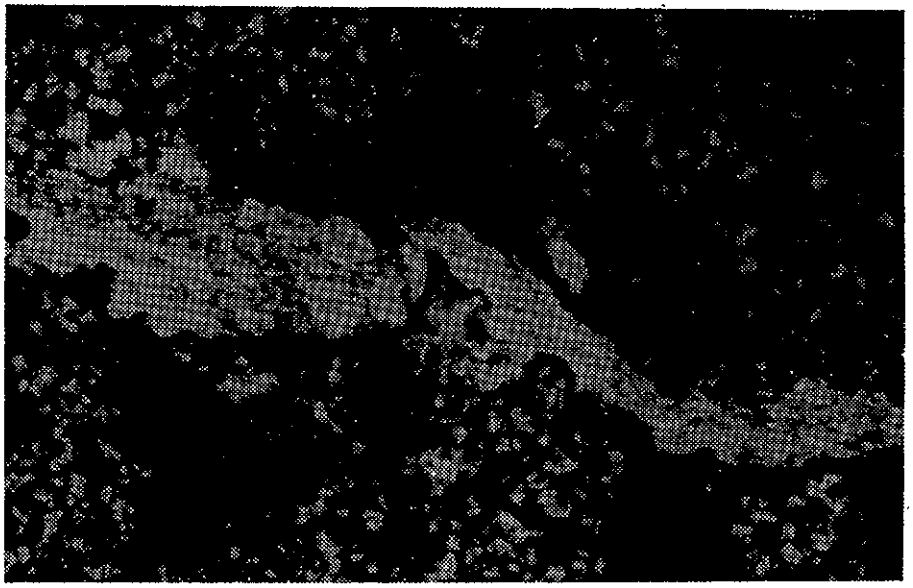

Figure 5.28—Photomicrograph of veinlet of alunite and quartz in silicified tuff.

replacement of primary minerals. It is generally intergrown with kaolinite and quartz. Identification of alunite is important because it indicates a low pH environment and alunite can be used in age determinations and isotopic studies.

5.5.12 Pyrophyllite, $Al_2(Si_4O_{10})(OH)_2$

Pyrophyllite occurs only in the silicified and massive silica/chert zones of the acid-sulfate alteration in the Steeple Rock district. It is fine-grained and occurs as disseminations, void-fillings, replacements of primary minerals, and as thin veinlets with quartz. In thin section, it commonly forms foliated and/or radiating lamellar aggregates (Fig. 5.29). Its identification in the district is primarily by XRD and petrographic studies. Pyrophyllite is an important mineral because it indicates desposition by acidic fluids $>200°C$ (Fig. 5.1).

5.5.13 Diaspore, $HAlO_2$

Diaspore is found in acid-sulfate altered rocks. It typically occurs as veins, some as wide as several centimeters, although locally it is disseminated throughout the altered rock. It is typically white to green to yellow to brown to colorless, transparent to translucent, and occurs with quartz, alunite, kaolinite, and iron oxides.

5.5.14 Despujolsite, $Ca_3Mn(SO_4)_2(OH)_6 \cdot 3H_2O$ (?)

Despujolsite is tentatively identified by XRD (Appendix 11.3) and occurs in the acid-sulfate altered areas, specifically the clay and silicified zones. It is yellow to brown, fine-grained, and intergrown with iron oxides. Whole-rock chemical analyses are consistent with the occurrence of this mineral. However, this is a less common mineral found in vein deposits (Fleischer, 1969) and microprobe and SEM studies are required before this mineral is confirmed.

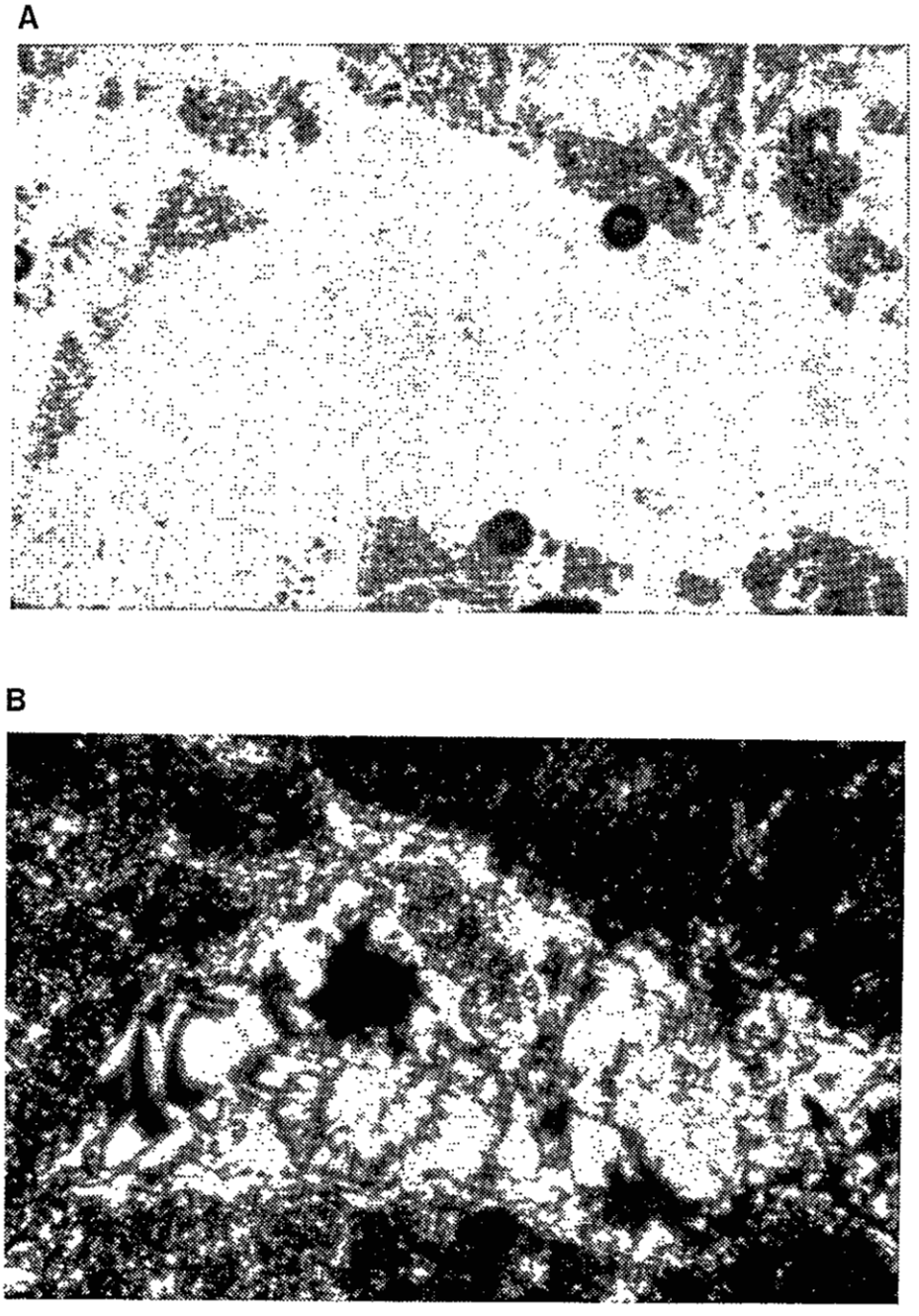

Figure 5.29—Photomicrograph of pyrophyllite filling vesicle in silicified andesite. a) plane light, b) crossed nicols. Field of view is approximately 0.5 mm.

5.6 Chemistry of alteration

Numerous surface and drill core samples of altered rocks from the Steeple Rock district were sampled and analyzed for major and trace elements (Appendix 11.4). The chemical variations produced by alteration reflect changes in the mineral assemblage which together are influenced by temperature and pressure, composition of the parent rock, composition of the altering fluids, permeability and duration of the alteration process (section 5.1).

The most extensive alteration in the district is by alkali-chloride waters and these altered rocks are characterized by differences in geochemistry (section 2.4). The mafic rocks are locally extensively altered to quartz, chlorite, pyrite, and other secondary minerals and exhibit a corresponding increase in silica, magnesium, and locally iron, relative to unaltered mafic rocks (Appendix 11.4c). The silicic rocks (rhyolites, ash-flow tuffs) exhibit variable changes in concentrations of silica and the alkali elements as a result of the alteration of feldspar and groundmass to quartz and clay minerals (kaolinite, illite, smectite, chlorite).

A vertical section through multiple flows of andesite of the Summit Mountain formation in USBM drill hole H9 was sampled and analyzed for major and trace elements (Appendix 11.4c, Figs. 5.30, 5.31). Although there is some scatter in the data, the andesites increase in K_2O, Ba, Rb, Sr and Zn concentrations and decrease in Al_2O_3 and Y concentrations toward the vein.

The acid-sulfate altered rocks exhibit more dramatic changes in the chemical composition as a result of dissolution by acid fluids and subsequent deposition of quartz, kaolinite, illite, alunite, and other secondary minerals. Differences in chemical composition between acid-sulfate and alkali-chloride altered rocks can be observed in the USBM drill hole H-10. The acid-sulfate altered rocks have higher concentrations of SiO_2 and Sr and lower concentrations of MgO, CaO, K_2O, Zn, and Rb relative to the alkali-chloride altered rocks (Figs. 5.32, 5.33). Elsewhere in the Steeple Rock district, many samples of acid-sulfate altered rocks have higher concentrations of SiO_2 and Al_2O_3 than typical host rocks within the

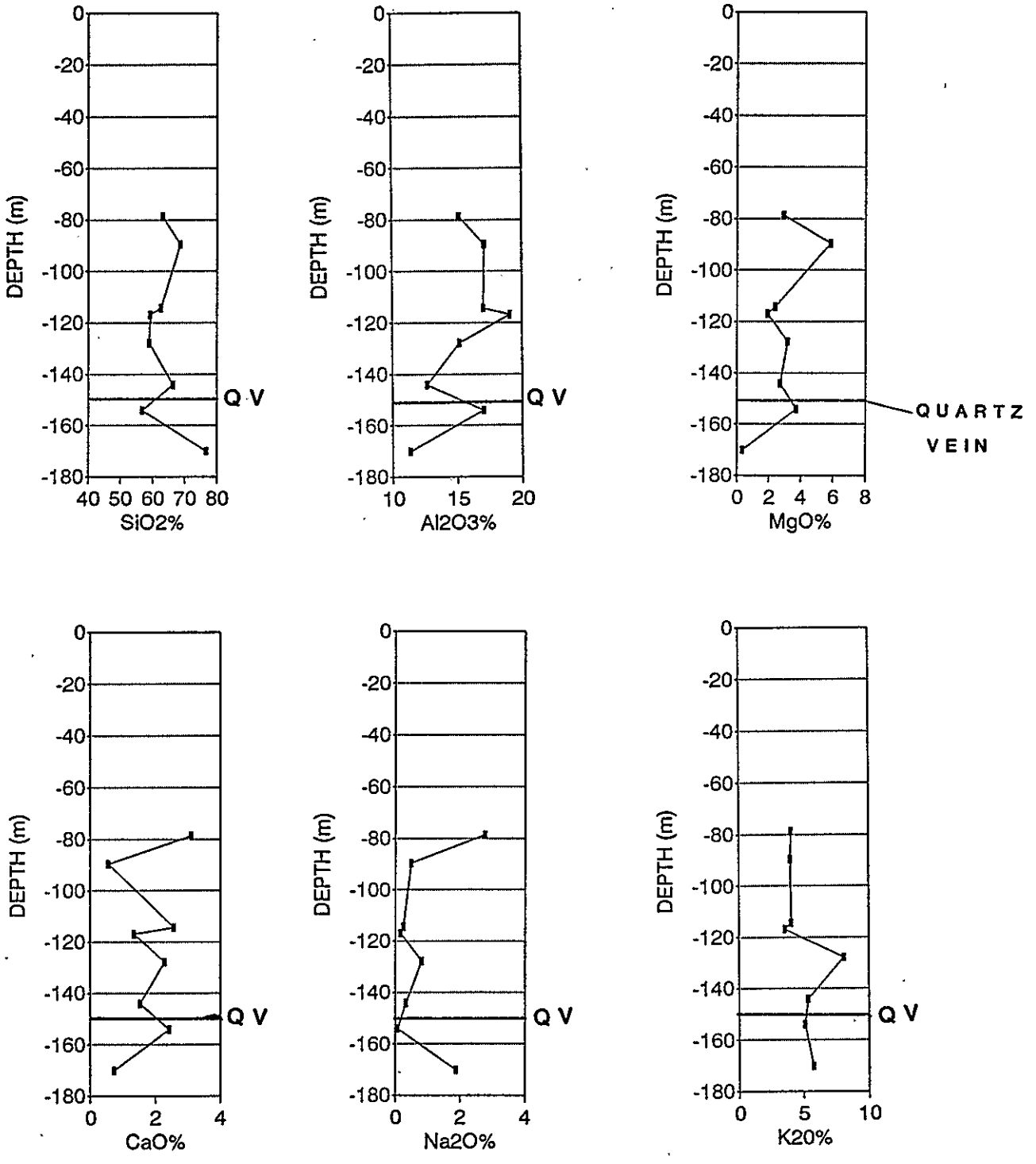

Figure 5.30—Concentrations of selected major elements with depth in USBM drill hole H9. H9 is located between the Carlisle and Center mines (Map 5) and consists of andesites, Summit Mountain formation. Quartz vein is at a depth of 151–153 m.

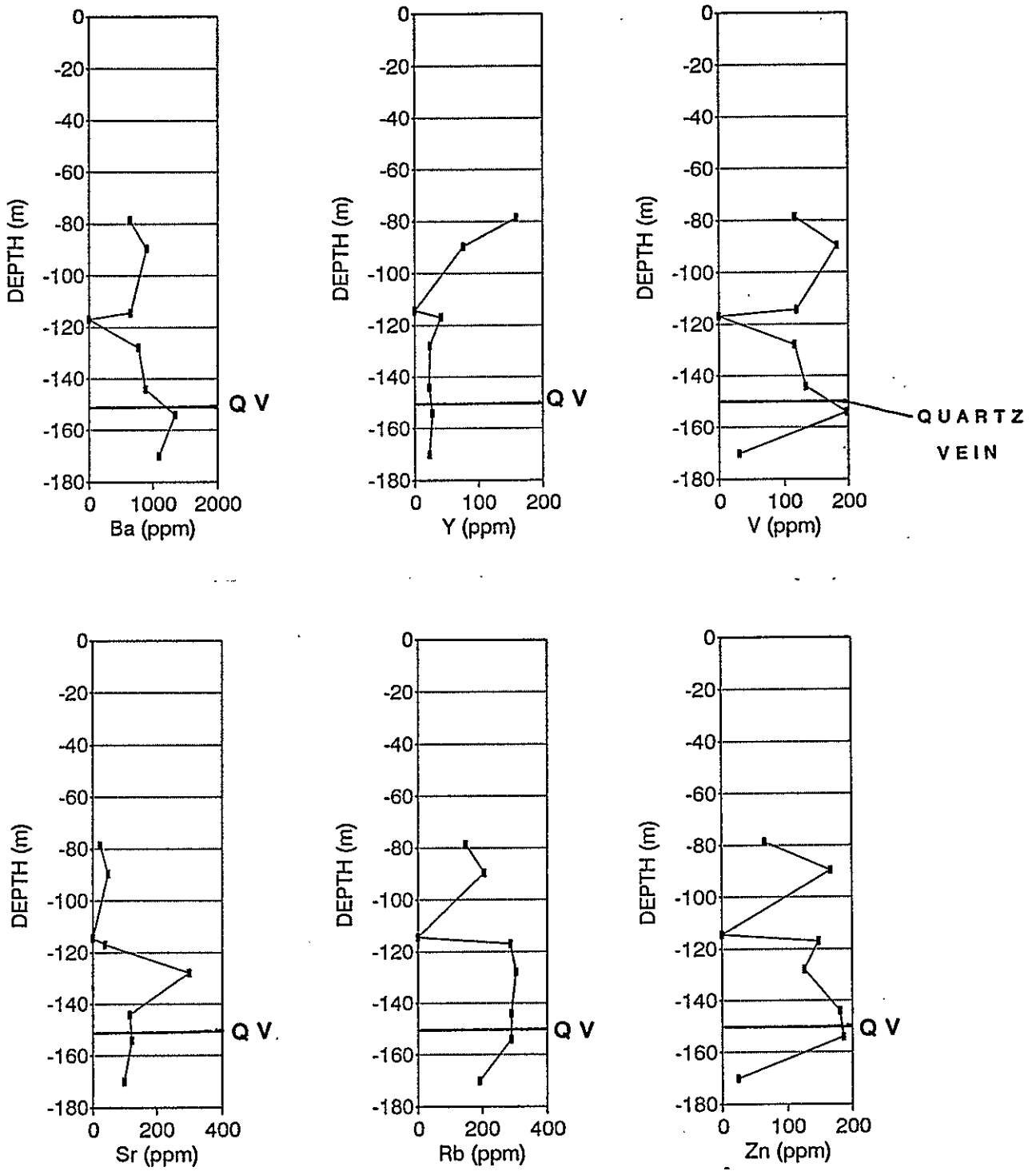

Figure 5.31—Concentrations of selected trace elements with depth in USBM drill hole H9.

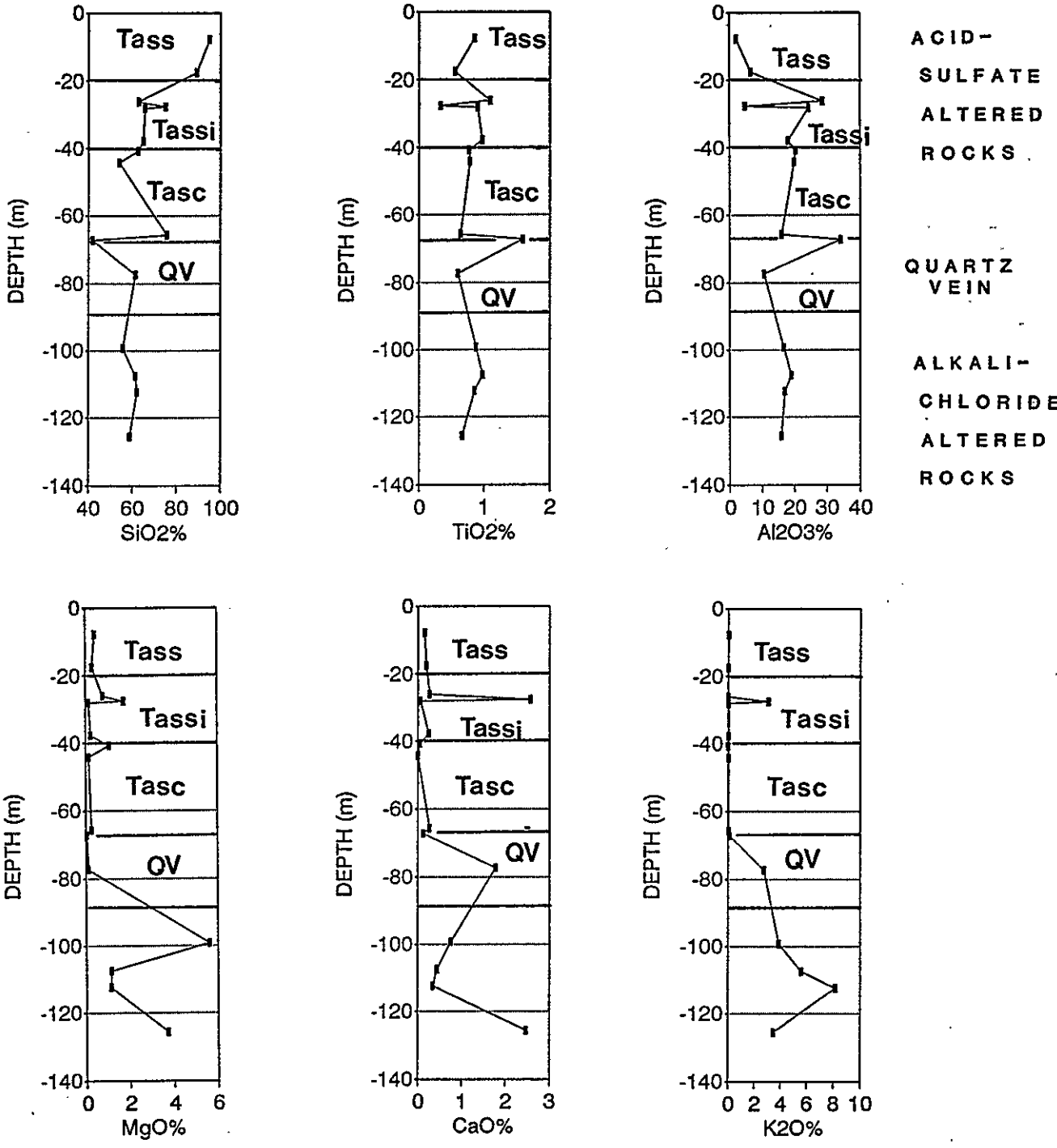

Figure 5.32—Alteration zonation and concentrations of selected major elements with depth in USBM drill hole H10. H10 is located at the Carlisle mine (Fig. 3.4, Map 5). The upper 67.1 m are in altered rocks (Tas) and the lower rocks are in andesites of Summit Mountain formation (Appendix 11.1).

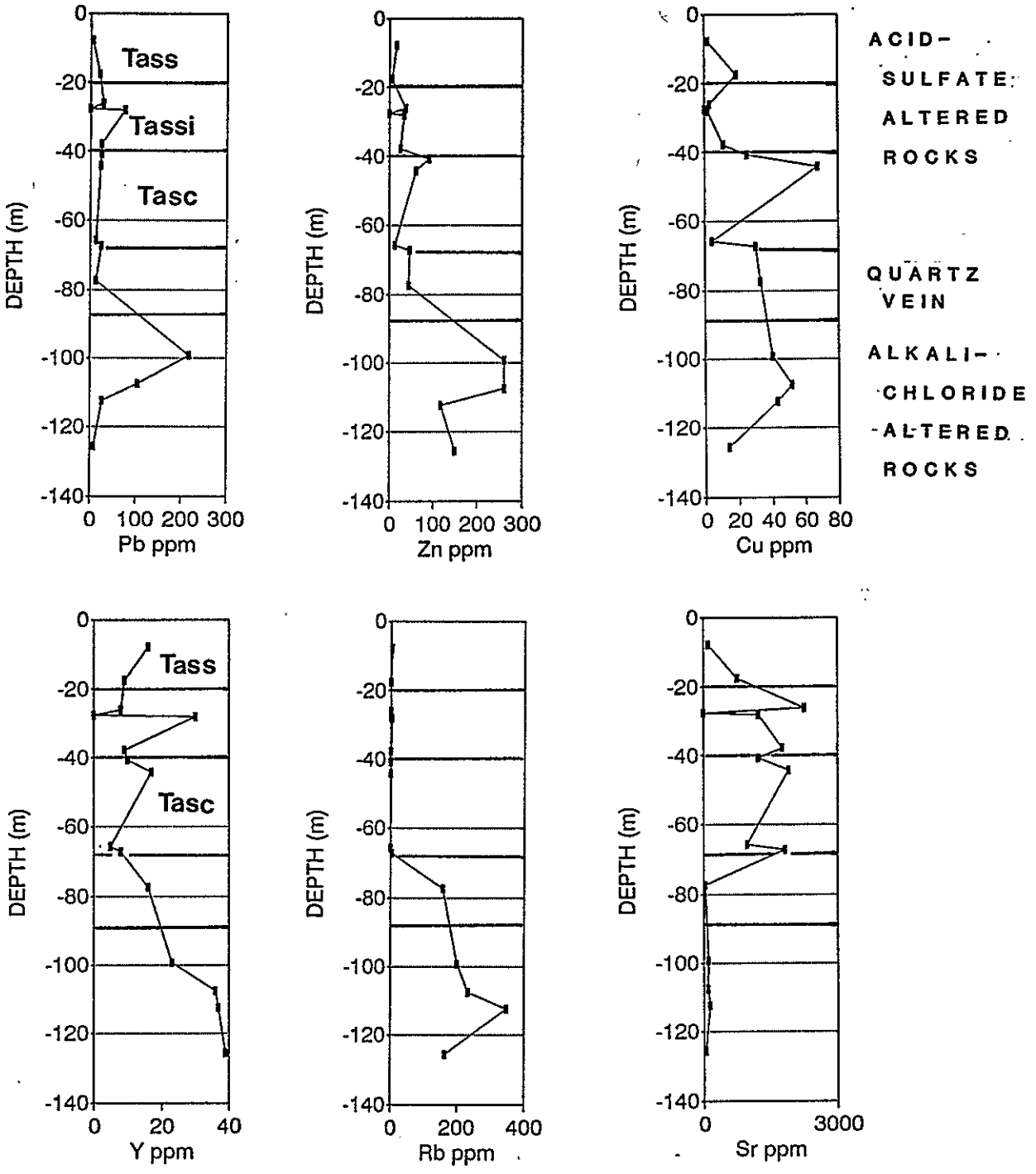

Figure 5.33—Alteration zonation and concentrations of selected trace elements with depth in USBM drill hole H10.

district (Fig. 5.34; Appendix 11.4). Many acid-sulfate altered rocks are also depleted in Rb (Fig. 2.24), Nb (Fig. 2.23), and Y (Fig. 2.23) relative to typical host rocks. Similar chemical trends are found at Telephone Ridge where the acid-sulfate altered rocks have higher concentrations of SiO_2 and lower concentrations of MgO, Na_2O, Rb, Zn, and Cu than underlying alkali-chloride altered rocks (Figs. 5.35, 5.36).

The acid-sulfate altered areas are typically zoned chemically, corresponding to the three mineralogical zones discussed earlier: central massive silica/chert zone, silicified zone, and outer clay zone. Three vertical sections through acid-sulfate altered rocks were sampled and analyzed for major and trace elements: USBM drill hole H10, west of Telephone Ridge (surface sampling only), and the south slope of Saddleback Mountain (surface sampling only) (Figs. 5.32, 5.33, 5.35, 5.36, 5.37).

The massive silica/chert zone (Tass) is characterized by $>90\%$ SiO_2 and is depleted in concentrations of most other elements (Figs. 5.32, 5.35, 5.37). The massive silica/chert zone is overlain by the silicified rocks at Saddleback Mountain and it overlies the silicified zone at all three localities. Maximum thickness rarely exceeds 20 m.

The silicified (Tassi) and clay (Tasc) zones are variable in chemical compositions. Silica and locally Pb decrease with depth away from the massive silica/chert zone, whereas Al_2O_3, Fe_2O_3, Na_2O, Ba, Cu, Zn, and Rb typically increase in concentration (Figs. 5.32, 5.33, 5.35, 5.36).

Changes in concentrations of many elements are erratic (Appendix 11.4). Indeed, some of the chemical trends previously discussed show erratic scatter in the data. This scatter may reflect differences in permeability which would allow or restrict flow of acidic fuids through the vertical section. The scatter also may reflect precipitation of secondary minerals during acid leaching. These chemical variations reflect complex fluid/rock interactions that would be expected in a near-surface hydrothermal environment.

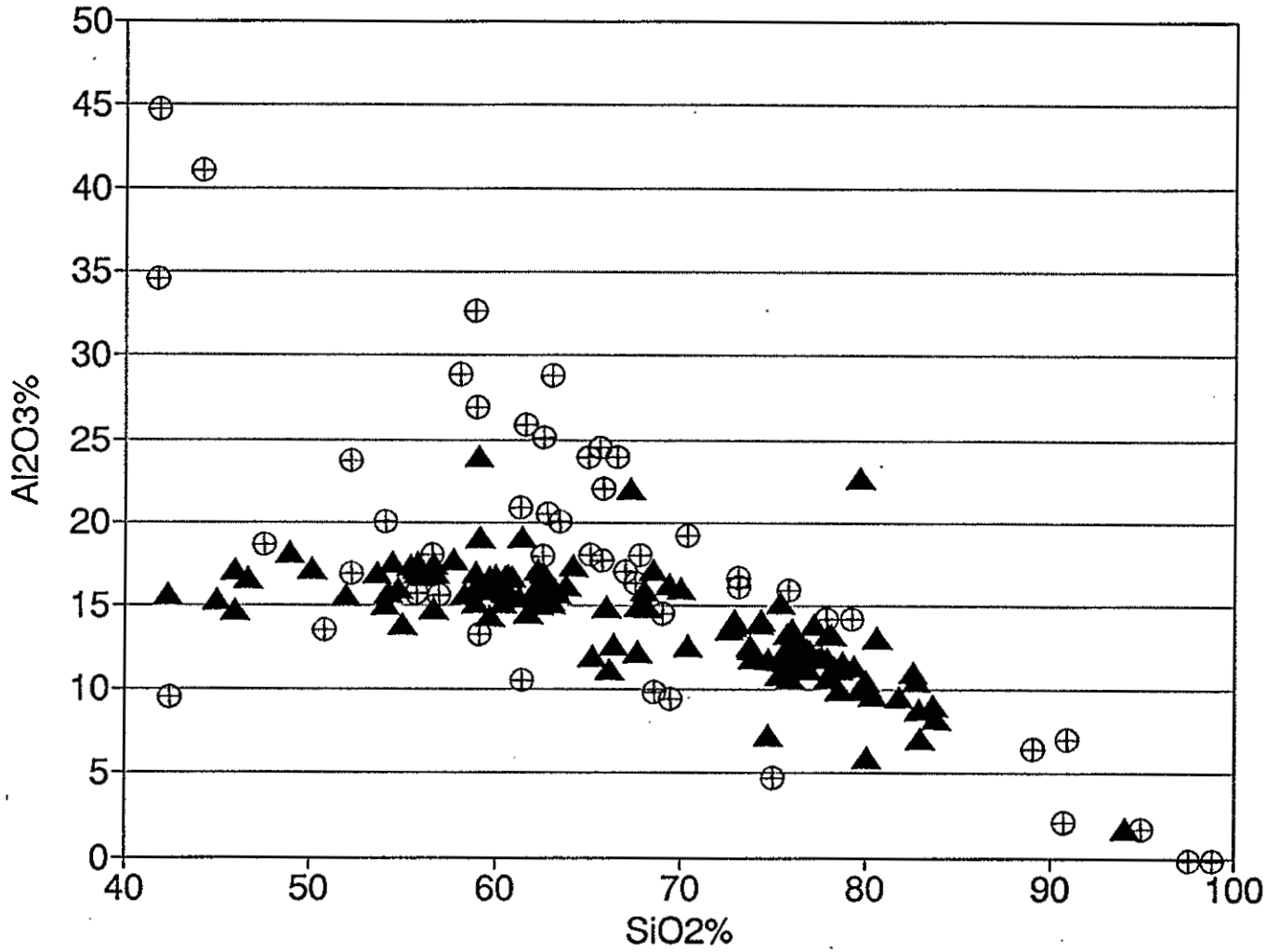

FIGURE 5.34 Al2O3 vs. SiO2 diagram of andesites, dacites, ash-flow tuffs, intrusive rhyolites (solid triangle) and acid-sulfate altered rocks (circle with cross). Note the scatter of the acid-sulfate altered rocks.

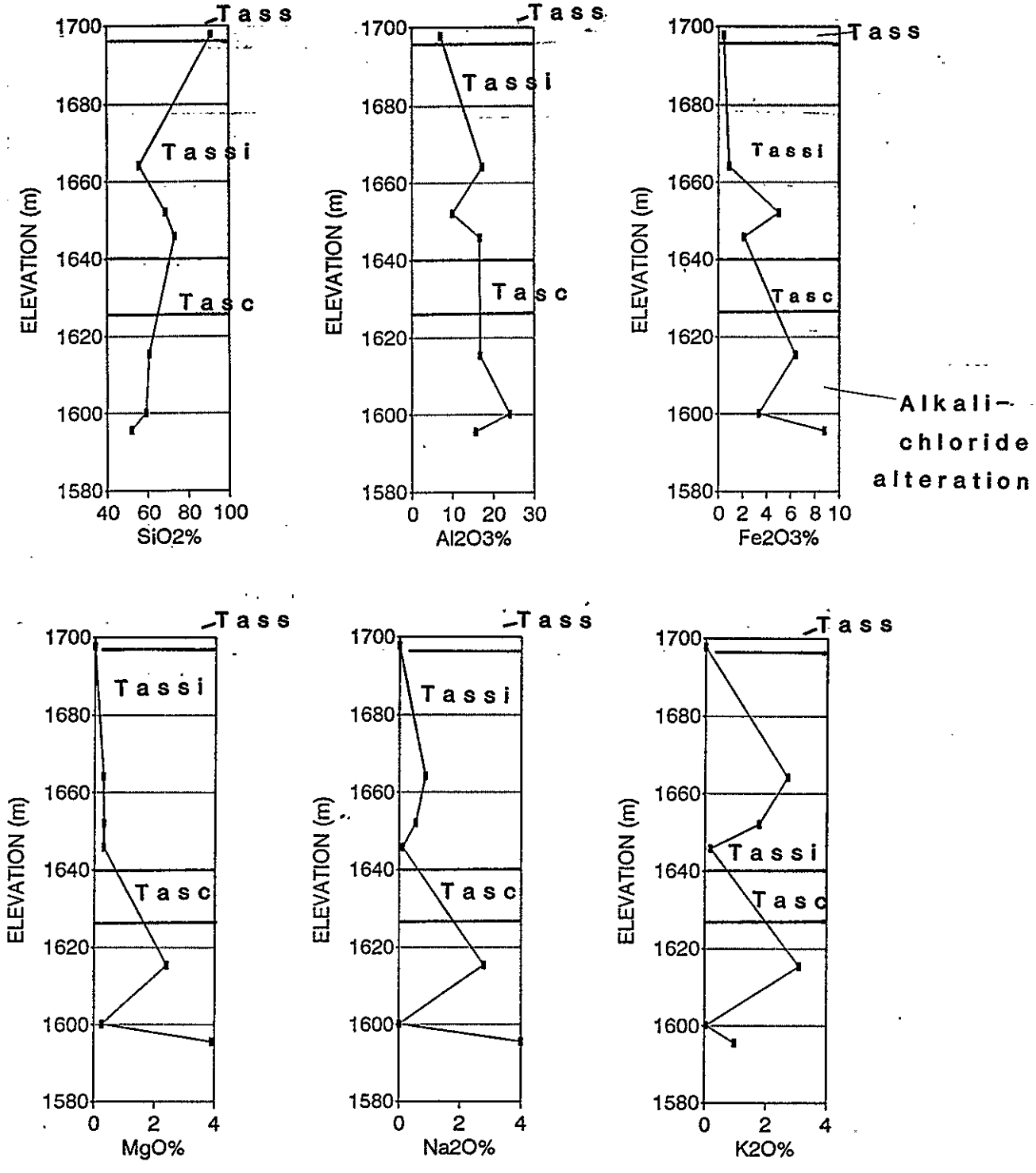

Figure 5.35—Concentrations of selected major elements with elevation west of Telephone Ridge. Sample locations are shown in Figures 5.11 and 5.18 (Map 2).

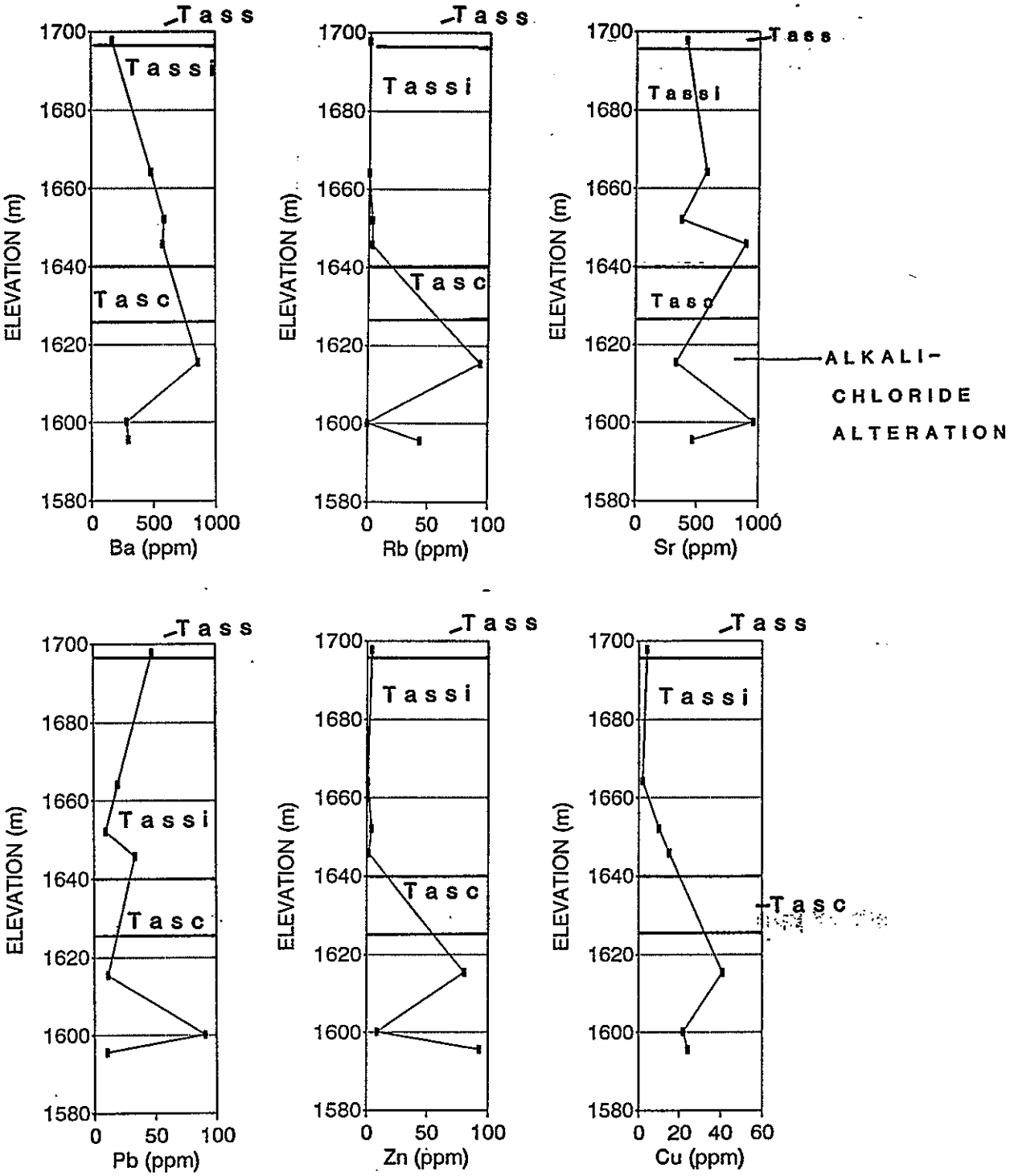

Figure 5.36—Concentrations of selected trace elements with elevation west of Telephone Ridge.

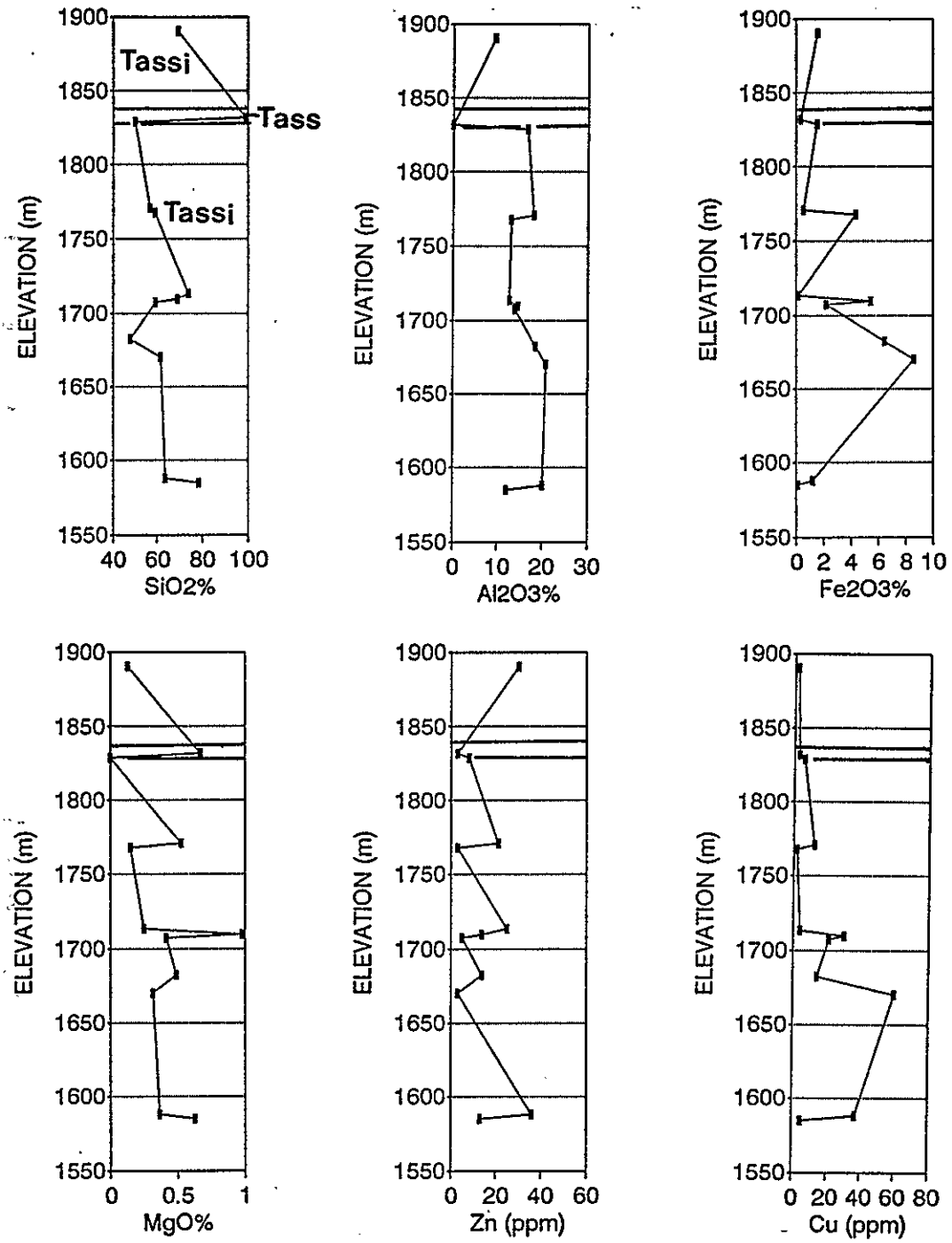

Figure 5.37—Concentrations of selected elements with elevation at Saddleback Mountain (south slope). Locations of samples are shown in Figure 5.21.

6. DISCUSSION

6.1 Alteration

6.1.1 General environment of acid-sulfate alteration

Acid-sulfate alteration is recognized in four specific types of hydrothermal environments (Fig. 6.1; Table 6.1): (1) magmatic-hydrothermal (hypogene), (2) magmatic-steam, (3) steam heated, and (4) supergene (Rye et al., 1992). These four environments are distinguished by field relationships, mineral assemblages, chemical composition, and textures. A brief description of these four environments follows in order to better understand the origin of this alteration in the Steeple Rock district.

6.1.1.1 Magmatic-hydrothermal environments—The magmatic-hydrothermal acid-sulfate altered environment is characterized by magmatic heat and significant magmatic components in the hydrothermal fluids. This type of environment has been termed "acid-sulfate" by Heald et al. (1987), "high-sulfidation" by Hedenquist (1987) and White and Hedenquist (1990), "kaolinite-alunite" by Berger and Henley (1989), quartz-alunite by Cox and Singer (1986), and may also include the enargite-bearing gold deposits described by Sillitoe (1983). These deposits are fracture controlled, horizontally zoned away from the acid solution channels, and have ages coeval with intrusive activity. Fumaroles, silicification, and hydrothermal brecciation are common features. Extensive acid-leaching of alkalis and aluminum produces a core of vuggy or sugary silica (silica residue) surrounded by successive zones of quartz-alunite-kaolinite, quartz-pyrophyllite-kaolinite, and quartz-kaolinite grading into argillic and finally propylitized wall rock. Base- and precious-metals mineralization may be associated with the acid-sulfate alteration in this environment in some areas. This type of alteration overlies some porphyry copper and porphyry molybdenum deposits (Bove et al., 1990).

Acid fluids are produced by the disproportionation of magmatic sulfur with decreasing temperatures (i.e. cooling), as represented by the following reaction:

$$4SO_2 + 4H_2O \rightleftarrows 3H_2SO_4 + H_2S.$$

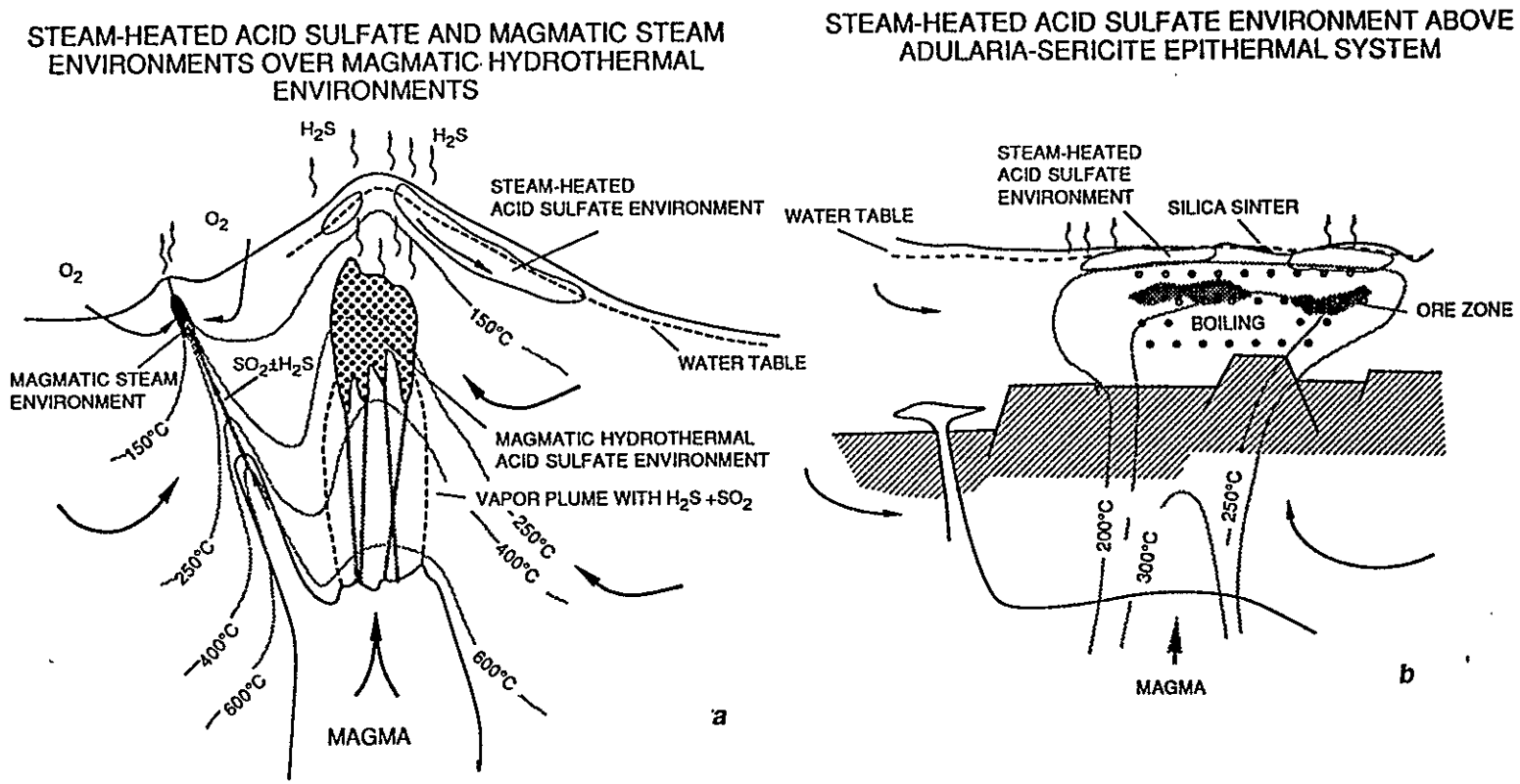

Figure 6.1 - Diagramatic sketch of types of acid-sulfate environments. a) Magmatic-hydrothermal and magmatic steam-heated environments. b) Steam-heated acid-sulfate environment above alkali-chloride (adularia-sericite) system. From Rye et al. (1992), modified from Henley and Ellis (1983).

Table 6.1—Summary of characteristics of environments of acid-sulfate alteration (from Rye et al., 1992; Thompson and Petersen, 1991; Henley and Ellis, 1983).

	Magmatic-hydrothermal	Magmatic steam	Steam heated	Supergene
Genesis	hypogene	hypogene	supergene	supergene
Structural controls	fracture controlled	fracture controlled	paleotopography	paleotopography, fault controlled
Timing	ages coeval with intrusive activity and mineralization	ages coeval with intrusive activity	much younger than host rocks, coeval with mineralization	much younger than host rocks and mineralization
Characteristics	fumaroles, hydrothermal brecciation and eruptions, horizontal and vertical zonation of mineral assemblages, silicification, vuggy silica common	fumaroles, hydrothermal brecciation and eruptions, veins	sinters, vertical zonation, at water table	oxidation at surface, blanket-like horizons
Associated metals	As, Au, Ag, Bi, Te, Sn, Sb, ± base metals	sulfides absent	Cu, As, Au, Ag deeper in system	either no mineralization or preserved mineralization from younger episodes
Alteration mineralization	alunite (>2 μm, heterogeneous composition), quartz diaspore, pyrophyllite, pyrite, enargite	monomineralic alunite veins, hematite, quartz, kaolinite	alunite (<2 μm homogeneous composition), quartz, kaolinite, cristobalite, opal, chalcedony, jarosite, hematite	alunite (<2 μm), quartz, kaolinite, halloysite, jarosite, iron oxides
Stable isotopes	$\delta^{34}S$ of alunite 10–18‰ greater than for pyrite, δD similar to magmatic water	δD similar to magmatic water	δD similar to meteoric water, $\delta^{34}S$ of alunite similar to associated sulfides	δD similar to meteoric water, low $\delta^{34}S$ of alunite (similar to $\delta^{34}S$ of pyrite)

HCl is also common in magmatic systems and further decreases the pH. The decrease in pH can also be a result of cooling without boiling (Reed and Spycher, 1985). The acid fluids dissolve most of the primary minerals in a rock, leaving silica residue. Sulfate minerals are deposited in the resulting voids.

6.1.1.2 Magmatic-steam environment—Recent work by Rye et al. (1992) and Cunningham et al. (1984) identified the magmatic-steam environment as a form of acid-sulfate alteration which is dominated by a vapor phase of magmatic origin. This environment is characterized by coarsely-crystalline monomineralic alunite veins up to several meters wide (Fig. 6.1; Cunningham et al., 1984). These deposits are rare, but have distinct stable isotope characteristics indicating a magmatic source; only four areas were studied by Rye et al. (1992). The genesis of these deposits is poorly understood, but available data indicate high temperatures, low pressures, and formation at shallow depths (Rye et al., 1992). Representative reactions are:

$$H_2S + 3/2O_2 \Rightarrow SO_2 + H_2O$$

$$SO_2 + 1/2O_2 + H_2O \Rightarrow H_2SO_4$$

6.1.1.3 Steam-heated environment—Steam-heated acid-sulfate alteration occurs in the near-surface, upper levels of hydrothermal systems (Fig. 6.1), at or above the water table. These environments are characterized by sinter, acid-leached silica residue, vertical zonation, and are controlled by topography. Alteration is vertically zoned from a sinter at the top, downward to quartz-alunite to quartz-kaolinite to argillic and propyllitic altered rocks (alkali-chloride alteration). Mineralization is absent in the altered area (Rye et al., 1992; Thompson and Petersen, 1991), but the alteration may overlie precious-metal mineralization which occurs at the boiling zone and possibly even deeper base-metal mineralization (Fig. 6.1b). The age of alteration is coincident with the age of underlying mineralization (Rye et al., 1992). Opal, jarosite, hematite, and chalcedony are common. The acidic fluids are formed by condensation of vapor and oxidation of dissolved H_2S, derived from deeper alkali-chloride waters, summarized by the following reaction:

$$H_2S + 2O_2 \Rightarrow H_2SO_4$$

6.1.1.4 Supergene environment—Supergene acid-sulfate alteration is produced by the oxidation at or near the surface of sulfide-rich deposits and therefore can be overprinted on mineralization formed by other types of acid-sulfate environments. Supergene environments are characterized by quartz, alunite, disordered kaolinite, halloysite, jarosite, and hydrous iron oxides. The alteration typically is controlled by topography, forming blanket-like horizons, that underlie gossans. Base- and precious-metals mineralization is older than supergene alteration and secondary enrichment may be common. Acid fluids may also descend along faults and become heated forming deep, thick, fault-controlled higher-temperature acid-sulfate alteration with alunite and pyrophyllite. These zones are difficult to distinguish from other types of acid-sulfate alteration, unless field relationships are preserved. The acid fluids are produced by oxidation of sulfides in the near-surface environment, represented by:

$$2FeS_2 + 7H_2O + 15/2O_2 \Rightarrow Fe_2O_3 \cdot 3H_2O + 4H_2SO_4.$$

6.1.1.5 Other environments—Alunite forms rarely in the sedimentary and metamorphic environments under restricted conditions. Alunite and jarosite form as precipitates of acid-hypersaline lakes in Australia (Bird et al., 1989; Alpers et al., 1992; Long et al., 1992). Mechanisms of precipitation are unknown, but stable isotope data are available and are similar to magmatic-hydrothermal alunite (Table 6.1). Alunite also occurs in some regolith profiles in Australia (Bird et al., 1989). Isotopic and other data led Bird et al. (1989) to postulate that alunite was formed by evaporative concentration of solutes in the regolith profile. Diagenetic, concretionary deposits of alunite occur in lagoonal sediments in Israel and Sinai (Goldberry, 1980). Alunite is formed by bacterial action on illite under anaerobic conditions, represented by:

$$KAl_2[OH_2Al_2Si_3O_{10}] + 4H^+ + 2SO_4^{-2} = 3SiO_2 + KAl_3(SO_4)_2(OH)_6.$$

Alunite is known to form in modern hot springs (Raymahashay, 1969; Schoen et al., 1974); data from some of these deposits is classified as steam-heated environment by Rye et al.

(1992). Alunite-group minerals also occur in low-grade metamorphic schist in South Africa (Schoch et al., 1985), however isotopic data are not available from these deposits.

6.1.2 Stable isotope studies

Although it is beyond the scope of this project to analyze samples for stable isotopes, Field (1966) reports sulfur isotope data for coexisting alunite and pyrite from the Bitter Creek area in the Steeple Rock district:

	$\delta^{34}S$ alunite ‰	$\delta^{34}S$ pyrite ‰
	12.5	-6.3
	12.7	0.7

Stable isotope studies of alunite and pyrite can provide information on (1) the origin of the components, (2) process and rates of formation, (3) physical-chemical environments, and (4) temperatures of formation.

An extensive literature search was conducted on alunite and stable isotope studies of alunite deposits, in order to interpret Field's (1966) data. Different geologic environments of alunite formation were identified and previously summarized in section 6.1.1. From these references, 62 areas were found with sulfur isotope data and many of these areas also had data on oxygen and hydrogen isotopes (Table 6.2). Rye et al. (1992) was the primary source, although other references were found. If more than one analysis was reported for an area, the data were averaged and both the average and the range were listed in Table 6.2. Each deposit was classified as (1) magmatic-hydrothermal (hypogene), (2) magmatic steam, (3) steam-heated, (4) supergene, (5) regolith, (6) diagenetic, or (7) acid lake by Rye et al. (1992) or specific author(s) from available geologic, mineralogic, and geochemical data. One natroalunite sample (no. 50) is included in Table 6.2. It is beyond the scope of this study to address any problems or discrepancies in classification of individual deposits. Two deposits, numbers 27 and 28, were not classified by the authors, and a steam-heated classification was assigned by this author on the basis of available data. It is also assumed that published stable

Table 6.2—Stable isotope data on alunite from different locations and geologic environments. *n = number of analyses (first number is for number of $\delta^{34}S$ analyses and second number is for other stable isotope analyses. magmatic - magmatic-hydrothermal, ms - magmatic steam, steam - steam-heated, super - supergene. Values are in ‰.

No.	Location	Setting*	$\delta^{34}S$ (min)	$\delta^{34}S$ (max)	$\delta^{34}S$ (avg)	Reference
1	Monte Negro, Dominican Republic	vein (n=1)	20	20	20	Muntean et al. (1990)
2	Pueblo Viejo, Dominican Republic	vein (n=1)	21.6	21.6	21.6	Kesler et al. (1981), Vennemann et al. (1993)
3	Goldfields, Nevada	replace (n=6)	11.6	23.3	17.5	Jensen et al. (1971)
4	Goldfields, Nevada	magmatic (n=1)	28.1	28.1	28.1	Rye et al. (1992)
5	Bitter Creek, New Mexico	hypogene (n=1)	12.7	12.7	12.7	Field (1966)
6	El Salvador, Chile	magmatic (n=2)	14.8	17	15.9	Field and Gustafson (1976), Rye et al. (1992)
7	Comstock, Nevada	(n-2/1)	21	21	21	Rye et al. (1992)
8	VA Range, Nevada	magmatic (n=5)	18	22.4	20.2	Rye et al. (1992)
9	Ramsey, Nevada	(n=1)	22.5	22.5	22.5	Rye et al. (1992)
10	Rodalquilar, Spain	stage 1 mag (n=9)	22.3	31	28.6	Rye et al. (1992)
11	Red Mountain, Colorado	stage 2 mag (n=7/3)	17.6	27.2	22.7	Bove et al. (1990), Rye et al. (1992)
12	Julcani, Peru	magmatic (n=11/6)	22.6	28.1	23.7	Rye et al. (1992)
13	Summitville, Colorado	magmatic (n=16/10)	13.4	24.5	21	Rye et al. (1992)
14	La Escondida, Chile	hypogene (n=2)	6.2	7	6.6	Alpers and Brimhall (1988)
15	Red Mountain, Colorado	stage 1 mag (n=6/5)	8.4	10.7	9.6	Bove et al. (1990), Rye et al. (1992)
16	Red Mountain, Colorado	stage 4 ms (n=2)	0.1	0.1	0.1	Bove et al. (1990), Rye et al. (1992)
17	Red Mountain, Colorado	stage 3 ms (n=3/2)	-3.9	-3.3	-3.6	Bove et al. (1990), Rye et al. (1992)
18	Marysvale, Utah	vein ms (n=4)	-0.8	-2.1	-1.5	Cunningham et al. (1984), Rye et al. (1992)
19	Cactus, California	magmatic steam (n=6)	-1	2.7	1.1	Rye et al. (1992)
20	Marysvale, Utah	steam (n=6)	7.4	15.4	12.5	Cunningham et al. (1984), Rye et al. (1992)
21	Yellowstone, Wyoming	steam (n=1)	0.9	0.9	0.9	Rye et al. (1992)
22	Steamboat Springs, Nevada	steam (n=1)	0.9	0.9	0.9	Rye et al. (1992)
23	National district, Nevada	steam (n=2)	-2.9	-2.9	-2.8	Rye et al. (1992), Vikre (1987)
24	Waiotapu, New Zealand	steam (n=1)	7.2	7.2	7.2	Rye et al. (1992)
25	Tolfa, Italy	steam (n=11)	1.9	7.6	5.3	Field and Lombardi (1972), Rye et al. (1992)
26	Buckskin, Nevada	steam (n=2)	-3.2	-2.8	3.7	Rye et al. (1992)
27	VA Range, Nevada	(n=1)	3.7	3.7	5.9	Rye et al. (1992)
28	Maggie Creek, Nevada	(n=1)	7.5	7.5	7.5	Rye et al. (1992)
29	Rodalquilar, Spain	stage 2 super (n=20)	5.6	10.2	7.5	Rye et al. (1992)
30	La Escondida, Chile	supergene (n=4)	-2.4	-0.5	-1.3	Alpers and Brimhall (1988)
31	El Salvador, Chile	super (n=3)	-1.48	3.64	1.83	Field and Gustafson (1976), Rye et al. (1992)
32	Wairakei, New Zealand	super (n=5)	-1.4	6.9	5.2	Steiner and Rafter (1966)
33	Waiotapu, New Zealand	super (n=3)	5.1	6.6	6.1	Steiner and Rafter (1966)
34	Chino Mine, New Mexico	super (n=1)	0.6	0.6	0.6	Field (1966), Rye et al. (1992)
35	Goldfield, Nevada	super (n=10)	-2.5	1.7	0.0	Jensen et al. (1971)
36	Goldfields, Nevada	(n=2)	2.8	2.9	2.9	Rye et al. (1992)
37	Post, Nevada	super (n=2)	9.2	11.1	10.1	Arehart et al. (1992)
38	Gold Quarry, Nevada	super (n=1)	8.4	8.4	8.4	Arehart et al. (1992)
39	Rain, Nevada	super (n=2)	9	10.9	10	Arehart et al. (1992)
40	Mineral Park, Arizona	super (n=2/1)	0.2	0.4	0.3	Field (1966), Rye et al. (1992)
41	Tolfa, Italy	super (n=14)	0.7	9.6	7.1	Cortecci et al. (1981)
42	Creede, Colorado	super (n=4/14)	-1.9	1.9	0.0	Rye et al. (1992)
43	Round Mountain, Nevada	super (n=13)	10.4	12.7	12.1	Rye et al. (1992)
44	Kidson, Australia	super (n=6/5)	1.5	6.9	4.7	Bird et al. (1989), Rye et al. (1992)
45	Vilacart, Riaza, Spain	super (n=3)	5.2	6	5.7	Rye et al. (1992)
46	Negredo, Riaza, Spain	super (n=2)	-1.2	-1.1	-1.1	Rye et al. (1992)
47	Mt. Leyshon, Australia	super (n=3/2)	8	9.8	9	Bird et al. (1989), Rye et al. (1992)
48	Sadler, Texas	super (n=1)	-1.1	-1.1	-1.1	Rye et al. (1992)

TABLE 6.2 (continued)

No.	Location	Setting*	$\delta^{34}S$ (min)	$\delta^{34}S$ (max)	$\delta^{34}S$ (avg)	Reference
49	Elura, New South Wales	super (n=1)	10.6	10.6	10.6	Taylor et al. (1984)
50	Marysvale, Utah	natro (n=3)	-5.5	-0.7	-2.5	Cunningham et al. (1984)
51	Springsure, Australia	regolith (n=3/1)	8.4	12.3	10.6	Bird et al. (1989)
52	Opal fields, Australia	regolith (n=6/5)	5.2	17.8	12.5	Bird et al. (1989)
53	Yilgarn, Australia	regolith (n=2/1)	15	19.5	17	Bird et al. (1989)
54	Kingscote, Australia	regolith (n=1)	20.6	20.6	20.6	Bird et al. (1989)
55	Noarlunga, Australia	diagenetic (n=3)	15.6	20.6	18	Bird et al. (1989)
56	Yilgarn, Australia	acid lake (n=3)	6	18	14	Bird et al. (1989)
57	Lake Tyrrell, Australia	acid lake (n=2/3)	16.7	19	17.8	Bird et al. (1989)
58	Lake Tyrrell, Australia	acid lake (n=1)	21.2	21.2	21.2	Alpers et al. (1992)
59	Eyre Penn., Australia	acid lake (n=4/3)	4.5	16.5	11	Bird et al. (1989)
60	Lake Chandler, Australia	acid lake (n=1)	19.8	19.8	19.8	Alpers et al. (1992)
61	Lake Hann, Australia	acid lake (n=1)	20.8	20.8	20.8	Alpers et al. (1992)
62	Lake Gilmore, Australia	acid lake (n=1)	19.6	19.6	19.6	Alpers et al. (1992)

isotope data utilized accepted standards, even though not all reports stated which isotopic standards were used. Analytical errors of data were not taken into account for this compilation. High-low graphs and histograms were plotted using a computer program (QUATTRO PRO).

Some potential problems may exist with stable isotope studies of alunite. Alunite forms a solid-solution series and substitution of other cations is common (Brophy et al., 1962). Alunite is locally fine-grained and difficult (impossible?) to separate from coexisting (not always cogenetic) minerals (such as quartz, kaolinite) and the effect on stable isotope studies is unknown. Different stages of alunite may be difficult to separate, especially when in fine-grained rocks. Recrystallization of alunite, which may be difficult to detect, may affect the isotopic chemistry. The isotopic chemistry of alunite may change as a result of later fluid migration, which is common in near-surface epithermal environments.

Alunite is found in several diverse geologic environments formed by different mechanisms. Alunite is a common product of acid-sulfate alteration. Weathering of sulfide deposits can also form alunite (supergene environment). Alunite is also found in modern hot springs (Raymahashay,, 1969; Schoen et al., 1974), acid lakes (Bird et al., 1989; Alpers et al., 1992), sedimentary rocks (Goldberry, 1980), and low-grade metamorphic rocks (Schoch et al., 1985). The majority of isotopic studies on alunite have been from the acid-sulfate environment, although some data exist from other environments (Table 6.2).

Early work by Field (1966) demonstrated the usefulness of stable isotope studies in differentiating between hypogene and supergene environments. Nearly identical isotopic compositions are found to exist between sulfate (i.e., alunite) and associated sulfides (i.e., pyrite) in the supergene environment. Dissimilarity of sulfur ratios between sulfate and associated sulfides supports a hypogene (i.e., magmatic-hydrothermal) origin. This is predicted by fractionation theory of sulfur isotopes and differences in sulfur bond strengths. Sulfate (i.e., alunite) will be enriched in $\delta^{34}S$ relative to coexisting sulfide (i.e., pyrite) in a magmatic-hydrothermal environment, provided that equilibrium is maintained. However,

fractionation of the sulfur isotopes does not occur in a supergene environment and the $\delta^{34}S$ is similar for both sulfide and sulfate (Field, 1966; Field and Lombardi, 1972). Rye et al. (1992) confirms the original observations by Field (1966) and provides additional stable isotopic data that can be utilized to differentiate between environments of formation.

The range in stable isotope values for various deposits can be shown by a high-low graph (Fig. 6.2) and is summarized in Table 6.3. $\delta^{34}S$ can be used with some reliability to distinguish magmatic-hydrothermal alunite from magmatic-steam, steam-heated, and supergene alunite, especially if the $\delta^{34}S$ values are high (above 13‰). However, caution is advised.

Table 6.3—Summary of range of stable isotope data from Table 6.1. All values are in ‰.

Type of Deposit	No. in Table 6.2	$\delta^{34}S$
Magmatic-hydrothermal	1-15	6-31
Magmatic steam	16-19	-3.9-2.7
Steam heated	20-28	-3.2-15.4
Supergene	29-49	-2.5-12.7
Natroalunite	50	-5.5-(-.7)
Regolith	51-54	-5.2-20.6
Diagenetic	55	15.6-20.6
Acid lake	56-62	4.5-21.2

Figure 6.3 is a histogram of $\delta^{34}S$ averaged values (Table 6.2) and it is apparent that there is overlap of $\delta^{34}S$ values from different environments. This is shown nicely in the cumulative frequency curve in Figure 6.4, which shows a curve with a slight break in slope at $\delta^{34}S$ = 13‰ and 20‰. The first break in slope is interpreted to correspond to the $\delta^{34}S$ value above which magmatic-hydrothermal and sedimentary (i.e., acid lake, diagenetic,regolith) environments are represented. However, $\delta^{34}S$ values alone can not be used to distinguish between alunites formed in the other environments. Other stable isotopes must be used, but these data are not available for the Steeple Rock samples. Data from Steeple Rock (i.e. Bitter

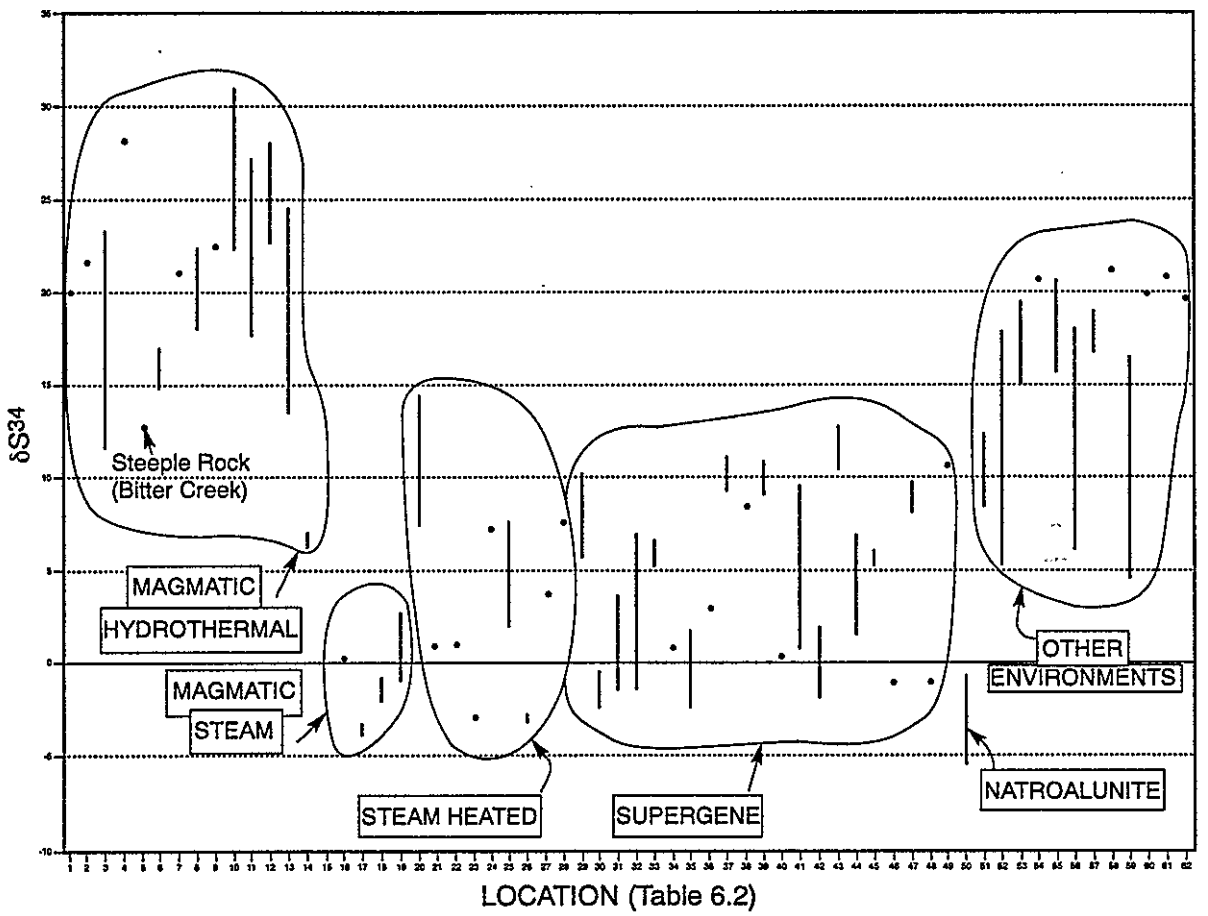

Figure 6.2. Range of stable isotope values of $\delta^{34}S$ in alunite. Dots and lines refer to range of values in Table 6.2.

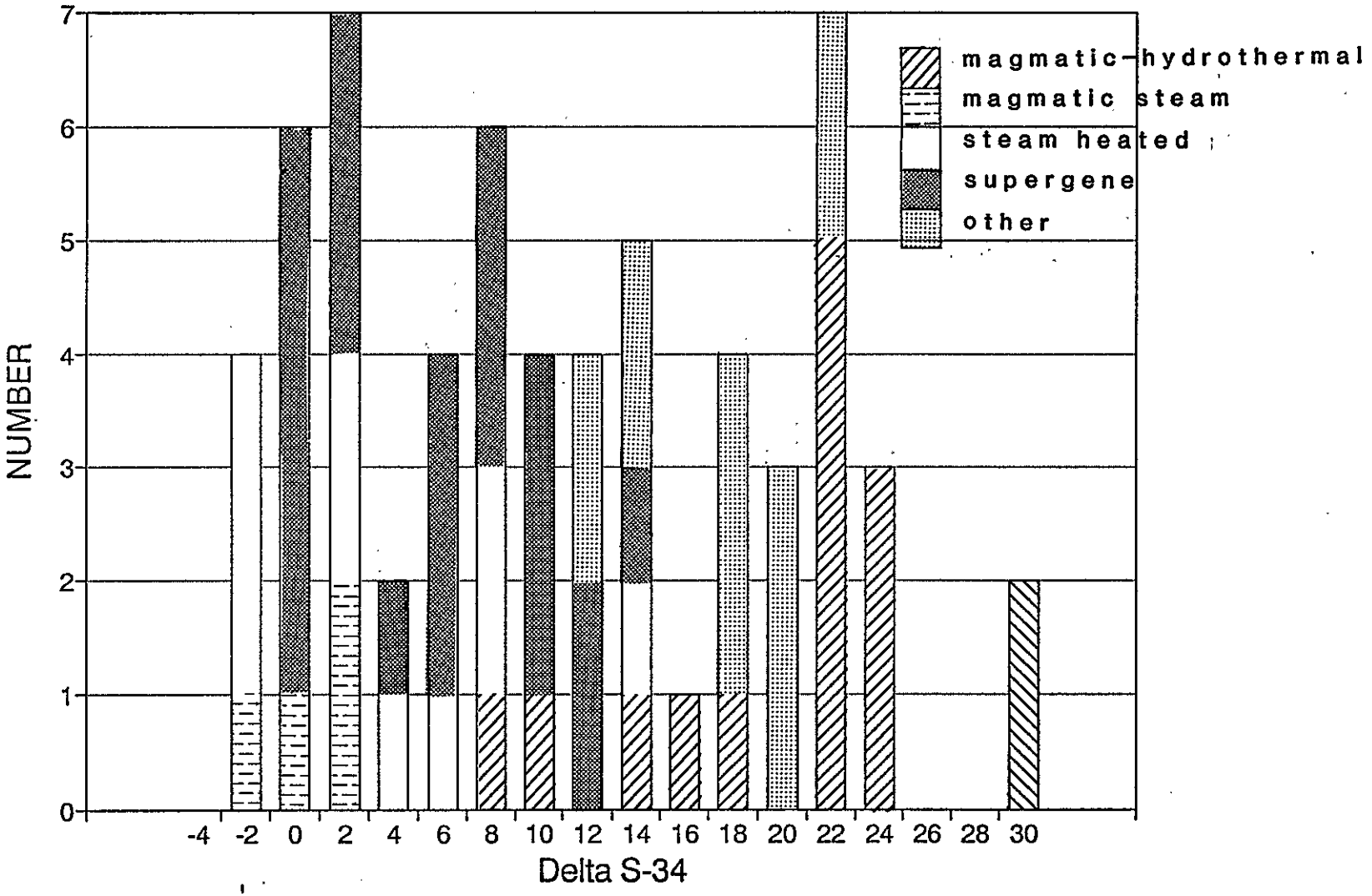

Figure 6.3 - Histogram of stable isotope values for delta s-34. Averaged values in Table 6.2 were used to avoid skewing by numerous analyses from one area.

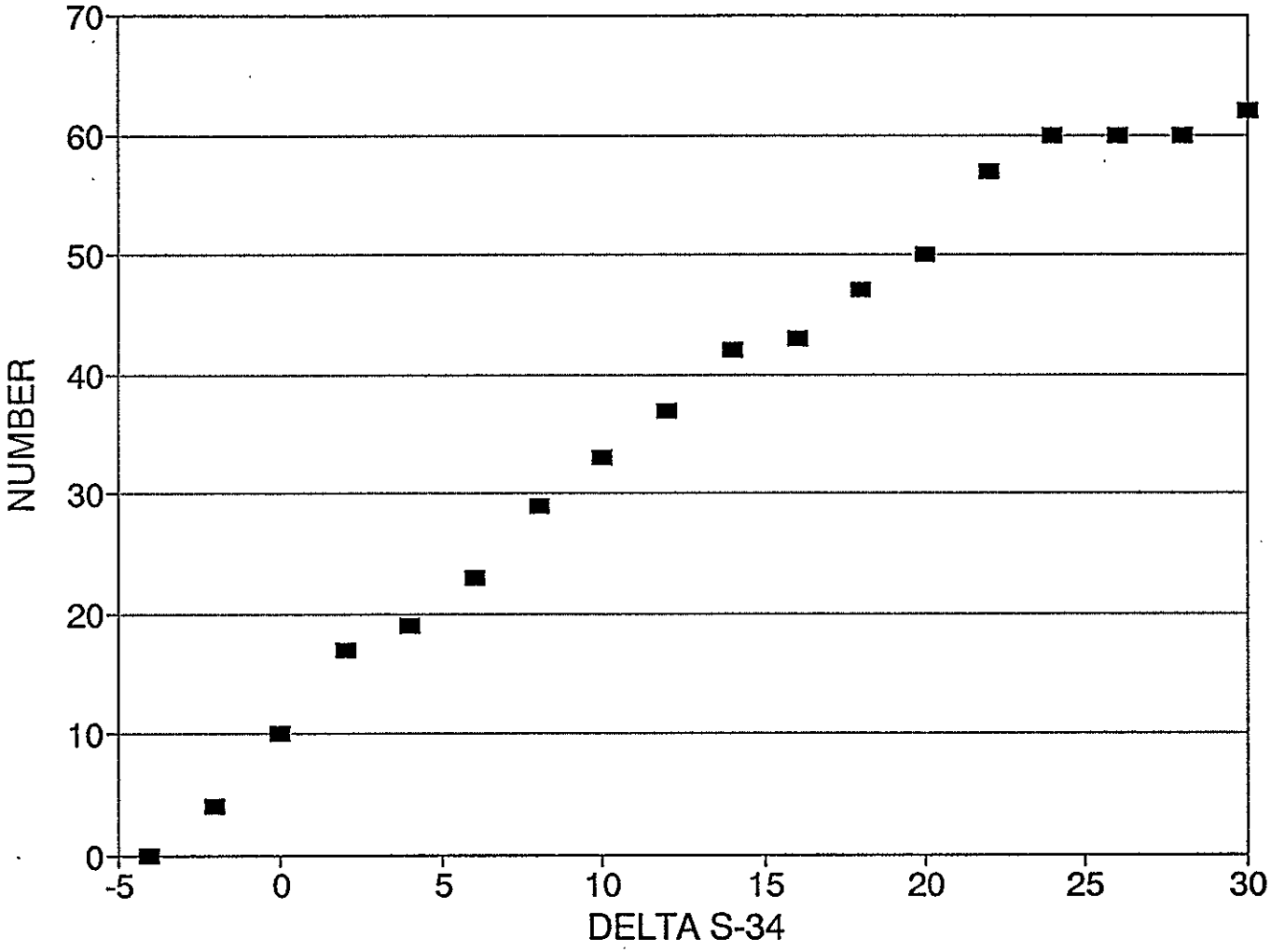

Figure 6.4 - Cummulative frequency curve of delta S-34 values.

TABLE 6.4—Alunite-pyrite $\delta^{34}S$ pairs and calculation of formation temperatures using fractionation factors from Ohmoto and Rye (1979).

No.	Location	Setting	$\delta^{34}S$ alun ‰	$\delta^{34}S$ py ‰	Temp °C
1	Monte Negro, Dom. Rep.	vein	20.0	-9.5	182
			21.6	-3.6	230
2	Pueblo Viejo, Dom. Rep.	vein	21.6	-3.6	230
5	Bitter Creek, New Mex.	hypogene	12.7	-6.3	339
			12.7	0.7	538
10	Rodalquilar, Spain	stage 1 magmatic	31	5.9	232
			28.8	5.7	260
			26.5	6.5	316
			22.3	4.9	380
11	Red Mt., Colo.	stage 2 magmatic	22.7	-6.9	181
12	Jucani, Peru	magmatic	22.7	-1.2	248
			24	1.9	277
			22.8	1.6	293
			22.5	0.8	283
			23.6	0.5	260
			23.8	-0.4	244
			22.7	0.2	270
			22.6	1.8	300
			28.1	1.6	214
13	Summitville, Colo.	magmatic	21.8	-3	236
			21.4	-8.1	182
			21.3	-3.6	234
			22.1	-7.6	180
			22.7	-5.4	196
			13.5	-2.2	435
15	Red Mt., Colo.	stage 1 magmatic	9.6	-8.1	372

Creek, Table 6.2) are consistent with formation in a magmatic-hydrothermal environment.

Sulfur isotope analyses of mineral pairs have potential for use as geothermometers, although several assumptions are required in using mineral-pairs for geothermometers. The mineral-pairs must be cogenetic and formed at the same temperature and from the same reservoir. The minerals must not have undergone any change in isotopic composition since formation. Fractionation factors must be available and have diverging slopes (Faure, 1986). Data in the literature are available for alunite-pyrite pairs (Table 6.4). It is difficult to be certain for each and every mineral-pair that the minerals were formed at the same time because the references did not provide enough information to ascertain that they were cogenetic, although it is assumed that they are cogenetic for this study. Calculated temperatures shown in Table 6.4 are derived using the fractionation factor listed below from Ohmoto and Rye (1979):

$$10^3 \ln \alpha_{\text{alun (SO4)-py}} = (4.86 \times 10^6 \times T^{-2}) + 6.0$$

where α is the fractionation factor and T is temperature in °K. Substituting the relationship

$$\delta^{34}S_{\text{alun}} - \delta^{34}S_{\text{py}} = 10^3 \ln \alpha_{\text{alun (SO4)-py}}$$

into the formula results in:

$$\delta^{34}S_{\text{alun}} - \delta^{34}S_{\text{py}} = (4.86 \times 10^6 \times T^{-2}) + 6.0.$$

Simplification and substituting T°C = T°K - 273 results in:

$$T(^\circ C) = \frac{2.205 \times 1000}{\sqrt{\delta^{34}S_{AL} - \delta^{34}S_{py} - 6}} - 273.$$

Most of the calculated temperatures in Table 6.4 from sulfur isotopes from magmatic-hydrothermal alunites are reasonable; however some are too high (no. 5, 13). Two temperatures calculated from the Steeple Rock data (Bitter Creek) are 339°C and 538°C. The lower temperature (339°C) is a reasonable estimate of the maximum temperature of the alteration, and is consistent with the alteration mineral assemblage (Table 5.1). It is important to determine the temperature of formation from isotope pairs because the altered rocks in the

Steeple Rock district do not have fluid inclusions that can be measured (section 4.2).

The available geologic, mineralogic, chemical, and isotopic data indicate that the acid-sulfate altered areas in the Steeple Rock district are a result of magmatic-hydrothermal fluids (Rye et al., 1991) as evidenced by the high $\delta^{34}S$ of alunite from Bitter Creek, the difference between $\delta^{34}S$ of cogenetic alunite and pyrite, mineral and chemical zonations (section 5) and the similarity in age of alunite with the host rocks (section 5, Table 2.1). Early hydrothermal systems developed consisting of alkali-chloride waters that interacted with the wall rocks to produce regional alkali-chloride alteration (White, 1981). Acid fluids were derived from magmatic waters by disproportionation of magmatic sulfate with decreasing temperatures and resulted in the acid-sulfate altered areas, which overlie alkali-chloride alteration. These features are similar to modern hot springs systems such as Norris Geyser Basin in Yellowstone National Park (White et al., 1988). High sulfidation gold deposits, yet to be discovered, may be associated with these areas in the district.

6.2 Mineralization

6.2.1 Boiling and mixing

Boiling has dynamic effects on the chemistry of a fluid and is commonly evoked to explain mineral deposition. Loss of even a small amount of steam and other gases results in a change in concentrations of metal complexes as well as other ions. Boiling results in loss of heat, an increase in pH, an increase in salinity, and a decrease in gas content (Reed and Spycher, 1985). For example, loss of CO_2 causes calcite to precipitate according to the following chemical equation:

$$Ca^{+2} + 2HCO_3^- \rightleftharpoons CaCO_3(s) + CO_2(g) + H_2O.$$

CO_2 is typically lost to the atmosphere making this an irreversible process. As calcite precipitates, the concentrations of other ions change. Therefore, it is important to recognize

zones of boiling because as gases are lost, metal solubilities decrease and deposition occurs. Boiling is episodic in many systems.

Several indicators can be used to recognize boiling in the low-sulfidation epithermal veins in the Steeple Rock district. Bladed calcite (lattice texture) is almost always found in zones of boiling fluids in modern geothermal systems (Talloch, 1982; R. R. L. Browne, unpubl. report, Spring, 1992; Mitchell and Leach, 1991; White and Hedenquist, 1990; Hedenquist, 1991; Simmons et al., 1992) and is one of the more distinctive indicators of boiling. This texture is common in epithermal vein deposits and is found along the East Camp-Twin Peaks fault system (including the Blue Bell fault).

In most natural waters, cooling without boiling causes calcite to dissolve (Fig. 6.5; Fournier, 1985b). However, when an ascending carbonate-rich fluid boils as a result of cooling adiabatically, then calcite will precipitate due to loss of CO_2 (Fournier, 1985b; Cunningham, 1985). Once CO_2 is lost, the boiling stops but the cooler water continues to ascend, dissolving the calcite. Quartz is deposited as a result of cooling of hydrothermal waters (Fig. 6.6; Fournier, 1985a) and therefore quartz simultaneously replaces bladed calcite. The rising fluids begin to boil again (as a result of adiabatic cooling) and the process is repeated until CO_2 is completely removed from the system.

In the Steeple Rock district, bladed quartz pseudomorphed after calcite and bladed calcite (Fig. 4.13) are found at the top of the Summit vein (elevation 1865.3 m) as well as at depths of 358 m in drill hole B91-17 (elevation 1290.8 m). Thus boiling occurred over a total interval of 574.4 m near the Summit mine and is associated with gold-silver deposition. Elsewhere in the Steeple Rock district, bladed quartz and/or calcite are rare and, if present, occur as late stage mineralization.

The presence of vapor-rich and two-phase fluid inclusions in the same sample is also indicative of zones of boiling (Roedder, 1984; Shepherd et al., 1985). However, liquid-rich inclusions also can form in the boiling zone by necking of two-phase inclusions. Thus fluid inclusion data for boiling need to be carefully evaluated. In samples from Steeple Rock, only

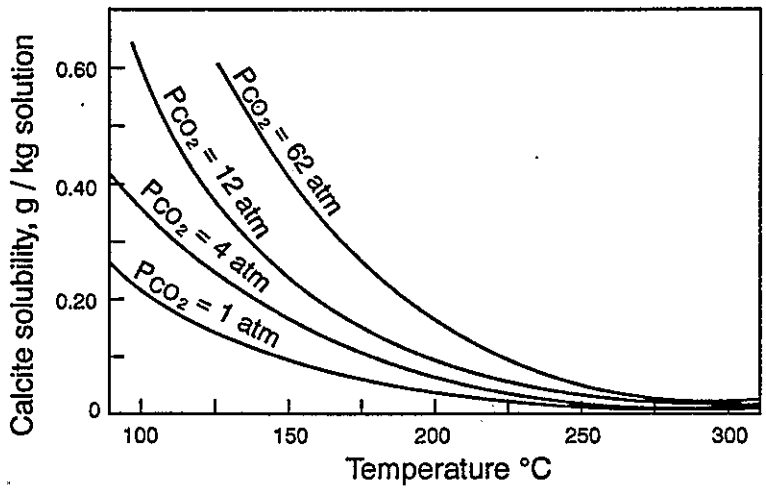

Figure 6.5 The solubility of calcite in water up to 300°C at various partial pressures of carbon dioxide (Fournier, 1895b; Ellis, 1959).

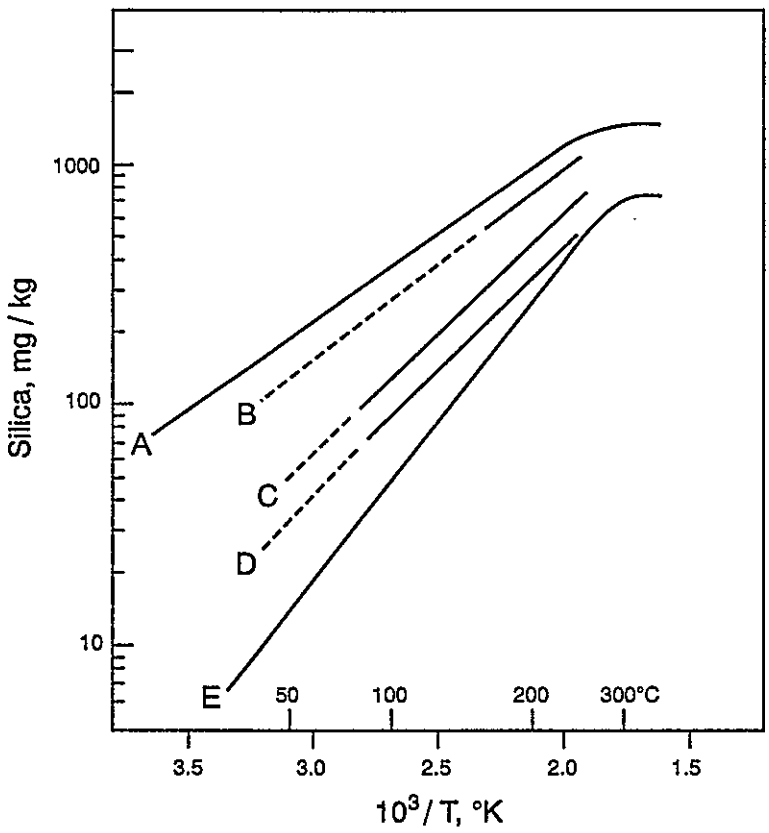

Figure 6.6 Solubilities of various silica phases in water at the vapor pressure of the solution. A= Amorphous silica, B= Opal-CT, C=α-Cristobalite, D= Chalcedony, E= Quartz (Fournier, 1985a).

a few contain both vapor-rich and two-phase inclusions and typically the vapor-rich inclusions are secondary inclusions (i.e., younger fluids). Therefore fluid inclusion evidence for boiling in the Steeple Rock district is inconclusive (section 4.2).

Additional mineralogic evidence for boiling includes (1) abundant quartz deposited as a result of cooling of supersaturated silica fluids (Fournier, 1985a), (2) veins of adularia as a result of an increase in pH resulting from boiling (P. R. L. Browne, unpubl. report, Spring. 1992), and (3) deposition of primary hematite as a result of oxidation of the fluids at the water table (Simmons et al., 1992; Cunningham, 1985). All of these features are present within the precious- and base-metal veins in the Steeple Rock district suggesting that boiling is a possible mechanism for mineral deposition, but not necessarily the only mechanism.

Cooling and mixing trends are difficult to determine in epithermal systems because they are not well defined by available data. Isotopic studies are required to define cooling and mixing trends and even isotopic data can be ambiguous. Fluid inclusion data can be used to indicate possible cooling and mixing trends (Shepherd et al., 1985). A plot of temperature vs. salinity of fluid inclusion data from Steeple Rock samples (Fig. 6.7) is consistent with cooling and mixing trends (Shepherd et al., 1985), but the effects of dilution and boiling are complex and specific models can not be derived from fluid inclusion data alone (Hedenquist and Henley, 1985).

6.2.2 Pressure and depth estimates

Data from fluid inclusion studies are widely used to estimate pressure and depth (Roedder and Bodnar, 1980). Two types of data are required to provide estimates of pressure at the time of formation of the fluid inclusions and presumably the host mineral: (1) composition of the fluid inclusions and (2) thermodynamic and geochemical data for the composition and temperature range of the fluid inclusions. These data are not always known exactly, thereby making any calculations of pressure and depth suspect.

The compositions of fluid inclusions from the Steeple Rock district are not known

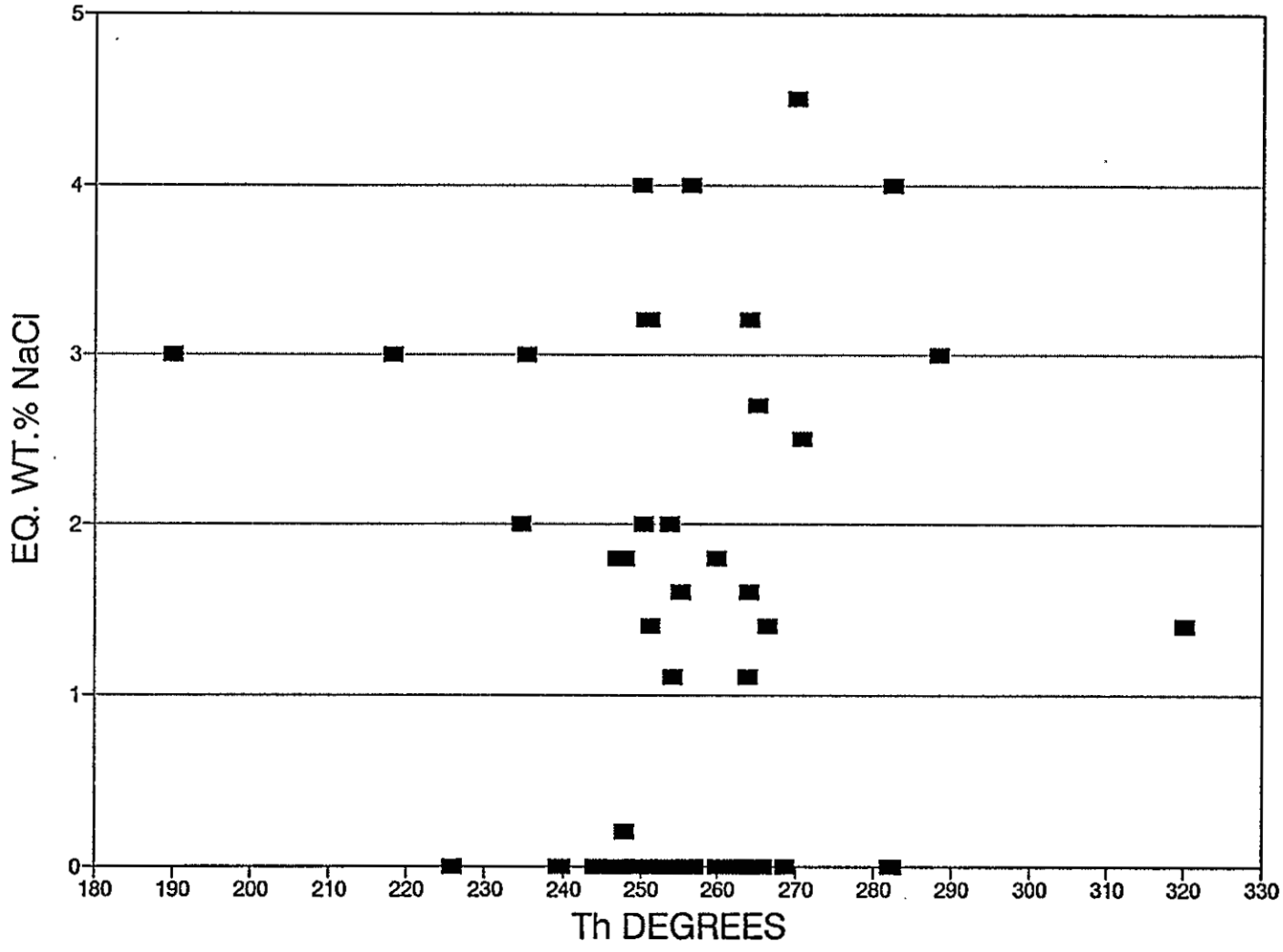

Figure 6.7 - Plot of temperature vs. salinity of fluid inclusions in quartz from the Steeple Rock district. This shotgun pattern is typical of cooling and mixing of fluids.

exactly. Last-ice melting temperatures indicate that calculated salinities are less than 5 eq. wt. % NaCl. Preliminary gas analyses of fluid inclusions from the district indicate anomalously high contents of CO_2 and H_2S are present locally (Ruff, 1993; Ruff and Norman, 1991); however, exact quantities are unknown but presumed low because most two-phase inclusions contain less than 30% gas by volume. Therefore it is assumed that most fluids which deposited epithermal vein minerals in the district were probably 0–5 eq. wt. % NaCl with only trace amounts of gases. The presence of bladed calcite in certain areas formed by boiling suggests that locally CO_2 contents may have been relatively high.

The minimum pressure which a fluid can have is its vapor pressure at any given composition and temperature. If the confining pressure falls below its vapor pressure, then the fluid will boil. The maximum pressure which a fluid can have is due to the weight of the overlying rocks (the lithostatic pressure), although it is possible to have overpressures from tectonic or other stresses. If the fluid is open to the surface via faults or cracks, then the confining pressure is due to a column of the overlying fluid or hydrostatic pressure. Typically the lithostatic pressure is greater than the hydrostatic pressure.

In a simple H_2O–NaCl system, assumed for the veins in the Steeple Rock district, the estimated depth can be determined by using calculations and boiling curves by Haas (1971). From fluid inclusion studies, the veins in the Steeple Rock district were deposited at temperatures between 240 and 320°C (Fig. 4.20, 4.21). Therefore, the Steeple Rock veins were emplaced at minimum depths of approximately 360–1300 m, assuming hydrostatic pressures (Fig. 6.8). This range in depths is reasonable because the Dark Thunder Canyon formation and lava flows of Crookson Peak most likely were present above the epithermal veins for a total approximate stratigraphic thickness of 1300 m.

Once the depth is determined, the pressure can be calculated from the following formula (Shepherd et al., 1985):

$$P = H\rho g$$

Where P = pressure (bars), H = depth (m), ρ = density of overlying material (1.00 gcm^{-3}

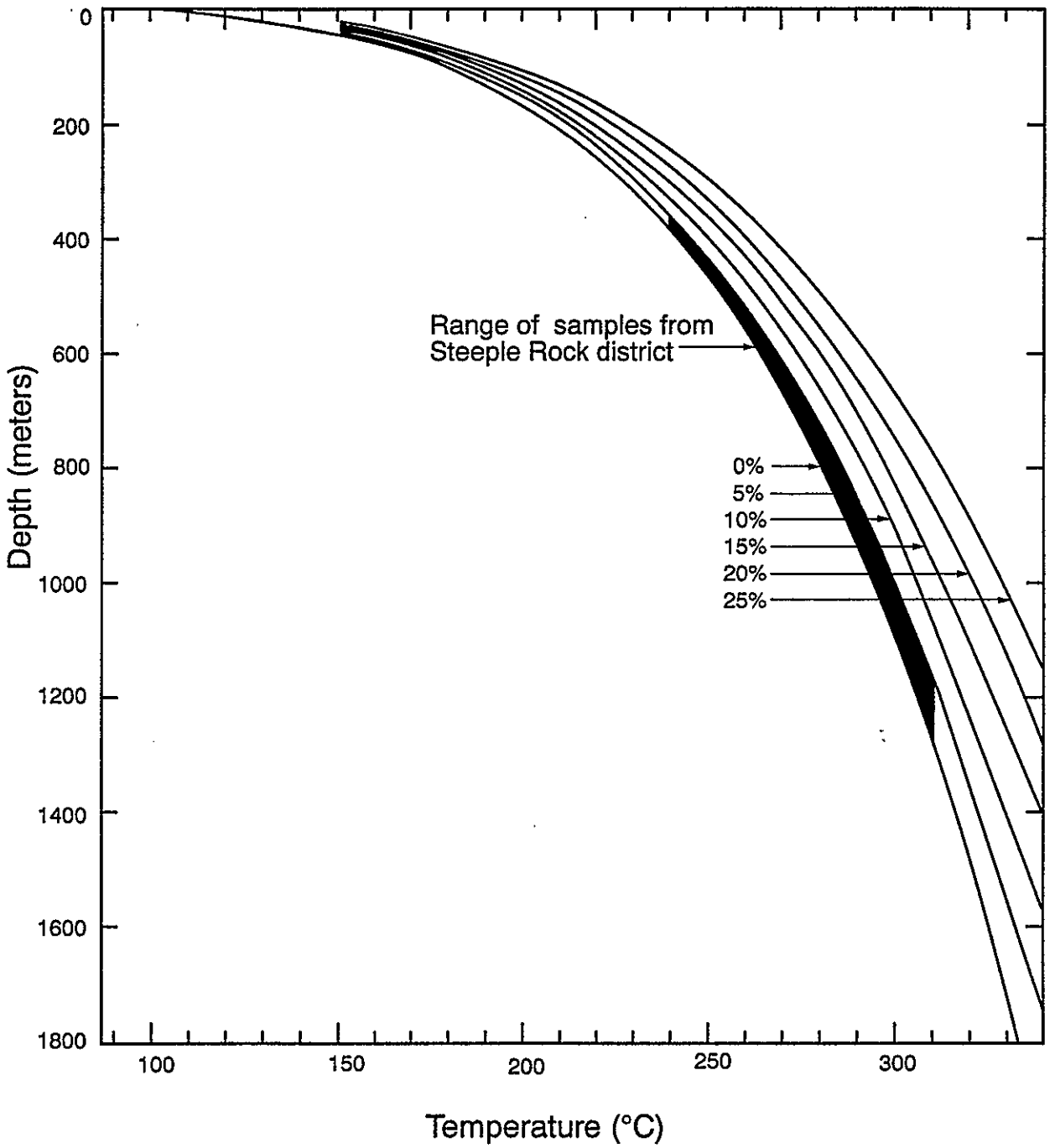

Figure 6.8 Boiling point curves under hydrostatic pressure for H_2O liquid (0 wt. percent) and for brine of constant composition given in wt. percent NaCl. The temperature at 0 meters of each curve is the boiling point for the liquid at 1.013 bars (1.0 atm) load pressure which is equivalent to the atmospheric pressure at sea level. From Haas (1971).

for hydrostatic and 2.70 gcm^{-3} for lithostatic overburden), and g = gravitational constant (981 dynes cm^{-2}). Note that 1 bar = 10^6 dynes cm^{-2}. Therefore approximate pressures of the formation of the veins in the Steeple Rock district are between 35 and 128 bars.

It must be emphasized that these pressure and depth estimates are only approximations because several assumptions exist. Furthermore, epithermal systems constantly seal and unseal, therefore the veins may be subjected to both hydrostatic and lithostatic conditions and overpressures may also occur. Epithermal systems are constantly changing, rarely in equilibrium, and dynamic.

However, from these calculations it is apparent that the veins in the Steeple Rock district formed at low pressures (< 150 bars) and near the surface at shallow depths (< 1.5 km). These estimates are typical of epithermal gold-silver districts throughout the world.

6.2.3 Geochemical constraints

Certain constraints on the geochemical and thermodynamic evolution of the epithermal vein deposits in the Steeple Rock district can be determined using the geologic, mineralogic, geochemical, and fluid inclusion data presented in sections 2 through 5 in conjunction with published experimental and theoretical geochemical and thermodynamic data. Detailed computer modeling of various data is possible (Reed and Spycher, 1985), but is not utilized here because it is time consuming and tedious and requires additional data not available for the Steeple Rock district. In addition, textural evidence of the Steeple Rock veins is consistent with a dynamic and constantly changing physical and chemical evolution, which increases the complexity and decreases the ultimate reliability of computer modeling.

The epithermal veins in the Steeple Rock district were deposited from low salinity fluids (< 5 eq. wt. % NaCl) at temperatures between 240° and 320°C (Fig. 4.20, 4.21, 4.22). Pressures were relatively low (< 150 bars, section 6.2.2). Deposition probably occurred under complex and constantly changing cycles of boiling, cooling, and mixing at shallow depths (< 1500 m; sections 6.2.1 and 6.2.2). Fluids, although low in total gas

content, probably contained elevated concentrations of CO_2 and H_2S as gases.

The veins consist predominantly of quartz which indicates that the fluids were supersaturated in silica (Fournier, 1985a; White and Hedenquist, 1990). Such supersaturated solutions generally indicate that large and rapid changes in the physical and chemical conditions of the fluid will occur and will ultimately affect the capacity of the fluid to transport and deposit ore minerals (Fournier, 1985a). Textures in vein samples from the Steeple Rock district suggest that some quartz was originally amorphous silica (section 4.1.2.1) and gold can be carried as a colloid with the amorphous silica (Herrington and Wilkinson, 1993). Therefore the transport and deposition of ore minerals is strongly dependent upon the solubility of silica with time.

The veins in the Steeple Rock district also consist of varying amounts of illite, adularia, calcite, and chlorite. Geochemistry of chlorite in epithermal systems has not been examined and thus chlorite will be ignored in this study. However, the presence of abundant illite and lesser amounts of adularia (K-feldspar) has important geochemical implications. Illite typically forms from acidic to slightly acidic solutions, depending upon the potassium concentration (Fig. 6.9; Henley, 1984; Reed and Spycher, 1985; Browne and Ellis, 1970). If the fluid is concentrated in CO_2 as well as Ca^{++}, then calcite will precipitate instead of the calc-silicate minerals (Fig. 6.9; Browne and Ellis, 1970). As the fluid evolves, the temperature most likely decreases, resulting in boiling, and resulting in an increase in pH. Thus deposition of illite may be followed by subsequent deposition of K-feldspar (adularia). This suggests that the Steeple Rock mineralizing fluids were probably acidic to slightly acidic and evolved toward neutral pH.

All types of veins in the Steeple Rock district typically contain pyrite and varying amounts of chalcopyrite, galena, and sphalerite. This mineral assemblage has important implications on the oxygen and sulfur fugacities. From the pH range established by the illite/adularia assemblage (3.5 to 5.6 at 250°C) and assuming a high to moderate potassium concentration, then the oxygen fugacity range can be estimated as log fo_2 = -41.8 to -30 (Fig.

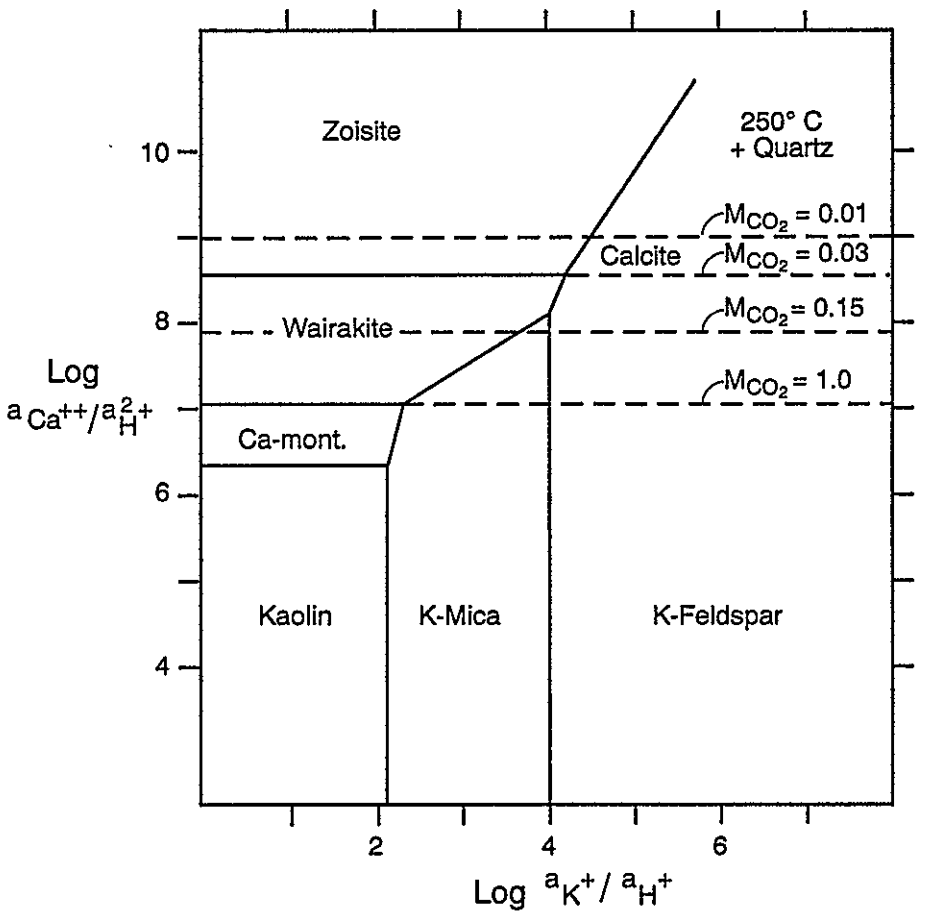

Figure 6.9 Activity diagram for the principal phases in the system $CaO\text{-}Al_2O_3\text{-}K_2O\text{-}H_2O$ at 250°C. Dashed lines repressent stability fields of calcite at different molarities of CO_2. Modified from Browne and Ellis (1970) and Henley (1984).

6.10; Barton, 1984). Then the sulfur fugacity can be estimated as log a_{S2} = -12.5 to -8.5 (Fig. 6.11; Barton, 1984). From this approach, it is apparent that the Steeple Rock mineralizing fluids were acidic to lightly acidic to neutral pH and had low to moderate oxygen and sulfur fugacities. These conditions are typical of low-sulfidation epithermal deposits (Table 1.1).

As the fluid evolved, the temperature decreased, pH increased, and the fluid became more oxidizing. This is consistent with the deposition of late adularia and primary hematite veins. Also influx of additional fluids probably occurred.

6.2.4 Relationship of mineralization to rhyolite intrusives

A common association between epithermal veins and rhyolite intrusions exists in many districts in the world (Cox and Singer, 1986; Buchanan, 1981; Burt and Sheridan, 1987). In the Steeple Rock district, some epithermal veins are related spatially to rhyolite dikes, especially in the Vanderbilt Peak (Alabama, New Years Gift, Laura, Jim Crow, Imperial mines), Apache Box, and Twin Peaks (Twin Peaks mine) areas. Locally, rhyolite dikes cut epithermal veins. However, in other areas of the Steeple Rock district, rhyolite intrusives are not present in the immediate vicinity of epithermal veins (East Camp, Summit, Bank mines). Mineralogic and geochemical data and statistical analyses described in sections 3 and 4 are consistent with, but not conclusive of, a genetic relationship between rhyolite intrusives and epithermal veins in the Steeple Rock district. Additional data supporting a rhyolite association include: (1) the tremendous amount of quartz deposition in the veins is best attributed to a rhyolitic magma rather than an andesitic magma, (2) the spatial association between the rhyolite dikes and epithermal veins, and (3) the epithermal veins are closer in age to the rhyolite intrusives than to the andesitic volcanism. However, this genetic association requires additional study.

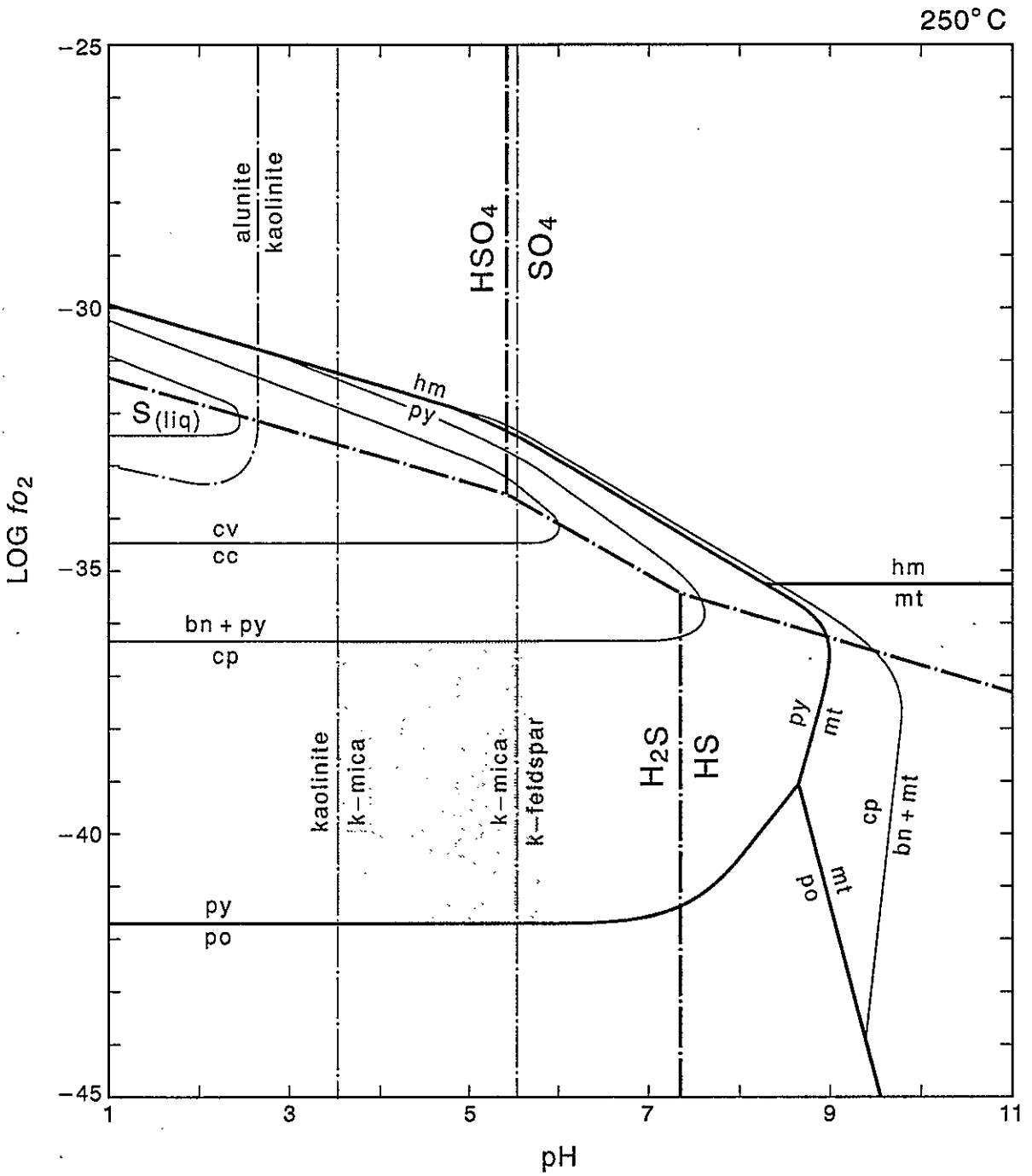

Figure 6.10– Log fo_2–pH diagram at 250° C. Log $a_{(k+)} = 1.5$. Bn–bornite; cc–chalcocite; cp–chalcopyrite; cv–covellite; hm–hematite; mt–magnetite; py–pyrite; po–pyrrhotite. Shaded field represents equilibrium stability field for Steeple Rock veins. Modified from Barton (1984) and Deng (1991).

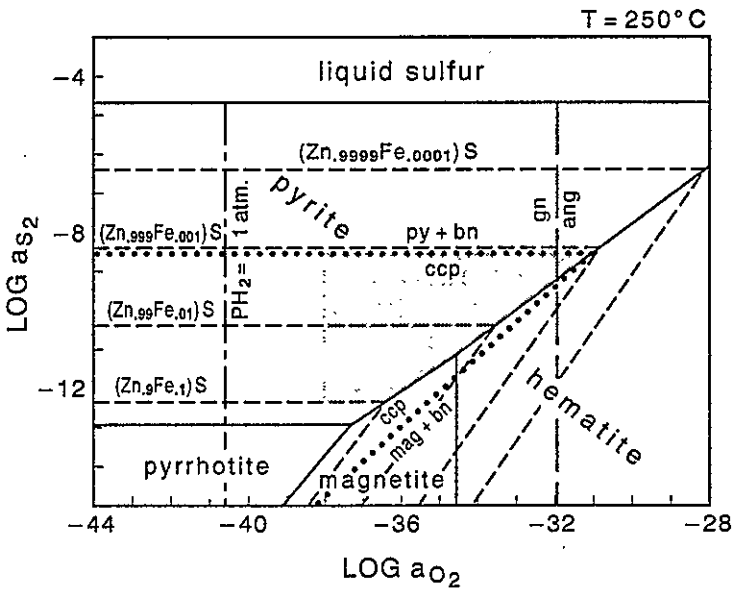

Figure 6.11 – Activity diagram for Fe–Pb–Cu–S–Zn system. Shaded field represents equilibrium stability field for Steeple Rock veins. Modified from Barton (1984).

6.3 District Zoning

6.3.1 Introduction

Systematic changes in the mineralogy, chemistry, and/or physical and chemical conditions within a mining district are referred to as district zoning. Zoning is also observed in much larger regional areas (regional zoning) and smaller, local areas (mine or deposit zoning). These systematic changes reflect changes in evolving fluids with time and distance from the source and provide excellent guides to ore deposits as well as to enhance our understanding of the genesis of ore deposits. By integrating and piecing together available data, district patterns emerge which are interpreted to represent district-wide zonations.

District zoning in epithermal districts is commonly difficult to interpret because the epithermal systems are dynamic and constantly changing. Overprinting of multiple epithermal (or geothermal) systems may also occur. In the Steeple Rock district, distribution of alteration assemblages, production, and vein mineral assemblages indicates that district zonations are partially preserved.

6.3.2 Alteration

Alkali-chloride alteration is common throughout the Steeple Rock district. Mineral assemblages containing epidote are indicative of deposition from fluids at temperatures greater than 200°C (Simmons et al., 1992) and are found at depth and near the epithermal veins in the Steeple Rock district. Mineral assemblages containing mordenite and smectite are indicative of lower temperatures (less than 180°C; Simmons et al., 1992) and are found distal to the epithermal veins (Fig. 6.12, 6.13).

Areas of acid-sulfate alteration are scattered throughout the Steeple Rock district (Fig. 5.4). The larger areas occur along the East Camp-Twin Peaks, Carlisle, and Bitter Creek faults. Sulfur isotopic data and mineralogy suggest maximum temperature of formation of 200–340°C (section 6.12; Fig. 5.1). Two areas are spatially associated with epithermal veins: Telephone Ridge area near the Carlisle and Center mines and Summit area near the Summit

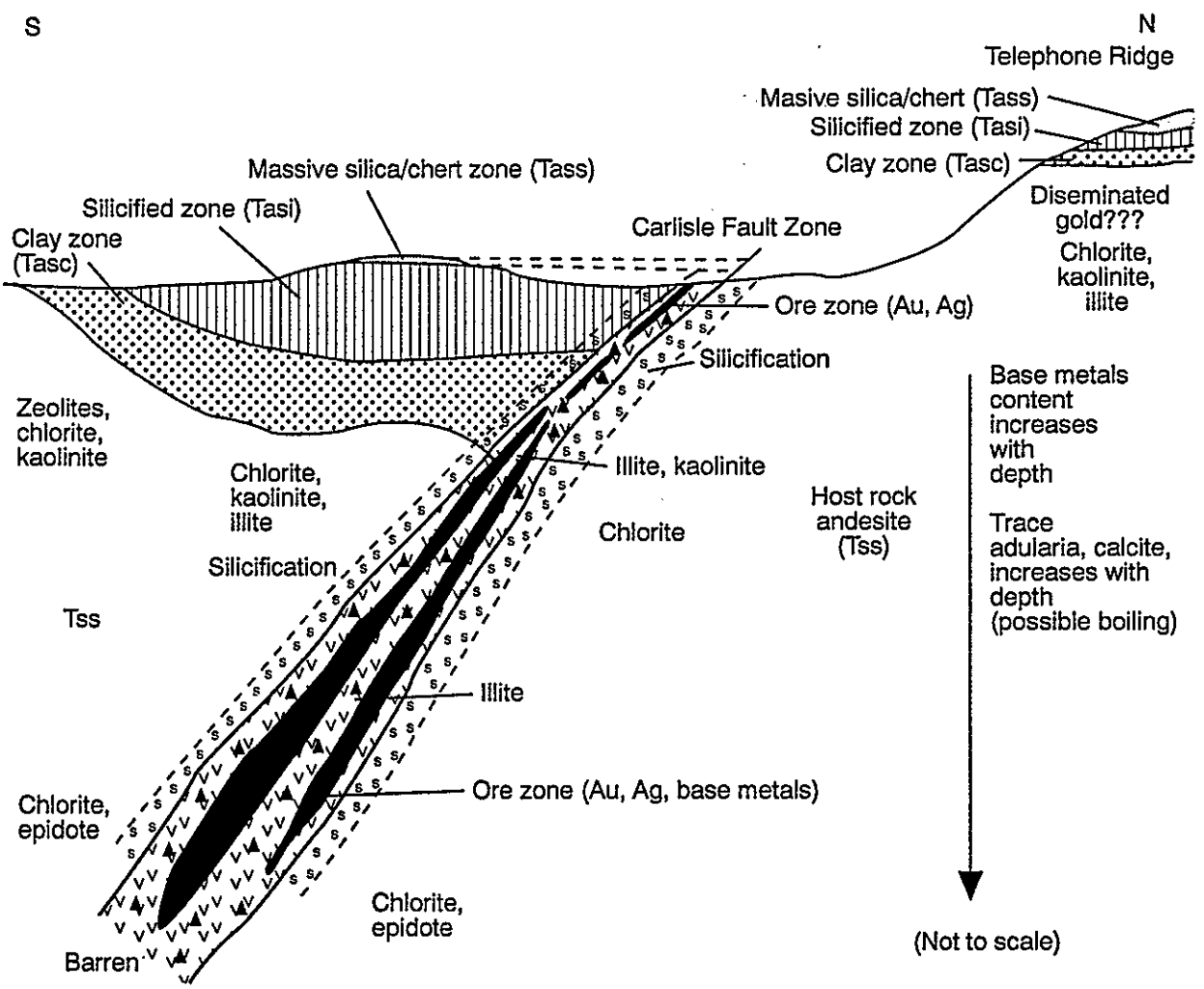

Figure 6.12 Relationship between alteration and vein deposits along the Carlisle fault (modified in part from Weacp drill data).

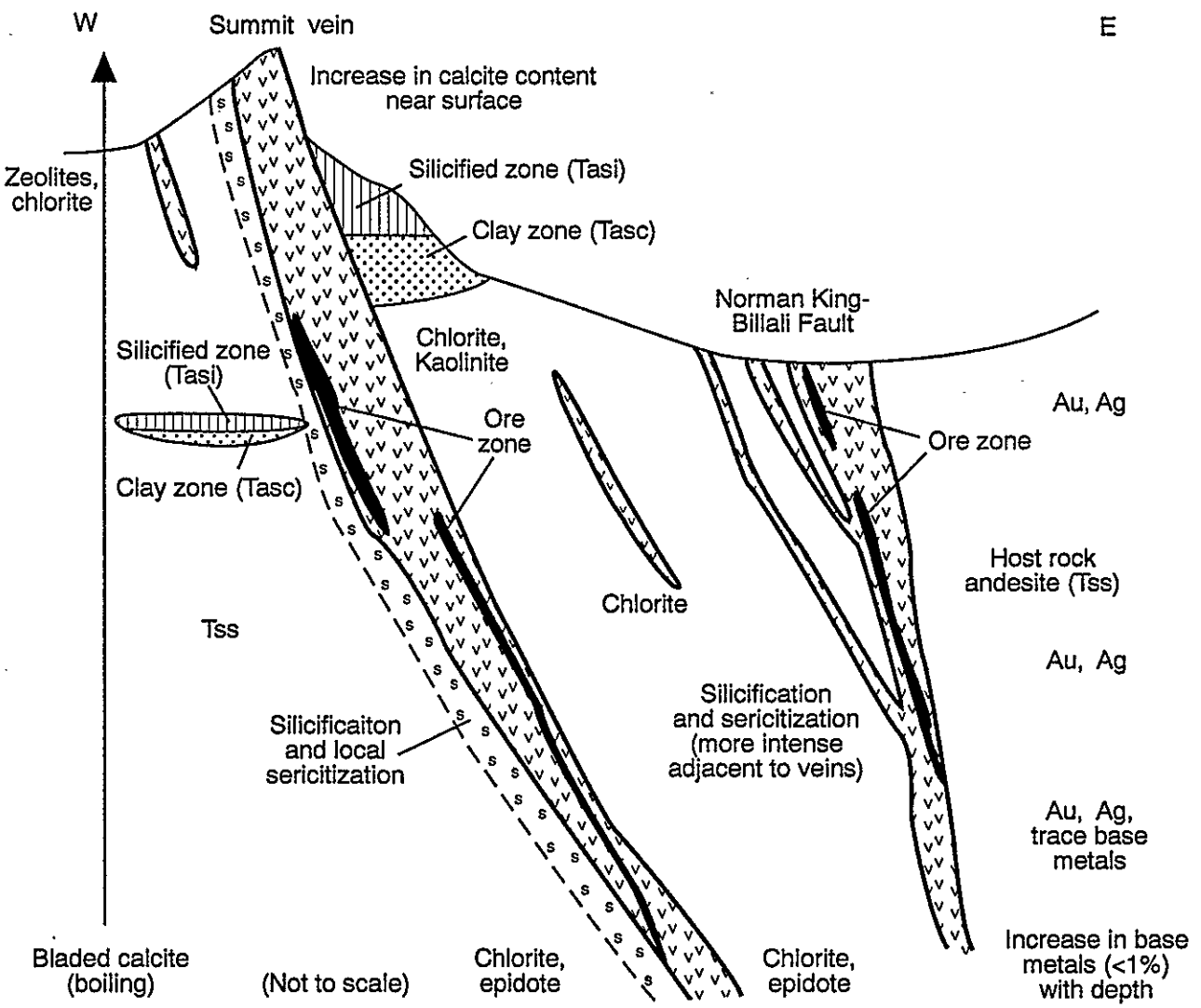

Figure 6.13 Relationship between alteration and vein deposits along the East Camp-Summit fault

and Bank mines (Fig. 6.12, 6,13). Acid-sulfate alteration caps or overlies base-metal veins at the Carlisle and Ontario mines and overlies precious-metal veins at the Bank mine. Furthermore, the Goat Camp Springs area is associated with fluorite veins.

Drilling at Telephone Ridge, Raeburn Hills, and Summit areas revealed minor intervals of disseminated gold mineralization. This acid-sulfate alteration overlies alkali-chloride alteration and locally mineralized veins. The drilling data, mineral assemblages, age reltionships, and zonation (section 5.3) suggest that the acid-sulfate altered areas may represent separate surface hydrothermal systems (i.e. hot springs, geysers) that are likely connected at depth, similar to modern geothermal fields (such as at Yellowstone and New Zealand; Elder, 1981). These acid-sulfate altered areas may overlie undiscovered epithermal vein deposits, similar to those at Carlisle mine or overlie undiscovered, disseminated gold deposits (Fig. 6.12).

6.3.3 Epithermal vein mineralization

Base-metal vein deposits (>10% base metals) with significant gold and silver contents occur only along the Carlisle fault, between the Carlisle and Ontario mines and possibly westward into section 2. This area may well represent the center of the district (Fig. 6.14). Stratigraphically the Center-Carlisle deposits and the gold-silver veins at East Camp and Summit are the same. Outward from the Carlisle-Center mines, low-sulfidation gold-silver veins occur along northwest- and north-trending faults which contain little or no base metals (<1%). The gold-silver veins along the East Camp-Twin Peaks fault system are associated with bladed calcite or bladed quartz after calcite. These deposits are not spatially associated with any rhyolite intrusives, but the gold-silver deposits in the vicinity of Twin Peaks and Vanderbilt Peak in the western portion of the district are associated with rhyolite intrusives. On the fringes or outer margins of the district, copper-silver veins occur, locally grading with precious-metal veins, and the outermost zone is represented by fluorite and manganese veins (Fig. 6.14). Late-stage fluorite was also deposited in local areas of base- and

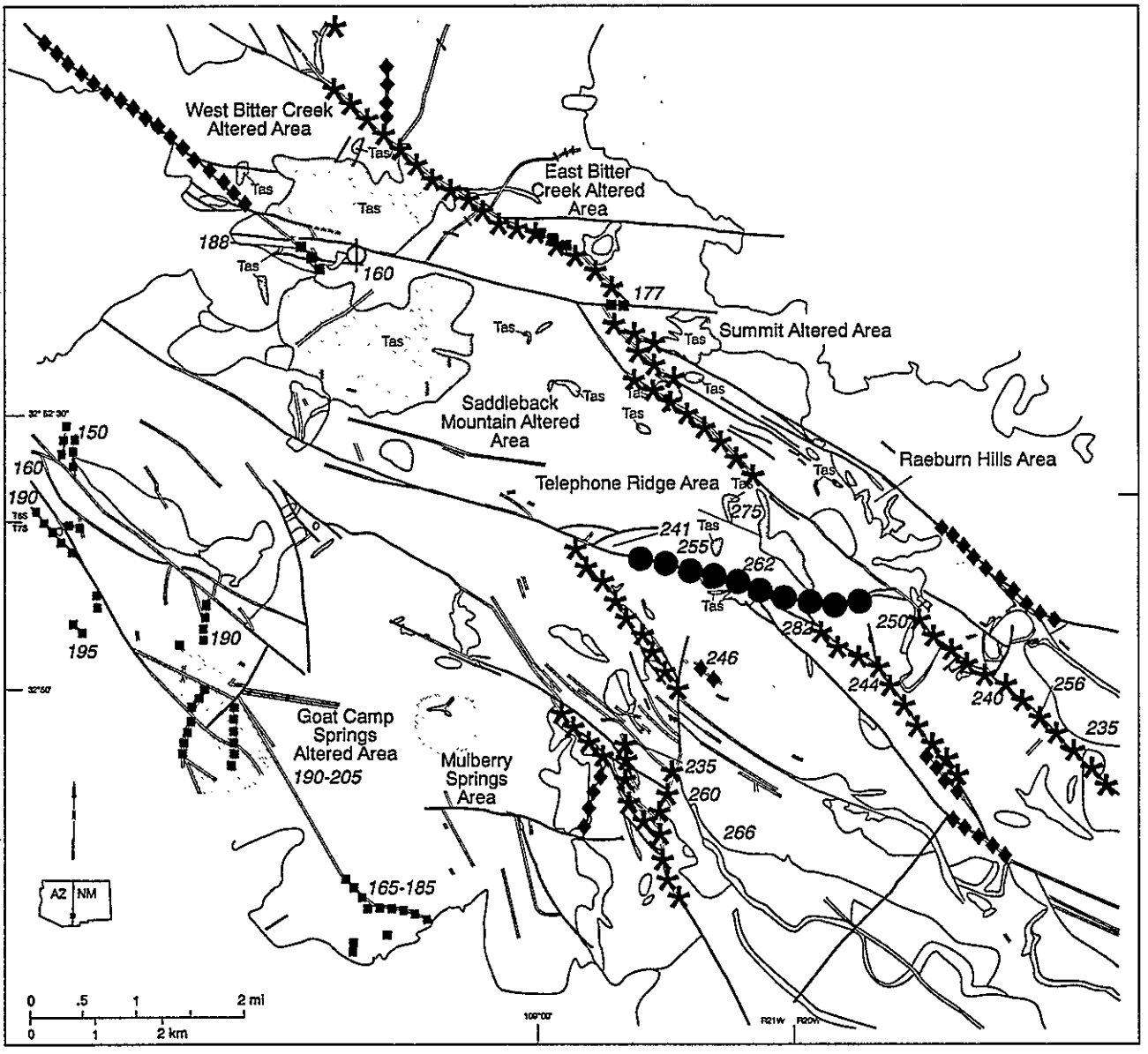

Figure 6.14 District zoning in the Steeple Rock mining district

precious-metal deposits.

6.3.4 Fluid inclusion data

Collectively, fluid inclusion data, especially temperature of homogenization, provide additional information on district zoning. The highest temperatures of homogenization in fluid inclusions come from sphalerites from the deeper levels of the Center mine (Table 4.2; 288–325°C). Some of the higher temperatures of homogenization of fluid inclusions in quartz also come from the Carlisle-Center mines area (Table 4.1, Appendix 11.7). Furthermore, the temperatures of homogenization increase with depth at the Carlisle-Center and Alabama mines (Table 4.1, Appendix 11.7). Fluid inclusion data are consistent with the center of the epithermal system located in the Carlisle-Center mines area.

Two or more centers of fluorite mineralization can be interpreted from fluid inclusion data of fluorite. The bimodal distribution of temperatures of homogenization (Fig. 4.22) is consistent with two centers of epithermal activity. The highest temperatures of homogenization are from fluorite from mines and prospects in the Goat Camp Springs area and the Forbis and Luckie mines (average 190–205°C, Fig. 6.14; Appendix 11.7). Temperatures of homogenization decrease away from the Goat Camp Springs area: Rattlesnake mines average 165–185°C, Fourth of July mines average 155–170°C, and Daniels Camp mines average 190°C (Table 4.3, Fig. 6.14). In the Bitter Creek area, temperatures of homogenization in fluorite from the Bitter Creek drill hole (BC1) are lower (160°C).

These data suggest that a second center of fluorite mineralization may occur north of Bitter Creek. This temperature difference could also be accounted for by variations in lateral fluid flow and/or mixing.

There are insufficient data to determine the significance of the Twin Peaks mine and prospects at Apache Box. The veins at the Twin Peaks mine and Apache Box could be part of the precious-metal zone centered at the Carlisle-Center mines or they could represent one or more separate systems. The fluorite veins in the Bitter Creek area could be part of either

system or a third independent system.

These data along with distribution of alteration (section 5), production (section 3), and mineral assemblages (section 4) suggest at least three possibilities. The fluorite and manganese mineralization represents the outer margins of an epithermal system centered at the Carlisle-Center mines. Alternatively, the fluorite mineralization could represent the top of separate epithermal systems that may grade into precious- and base-metals with depth. These separate epithermal fluorite systems could also be barren of metal mineralization. A combination of these hypotheses is also possible.

6.4 Paragenesis

Field observations, petrographic studies, descriptions of drill core, and other geologic data have resulted in a paragenetic sequence of events in the Steeple Rock district (Figs. 6.15 and 6.16). The paragenesis of alteration and mineralization can be divided into six stages: premineralization, four mineralization stages (stage 1, stage 2, stage 3, late), and post-mineralization. Two paragenic models are consistent with the geologic data: a episodic model (Fig. 6.15) and a continuous model (Fig. 6.16).

The pre-mineralization stage is characterized by regional and successive multiple periods of silicification and alkali-chloride and acid-sulfate alteration with deposition of disseminated pyrite. Intensity and rank of alteration varies according to physical and chemical conditions. Permeability of the altered rocks decreased as alteration increased, because secondary minerals filled the void spaces (section 5.5). The presence of coexisting epidote and chlorite at depth in alkali-chloride altered rocks indicates that temperatures ranged as high as 240°–300°C (Beaufort et al., 1992; Arnorsson et al., 1983; Simmons et al., 1992). Locally in the Steeple Rock district, steam-heated condensates formed at temperatures of 200–340°C and produced acid-sulfate altered areas near the surface, above the alkali-chloride altered rocks (section 6.1). Mineral and textural zoning (Figs. 6.12, 6.13) and limited isotopic data (Table 6.2; Field, 1966) suggest that this acid-sulfate alteration involved magmatic sources (i.e.

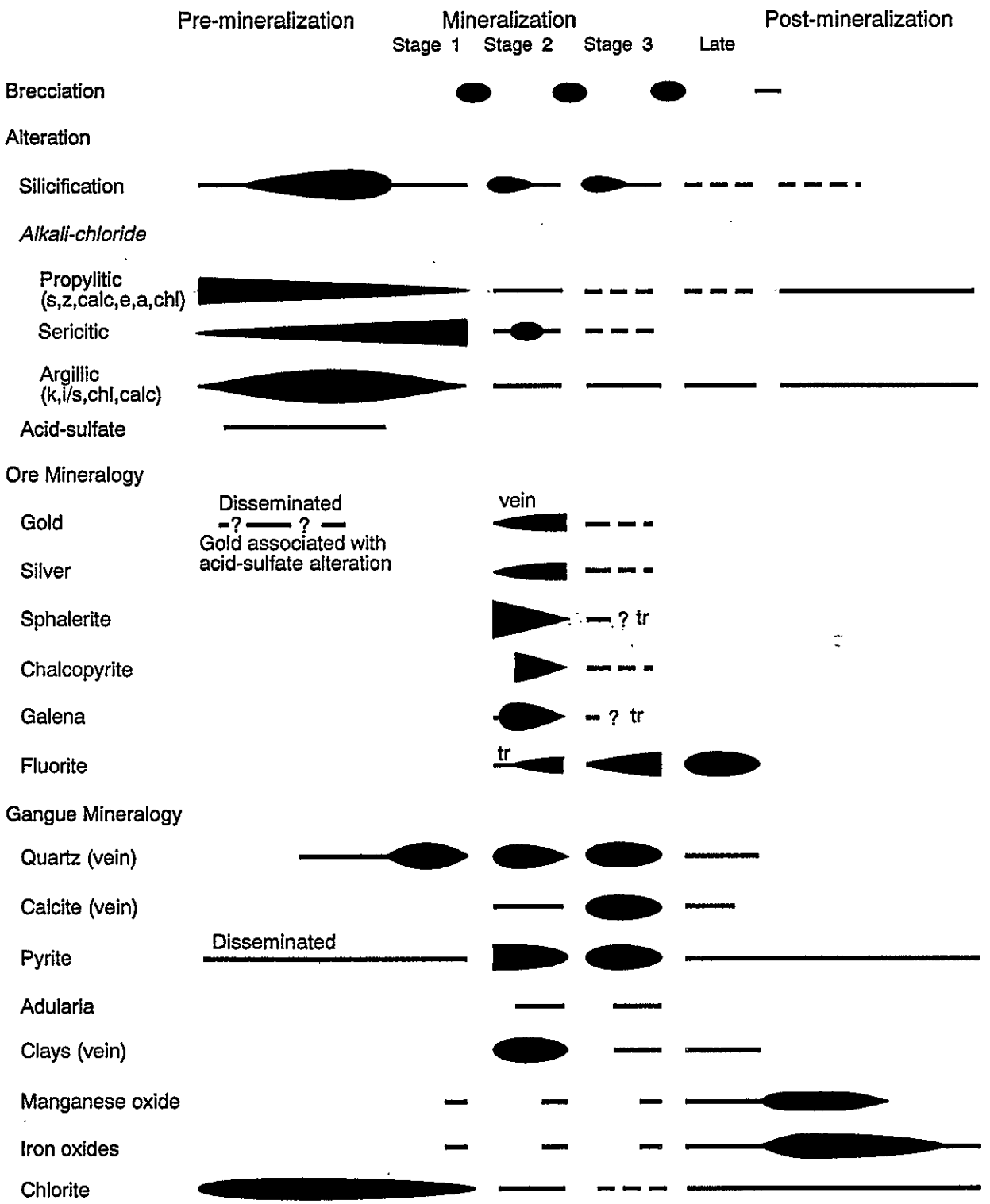

Figure 6.15 Simplified paragenetic sequence of events in the Steeple Rock District, assuming separate episodic events. s-sericite, z-zeolite, calc-calcite, e-epidote, a-adularia, chl-chlorite, i/s-illite/smectite, k-kaolinite

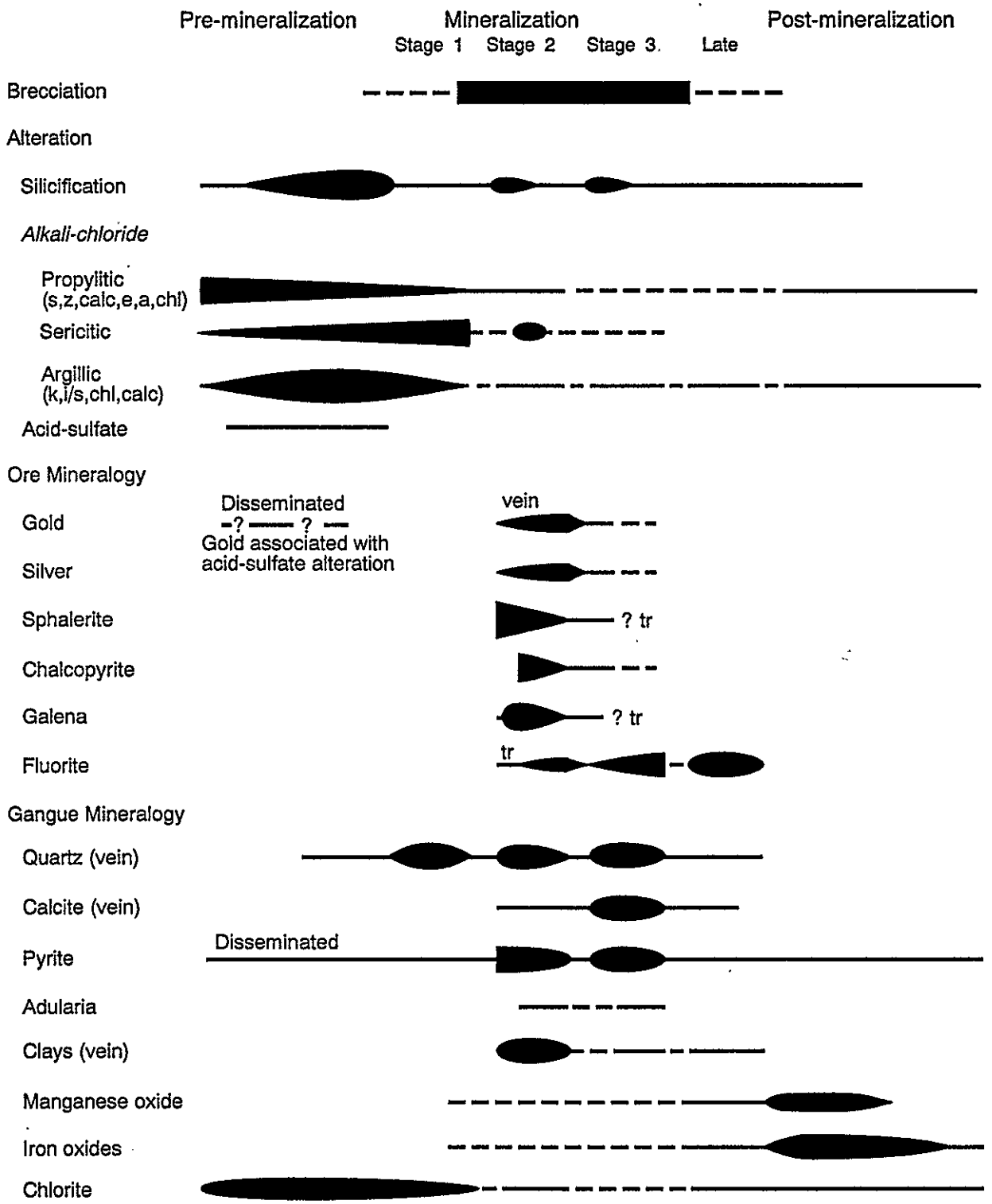

Figure 6.16 Simplified paragenetic sequence of events in the Steeple Rock District, assuming continuous alteration, mineralization and brecciation. s-sericite, z-zeolite, calc-calcite, e-epidote, a-adularia, chl-chlorite, i/s-illite/smectite, k-kaolinite

hypogene origin). The potential for high-sulfidation disseminated gold deposits related to the acid-sulfate alteration is fair to excellent. Faulting and brecciation of this early alteration followed. Fragments of the altered rocks dominated by quartz, chlorite, and pyrite occur in the mineralized veins. Locally along the East Camp-Twin Peaks and Carlisle faults, acid-sulfate altered rocks were offset and placed adjacent to deeper-level alkali-chloride altered rocks (Maps 1, 2). The faults were subsequently filled with younger mineralization.

The mineralization period is divided into four stages, each stage may be separated by a period of brecciation: stage 1, stage 2, stage 3, and late mineralization (Fig. 6.15). However, brecciation could also have been continuous throughout the four mineralization stages (Fig. 6.16). Figure 4.12 illustrates the four stages of mineralization in one boulder. In general, stage 1 is characterized by white to gray to green chalcedonic to microcrystalline, barren quartz and pyrite, which occurs as breccia fragments within Stage 2 veins or occurs as thin bands along the contact with the host rock. Textures suggest that some chalcedony may be recrystallized amorphous silica (section 4.1.2.1). Stage 2 is the main ore-bearing event and consists of banded, rhythmically-layered, and brecciated quartz with gold, silver, and sulfides forming thin black to blue bands (Fig. 3.6) in a gangue of fluorite, calcite, adularia, clays, hematite, chlorite, and silicification. In some areas, stage 2 veins are brecciated and cemented by stage 3 quartz (Fig. 4.12). Stage 2 veins crosscut stage 1 veins. Recrystallized chalcedony or amorphous silica is rare in Stage 2, but occurs as small fragments interstitial to vein quartz. Multiple periods of this rhythmically-banded sulfide-quartz deposition occurred locally; however, detailed paragenesis is complex and only simplified in Figures 6.15 and 6.16. In some veins, sphalerite was deposited first prior to chalcopyrite as evidenced by replacement textures and chalcopyrite disease. Galena and pyrite were deposited after chalcopyrite. However, in other veins all four sulfide minerals coprecipitated (Fig. 4.7). Fluorite, calcite, and additional quartz were deposited during the waning stages of stage 2 mineralization, because these minerals occur in bands within the center of the stage 2 veins. Stage 3 mineralization is characterized by quartz, calcite, pyrite, and local adularia, clays,

chlorite, and iron and manganese oxides, which crosscuts stage 1 and 2 veins. Locally gold and silver mineralization with a trace of base-metal sulfides were also deposited. Temperatures of all stage 2 and 3 veins ranged from 240 to 330°C (Tables 4.1, 4.2, 4.3; Figs. 4.20, 4.21, 4.22). The temperature of stage 1 veins is unknown, but presumed to be <300°C on the basis of mineralogy. Late stage mineralization consisted of lower temperature fluorite (Table 4.3), drusy quartz, calcite, pyrite, clays, chlorite, and iron and manganese oxides in veins crosscutting stage 1, 2 and 3 veins, vugs, fractures, and other open spaces.

The mineralization stages were followed by post-mineralization alteration and oxidation (Figs. 6.15, 6.16). Alkali-chloride alteration with deposition of pyrite occurred. Thin veins of quartz-chlorite, quartz-calcite, and quartz-hematite crosscut mineralizing veins and older altered rock (Fig. 5.2, 5.3). Oxidation of near-surface base-metal veins occurred locally and may have concentrated gold and silver in some places by supergene enrichment processes. Some oxidation is currently active, especially at the Carlisle mine where nantokite and chalcanthite are forming along the adit walls. The pH of water in the Carlisle adit is 2.5–3.5. Iron and manganese oxides are also a result of this final alteration.

6.5 Age of alteration and mineralization

The age and duration of these six stages of alteration and mineralization are uncertain and are based upon a few age determinations (Table 2.1) and field relationships (section 2, Map 1). Alkali-chloride alteration probably began as soon as the permeable flows were emplaced and cooled as convective geothermal systems developed in response to high heat-flow produced by continuing andesite and/or rhyolite volcanism during the Oligocene (section 5.2). Acid-sulfate alteration is closely related to alkali-chloride alteration (section 5.3). One age date of a quartz-alunite sample from Saddleback Mountain (acid-sulfate altered Summit Mountain formation) is reported as 31.3 Ma (Hedlund, 1993) and represents a maximum age of the acid-sulfate alteration and of the upper flows of the Summit Mountain formation. An additional age date of a relatively unaltered andesite from the Summit Mountain formation is

also reported as 31.3 Ma (Hedlund, 1993). However, younger rocks are also altered by acid-sulfate fluids in the Steeple Rock district and these rocks are 27–28 Ma or younger (ash-flow tuffs, sedimentary rocks, and andesites of the Dark Thunder Canyon formation; Table 2.1; Fig. 5.7).

Most modern geothermal systems have durations of activity of less than 3 million years, and most are less than a few hundred thousand years (Table 6.5; P. L. R. Browne, unpubl. report, Spring 1992). However, the activity in the Steeple Rock district spanned at least 3-4 million years. It was unlikely that one single hydrothermal system was active in the district. Multiple hydrothermal systems of unknown duration were probably active intermittently in the Steeple Rock district at least between 31–27 Ma and perhaps even more recently. The distribution (Figs. 5.4, 6.12, 6.13), zonations (section 5), and timing of alteration and vein mineralization (Table 2.1, section 2) are consistent with different periods of hydrothermal activity. The acid-sulfate alteration is clearly offset and cut by younger mineralized faults. These convective systems would develop in permeable rocks in response to continuing periods of volcanism followed by periods of nonvolcanism in the area. Migration of systems throughout time from one area to another probably occurred as well.

The age of epithermal mineralization is also uncertain. Epithermal veins fill faults that cut the Tertiary volcanics in the Steeple Rock district, the youngest of which are lava flows of Crookson Peak dated as 27.6 Ma (Hedlund, 1990c). Wahl (1983) reports that adularia from the East Camp vein has an age date of 18 Ma, but provides no additional data. Adularia from the Mogollon district, northeast of the Steeple Rock district (Fig. 1.1), has an age date of 18 Ma ($^{39}Ar/^{40}Ar$; W. C. McIntosh, pers. comm. December 1992). Since the adularia in both districts may be younger than the metal mineralization, these age dates are probably minimum ages. The adularia occurs late in stage 2 and in stage 3 mineralization in the Steeple Rock district. In Mogollon, the adularia occurs as late crystals on the quartz breccia (personal observation). It is also interesting to note that the second stage of supergene enrichment at the Tyrone porphyry copper deposit occurred at 19.5 Ma (Cook, 1993) and a similar age is

Table 6.5—Summary of duration of activity of modern geothermal systems (modified from P. L. R. Browne, written communication, Spring 1992).

Geothermal field	Age (years)	Remarks	Reference
Kawerau, NZ	>200,000	surface activity	Browne (1978)
Waimangu, NZ	97	likely in error	---
Broadlands, NZ	370,000	---	Grindley (1965)
Orakeikorabo, NZ	>20,000	one of the oldest systems in New Zealand	---
Wairakei, NZ	10,000	residence time of deep water (radiocarbon dating)	Elder (1981)
Taupo, NZ	>500,000	---	Elder (1981)
Nesjavellir, Iceland	2,000	---	Kristmannsdotter and Tomasson (1974)
Valles, NM	1.2 million	multiple periods of activity	White (1979); Woldegabriel (1990)
Long Valley, CA	300,000	intermittent	White (1979)
Steamboat Springs, NV	3 million	intermittent	White (1979)
Yellowstone, WY	400,000–600,000	multiple systems	White (1979); White et al. (1988)
The Geysers, CA	>57,000	stored heat calculation	White (1979)
Sulfur Bank, CA	27,000	---	White (1979)
Larderello, Italy	3 million	Rb/Sr and K/Ar age dates	Del Moro et al. (1982); Minissale (1991)

reported for the second stage of supergene enrichment at the Morenci copper porphyry deposit (S. S. Cook, pers. comm. February 1993).

In the Steeple Rock district, epithermal veins in some areas are spatially related to rhyolite dikes. Some rhyolite dikes in places offset some epithermal veins (Maps 1, 2). Wahl (1983) reports an age of a rhyolite dike as 18 Ma, but provides no additional data. Hedlund (1990a) reports an age of 21.4 Ma (fission track on zircon) from the quartz monzonite which intrudes the rhyolite of Steeple Rock (Table 2.1). A vitrophyre from a rhyolite dome west of Saddleback Mountain has an $^{39}Ar/^{40}Ar$ age of 25.3 Ma (Table 2.1; W. C. McIntosh and R. Appelt, pers. commun. Aug. 1993). Other ages of rhyolite intrusives in the Mule Creek-Summit Mountains area range from 28.7 to 17.7 Ma (Table 2.1). Therefore, epithermal veins in the Steeple Rock district are probably between 27 and 18 Ma and may be closer to 20 to 18 Ma in age.

6.6 Tectonic Setting

Many epithermal districts in southwestern New Mexico and the United States occur along ring-fracture zones of mid-Tertiary calderas (Fig. 1.1; Buchanan, 1981; Rytuba, 1981). However, there is no evidence to support a caldera in the vicinity of the Steeple Rock district, contrary to earlier interpretations (Biggerstaff, 1974; Elston, 1978). However, the Steeple Rock district lies in a tectonically active area that was dominated by a succession of dynamic and sometimes rapidly changing plate tectonic settings since Precambrian times, and especially since the Laramide period of compressional tectonics. Each tectonic period had lasting effects (section 2.3.1), but the most important events affecting the area are the more recent.

The Steeple Rock district lies on the southern edge of the Mogollon-Datil volcanic field (late Eocene-Oligocene), on the northern edge of the Burro uplift (Laramide), and near the intersection of the west-northwest-trending Texas and northeast-trending Morenci lineaments. Although only Oligocene-Miocene rocks are exposed in the Steeple Rock district, the regional faults have a trend similar to Laramide structural features and the Texas and

Morenci lineaments. These major regional structural features probably reactivated throughout geologic time and in the Steeple Rock area may have acted as conduits and controlled emplacement of magma and subsequent hydrothermal activity.

The Burro uplift probably defines the northern edge of the Texas lineament in western New Mexico which remained a highland throughout most of geologic time. Paleogeographic and isopach maps suggest it was a highland from the Cambrian to the Cretaceous (Ross and Ross, 1986). Cretaceous marine sedimentary rocks onlap Proterozoic granitic rocks at Riley Peaks, south of Steeple Rock as well as in the northern Burro Mountains (Drewes et al., 1985). The Cretaceous rocks at Riley Peaks are relatively thin (<300 m; Hedlund, 1980b), suggesting that much of the Burro uplift was a highland prior to Laramide time (Drewes, 1991). However, a thicker section of Cretaceous rocks could have been deposited on the Burro uplift and subsequently been uplifted and eroded during the Eocene. The Virden Formation (Eocene; Elston, 1960; Hedlund, 1990b) consists of fluvial sediments that contain large boulders of Proterozoic granite, presumably eroded from the Burro uplift. The northern Burro uplift is probably part of the Morenci uplift of Cather and Johnson (1986) during the Eocene and may have been a source of sediment to the Eocene Baca Basin.

As Laramide compressional tectonics ceased, mid-Tertiary extensional tectonics began. In the Datil-Quemado area, this transition occurred at about 36 Ma. In the Steeple Rock area, this shift in tectonic styles is marked by eruption of bimodal volcanism at about 34 Ma with the emplacement of the andesite of Mud Springs, andesite of Mt. Royal, and rhyolite of Steeple Rock. From about 34 Ma to 27 Ma, as much as 2440 m or more of bimodal volcanic rocks were deposited in the Steeple Rock district on the northern Burro uplift, followed by intrusion of rhyolite dikes, and domes, and plugs from 28 to 17 Ma (section 2). It is speculated that this extensive pile of volcanics may have resulted in subsidence of the northern Burro uplift and was uplifted during late Tertiary as part of Basin and Range faulting.

The Texas and Morenci lineaments are defined by primarily structural features,

although Laramide copper porphyries also occur along the Morenci lineament. Epithermal deposits tend to form on the flanks of these lineaments (Fig. 1.1, 2.2). The lineaments are reactivated, deep crustal flaws that locally control emplacement of magma and subsequently hydrothermal fluids. These hydrothermal fluids migrate onto edges of highlands such as the Burro uplift and ultimately form epithermal deposits, for example, in the Steeple Rock district. Even today many hot springs in southwestern New Mexico occur over Laramide uplifts and along regional structures (Witcher, 1988), suggesting that Laramide structures have controlled regional heat-flow ever since.

6.7 Geologic History

The Steeple Rock district occurs in a tectonically complex area. Regional lineaments and faults localized and controlled magmatic activity and subsequent hydrothermal fluids. Andesites, basaltic andesites, ash-flow tuffs, rhyolite intrusives and volcaniclastic rocks were deposited during a series of cyclic volcanic events from approximately 34 Ma to at least as young as 17 Ma (event 1, Fig. 6.17; Table 2.1). Minor rhyolite intrusion and extensive faulting may have occurred as early as 28 Ma, if not before (event 2, Table 2.1).

An older hydrothermal system developed in response to high heat flow produced by regional and local volcanism at approximately 31 Ma and younger (event 3, Fig. 6.17). More than one system probably developed in different localities and at different times; some systems may have migrated from one locality to another. This is supported by the complex and overlapping vents found in some of the altered areas (section 5). Regional alkali-chloride alteration affected most of the district during these events. Locally, acid-sulfate alteration, possibly associated with disseminated gold deposits (high sulfidation) yet to be discovered, occurred at or near the surface and was probably accompanied by hot springs and geysers. The abundant hydrothermal brecciation and presence of fossil fumaroles in the altered areas is supportive of this surface activity. Similar environments occur in modern geothermal systems, for example Norris Geyser Basin at Yellowstone National Park (White et al., 1988), Bacon-

1.) Deposition (33-27 Ma)

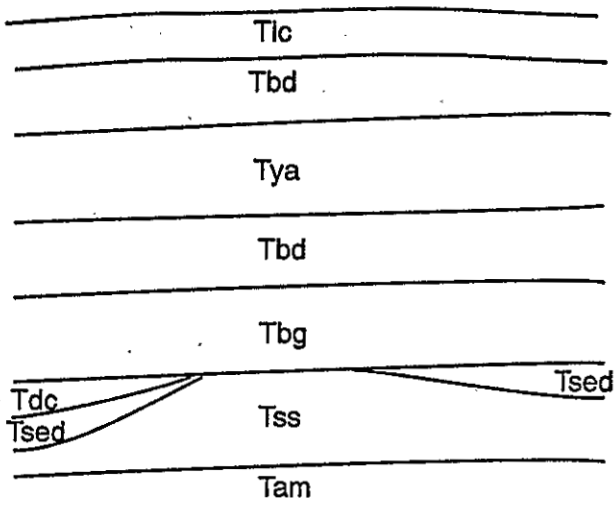

2.) Minor faulting and possible intrusion of rhyolites.

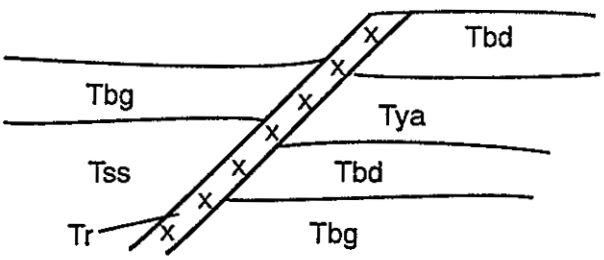

3.) Regional alteration (~ 31 Ma and younger).

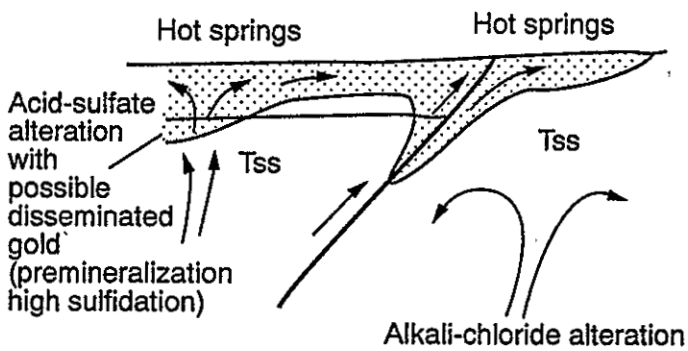

4.) Burial (?), faulting and intrusion of rhyolites.

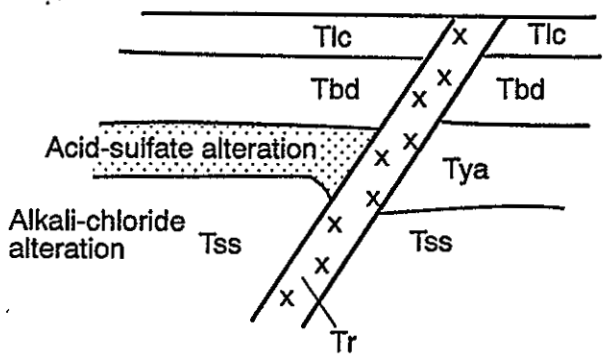

5.) Epithermal veins (mineralization stage-low sulfidation).

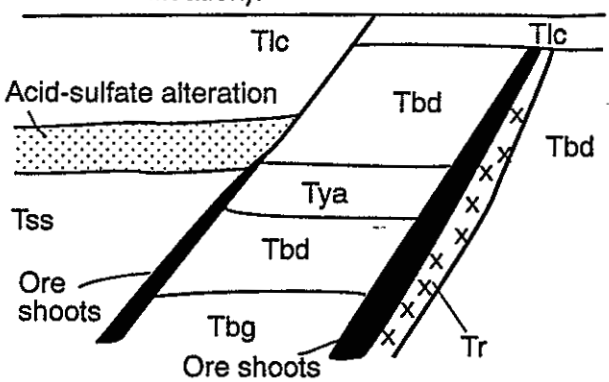

6.) Regional alkali-chloride alteration, erosion, and possible uplift.

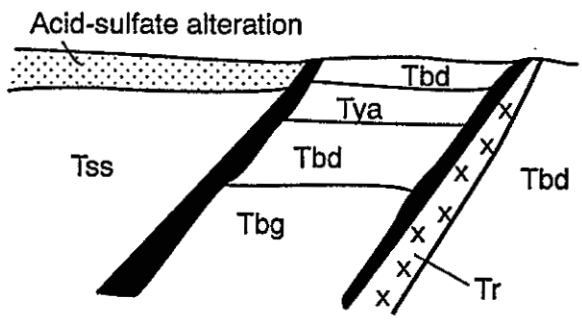

Figure 6.17 Sequence of events in the Steeple Rock district

Manito in the Philippines (Reyes, 1990), and Wasotapa in New Zealand (Simmons et al., 1992).

Faulting occurred after this alteration event because some areas of acid-sulfate alteration have been offset (event 4, Fig. 6.17; Maps 1, 2). A second hydrothermal system developed, probably in response to continued rhyolite intrusive activity. Low-sulfidation epithermal vein deposits (mineralization stage, Figs. 6.15, 6.16) formed along these faults and are associated with syn-mineralization alkali-chloride alteration (event 5; Fig. 6.17). Some ore shoots are capped by older acid-sulfate alteration, whereas other ore shoots cut acid-sulfate alteration (Figs. 6.12, 6.13). Some ore shoots are spatially associated with rhyolite intrusives (Map 2). Other geologic data (fluid inclusion analyses, section 4.2; mineralogy, section 4.1; and geochemistry, section 4.3) suggest that epithermal veins formed by chemically complex and diverse fluids (see section 6.2). The deposits were formed from low salinity, acidic to slightly acidic to neutral pH fluids at temperatures between 240° and 320°C at relatively shallow depths (360–1300 m). Ore minerals precipitated as a result of cyclic periods of boiling, cooling, and mixing. Four stages of mineralization occurred: brecciation accompanied mineralization (Figs. 6.15, 6.16). Regional faulting occurred during and after epithermal mineralization.

A third hydrothermal system developed and produced regional alkali-chloride alteration which overprinted older alteration and mineralization (event 6, Fig. 6.17). Erosion and possible uplift followed. Oxidation, supergene alteration, and weathering of some deposits occurred, however, most deposits were not affected by oxidation and supergene alteration as evidenced by the mineralogy and chemistry of the deposits (section 3).

6.8 Relationship of the Steeple Rock district to other epithermal deposits and modern geothermal systems

This study illustrates numerous similarities between the Steeple Rock district and other epithermal vein deposits and modern geothermal systems. Several compilations with

brief descriptions of epithermal deposits have been previously published and the reader is referred to them for details (Moiser et al., 1986, North and McLemore, 1986, 1988; Buchanan, 1981; Hayba, 1983; Heald et al., 1987; Hayba et al., 1985; White and Hedenquist, 1990; Rye et al., 1992). Numerous modern geothermal systems have likewise been examined and descriptions have been published (Mitchell and Leach, 1991; Browne, 1978; White, 1981; Elder, 1981). There are three common factors controlling the occurrence of geothermal systems: (1) most occur in areas containing deep-seated intrusives that provide heat for convective hydrothermal systems consisting of meteoric, magmatic, and locally formation waters; (2) all are formed at shallow crustal depths in permeable rocks; and (3) all are located along major regional structures, including crustal lineaments and calderas.

However, there are some differences between the Steeple Rock district and other epithermal deposits and modern geothermal systems. Many older epithermal mineral deposits are common in modern geothermal systems; for example, McLaughlin at Geysers-Clear Lake geothermal system (Donnelly-Nolan et al., 1993); Mesquite at the Salton Sea trough system (McKibben, 1991); and numerous gold districts in the Philippines geothermal systems (Mitchell and Leach, 1991). However, the Steeple Rock district is one example of the early development of a geothermal system with both alkali-chloride and acid waters that cooled and were followed by younger epithermal mineralization and even later regional alkali-chloride alteration. Consequently, other epithermal districts and areas of acid-sulfate alteration need to be thoroughly examined to determine the relationship between alteration and mineralization in time and space and to determine if more than one hydrothermal event occurred.

7. CONCLUSIONS

Integration of Steeple Rock and other data and the resulting interpretations indicate that the alteration and mineralization of the Steeple Rock district are a result of successive, multiple cycles of volcanic and geothermal activity which occurred sporadically from 34 to 17 Ma (section 2). These systems had variable hydrologic and geochemical constraints which gave rise to complex, superimposed alteration and mineralization assemblages seen in the district (sections 3, 4, 5). Exact timing and duration of these events is partly speculative and based upon published age determinations (Table 2.1) and field relationships. There is no supporting evidence that these events were continuous; instead the alteration and mineralization were probably episodic, waning, and migrating from one locality to another. While many older epithermal deposits occur in areas of modern geothermal systems (section 6.8), the Steeple Rock district is one example of the early development of a geothermal system followed by younger epithermal mineralization.

Available data suggest that the acid-sulfate alteration in the Steeple Rock district was produced in a magmatic-hydrothermal environment (section 6.1). Sulfur isotope data, including geothermometric calculations, strongly support a magmatic-hydrothermal origin. Furthermore, the mineral assemblages, chemical changes, zonation, intense silicification, hydrothermal brecciation and hydrofracturing, and the presence of fossil fumaroles are consistent with a magmatic-hydrothermal origin (section 5). Alkali-chloride alteration is more pervasive in the district than acid-sulfate alteration and surrounds and underlies the acid-sulfate alteration (section 5). This relationship is also consistent with a magmatic-hydrothermal environment for both types of alteration.

Available data also suggest that the low-sulfidation mineralization in the Steeple Rock district was deposited by low salinity (<5 eq. wt. % NaCl), neutral to slightly acidic fluids at temperatures between 240° and 320°C and relatively shallow depths (360–1300 m) and at low pressures (<500 bars; section 6.2). Locally, arsenic, antimony and mercury values occur at elevated levels within the mineralization and alteration (Appendix 11.6, section 4.3). A

combination of alternating cycles of boiling, mixing, and cooling hydrothermal fluids was involved in forming these deposits. The veins were emplaced along pre-existing faults and are younger than the alkali-chloride and acid-sulfate alteration. Faulting probably occurred throughout the mineralization epoch as evidenced by multiple brecciation in the veins.

Some general guides to ore mineralization can be summarized from sections 3 and 4. Known epithermal mineralization occurs along prominent silicified and brecciated faults. Precious and base metals occur in banded and rhythmically layered and brecciated quartz within aggregates or thin black bands or streaks of sulfides. The best ore shoots occur at inflections of strike and dip of the fault, especially at the intersection of cross faults. Ore occurs below and within zones of boiling as evidenced by bladed calcite and bladed quartz pseudomorphed after calcite. Predominant gangue mineralogy consists of chlorite, pyrite, illite, amethyst, and coatings of mottramite and/or mimetite are common if the ore is oxidized. Mineralized veins consist of high gold and silver values as well as elevated lead and zinc, and to a lesser extent, copper (sections 3, 4.3). Elevated arsenic concentrations commonly occur in the country rock above some ore zones (section 4.3).

Regional structures probably controlled magmatic and volcanic activity (which resulted in areas of high flow) and subsequent convective migration of hydrothermal fluids (section 2, section 6.6). The district lies on the southern edge of the Mogollon-Datil volcanic field (late Eocene-Oligocene), on the northern edge of the Burro uplift, and near the intersection of the west-northwest-trending Texas and northeast-trending Morenci lineaments (Fig. 2.2). Furthermore, the Santa Rita lineament (New Mexico mineral belt) occurs to the southeast. Faulting in the Oligocene-Miocene volcanic rocks in the district parallels these regional features as well as older Laramide structures as a result of compressional tectonics. This suggests that the Mid-Tertiary extensional tectonic features may be along reactivated Laramide features, at least in part. These regional features represent deep crustal flaws and acted as conduits for and controlled magma migration, heat flow, and subsequent hydrothermal fluids.

This study also resulted in a few additional observations concerning alteration and stratigraphy. Major and trace element analyses must be used with care in volcanic terranes in characterizing the igneous rocks because silica was introduced early in the alteration process (section 2.4). Some rocks called dacites, because of tiny but visible quartz, are actually andesite with secondary quartz filling small amygoidals and other open spaces.

At least four ash-flow tuffs are exposed in the district (section 2.2). Two of the tuffs were derived from the Bursum caldera in the Mogollon Mountains. The younger ash-flow tuffs are perhaps from younger, less known calderas to the west and south. Some of the ash-flow tuffs also may be from local rhyolite doming (Fig. 2.5). Understanding the origin and distribution of these tuffs will aid our understanding of extent of regional ash-flow tuffs from distal calderas.

The economic potential of the Steeple Rock district for discovery of base- and precious-metals veins is excellent (section 4.4). Current exploration and past production (section 3) suggest that most orebodies are several thousands to several tens of thousands of tons in size, but it is possible to discover larger orebodies. Numerous mineralized faults have not been adequately explored at depth. Faults in the Alabama Ridge–Jim Crow mine area contain detectable gold and silver values and represent one area of future exploration. Geophysical surveys, geochemical sampling programs, and extensive drilling programs are required to identify and delineate additional areas of mineralization. Locally, elevated arsenic concentrations form a halo above mineralized veins which may serve as an exploration guide. In addition, the district has some potential for development of high-sulfidation disseminated gold deposits associated with the acid-sulfate alteration. Alunite deposits, specialty clay deposits, decorative stone, and perhaps fluorite also may have some economic potential.

8. FUTURE RESEARCH

Recommendations for future studies are summarized below.

(1) Geochronologic studies of vein deposits and alteration in the Steeple Rock area are needed to confirm age relationships described in this study (sections 4, 5). These studies will aid in better understanding of the time involved in epithermal systems and the formation of gold-silver epithermal deposits.

(2) Stable isotope studies of acid-sulfate altered rocks and vein deposits are necessary to confirm an input from magmatic-hydrothermal sources, define patterns of fluid flow, and provide additional data on temperatures of formation (section 6.1). Analyses of alunite are especially important because alunite can provide age constraints, information on sources, and constraints in temperatures of formation.

(3) Paleomagnetic, geochronologic, and geochemical analyses of rhyolite domes, plugs and dikes should be done to determine information on age, source, and possible relationship to epithermal vein mineralization (section 2.2).

(4) Paleomagnetic analyses of altered rocks, especially acid-sulfate altered rocks are needed to determine original lithology and age constraints. Also these studies could be used to determine the effects of alteration on paleomagnetic data.

(5) More detailed mineralogic analyses, on the gold-silver veins are needed to aid in recovery of the precious metals and to aid in grade control (section 4.1). What are the silver minerals and where is the gold and silver in the veins? This information may also refine the genesis of these deposits.

(6) Detailed geologic mapping and geochemical analyses of future mines should be done to provide better guidelines on ore controls and further our understanding of the chemistry and origin of these deposits (section 3).

(7) Experimental work on chalcopyrite disease in sphalerite needs to be performed. What is the origin of chalcopyrite disease in epithermal environments? Are the minerals coprecipitated or does chalcopyrite replace sphalerite? Does chalcopyrite disease affect

microthermometric measurements of fluid inclusions?

(8) Detailed mapping, petrologic, and geochemical studies of the older volcanic rocks of Steeple Rock and Mt. Royal are necessary in order to understand in more detail the emplacement of these rocks, including the Steeple Rock dome (section 2).

(9) Experimental studies involving chlorite, quartz, and calcite/dolomite are required at different pHs and temperatures to produce needed phase diagrams in order to begin to understand the significance of chlorite deposition in the epithermal environment.

9. REFERENCES

Abbey, S., 1979, Reference mateials–rock samples S4-2, S4-3, MRG-1: Canmet Report 79-35, 66 p.

Albino, G. V. and Margolis, J., 1991, Differing styles of adularia-sericite epithermal deposits—contrasts in geologic setting and mineralogy (abstr.): Geological Society of America, Abstracts with Programs, p. A464.

Alpers, C. N. and Brimhall, G. H., 1988, Middle Miocene climatic change in the Atacama Desert, northern Chile: Evidence from supergene mineralization at La Escondida: Geological Society of America Bulletin, v. 100, p. 1640-1656.

Alpers, C. N., Rye, R. O., Nordstrom, D. K., White, L. D., and King, B. S., 1992, Chemical, crystallographic and stable isotope properties of alunite and jarosite from acid-hypersaline Australian lakes: Chemical Geology, v. 96, p. 203-226.

Altaner, S. P., Fitzpatrick, J. J., Krohn, M. D., Bethke, P. M., Hayba, D. O., Goss, J. A., and Brown, Z. A., 1988, Ammonium in alunites: American Mineralogist, v. 73, p. 145–152.

American Public Health Association, 1992, Standard methods: 18th ed., U.S. American Public Health Association.

Anderson, E. C., 1957, The metal resources of New Mexico and their economic features through 1954: New Mexico Bureau of Mines and Mineral Resources, Bulletin 39, 183 p.

Anthony, J. W., Bideaux, R. A., Bladh, K. W., and Nichols, M. C., 1990, Handbook of Mineralogy, volume 1: Elements, sulfides, sulfosalts: Mineral Data Publishing, Tucson, Arizona, 588 p.

Appelt, R. M., 1993, Paleomagnetic correlation of ignimbrites in the Steeple Rock mining district, southwestern New Mexico (abst.): Geological Society of America, Abstracts with Programs, v. 25, no. 5, p. 4.

Arehart, G. B., Kesler, S. E., O'Neil, J. R., and Foland, K. A., 1992, Evidence for the

supergene origin of alunite in sediment-hosted micron gold deposits, Nevada: Economic Geology, v. 87, p. 263-270.

Arnorsson, S., Gunnlaugsson, E., and Suavarsson, H., 1983, The chemistry of geothermal waters in Iceland. II. Mineral equilibria and independent variables controlling water compositions: Geochimica et Cosmochimica Acta, v. 47, p. 547–566.

Bagby, W. C. and Berger, B. R., 1985, Geologic characteristics of sediment-hosted, disseminated precious-metal deposits in the western United States; *in* Berger, B. R. and Bethke, P. M., eds., Geology and geochemistry of epithermal systems: Reviews in Economic Geology, v. 2, p. 169-202.

Barton, P. B., Jr., 1984, Redox reactions in hydrothermal fluids; *in* Henley, R. W., Truesdell, A. H., and Barton, P. B. Jr., Fluid-mineral equilibrium in hydrothermal systems: Economic Geology, Reviews in Economic Geology, v. 1, p. 99–114.

Barton, P. B., and Bethke, P. M., 1987, Chalcopyrite disease in sphalerite: palthology and epidemiology: American Mineralogist, v. 72, p. 451-467.

Bates, R. L. and Jackson, J. A., eds., 1980, Glossary of geology: American Geological Institute, Virginia, 751 p.

Beane, R., 1991, Oxidation of a gold-bearing quartz-sericite-pyrite solution: Calculations and an example from the El Indio district, Chile (abstr.): Geological Society of America, Abstracts with Programs, p. A464.

Beaufort, D., Patrier, P., Meunier, A., and Ottariani, M. M., 1992, Chemical variations in assemblages including epidote and/or chlorite in the fossil hydrothermal system of Saint Martin (Lesser Antilles): Journal of Volcanology and Geothermal Research, v. 51, p. 95–114.

Berger, B. R. and Henley, R. W., 1989, Advances in the understanding of epithermal gold-silver deposits, with special reference to the western United States; *in* Eays, R. R., Ramsay, W. R. H., and Groves, D. I., eds. The geology of gold deposits: The perspective in 1988: Economic Geology, Monograph 6, p. 405-423.

Biggerstaff, B. P., 1974, Geology and ore deposits of the Twin Peaks area, Grant County, New Mexico: unpublished M.S. thesis, University of Texas at El Paso, 102 p.

Bingler, E. C., Trexler, D. T., Kemp, N. R., and Bonham, H. F., Jr., 1976, PETCAL: A BASIC language computer program for petrologic calculations: Nevada Bureau of Mines and Geology, Report 28, 27 p.

Bird, M. I., Andrew, A. S., Chivas, A. R., and Lock, D. E., 1989, An isotopic study of surficial alunite in Australia: 1. Hydrogen and sulfur isotopes: Geochimica et Cosmochimica Acta, v. 53, p. 3223-3237.

Bodner, R. J., Reynolds, T. J., and Kuehn, C. A., 1985, Fluid inclusion systematics in epithermal systems; *in* Berger, B. R. and Bethke, P. M., eds., Geology and geochemistry of epithermal systems: Reviews in Economic Geology, v. 2, p. 73-98.

Borland International Inc., 1991, Quattro Pro 3.0: Borland International Inc., Scotts Valley, California, 807 p.

Bornhorst, T. J., 1980, Major- and trace-element geochemistry and mineralogy of upper Eocene to Quaternary volcanic rocks of the Mogollon-Datil volcanic field, southwestern New Mexico [Ph.D. dissertation]: Albuquerque, University of New Mexico, 1108 p.

Bornhorst, T. J., 1986, Granophile elements in mid-Cenozoic calc-alkalic rhyolitic volcanic rocks, Mogollon–Datil volcanic field, southwestern New Mexico; *in* Taylor, R. P. and Strong, D. F., eds., Recent advances in the geology of granite-related mineral deposits: The Canadian Institute of Mining and Metallurgy, Special Volume 39, p. 331–341.

Bornhorst, T. J., 1988, Character of mid-Cenozoic andesites, basaltic andesites and related volcanic rocks, Mogollon-Datil volcanic field, southwestern New Mexico; *in* Drexler, J. W., and Larson, E. E., Cenozoic volcanism in the Southern Rocky Mountains updated: A tribute to Rudy C. Epis—Part 2: Colorado School of Mines Quarterly, v. 83, p. 1–13.

Bortnikov, N. S., Genkin, A. D., Dobrovolskaya, M. G., Muravitskaya, G. N., and Filimmora, A. A., 1991, The nature of chalcopyrite inclusions in sphalerite: exsolution, coprecipitation, or "disease?": Economic Geology, v. 86, p. 1070-1082.

Bove, D. J., Rye, R. O., and Hon, K., 1990, Evolution of the Red Mountain alunite deposit, Lake City, Colorado: U.S. Geological Survey, Open-file Report OF-90-235, 30 p.

Briggs, J. P., 1981, Mines and prospects map of the Hells Hole further planning area (RARE II), Greenlee County, Arizona, and Grant County, New Mexico: U.S. Geological Survey, Miscellaneous Field Studies Map MF-1344-C, scale 1:62,500.

Briggs, J. P., 1982, Mineral investigation of the Hells Hole Roadless area, Greenlee County, Arizona and Grant County, New Mexico: U.S. Bureau of Mines, Open-file Report MLA 137-82, 22 pp.

Brooks, W. E. and Ratté, J. C., 1985, Geologic map of the Bear Mountain quadrangle, Grant County, New Mexico: U.S. Geological Survey, Miscellaneous Field Studies Map MF-1782, scale 1:24,000.

Brophy, G. P., Scott, E. S., and Snellgrove, R. A., 1962, Sulfate studies II. Solid solution between alunite and jarosite: American Mineralogist, v. 47, p. 112-126.

Browne, P. R. L., 1978, Hydrothermal alteration in active geothermal fields: Annual Reviews of Earth and Planetary Science, v. 6, p. 229–250.

Browne, P. R. L. and Ellis, A. J., 1970, the Ohaki-Broadlands hydrothermal area, New Zealand: Mineralogy and related geochemistry: American Journal of Science, v. 269, p. 97–131.

Buchanan, L. J., 1981, Precious metal deposits associated with volcanic environments in the southwest; *in* Dickinson, W. R. and Payne, W. D., Relations of tectonics to ore deposits in the southern Cordillera: Arizona Geological Society Digest, v. 14, p. 237-262.

Burt, D. M., and Sheridan, M. F., 1987, Types of mineralization related to fluorine-rich silicic lava flows and domes; *in* Fink, J. H., ed., The emplacement of silicic domes

and lava flows: Geological Society of America, Special paper 212, p. 103–110.

Cather, S. M., 1990, Stress and volcanism in the northern Mogollon-Datil volcanic field, New Mexico: Effects of the post-Laramide tectonic transition: Geological Society of America Bulletin, v. 102, p. 1447–1458.

Cather, S. M. and Johnson, B. D., 1986, Eocene depositional systems and tectonic framework of west-central New Mexico and eastern Arizona: *in* Peterson, J. A., ed., Paleotectonics and sedimentation in the Rocky Mountain Regional, United States: American Association of Petroleum Geologists, Memoir 41, p. 623-652.

Cather, S. M., McIntosh, W. C., and Chapin, C. E., 1987, Stratigraphy, age, and rates of deposition of the Datil Group (Upper Eocene-Lower Oligocene), west-central New Mexico: New Mexico Geology, v. 9, p. 50-54.

Chapin, C. E., Chamberlin, R. M., and Hawley, J. W., 1978, Socorro to Rio Salado; *in* Hawley, J. W., ed., Guidebook to the Rio Grande rift in New Mexico and Colorado: New Mexico Bureau of Mines and Mineral Resources, Circular 163, p. 121-137.

Coney, P. J., 1978, The plate tectonic setting of southeastern Arizona: New Mexico Geological Society, Guidebook 29, p. 285-290.

Coney, P. J., and Reynolds, S. J., 1977, Cordilleran Benioff zones: Nature, v. 270, p. 403-406.

Cook, S. S., 1993, Supergene copper mineralization at the Tyrone mine, Grant County, New Mexico (abstr.): Society for Mining, Metallurgy and Exploration, Inc., 1993 Annual Meeting and Exhibit, Program with Abstracts, p. 139.

Cortecci, G., Lombardi, G., Reyes, E., and Turi, B., 1981, A sulfur isotopic study of alunites from Latium and Tuscany, central Italy: Mineralium Deposita, v. 16, p. 147-156.

Cox, D. P., and Singer, D. A., editors, 1986, Mineral deposit models: U.S. Geological Survey, Bulletin 1693, 379 p.

Craig, J. R., and Vaughan, D. J., 1981, Ore microscopy and ore petrography: John Wiley

and Sons, Inc., New York, New York, 406 p.

Criss, J., 1980, Fundamental-parameters calculations in a laboratory microcomputer: Advances in X-ray Analysis, v. 23, p. 93-97.

Cunningham, C. G., 1985, Characteristics of boiling-water-table and carbon dioxide models for epithermal gold deposition; *in* Tooker, E. W., ed., Geologic characteristics of sediment- and volcanic-hosted disseminated gold deposits— search for an occurrence model: U.S. Geological Survey, Bulletin 1646, p. 43–46.

Cunningham, C. G., Rye, R. O., Steven, T. A., and Mehnert, 1984, Origins and exploration significance of replacement and vein-type alunite deposits in the Marysvale volcanic field, west-central Utah: Economic Geology, v. 79, p. 50-71.

Davies, J. F., 1989, Some temporal-spatial aspects of North American porphyry deposits: Economic Geology, v. 84, p. 2300-2306.

De Cserna, Z., 1989, An outline of the geology of Mexico; *in* Bally, A. W., and Palmer, A. R., eds., The geology of North America—An overview: Geological Society of America, DNAG, v. A., p. 233-264.

Deer, W. A., Howie, R. A., and Zussman, J., 1975, Rock-forming minerals, v. 5, Non-silicates: Longman Group, Ltd., London, 371 p.

De La Roche, H., Leterrier, J., Grandclaude, P., and Marchal, M., 1980, A classification of volcanic and plutonic rocks using R_1R_2-diagram and major-element analyses—its relationships with current nomenclature: Chemical Geology, v. 29, p. 183–210.

Del Moro, A., Puxeddu, M., Radicatidi Brozolo, F., and Villa, J. M., 1982, Rb-Sr and K-Ar ages on minerals at temperatures of 300°C–400°C from deep wells in the Larderello geothermal field (Italy): Contributions to Mineralogy and Petrology, v. 81, p. 340–349.

Deng, Q., 1991, Geology and trace element geochemistry of the Hollister gold deposit, Ivanhoe district, Elko County, Nevada: Ph.D. dissertation, University of Texas at El Paso, 288 p.

DeRonde, C. E. J. and Blattner, P., 1988, Hydrothermal alteration, stable isotopes and fluid inclusions of the Golden Cross epithermal gold-silver deposit, Waihi, New Zealand: Economic Geology, v. 83, p. 896-917.

Dickinson, W. R., 1981, Plate tectonic evolution of the southern Cordillera; *in* Dickinson, W. R., and Payne, W. D., eds., Relations of tectonics to ore deposits in the southern Cordillera: Arizona Geological Society Digest, v. 14, p. 113-136.

Donnelly-Nolan, J. M., Burns, M. G., Goff, F. E., Peters, E. K., and Thompson, J. M. , 1993, The Geysers-Clear Lake area, California: Thermal waters, mineralizatin, volcanism, and geothermal potential: Economic Geology, v. 88, p. 301–316.

Dowling, K., and Morrison, E., 1989, Application of quartz textures to the classification of gold deposits using North Queensland examples; *in* The geology of gold deposits: The perspective in 1988: Economic Geology Monograph 6, p. 342-355.

Drewes, H., 1991, Description and development of the Cordilleran orogenic belt in the southwestern United States and northern Mexico: U.S. Geological Survey, Professional Paper 1512, 92 p.

Drewes, H., Houser, B. B., Hedlund, D. C. Richter, D. H., Thorman, C. H., and Finnell, T. L., 1985, Geologic map of the Silver City 1 degree x 2 degree quadrangle, New Mexico and Arizona: U.S. Geological Survey, Map I-1310C, scale 1:250,000.

Duval, J. S., 1988, Aerial gamma-ray contour maps of regional surface concentrations of uranium, potassium, and thorium: U.S. Geological Survey, Geophysical Investigations GP-979, scale 1:750,000.

Eimon, P. I. and Bazrafshan, K., 1989, Hydrothermal modeling, Steeple Rock district, New Mexico (abstr.): New Mexico Geology, v. 11, p. 43.

Elder, J., 1981, Geothermal systems: Academic Press, Inc., New York, New York, 508 p.

Elders, N. A., Jr., Hoagland, J. R., and Williams, A. E., 1981, Distribution of hydrothermal mineral zones in the Cerro Prieto geothermal field of Baja California, Mexico: Geothermics, v. 10, p. 245–253.

Eldridge, C. S., Bourcier, W. L., Ohmoto, H., and Barnes, H. L., 1988, Hydrothermal inoculation and incubation of the chalcopyrite disease in sphalerite: Economic Geology, v. 83, p. 978-989.

Ellis, A. J., 1959, The solubility of calcite in carbon dioxide solutions: American Journal of Science, v. 257, p. 354–365.

Elston, W. E., 1956, Reconnaissance geology of the Virden quadrangle, Grant and Hidalgo Counties, New Mexico (abstr.): Geological Society of America, v. 67, p. 1691-1692.

Elston, W. E., 1960, Reconnaissance geologic map of the Virden quadrangle: New Mexico Bureau of Mines and Mineral Resources, Geologic Map 15, scale 1:126,720.

Elston, W. E., 1961, Upper Cretaceous volcanism and mineralization, Steeple Rock mining district, Grant County, New Mexico (abstr.): New Mexico Geological Society, Guidebook 12, p. 193.

Elston, W. E., 1978, Mid-Tertiary cauldrons and their relationship to mineral resources, southwestern New Mexico: A brief overview; *in* Chapin, C. E., Elston, W. E., and James, H. L., Field guide to selected cauldrons and mining districts of the Datil-Mogollon volcanic field, New Mexico: New Mexico Geological Society, Special Publication No. 7, p. 107–113.

Elston, W. E., 1984, Subduction of young oceanic lithosphere and extension orogeny in southwest North America during Mid-Tertiary times: Tectonics, v. 3, p. 229-250.

Elston, W. E., 1989, Overview of the Mogollon-Datil volcanic field; *in* Field excursions to volcanic terranes in the region: New Mexico Bureau of Mines and Mineral Resources, Memoir 46, p. 43-46.

Engebretson, D. C., Cox, A., and Thompson, G. A., 1984, Correlation of plate motions with continental tectonics: Laramide Basin and Range: Tectonics, v. 3, p. 115-119.

Environmental Protection Agency (EPA), 1979, Methods for chemical analysis of water and wastes: U.S. Environmental Protection Agency, 600/4-79-020.

Farnham, L. L., Stewart, L. A., and DeLong, C. W., 1961, Manganese deposits of eastern

Arizona: U.S. Bureau of Mines, Information Circular 7990, 178 p.

Faure, G., 1986, Principles of isotopic geology (2nd ed.): New York, John Wiley and Sons, 589 p.

Favorskaya, M. A. and Vinogradov, N. V., 1991, Geological evolution of ore-concentrating lineaments: Global Tectonics and Metallogeny, v. 4, p. 75-84.

Field, C. W., 1966, Sulfur isotope method for discriminating between sulfates of hypogene and supergene origin: Economic Geology, v. 61, p 1428-1435.

Field, C. W. and Gustafson, L. B., 1976, Sulfur isotopes in the porphyry copper deposit at El Salvador, Chile: Economic Geology, v. 71, 1533-1548.

Field, C. W. and Lombardi, G., 1972, Sulfur isotopic evidence for the supergene origin of alunite deposits: Mineralium Deposits, v. 7, p. 113-125.

Finnell, T. L., 1987, Geologic map of the Cliff quadrangle, Grant County, New Mexico: U.S. Geological Survey, Miscellaneous Investigations Series Map I-1768, scale 1:50,000.

Fisher, R. A., 1953, Dispersion on a sphere: Proceedings of the Royal Society of London, Series A, v. 217, p. 295-305.

Fleischer, M., 1969, Despujolsite: American Mineralogist, v. 54, p. 326.

Fournier, R. O., 1985a, The behavior of silver in hydrothermal solutions; *in* Berger, B. R., and Bethke, P. M., eds., Geology and geochemistry of epithermal systems: Reviews in Economic Geology, v. 2, p. 45-62.

Fournier, R. O., 1985b, Carbonate transport and deposition in the epithermal environment; *in* Berger, B. R., and Bethke, P. M., eds., Geology and geochemistry of epithermal systems: Reviews in Economic Geology, v. 2, p. 63-72.

Fournier, R. O., Thompson, J. M., Cunningham, C. G., and Hutchinson, R. A., 1991, Conditions leading to a recent small hydrothermal explosion at Yellowstone National Park: Geological Society of America, Bulletin, v. 103, p. 1114–1120.

Gillerman, E., 1964, Mineral deposits of western Grant County, New Mexico: New Mexico

Bureau of Mines and Mineral Resources, Bulletin 83, 213 p.

Goff, F., Gardner, J. N., Baldridge, W. S., Hulen, J. B., Nielson, D. L., Vaniman, D., Heiken, G., Dungan, M. A., and Broxton, D., 1989, Excursion 17B: Volcanic and hydrothermal evolution of Valles caldera and Jemez volcanic field; *in* Field excursions to volcanic terranes in the western United States, volume 1: Southern Rocky Mountain region: New Mexico Bureau of Mines and Mineral Resources, Memoir 46, p. 381-434.

Goldberry, R., 1980, Early diagenetic, Na-alunites in Miocene algal mat intertidal facies, Ras Sudar, Sinai: Sedimentology, v. 27, p. 189-198.

Griggs, R. L. and Wagner, H. C., 1966, Geology and ore deposits of the Steeple Rock mining district, Grant County, New Mexico: U.S. Geological Survey, Bulletin 1222-E, 29 p.

Grindley, G. W., 1965, The geology, structure, and exploitation of the Wairukei geothermal field, Taupo, New Zealand: New Zealand Geological Survey Bulletin 75, 131 p.

Guilbert, J. M., and Park, C. F., Jr., 1986, The geology of ore deposits: W. H. Freeman and Company, New York, New York, 985 p.

Haas, J. L., Jr., 1971, The effect of salinity on the maximum thermal gradient of a hydrothermal system at hydrostatic pressure: Economic Geology, v. 66, p. 940–946.

Hafty, J., Riley, L. B., and Goss, W. R., 1977, A manual on fire assaying and determination of the noble metals in geological materials: U.S. Geological Survey, Bulletin 1445, 58 p.

Hall, R. G., 1978, World nonbauxite aluminum resources—Alunite: U.S. Geological Survey, Professional Paper 1076A, 35 p.

Hassemer, J. R., Watts, K. C., Forn, C. L., and Moseer, E. L., 1983, Maps showing the distribution and relationship and relationships of selected metals in heavy-mineral concentrates of the Hells Hole further planning area (RARE II), Greenlee County, Arizona and Grant County, New Mexico: U.S. Geological Survey, Miscellaneous

Field Studies Map MF-1344D, scale 1:100,000.

Hayba, D. O., 1983, A compilation of fluid-inclusion and stable-isotope data on selected precious- and base-metal epithermal deposits: U.S. Geological Survey, Open-file Report 83-450, 24 p.

Hayba, D. O., Bethke P. M., Heald, P. and Foley, N. K., 1985, Geologic, mineralogic, and geochemical characteristics of volcanic-hosted epithermal precious-metal deposits; *in* Berger, B. R. and Bethke, P. M., eds., Geology and geochemistry of epithermal systems: Reviews in Economic Geology, v. 2, p. 129-168.

Hayes, P. T., 1978, Cambrian and Ordovician rocks of southeastern Arizona and southwestern New Mexico: New Mexico Geological Society, Guidebook 29, p. 165-173.

Hayes, P. T. and Drewes, H., 1978, Mesozoic depositional history of southeastern Arizona: New Mexico Geological Society, Guidebook 29, p. 201-208.

Heald, P., Foley, N. K., and Hayba, D. O., 1987, Comparative anatomy of volcanic-hosted epithermal deposits: acid-sulfate and adularia-sericite types: Economic Geology, v. 82, p. 1-26.

Hedenquist, J. W., 1987, Mineralization associated with volcanic-related hydrothermal systems in the circum-Pacific basin; *in* Horn, M. K., ed., Transactions, Fourth Circum-Pacific Energy and Mineral Resources Conference, Singapore: Tulsa, Oklahoma, American Association of Petroleum Geologists, p. 513–524.

Hedenquist, J. W., 1991, Boiling and dilution in the shallow portion of the Waiotapu geothermal system, New Zealand: Geochimica et Cosmochimica Acta, v. 55, p. 2753–2765.

Hedenquist, J. W. and Henley, R. W., 1985, The importance of CO_2 on freezing point measurements of fluid inclusions: evidence from active geothermal systems and implications for epithermal ore deposition: Economic Geology, v. 80, p. 1379-1406.

Hedlund, D. C., 1990a, Geologic map and sections of the Steeple Rock quadrangle, Grant

and Hidalgo Counties, New Mexico: U.S. Geological Survey, Open-file Report 90-240, scale 1:24,000, 14 p.

Hedlund, D. C., 1990b, Geology and mineral deposits of the Steeple Rock and Duncan mining districts, Grant and Hidalgo Counties, New Mexico and Greenlee County, Arizona: U.S. Geological Survey, Open-file Report 90-239, 27 p.

Hedlund, D. C., 1990c, Preliminary geologic map of the Goat Camp Spring quadrangle, Grant and Hidalgo Counties, New Mexico and Greenlee County, Arizona: U.S. Geological Survey, Open-file Report 90-490, scale 1:24,000.

Hedlund, D. C., 1993, Geologic map of the Tillie Hall Peak quadrangle, Greenlee County, Arizona and Grant County, New Mexico: U.S. Geological Survey, Map GQ-1715, scale 1:24,000.

Hemley, J. J., Montoya, J. W., Marienenko, J. W., and Luce, R. W., 1980, Equilibrium in the system Al_2O_3-SiO_2-H_2O and some general implications for alteration/mineralization processes: Economic Geology, v. 75, p 210-228.

Henley, R. W., 1984, Hydrolysis reactions in hydrothermal fluids; *in* Henley, R. W., Truesdell, A. H., and Barton, P. B., Jr., Fluid-mineral equilibrium in hydrothermal systems: Economic Geology, Reviews in Economic Geology, v. 1, p. 65–80

Henley, R. W., 1985, The geothermal framework for epithermal deposits; *in* Burger, B. R. and Bethke, P. M., eds., Geology and geochemistry of epithermal systems: Reviews in Economic Geology, v. 2, p. 1-24.

Henley, R. W. and Brown, K. L., 1985, A practical guide to the thermodynamics of geothermal fluids and hydrothermal ore deposits; *in* Berger, B. R. and Bethke, P. M., eds., Geology and geochemistry of epithermal systems: Reviews in Economic Geology, v. 2, p. 25-44.

Henley, R. W., and Ellis, A. J., 1983, Geothermal systems, ancient and modern: a geochemical review: Earth Science Reviews, v. 19, p. 1–50.

Henneberger, R. C., and Browne, P. R. L., 1988, Hydrothermal alteration and evolution of

the Ohakur, hydrothermal system, Taupo volcanic zone, New Zealand: Journal of Volcanology and Geothermal Research, v. 34, p. 211–231.

Henry, C. D. and Price, J. G., 1984, Variations in caldera development in the Tertiary volcanic field of Trans-Pecos Texas: Journal of Geophysical Research, v. 89, p. 8765–8786.

Henry, C. D. and Price, J. G., 1986, Early Basin and Range development in Trans-Pecos Texas and adjacent Chihuahua: Magmatism and orientation, timing, and style of extension: Journal of Geophysical Research, v. 91, p. 6213-6224.

Henry, C. D., Price, J. G., Parker, D. F., and Wolff, J. A., 1989, Excursion 9A: Mid-Tertiary silicic alkaline magmatism of Trans-Pecos Texas: Rheomorphic tuffs and extensive silicic lavas; *in* Field excursions to volcanic terranes in the western United States, volume 1: Southern Rocky Mountain region: New Mexico Bureau of Mines and Mineral Resources, Memoir 46, p. 231-274.

Herrington, R. J. and Wilkinson, J. J., 1992, Colloidal gold and silica in mesothermal vein systems: Geology, v. 21, p. 539–542.

Heyl, A. V., 1983, Some major lineaments reflecting deep-seated fracture zones in the central United States, and mineral districts related to the zones: Global Tectonics and Metallogeny, v. 2, p. 75-77.

Hildreth, W., and Mahood, G., 1985, Correlation of ash-flow tuffs: Geological Society of America Bulletin, v. 96, p. 968-974.

Hutchison, M. N., and Scott, S. P., 1981, Sphalerite geobarometry in the system Cu-Fe-Zn-S: Economic Geology, v. 76, p. 143-153.

Irvine, T. N. and Baragar, W. R. A., 1971, A guide to the chemical classification of the common volcanic rocks: Canadian Journal of Earth Sciences, v. 8, p. 523–548.

Jensen, M. L., Ashley, R. P., and Albers, J. P., 1971, Primary and secondary sulfates at Goldfield, Nevada: Economic Geology, v. 66, p. 618-626.

Johnson, C. H., 1943, Steeple Rock district, Grant County, New Mexico: U.S. Bureau of

Mines, War Minerals Report 188, 11 p.

Karlstrom, K. E., and Bowring, S. A., 1988, Early Proterozoic assembly of tectonostratigraphic terranes in southwestern North America: Journal of Geology, v. 96, p. 561-576.

Karlstrom, K. E., Doe, M. F.,, Wessels, R. L., Bowring, S. A., Dönn, J. C., and Williams, M. L., 1990, Juxtaposition of Proterozoic crustal blocks: 1.65-1.60 Ga Mazatzal orogeny: Arizona Geological Survey, Special Paper 7, p. 114-123.

Keith, S. B., 1978, Paleosubduction geometries inferred from Cretaceous and Tertiary magmatic patterns in southwestern North America: Geology, v. 6, p. 516–521.

Keith, S. B., Gest, D. E., DeWitt, E., Tull, N. W., and Everson, B. A., 1983, Metallic mineral districts and production in Arizona: Arizona Bureau of Geology and Mineral Technology, Bulletin 194, 58 p.

Kesler, S. E., Russell, N., Seaward, M., Rivera, J., McCurdy, K., Cumming, G. L., and Sutter, J. F., 1981, Geology and geochemistry of sulfide mineralization underlying the Pueblo Viejo gold-silver oxide deposit, Dominican Republic: Economic Geology, v. 76, p. 1096-1117.

Kirschvink, J. L., 1980, The least-squares line and plane and the analysis of palaeomagnetic data: Geophysical Journal Royal Astron. Society, v. 62, p. 699-718.

Klein, D. P., 1987, Aeromagnetic map of the Silver City 1° x 2° quadrangle, New Mexico and Arizona: U.S. Geological Survey, Map I-1310D, scale 1:250,000.

Kojima, S., 1992, The nature of chalcopyrite inclusions in sphalerite: exsolution, coprecipitation, or "disease?"—A discussion: Economic Geology, v. 87, p. 1191-1192.

Krauskopf, K. B., 1979, Introduction to geochemistry: McGraw-Hill Book Co., New York, New York, 617 p.

Kristmannsdottir, H., and Tomasson, J., 1974, Neojavellir hydrothermal alteration in a high temperature area: Proceedings of the International Symposium on Water-Rock

Interaction, Prague, p. 170–177.

Le Bas, M. J., Le Martre, R. W., Streckusen, A., and Zanettin, B., 1986, A chemical classification of volcanic rocks based on the total alkali-silica diagram: Journal of Petrology, v. 27, p. 745–750.

LeMaitre, R. W., ed., 1989, A classification of igneous rocks and glossary of terms: Blackwell Scientific Publications, Oxford, Great Britain, 193 p.

Lindgren, W., 1922, A suggestion for the terminology of certain mineral deposits: Economic Geology, v. 17, p. 202-294.

Lindgren, W., 1933, Mineral deposits; fourth edition, McGraw-Hill, New York, 930 p.

Lindgren, W., Graton, L. C., and Gordon, C. H., 1910, The ore deposits of New Mexico: U.S. Geological Survey, Professional Paper 68, p. 327-328.

Lipman, P. W., compiler, 1989, Excursion 16B: Oligocene-Miocene San Juan volcanic field, Colorado; *in* Field excursions to volcanic terranes in the western United States, volume 1: Southern Rocky Mountain region: New Mexico Bureau of Mines and Mineral Resources, Memoir 46, p. 303-380.

Lipman, P. W. and Reed, J. C., Jr., 1989, Geologic map of the Latir volcanic field and adjacent areas, northern New Mexico: U.S. Geological Survey, Miscellaneous Investigations Map I-1907, scale 1:48,000.

Long, D. T., Fegan, N. E., McKee, J. D., Lyons, W. B., Hines, M. E., and Macumber, P. G., 1992, Formation of alunite, jarosite, and hydrous iron oxides in hypersaline systems: Lake Tyrrell, Victoria, Australia: Chemical Geology, v. 96, p. 183–202.

Lowell, J. D., 1974, Regional characteristics of porphyry copper deposits of the southwest: Economic Geology, v. 69, p. 601-617.

Mack, G. H. and Clemons, R. E., 1988, Structural and stratigraphic evidence for the Laramide (early Tertiary) Burro uplift in southwestern New Mexico: New Mexico Geological Society, Guidebook 39, p. 59–66.

MacKenzie, W. S., Donaldson, C. H., and Guilford, C., 1991, Atlas of igneous rocks and

their textures: Longman Scientific and Technical and John Wiley and Sons, Inc., New York, New York, 148 p.

Magee, R. W., Moore, J. M., and Brunner, J., 1986, Thermatic mapper data applied to mapping hydrothermal alteration in southwest New Mexico: Fifth Thermatic Conference, Remote sensing for exploration geology, Reno, Nevada, Sept. 29–Oct. 2, 10 p.

Mango, H. N., Conrad, M. E., and Zantop, H., 1991, The Guanajuato mining district: A "classic" epithermal deposit? (abstr.): Geological Society of America, Abstracts with Programs, v. 23, p. A229.

Margolis, J., Reed, M. H., and Albino, G. V., 1991, A process-oriented classification of epithermal systems: magmatic volatile-rich versus volatile-poor fluid paths (abstr.): Geological Society of America, p. A230.

Marshak, S., and Mitra, G., 1988, Basic methods of structural geology: Prentice-Hall, Inc., Englewood Cliffs, New Jersey, 445 p.

Marvin, R. F., Mehnert, H. H., and Naeser, C. W., 1988, U.S. Geological Survey radiometric ages—compilation C: part 2: Arizona and New Mexico: Isochron/West, v. 51, p. 5-13.

Marvin, R. F., Naeser, C. W., Bikerman, M., Mehnert, H. H., and Ratté, J. C., 1987, Isotopic ages of post-Paleocene igneous rocks within and bordering the Clifton 1 degree x 2 degree quadrangle, Arizona-New Mexico: New Mexico Bureau of Mines and Mineral Resources, Bulletin 118, 63 p.

Mayo, E. B., 1958, Lineament tectonics and some ore districts of the southwest: Mining Engineering, v. 11, p. 1169-1175.

McAnulty, W. N., 1978, Fluorspar in New Mexico: New Mexico Bureau of Mines and Mineral Resources, Memoir 34, 64 p.

McDowell, T. W. and Claubagh, S. E., 1979, Ignimbrites of the Sierra Madre Occidental and their relation to the tectonic history of western Mexico: Geological Society of

America, Special Paper 180, p. 113–124.

McIntosh, W. C., 1991, Evaluation of paleomagnetism as a correlation criterion for Mogollon-Datil ignimbrites, southwestern New Mexico: Journal of Geophysical Research, v. 96, no. B8, p. 13,459-13,483.

McIntosh, W. C., Chapin, C. E., Ratté, J. C., and Sutter, J. F., 1992a, Time-stratigraphic framework for the Eocene-Oligocene Mogollon-Datil volcanic field southwestern New Mexico: Geological Society of America Bulletin, v. 104, p. 851-871.

McIntosh, W. C., Geissman, J. W., Chapin, C. E., Kunk, M. J., and Henry, C. D., 1992b, Calibration of the latest Eocene-Oligocene geomagnetic polarity time sale using $^{40}Ar/^{39}Ar$ dated ignimbrites: Geology, v. 20, p. 459-463.

McIntosh, W. C., Sutter, J. F., Chapin, C. E., and Kedzie, L. L., 1990a, High-precision $^{40}Ar/^{39}Ar$ sanidine geochronology of ignimbrites in the Datil-Mogollon volcanic field, southwestern New Mexico: Bulletin of Volcanology, v. 52, p. 584-601.

McIntosh, W. C., Kedzie, L. L., and Sutter, J. F., 1990b, Paleomagnetic and $^{40}Ar/^{39}Ar$ dating database for Mogollon-Datil ignimbrites, southwestern New Mexico: New Mexico Bureau of Mines and Mineral Resources, Bulletin 135, 79 p.

McKibben, M. A., 1991, Introduction to the Salton Trough Rift; *in* McKibben, M. A., ed., The diversity of mineral and energy resources of southern California: Society of Economic Geologists, Guidebook Series, v. 12, p. 77–86.

McLemore, V. T., 1991, Alteration and mineralization in the Carlisle-Center and East Camp area of the Steeple Rock mining district, Grant County, New Mexico—Preliminary observations (abstr.): New Mexico Geology, v. 13, p. 94.

McLemore, V. T., and Clark, K. F., 1993, Alteration and epithermal mineralization in the Steeple Rock mining district, Grant County, New Mexico and Greenlee County, Arizona (abstr.): Conference Program and extended abstracts, Integrated Methods in Exploration and Discovery, Society of Economic Geologists, AB69–70.

McLemore, V. T. and McKee, C., 1988a, A preliminary geochemical study of the Redrock

anorthosite and granite, Burro Mountains, southwestern New Mexico: New Mexico Geological Society, Guidebook 39, p. 83-88.

McLemore, V. T. and McKee, C., 1988b, Geochemistry of the Burro Mountains syenites and adjacent Proterozoic granite and gneiss and the relationships to a Cambrian-Ordovician alkalic magmatic event in New Mexico and southern Colorado: New Mexico Geological Society, Guidebook 39, p. 89-98.

McLemore, V. T. and Quigley, T., 1992, Epithermal gold-silver mineralization at the Alabama mine, Steeple Rock district, Grant County, New Mexico (abst.): New Mexico Geology, v. 14, p. 65.

Meeves, H. C., 1966, Nonpegmatitive beryllium occurrences in Arizona, Colorado, New Mexico, Utah, and four adjacent states: U.S. Bureau of Mines, Report of Investigations RI-682, 68 p.

Minissale, A., 1991, The Larderello geothermal field: a review: Earth Science Reviews, v. 31, p. 133–151.

Mitchell, A. H. G., and Leach, T. M., 1991, Epithermal gold in the Philippines: Island arc metallogenesis, geothermal systems and geology: Academic Press, San Diego, California, 457 p.

Moolick, R. T., and Durek, J. J., 1966, The Morenci district; *in* Titley, S. R. and Hicks, C. L., eds., Geology of the porphyry copper deposits, southwestern North America: The University of Arizona Press, Tucson, Arizona, p. 221–232.

Morgan, P., Seager, W. R., and Golombek, M. P., 1986, Cenozoic thermal, mechanical, and tectonic evolution of the Rio Grande rift: Journal of Geophysical Research, v. 91, p. 6263-6276.

Morrison, R. B., 1965, Geologic map of the Duncan and Canador Peak quadrangles, Arizona and New Mexico: U.S. Geological Survey, Map I-442.

Mosier, D. L., Menzie, W. D., and Kleinhampl, F. J., 1986, Geologic and grade-tonnage information on Tertiary epithermal precious- and base-metal vein districts associated

with volcanic rocks: U.S. Geological Survey, Bulletin 1666, 39 p.

Muehlberger, W. R., 1980, Texas lineament revisited: New Mexico Geological Society, Guidebook 31, p. 113-121.

Muffler, L. J. P., White, D. E., and Truesdell, A. H., 1971, Hydrothermal explosion craters in Yellowstone National Park: Geological Society of America, Bulletin, v. 82, p. 723–740.

Muntean, J. L., Kesler, S. E., Russell, N., and Palanco, J., 1990, Evolution of the Monte Negro sulfate Au-Ag deposit, Pueblo Viejo Dominican Republic: Important factors in grade development: Economic Geology, v. 85, p. 1738-1758.

New Mexico Geological Society (NMGS), 1982, Geologic highway map of New Mexico: New Mexico Geological Society, scale 1:1,000,000.

Nie, N. H., Hull, C. H., Jenkins, J. G., Steinbrenner, K., and Bent, P. H., 1975, SPSS, Statistical package for the Social Sciences: New York, McGraw-Hill Book Co., 675 p.

Norrish, K. and Hutton, J. T., 1969, An accurate x-ray spectrographic method for the analysis of a wide range of geologic samples: Geochimica et Cosmochimica Acta, v. 33, p. 431-454.

North, R. M. and McLemore, V. T., 1986, Silver and gold occurrences in New Mexico: New Mexico Bureau of Mines and Mineral Resources, Resource Map 15, 32 p.

North, R. M. and McLemore, V. T., 1988, A classification of the precious metal deposits of New Mexico; *in* Bulk minable precious metal deposits of the western United States: Geological Society of Nevada, symposium proceedings, p. 625-659.

Obenaulf, R. H. and Bostwick, R., eds., 1988, SPEX handbook of sample preparation and handling: SPEX Industries, Inc., 94 p.

Ohmoto, H. and Rye, R. O., 1979, Isotopes of sulfur and carbon; *in* Barnes, H. L., ed., Geochemistry of hydrothermal ore deposits: New York, Wiley Interscience, p 509-567.

Pattrick, R. A. D., Dorling, M., and Polya, D. A., 1993, TEM study of indium- and copper-bearing growth-banded sphalerite: Canadian Mineralogist, v. 31, p. 105–117.

Pearce, J. A., Harris, N. B. W., and Tindle, A. G., 1984, Trace element discrimination diagrams for the tectonic interpretation of granitic rocks: Journal of Petrology, v. 24, p. 956–983.

Perkins, M., and Nieman, B., 1983, Epithermal gold mineralization in the South Mountain volcanic dome, Summitville, Colorado; *in* Genesis of Rocky Mountain ore deposits; changes with time and tectonics: Denver Region Exploration Geologists Society Proceedings, p. 71–78.

Phillips, W. J., 1972, Hydraulic fracturing and mineralization: Journal of Geological Society of London, v. 128, p. 337–359.

Powers, R. S., 1976, Geology of the Summit Mountains and vicinity, Grant County, New Mexico and Greenlee County, Arizona: unpublished M.S. thesis, University of Houston, 107 p.

Price, J. C. and Henry, C. D., 1984, Stress orientations during Oligocene volcanism in Trans-Pecos Texas: Timing the transition from Laramide compression to Basin and Range extension: Geology, v. 12, p. 238-241.

Raines, G. L., 1984, Limonite alteration map of the Silver City 1 degree x 2 degree quadrangle, New Mexico and Arizona: U.S. Geological Survey, Miscellaneous Field Investigations Map MF-1183-Q, scale 1:250,000.

Ramdohr, P., 1969, The ore minerals and their intergrowths: Pergamon Press, New York, New York, 1174 p.

Ratté, J. C. and Gaskill, D. L., 1975, Reconnaissance geologic map of the Gila Wilderness study area, southwestern New Mexico: U.S. Geological Survey, Miscellaneous Investigations Map I-886, scale 1:62,500.

Ratté, J. C., Marvin, R. F., Naeser, C. W., and Bikerman, M., 1984, Calderas and ash-flow tuffs of the Mogollon Moutains, southwestern New Mexico: Journal of Geophysical

Research, v. 89, p. 8713-8732.

Ratté, J. C. and Hedlund, D. C., 1981, Geologic map of the Hells Hole further planning area (RARE II), Greenlee County, Arizona and Grant County, New Mexico: U.S. Geological Survey Map MF-1344-A, scale 1:62,500.

Ratté, J. C., Hassemer, J. R., Marton, R. A., and Briggs, J. P., 1982, Mineral resource potential of the Hells Hole further planning area (RARE II) Greenlee County, Arizona and Grant County, New Mexico: U.S. Geological Survey, Map MF-1344-E, 7 p.

Ratté, J. C. and Brooks, W. E., 1983, Geologic map of the Mule Creek quadrangle, Grant County, New Mexico: U.S. Geological Survey, Map MF-1666, scale 1:24,000.

Raymahashay, B. C., 1969, A geochemical study of rock alteration by hot springs in the Paint Pot Hill area, Yellowstone Park: Geochimica et Cosmochimica Acta, v. 32, p. 499-522.

Reed, M. H., and Spycher, N., 1985, Boiling, cooling, and oxidation in epithermal systems: a numerical modeling approach; *in* Berger, B. R., and Bethke, P. M., eds., Geological geochemistry of epithermal systems: Reviews in Economic Geology, v. 2, p. 249–272.

Renault, J., 1984, Turbine drive sample spinner for x-ray diffraction: Rev. Sci. Instrum., v. 55, p. 805-806.

Reyes, A. G., 1990, Petrology of Philippine geothermal systems and the application of alteration mineralogy to their assessment: Journal of Volcanology and Geothermal Resources, v. 43, p. 274–309.

Richter, D. H. and Lawrence, V. A., 1983, Mineral deposit map of the Silver City 1 degree x 2 degree quadrangle, New Mexico and Arizona: U.S. Geological Survey, Map I-1319-B, scale 1:250,000.

Richter, D. H., Sharp, W. N., Watts, K. C., Raines, G. L., Houser, B. B., and Klein, D. P., 1986, Maps showing mineral resource assessment of the Silver City 1 degree x 2 degree quadrangle, New Mexico and Arizona: U.S. Geological Survey, Map I-1310-

F, scale 1:250,000.

Robinson, R. W., 1984, Geology, structure, and mineralization in the Steeple Rock mining district (abstr.): New Mexico Bureau of Mines and Mineral Resources, Circular 199, p. 54.

RockWare, Inc., 1991, ROCKSTAT: RockWare, Inc., Wheat Ridge, Colorado, 54 p.

RockWare, Inc., 1992a, MSTAT: Srie Ptg., Ltd., Dee Why, NSW, 77 p.

RockWare, Inc., 1992b, STEREO: The stereographic projection program: RockWare, Inc., Wheat Ridge, Colorado, 41 p.

Roedder, E., ed., 1984, Fluid inclusions: Reviews in Mineralogy, v. 12, Mineralogical Society of America, 646 p.

Roedder, E., and Bodnar, R. J., 1980, Geologic pressure determinations from fluid inclusion studies: Annual Reviews Earth Science, v. 8, p. 263-301.

Rose, A. W., and Baltosser, W. W., 1966, The porphyry copper deposit at Santa Rita, New Meixco; *in* Titley, S. R. and Hicks, C. L., eds., Geology of the porphyry copper deposits, southwestern North America: The University of Arizona Press, Tucson, Arizona, p. 205–220.

Ross, C. A., 1973, Pennsylvanian and Early Permian depositional history, southeastern Arizona: American Association of Petroleum Geologists Bulletin, v. 57, p. 887-912.

Ross, C. A. and Ross, J. R. P., 1986, Paleozoic paleotectonics and sedimentation in Arizona and New Mexico; *in* Peterson, J. A., ed., Paleotectonics and sedimentation in the Rocky Mountain Region, United States: American Association of Petroleum Geologists, Memoir 41, p. 653-668.

Rothrock, H. E., Johnson, C. H., and Hahn, A. D., 1946, Fluorspar resources in New Mexico: New Mexico Bureau of Mines and Mineral Resources, Bulletin 21, 245 p.

Ruff, R. K., 1993, Gas analysis of fluid inclusions: Application toward precious metal exploration, Steeple Rock mining district, Grant County, New Mexico: M.S. thesis, New Mexico Institute of Mining and Technology, 89 p.

Ruff, R. K. and Norman, D. I., 1991, Gas analysis of fluid inclusions: Applications toward precious metal exploration, Steeple Rock district, Grant County, New Mexico (abstr.): New Mexico Geology, v. 13, p. 64.

Russell, P. L., 1947, Steeple Rock zinc-lead district, Grant County, New Mexico: U.S. Bureau of Mines, RI 4073, 13 p.

Rye, R. O., Bethke, P. M., and Wasserman, M. D., 1992, The stable isotope geochemistry of acid-sulfate alteration: Economic Geology, v. 87, p. 225-264.

Rytuba, J. J., 1981, Relation of calderas to ore deposits in the western United States; *in* Relations of tectonics to ore deposits in the southern Cordillera: Arizona Geological Society Digest, v. 14, p. 22

Sander, M. V. and Black, J. E., 1988, Crystallization and recrystallization of growth-zoned vein quartz crystals from epithermal systems—implications for fluid inclusion studies: Economic Geology, v. 83, p. 326.

Schmitt, H. A., 1966, The porphyry copper deposits in their regional setting; *in* Titley, S. R. and Hicks, C. L., eds., Geology of the porphyry copper deposits, southwestern North America: The University of Arizona Press, Tucson, Arizona, p. 17–33.

Schoch, A. E., Beukes, G. J., and Praelkelt, H. E., 1985, A natroalunite-zaherite-hotsonite paragenesis from Pofadder, Bushmanland, South Africa: Canadian Mineralogist, v. 23, p. 29–34.

Schoen, R., White, D. E., and Hemley, J. J., 1974, Argillization by descending acid at Steamboat Springs, Nevada: Clays and Clay Minerals, v. 22, p. 1-22.

Scholle, P. A., 1979, A color-illustrated guide to constituents, textures, cements, and porosities of sandstones and associated rocks: American Association of Petroleum Geologists, Memoir 28, 201 p.

Schumacher, D., 1978, Devonian stratigraphy and correlations in southeastern Arizona: New Mexico Geological Society, Guidebook 29, p. 175-182.

Seager, W. R. and Mack, G. H., 1986, Laramide paleotectonics of southern New Mexico: *in*

Peterson, J. A., ed., Paleotectonics and sedimentation in the Rocky Mountain Regional, United States: American Association of Petroleum Geologists, Memoir 41, p. 669-685.

Seager, W. R., Mack, G. H., Raimonde, M. S., and Ryan, R. G., 1986, Laramide basement-cored uplift and basins in south-central New Mexico: New Mexico Geological Society, Guidebook 37, p. 123-130.

Sharp, R. R., Morris, W. A., and Aamodt, P. L., 1978, Uranium hydrogeochemical and stream sediment reconnaissance data release for the New Mexico portions of the Douglas, Silver City, Clifton, and St. Johns NTMS quadrangles, New Mexico/Arizona: U.S. Department of Energy, Report GJBX-69(78), 123 p.

Sharp, W. N., 1991, Petrochemistry of igneous rocks, Silver City 1 x 2 degree quadrangle, New Mexico and Arizona: U.S. Geological Survey, Miscellaneous Investigations Series Map I-1310H, scale 1:250,000.

Shepherd, T., Rankin, A. H., and Alderton, D. H., M., 1985, A practical guide to fluid inclusion studies: Blackie and Son, Ltd., Glasgow, Great Britain, 239 p.

Sigvaldason, G. E., 1992, Recent hydrothermal explosion craters in an old hyaloclastite flow, central Iceland: Journal of Volcanology and Geothermal Research, v. 54, p. 53—63.

Silberman, M. L. and Berger, B. R., 1985, Relationship of trace-element patterns to alteration and morphology in epithermal precious-metal deposits; *in* Berger, B. R. and Bethke, P. M., eds., Geology and geochemistry of epithermal systems: Reviews in Economic Geology, v. 2, p. 203-232.

Sillitoe, R. H., 1983, Enargite-bearing massive sulfide deposits high in porphyry copper systems: Economic Geology, v. 78, p. 348-352.

Simmons, S. F., Browne, P. R. L., and Brathwaite, R. L., 1992, Active and extinct hydrothermal systems of the North Island, New Zealand: Society of Economic Geologists, Guidebook Series, v. 15, 121 p.

Stacey, J. S. and Hedlund, D. C., 1983, Lead-isotopic composition of diverse igneous rocks

and ore deposits from southwestern New Mexico and their implications for early Proterozoic crustal evolution in the western United States: Geological Society of America Bulletin, v. 94, p. 43-57.

Steiner, A. and Rafter, T. A., 1966, Sulfur isotopes in pyrite, pyrrhotite, alunite, and anhydrite from steam wells in the Taupo volcanic zone, New Zealand: Economic Geology, v. 61, p. 1115-1129.

Stoffregen, R. E., 1987, Genesis of acid-sulfate alteration and Au-Cu-Ag mineralization at Summitville, Colorado: Economic Geology, v. 82, p. 1575–1591.

Stoffregen, R. E., and Alpers, C. N., 1987, Woodhouseite and suanbergite in hydrothermal ore deposits: products of apatite destruction during advance argillic alteration: Canadian Mineralogist, v. 25, p. 201–211.

Stoffregen, R. E., and Cygan, G. L., 1990, Experimental study of Na-K exchange between alunite and aqueous sulfate solutions: American Mineralogist, v. 75, p. 209–220.

Strangway, D. E., Simpson, J., and York, D., 1976, Paleomagnetic studies of volcanic rocks from the Mogollon Plateau area of Arizona and New Mexico: New Mexico Geological Society, Special Publication 5, p. 119–124.

Swanson, R. G., 1981, Sample examination manual: American Association of Petroleum Geologists, Methods in Exploration Series,

Talloch, A. J., 1982, Mineralogical observations on carbonate scaling in geothermal wells at Kawerau and Broadlands: Proceedings of the Pacific Geothermal Conference, Part I, p. 131-134.

Taylor, B. E., Wheeler, M. C., and Nordstrom, D. K., 1984, Stable isotope geochemistry of acid mine drainage: experimental oxidation of pyrite: Geochimica et Cosmochimica Acta, v. 48, p. 2669-2678.

Texas Instruments, Inc., 1978, Aerial radiometric and magnetic reconnaissance survey of portions of Arizona, New Mexico: Silver City quadrangle: U.S. Department of Energy, Report GJBX-23(79), vol. 2-D, 205 p.

Thompson, A. J. B. and Petersen, E. U., 1991, Alunite compositions and textures: Indicators of the environment of formation (abstr.): Geological Society of America, Abstracts with Programs, v. 23, p. A229.

Tingley, J. V. and Berger, B. R., 1985, Lode gold deposits of Round Mountain, Nevada: Nevada Bureau of Mines and Geology, Bulletin 100, 62 p.

Titley, S. R., 1982, Geologic setting of porphyry copper deposits: southeastern Arizona; *in* Titley, S. R., ed., Advances in geology of the porphyry copper deposits, southwestern North America: University of Arizona Press, Tucson, Arizona, p. 37-58.

Tooker, E. W. and Vercoutere, T. L., 1986, Gold in the conterminous United States, perspective of 1986, Preliminary map of selected geographic, economic, and geologic attributes of productive (> 10,000 oz) gold districts: U.S. Geological Survey, Open-file Report 86-209, 32 p.

Trace, R. D., 1947, The Fourth of July and Luckie No. 1 and No. 2 fluorspar veins, Greenlee County, Arizona: U.S. Geological Survey, Strategic Minerals Investigations Report 3-207, 6 p.

Trauger, F. D., 1972, Water resources and general geology of Grant County, New Mexico: New Mexico Bureau of Mines and Mineral Resources, Hydrologic Report 2, 211 p.

Turner, G. L., 1962, The Deming axis, southeastern Arizona, New Mexico, and Trans-Pecos Texas: New Mexico Geological Society, Guidebook 13, p. 59-71.

U.S. Bureau of Mines, 1992, Mineral commodity summaries 1992: U.S. Department of the Interior, 204 p.

Vennemann, T. W., Muntean, J. L., Kesler, S. E., O'Neil, J. R., and Valley, J. W., 1991, Stable isotope evidence for magmatic fluids: Pueblo Viejo acid-sulfate Au-Ag deposits, Dominican Republic (abstr.): Geological Society of America, Abstracts with Programs, p. A229.

Vennemann, T. W., Muntean, J. L., Kesler, S. E., O'Neil, J. R., Valley, J. W., and Russell, N., 1993, Stable isotope evidence for magmatic fluids in the Pueblo Viejo

epithermal acid sulfate Au-Ag deposit, Dominican Republic: Economic Geology, v. 88, p. 55–71.

Vikre, P. G., 1987, Paleohydrology of Buckskin Mountain, National district, Humbolt County, Nevada: Economic Geology, v. 82, p. 934–950.

Wahl, D. E., 1980, Mid-Tertiary volcanic geology in parts of Greenlee County, Arizona and Grant County, New Mexico: unpublished Ph.D. dissertation, Arizona State University, 144 p.

Wahl, D. E., 1983, Comments on economic volcanology between Redrock, New Mexico and Clifton, Arizona (abstr.): New Mexico Geology, v. 5, p. 67.

Walthier, T. N., Araneda, G. R., and Crawford, J. W., 1982, The El Indio gold, silver, and copper deposit region of Coquimbo, Chile; *in* Watson, S. T., ed., Transactions of the Third Circum-Pacific Energy and Mineral Resources Conference: Honolulu, The Circum-Pacific Council for Energy and Mineral Resources, p. 349–355.

Wargo, J. G., 1959, The geology of the Schoolhouse Mountain quadrangle, Grant County, New Mexico: unpublished Ph.D. dissertation, University of Arizona,, Tucson, 187 p.

Watts, K. C. and Hassemer, J. R., 1988, Geochemical interpretive and summary maps, Silver City 1 degree x 2 degree quadrangle, New Mexico and Arizona: U.S. Geological Survey, Map I-1310-E, scale 1:250,000.

Wertz, J. B., 1970a, Arizona's copper province and the Texas lineament: Mining Engineering, v. 5, p. 80-81.

Wertz, J. B., 1970b, The Texas lineament and its economic significance in southeastern Arizona: Economic Geology, v. 65, p. 166-181.

White, D. E., 1955, Thermal springs and epithermal ore deposits: Economic Geology, 50th anniv. volume, p. 99-154.

White, D. E., 1979, Duration of hydrothermal activity at Steamboat Springs, Nevada from ages of spatially associated volcanic rocks: U.S. Geological Survey, Professional Paper 4580, 13 p.

White, D. E., 1981, Active geothermal systems and hydrothermal ore deposits: Economic Geology, 75th anniv. volume, p. 392-423.

White, D. E., Hutchinson, R. A., and Keith, T. E. C., 1988, The geology and remarkable thermal activity of Norris Geyser Basin, Yellowstone National Park, Wyoming: U.S. Geological Survey, Professional Paper 1456, 84 p.

White, D. L. and Foster, M. G., 1981, Uranium resource evaluation, Clifton quadrangle, ARizona and New Mexico: U.S. Department of Energy, Report PGJ/F--116-82, 53 p.

White, N. C. and Hedenquist, J. W., 1990, Epithermal environments and styles of mineralization: variations and their causes, and guidelines for exploration: Journal of Geochemical Exploration, v. 36, p. 445–474.

Wiggins, L. B., and Craig, J. R., 1980, Reconnaissance of the Cu-Fe-Zn-S system: sphalerite phase relationships: Economic Geology, v. 75, p. 742-751.

Williams, F. E., 1966, Fluorspar deposits of New Mexico: U.S. Bureau of Mines, Information Circular 8307, 143 p.

Wilson, E. D., 1950, Fluorspar in Arizona: Arizona Bureau of Mines, Circular 151, 13 p.

Wilson, M., McLemore, V. T., and Gundiler, I., 1993, Geology and ore-mineralogy of the Center mine, Steeple Rock mining district, New Mexico: A process mineralogy perspective: New Mexico Bureau of Mines and Mineral Resources, Open-file Report ___, 26 p.

Winchester, J. A. and Floyd, P. A., 1977, Geochemical discrimination of different magma series and their differentiation products using immobile elements: Chemical Geology, v. 20, p. 325–343.

Witcher, J. C., 1988, Geothermal resources of southwestern New Meixco and southeastern Arizona: New Mexico Geological Society, Guidebook 39, p. 191–198.

Woldegabriel, G., 1990, Hydrothermal alteration in the Villes caldera ring fracture zone and core hole VC–1: evidence for multiple hydrothermal systems: Journal of Volcanology and Geothermal Research, v. 40, p. 105–122.

Wynn, J. C., 1981, Complete Bouguer gravity anomaly map of the Silver City 1° x 2° quadrangle, New Mexico-Arizona: U.S. Geological Survey, Map I–1310A, scale 1:250,000.

Yau, Yu-Chyi, Peacor, D. R., Beane, R. E., Essene, E. J., and McDowell, S. D., 1988, Microstructures, formation mechanisms, and depth-zoning of phyllosilicates in geothermally altered shales, Salton Sea, California: Clays and Clay Minerals, v. 36, p. 1-10.

Zijderveld, J. P. A., 1967, A. C., Demagnetization of rocks: analysis of results; *in* Collinson, D. W., Creer, K. M., and Runcorn, S. K., eds., Methods in paleomagnetism: Elsevier, Amsterdam, p. 254-286.

10. LIST OF ABBREVIATIONS AND ACRONYMS

ASARCO	American Smelting and Refining Co.
CUSMAP	Contiguous United States Mineral Appraisal Project
EPA	Environmental Protection Agency (United States)
FMC	Foote Minerals Corp.
NMBMMR	New Mexico Bureau of Mines and Mineral Resources (Socorro, NM)
NMIMT	New Mexico Institute of Mining and Technology (Socorro, NM)
SEM	Scanning electron microscopy
USBM	United States Bureau of Mines
USGS	United States Geological Survey
UTEP	University of Texas at El Paso
XRD	X-ray diffraction spectrometry
XRF	X-ray fluorescent spectrometry

11.1 APPENDIX 1

DESCRIPTION OF DRILL CORE

This appendix includes brief petrologic descriptions and chemical analyses of drill core from throughout the Steeple Rock district. Not all of the core was available for study and the descriptions presented here are a synopsis of available data. In some cases, there was insufficient time to examine all of the core that was available. Most of the core examined is diamond drill core, although some data are based on drill cuttings from reversed circulation drilling. Descriptions designated by * indicate holes examined for this study. Each interval is assigned to a specific formation as used in this study by the author. Samples were collected from drill core examined and data from these samples are in Appendices 11.2, 11.3, 11.4, 11.5, 11.6, and 11.7. Assay data are typically as reported by the corresponding company, although some samples were assayed for this study and are included. All depths are drill depths unless otherwise specified (i.e., have not been converted to true thickness or depths).

11.1.1 Carlisle – Center mines

Brief descriptions and summary of drill data (Tables 11.1, 11.2, 11.3, 11.4) from holes in the Carlisle and Center mines area are below. The USBM drilled 14 diamond drill holes in 1942 (Russell, 1947) and the core is stored at the USGS Core Facility in Denver, Colorado (see Fig. 3.4, 5.11 and Map 5 for location). Drill holes H-1 through H-8 were drilled on the 700 ft level. Weaco, Ltd. drilled 20 holes at the Carlisle mine and one hole at the Section 2 adit in 1991 (see Fig. 3.4, 4.25 and Maps 2, 5 for location of drill holes). Splits of the cuttings are on file at NMBMMR. R&B Mining Co. drilled 5 diamond drill holes on the 10th level (Map 4). All holes were in the Summit Mountain formation and were examined for this study. Dresser Minerals also drilled 12 holes at the Center mine (Map 4, 5), but the core is not available for study. HD = Hole declination in degrees. DI – Drill depth interval in meters.

Hole no.	HD	DI (m)	Description
Holes drilled by the USBM (1942)			
H-1	-67	0-53.8	Dark gray to gray andesite porphyry (Summit Mountain formation) with thin stringers of quartz and sulfide veins. Epidote common in trace amounts.
		53.8-56.5	Quartz breccia vein locally with small fluorite cubes (< 1 mm diameter).
		56.5-103.6	Gray to green-gray andesite porphyry (Summit Mountain formation).
H-2	-84	0-53.9	Gray andesite porphyry (Summit Mountain formation) with disseminated chlorite, epidote, and pyrite.
		53.9-75.0	Green-gray andesite porphyry with abundant chlorite and pyrite.
		75.0-79.4	Quartz breccia vein.
		79.4-94.6	Green-gray andesite porphyry (Summit Mountain formation).
H-3	-68	0-64.5	Gray andesite porphyry (Summit Mountain formation).
		64.5-72.4	Quartz vein
		72.4-	Green-gray andesite porphyry (Summit Mountain formation).
H-4	-39	0-36.6	Green-gray andesite porphyry (Summit Mountain formation) with thin veins of quartz, calcite, chlorite, and pyrite.
		36.6-44.8	Quartz breccia vein.
		44.8-49.4	Silicified green to green-gray andesite porphyry with abundant chlorite and trace epidote.
		49.4-82.7	Green-gray andesite porphyry (Summit Mountain formation).

Hole no.	HD	DI (m)	Description
H-5	-44	0-50.3	Green-gray andesite porphyry (Summit Mountain formation).
		50.3-52.3	Quartz breccia vein.
		52.3-55.5	Silicified light-green andesite porphyry.
		55.5-57.9	Red-brown to green andesite porphyry, silicified and iron stained with abundant chlorite.
		57.9-56.1	Green-gray andesite porphyry
		56.1-58.2	Quartz breccia vein.
		58.2-65.7	Green-gray andesite porphyry (Summit Mountain formation).
H-6	-26.5	0-53.7	Gray andesite porphyry (Summit Mountain formation).
		53.7-68.9	Quartz breccia vein with chalcopyrite, pyrite, galena and sphalerite.
		68.9-85.5	Gray andesite porphyry (Summit Mountain formation).
H-7	-44	0-36.0	Dark gray to gray andesite porphyry (Summit Mountain formation) with disseminated chlorite, pyrite, and epidote.
		36.0-40.6	Quartz breccia vein.
		40.6-66.1	Gray to green-gray andesite porphyry, locally brecciated, silicified, and cut by quartz, calcite, and chlorite veins (Summit Mountain formation).
H-8	-21	0-57.0	Gray andesite porphyry (Summit Mountain formation).
		57.0-62.0	Quartz breccia vein.
		62.0-70.5	Green-gray andesite porphyry.
		70.5-75.7	Quartz breccia vein.
		75.7-90.0	Green-gray to gray andesite porphyry with silicified zones (Summit Mountain formation).
*H-9	-73	0-112.8	Dark gray to gray to purple andesite porphyry with intervals of thin veinlets of quartz and chlorite (< 1 cm wide), Summit Mountain formation.
		112.8-115.8	Green-gray andesite porphyry with disseminated pyrite and thin quartz-pyrite veinlets (< 1 cm wide).
		115.8-143.2	Gray to green-gray andesite porphyry, Summit Mountain formation.
		143.2-151.2	Silicified gray to green-gray andesite porphyry, Summit Mountain formation.
		151.2-153	Quartz and quartz breccia vein with sulfides.

Hole no.	HD	DI (m)	Description
		153-167.1	Green-gray andesite porphyry, Summit Mountain formation.
*H-10	-45	0-67.1	Variegated yellow, purple, pink, black, to white altered tuff with zones of pyrite disseminations and thin quartz veinlets. Sedimentary rocks, undifferentiated.
		67.1-82.3	Brecciated, silicified andesite and quartz.
		82.3-85.3	White quartz vein with chlorite and sulfides (pyrite, chalcopyrite, galena, sphalerite).
		85.3-91.5	Silicified gray to green-gray andesite porphyry, Summit Mountain formation.
		91.5-125.8	Green-gray andesite porphyry, Summit Mountain formation.
*H-11	-67	0-59.4	Variegated yellow, purple, pink, to white altered tuff, sedimentary rocks, undifferentiated.
		59.4-61.0	Quartz vein with amethyst.
		61.0-67.0	Gray silicified tuff.
		67.0-88.4	Gray volcanic breccia, minor silicification.
		88.4-94.6	Green-gray andesite porphyry, Summit Mountain formation.
		94.6-101.8	Quartz vein with sulfides (galena, chalcopyrite, sphalerite, pyrite).
		101.8-109.7	Chloritized and silicified green-gray andesite porphyry, Summit Mountain formation.
		109.7-124.9	Green-gray to gray andesite porphyry, Summit Mountain formation.
*H-12	-40	0-12.2	Poor core recovery—soil.
		12.2-15.7	Brown to gray to green-gray andesite porphyry.
		15.7-16.5	Quartz vein (amethyst, pyrite, chalcopyrite, malachite, azurite, galena, sphalerite).
		16.5-21.9	Silicified green-gray andesite porphyry, Summit Mountain formation.
		21.9-23.2	Quartz vein (pyrite, chalcopyrite, malachite, azurite, galena, sphalerite).
		23.2-41.1	Gray andesite porphyry, Summit Mountain formation.
*H-13	-50	0-25.6	Gray andesite porphyry, Summit Mountain formation.
		25.6-31.1	Quartz vein (fluorite, galena, sphalerite, chalcopyrite, pyrite, malachite).
		31.1-48.8	Green-gray to gray porphyritic andesite, Summit Mountain formation.

Hole no.	HD	DI (m)	Description
*H-14	-67	0-43.3	Purple tuff, sedimentary rocks, undifferentiated.
		43.3-69.5	Variegated purple, green, yellow, to white altered tuff.
		69.5-89.6	White to gray altered tuff (silicified).
		89.6-104.8	Green-gray to gray andesite porphyry, Summit Mountain formation.
		104.8-107.5	Quartz vein (chlorite, galena, chalcopyrite, pyrite, sphalerite).
		107.5-111.2	Gray andesite porphyry, Summit Mountain formation.

Table 11.1—Summary of drill data along the Carlisle fault, USBM, 1942. *All holes were examined for this study. Az = Azimuth in degrees. HD = Hole declination in degrees. Depths are drill depths not true depths.

Hole no. (USBM prefix)	Collar elevation (m)	Az	HD	Total depth (m)	Vein intercept (m)	Sample intercept (m)	Au oz/ton	Ag oz/ton	Cu%	Pb%	Zn%	Reference	Comments
H-1*	1366.1	35	-67	103.6	53.8-54.7	53.8-54.7	tr	0.64	0.5	5.4	3.7	Russell (1947)	Drilled at 213.3 m level of Carlisle.
						55.7-56.5	tr	0.56	1.0	0.9	1.5		
H-2*	1366.1	35	-84	94.6	75.0-79.4	75.0-75.4	0.02	3.0	1.2	1.7	2.0	Russell (1947)	Drilled at 213.3 m level of Carlisle.
H-3*	1366.1	77	-68		64.5-72.4	70.8-72.4	tr	0.24	0.6	3.0	0.5	Russell (1947)	Drilled at 213.3 m level of Carlisle.
H-4*	1366.1	35	-39	82.7	36.6-44.8	36.7-37.8	0.02	2.78	1.24	3.3	6.0	Russell (1947)	Drilled at 213.3 m level of Carlisle.
						37.8-42.8	tr	0.52	0.64	0.60	0.50		
						42.8-43.1	0.01	1.48	1.24	2.5	3.6		
						43.1-43.6	0.0	0.56	0.90	1.3	2.2		
						43.6-43.9	0.0	0.16	0.17	0.20	2.2		
						43.9-44.5	tr	0.60	0.33	1.2	1.8		
H-5*	1366.1	65	-44	65.7	50.3-52.3	50.8-51.8	0.0	0.0	0.2	1.4	2.1	This report	Drilled at 213 m level of Carlisle.
						51.3-51.8	0.02	1.22	1.0	4.1	7.8	Russell (1947)	
H-6*	1366.1	75	-26.5	85.5	53.7-68.9	64.8-65.5	tr	0.56	0.31	1.2	1.5	Russell (1947)	Drilled at 213 m level of Carlisle.
H-7*	1366.1	3	-44	66.1	36.0-40.6	39.3-39.6	tr	0.2	0.04	0.15	0.38	Russell (1947)	Drilled at 213.3 m level of Carlisle.
H-8*	1366.1	80	-21	90.0	57.0-62.0	57.7-58.1	0.01	0.8	0.35	1.2	1.9	Russell (1947)	Drilled at 213.3 m level of Carlisle.
					70.5-75.7	60.9-61.2	0.04	3.68	1.1	3.15	3.0		
H-9*	1612.6	358	-73	167.1	151.2-153	151.8-152.5	tr	0.16	2.0	0.3	0.5	Russell (1947)	Between Carlisle and Center mines.
H-10*	1580.4	37	-45	125.8	67.1-91.5	27.4-27.7	0.0	0.0	0.001	0.0071	0.0027	This report	West of Carlisle mine.
						83.3-83.7	0.0	0.0	0.003	0.0057	0.0053	This report	
						85.0-85.3	0.016	0.0	0.079	0.2	0.072	This report	
						78.8-80.9	tr	0.12	tr	0.06	0.5		
H-11*	1611.9	12	-67	124.9	94.6-101.8	94.6-94.9	0.02	0.48	0.31	1.14	2.0	Russell (1947)	Test ore intercept at Center mine.
						94.9-95.9	0.04	0.16	0.12	0.36	0.3		
						97.4-98.4	0.0	0.04	tr	0.06	0.25		
H-12*	1597.3	10	-40	41.1	15.7-16.5	15.7-16.5	0.08	0.72	0.14	1.6	2.8	Russell (1947)	East of Pennsylvania mine.
					21.9-23.2	21.9-23.2	0.11	0.7	0.19	0.3	0.25		
H-13*	1595.0	10	-50	48.8	25.6-31.1	25.9-28.6	0.0	tr	0.0	0.0	0.2	Russell (1947)	Below H12.
						30.0-31.1	0.05	0.45	0.08	tr	0.3		
H-14*	1603.7	16	-67	111.2	104.8-107.3	56.2-56.4	0.0	0.0	0.001	0.0011	0.0029	This report	Test ore intercept at Center mine.
						104.8-105.4	tr	0.8	0.25	1.7	2.2	Russell (1947)	
						105.4-106.3	0.01	0.28	0.26	0.53	0.98		
						106.3-107.3	0.0	0.2	0.07	tr	0.4		

Hole no.	HD	DI (m)	Description
Holes drilled by Weaco Minerals, Ltd.			
CR91-1	-50	0-12.2	Silicified tuff cut by quartz veins.9
		12.2-13.7	Quartz vein with amethyst and pyrite.
		13.7-16.8	Quartz vein with galena, sphalerite and chalcopyrite.
		16.8-36.6	Quartz vein.
		36.6-54.9	Silicified tuff cut by quartz veins with pyrite and sericite.
CR91-2	-50	0-42.7	Green-gray andesite porphyry, Summit Mountain formation, chloritized and silicified.
		42.7-61.0	Black to dark gray andesite with epidote, pyrite, and silicified, Summit Mountain formation.
		61.0-73.1	Dark gray to green-gray andeiste with increasing chlorite and sericite.
		73.1-103.6	Hematite increases.
CR91-3	-60	0-13.7	Silicified tuff.
		13.7-19.8	Quartz vein.
		19.8-39.6	Silicified andesite with sericite and pyrite, Summit Mountain formation.
		39.6-67.1	Chloritized, silicified andesite with epidote and pyrite.
CR91-4	-60	0-33.5	Green to brown to red tuff with increasing amount of epidote, pyrite, sericite, and quartz with depth.
		33.5-38.1	Stope, no sample.
		38.1-61.0	Quartz vein with pyrite.
		61.0-73.1	Green-gray andesite with pyrite and quartz, Summit Mountain formation.
CR91-5	-90	0-9.1	Silicified tuff.
		9.1-21.3	Quartz vein with pyrite, amethyst, sphalerite, and galena.
		21.3-29.0	Stope, no sample.
		29.0-36.6	Silicified green-gray andesite, Summit Mountain formation.
CR91-6	-60	0-1.5	Silicified tuff.
		1.5-9.1	Quartz vein with pyrite.
		9.1-13.7	Stope, limited sample.
		13.7-15.2	Quartz vein.
		15.2-18.3	Gray to black, chloritized and silicified andesite porphyry, Summit Mountain formation.
CR91-7	-60	0-1.5	Overburden.
		1.5-16.8	Quartz vein with pyrite and sulfides.
		16.8-19.8	Stope, no sample.

Hole no.	HD	DI (m)	Description
		19.8-22.9	Quartz vein.
		22.9-24.4	Dark gray, silicified andesite with pyrite and epidote.
		24.4-36.6	Stope, no sample.
		36.6-42.7	Dark gray, silicified andesite with pyrite and epidote, Summit Mountain formation.
CR91-8	-90	0-3.0	Dump material.
		3.0-13.7	Green-gray silicified andesite, Summit Mountain formation.
		13.7-61.0	Silicified andesite, Summit Mountain formation.
		61.0-67.1	Silicified andesite, Summit Mountain formation.
CR91-9	-60	0-1.5	Overburden.
		1.5-10.7	Quartz vein with pyrite.
		10.7-24.4	Green-gray, silicified andesite porphyry with epidote and pyrite, Summit Mountain formation.
CR91-10	-60	0-1.5	Overburden.
		1.5-61.0	Green-gray to brown andesite porphyry with varying amounts of quartz, pyrite, chlorite, and epidote; Summit Mountain formation.
CR91-11	-60	0-1.5	Overburden.
		1.5-48.8	Green-gray to brown andesite porphyry with varying amounts of quartz, pyrite, chlorite, and epidote; Summit Mountain formation.
CR91-12	-90	0-1.5	Overburden.
		1.5-18.3	Silicified and brecciated tuff.
		18.3-59.4	Quartz breccia vein with fragments of andesite and pyrite and sulfides. Wood in some samples suggesting stopes nearby.
		59.4-67.1	Green-gray, chloritized and silicified andesite porphyry, Summit Mountain formation.
CR91-13	-60	0-3.0	Overburden.
		3.0-10.7	Silicified tuff.
		10.7-97.5	Quartz breccia vein with pyrite, amethyst, and sulfides and breccia fragments of tuff.
CR91-14	-90	0-24.4	Green-gray to brown tuff, silicified.
		24.4-61.0	Green-gray to brown, chloritized and silicified andesite with varying amounts of quartz, epidote, and pyrite.

Hole no.	HD	DI (m)	Description
CR91-15	-90	0-6.1	Silicified tuff.
		6.1-33.5	Quartz breccia vein with fragments of andesite and tuff and pyrite and sulfides, locally.
		33.5-61.0	Silicified and chloritized andesite porphyry, Summit Mountain formation.
CR91-17	-60	0-1.5	Overburden.
		1.5-48.8	Silicified, hematized tuff.
		48.8-103.6	Quartz breccia vein.
CR91-18	-60	0-1.5	Soil.
		1.5-24.4	Silicified tuff.
		24.4-97.5	Quartz breccia vein.
		97.5-103.6	Silicified tuff.
		103.6-106.7	Green-gray andesite, locally chloritized and silicified, Summit Mountain formation.
CR91-19	-60	0-12.2	Green-gray to brown chloritized andesite, Summit Mountain formation.
		12.2-42.7	Quartz breccia vein with fragments of silicified tuff and andesite.
		42.7-61.0	Green-gray to brown chloritized and silicified andesite, Summit Mountain formation.
CR91-20	-60	0-1.5	Overburden.
		1.5-83.8	Silicified tuff.
		83.8-91.4	Green-gray silicified and chloritized andesite, Summit Mountain formation.
		91.4-100.6	Silicified tuff.
		100.6-112.8	Quartz breccia vein with pyrite.
CR91-21	-90	0-1.5	Overburden.
		1.5-6.1	Silicified tuff.
		6.1-18.3	Quartz breccia vein.
		18.3-54.9	Silicified tuff.

TABLE 11.2—Summary of drill data at the Carlisle mine by WEACO, Ltd., 1991. Holes were drilled by reverse circulation and only drill cuttings are available. Samples were typically taken every 1.5 m and assayed (few exceptions). Only selected assays of drill intercepts are reported here. Depths are drill depths. Note holes CR91-2, -10, -11, -14, and -15 did not intercept the Carlisle vein.

Hole no.	Collar elevation (m)	Az	HD	Total depth (m)	Vein intercept (m)	Sample intercept (m)	Au oz/ton	Ag oz/ton	Cu ppm	Pb ppm	Zn ppm	Comments
CR91-1	1610.8	230	-50	54.9	12.2-36.6	12.2-13.7	0.006	<0.01	170	790	160	
						13.7-15.2	0.105	1.94	190	1450	195	
						15.2-16.8	0.755	11.49	300	1900	340	
						16.8-18.3	0.016	0.45	80	730	280	
CR91-2	1609.3	230	-50	103.6	-----	65.5-67.1	0.01	<0.01	60	4	80	Did not intersect vein?
CR91-3	1609.3	360	-60	67.1	13.7-19.8	12.2-13.7	0.016	<0.01	75	24	320	
						13.7-15.2	0.002	<0.01	100	210	305	
CR91-4	1606.2	357	-60	73.1	33.5-61.0	38.1-39.6	<0.002	0.02	60	26	485	Stope at 33.5-38.1.
CR91-5	1610.8	vertical	-90	36.6	9.1-29.0	16.8-18.3	0.09	3.97	130	760	940	Stope at 21.3-29.0 m.
						18.3-19.8	0.092	0.6	230	1600	1850	
						19.8-21.3	0.37	0.96	370	1250	1300	
						29.0-30.5	0.016	<0.01	195	265	1900	
CR91-6	1610.8	57	-60	18.3	1.5-15.2	12.2-13.7	0.004	0.01	450	1250	690	Stope at 9.1-13.7
CR91-7	1610.8	5	-60	42.7	1.5-22.9	7.6-9.1	0.34	0.25	670	1200	910	Stopes at 16.8-19.8, 24.4-36.6.
					24.4-36.6	9.1-13.7	0.04	<0.01	190	1300	425	
						13.7-15.2	0.028	0.27	1650	5700	6850	
						15.2-16.8	0.002	0.83	4200	2150	4400	
CR91-8	1610.8	vertical	-90	67.1	13.7-61.0	50.3-51.8	0.13	2.53	450	1600	3150	
						51.8-53.3	0.62	2.2	490	1150	3400	
						53.5-54.9	0.032	0.15	145	155	450	
CR91-9	1578.8	55	-60	24.4	0-10.7	6.1-7.6	0.002	1.64	22000	17000	41500	Drilled in pit.
						7.6-9.1	0.008	2.54	15000	9850	22500	
CR91-10	1606.2	215	-60	61.0	-----	19.8-21.3	0.014	0.31	110	85	235	Did not intersect vein.
						27.4-29.0	<0.002	1.76	70	55	170	
CR91-11	1606.2	215	-60	48.8	-----	16.8-18.3	0.01	<0.01	60	6	150	Did not intersect vein.
						30.5-32.0	<0.002	0.17	75	14	315	
						32.0-33.5	0.022	0.03	65	36	175	
CR91-12	1609.3	vertical	-90	67.1	18.3-59.4	24.4-25.9	0.012	0.03	180	100	100	Wood in some sample - backfilled stope?
						25.9-27.4	0.28	0.01	65	65	120	
						27.4-29.0	0.075	0.32	120	70	90	
						39.6-41.1	0.022	0.18	170	70	135	
CR91-13	1594	55	-60	97.5	10.7-97.5	88.4-89.9	0.046	0.42	1600	8950	7900	
						89.9-91.4	0.002	0.09	1100	1750	1800	
						91.4-93.0	0.034	0.19	1600	3400	2400	
CR91-14	1597.1	vertical	-90	61.0	-----	51.8-53.3	<0.002	<0.01	44	65	145	Did not intersect vein.
CR91-15		vertical	-90	42.7	-----	30.5-32.0	<0.002	<0.01	75	14	90	Section 2 mine, did not intersect vein.
CR91-16		vertical	-90	61.0	6.1-33.5	13.7-15.2	0.038	0.22				
						21.3-22.9	0.41	0.16	185	50	36	
CR91-17		60	-60	103.6	48.8-103.6	74.7-76.2	0.026	<0.01				
CR91-18		50	-60	106.7	24.4-97.5	77.7-79.2	0.016	<0.01	42	16	85	
						79.2-80.8	<0.002	<0.01	180	200	230	
CR91-19		50	-60	61.0	12.2-42.7	13.7-15.2	0.006	<0.01	34	8	24	
						15.2-16.8	0.008	<0.01	34	8	24	
CR91-20		50	-60	112.8	100.6-112.8	54.9-56.4	0.002	<0.01	28	2	75	
						99.1-100.6	0.002	0.18	30	110	90	
						100.6-120.1	0.002	0.02	1050	910	1300	
CR91-21		vertical	-90	54.9	6.1-18.3	19.8-21.3	<0.002	0.07	100	48	325	

Hole no.	HD	DI (m)	Description
Holes drilled by R&B Mining Co. on 10th level, Center mine (1992).			
*C-1S	+3	0–26.5	Green-gray, silicified andesite porphyry of Summit Mountain formation with disseminated chlorite, epidote, and pyrite and quartz and chlorite veins.
		26.5–29.5	Quartz vein with zones of galena, chalcopyrite, sphalerite, pyrite and fluorite.
		29.5–29.7	Green-gray silicified andesite porphyry with quartz, pyrite, and chlorite, Summit Mountain formation.
*C-2N	-18	0–150	Green-gray, silicified andesite porphyry of Summit Mountain formation with quartz, pyrite, and epidote veins.
	NOTE: Vein not intersected.		
*C-2S		0–4.3	Missing core.
		4.3–5.8	Gray silicified andesite porphyry with quartz and chlorite veins, Summit Mountain formation.
		5.8–7.3	Missing core.
		7.3–12.8	Gray silicified andesite porphyry with chlorite and pyrite veins, Summit Mountain formation.
		12.8–14.6	Quartz vein with pyrite and galena.
		14.6–16.5	Gray silicified andesite porphyry, Summit Mountain formation.
		16.5–18.6	Quartz vein with pyrite and galena.
*C-3S		0–10.4	Green-gray, silicified andesite porphyry with chlorite, pyrite, epidote, and quartz; Summit Mountain formation.
		10.4–11.9	Quartz vein with pyrite, galena, sphalerite, and chalcopyrite.
		11.9–19.8	Green-gray, silicified andesite porphyry; Summit Mountain formation.
		19.8–27.4	Quartz vein with zones of galena, pyrite, sphalerite, chalcopyrite, and trace fluorite.
		27.4–29.3	Green-gray, silicified andesite, Summit Mountain formation.

C-1S core not available.

Table 11.3—Summary of drill data of holes drilled at Center mine by R and B Mining Co. (1992-1993). Holes drilled on 10th level. Au, Ag and F by Robert Schantz. Cu, Pb, Zn, and Hg by NMBMMR chemical laboratory. C-1S, C-2N, and C-1N drilled at Drill Station No. 1 and C-2N and C-3N drilled at Drill Station No. 2 (Map 4). Depths are drill depths.

Hole no.	AZ	HD	Total depth (m)	Sample intercept (m)	Au oz/ton	Ag oz/ton	F%	Cu ppm	Pb ppm	Zn ppm	Hg%
C-1S*	S10W	+3	34.1	24.4-25.0	0.011	0.71	0.87	157	775	596	0.09
				25.6-26.2	0.076	0.59	0.22	56	33	234	<0.02
				26.2-26.8	0.077	3.58	1.1	1600	2300	4200	0.02
				26.8-27.4	0.24	11.00	0.82	1900	7400	4100	<0.02
				27.4-28.0	1.55	75.8	0.54	1100	4000	8300	<0.02
				28.0-28.6	0.008	0.63	0.35	3000	1300	3200	0.21
				28.6-29.7	0.63	1.56	1.31	477	5500	2900	0.03
C-2N*	N70W	-18	45.7	36.6-38.1	0.001	<0.05	0.14	--	--	--	--
				38.1-39.6	0.003	0.53	0.1	--	--	--	--
				39.6-41.1	0.007	0.2	0.12	--	--	--	--
				41.1-42.7	0.002	0.2	0.17	--	--	--	--
				42.7-45.7	0.003	<0.05	0.11	--	--	--	--
				45.7-47.2	0.003	0.25	0.13	--	--	--	--
C-3S	N6SE	0	29.3	10.4-11.9	0.005	0.29	0.38	--	--	--	--
				19.8-21.3	0.003	<0.05	0.102	--	--	--	--
				21.3-22.2	0.003	0.23	0.281	--	--	--	--
				22.2-23.5	0.053	<0.05	0.046	--	--	--	--
				23.5-24.4	0.035	0.74	0.054	--	--	--	--
				24.4-25.2	0.022	1.10	0.045	--	--	--	--
				25.2-26.5	0.215	8.91	0.042	--	--	--	--
				26.5-27.4	0.023	0.09	0.144	--	--	--	--
C-2S	N30E	0	18.6	12.8-13.7	0.031	1.38	0.03	--	--	--	--
				13.7-14.6	*12.35	7.37	0.19	--	--	--	--
				14.6-15.5	0.002	0.02	0.07	--	--	--	--
				15.5-16.5	0.161	17.94	0.04	--	--	--	--
				16.5-18.6	0.139	3.45	0.05				

*Reassayed sample 12.8-13.7 and obtained 12.01 oz/ton Au.

Table 11.4 - Summary of limited data of holes drilled at the Center mine by Dresser Minerals (file maps 1976, 1978). Depths are assumed to be true depths. AZ = Azimuth in degrees; HD = hole declination in degrees.

Hole no.	Collar elev. (m)	Az	HD	Sample intercept (m)	Au oz/ton	Ag oz/ton	Cu%	Pb%	Zn%
BC1	1619.6	N0E	-73	--	0.06	1.35	--	--	--
BC2	1602.6	N16E	-65	--	no values				
BC3	1600.4	N23E	-62.5	109.7-114.0	0.67	26.0	--	--	--
				166.4-168.5	0.30	0.81	0.21	3.5	4.44
BC4	1600.4	N23E	-48.5	95.4-96.0	0.4?	2.7	--	--	--
				127.4-128.0	0.3	17.9	0.9	1.2	1.8
BC5	1596.2	N23E	-44	113.7-114.9	0.61	30.3	--	--	--
				121.0-121.9	0.58	3.24	--	--	--
				122.8-123.4	0.38	0.4	0.24	6.9	7.2
BC7	1602.2	N3W	-60	123.0-124.3	0.64	16.6	0.05	1.3	0.5
BC8	1602.6	N16E	-51	103.0-118.0	low grade values				
BC9	1595.9	N16E	-65	139.9-141.1	0.22	4.73	--	--	--
				139.9-150.9	0.01	0.3	0.5	2.5	3.9
BC10	1589.1	N14E	-67	196.0-205.7	--	0.36	--	--	--
BC11	1594.3	N0E	-82	166.4-175.6	0.01	0.94	0.5	nil	0.7
BC6	1596.2	N20E	-60.5		no values				
P1	1590.4	N10E	-54	96.6-97.5	0.03	4.57	1.5	0.1	0.1

11.1.2 Alabama mine

Brief descriptions and summary of drill data (Table 11.5) from two holes drilled by Great Lakes Exploration, Inc. at the Alabama mine are below. Location of holes in Figure 2.19. The core is stored at NMBMMR. Az - azimuth in degrees. HD - hole declination in degrees. DI - drill depth interval.

Hole no.	Az	HD	DI (m)	Description
*A1	N76E	-45	0-34.7	Green-gray to gray, chloritized porphyritic to amygdaloidal andesite of Dark Thunder Canyon formation. Locally cut by veins of quartz, chlorite, pyrite, and epidote.
			34.7-37.6	Silica-hematite breccia vein consisting of brecciated fragments of andesite and rhyolite in quartz-hematite matrix with local disseminated pyrite and other sulfides.
			37.6-44.1	Silicified intrusive rhyolite with local hematite.
			44.1-56.1	Green-gray, chloritized porphyritic to amygdaloidal andesite of Dark Thunder Canyon formation.
*A2	S75S	-65	0-61.9	Green-gray to gray, chloritized porphyritic to amygdaloidal andesite of Dark Thunder Canyon formation. Locally cut by quartz, chlorite, pyrite, and epidote veins.
			61.9-66.4	Brecciated andesite, bleached and hematized.
			66.4-68.9	Silica-hematite breccia vein consisting of brecciated fragments of andesite and rhyolite in quartz-hematite matrix with local disseminated pyrite and other sulfides. Visible gold reported. Cut by late calcite veins.
			68.9-70.1	Silicified rhyolite intrusive.
			70.1-77.4	Green-gray to gray, chloritzed and silicified porphyritic to amygduloidal andesite of Dark Thunder Canyon formation.

Table 11.5 - Summary of drill data at the Alabama mine by Great Lakes Exploration, Inc. (1991). Drill core from both holes examined for this study. AZ = Azimuth in degrees; HD = hole declination in degrees. Depths are drill depths.

Hole no.	Collar elev. (m)	Az	HD	Total depth (m)	Vein intercept (m)	Au oz/ton	Ag oz/ton	Comments
*A-1	1577.3	N76 E	-45	56.1	34.7-37.6	0.005	0.28	Test beneath south ore zone.
*A-2	1571.2	S75 S	-65	77.4	66.4-70.1			Test beneath south ore zone.
					66.4-67.1	0.134	0.32	

11.1.3 Jim Crow-Imperial mines (Queenstake Resources, Ltd., 1984, 1987).

Below are brief descriptions of the drill core and a summary of drill data is in Table 11.6. Core from holes J84-2 and J84-3 were were examined for this study. Remaining descriptions are from unpublished reports by Queenstake Resources, Inc. Formation names in parentheses. HD = hole declination in degrees; DI = Drill depth interval.

Hole no.	HD	DI (m)	Description
J84-1	-60	0-25.3	Amygdaloidal andesite flows (Dark Thunder Canyon formation).
		25.3-56.6	Lithic-rich younger ash-flow tuff, top is poorly welded, whereas the rest of the unit is densely to moderately welded.
		56.6-74.7	Green-gray amygdaloidal andesite flows. Chloritization increases with depth (Dark Thunder Canyon formation).
		74.7-111.2	Quartz-sulfide veins in silicified hematite breccia zone.
		111.2-111.6	Andesite altered to gray clay (andesite of Mt. Royal?).
*J84-2	-75	0-3.7	Rotary drilled—no core.
		3.7-21.3	Amygdaloidal andesite flows of Dark Thunder Canyon formation with chlorite, hematite and calcite.
		21.3-47.9	Lithic-rich, younger ash-flow tuff. Densely welded in center. Hematized zones.
		47.9-89.0	Amygdaloidal andesite flows of Dark Thunder Canyon formation with chlorite, hematite, calcite and local quartz.
		89.0-93.3	Quartz-sulfide veins in hematite quartz breccia veins.
		93.3-111.6	Andesite, silicified, Dark Thunder Canyon formation.
		111.6-124.7	Quartz-sulfide-calcite veins
		124.7-130.8	Andesite of Mt. Royal.
*J84-3	-57	0-24.4	Amygdaloidal andesite flows of Dark Thunder Canyon formation with calcite, hematite, and chlorite.
		24.4-53.6	Lithic-rich, younger ash-flow tuff. Densely welded in the center. Hematized zones.
*J84-3		53.6-73.1	Amygdaloidal andesite flows of Dark Thunder Canyon formation with calcite, hematite, chlorite, and quartz.
		73.1-92.7	Quartz-hematite breccia with quartz-sulfide veins.
		92.7-93.6	Andesite of Mt. Royal(?).
J87-1	-60	0-18.3	Amygdaloidal andesite flows (Dark Thunder Canyon formation). Propyllic alteration. Veinlets of calcite, chlorite, quartz, and clay.
		18.3-47.3	Lithic-rich, younger ash-flow tuff with densely welded center.
		47.3-80.3	Amygdaloidal andesite flows (Dark Thunder Canyon formation). Highly sheared and fractured.
		80.8-96.9	Quartz-sulfide veins in silicified hematite breccia zone.
		96.9-101.5	Andesite of Mt. Royal(?).

Hole no.	HD	DI (m)	Description
J87-2	-55	0-18.3	Amygdaloidal andesite flows (Dark Thunder Canyon formation). Propyllic alteration. Veinlets of calcite, chlorite, quartz, and clay.
		18.3-48.8	Lithic-rich younger ash-flow tuff with densely welded center.
		48.8-74.7	Amygdaloidal andesite flows (Dark Thunder Canyon formation). Highly sheared and fractured. Veinlets of quartz, calcite, and hematite.
		74.7-83.2	Quartz-sulfide veins in silicified hematite breccia zone.
		83.2-88.1	Andesite of Mt. Royal(?).
J87-3	-65	0-18.9	Amygdaloidal andesite flows (Dark Thunder Canyon formation). Propyllic alteration. Veinlets of calcite, quartz, chlorite, hematite, and clay.
		18.9-42.7	Lithic-rich, younger ash-flow tuff with densely welded center.
		42.7-82.3	Amygdaloidal andesite flows (Dark Thunder Canyon formation). Highly sheared and fractured. Veinlets of quartz, calcite and hematite.
		82.3-90.6	Quartz-sulfide veinlets in silicified hematite breccia zone.
		90.6-93.0	Andesite of Mt. Royal(?).
J87-4	-45	0-24.7	Amygdaloidal andesite (Dark Thunder Canyon formation). Propyllitic alteration.
		24.7-61.3	Lithic-rich, younger ash-flow tuff with densely welded center.
		61.3-78.1	Amygdaloidal andesite flows (Dark Thunder Canyon formation). Highly sheared and fractured.
		78.1-85.7	Quartz-sulfide veinlets in silicified hematite breccia zone.
		85.7-88.7	Andesite of Mt. Royal(?).

Table 11.6 - Summary of drill data at Jim Crow-Imperial mines by Queenstake Resources, Inc., 1984, 1987. AZ = Azimuth in degrees; HD = hole declination in degrees. *Assayed by NMBMMR chemical laboratory (zones in the younger ash-flow tuff). Depths are drill depths.

Hole no.	Collar elev. (m)	AZ	HD	Total depth (m)	Vein/Sample intercept (m)	Au oz/ton	Ag oz/ton	Comments
J84-1	1445.6	N90E	-60	111.6	74.7-111.2	--	--	Imperial vein
					93.1-96.0	0.071	1.98	--
					93.1-94.2	0.115	2.6	--
J84-2	1445.6	N90E	-75	130.8	*68.0-68.2	0	0	Imperial vein
					94.5-112.2	--	--	--
					101.6-102.0	0.044	0.72	--
					114.0-114.8	0.016	1.16	--
J84-3	1438.6	N80E	-57	93.6	*52.7-53.0	0	0	Imperial vein
					68.4-84.4	--	--	--
					77.1-78.3	0.099	1.96	--
					80.8-83.8	0.269	45.53	--
J87-1	1438.6	N80E	-80	101.5	71.9-75.5	--	--	Imperial vein
					73.9-75.5	0.035	0.01	--
					85.2-96.6	--	--	--
					83.0-95.4	0.021	2.2	--
J87-2	1438.6	N80E	-55	88.1	64.2-65.7	--	--	Imperial vein
					64.2-64.5	0.025	0.1	--
					67.8-83.2	--	--	--
					78.9-81.1	0.51	1.53	--
J84-3	1438.6	N80E	-65	93.0	82.9-90.9	--	--	Imperial vein
					86.0-87.5	0.037	2.67	--
J84-4	1438.6	N80E	-45	88.7	63.2-63.5	<0.005	0.05	Imperial vein
					65.2-68.7	--	--	--
					67.2-67.6	0.005	0.38	--
					75.6-85.6	--	--	--
					81.0-84.1	0.066	3.54	--

11.1.4 Summit area

The most extensive drilling in the Steeple Rock district has been along the East Camp-Summit fault from south of the Summit mine northwestward to north of the Mohawk mine. Inspiration Minerals, Inc. drilled 15 holes underneath the Apex-Summit workings and delineated additional ore (Table 11.7). Subsequently NovaGold Resources, Ltd. drilled along the vein in 1988–1989. In 1989 NovaGold entered a joint venture agreement with Biron Bay Resources, Ltd. and additional holes were drilled in 1990, 1991, and 1992 (Table 11.8). Biron Bay Resources, Ltd. is the controlling partner in the joint venture. Most of this drill core is available for study, however, only five holes were examined for this project due to time constraints. Three descriptions are presented here.

Hole no.	HD	DI (m)	Description
S88-5	-36	0-21.3	Brown to white silicified and iron-stained tuff.
		21.3-64.3	Gray andesite porphyry (Summit Mountain formation), locally silicified, brecciated and with abundant chlorite.
		64.3-70.1	Brown, poorly sorted, fine-grained sandstone.
		70.1-77.4	Brown to gray conglomerate.
		77.4-108.4	Gray andesite porphyry.
		108.4-110.8	Quartz breccia vein with pyrite.
		110.8-164.9	Interbedded gray andesite porphyry, volcanic breccias, and thin brown sandstones, locally brecciated, silicified, and iron-stained (Summit Mountain formation).
B91-17	-77	0-10.7	Silicified, white to tan tuff.
		10.7-128.6	Green-gray andsite porphyry with thin veins of quartz, chlorite, pyrite, and disseminated pyrite and chlorite (Summit Mountain formation).
		128.6-132.3	Quartz breccia vein with pyrite.
		132.3-166.1	Silicified gray to green-gray andesite porphyry.
		166.1-286.5	Green-gray andesite porphyry with zones of gray to white silicification and green chlorite.
		286.5-309.0	Quartz breccia veins with zones of silicified andesite porphyry.
		309.0-324.4	Green-gray to gray andesite porphyry with silicified zones.
		324.4-366.0	Silicified green-gray to gray andesite porphyry (Summit Mountain formation).
M91-4	-60	0-9.8	Silicified iron-stained white to tan tuff.
		9.8-85.6	Gray to green-gray andesite porphyry with thin veins of quartz, calcite, chlorite, and pyrite (Summit Mountain formation).
		85.6-89.6	Silicified gray to white andesite porphyry.
		89.6-271.6	Green-gray andesite porphyry.
		271.6-274.3	Gray to brown, poorly sorted, matrix-supported volcanic breccia (Summit Mountain formation).
		274.3-279.2	Green-gray to gray andesite porphyry with zones of white silicification.
		279.2-457.8	White to gray silicified andesite porphyry with veins of quartz, bladed calcite, pyrite, and local fluorite.
		457.8-469.4	White to light gray silicified andesite porphyry with disseminated pyrite, chalcopyrite, galena, and sphalerite.
		469.4-522.4	White to light gray silicified andesite porphyry
		522.4-618.5	Gray to green-gray andesite porphyry with white silicified zones and zones of veins of quartz, calcite, pyrite, and chalcopyrite-galena-sphalerite. Chlorite increases toward bottom of hole (Summit Mountain formation).

Table 11.7—Summary of drill data by Inspiration Mines, Inc., 1983-1984. Depths are drill depths.

Hole no.	Collar elev. (m)	Az	HD	Total depth (m)	Vein intercept (m)	Au oz/ton	Ag oz/ton	Comments
S-1	1757.8	S48 12'W	-35	158.2	100.5-146.6	0.025	1.376	Beneath stopes in Summit
					114.6-118.6	0.042	2.728	adit
S-2	1758.6	S66W -	-25	174.3	122.5-134.1	0.027	1.808	Beneath stopes in Summit
					130.4-134.1	0.034	2.733	adit
S-3	1762.1	S53 25'W	-20	154.5	128.9-143.6	---	---	Beneath surface outcrop
					136.5-142.3	0.083	17.55	
S-4	1761.5	S52 5'W	-45	203.9	155.1-191.1	---	---	Beneath hole S-3
					173.4-181.3	0.8	6.78	
S-5	1755.8	S49 7'W	-15	92.3	74.7-84.4	---	---	Beneath surface outcrop
					80.8-84.4	0.024	1.32	
S-6	1755.6	S46 40'W	-45	110.0	83.8-98.8	minor	minor	Beneath hole S-5.
S-7	1750.5	S5 9'E	-15	77.4	52.7-69.9	---	---	Test northwest extension of
					63.7-68.3	0.051	3.88	Apex level
S-8	1750.4	S31 47'W	-15	79.8	57.3-73.5	---	---	Test beneath hole S-7
					68.3-72.5	0.023	1.64	
S-9	1750.2	S55 28'W	-15	131.4	76.2-107.9	---	---	Test northwest of S-8
					83.5-89.8	0.035	2.15	
					93.0-96.0	0.035	2.31	
					99.1-105.2	0.053	2.36	
S-10	1761.7	S37 28'W	-22	185.9	133.8-179.2	---	---	Test below Summit level
					158.8-164.6	0.048	2.085	
S-11	1728.4	N88 43'W	-28	128.3	96.0-122.2	---	---	Test below Juan's stope
					97.5-102.4	0.016	1.996	Hanging wall
					119.2-122.2	0.115	16.25	Footwall
S-12	1753.2	S8 43'W	-14	123.7	77.1-114.4	---	---	Test Billali ore shoot
					95.1-100.9	0.036	1.38	
					105.2-106.7	0.04	2.2	
S-13	1752.5	S50 W	-13	152.1	71.0-94.5	0	0	Test west of hole S-12
					119.8-147.2	---	---	
					128.3-137.5	0.013	1.105	
S-14	1706.8	N5 E	-35	119.2	38.4-99.1	---	---	Test extension of Apex level
					58.2-63.1	0.019	1.69	
S-15	1706.8	N35 E	-30	57.3	39.9-57.3	minor	minor	Test east of hole S-14

Table 11.8—Summary of drill data along the East Camp-Summit fault, Nova Gold Resources, Ltd. and Biron Bay Resources, Ltd., 1988–1992. Data from some holes are unavailable. Assays are either high zones (less than 1.0 m intercept) or calculated over a specified depth interval. AZ — Azimuth in degrees. HD – Hole declination in degrees. * Holes examined for this study. Depths are drill depths.

Hole no.	Collar elevation (m)	Az	HD	Total depth (m)	Sample intercept (m)	Au oz/ton	Ag oz/ton	Comments
S88-1	1726.6	235	-47	196.0	156.4-158.1	0.016	1.32	--
S88-2	1744.9	223	-46	366.4	205.7-228.0	0.094	3.13	--
S88-3	1726.6	235	-80	317.0	268.9-290.0	tr	0.05	--
S88-4	1744.9	223	-68	424.9	322.5-333.1	0.028	1.55	--
S88-5*	1709.2	48	-36	164.9	108.4-110.8	0.201	5.21	--
S88-6	1673.9	238	-50	146.9	83.8-85.3	0.190	0.25	--
S88-7	1655.3	235	-63	299.9	229.8-231.9	0.045	3.17	--
S88-8	1738.5	225	-45	294.4	258.8-264.9	0.044	4.77	--
S88-9	1746.7	225	-53	318.2	262.4-298.9	0.145	16.8	--
S88-10	1738.5	225	-66	388.3	356.8-358.3	0.023	2.76	--
S88-11	1655.3	225	-71	464.8	390.4-404.1	0.007	0.69	--
S88-12	1694.6	225	-52	211.2	169.3-170.5	0.008	0.91	--
S88-13	1749.5	210	-43	305.1	167.5-176.5	0.052	4.69	--
S88-14	1741.8	210	-43	287.8	79.2-80.8	0.014	1.54	--
S88-15	1749.5	210	-70	324.3	245.0-271.6	0.073	5.04	--
S89-1	1746.7	220	-42	284.1	179.9-180.7	0.081	11.5	--
					225.5-232.2	0.061	3.58	--
					229.2-232.2	0.07	3.81	--
S89-2	1746.7	220	-62	367.0	310.3-311.5	0.124	1.0	--
					317.6-321.9	0.22	19.2	--
S89-3	1738.5	222	-30	276.4	191.4-195.1	0.017	1.3	--
					191.4-193.5	0.024	1.97	--
S89-4	1738.5	225	-55	329.5	291.7-294.1	0.021	2.37	--
S89-5	1746.7	225	-53	75.4	256.6-289.2	0.032	23.95	--
					274.3-276.4	0.056	1.95	--
					284.1-289.2	0.368	55.929	--
S89-6	1781.5	230	-45	204.8	158.5-169.5	0.157	4.626	--
					163.1-169.5	0.258	7.36	--
					166.1-169.5	0.444	12.6	--
S89-7	1741.8	210	-57	229.8	84.2-87.5	0.035	2.736	--
					191.1-192.9	0.006	1.0	--
S89-8	1741.8	210	-65	256.6	95.7-105.8	0.043	2.55	--
					103.0-105.8	0.087	6.83	--
					213.3-218.2	0.015	1.22	--
S89-9	1728.1	210	-55	321.5	261.2-263.0	0.075	6.025	--
					263.0-263.9	0.01	0.45	--
					263.9-264.9	0.054	2.65	--
S89-10	1728.1	210	-65	360.9	310.0-313.3	0.022	3.54	--
					331.3-332.2	0.04	4.45	--
S89-11	1694.6	229	-45	153.6	--	--	--	--
S89-12	1694.6	229	-70	209.1	--	--	--	--
S89-13	1682.4	211	-60	273.4	--	--	--	--
S89-14	1682.4	211	-69	284.4	--	--	--	--
S90-1	1749.5	210	-60	280.4	220.7-224.3	0.034	1.07	--
S90-2	1664.1	210	-45	489.5	--	--	--	--
S90-3	1751.0	229	-62	312.7	214.6-216.7	0.305	8.68	--
					228.3-233.5	0.056	4.94	--

Table 11.8 (continued)

Hole no.	Collar elevation (m)	Az	HD	Total depth (m)	Sample intercept (m)	Au oz/ton	Ag oz/ton	Comments
					2253.6-258.5	0.289	0.47	--
S90-4	1741.0	229	-70	362.4	285.3-290.5	0.076	7.23	--
					287.1-288.9	0.11	13.35	--
					299.9-301.1	0.096	0.05	--
S90-5	1664.1	200	-45	504.7	--	--	--	--
S90-6	1751.0	229	-50	274.3	174.0-174.6	0.352	6.75	--
					185.3-187.1	0.107	8.275	--
S90-7	1743.4	229	-45	320.1	267.0-267.3	0.097	5.95	--
S90-8	1715.9	229	-52	480.0	396.1-396.4	0.665	111.0	--
S90-9	1743.4	229	-56	376.1	324.0-327.3	0.039	3.75	--
S90-10	1604.7	43	-45	169.8	100.9-121.9	0.071	0.32	Norman King
					134.4-135.3	0.098	0.3	--
S90-11	1604.7	43	-60	232.2	117.0-118.3	0.102	0.15	Summit
S90-12	1633.6	50	-47	170.7	116.1-123.0	0.109	0.05 FW	Norman King
					137.5-141.1	0.046	3.73 HW	--
S90-13	1633.6	50	-60	247.2	163.4-164.3	0.297	0.25	Norman King
S90-14	1621.5	235	-45	181.0	123.9-124.8	1.28	0.75 FW	Billali
S90-15	1621.5	247	-65	202.5	151.5-152.1	0.043	0.05	Summit
					166.1-167.3	0.056	0.05	--
S90-16	1624.5	222	-45	211.2	88.4-89.0	0.179	8.25	--
S90-17	1624.5	222	-75	175.3	122.8-124.0	0.079	0.2	--
S90-18	1624.5	222	-7	112.5	67.4-71.3	0.091	6.47	Billali
S90-19	1630.6	224	-68	239.3	54.3-55.2	0.128	9.1	Summit
S90-20	1744.9	227	-40	201.2	164.9-166.7	0.091	7.93	Summit
S90-21	1630.6	224	-40	171.0	105.8-108.2	0.52	23.86	Billali
S90-22	1630.6	224	0	119.5	106.7-109.4	0.096	7.46	Billali
S90-23	1636.7	227	-54	144.8	83.2-86.6	0.142	10.3	Billali
S90-24	1744.9	227	-58	257.2	203.0-205.4	0.046	4.07	Summit
S90-25	1636.7	227	-76	187.1	89.1-89.9	0.035	3.05	--
S90-26	1744.9	227	-71	274.0	255.7-260.3	0.288	15.211	--
S90-27	1636.7	226	-23	121.9	39.6-40.6	0.048	0.8	--
S90-28	1744.3	227	-58	295.6	252.7-255.4	0.089	6.43	--
S90-29	1667.2	270	-45	158.2	67.7-68.6	0.018	3.2	--
S90-29R	1667.2	268	-45	77.1	--	--	--	--
S90-30	1744.3	227	-29	213.3	178.9-179.8	0.254	10.7	--
S90-31	1652.8	270	-45	156.7	--	--	--	--
S90-32	1652.8	270	-65	213.7	--	--	--	--
S90-33	1749.5	180	-60	223.7	201.5-204.2	0.08	3.37	--
S90-34	1712.9	227	-55	487.7	338.8-339.8	0.046	1.05	--
S90-35	1749.5	180	-42	192.0	146.6-149.3	0.1	5.25	--
S90-36	1749.5	180	-70	360.9	288.6-289.2	0.182	8.2	--
S90-37	1712.9	225	-62	621.8	243.8-244.7	0.118	6.65	--
S90-38	1749.5	206	-55	222.5	177.7-180.4	0.368	2.83	--
S90-39	1749.5	206	-72	397.4	204.2-206.9	0.028	2.3	--
S91-1		229	-50	378.5	337.7-338.6	0.041	4.58	--
					338.6-339.5	0.032	3.33	--
					339.5-340.4	0.075	7.22	--
					340.4-341.4	0.028	2.03	--
S91-2	--	211	-36	439.8	258.6-259.2	0.043	0.05	--
					259.2-259.5	0.007	<0.05	--
					259.5-260.0	0.018	0.45	--
					395.7-396.5	0.005	0.05	--

Table 11.8 (continued)

Hole no.	Collar elevation (m)	Az	HD	Total depth (m)	Sample intercept (m)	Au oz/ton	Ag oz/ton	Comments
S91-3		227	-38	358.1	87.2-91.4	tr	0.3	--
					298.7-299.3	0.012	0.7	--
					299.3-300.2	0.011	0.6	--
					328.6-329.5	0.006	0.6	--
S91-4		210	-50	568.1	242.6-243.8	0.012	0.1	--
S91-5		229	-55	247.2	210.5-212.6	0.034	2.75	--
					217.0-219.4	0.039	1.775	--
S91-6	1673.3	229	-38	219.8	171.6-173.4	0.093	6.04	Summit
S91-7		235	-39	177.7	153.9-158.2	0.159	29.77	Summit
S91-8		206	-49	506.6	279.2-280.0	0.011	0.04	Summit
S91-9		235	-57	229.5	205.1-206.3	0.05	8.8	Summit
S91-10		235	-70	303.3	236.5-237.4	0.03	0.35	--
S91-11		196	-33	107.3	83.8-88.4	0.176	13.77	--
S91-12		--	--	--	--	--	--	--
S91-13		206	-66	318.2	266.7-268.5	0.06	2.12	--
S91-14		206	-35	270.0	180.0-180.9	0.006	0.2	--
S91-15		235	-51	376.7	335.6-336.5	0.006	0.25	--
S91-16		207	-45	189.9	108.5-109.4	0.038	1.25	--
S91-17		206	-61	586.4	287.4-288.3	0.025	0.2	--
S91-18		207	-62	263.3	212.3-213.0	0.259	0.8	--
S91-19		230	-40	300.2	200.0-200.8	0.016	0.25	--
S91-20		207	-73	318.5	122.8-127.1	0.059	3.89	--
					132.6-135.0	0.064	3.73	--
					141.1-145.1	0.047	7.2	--
					154.2-156.0	0.098	5.18	--
S91-21		196	-38	265.5	203.6-203.9	0.281	2.55	--
S91-22		--	--	--	--	--	--	--
		0.048	3.15	--	--	--	--	--
S91-23		196	-48	332.8	216.1-220.1	0.84	3.87	--
					273.7-277.4	0.043	5.36	--
S91-24		196	-57	387.4	329.8-330.4	0.052	2.1	--
B91-16		224	-45	189.9	70.7-75.1	0.301	21.8	Billali
B91-17*		228	-77	366.0	324.4-343.6	0.033	0.08	--
					289.5-290.5	0.043	0.2	--
					304.5-305.4	0.025	0.45	--
					305.4-306.3	0.022	0.3	--
B91-18		Vert	Vert	477.3	342.4-343.6	0.034	0.05	--
					94.2-95.7	0.03	0.1	--
					118.3-119.2	0.04	0.05	--
B91-19		Vert	Vert	306.0	--	--	--	--
B91-20		Vert	Vert	275.5	81.1-84.7	0.113	6.0	--
					92.7-96.5	0.205	8.73	--
					158.6-155.4	0.098	5.27	--
					133.5-139.6	0.286	16.93	--
B91-21		Vert	Vert	394.4	191.4-193.5	0.021	0.78	--
					200.5-201.8	0.022	0.35	--
					216.4-220.4	0.024	0.13	--
					224.9-226.2	0.035	0.45	--
B91-22		226	-80	199.3	--	--	--	--
B92-1		226	-76	182.9	--	--	--	--
M91-1		228	-45	274.3	--	--	--	Mohawk
M91-3		45	-45	515.7	--	--	--	--

Table 11.8 (continued)

Hole no.	Collar elevation (m)	Az	HD	Total depth (m)	Sample intercept (m)	Au oz/ton	Ag oz/ton	Comments
M91-4*		45	-60	613.5	461.1-462.7	0.299	14.0	--
SE91-1		3	-45	292.6	212.5-213.3	0.097	0.2	--
SE91-2		3	-60	253.9	--	--	--	--

11.1.5 Telephone Ridge-Raeburn Hills areas

Limited drill data were available from holes drilled on Telephone Ridge by Pioneer Nuclear, Inc. in 1984 (Table 11.9) and in the Raeburn Hills area by FMC Gold Co. in 1988 (Table 11.10). Neither cuttings nor core were available. Location of drill holes in Figs. 5.7, 5.11, and Map 2. Both areas were drilled to located potential gold deposits related to the acid-sulfate alteration. Brief description of drill core from Telephone Ridge from Pioneer Nuclear, Inc. maps is below.

Hole no.	HD	DI (m)	Description
SRIC	-45	0-4.2	Soil
		4.2-45.7	Bleached argilized acid-sulfate, silicified zones.
		45.7-49.7	Ash-flow tuff (Bloodgood Canyon Tuff??).
		70.1	Fluorite veins with pyrite.
		75.0-153.6	Altered ash-flow tuff or tuffaceous sediments.
		153.6-349.9	Green gray to dark gray andesite of Summit Mountain formation.
SR2C	-60	0-26.2	Green-gray andesite of Summit Mountain formation.
		26.2-60.0	Maroon to green to gray acid-sulfate altered tuffs or andesite.
		60.0-86.3	Quartz veins cutting altered rock.
		86.3-97.2	Tuff.
SR3C	-50	0-27.7	Green-gray andesite of the Summit Mountain formation.
		27.7-117.0	Acid-sulfate altered rock with thin quartz veins.
		117.0-289.2	Green-gray andesite of the Summit Mountain formation.
SR4C	-50	0-20.0	Green-gray andesite of the Summit Mountain formation.
		20.0-?	Acid-sulfate altered rock. (Additional data not available.)

Table 11.9—Summary of drill data from Telephone Ridge area by Pioneer Nuclear, Inc., 1984. Az = Azimuth in degrees; HD = hole declination in degrees. Depths are drill depths.

Hole no.	Collar elev. (m)	Az	HD	Total depth (m)	Sample intercept (m)	Au oz/ton	Ag oz/ton	Comments
SR1C	1670.2	S33W	-45	349.9	10.7-12.1	0.002	0.05	Thin veinlets. Argillic altered.
					19.8-21.3	0.005	<0.05	Brecciated. Argillic altered.
					21.3-22.2	0.004	0.05	Silicified rubble zone.
					32.9-34.4	0.002	0.05	Strongly fractured zone.
					71.6-73.1	0.005	0.15	Strongly fractured zone.
					83.5-85.6	0.077	0.05	Silicified rubble zone.
					85.6-87.2	0.004	0.05	Breccia zone.
					87.2-87.5	0.006	<0.02	Pyrite disseminations.
					182.0-184.4	0.001	0.25	Thin quartz-pyrite vein.
SR2C	1670.2	S33W	-60	97.2				
SR3C	1670.2	S70W	-50	289.2	9.1-10.7	0.002	0.05	Thin veins
					15.2-16.7	0.007	0.1	Clay zone
					21.3-22.8	0.008	0.05	Quartz veinlets
					42.7-44.2	0.011	<0.05	Silicified breccia
					44.2-45.8	0.02	0.01	Silicified breccia
					45.8-47.2	0.006	0.1	Silicified breccia with pyrite.
					47.2-48.8	0.012	0.05	Silicified breccia with pyrite.
					48.8-50.3	0.016	0.05	Silicified breccia with pyrite.
					50.3-51.8	0.012	<0.05	Silicified zone
					51.8-53.3	0.011	tr	Silicified zone
					91.7-92.3	0.003	0.15	Quartz-pyrite veins
					99.1-100.6	tr	0.2	Quartz-pyrite vines
					218.4-218.7	0.001	0.1	Quartz-clay-pyrite veins
SR4C		S70W	-50	354.8	234.7-235.9	tr	1.1	Quartz-pyrite veins

Table 11.10—Summary of drill data from the Raeburn Hills area by FMC Gold Co. (1988). Only some cuttings left at the drill sites could be examined for this study. Data is from E. M. Crist (unpublished report, October 1988). Az = Azimuth in degrees; HD = hole declination in degrees. Depths are drill depths.

Hole no.	Collar elev.	Az	HD	Total depth (m)	Au range oz/ton	Comments
M-1	1639.7	S43 W	?	?		Test Blue Bell fault.
M-2	1636.7	N43 E	?	?		Test Blue Bell fault.
M-3	1648.9	S70 E	?	?		North end of the Knob.
M-4	1731.2	S40 W	?	?		Test the Knob.
M-5	1661.1	S43 W	?	?		Test south end of Raeburn Hills.
M-6	1731.2	vertical	90	254.5	0.005-0.07	Test the Knob.
M-7	1731.2	vertical	90	170.7	0.005	Test the Knob.
M-8	1706.8	vertical	90	152.4	0.005-0.015	Test the Knob.
M-9	1731.2	vertical	90	175.3	none	Test south end of Raeburn Hills.
M-10	1740.3	vertical	90	85.3	none	Test silicified zone east of Raeburn Hills.
M-11	1676.3	vertical	90	157.0	0.02	Raeburn Hills.
M-12	1679.4	vertical	90	121.9	0.005	Test East Camp fault near Carnation mine.

11.1.6 Bitter Creek BCl (Kennecott Co., sec. 20, T16S, R21W, 1954)

A brief description of available core from the Kennecott hole in Bitter Creek is below. The hole was drilled to a total depth of 746 m (Hedlund, 1990b), but some of the core is missing. This drill core is stored at the USGS core facility in Denver, CO, and was examined for this study because it provides the only subsurface data in the Bitter Creek area. The collar elevation, exact location, azimuth, and hole declination are unknown, but it is assumed that the hole was vertical. Approximate location of the drill hole is plotted on Map 2. It is possible that some of the missing core may represent altered or mineralized zones. Assays are not available, but several samples were collected and assayed for this study (Table 11.12). Data for samples collected are in Appendices 11.3, 11.4, 11.5, and 11.6. Depths are drill depths.

Hole No.	Hole declination	Depth interval (m)	Description
*BCl	vertical(?)	0-29	Core missing
		29-33.5	Gray to bleached yellow andesite porphyry of the Summit Mountain formation with chlorite altered zones and zones of disseminated pyrite (Appendix 11.3). Calcite veins.
		33.5-58.0	Core missing.
		58.0-62.2	Green-gray andesite porphyry with chlorite alteration; Summit Mountain formation.
		62.2-71.6	Core missing.
		71.6-82.6	Gray to brown andesite porphyry of Summit Mountain formation. Feldspars altered to white to yellow clay. Calcite veins.
		82.6-85.3	Green to colorless fluorite vein with some quartz, calcite, and manganese oxides.
		85.3-114.0	Green-gray andesite porphyry. Summit Mountain formation with thin veinlets (<2 cm wide) of quartz, calcite, galena, pyrite, sphalerite, chalcopyrite and fluorite. (Assays of a sample in Table 11.10.) Chlorite and mixed clays in host (Appendix 11.3).
		114.0-116.4	Brecciated zone (hematite, chlorite). Assays in Table 11.10.
		116.4-117.0	White clay zone.
		117.0-118.0	Green to colorless fluorite veins.
		118.0-177.4	Green-gray andesite porphyry, Summit Mountain formation, chlorite alteration. Pyrite disseminated throughout most of the interval.
		177.4-183.5	Missing core.
		183.5-255.1	Green-gray to black andesite porphyry of the Summit Mountain formation. Pyrite and chlorite throughout. Thin veinlets (<1 cm) of quartz, calcite, pyrite, chalcopyrite, galena, and sphalerite.
		255.1-258.5	Core missing.
		258.5-277.7	Green-gray andesite porphyry, Summit Mountain formation. Chlorite alteration with disseminated pyrite. Veinlets. Some zones of black andesite porphyry.
		277.7-428.8	Green-gray andesite porphyry, Summit Mountain formation. Alteration minerals consists of epidote,

Hole No.	Hole declination	Depth interval (m)	Description
			chlorite, pyrite, and quartz (Appendix 11.3).
		428.8-434.6	Core missing.
		434.6-446.5	Green-gray andesite similar to above.
		446.5-449.2	Green-gray to red-brown andesite porphyry, Summit Mountain formation with hematite and carbonate alteration. Minor chlorite and epidote (confirmed by XRD, Appendix 11.3).
		449.2-477.3	Green-gray andesite porphyry, Summit Mountain formation with chlorite, hematite, pyrite, and locally, epidote. Minor silicified zones.
		477.3-480.3	White silicified zone. Assays of sample in Table 11.10.
		480.3-525.8	Green-gray andesite porphyry, Summit Mountain formation with chlorite, hematite, pyrite, and epidote.
		525.8-527.9	Brecciated and fractured andesite with quartz veins and hematite.
		527.9-549.2	Green-gray andesite porphyry, Summit Mountain formation with chlorite, hematite, pyrite, and epidote. Brecciated zones locally.
		549.2-561.4	Green-gray, lithic volcanic breccia (andesitic).
		561.4-577.3	Green-gray andesite porphyry, Summit Mountain formation with chlorite, pyrite, epidote, and calcite.
		577.3-579.7	Core missing.
		579.7-608.4	Green-gray andesite porphyry, Summit Mountain formation with chlorite, pyrite, epidote, calcite, and minor quartz.
		608.4-609.6	Gray silicified zone with disseminated pyrite.
		609.6-615-7	Core missing.
		615.7-633.3	Green-gray andesite porphyry, Summit Mountain formation with chlorite, pyrite, epidote, calcite, and minor quartz and fluorite veinlets (<2 cm). Silicified zones present.
		633.3-649.8	Core missing.
		649.8-741.2	White to green-gray, silicified andesite or dacite porphyry with chlorite, epidote, pyrite, and calcite. Veinlets of amethyst.
		741.2-746.0	Core missing.

TABLE 11.12—Chemical analyses of drill core from the Bitter Creek BC1 hole (analyses by NMBMMR chemical laboratory). Au and Ag are in oz/ton; Cu, Pb, Zn, Mo, and Hg are in ppm.

Sample	BC1-292-294	BC1-374-476	BC1-1566-1568	BC1-1568-1572	BC1-1572-1576
Au	0	0	0	0	0
Ag	0	0	0	0	0
Cu	250	7.9	16	16	8.6
Pb	530	32	39	53	22
Zn	47	55	35	57	24
Mo	46	54	1.7	1.7	2.2
Hg	0.06	0.09	0.05	0.04	0.06
Drill Depth (m)	89.0-89.6	114.0-114.6	477.3-477.9	477.9-479.1	479.1-480.3

Appendix 11.2 - Petrography - This appendix includes mineral abundance and alteration intensity (visual estimation explained in sections 1.5.3 and 5.1). * denotes samples also analyzed by XRD (Appendix 11.3). Alt int - alteration intensity (section 5.1), Poro - porosity, Plag - plagioclase, Hbd - hornblende, Bio - biotite, Chl - chlorite, Mag - magnetite, Tit - titanite (sphene), Grdmass - groundmass, I/S - illite/smectite, Q - quartz, K - kaolinite, Pyr - pyrophyllite, Hem - hematite, Leuc - leucoxene/anatase, Alu - alunite, Py - pyrite, Ep - epidote, Calc - calcite, K-feld - K-feldspar, FM -formation (symbols explained in Figure 2.1).

	Lithology	Texture	Alt int	Poro	Plag	Hbd	Bio	Chl	Mag	Tit	Grd-mass	I/S	Q	K	Pyr	Hem	Leuc	Alu	Py	Ep	Calc	adularia	K-feld	Other	Fm
Diabase dike (Td)																									Td
169	diabase	glomerophyritic	32	(5)	20	--	1	(40)	5	tr	--	(3)	2(5)	--	--	(5)	(5)	--	(3)	(5)	--	(1)	--	--	Td
187	diabase	porphyrtic	77	(3)	15	1	1	(50)	5	1	--	--	(3)	--	--	(10)	(5)	--	(3)	(5)	--	(3)	--	--	Td
Quartz monzonite dike (Tq)																									Tq
651	--	--	30	--	20	tr	2	--	5	3	(15)	(10)	20	--	--	(5)	--	--	--	--	--	--	20	tr-zircon	Tq
Ryholite intrusives (Tr)																									
42a	rhyolite	porphyritic	25	(2)	20	--	2	(5)	5	--	--	(10)	38	--	--	(10)	(2)	--	--	(1)	(5)	--	--	5-rock fragments	Tr
56	rhyolite	--	80	--	1	--	2	--	--	2	--	(20)	15(20)	(30)	--	(10)	--	--	--	--	--	--	--	--	Tr
59*	rhyolite	holocrystalline	8	--	--	--	1	--	tr	1	--	--	65	--	--	(5)	(3)	--	tr	--	--	--	25	--	Tr
172	rhyolite	microcrystalline	75	(5)	--	--	--	--	--	--	--	(30)	25	(20)	--	(20)	--	--	--	--	--	--	--	--	Tr
199	rhyolite	porphyritic	42	(5)	2	--	1	--	--	tr	--	(30)	50	--	--	(2)	--	--	--	--	--	(5)	5	--	Tr
203	rhyolite	porphyritic	58	(10)	--	--	tr	--	--	2	--	(30)	40	--	--	(5)	(10)	--	--	--	--	(3)	--	tr-zircon	Tr
239b*	rhyolite	--	49	--	--	--	--	--	--	1	--	(5)	40(40)	--	--	(2)	(1)	--	(1)	--	--	--	--	--	Tr
251	rhyolite	--	45	--	--	--	--	--	--	tr	--	(15)	50(20)	--	--	(5)	--	--	(5)	--	--	tr	5	quartz veins	Tr
280	rhyolite	breccia	25	--	--	--	--	--	5	5	--	(10)	55	--	--	(10)	--	--	--	--	(5)	--	10	--	Tr
314*	rhyolite	porphyritic	35	--	10	--	5	--	--	5	--	(10)	30(20)	--	--	(5)	--	--	tr	--	--	--	15	tr-zircon	Tr
315*	rhyolite	porphyritic	25	--	10	--	5	--	5	5	--	(15)	35	--	--	(10)	--	--	--	--	--	--	15	--	Tr
366	rhyolite	--	60	--	--	--	tr	--	--	--	--	(10)	50(30)	tr	--	(5)	(5)	--	--	--	--	--	tr	tr-goethite, rutile	
598*	rhyolite	porphyritic	48	(4)	2	--	--	--	--	1	--	(10)	50(20)	--	--	(5)	(1)	--	--	--	(2)	--	5	--	Trp
717*	rhyolite	spherulitic	38	--	5	--	1	(1)	--	1	--	(10)	50(20)	--	--	--	(1)	--	(1)	--	(5)	--	5	--	Tr
936*	rhyolite	--	49	--	10	--	--	--	--	1	--	(25)	40(20)	--	--	(2)	(1)	--	(1)	--	--	--	--	--	--
988*	rhyolite	spherulitic	41	(10)	--	--	--	--	--	2	--	--	40(20)	--	--	(5)	--	--	(tr)	--	--	(1)	10	2-pyroxene	Tr
1028*	TwinPeaks	porphyritic	29	(5)	--	--	1	--	3	2	--	(20)	45	--	--	(10)	(3)	--	(1)	--	--	(tr)	10	tr-hedenbergite	Tr
1045*	rhyolite	porphyritic	48	(5)	--	--	--	--	--	2	--	--	50(20)	(10)	--	(2)	(2)	--	--	--	--	--	--	(10)-illite	Tr
1046*	rhyolite	microcrystalline	28	(5)	--	--	tr	--	--	2	--	(20)	60	--	--	(2)	(2)	--	--	--	--	--	10	1-fluorite, (20)-illite	Tr
1047*	rhyolite	porphyritic	20	--	--	--	--	--	3	2	--	(10)	65	--	--	(5)	(3)	--	(2)	--	--	--	10	tr-zircon,fluorite	Tr
1048*	Apache Box	holocrystalline	56	--	--	--	--	(1)	--	2	--	--	37(35)	--	--	(5)	--	--	--	--	--	--	10	(10)-illite	Tr
Rhyolite flows and/or domes																									
955a	rhyolite	--	5	--	--	--	5	--	--	--	--	--	5	--	--	(5)	--	--	--	--	--	--	5	70-volcanic glass	Twr
977*	rhyolite	--	43	(15)	10	--	--	--	--	2	--	--	45(20)	--	--	(1)	(1)	--	(1)	--	--	--	--	(5)-illite	Twr
Rhyodacite of Willow Creek (Twd)																									
553	spherulitic	--	47	--	1	--	--	--	2	--	--	(15)	40(20)	--	--	(10)	(1)	--	--	--	(1)	--	10	--	Twd
Dark Thunder Canyon formation (Tbd)																									
3	andesite	trachytic,amygd.	40	(3)	36	5	5	(10)	10	--	(25)	--	--	--	--	(5)	--	--	--	(1)	--	--	--	--	Tbd
4 dike*	andesite	trach.,porp.	60	--	25	10	--	(10)	5	tr	(20)	(10)	--	--	--	(10)	--	--	--	(5)	(5)	--	--	--	Tbd

Appendix 11.2 (continued)

	Lithology	Texture	Alt int	Poro	Plag	Hbd	Bio	Chl	Mag	Tit	Grd-mass	I/S	Q	K	Pyr	Hem	Leuc	Alu	Py	Ep	Calc	adularia	K-feld	Other	Fm
21	andesite	breccia	80	--	10	3	--	(20)	2	tr	(30)	(5)	(10)	--	--	(10)	--	--	--	(5)	(5)	--	--	--	Tbd
31*	volc brec	breccia	75	(5)	15	--	5	(10)	5	--	(15)	--	(20)	(2)	--	(5)	--	--	(1)	(2)	(5)	(5)	--	(5)-malachite,tr-anatase	Tbd
39*	porphyritic andesite	porphyritic --	63	--	25	2	tr	(10)	10	tr	(25)	(5)	(5)	--	--	(2)	--	--	(1)	(3)	(5)	(5)	--	tr-apatite,(2)-siderite, tr-malachite	Tbd Tbd
55	bas and	--	70	--	20	5	--	(10)	5	tr	--	(5)	(25)	--	--	(25)	--	--	(5)	--	--	--	--	--	--
61*	bas and	trach.,porp.	70	--	20	2	3	(15)	--	--	--	(10)	25	--	--	(15)	--	--	--	--	--	--	--	5-anatase,(5)-malachite	Tbd
220	andesite	porphyritic	75	--	15	1	--	(50)	4	--	--	(5)	--	--	--	(7)	(5)	--	--	(3)	(5)	--	--	5-pyroxene	Tbd
221	andesite	porphyritic	80	(5)	15	2	--	--	5	--	--	(3)	--	--	--	(5)	(3)	--	--	--	(2)	--	--	--	Tbd
226	andesite	porphyritic	95	(5)	5	--	--	(60)	--	--	--	--	--	--	--	(15)	--	--	--	(5)	(10)	--	--	--	Tbd
292	andesite	porpyritic	70	(2)	20	--	--	(2)	--	--	(40)	(10)	(5)	--	--	(10)	--	--	(1)	--	--	--	10	--	Tbd
602	andesite	trachytic	57	(2)	40	--	--	--	3	--	--	(10)	--	--	--	(15)	(5)	--	--	--	(5)	--	--	20-clay	Tbd
613	andesite	trachytic	55	--	40	--	--	--	--	--	--	--	(2)	--	--	(10)	(3)	--	--	--	--	--	--	5-pyroxene,40-clay	Tbd
703*	andesite	trachytic	50	--	40	2	--	(5)	3	tr	(40)	--	tr	--	--	(5)	--	--	--	--	--	--	--	10-augite	Tbd
Younger ash-flow tuff, undifferientiated (Ta)																									
42b	tuff	--	83	(2)	5	--	2	--	--	--	--	(35)	10(40)	--	--	(5)	(1)	--	--	--	--	--	--	tr-zircon	Ta
270	tuff	--	39	(7)	--	--	--	--	--	1	--	(5)	50(20)	--	--	(5)	(2)	--	--	--	--	--	10	--	Tya1
274*	tuff	--	36	--	--	--	1	--	2	1	--	(10)	50(20)	--	--	(5)	(1)	--	--	--	--	--	10	--	Tya1
281	tuff	relict pumice	48	(5)	10	--	--	--	--	2	--	(5)	40(30)	(5)	--	(2)	--	--	(1)	--	--	--	--	--	Tya
293*	tuff	bimodal sorting	31	(2)	--	--	--	--	--	1	--	(7)	60(20)	--	--	(2)	--	--	--	--	--	--	5	tr-zircon, tr-apatite, 3-rock fragments	Ta Ta
326	breccia	--	49	(5)	--	--	--	--	--	1	--	--	50(25)	--	--	(2)	(1)	--	(1)	--	--	--	--	(15)-illite	Ta
370	tuff	--	75	--	20	--	--	--	--	--	(65)	(5)	5	--	--	(4)	--	--	(1)	--	--	--	--	--	Ta
428	tuff	bimodal sorting	28	(2)	--	--	5	--	1	1	--	(5)	55(20)	--	--	(1)	--	--	--	--	--	--	10	--	Tya1
438	tuff	bimodal sorting	29	(3)	--	--	2	--	2	2	--	(4)	55(20)	--	--	(2)	--	--	--	--	--	--	10	--	Ta
445	tuff	--	--	--	--	--	--	--	--	--	--	--	--	--	--	--	--	--	--	--	--	--	--	--	Ta
446	tuff	--	--	--	--	--	--	--	--	--	--	--	--	--	--	--	--	--	--	--	--	--	--	--	Ta
448	tuff	--	--	--	--	--	--	--	--	--	--	--	--	--	--	--	--	--	--	--	--	--	--	--	Ta
520	tuff	relict pumice	36	(2)	--	--	2	--	1	1	--	(10)	50(20)	--	--	(4)	--	--	--	--	--	--	10	--	Tya1
726b*	tuff	relict pumice	31	(5)	--	--	1	--	2	1	--	(5)	55(20)	--	--	--	(1)	--	--	--	--	--	10	--	Tya2
727*	tuff	relict pumice	29	(6)	1	--	2	--	1	1	--	(5)	55(20)	--	--	(2)	(1)	--	--	--	--	--	10	--	Tya2
728*	tuff	relict pumice	37	(5)	5	--	1	--	1	1	--	(10)	45(20)	--	--	(1)	(1)	--	--	--	--	--	10	--	Tya1
729	tuff	relict pumice	46	(5)	1	--	1	--	1	1	--	(15)	40(20)	--	--	(5)	(1)	--	--	--	--	--	10	--	Tya1
730*	tuff	relict pumice	36	(5)	1	--	1	--	1	1	--	(10)	50(20)	--	--	(1)	--	--	--	--	--	--	10	--	Tya1
732*	tuff	bimodal sorting	32	(5)	--	--	--	--	--	1	--	(5)	55(20)	--	--	(2)	--	--	(2)	--	--	--	5	5-rock fragments	Ta
733*	tuff	bimodal sorting	35	(3)	2	--	1	--	1	1	--	(10)	45(20)	--	--	(1)	(1)	--	--	--	--	--	10	5-rock fragments	Tya2
1083*	tuff	bimodal sorting	38	(5)	--	--	--	--	--	2	--	--	50(20)	--	--	(1)	(1)	--	(1)	--	--	--	10	(10)-illite	Ta
1088	tuff	bimodal sorting	41	(5)	2	--	1	--	--	1	--	(15)	40(10)	--	--	(5)	(1)	--	--	--	--	--	10	5-rock fragments, (5)-zeolites	Ta

Appendix 11.2 (continued)

	Lithology	Texture	Alt int	Poro	Plag	Hbd	Bio	Chl	Mag	Tit	Grd-mass	I/S	Q	K	Pyr	Hem	Leuc	Alu	Py	Ep	Calc	adularia	K-feld	Other	Fm
NM989	tuff	relict pumice	15	(5)	1	--	1	--	1	2	--	(10)	70	--	--	--	--	--	--	--	--	--	10	--	Ta
Summit Mountain formation (Tss)																									
403s	andesite	porphyritic	15	--	20	5	5	--	--	5	50	--	(5)	(5)	--	(5)	--	--	--	(tr)	--	--	--	--	Tss
BC1-2250*	andesite	porphyritic	95	--	5	--	--	(30)	--	(5)	--	(15)	(tr)	--	--	(4)	(10)	--	(1)	--	--	(5)	--	25-anhydrite	Tss
H7-33.8	andesite	porphyritic	93	(3)	5	--	1	(15)	--	1	--	(15)	(30)	(10)	--	(10)	(1)	--	(1)	--	--	(3)	--	--	Tss
H7-143.2	andesite	porphyritic	93	(2)	5	--	1	(15)	--	1	--	(20)	(30)	--	--	(15)	(1)	--	(2)	--	--	(3)	--	--	Tss
H7-213	andesite	trachytic	86	(3)	10	--	2	(10)	--	1	--	(20)	(35)	--	--	(2)	(1)	--	(5)	(1)	(10)	--	--	--	Tss
H9-259.7	andesite	--	80	--	15	--	--	(15)	--	5	--	--	(5)	(30)	--	(15)	--	--	(5)	(5)	(5)	--	--	--	Tss
H9-558	andesite	--	100	--	--	--	--	--	--	(5)	--	--	(40)	(30)	--	(10)	--	--	(5)	--	--	(5)	--	(5)-chalcopyrite	Tss
H10-326	andesite	porp,trachytic	85	--	15	--	--	(15)	--	--	--	(35)	(5)	--	--	(15)	--	--	(5)	--	--	(5)	--	(5)-anatase	Tss
H10-369	dacite	porphyritic	93	(5)	10	--	--	(5)	2	--	--	(25)	5(10)	(25)	--	(1)	--	--	(5)	(2)	--	--	--	(5)-dolomite	Tss
H10-412	andesite	porphyritic	90	--	10	--	--	(20)	--	--	--	(10)	(5)	(25)	--	(5)	--	--	(5)	--	(10)	(5)	--	(5)-anatase	Tss
H14-16	tuff	--	95	(5)	5	--	--	--	--	--	--	(20)	(10)	--	--	(40)	(5)	--	--	--	--	(10)	--	5-smectite	Tss
H14-188*	tuff	--	100	(tr)	--	--	--	--	--	--	--	--	(30)	(20)	(20)	(5)	(5)	--	(5)	--	--	--	--	(15)-jarosite	Tss
H14-225.5*	tuff	--	95	(3)	--	--	--	--	--	3	--	(15)	2(40)	(20)	(5)	(5)	(5)	--	(2)	--	--	--	--	--	Tss
H14-231*	tuff	--	99	(2)	--	--	--	--	--	--	--	(15)	1(50)	(20)	(5)	(1)	(5)	--	(1)	--	--	--	--	--	Tss
H14-243.6*	tuff	--	98	(5)	--	--	--	--	--	2	--	(10)	(40)	(30)	--	(3)	(5)	--	(5)	--	--	--	--	--	Tss
H14-259	andesite	--	100	--	--	--	--	--	--	--	--	(30)	(60)	--	--	(5)	(5)	--	(tr)	--	--	--	--	--	Tss
H14-269-270*	tuff	--	99	(5)	--	--	--	--	--	tr	--	(15)	1(30)	(40)	--	(1)	(3)	--	--	--	--	(5)	--	--	Tss
H14-291*	tuff	--	100	(3)	--	--	--	--	--	--	--	(20)	(30)	(20)	--	(5)	(5)	--	(2)	--	--	(15)	--	--	Tss
H6-187	andesite	--	100	--	--	--	--	(45)	--	--	--	--	(40)	--	--	(5)	--	--	(5)	--	--	(4)	--	1-chalcopyrite	Tss
B91-17-651	andesite	trachytic	92	(5)	3	--	2	(20)	--	1	--	(20)	(35)	--	--	(5)	(1)	--	(2)	(2)	(2)	--	--	2-pyroxene	Tss
S88-5-463	andesite	trachytic	92	(5)	5	--	2	(10)	--	1	--	(15)	(35)	(15)	(2)	(1)	(1)	(2)	(5)	(2)	--	--	--	(1)-diaspore	Tss
M91-4-689-690	andesite	--	87	(5)	5	--	2	(10)	--	1	--	(15)	(30)	(10)	--	(1)	--	--	(5)	--	(10)	--	5	--	Tss
M91-4-742.8	andesite	porphyritic	90	(5)	10	--	--	(15)	--	--	--	(35)	(10)	--	--	--	(5)	--	(10)	--	(5)	(5)	--	--	Tss
51a	porp and	glomerophyritic	86	(3)	5	--	2	(15)	--	2	--	(20)	(40)	--	--	(5)	--	--	(3)	--	(5)	--	--	--	Tss
68	sandstone	--	90	(5)	tr	--	--	(40)	--	--	--	(20)	10	--	--	(20)	--	--	(5)	--	--	--	--	--	Tss
73	volc bx	--	85	(10)	5	--	--	--	--	--	--	--	10	(10)	(5)	(35)	(5)	--	(5)	--	--	--	--	(5)-rock fragments	Tss
74	volc bx	--	98	(4)	--	--	--	--	--	--	--	(10)	2(30)	(30)	(5)	(10)	(2)	(5)	(5)	--	--	--	--	--	Tss
75*	tuff?	--	98	(10)	--	--	--	--	--	--	--	(10)	2(30)	(30)	(2)	(1)	(2)	(20)	(2)	--	--	--	--	(2)-diaspore,tr-anatase	Tss
79	tuff	--	99	(5)	--	--	--	--	--	--	--	--	(40)	(20)	(5)	(5)	(2)	(20)	(1)	--	--	--	--	(2)-diaspore	Tss
85*	tuff?	--	98	(10)	--	--	--	--	--	--	--	--	(35)	(30)	(2)	(5)	--	(15)	--	--	--	--	--	2-anatase,greigite	Tss
92	tuff	--	100	(5)	--	--	--	--	--	--	--	--	(35)	(30)	(2)	(3)	--	(20)	--	--	--	--	--	(5)-anatase	Tss
98	breccia	--	100	(10)	--	--	--	--	--	--	--	--	(30)	(25)	(5)	(10)	--	(5)	--	--	--	--	--	(10)-anatase,tr-zircon	Tss
107	breccia	--	97	(5)	--	--	--	--	--	--	--	--	3(35)	(30)	(15)	(5)	(5)	(2)	--	--	--	--	--	--	Tss
111*	and flow	--	65	--	20	--	1	--	2	2	(35)	(5)	(10)	--	--	(10)	--	--	--	(1)	(4)	--	--	5-enstatie,5-rock fragments	Tss
112	?	--	100	(10)	--	--	--	--	--	--	--	--	(50)	(20)	(10)	(5)	(5)	--	--	--	--	--	--	--	Tss

Appendix 11.2 (continued)

	Lithology	Texture	Alt int	Poro	Plag	Hbd	Bio	Chl	Mag	Tit	Grd-mass	I/S	Q	K	Pyr	Hem	Leuc	Alu	Py	Ep	Calc adularia	K-feld	Other	Fm
115*	?	--	100	(5)	--	--	--	--	--	--	--	--	(45)	(20)	--	(5)	(10)	--	--	--	--	--	tr-zircon,(15)-diaspore	Tss
123	tuff	--	40	(5)	15	--	5	--	5	--	(25)	--	10	--	--	(10)	--	--	tr	--	--	10	(5)-anatase,10-rock frag	Tss
128	sandstone	--	70	(25)	10	--	--	--	--	--	--	--	15	(25)	--	(10)	(5)	--	--	--	--	--	(5)-diaspore,5-rock frag	Tss
144*	?	--	98	(5)	--	--	--	--	--	2	--	--	(40)	(20)	(10)	(3)	(5)	--	--	--	--	--	(15)-illite,tr-fluorite	Tss
159	sandstone	--	80	(5)	--	--	--	(10)	--	5	(10)	(20)	15(15)	--	--	(20)	--	--	--	--	--	--	--	Tss
327*	andesite	porphyritic	68	(5)	30	1	1	(3)	--	(5)	--	(15)	(10)	(15)	--	(10)	--	--	--	--	(5)	--	--	Tss
329*	ss/tuff	--	94	(5)	--	--	--	(5)	--	1	--	--	5(20)	(40)	--	(10)	(2)	--	(2)	--	--	--	(10)-diaspore	Tss
332*	andesite	porp, trachytic	81	--	15	2	2	(10)	--	--	(30)	(10)	(5)	--	--	(25)	--	--	--	--	(1)	--	tr-apatite	Tss
341*	andesite	porphyritic	30	(5)	25	6	6	(5)	10	--	20(10)	(7)	tr	(6)	--	tr	tr	--	--	--	--	--	tr-diaspore	Tss
345*	andesite	porphyritic	70	--	20	--	--	(20)	10	--	(25)	(10)	(5)	--	--	(5)	(5)	--	tr	--	--	--	--	Tss
346*	tuff/ss	--	90	(10)	--	--	--	--	--	--	--	(10)	10(10)	(30)	--	(25)	--	--	(5)	--	--	--	--	Tss
352*	andesite	porphyritic	90	--	5	--	tr	(20)	--	5	--	(30)	(5)	(20)	--	(10)	--	--	--	(5)	--	(5)	--	Tss
353*	andesite	porphyritic	84	(5)	15	--	--	(15)	--	1	(30)	(15)	(5)	--	--	(5)	--	--	(4)	--	--	(5)	--	Tss
369*	andesite	porphyritic	83	(5)	10	--	--	(10)	5	2	(45)	--	(3)	--	--	--	--	--	--	(2)	(10)	(3)	--	Tss
687*	andesite	--	75	--	20	--	--	(10)	--	5	--	--	(10)	(30)	--	(15)	--	--	(5)	(5)	--	--	--	Tss
714*	andesite	porphyritic	95	(10)	3	--	--	(15)	--	--	--	(5)	(30)	(20)	(2)	(10)	--	--	--	--	--	--	2	Tss
715*	andesite	trach, porp	87	(5)	15	--	2	(10)	--	1	--	(15)	(30)	--	--	(5)	(1)	--	(5)	(1)	(5)	--	5	Tss
736	andesite	porphyritic	77	--	20	--	2	(5)	--	1	(60)	--	(5)	--	--	(5)	(1)	--	(1)	--	(5)	--	--	Tss
882	andesite	porphyritic	77	(5)	20	--	2	--	--	1	(50)	(5)	(5)	(5)	--	(5)	(1)	--	(1)	--	--	--	--	Tss
907	and porp	trachytic	75	(5)	15	--	5	(5)	--	--	(40)	(10)	(5)	--	--	(10)	--	--	--	--	--	--	5-pyroxene	Tss
913	andesite	porphyrtic	94	(5)	5	--	1	(5)	--	--	--	(20)	(30)	(10)	--	(10)	--	--	(2)	--	(10)	(1)	(1)-fluorite	Tss
914	dacite	porphyrtic	69	--	20	--	2	(15)	--	2	(40)	--	2(3)	--	--	(5)	--	--	(1)	--	(5)	--	5-pyroxene	Tss
1091	andesite	trachytic	88	(5)	5	--	3	(15)	--	2	--	(25)	(30)	--	--	(10)	(1)	--	--	(1)	--	(1)	2-pyroxene	Tss
Bloodgood Canyon Tuff (Tbg)																								
40	tuff	--	18	(5)	5	--	1	(2)	2	2	65	(5)	5	--	--	(5)	(1)	--	--	--	--	--	2-rock fragments	Tbg
53	tuff	--	10	(5)	10	--	2	--	1	2	65	--	10	--	--	(5)	--	--	--	--	--	--	--	Tbg
288	tuff	--	32	(3)	10	--	1	--	--	1	--	(5)	55(20)	--	--	(3)	(1)	--	(1)	--	--	--	--	Tbg
527	tuff	--	27	(1)	--	--	1	--	1	1	--	(5)	65(20)	--	--	(1)	--	--	--	--	--	--	5	Tbg?
529	tuff	relict pumice	32	(2)	2	--	3	--	2	1	--	(5)	50(20)	--	--	(5)	--	--	--	--	--	--	10	Tbg
637	tuff	relict pumice	33	(3)	--	--	2	--	1	1	--	(5)	50(20)	--	--	(5)	--	--	--	--	--	--	10	3-rock fragments Tbg
645*	tuff	relict pumice?	31	(1)	--	--	3	--	--	1	--	(5)	50(20)	--	--	(5)	--	--	--	--	--	--	10	5-rock fragments Tbg
739*	tuff	--	36	(5)	2	--	2	--	2	1	--	(10)	50(20)	--	--	(1)	--	--	--	--	--	--	5	2-rock fragments Tbg
916*	tuff	bimodal sorting	37	(5)	2	--	2	--	1	1	--	(10)	45(20)	--	--	(2)	--	--	--	--	--	--	10	2-rock fragments Tbg
1031*	tuff	relict pumice	41	(4)	--	--	2	--	1	1	--	(15)	45(20)	--	--	(2)	--	--	--	--	--	--	10	-- Tbg
1036*	tuff	relict pumice	43	(10)	5	--	2	--	1	1	--	(10)	45(20)	--	--	(1)	--	--	--	--	--	(2)	5	-- Tbg
1039*	tuff	bimodal sorting	41	(5)	5	--	2	--	1	1	--	(15)	45(20)	--	--	(1)	--	--	--	--	--	--	5	-- Tbg
NM987	tuff	--	16	(5)	1	--	1	--	1	1	--	(10)	70	--	--	(1)	--	--	--	--	--	--	10	-- Tbg

Appendix 11.2 (continued)

	Lithology	Texture	Alt int	Poro	Plag	Hbd	Bio	Chl	Mag	Tit	Grd-mass	I/S	Q	K	Pyr	Hem	Leuc	Alu	Py	Ep	Calc	adularia	K-feld	Other	Fm
Altered rocks, undifferientiated (Tas)																									
71*	altered	--	99	(20)	--	--	--	--	--	1	--	--	(35)	(30)	--	(10)	(3)	--	(1)	--	--	--	--	tr-zircon	Tassi
101	silica	--	100	(3)	--	--	--	--	--	--	--	--	(70)	(10)	(10)	(1)	(5)	--	tr	--	--	--	--	(1)-anatase,tr-apatite	Tass
139*	silica cap	--	96	(5)	2	--	--	--	--	1	--	(15)	(50)	(15)	--	(5)	--	--	--	--	--	(1)	--	(5)-anatase	Tass
217a	--	--	93	(3)	5	--	--	--	--	2	--	(10)	(60)	--	--	(20)	--	--	--	--	--	--	--	--	Tasc
331*	--	--	100	--	--	--	--	--	--	--	--	--	(50)	(20)	--	(5)	--	--	--	--	--	--	--	(25)-diaspore,tr-anatase,tr-apatite	Tassi
333*	ss/tuff	breccia	100	(3)	--	--	--	--	--	--	--	--	(20)	(50)	--	(17)	(2)	(5)	(3)	--	--	--	--	--	Tassi
334*	ss/tuff	--	95	(20)	--	--	--	--	--	--	--	--	5(20)	(30)	(5)	(3)	--	(10)	(2)	--	--	--	--	(5)-diaspore	Tassi
335*	--	--	92	(3)	2	--	--	--	1	tr	--	--	5(20)	(45)	--	(3)	(5)	(15)	(1)	--	--	--	--	tr-apatite,tr-diaspore	Tassi
336*	--	v. fine grained	99	(10)	--	--	--	--	--	1	--	--	(30)	(40)	--	(10)	(5)	(1)	(3)	--	--	--	--	--	Tassi
337*	--	v. fine grained	100	(5)	--	--	--	--	--	--	--	--	(30)	(40)	(15)	(5)	(3)	(1)	(1)	--	--	--	--	--	Tassi
338*	--	v. fine grained	97	(5)	--	--	--	--	--	3	--	--	(30)	(30)	(15)	(10)	(4)	--	(3)	--	--	--	--	--	Tassi
339*	--	v. fine grained	98	(5)	--	--	--	--	--	2	--	--	(30)	(45)	--	(3)	(5)	(5)	(5)	--	--	--	--	--	Tassi
342*	volc brec	--	100	(10)	--	--	--	--	--	--	--	--	(35)	(35)	(10)	(8)	(2)	--	tr	--	--	--	--	--	Tassi
343*	ss/tuff	--	95	(15)	--	--	--	--	--	tr	--	--	5(30)	(35)	--	(3)	(2)	(10)	tr	--	--	--	--	--	Tsssi
344a*	--	--	100	(30)	--	--	--	--	--	--	--	--	(20)	(35)	--	(3)	(5)	(5)	(2)	--	--	--	--	gypsum	Tassi
344b	--	--	100	(5)	--	--	--	--	--	tr	--	--	tr	(35)	--	(3)	(5)	(10)	(2)	--	--	(5)	--	(35)-diaspore,tr-gypsum	Tassi
368*	--	--	100	(10)	--	--	--	--	--	tr	--	--	(43)	--	--	--	--	--	--	--	--	--	--	(5)-anatase,jarosite,(42)-illite,tr-jarosite	Tasc
419f*	andesite	trachytic	93	(5)	5	--	--	--	--	2	--	(10)	(25)	(35)	--	(20)	(3)	--	--	--	--	--	--	--	Tassic
534*	andesite?	porphyrtic	94	(5)	5	--	--	--	--	1	--	(35)	(40)	(5)	--	(5)	(2)	--	--	--	--	--	--	(2)-natroalunite	Tasc
541*	--	--	99	(5)	--	--	--	--	--	1	--	--	(40)	(45)	--	(5)	(2)	(2)	--	--	--	--	--	--	--
582*	--	porphyrtic	99	(10)	--	--	--	--	--	1	--	(5)	(58)	(20)	--	(5)	(1)	--	--	--	--	--	--	--	Tassi
601a*	--	porphyrtic	99	(10)	--	--	--	--	--	1	--	(10)	(70)	--	--	(2)	(1)	--	(2)	--	--	--	--	(5)-jarosite	Tassi
608c*	tuff	bimodal sorting	85	(5)	--	--	--	--	--	1	--	(15)	10(45)	(15)	--	(5)	--	--	--	--	--	--	4	--	Tassi
628*	andesite?	porphyritic	99	(2)	--	--	--	--	--	1	--	--	(45)	(45)	--	(5)	(1)	--	(1)	--	--	--	--	--	Tasc
629	--	--	99	(2)	--	--	--	--	--	1	--	(5)	(40)	(40)	--	(9)	(1)	(1?)	(1)	--	--	--	--	--	Tassi
630*	--	--	99	(5)	--	--	--	--	--	1	--	--	(40)	(40)	--	(10)	(1)	(2)	(1)	--	--	--	--	--	Tas
631*	--	--	99	(2)	--	--	--	--	--	1	--	--	(40)	(40)	--	(10)	(1)	(5)	(1)	--	--	--	--	--	Tas
792a*	--	--	99	(5)	--	--	--	--	--	1	--	(3)	(30)	(30)	--	(5)	(5)	--	(1)	--	--	--	--	(10)-illite	Tasc
868b*	sandstone	--	95	--	--	--	--	--	--	--	--	--	5(40)	(40)	--	(5)	(5)	(5)	--	--	--	--	--	--	Tasc
944b*	--	--	99	(10)	--	--	--	--	--	1	--	--	(25)	(40)	--	(5)	(5)	--	--	--	--	--	--	(5)-greigite, (10)-natroalunite	Tassi
944e*	tuff	bimodal soting	93	--	--	--	--	--	--	2	--	--	5(90)	--	--	--	(3)	--	--	--	--	--	--	--	Tass
948a*	--	--	98	(3)	1	--	--	--	--	1	--	--	(60)	(20)	--	--	--	--	--	--	--	--	--	(5)-illite, (10)-natroalunite	Tassi
951*	--	--	99	(10)	--	--	--	--	--	1	--	--	(50)	(15)	--	(10)	(5)	--	(4)	--	--	--	--	(5)-illite	Tassi
952*	--	--	100	(10)	--	--	--	--	--	tr	--	--	(60)	(25)	--	(2)	--	(3)	--	--	--	--	--	--	Tassi

Appendix 11.2 (continued)

Lithology	Texture	Alt int	Poro	Plag	Hbd	Bio	Chl	Mag	Tit	Grd-mass	I/S	Q	K	Pyr	Hem	Leuc	Alu	Py	Ep	Calc	adularia	K-feld	Other	Fm
H10-123.9-124*?	--	100	(5)	--	--	--	--	--	(5)	--	--	(30)	(40)	--	(10)	(5)	--	(5)	--	--	--	--	--	Tassi
H10-134.2-.4*?	--	100	(5)	--	--	--	--	--	(5)	--	--	(35)	(40)	--	(5)	(5)	--	(5)	--	--	--	--	--	Tasc
H10-26.4-.5* tuff	--	98	(5)	--	--	--	--	--	tr	--	(2)	2(78)	(2)	(5)	(2)	(2)	--	(tr)	--	--	--	--	--	Tassi
H10-57-57.2 tuff	--	95	(5)	--	--	--	--	--	5	--	(10)	(80)	--	--	(2)	(3)	--	--	--	--	--	--	--	Tassi
H10-57.8-.9* tuff	--	98	(10)	--	--	--	--	--	2	--	(10)	(70)	--	--	(3)	(5)	--	--	--	--	--	--	--	Tassi
H10-85.9-86.1* tuff	--	95	(3)	--	--	--	--	--	5	--	--	(30)	(20)	(10)	(2)	(5)	--	--	--	--	--	--	(25)-diaspore	Tassi
H10-90.6* tuff	--	100	(5)	--	--	--	(15)	--	(5)	--	(15)	(40)	(5)	--	--	--	--	(10)	--	--	--	(5)	--	Tassi
H10-92-92.1* tuff	--	100	(5)	--	--	--	--	--	--	--	(20)	(40)	(15)	(10)	--	--	--	(5)	--	--	--	--	(5)-anatase	Tassi
H10-145.5-.8	breccia	99	(3)	--	--	--	--	--	1	--	(40)	(25)	--	(5)	(20)	(2)	--	(5)	--	--	--	--	--	
Davis Canyon Tuff (Tdc)																								
649 --	--	55	--	tr	3	--	--	--	--30(33)		--	5	--	--	(2)	--	--	--	--	--	--	2	20-clay, 5-rock fragments	Tdc
NM960 --	--	5	--	--	tr	--	--	--	--	75	--	5	--	--	(5)	--	--	--	--	--	--	5	10-pumice	Tdc
Veins (qv)																								
Center C*	--	--	2	--	--	--	7	--	--	--	4	75	--	--	3	--	--	--	--	--	1	--	5-galena,3-chalcopyrite	qv
Center dump*	--	--	10	--	--	--	--	--	--	--	40	40	--	--	3	--	--	--	--	--	2	--	5-galena	qv
H14-259 vein	--	--	3	--	--	--	2	--	--	--	2	90	--	--	--	--	--	tr	--	--	2	--	1-galena with chalcopyrite	qv
H14-344 vein	--	--	--	--	--	--	--	--	1	--	15	80	--	--	--	1	--	tr	--	--	1	--	1-galena,.5-sphalerite-.5-chalcopyrite, tr-chalcocite,acanthite?	qv
McDonald A	--	--	5	--	--	--	tr	--	--	--	1	90	--	--	tr	--	--	2	--	tr	1	--	tr-chalcopyrite,1-enargite, tr-galena	qv
McDonald B	--	--	3	--	--	--	1	--	--	--	1	92	--	--	1	--	--	tr	--	1	1	--	--	qv
ML1* --	--	--	5	--	--	--	--	--	--	--	2	88	--	--	--	--	--	1	--	--	1	--	(1)-anatase,2-sphalerite	qv
Ontario shaft*	--	--	--	--	--	--	5	--	--	--	5	70	--	--	5	--	--	3	--	1	1	--	2-sphalerite,3-galena,3-chalcopyrite,2-bornite, tr-nantokite	qv qv
4vein vein	--	--	5	--	--	5	3	--	--	--	--	75	--	--	12	--	--	--	--	--	--	--	--	qv
47* vein bx	--	--	--	--	--	--	5	--	--	--	25	25	--	--	10	--	--	5	--	--	5	--	(5)-malachite,(20)-rock frag	qv
48 vein bx	--	--	5	--	--	--	--	--	--	--	20	35	--	--	10	--	--	5	--	--	5	--	(20)-rock fragments	qv
51b vein	--	--	5	--	--	--	10	--	--	--	25	45	--	--	5	--	--	5	--	--	5	--	--	qv
340c* --	--	--	5	3	--	--	--	--	--	2	--	40	15	--	5	3	--	2	--	--	--	--	25-illite	qv
708* --	--	--	3	--	--	--	1	--	--	--	--	88	1	--	1	--	--	1	--	--	tr	--	1-chalcopyrite, galena, sphalerite,tr-chrysocolla	qv
																							(1)-anatase,(3)-rock frag	qv

Appendix 11.3—X-ray diffraction data. K - kaolinite, I/S - illite (sericite)/smectite mixed layered clays, I - illite (sericite), S - smectite, Chl - chlorite, Q - quartz, Feld - feldspar, Alu - alunite, Pyr - pyrophyllite, Jar - jarosite, Hem - hematite, Calc - calcite, Dias - diaspore, Gyp - gypsum, Fluor - fluorite, Ana - anatase, Py - pyrite, Ep - epidote.
* denotes thin section samples described in Appendix 11.2. @ denotes chemical assays in Appendix 11.6.

Sample no.	Clay analysis	K	I/S	I	S	Chl	Q	Feld	Alu	Pyr	Jar	Hem	Calc	Dias	Gyp	Fluor	Ana	Py	Ep	Other
Sinter (Qs)																				
Sinter	--	?	?	--	--	--	--	--	--	--	--	--	--	--	x	--	--	--	--	--
Diabase dike (Td)																				
584	--	--	--	x	--	x	x	x	--	--	--	--	x	--	--	--	--	--	--	--
Rhyolite/rhyodacite dikes (Tr, Trd)																				
59*	--	--	--	--	--	--	x	x	--	--	--	--	--	--	--	--	--	tr	--	--
204*	--	x	--	x	--	--	x	--	--	--	--	--	--	--	--	--	x	--	--	--
239b*	--	--	--	--	--	--	x	x	--	--	--	--	--	--	--	--	--	x	--	titanite
314*	--	--	--	--	--	--	x	x	--	--	--	--	--	--	--	--	--	--	--	--
315*	--	--	--	--	--	--	x	x	--	--	--	--	--	--	--	--	--	--	--	--
366	--	tr	tr	--	--	--	x	--	--	--	--	--	--	--	--	--	x	--	--	goethite, rutile
409*	--	--	--	--	--	--	x	x	--	--	--	--	--	--	--	--	--	--	--	titanite, hedenbergite
452*	--	--	x	--	--	--	x	x	--	--	--	--	--	--	--	--	--	--	--	--
514*	--	--	--	x	--	--	x	x	--	--	--	--	--	--	--	--	--	--	--	titanite
537	yes.	x	x	--	--	--	x	--	--	--	--	--	--	--	x	--	--	x	--	--
598*	--	--	x	--	--	--	x	x	--	--	--	--	x	--	--	--	--	--	--	--
717*	--	--	--	x	--	--	x	x	--	--	--	--	x	--	--	--	--	--	--	--
936	--	--	tr	--	--	--	x	x	--	--	--	--	--	--	--	--	--	--	--	--
958	--	--	--	--	--	--	x	--	x	--	x	x	--	--	--	--	--	--	--	goethite
988*	--	--	--	x	--	--	x	x	--	--	--	--	--	--	--	--	--	--	--	titanite, hedenbergite
1028*	--	--	--	--	--	--	x	x	--	--	--	--	--	--	--	--	--	--	--	titanite
1045*	--	--	x	--	--	--	x	x	--	--	--	--	--	--	--	--	--	--	--	titanite
1046*	--	--	--	x	--	--	x	x	--	--	--	--	--	--	--	x	--	--	--	--
1047*	--	--	x	--	--	--	x	x	--	--	--	--	--	--	--	tr	--	--	--	--
1048*	--	--	--	--	--	--	x	x	--	--	--	--	--	--	--	--	--	--	--	titanite
1108	--	x	--	--	--	--	x	--	--	x	--	--	--	--	--	--	--	--	--	--
1109	--	x	--	--	--	--	x	--	--	x	--	--	--	--	--	--	--	--	--	--
Rhyolite flows and/or domes (Twr)																				
977*	--	x	--	--	--	--	x	x	--	--	--	x	--	--	--	--	--	x	--	titanite
Dark Thunder Canyon formation (Tbd)																				
4dike*	--	--	x	--	x	x	x	x	--	--	--	x	x	--	--	--	--	--	x	titanite, hornblende, magnetite
31*	yes	x	--	--	x	--	x	x	--	--	--	x	x	--	--	--	x	--	x	titanite, magnetite
39*	yes	--	x	--	--	x	x	x	--	--	--	x	x	--	--	--	--	x	x	titanite, biotite, magnetite, malachite
61*	--	--	--	x	--	x	x	x	--	--	--	x	--	--	--	--	x	--	--	malachite, biotite, hornblende
68	--	x	--	--	--	--	x	--	x	x	--	--	--	--	--	--	--	--	--	minamiite
699	--	--	--	--	--	x	--	--	--	--	--	--	--	--	--	--	--	--	--	--
701	--	x	--	--	--	--	x	--	--	--	--	--	--	--	--	--	--	--	--	--
703*	--	--	--	--	--	x	x	x	--	--	--	--	--	--	--	--	--	--	--	titanite, augite
910	--	x	--	--	--	--	x	x	--	--	--	--	--	--	--	--	--	--	--	titanite

Appendix 11.3 (continued)

Sample no.	Clay analysis	K	I/S	I	S	Chl	Q	Feld	Alu	Pyr	Jar	Hem	Calc	Dias	Gyp	Fluor	Ana	Py	Ep	Other
1026	--	--	--	x	--	x	x	x	--	--	--	--	--	--	--	--	--	x	--	--
1026b	--	--	--	--	x	--	x	x	--	--	--	x	x	--	--	--	--	x	--	titanite, aegirine
Younger ash-flow tuff (Tya)																				
274*	--	--	--	--	--	--	x	x	--	--	--	--	--	--	--	--	--	x	--	titanite
Ash-flow tuff (Ta)																				
293*	--	--	--	x	--	--	x	x	--	--	--	--	--	--	--	--	--	--	--	titanite
674*	--	x	--	--	--	--	x	--	--	--	--	--	--	--	--	--	--	--	--	--
725	--	x	--	x	--	--	x	x	--	--	--	--	--	--	--	--	--	--	--	--
726b*	--	--	--	x	--	--	x	x	--	--	--	--	--	--	--	--	--	--	--	pseudobrookite
727*	--	--	--	x	--	--	x	x	--	--	--	--	--	--	--	--	--	--	--	--
728*	--	--	--	--	--	--	x	x	--	--	--	--	--	--	--	--	x	--	--	--
730*	--	--	--	x	--	--	x	x	--	--	--	--	--	--	--	--	--	--	--	--
732*	--	--	--	--	--	--	x	x	--	--	--	--	--	--	--	--	--	--	--	--
733*	--	--	--	--	--	--	x	x	--	--	--	--	--	--	--	--	--	--	--	--
736*	--	x	--	x	--	--	x	x	--	--	--	--	--	--	--	--	--	--	--	--
739*	--	--	x	--	--	--	x	x	--	--	--	--	--	--	--	--	--	--	--	titanite
741*	yes	x	--	tr	--	--	x	--	--	--	--	--	--	x	--	--	--	--	--	--
741a*	yes	x	--	--	?	--	x	--	--	--	--	--	--	--	--	--	--	--	--	--
1036*	--	--	x	--	--	--	x	--	--	--	--	--	--	--	--	--	--	--	--	--
1039*	--	--	--	x	--	--	x	x	--	--	--	--	--	--	--	--	--	--	-	titanite
1083	--	--	--	x	--	--	x	x	--	--	--	--	--	--	--	--	--	--	--	--
1088	--	--	--	--	--	--	x	x	--	--	--	--	--	--	--	--	--	--	--	clinoptilolite, heulandite, natroapopyllite, diopside, stilbite
NM987	--	--	--	--	--	--	x	x	--	--	--	--	--	--	--	--	--	--	--	titanite
Summit Mountain formation (Tss)																				
75*	--	?	--	x	--	--	x	--	--	--	--	--	--	--	--	--	x	--	--	--
85*	--	--	--	--	--	--	x	--	x	--	--	--	--	--	--	--	x	--	--	greigite
111*	--	--	--	--	--	?	x	x	--	--	--	--	--	--	--	--	--	--	--	titanite, enstatite
115*	--	x	--	--	--	--	x	--	--	--	--	--	--	x	--	--	--	--	--	--
139*	--	--	x	--	--	x	x	--	--	--	--	--	--	--	--	--	--	--	--	--
144*	--	x	--	x	--	--	x	--	--	--	--	--	--	--	--	x	--	--	--	--
227a*	--	--	x	--	--	x	x	x	--	--	--	x	--	--	--	x	--	--	--	titanite, hedenbergite
227c	--	--	x	--	--	--	x	x	--	--	--	x	--	--	--	x	--	--	--	despujolsite?
327*	yes	x	x	--	x	x	x	x	--	--	--	--	x	--	--	--	--	--	--	--
329*	yes	x	--	--	--	tr	x	--	--	--	--	--	--	--	--	--	--	--	--	--
332*	yes	x	--	x	--	x	x	--	x	--	--	--	--	--	--	--	--	x	--	--
332g*	yes	x	--	x	--	x	x	--	--	--	--	--	--	--	--	--	--	--	--	--
333*	yes	x	x	--	--	--	x	--	x	--	--	x	--	--	--	--	--	--	--	--
334*	--	x	--	--	--	--	x	--	tr	x	--	x	--	x	--	--	--	x	--	apatite
335*	yes	x	--	--	--	--	x	x	x	--	--	x	--	x	--	--	--	x	--	leucoxene, magnetite

Appendix 11.3 (continued)

Sample no.	Clay analysis	K	I/S	I	S	Chl	Q	Feld	Alu	Pyr	Jar	Hem	Calc	Dias	Gyp	Fluor	Ana	Py	Ep	Other
341*	yes	x	--	tr	x	x	x	x	--	--	--	x	--	--	--	--	--	--	--	hornblende, biotite, magnetite
342*	yes	x	--	--	--	--	x	--	--	x	--	x	--	--	--	--	--	x	--	leucoxene
343*	yes	x	--	--	--	--	x	--	x	--	--	x	--	--	--	--	--	x	--	leucoxene, titanite
344	yes	x	--	tr	--	--	x	--	x	--	--	tr	--	x	x	--	--	x	--	leucoxene, adularia
345*	yes	--	--	x	--	x	x	x	--	--	--	x	--	--	--	--	--	x	--	leucoxene, magnetite
346*	yes	x	--	--	--	--	x	--	--	--	--	--	--	--	--	--	--	--	--	--
348*	yes	x	--	--	x	--	x	--	--	--	--	--	--	--	x	--	--	--	--	--
352*	yes	x	x	--	--	x	x	x	--	--	--	--	--	--	--	--	--	--	--	--
353*	--	--	--	--	--	--	x	x	--	--	--	--	--	--	--	--	--	--	--	dolomite
369b*	--	x	--	--	--	x	x	x	--	--	--	--	--	--	--	--	--	x	--	titanite
687*	--	--	x	--	--	--	x	x	--	--	--	--	--	--	--	--	--	--	--	titanite
696	yes	x	x	--	x	x	x	x	--	--	--	--	--	--	--	--	--	--	--	--
714*	yes	--	--	--	x	x	x	x	--	x	x	--	--	--	--	--	--	--	--	--
715*	--	--	--	x	--	x	x	x	--	--	--	--	--	--	--	--	--	x	--	titanite
822e	--	--	--	x	--	--	x	--	--	--	--	--	--	--	--	--	--	--	--	--
829*	--	--	?	--	--	--	x	x	--	--	--	--	--	--	--	--	--	--	--	--
840	--	x	--	x	--	--	x	x	--	--	--	--	x	--	--	--	--	--	--	--
882	--	?	--	--	?	?	x	x	--	--	--	--	--	--	--	--	--	--	--	gismondine
906	--	x	--	x	--	--	x	x	--	--	--	--	x	--	--	--	--	x	--	--
913	--	--	--	--	x	x	x	x	--	--	--	x	x	--	--	x	--	--	--	--
928	--	x	--	--	--	--	x	--	--	x	--	--	--	--	--	--	x	--	--	natroalunite
1029	--	--	--	--	--	--	x	x	--	--	--	--	x	--	--	--	--	x	--	hydrobiotite
1077	--	--	--	x	--	x	x	x	--	--	--	--	--	--	--	--	--	--	--	--
1078	--	x	x	--	--	x	x	--	--	--	--	--	--	--	--	--	--	--	--	--
1079	--	x	x	--	--	x	x	--	--	--	--	--	--	--	--	--	x	x	--	nantokite, sphalerite
1081	--	--	--	x	--	--	x	--	--	--	--	--	x	--	--	--	--	x	--	pseudomalacite
1118	--	--	x	x	--	--	x	x	--	--	--	--	x	--	--	--	--	x	--	titanite
Bloodgood Canyon Tuff (Tbg)																				
645*	--	--	--	--	--	--	x	x	--	--	--	--	--	--	--	--	--	x	--	titanite
916*	--	--	--	x	--	--	x	x	--	--	--	--	--	--	--	--	--	--	--	titanite
1031*	--	--	--	--	--	--	x	x	--	--	--	--	--	--	--	--	--	--	--	gismondine
Sedimentary rocks (Tsed)																				
178	--	--	--	--	x	--	x	x	--	--	--	x	--	--	--	--	--	--	--	wairakite, clinoenstatite
291c*	--	--	x	x	--	--	x	x	--	--	--	--	x	--	--	--	--	--	--	--
331*	yes	x	--	--	--	--	x	--	--	--	--	--	--	x	--	--	--	--	--	--
578	--	--	--	--	--	--	x	--	--	--	--	--	--	--	--	x	--	--	--	--
632	--	--	--	--	--	--	x	--	--	--	--	x	--	--	--	--	--	--	--	--
662*	--	--	x	--	--	x	x	x	--	--	--	--	--	--	--	--	--	--	--	--
718	yes	--	--	x	--	--	x	--	--	--	x	x	--	--	--	--	--	--	--	goethite, hydromagnesite
820	--	x	--	--	--	--	x	--	--	--	--	x	--	--	--	--	x	--	--	--
834	--	x	--	--	--	--	x	--	--	--	--	--	--	--	--	--	x	--	--	tridymite

Appendix 11.3 (continued)

Sample no.	Clay analysis	K	I/S	I	S	Chl	Q	Feld	Alu	Pyr	Jar	Hem	Calc	Dias	Gyp	Fluor	Ana	Py	Ep	Other
1102*	--	--	--	x	--	--	x	x	--	--	--	--	--	--	--	--	--	--	--	--
1104*	--	x	--	x	--	x	x	x	--	--	--	--	--	--	--	--	--	--	--	titanite
Altered, undifferientaited (Tas)																				
BA1@	--	--	--	--	--	--	x	x	--	--	--	--	--	--	--	--	--	--	--	titanite, wulfenite
BA2	--	--	?	--	--	--	x	--	--	--	--	x	--	--	--	--	--	--	--	--
CT1	yes	--	x	--	--	--	x	x	--	--	--	--	--	--	--	--	--	--	--	--
CT2	yes	--	x	--	--	--	x	x	--	--	--	--	--	--	--	--	--	--	--	--
L Quarry	x	--	--	--	--	--	x	--	--	--	--	--	--	--	x	--	--	--	--	--
SB1-2	--	--	--	--	--	--	x	--	--	--	x	--	--	--	--	--	--	--	--	--
T Raeb N	x	--	--	--	--	--	x	--	x	x	--	--	--	--	--	--	--	--	--	--
TR Pit 1	--	--	--	--	--	--	x	--	--	--	--	--	--	x	--	--	--	--	--	--
TR Pit 2	--	x	--	--	--	--	x	--	--	x	--	--	--	--	--	--	--	--	--	--
t1	--	x	--	--	--	--	x	--	x	--	--	--	--	--	--	--	x	--	--	greigite
t2	--	--	--	--	--	--	x	--	--	--	--	--	--	--	--	--	x	--	--	--
tr5	yes	x	--	--	--	--	x	--	--	--	--	--	--	--	--	--	--	--	--	--
71	--	x	--	--	--	--	x	--	--	--	--	x	--	--	--	--	--	--	--	--
71 yellow clay*	--	x	--	--	--	--	--	--	--	--	--	--	--	--	--	--	--	--	--	--
101*	yes	x	x	--	--	--	x	--	--	tr	--	--	--	--	--	--	x	x	--	leucoxene
103*@	--	tr	--	--	--	--	x	--	--	tr	--	--	--	--	--	--	--	--	--	--
275*	--	--	--	--	--	--	x	--	--	--	--	--	--	--	--	--	--	--	--	--
322*	yes	x	--	--	--	--	x	--	--	x	--	--	?	--	--	--	--	--	--	--
326	yes	x	x	--	x	--	x	--	--	--	--	--	--	--	--	--	--	--	--	--
328*	yes	--	--	x	--	--	x	--	--	--	--	--	--	--	--	--	--	--	--	--
330*	--	x	--	--	--	--	x	--	x	x	--	--	--	--	--	--	x	--	--	greigite
336*	yes	x	--	--	--	--	x	--	--	--	--	--	--	x	--	--	--	--	--	--
337*	yes	x	--	--	--	--	x	--	--	x	--	--	--	--	--	--	--	--	--	--
338*	yes	x	--	--	--	--	x	--	--	x	--	--	--	--	--	--	--	--	--	--
339*	--	x	--	--	--	--	x	--	x	--	--	--	--	--	--	--	--	--	--	--
351*	yes	x	x	--	--	--	x	--	--	--	--	--	--	--	--	--	--	--	--	--
354*	yes	x	--	--	--	--	x	--	--	x	--	--	--	--	--	--	--	--	--	--
355	yes	x	--	x	--	--	x	x	--	--	--	--	--	--	--	--	x	--	--	--
357*	--	x	x	--	--	--	x	--	--	--	--	--	--	--	--	--	--	x	--	--
359*	--	x	--	--	--	--	x	--	--	x	--	--	--	--	--	--	--	--	--	--
362*	yes	x	--	--	--	--	x	--	--	x	--	--	--	--	--	--	--	--	--	--
364*	yes	x	--	--	--	--	x	--	--	--	--	--	x	--	--	--	--	--	--	--
364purple	--	x	--	--	--	--	x	--	--	x	--	--	--	--	--	--	--	--	--	--
364white	--	x	--	--	--	--	x	--	x	--	--	--	--	x	--	--	--	--	--	--
365*	yes	x	--	--	--	--	x	--	--	--	--	--	--	--	--	--	--	--	--	--
368*@	yes	--	--	x	--	--	x	--	--	--	tr	--	--	--	--	--	x	--	--	titanite
368b@	yes	--	--	--	--	x	x	x	--	--	--	--	--	--	--	--	--	x	--	titanite, aegirine

Appendix 11.3 (continued)

Sample no.	Clay analysis	K	I/S	I	S	Chl	Q	Feld	Alu	Pyr	Jar	Hem	Calc	Dias	Gyp	Fluor	Ana	Py	Ep	Other
419f*	yes	x	tr	--	x	--	x	x	--	--	--	x	--	--	--	--	--	--	--	titanite
504b	yes	x	--	--	--	--	x	x	--	--	--	--	--	--	x	--	--	--	--	--
532*@	yes	x	--	--	--	--	x	--	--	--	--	--	--	--	x	--	--	x	--	--
533*@	yes	x	--	--	--	--	x	--	--	--	--	--	--	--	--	--	--	--	--	--
534*	yes	?	--	x	--	--	x	x	x	--	tr	--	--	--	--	--	--	--	--	--
541*	yes	x	--	--	--	--	x	--	x	--	--	--	--	--	--	--	x	--	--	--
542*@	yes	x	--	--	--	--	x	--	x	--	--	--	--	--	--	--	--	--	--	--
582	yes	x	--	--	--	--	x	--	--	--	--	--	--	--	--	--	--	--	--	--
600@	yes	x	--	tr	--	--	x	--	--	--	--	--	--	--	--	--	--	x	--	mottramite
601a*@	--	--	--	x	--	--	x	--	--	--	x	--	--	--	--	--	--	--	--	pseudomalachite?, ferrihydrite
608c*	--	--	--	x	--	--	x	x	--	--	--	--	--	--	--	--	--	--	--	gismondine
615@	--	x	--	--	--	--	x	--	--	--	--	--	--	--	--	--	--	--	--	--
628*	yes	x	--	--	--	--	x	--	--	--	--	--	--	--	--	--	--	--	--	--
630*	--	--	--	--	--	--	x	--	tr	--	--	--	--	--	--	--	--	--	--	greigite, minamiite, melanterite
631*	--	--	--	?	--	--	x	--	x	--	x	--	--	--	--	--	--	--	--	minamiite
644	--	--	--	--	--	--	x	x	--	--	--	--	--	--	--	--	--	--	--	titanite
652a@	yes	--	--	x	--	x	x	--	--	--	x	--	--	--	--	--	x	x	--	pseudomalachite
652b@	--	--	--	x	--	--	x	--	--	x	--	--	--	--	--	--	--	--	--	--
679@	--	x	x	--	--	--	x	--	--	--	--	--	--	--	--	--	--	x	--	cerussite, goethite, clinochlore
713*	yes	--	--	x	--	--	x	x	--	--	--	--	x	--	--	--	x	--	--	--
716a	yes	--	x	--	--	--	x	x	--	x	--	--	--	--	--	--	--	--	--	--
716b	yes	--	x	--	tr	--	x	x	--	--	x	--	--	--	x	--	--	--	--	--
716c	--	--	--	x	--	x	x	x	x	--	--	--	--	--	x	--	--	--	--	--
817c	--	--	--	?	--	x	x	--	--	--	--	--	--	--	--	x	--	x	--	--
719@	yes	tr	x	--	--	--	x	x	--	--	--	--	--	--	--	--	--	x	--	--
720	--	--	--	--	--	x	x	x	--	--	--	--	--	--	--	--	--	--	--	titanite, johannsenite
722*	yes	x	x	--	--	--	x	--	--	--	--	--	--	--	--	--	--	--	--	--
723@	yes	x	x	--	--	--	x	x	--	--	--	--	--	--	--	--	--	--	--	goethite
724c	yes	--	--	--	x	--	x	x	--	--	--	--	--	--	--	--	--	--	--	--
742*@	yes	x	--	--	--	tr	x	--	--	x	?	--	--	--	--	--	--	--	--	--
744*	yes	x	--	--	--	--	x	--	--	--	--	--	--	--	--	--	x	--	--	--
746	yes	x	--	--	--	--	x	--	--	--	--	--	--	--	--	--	x	--	--	--
747*@	--	--	--	--	--	--	x	--	--	--	--	--	--	--	--	--	--	--	--	--
748@	yes	x	--	--	--	--	x	--	--	--	--	--	--	--	--	--	--	--	--	--
750*@	--	x	x	--	--	--	x	--	--	--	--	--	--	--	--	--	x	--	--	--
752a*	yes	x	--	--	--	--	x	--	--	--	--	--	--	--	--	--	--	--	--	rutile
752b*	yes	x	--	--	--	--	x	--	--	--	--	--	--	--	--	--	--	--	--	rutile
753	yes	x	--	--	x	--	x	x	x	--	--	--	x	--	--	--	--	--	--	titanite
754*@	yes	x	--	tr	--	--	x	--	--	--	--	--	--	--	--	--	--	--	--	--
755	yes	x	--	x	--	--	x	x	--	--	x	--	--	--	x	--	--	--	--	tennantite
756@	--	--	--	--	--	--	x	--	--	--	--	--	--	--	--	--	x	x	--	sphalerite

Appendix 11.3 (continued)

Sample no.	Clay analysis	K	I/S	I	S	Chl	Q	Feld	Alu	Pyr	Jar	Hem	Calc	Dias	Gyp	Fluor	Ana	Py	Ep	Other
757	yes	x	--	--	x	--	?	--	--	--	--	--	--	--	--	--	--	--	--	goethite
759	yes	x	--	--	--	--	x	--	--	--	--	--	--	--	--	--	--	--	--	rutile
760a@	yes	x	x	--	--	x	x	--	--	--	--	--	--	--	--	--	--	--	--	--
760b	--	x	--	x	--	--	x	--	--	x	--	--	x	--	--	--	--	x	--	--
761@	yes	x	--	--	x	--	x	--	--	--	--	--	--	--	--	--	x	--	--	--
762	yes	x	--	--	x	--	x	--	--	--	--	--	--	--	--	--	--	--	--	--
763	yes	--	--	--	--	--	x	--	--	--	--	--	--	--	--	--	x	--	--	--
765	--	x	--	--	--	--	--	--	--	--	--	--	--	x	--	--	--	--	--	tridymite, clinoclase
767	--	x	--	x	--	--	x	--	--	--	x	x	--	--	--	--	--	--	--	goethite
769@	--	--	--	x	--	--	x	--	--	--	--	--	--	--	--	--	--	--	--	--
770*@	--	x	--	x	--	--	x	--	--	--	--	--	--	--	--	--	--	--	--	--
771*@	--	?	--	--	--	--	x	--	x	--	--	--	--	--	--	--	--	--	--	greigite, minamiite, natoalunite
772@	--	x	--	--	--	--	x	--	--	--	--	--	--	--	--	--	--	--	--	--
773*@	--	--	--	--	--	--	x	--	--	--	--	--	--	--	--	--	?	--	--	--
775*@	--	x	--	x	--	x	x	--	--	--	--	x	--	--	--	--	--	--	--	--
776*@	--	x	--	--	--	--	x	--	--	--	--	--	--	x	--	--	--	--	--	--
777*@	--	?	--	?	--	--	x	--	x	--	--	--	--	--	--	--	--	--	--	greigite, minamiite
779@	--	x	x	--	--	--	x	--	--	--	--	--	--	x	--	--	x	--	--	--
780@	--	x	--	x	--	--	x	--	--	--	--	--	--	--	--	--	--	--	--	--
781*@	--	x	--	--	--	--	x	--	--	--	--	x	--	--	--	--	x	--	--	--
785@	--	x	--	--	--	--	x	--	--	--	--	--	--	x	--	--	x	--	--	--
786	--	?	--	--	--	x	x	x	--	--	--	--	--	--	--	--	--	--	--	--
789	--	--	--	--	--	--	--	--	--	--	--	--	--	x	--	--	--	--	--	--
791*	--	x	--	--	--	--	x	--	x	x	--	--	--	--	--	--	--	--	--	--
792a*	--	--	x	--	--	--	x	--	--	--	--	--	--	--	--	--	--	--	--	--
793*	--	--	--	x	?	--	?	--	--	--	--	--	--	--	--	--	--	--	--	--
794	--	x	--	--	--	--	x	--	--	--	--	--	--	--	--	--	x	--	--	--
795	--	?	--	?	--	--	x	--	--	--	--	--	--	--	--	--	x	--	--	--
796	yes	x	x	--	--	--	x	x	--	--	--	--	--	--	--	--	--	--	--	titanite, esseneite
797	--	--	--	--	--	--	x	--	--	--	--	--	--	--	--	--	--	--	--	--
798	--	x	--	--	--	--	x	--	--	--	--	--	--	--	--	--	x	--	--	--
799	--	x	x	--	--	--	x	x	--	--	--	--	--	--	--	--	--	--	--	goethite, gismondine
811*	--	--	x	--	--	--	x	--	--	--	--	--	--	--	--	--	--	--	--	--
812*	--	--	--	x	x	--	x	--	--	--	--	--	--	--	--	--	--	--	--	--
814*	--	x	--	--	--	--	x	x	--	--	--	--	--	--	--	--	--	x	--	tridymite, opal
821	--	x	--	--	--	--	x	--	--	--	--	--	--	--	--	--	--	--	--	--
822	--	--	x	--	--	--	x	--	--	--	x	--	--	--	--	--	--	--	--	pseudomalachite
822a	--	--	x	--	--	x	x	--	--	--	--	--	--	--	--	--	--	--	--	--
822c	--	--	--	x	--	--	x	--	--	--	--	--	--	--	--	--	--	--	--	prehnite?
822d@	--	--	--	x	--	--	x	x	--	--	x	--	--	--	--	--	--	--	--	--
823a*	--	x	--	--	--	--	x	--	--	--	--	--	--	--	--	--	--	--	--	tridymite

Appendix 11.3 (continued)

Sample no.	Clay analysis	K	I/S	I	S	Chl	Q	Feld	Alu	Pyr	Jar	Hem	Calc	Dias	Gyp	Fluor	Ana	Py	Ep	Other
823b	--	x	--	--	--	--	x	--	--	--	--	--	--	x	--	--	--	--	--	--
827*	--	--	--	x	--	--	x	--	--	--	--	--	--	--	--	--	--	--	--	--
828*	--	x	--	--	--	--	x	--	--	--	--	--	--	--	--	--	--	--	--	despujolsite(?)
833	--	x	--	x	--	--	x	--	--	--	--	--	--	--	--	--	--	--	--	goethite, despujolsite(?)
835	--	--	--	x	--	--	x	--	--	--	--	--	--	--	--	--	--	--	--	--
838	--	x	--	--	--	--	x	--	--	--	--	--	--	--	--	--	--	--	--	rutile
842	--	x	--	x	--	--	x	--	--	--	--	--	--	--	--	--	--	--	--	--
843a	--	x	--	--	--	--	x	--	--	--	--	--	--	--	--	--	--	--	--	--
843b	--	x	--	--	--	--	x	--	--	--	--	--	--	--	--	--	--	--	--	--
844	yes	--	--	x	--	--	x	--	--	--	--	--	--	--	--	--	--	--	--	--
845*	--	x	--	x	--	--	x	--	--	--	--	--	--	--	--	--	--	--	--	natrojarosite
868b	--	x	--	--	--	--	x	--	x	--	--	--	--	--	--	--	--	--	--	greigite, minamiite, anhydrite
870	--	x	--	--	?	--	x	--	--	--	--	--	--	--	--	--	--	--	--	--
871b*	yes	x	x	--	--	--	x	x	--	--	--	--	--	--	--	--	--	--	--	--
873	--	--	--	x	--	--	x	x	--	--	--	x	--	--	--	--	--	--	--	--
875	--	--	--	?	--	?	x	x	--	--	--	--	x	--	--	--	--	--	--	--
875b@	--	?	--	x	--	?	x	x	--	--	--	--	--	--	--	--	--	x	--	--
876@	--	--	--	x	--	x	x	--	--	--	--	--	x	--	x	--	--	--	--	--
878a	--	--	x	--	--	--	x	--	--	--	x	--	--	--	--	--	--	--	--	--
878b@	--	--	--	--	--	--	x	--	--	--	--	--	--	--	--	--	--	--	--	rutile
878c	--	--	?	--	--	--	x	--	--	--	x	x	--	--	--	--	--	--	--	rutile
879a	--	x	--	--	--	--	x	--	--	--	--	--	--	--	--	--	x	--	--	goethite, tridymite
879b	--	--	--	--	--	--	x	--	--	--	--	--	--	--	--	--	--	--	--	greigite, minamiite
879c	--	--	--	--	--	x	x	--	--	--	--	--	--	--	--	--	x	--	--	gismondine
884	--	--	x	--	--	--	x	x	--	--	--	--	--	--	--	--	--	--	--	pseudomalachite
885	--	x	--	--	x	--	x	--	--	--	--	--	--	--	--	--	--	--	--	clinoclase
886@	--	--	--	--	--	--	x	--	--	--	--	--	--	--	--	--	x	--	--	--
893	--	x	--	--	--	--	x	--	--	--	--	--	--	--	--	--	--	--	--	natroalunite
895a*	--	x	--	?	--	--	x	--	x	--	--	--	--	--	--	--	--	--	--	greigite, minamiite
895b*	--	x	--	--	--	--	x	--	--	--	--	--	--	--	--	--	--	--	--	tridymite
909b*	--	--	--	x	?	--	x	--	--	--	--	--	--	--	--	--	--	--	--	--
929	--	x	--	--	--	--	x	--	--	--	--	--	--	--	--	--	--	--	--	natroalunite
930	--	x	--	--	--	--	x	--	x	--	--	--	--	--	--	--	--	--	--	--
931	--	x	--	--	--	--	x	--	--	--	--	--	--	--	--	--	--	--	--	goethite
933	--	--	--	x	--	--	x	--	--	--	--	--	--	--	--	--	x	--	--	--
943	--	x	--	--	--	--	x	--	--	--	--	--	--	--	--	--	--	--	--	--
943a	--	x	--	--	--	--	x	--	--	--	--	--	--	--	--	--	--	--	--	galena?
943b	--	--	--	--	--	x	x	x	--	--	--	--	x	--	--	--	--	--	x	--
944a	--	x	x	--	--	--	x	x	--	--	--	--	--	--	--	--	--	--	--	natrojarosite
944b*	--	--	--	--	--	--	x	--	x	--	--	--	--	--	--	--	x	--	--	natroalunite, greigite
944c	--	--	--	x	--	--	x	--	--	--	--	--	--	--	--	--	x	--	--	--

Appendix 11.3 (continued)

Sample no.	Clay analysis	K	I/S	I	S	Chl	Q	Feld	Alu	Pyr	Jar	Hem	Calc	Dias	Gyp	Fluor	Ana	Py	Ep	Other
944c*	--	--	--	--	--	--	x	--	--	--	--	--	--	--	--	--	--	--	--	--
944	--	x	--	--	--	--	--	--	--	--	--	--	--	--	--	--	--	--	--	--
945	--	x	--	--	--	--	x	--	--	--	--	x	--	--	--	--	x	--	--	tridymite
946	--	x	--	--	--	--	--	--	--	--	--	--	--	--	--	--	--	--	--	--
948a	--	--	--	x	--	--	x	x	x	--	--	--	--	--	--	--	--	--	--	--
948b	--	?	--	--	--	--	x	x	--	--	--	--	--	--	--	--	--	--	--	--
948c	--	--	--	--	--	--	--	--	--	--	--	--	--	--	--	--	--	--	--	natroalunite
949*@	--	--	--	x	--	--	x	--	--	--	x	--	--	--	--	--	--	--	--	--
950	--	--	--	x	--	--	x	--	x	x	--	--	--	--	--	--	--	--	--	--
951*	--	x	--	x	--	--	x	--	--	--	--	--	--	--	--	--	--	--	--	--
951c	--	x	--	x	--	--	x	--	--	--	--	--	--	--	--	--	--	--	--	--
951m	--	--	--	x	--	--	x	x	x	--	--	--	--	--	--	--	--	--	--	--
952*	--	x	--	x	--	--	x	--	x	--	--	--	--	--	--	--	--	--	--	greigite
953	--	--	x	x	--	x	x	x	--	--	--	--	--	--	--	--	--	--	--	--
959*	--	--	--	x	--	--	x	--	x	--	--	--	--	--	--	--	x	--	--	natroalunite, greigite
960*	--	--	--	--	?	--	x	--	x	--	x	--	--	--	--	--	--	--	--	natroalunite, minamiite
961	--	x	--	--	--	--	x	--	x	--	--	--	--	--	--	--	--	--	--	greigite, minamiite
962	--	x	--	--	--	--	x	--	--	--	--	--	x	--	--	--	x	x	--	--
963*	--	--	?	--	--	--	x	--	--	--	--	--	--	--	--	--	--	--	--	manganosite, galena, chrysocolla
970*	--	--	--	--	--	--	x	--	x	--	--	--	--	--	--	--	--	--	--	greigite
986	--	--	--	--	--	--	x	--	--	--	--	x	--	--	--	--	--	--	--	--
994	--	x	--	--	--	--	x	--	--	x	--	x	--	--	--	--	--	x	--	--
999	--	x	--	--	--	--	x	--	--	--	--	--	--	--	--	--	--	--	--	tridymite
1000	--	x	--	--	--	--	x	--	--	--	--	x	--	--	--	--	--	--	--	--
1001*	--	x	x	--	--	x	--	--	--	--	--	--	--	--	--	--	--	--	--	tridymite?, galena?
1004	--	--	--	x	--	--	x	x	--	--	--	--	--	--	--	--	--	x	--	titanite
1020	--	x	--	--	--	--	x	--	--	x	--	--	--	--	--	--	--	--	--	--
1021	--	x	--	--	--	--	x	--	--	--	--	--	--	--	--	--	--	--	--	--
1023*	--	--	--	--	--	--	x	--	--	--	--	--	--	--	--	--	x	--	--	--
1025a	--	x	--	--	--	x	x	x	--	--	--	--	x	--	--	--	--	--	--	rutile, hedenbergite
1062	--	--	--	--	--	--	x	--	--	--	x	--	--	--	--	--	--	--	--	--
1063	--	--	--	x	--	--	x	--	--	--	x	x	--	--	--	--	--	--	--	--
1066	--	x	--	--	--	--	x	--	--	--	--	--	--	--	--	--	--	--	--	--
1067	--	--	--	--	--	--	x	--	--	--	--	--	--	--	--	--	--	--	--	--
1074	--	--	x	--	--	--	x	--	--	--	--	x	--	--	--	--	--	--	--	--
1075@	yes	x	x	--	--	--	x	x	--	--	--	--	--	--	--	--	x	x	--	chalcopyrite, nantokite
1082	--	x	x	--	--	x	x	--	--	--	--	--	--	--	--	--	--	--	--	--
1105	--	x	x	--	--	--	x	--	--	x	x	--	--	--	--	--	--	--	--	natrojarosite
1107	--	--	--	x	--	--	x	--	--	--	--	--	--	--	--	--	--	--	--	--
1110	--	x	--	--	--	--	--	--	--	--	--	x	--	--	--	--	--	--	--	--

Quartz veins (qv)

Appendix 11.3 (continued)

Sample no.	Clay analysis	K	I/S	I	S	Chl	Q	Feld	Alu	Pyr	Jar	Hem	Calc	Dias	Gyp	Fluor	Ana	Py	Ep	Other
Carl pit west-8814@		x	--	x	--	--	x	--	--	--	--	--	--	--	--	--	--	--	--	pseudomalachite
East Camp Dump-8816@			--	--	x	x	x	--	--	--	--	--	--	--	--	--	--	--	--	--
Goldenrod@	--	--	--	--	--	x	x	x	--	--	--	--	--	--	--	--	--	x	--	titanite, hedenbergite
ML-1-8496@	--	--	--	x	--	x	x	--	--	--	--	--	--	--	--	--	x	--	--	--
ML-2@	--	--	?	--	--	--	x	x	--	--	--	--	--	--	--	--	--	--	--	aegirine, titanite
ML-3@	--	--	x	--	--	--	x	x	--	--	--	--	--	--	--	--	--	--	--	titanite
ML4	yes	--	x	--	--	--	x	x	--	--	--	--	--	--	--	--	--	--	--	--
Mcdon upper adit@		--	--	--	--	--	x	x	--	--	--	--	--	--	--	--	--	--	--	--
O-1@	--	x	--	--	--	--	x	--	--	--	--	--	--	--	--	--	--	--	--	galena, nantokite, sphalerite, chalcopyrite
Ontario shaft@	--	--	--	--	--	x	--	--	--	--	--	--	x	--	--	--	--	--	--	sphalerite
Ontario top l-1 sad	--	--	--	x	--	x	x	--	--	--	--	--	--	--	--	--	--	--	--	sphalerite
Ontario top pit	--	--	--	x	--	x	--	--	--	--	--	--	--	--	--	--	--	--	--	--
P1@	--	x	--	--	--	--	x	--	--	--	--	--	--	--	--	--	--	--	--	--
P2@	--	--	--	--	--	--	x	--	--	--	--	--	--	--	--	--	--	--	--	--
S-1@	--	--	x	--	--	x	x	x	--	--	--	--	--	--	--	--	--	--	--	titanite
S-2@	--	--	--	--	--	--	x	x	--	--	--	--	--	--	--	x	--	--	--	titanite
S-3@	--	x	--	x	--	x	x	x	--	--	--	--	--	--	--	--	--	--	--	sphalerite, nantokite
Sec 2*@	--	--	--	--	--	--	--	--	--	--	--	--	--	--	--	--	--	--	--	adularia
Bluegoosc@	--	--	x	--	--	x	--	--	--	--	--	--	--	--	--	--	--	x	--	pseudomalachite
m-1@	--	--	--	--	--	--	x	--	--	--	--	--	x	--	--	--	--	--	--	--
m-2@	--	--	--	--	?	?	x	x	--	--	--	--	--	--	--	--	--	--	--	titanite, clinopyroxene
m-5	--	--	x	--	--	?	x	--	--	--	--	--	x	--	--	--	--	--	--	--
ms-1	--	x	--	--	--	--	x	--	--	--	--	--	--	--	--	--	--	--	--	--
ms-2	--	x	--	--	--	--	x	--	--	--	--	--	--	--	--	--	--	--	--	tridymite
A15028	--	--	--	--	--	--	--	--	--	--	--	--	--	--	--	--	--	--	--	--
A15036	--	--	--	--	--	--	--	--	--	--	--	--	--	--	--	--	--	--	--	--
15@	--	--	--	--	--	--	x	x	--	--	--	--	--	--	--	--	--	--	--	--
20@	--	?	x	--	--	--	x	x	--	--	--	--	--	--	--	--	--	--	--	titanite
27b@	--	--	--	--	--	--	x	--	--	--	--	--	--	--	--	--	--	--	--	--
27c@	--	--	--	--	x	x	x	--	--	--	--	--	--	--	--	--	--	--	--	--
32@	--	--	?	--	--	--	x	--	--	--	--	--	x	--	--	--	--	--	--	--
47*@	--	--	x	--	--	tr	x	x	--	--	--	x	--	--	--	--	--	x	--	--
60@	--	--	x	--	--	x	x	x	--	--	--	--	--	--	--	--	--	--	--	titanite, hedenbergite
71white vein*	x	--	--	--	--	--	--	--	--	--	--	--	--	--	--	--	--	--	--	--
219b	--	--	--	--	x	--	x	--	--	--	--	--	--	--	--	--	--	--	--	--
233*@	--	?	--	--	?	--	x	x	--	--	--	--	--	--	--	--	--	--	--	gismodine
236@	--	--	--	--	--	x	x	--	--	--	--	--	--	--	--	--	--	x	--	cerusite
243*	--	x	--	--	--	--	x	--	--	--	--	x	--	--	--	--	--	x	--	galena
244@	--	--	x	--	--	--	x	x	--	--	--	--	--	--	--	--	x	x	--	--
246@	--	--	--	--	--	--	x	--	--	--	--	--	--	--	--	--	--	--	--	--
257a	--	--	--	--	--	--	--	--	--	--	--	--	--	--	--	--	--	--	--	mimetite

Appendix 11.3 (continued)

Sample no.	Clay analysis	K	I/S	I	S	Chl	Q	Feld	Alu	Pyr	Jar	Hem	Calc	Dias	Gyp	Fluor	Ana	Py	Ep	Other
263@	--	?	--	--	--	?	x	x	--	--	--	--	--	--	--	--	--	--	--	malachite
287@	--	--	x	--	--	--	x	x	--	--	--	--	--	--	--	x	--	--	--	titanite
297c	--	?	--	x	--	--	x	x	--	--	--	--	x	--	--	--	--	--	--	--
309*@	--	--	--	--	--	x	x	--	--	--	--	--	--	--	--	--	--	--	--	galena
311*@	--	--	--	--	--	--	x	--	--	--	--	--	--	--	--	--	--	--	--	--
323@	--	--	--	--	--	--	x	x	--	--	--	--	--	--	--	x	--	--	--	hedenbergite
349@	yes	x	x	--	--	--	x	x	--	--	--	--	--	--	--	--	--	--	--	pyrrhotite
340c*@	yes	--	--	x	--	--	x	--	--	--	--	--	--	--	--	--	--	--	--	--
350*@	yes	tr	--	x	--	--	x	--	--	--	--	--	--	--	x	--	--	--	--	--
367*	--	x	--	--	--	--	x	x	--	--	x	--	--	--	--	--	--	x	--	titanite
372@	--	--	--	--	--	--	--	--	--	--	--	--	--	--	--	--	--	--	--	malachite
434*@	--	--	--	--	--	--	x	--	--	--	--	--	--	--	--	--	--	--	--	--
434c@	--	--	--	--	--	x	x	x	--	--	--	--	--	--	--	x	--	x	--	titanite
469@	--	--	--	--	--	--	x	--	--	--	--	--	--	--	--	--	x	--	--	opal
486@	--	--	--	--	--	--	x	x	--	--	--	--	x	--	--	--	--	--	--	--
510b-2*@	yes	x	x	--	--	--	--	--	--	--	--	--	--	--	--	x	--	--	--	--
512b	yes	--	x	--	--	--	x	--	--	--	--	--	--	--	--	--	--	--	--	--
513@	yes	x	x	--	--	--	x	--	--	--	--	--	--	--	--	x	--	--	--	--
516b	--	--	--	x	--	--	x	--	--	x	--	--	--	--	--	--	--	--	--	--
536*	--	x	--	x	--	--	x	x	x	--	--	--	--	--	--	--	--	x	--	--
538	yes	x	x	--	--	--	x	x	--	--	--	--	--	x	--	--	--	--	--	azurite
544	yes	x	x	--	--	--	x	x	--	x	--	--	--	--	--	--	x	--	--	--
545@	yes	x	x	--	--	--	x	--	--	--	--	--	--	--	--	x	x	--	--	--
546*@	yes	--	x	--	--	--	x	x	--	--	--	--	--	--	--	--	--	--	--	chalcopyrite
546b	--	--	--	--	--	--	x	--	--	x	--	x	--	--	--	--	--	--	--	--
549*@	yes	--	--	--	x	--	x	x	--	--	--	--	--	--	x	--	--	--	--	--
588@	--	x	--	x	--	--	x	x	--	--	--	--	--	--	--	--	--	--	--	--
594@	yes	x	--	--	--	--	x	--	--	--	--	--	--	--	x	--	--	--	--	--
605@	--	--	x	--	--	x	x	x	--	--	--	--	--	--	--	--	--	--	--	titanite
608b@	--	?	?	--	--	--	x	x	--	--	--	--	--	--	--	--	--	--	--	titanite
634@	yes	x	x	--	--	--	x	--	--	--	--	--	--	--	--	--	--	--	--	--
695@	--	--	--	--	--	--	x	x	--	--	--	--	--	--	--	--	--	--	--	goethite, titanite
708*@	--	x	--	--	--	?	x	x	--	--	--	--	--	--	--	--	x	--	--	goethite, chrysocolla
710*@	--	--	--	--	--	x	x	--	--	--	--	--	--	--	--	--	--	--	--	galena
724a*	yes	--	--	--	x	--	x	--	x	--	--	--	--	x	--	--	--	x	--	--
724b@	yes	x	x	--	--	--	x	x	x	--	--	--	--	--	--	--	--	x	--	titanite
743	yes	--	--	--	--	--	x	--	--	--	--	--	--	--	--	--	--	--	--	--
783	--	--	--	x	--	--	x	--	--	--	--	--	--	--	--	--	--	--	--	--
800	--	x	--	x	--	--	x	--	--	--	--	--	--	--	--	--	--	--	--	--
801	--	--	--	--	?	?	x	x	--	--	--	--	--	--	--	--	--	--	--	titanite, aegirine
813b@	--	x	--	x	--	--	x	--	--	--	--	--	--	--	--	--	--	--	--	--

Appendix 11.3 (continued)

Sample no.	Clay analysis	K	I/S	I	S	Chl	Q	Feld	Alu.	Pyr	Jar	Hem	Calc	Dias	Gyp	Fluor	Ana	Py	Ep	Other
817b	--	--	--	x	--	--	x	--	--	--	--	--	--	--	--	--	--	--	--	cristobalite
837@	--	--	--	--	--	--	x	--	--	--	--	--	--	--	--	--	x	--	--	--
850@	--	--	--	x	--	--	x	--	--	--	--	--	--	--	--	--	--	--	--	--
850a@	--	--	--	--	--	--	x	x	--	--	--	--	--	--	--	--	--	x	--	--
888-1@	--	x	--	--	--	--	x	--	--	--	--	--	--	--	--	--	--	--	--	--
888-2	--	?	--	?	--	?	x	--	--	--	--	--	x	--	--	x	--	--	--	sphalerite, diopside
888-3@	--	--	--	--	--	--	x	--	--	--	--	--	--	--	--	--	--	--	--	--
888-4	--	--	x	--	--	--	x	--	--	--	--	--	--	--	--	--	--	x	--	pseudomalachite
889-1@	--	?	--	x	--	?	x	x	--	--	--	--	--	--	--	x	--	--	--	titanite
889-2@	--	--	--	x	--	x	x	x	--	--	--	--	--	--	--	--	--	--	--	--
890-1	--	--	--	--	--	--	x	x	--	--	x	--	--	--	--	--	--	--	--	--
890-2@	--	--	--	?	--	--	x	x	--	--	--	--	--	--	--	--	--	x	--	titanite
890-3@	--	--	--	--	--	--	x	x	--	--	--	--	--	--	--	--	x	--	--	titanite
890-4	--	x	--	x	--	--	x	x	--	--	x	--	--	--	x	--	--	--	--	ferrihydrite
890-5	--	--	--	x	--	--	x	x	--	--	--	--	--	--	--	--	--	--	--	titanite
903@	--	--	--	--	--	--	x	--	--	--	--	--	--	--	--	--	?	--	--	--
909a@	--	?	--	?	--	?	x	x	--	--	--	--	--	--	--	--	--	x	--	titanite
917a@	--	x	--	x	--	--	x	--	--	--	--	--	--	--	--	--	--	--	--	rutile
917b	--	x	--	--	--	--	x	--	--	--	--	x	--	--	--	--	--	--	--	--
917c	--	--	--	--	--	x	x	--	--	--	--	--	--	--	--	--	--	--	--	maghemite
917d@	--	x	--	--	?	?	x	x	--	--	--	--	--	--	--	--	--	--	--	titanite, hedenbergite
918@	--	--	--	--	--	x	x	x	--	--	--	--	--	--	--	x	--	--	--	titanite
920@	--	--	--	?	--	--	x	--	--	--	--	x	--	--	--	--	--	--	--	gismondine
922@	-	x	?	--	--	x	x	x	--	--	--	--	--	--	--	--	--	--	--	cerussite, brookite, anhydrite
923@	--	x	--	--	--	x	x	x	--	--	--	--	--	--	--	--	--	--	--	manganosite
927@	--	?	--	--	--	--	x	x	--	--	--	--	--	--	--	--	--	--	--	titanite
984@	--	--	--	?	--	--	x	--	--	--	x	--	--	--	--	x	--	x	--	goethite
992	--	--	--	--	--	--	x	--	--	--	--	--	--	--	--	x	--	x	--	goethite
1011@	--	--	--	x	--	--	x	x	--	--	--	--	--	--	--	--	--	x	--	pyrolusite
1017@	--	--	--	x	--	--	x	x	--	--	--	--	--	--	--	--	--	--	--	gismondine, goethite
1033a@	--	x	--	--	--	--	x	x	--	--	--	--	--	--	--	--	--	--	--	--
1041@	--	--	--	--	--	--	x	--	--	--	--	--	x	--	--	--	--	--	--	--
1043@	--	--	x	--	--	--	x	--	--	--	--	--	--	--	--	x	--	--	--	--
1050@	--	--	--	x	--	--	x	x	--	--	--	--	--	--	--	--	--	--	--	titanite
1053@	--	x	x	--	--	?	x	x	--	--	--	--	--	--	--	x	--	--	--	rutile, manganosite
1064a*	--	x	--	--	--	--	x	x	--	--	--	--	--	--	--	--	--	--	--	greigite, minamiite, anhydrite, pseudobrookite
1068a@	--	?	x	--	--	?	x	x	--	--	--	--	--	--	--	x	--	--	--	azurite
1068b@	--	x	--	--	--	--	x	x	--	--	--	--	--	--	--	--	--	--	--	goethite
1071@	--	--	--	--	--	--	x	--	--	--	--	--	--	--	--	x	--	--	--	--
1080	--	--	--	x	--	--	x	--	--	--	x	--	--	--	--	--	--	--	--	--
1086b	--	--	?	--	--	--	x	x	--	--	--	--	--	--	--	--	--	--	--	titanite

Appendix 11.3 (continued)

Sample no.	Clay analysis	K	I/S	I	S	Chl	Q	Feld	Alu	Pyr	Jar	Hem	Calc	Dias	Gyp	Fluor	Ana	Py	Ep	Other
Drill core																				
Summit S88-s																				
S-885-5-10	yes	x	x	--	--	--	x	--	--	--	--	--	--	--	x	--	--	--	--	--
21-27	yes	x	x	--	--	--	x	--	--	--	x	--	--	--	--	--	--	--	--	--
38-43	yes	x	x	--	--	--	--	--	--	--	--	--	--	--	--	--	--	--	--	--
58-64	yes	x	x	--	--	--	x	--	--	--	--	--	--	--	--	--	--	--	--	--
70-73	yes	x	x	--	--	--	--	--	--	--	--	--	--	--	--	--	--	--	--	--
114.5	yes	x	--	x	--	--	x	--	--	x	--	--	--	--	--	--	--	--	--	--
124-135	yes	x	--	x	--	--	x	--	--	--	--	--	--	--	--	--	--	--	--	--
145.5-146.5	yes	x	x	--	--	--	--	--	--	--	--	--	--	--	--	--	--	--	--	goethite
181-183	yes	x	x	--	--	--	x	x	--	--	--	--	--	--	--	--	--	--	--	--
194-196	--	x	--	x	--	--	x	x	--	--	--	--	--	--	--	--	--	x	--	titanite
212	--	x	--	x	--	--	x	x	--	--	--	--	--	--	--	--	--	--	--	rutile
237	--	x	--	x	--	--	x	x	--	--	--	--	--	--	--	--	--	--	--	--
273	yes	x	--	x	--	--	x	x	--	--	--	--	--	--	--	--	--	--	--	--
241.5-246	yes	x	x	--	--	--	--	--	--	--	--	--	--	--	--	--	--	--	--	--
266-267	yes	x	x	--	--	--	x	x	--	--	--	--	--	--	--	--	--	--	--	--
267-268	yes	x	x	--	--	--	x	x	--	?	--	x	--	--	--	--	--	--	--	--
282-282.5	yes	x	x	--	--	--	x	--	--	--	--	--	--	--	--	--	--	--	--	--
288.5-289	yes	x	x	--	--	--	x	--	--	--	--	--	--	--	--	--	--	--	--	--
295.5	--	--	--	x	--	--	x	x	--	--	--	--	--	--	--	--	--	--	--	titanite, hedenbergite, chalcopyrite
338-339	yes	x	--	--	--	--	x	--	--	--	--	--	--	--	--	--	--	--	--	--
360.5	--	x	--	--	x	x	x	--	--	--	--	--	x	--	--	--	--	--	--	--
372	yes	x	x	--	--	--	x	x	--	--	--	--	--	--	--	--	--	--	--	titanite
430	yes	x	--	tr	--	--	--	--	--	--	--	--	--	--	--	--	--	--	--	--
432.5-433	yes	x	--	tr	--	--	x	--	--	--	--	x	--	--	--	--	--	--	--	tridymite
440.5-443	yes	x	x	--	--	--	x	x	--	--	--	--	--	--	--	--	--	--	--	titanite
462.5	yes	x	--	--	--	--	--	--	--	--	--	--	--	--	--	--	--	--	--	--
463	--	x	x	--	--	x	x	x	x	x	--	--	--	x	--	--	--	--	--	--
S89-8-12	--	--	--	--	--	--	--	--	--	--	--	--	--	--	--	--	--	--	--	--
24	x	x	x	x	--	--	--	--	--	--	--	--	--	--	--	--	--	x	--	--
40	x	x	x	--	--	--	--	--	--	--	--	--	--	--	--	--	--	--	--	--
63	x	x	--	--	--	--	--	--	--	--	--	--	--	--	--	--	--	--	--	--
71	x	x	--	--	--	--	--	--	--	--	--	--	--	--	--	--	--	--	--	--
108	x	x	x	--	--	--	--	--	--	--	--	--	--	--	--	--	--	--	--	--
125	x	x	--	--	--	--	--	--	--	--	--	x	--	--	--	--	--	--	--	--
136	x	x	x	--	--	--	--	--	--	--	--	--	--	--	--	--	--	x	--	tridymite
146	x	x	--	--	--	--	--	--	--	--	--	--	--	--	--	--	--	--	--	--
153	x	x	x	--	--	--	--	--	--	--	--	--	x	--	--	--	--	--	--	--
160	x	x	--	--	--	--	--	--	--	--	--	--	--	--	--	--	--	--	--	--
172	x	x	--	--	--	--	--	--	--	--	--	--	--	--	--	--	--	--	--	--

Appendix 11.3 (continued)

Sample no.	Clay analysis	K	I/S	I	S	Chl	Q	Feld	Alu	Pyr	Jar	Hem	Calc	Dias	Gyp	Fluor	Ana	Py	Ep	Other
254.2	x	x	—	--	--	--	--	--	--	--	--	--	--	--	--	--	--	--	--	--
256	x	x	--	--	--	--	--	--	--	--	--	--	--	—	—	--	--	--	--	jacobsite
262	x	x	x	--	--	--	--	--	--	--	--	--	--	—	--	--	--	--	--	jacobsite
271.5	x	x	x	--	--	--	--	--	--	—	--	--	--	--	--	--	--	--	--	--
421	x	x	--	--	--	--	--	--	--	--	--	--	--	—	--	--	--	--	--	jacobsite
Summit																				
B91-17-18	--	x	--	--	--	--	x	--	x	--	--	--	--	--	--	--	--	--	--	--
B91-17-112	--	x	x	--	--	x	x	x	--	--	--	--	x	--	--	--	x	--	--	--
B91-17-224	--	x	—	--	--	--	x	--	--	--	--	--	--	--	--	x	--	--	--	--
B91-17-371.5	--	--	x	--	--	--	x	--	--	--	--	--	--	--	--	--	--	--	--	dolomite
B91-17-469	--	--	--	--	--	--	x	--	--	--	--	--	--	--	--	--	--	--	--	rhodochrosite
B91-17-478	--	--	--	x	--	--	x	x	x	--	--	--	--	--	--	--	x	--	--	--
B91-17-480	--	x	--	--	--	--	x	--	--	--	--	--	--	--	--	--	--	--	--	siderite
B91-17-481	--	--	--	--	--	--	x	--	--	--	--	--	--	--	--	--	--	--	--	siderite
B91-17-489	--	--	x	--	--	--	x	--	--	--	--	--	--	--	--	--	--	--	--	marcasite
B91-17-534-535	--	--	—	--	--	x	x	x	--	--	--	--	--	x	--	--	--	--	--	tennantite
B91-17-573-583	--	--	--	x	--	x	--	--	--	--	--	--	--	--	--	--	--	--	--	--
B91-17-633	yes	x	x	--	--	x	x	x	--	--	--	--	x	--	--	--	--	--	--	aegirine
B91-17-651	--	--	--	--	--	x	x	x	--	--	--	--	--	--	--	--	--	--	--	aegirine, titanite, sphalerite
B91-17-775	--	--	--	x	--	x	x	x	x	--	--	--	--	--	--	--	--	--	--	dolo, sphalerite
B91-17-776	--	--	--	--	--	x	x	--	--	--	--	--	--	--	--	--	--	--	--	sphalerite
B91-17-798	--	x	—	--	--	--	x	--	--	—	--	--	--	--	--	--	--	--	--	dolomite
B91-17-798-805	--	--	x	--	--	x	x	--	--	x	--	--	--	?	--	x	--	x	--	--
B91-17-839	--	--	x	--	--	x	x	--	x	--	--	--	--	--	--	--	--	--	--	--
B91-17-886	--	--	--	--	--	--	--	--	--	--	--	--	--	--	--	--	--	--	--	dolomite
B91-17-886	--	--	--	--	--	--	x	--	--	--	--	--	--	--	--	--	--	--	--	dolomite
B91-17-941	--	--	x	--	--	--	x	x	x	--	--	--	--	x	--	--	--	x	--	--
B91-17-1074	--	--	x	--	--	x	x	--	--	--	?	--	x	--	--	--	--	x	--	--
B91-17-1025	--	--	--	--	--	--	--	--	--	--	--	--	--	--	--	--	--	--	--	rhodochrosite
Summit																				
B92-1-694	--	--	x	—	--	--	x	--	--	--	--	--	--	--	--	--	--	--	--	dolomite
Summit																				
M91-4-200	--	x	--	x	--	--	x	--	--	x	--	--	x	--	--	--	--	x	--	--
M91-4-208	--	--	x	--	--	--	x	x	--	--	--	--	--	--	--	--	--	--	--	chalcopyrite, hornblende, sphalerite
M91-4-510	--	x	x	--	—	x	x	x	--	--	--	--	--	--	--	--	—	x	--	sphalerite
M91-4-689-690	--	?	x	--	?	x	x	x	--	--	--	--	x	--	--	--	--	x	--	--
M91-4-797-798	--	--	--	x	--	--	x	--	--	--	--	--	--	--	--	--	--	x	--	--
M91-4-800.6-801.6	--	—	x	--	--	--	x	--	--	--	--	--	--	--	--	--	--	--	--	--

Appendix 11.3 (continued)

Sample no.	Clay analysis	K	I/S	I	S	Chl	Q	Feld	Alu	Pyr	Jar	Hem	Calc	Dias	Gyp	Fluor	Ana	Py	Ep	Other
Jim Crow-Imperial																				
J84-2-189-190	--	x	--	--	--	--	x	x	--	--	x	--	x	--	--	--	--	x	--	--
J84-2-223.3-223.7		--	--	--	--	x	x	x	--	--	--	--	--	--	--	--	--	--	--	titanite, hedenbergite
J84-3-228-228.2	--	--	--	x	--	x	x	--	--	--	--	x	x	--	--	--	--	--	--	--
J84-3-304-307	--	x	x	--	--	--	x	x	?	--	--	--	--	--	--	--	--	--	--	--
J84-3-423	yes	--	x	--	--	x	x	--	--	--	--	--	x	--	--	--	--	--	--	--
USBM Carlisle-Center mines																				
H1-54	--	x	--	--	--	x	x	x	--	--	--	--	--	--	--	--	--	--	--	titanite
H1-134	--	?	--	--	--	x	x	x	--	--	--	--	--	--	--	--	--	--	--	titanite, aegirine
H1-173.5	--	--	--	--	--	--	x	x	--	--	--	--	x	--	--	--	--	--	--	sphalerite, galena
H1-175-176	--	--	--	--	--	x	x	x	--	--	--	--	--	--	--	--	--	--	--	aegirine-augite, galena, titanite
H1-235	--	--	--	x	--	x	x	x	--	--	--	--	--	--	--	--	--	x	--	wulfenite
H1-307	--	--	--	--	--	x	x	x	--	--	--	--	--	--	?	--	--	--	--	anhydrite
H2-223.1-223.2	yes	--	--	x	--	x	x	--	--	--	--	--	--	--	--	--	--	x	--	--
H4-148-148.4	yes	tr	--	x	x	?	x	--	--	--	--	--	--	--	--	--	--	--	--	--
H4-162-162.5	--	x	?	--	--	?	x	--	--	--	--	--	x	--	--	--	--	--	--	--
H5-166.6-170	--	--	--	--	--	x	x	--	--	--	--	--	--	--	--	--	--	x	--	galena
H5-171	--	x	--	x	--	?	x	--	--	--	--	--	--	--	--	--	--	--	--	--
H5-176	--	?	--	?	--	x	x	--	--	--	--	--	--	--	--	--	--	--	--	--
H5-184	yes	x	--	x	--	--	x	--	--	--	--	--	--	--	--	--	--	--	--	--
H5-188	--	x	--	--	--	--	x	x	--	--	--	--	--	--	--	--	--	x	--	--
H6-45	--	--	--	--	--	x	x	x	--	--	--	--	--	--	--	--	--	x	--	enstatite
H6-216.4	yes	x	--	--	--	x	x	--	--	--	--	--	--	--	--	--	--	--	--	sphalerite
H7-33.8-34.4	--	?	--	?	--	?	x	x	--	--	--	--	--	--	--	--	--	--	--	titanite, gismondine
H7-162-163	yes	x	--	x	--	--	x	--	--	--	--	--	--	--	--	--	--	x	--	--
H7-213	--	x	--	--	--	--	x	x	--	--	--	--	--	--	--	--	--	x	--	chalcopyrite
H9-53.5	--	x	--	--	--	--	x	--	--	x	--	--	x	--	--	--	--	--	--	azurite, enstatite
H9-209	--	--	--	--	--	x	x	x	--	--	--	--	x	--	--	--	--	--	--	wulfenite?
H9-250.5	--	--	--	--	--	--	--	--	--	--	--	--	--	--	--	--	--	--	--	goethite, titanite
H9-211	--	--	--	--	x	--	x	x	--	--	--	--	--	--	--	--	--	--	--	--
H9-225	--	--	x	--	--	x	tr	x	--	--	--	--	--	--	--	--	--	--	--	clinoenstatite, titanite
H9-259-7-260.2	x	--	--	--	x	x	x	?	--	--	--	--	x	--	--	--	--	--	--	--
H9-270.5	--	--	--	--	--	x	x	x	--	--	--	--	--	--	--	--	--	x	--	titanite
H9-295	--	?	--	x	?	x	x	--	--	--	--	--	--	--	--	--	--	--	--	gismondine
H9-312-314	--	x	--	x	x	--	x	--	--	--	--	--	--	--	--	--	--	--	--	--
H9-315-318	--	--	?	x	--	x	x	--	--	--	--	--	--	--	--	--	--	--	--	--
H9-330	--	--	--	x	--	--	x	--	--	--	--	--	x	--	--	--	x	--	--	--
H9-328-334	--	--	--	x	--	--	x	--	--	--	--	--	--	--	--	--	--	--	--	--
H9-367.6	--	x	x	--	--	--	x	--	--	--	--	x	x	--	--	--	--	?	--	chalcopyrite?, cuprite
H9-369.6	--	?	--	x	--	?	x	--	--	--	--	--	x	--	--	--	--	--	--	--

Appendix 11.3 (continued)

Sample no.	Clay analysis	K	I/S	I	S	Chl	Q	Feld	Alu	Pyr	Jar	Hem	Calc	Dias	Gyp	Fluor	Ana	Py	Ep	Other
H9-376-376.8	--	--	--	x	--	x	x	--	--	--	--	--	x	--	--	--	--	--	--	--
H9-379.6-388	--	x	x	--	--	x	x	x	--	--	--	--	x	--	--	--	--	--	--	--
H9-420-421	--	x	x	--	--	x	x	x	?	--	--	--	x	--	--	--	--	x	--	--
H9-429	--	--	--	--	--	x	x	x	--	--	--	--	--	--	--	--	--	--	--	titanite
H9-472.9-473.2	--	--	x	--	x	x	x	?	--	--	--	--	--	--	--	--	--	--	--	--
H9-497	--	--	--	x	--	x	x	x	--	--	--	--	--	--	--	--	--	x	--	sphalerite, galena
H9-501	--	x	--	--	--	--	x	x	--	--	--	--	x	--	--	--	--	x	--	galena
H9-502	--	--	--	x	--	x	x	--	--	--	--	--	--	--	--	--	--	x	--	pseudomalachite
H9-506.6-507.2	x	x	--	--	x	x	x	--	--	--	--	--	x	--	--	--	--	x	--	--
H9-542	--	--	--	--	--	x	x	x	--	--	--	--	x	--	--	--	--	x	--	chalcopyrite, galena
H9-558-559	yes	x	--	--	x	--	x	x	--	--	--	--	--	--	--	--	--	--	--	titanite, chalcopyrite
H10-26.4-26.5	yes	x	x	--	--	--	x	--	--	x	--	--	--	--	--	--	x	--	--	--
H10-57.8-57.9	--	x	--	--	--	--	x	--	--	x	--	--	--	--	--	--	--	--	--	--
H10-85.9-86.1	--	x	--	--	--	--	x	--	--	x	--	--	--	x	--	--	--	--	--	--
H10-90.6-91	--	?	--	x	--	?	x	x	--	--	--	--	--	--	--	--	--	--	--	titanite
H10-92-92.1	--	x	--	x	--	--	x	--	--	x	--	--	--	--	--	--	x	--	--	--
H10-123.9-124	--	x	--	--	--	--	x	--	--	--	--	--	--	--	--	--	--	--	--	--
H10-134.2-134.4	--	x	--	--	--	--	x	--	--	--	--	--	--	--	--	--	--	x	--	--
H10-145.5-.8	yes	x	--	--	--	--	x	--	--	x	--	--	--	--	--	--	--	x	--	--
H10-215.8-216.4	--	x	--	--	--	--	x	x	--	--	--	--	--	--	--	--	--	--	--	--
H10-219.9-220.7	--	x	--	--	--	--	x	--	--	x	--	--	--	--	--	--	--	x	--	--
H10-253.6-255.9	--	--	--	x	--	--	x	--	--	--	--	--	--	--	--	--	--	x	--	fluorite
H10-273.3-274.7	--	--	--	x	--	--	x	--	--	--	--	--	--	--	--	--	--	x	--	goethite
H10-279-279.8	--	x	--	--	--	--	x	--	--	--	--	--	--	--	--	--	--	x	--	cerussite
H10-284	--	--	--	--	--	x	x	x	--	--	--	--	--	--	--	--	--	--	--	titanite
H10-326-326.5	--	--	x	--	--	x	x	x	--	--	--	--	--	--	--	--	--	--	--	--
H10-369-369.4	--	x	x	--	--	x	x	x	?	--	--	--	--	--	--	--	--	--	--	dolomite
H10-353.3	--	x	--	x	--	--	x	x	--	--	--	--	--	--	--	--	--	--	--	--
H10-404.8	--	x	x	--	--	--	x	x	--	--	--	--	--	--	--	--	--	--	--	--
H10-412-412.6	yes	x	x	--	--	x	x	x	--	x	--	--	--	--	--	--	--	--	--	--
H11-250	--	--	--	x	--	--	--	--	--	--	--	--	--	--	--	--	--	--	--	brookite, pseudomalachite
H11-251.2	yes	x	--	x	--	--	x	--	--	--	--	--	--	--	--	--	--	x	--	--
H11-254.8	--	--	--	x	--	--	x	--	--	--	--	--	--	--	--	--	--	?	--	pseudomalachite, sphalerite
H12-134.6	--	x	x	--	--	x	x	x	--	--	--	--	--	--	--	--	--	--	--	--
H14-184.5-185	--	--	--	--	--	--	x	--	--	x	--	x	--	--	--	--	--	x	--	sphalerite
H14-188	--	x	--	--	--	--	x	--	--	x	x	--	--	--	--	--	--	--	--	--
H14-218.9-219	--	x	--	x	--	--	x	x	--	--	--	--	--	--	--	--	x	--	--	dolomite, cinnabar?
H14-225.5	--	x	--	x	--	x	x	x	--	--	--	--	--	--	--	--	x	--	--	--
H14-228.4-229.6	--	x	--	x	--	--	x	x	--	x	--	--	--	--	--	--	--	--	--	anhydrite?
H14-237	yes	x	--	x	--	--	x	x	--	x	x	--	--	x	--	--	x	--	--	--
H14-231	--	x	--	x	--	--	x	--	--	x	--	--	--	--	--	--	--	--	--	--

Appendix 11.3 (continued)

Sample no.	Clay analysis	K	I/S	I	S	Chl	Q	Feld	Alu	Pyr	Jar	Hem	Calc	Dias	Gyp	Fluor	Ana	Py	Ep	Other
H14-243.6	--	--	--	--	--	--	x	--	--	--	--	--	--	--	--	--	--	--	--	--
H14-269	--	x	--	x	--	--	x	--	--	x	--	--	--	--	--	--	--	--	--	--
H14-291	--	x	x	--	--	x	x	x	--	--	--	--	--	--	--	--	--	--	--	--
Alabama																				
A1-19	--	--	--	--	--	x	x	x	--	--	--	--	--	--	--	--	--	--	--	--
A1-67-67.5	--	--	--	--	--	--	x	x	--	--	--	--	x	--	--	--	--	--	--	--
A1-122	--	x	--	--	--	--	x	--	--	--	--	--	--	--	--	--	--	--	--	--
A1-177	--	--	--	--	--	x	x	x	--	--	--	--	x	--	--	--	x	x	--	--
A2-9	--	x	x	--	--	x	x	x	--	--	--	--	x	--	--	--	--	--	--	--
A2-31.5	--	--	--	--	--	x	--	--	--	--	--	--	--	--	x	--	--	--	--	--
A2-54.8	--	x	--	--	--	x	x	--	--	--	--	--	--	--	x	--	--	--	--	--
A2-60	--	--	x	--	--	x	x	--	--	--	--	--	--	--	--	--	--	--	--	--
A2-65.5	--	--	--	--	--	x	--	--	--	--	--	--	x	--	--	--	--	--	--	--
A2-128.3	--	x	x	--	--	x	--	--	--	--	--	--	x	--	--	--	--	--	--	--
A2-171.8-172.1	x	x	--	--	x	x	--	--	--	--	--	--	--	--	--	--	--	--	--	--
Center mine samples																				
C3-48	--	x	--	--	--	--	x	x	--	--	--	--	--	--	--	--	--	--	--	galena, sphalerite
C-141	--	--	x	--	--	--	x	--	--	--	--	--	x	--	--	x	--	--	--	sphalerite
C-357	--	--	--	--	--	--	--	--	--	--	--	--	--	--	--	x	--	--	--	sphalerite?
C-369	--	--	--	--	--	--	--	--	--	--	--	x	x	--	--	--	--	--	--	--
C-389	--	--	--	--	--	x	x	x	--	--	--	--	x	--	--	x	--	--	x	--
Center min id	--	x	--	--	--	x	x	--	--	--	--	--	--	--	--	--	--	--	--	sphalerite, galena, clinochlore
Center ore	--	--	--	--	--	?	x	x	--	--	--	--	--	--	--	x	--	--	--	chalcopyrite
Center dump	--	--	--	x	--	--	x	--	--	--	--	--	--	--	--	--	--	x	--	--
Center level 2-3 366	yes	x	--	x	--	--	x	--	--	--	--	--	--	--	--	--	--	--	--	--
Center level 3-124	--	--	--	--	x	x	x	--	--	--	--	--	--	--	--	--	--	--	--	sphalerite, galena
Center 4th xcut 20	yes	--	x	--	--	--	x	--	--	--	--	--	--	--	--	--	--	--	--	--
Center 4th xcut 43	yes	x	--	x	tr	--	--	--	--	--	--	--	--	--	--	--	--	--	--	--
Center 4th 49e n wall	yes	x	--	--	x	x	x	--	--	--	--	--	--	--	--	--	--	--	--	--
Center 5 to 6-45	--	--	x	--	--	x	x	x	--	--	--	--	--	--	--	--	--	--	--	titanite, aegirine
Center 6th	yes	x	--	x	--	--	x	--	--	--	--	--	x	--	--	--	--	--	--	--
Center 6th fan	--	--	--	x	--	x	--	--	--	--	--	--	--	--	--	--	--	x	--	chalcopyrite, sphalerite
Center 7th xfault	--	--	--	--	--	--	x	--	--	--	--	--	--	--	x	--	--	--	--	--
Center 8th xcut 10E	yes	x	--	x	--	--	--	--	--	--	--	--	--	--	--	--	--	--	--	--
Center 8th xcut 2v 21	yes	x	x	--	--	--	--	--	--	--	--	--	--	--	--	--	--	--	--	--
Center level 10-1	--	--	--	x	--	--	x	--	--	--	--	--	--	--	--	--	--	x	--	--
Center level 10-52	--	--	x	--	--	x	--	--	--	--	--	--	--	--	--	--	--	--	--	--
Center level 10-53	--	--	--	--	--	x	x	--	--	--	--	--	--	--	--	--	--	--	--	--
Center level 10-56	--	--	x	--	--	x	--	--	--	--	--	--	--	--	--	--	--	x	--	rutile

Appendix 11.3 (continued)

Sample no.	Clay analysis	K	I/S	I	S	Chl	Q	Feld	Alu	Pyr	Jar	Hem	Calc	Dias	Gyp	Fluor	Ana	Py	Ep	Other
Center drill core samples																				
c1-67.6-68	yes	x	x	--	--	--	x	x	--	--	--	--	--	--	--	--	--	--	--	--
c1-68.6	yes	--	x	--	--	x	x	x	--	--	--	--	--	--	--	--	--	x	--	--
C1-92	yes	x	--	x	--	--	x	x	x	--	--	--	--	--	--	x	--	--	--	--
Bitter Creek hole																				
BC1-95.2-95.7	yes	x	x	--	--	x	x	x	--	--	--	--	--	--	--	--	--	x	--	--
BC1-112-113	--	--	--	x	--	x	x	x	--	--	--	--	--	--	--	--	--	--	--	--
BC1-124-129	--	--	--	x	x	x	x	x	--	--	--	--	--	--	--	--	--	x	--	--
BC1-126	--	--	--	--	--	x	x	x	--	--	--	--	--	--	--	--	--	x	--	magnetite
BC1-153	--	--	--	--	--	x	x	--	--	--	--	--	--	--	--	x	x	--	--	--
BC1-154-160	--	--	--	--	--	x	x	x	--	--	--	--	--	--	--	--	--	--	--	--
BC1-292-294	--	x	--	--	--	x	x	x	--	--	--	--	--	--	--	--	--	x	--	--
BC1-275-277	--	--	--	--	x	--	x	--	--	--	--	--	--	--	--	x	--	--	--	sphalerite
BC1-271.8	--	--	--	x	x	--	x	--	--	--	--	--	--	--	--	x	--	--	--	sphalerite
BC1-277	--	--	--	--	--	--	x	x	--	--	--	--	--	--	--	--	--	x	--	--
BC1-284	--	--	--	x	--	x	x	x	--	--	--	--	--	--	--	--	--	x	--	despujolsite(?)
BC1-315.8	--	--	--	--	--	--	x	x	--	--	--	--	--	--	--	--	--	x	--	titanite, hedenbergite
BC1-320	--	--	--	--	--	x	x	x	--	--	--	--	--	--	--	x	--	x	--	--
BC1-374-376	--	--	--	x	--	--	x	x	--	--	--	--	--	--	--	--	--	x	--	--
BC1-382-384	--	--	--	--	--	x	x	x	--	--	--	--	--	--	--	--	--	x	--	--
BC1-386.5	--	--	--	--	--	--	x	--	--	--	--	--	--	--	--	x	--	x	--	sphalerite
BC1-492-500	--	?	--	x	--	?	x	x	--	--	--	--	--	--	--	--	--	--	--	--
BC1-650	--	--	--	x	--	x	x	x	--	--	--	--	--	--	--	--	--	x	--	--
BC1-703-704	--	--	--	x	x	x	x	x	--	--	--	--	--	--	--	--	--	x	--	--
BC1-761.8	--	x	--	x	--	--	x	x	--	--	--	--	--	--	--	--	--	--	--	--
BC1-933.2	--	--	--	--	--	x	x	x	--	--	--	--	--	--	--	--	--	x	--	titanite
BC1-951-953	--	?	--	--	--	?	x	x	--	--	--	--	x	--	--	--	--	--	--	--
BC1-1023	--	--	--	x	--	x	x	x	--	--	--	--	--	--	--	--	--	x	--	titanite
BC1-1023	--	--	--	--	?	--	x	x	--	--	--	--	--	--	--	--	--	--	--	gismondine
BC1-1189.8	--	--	x	--	--	x	x	x	--	--	--	--	--	--	--	--	--	x	--	--
BC1-1400	--	--	--	--	x	--	x	x	--	--	--	--	--	--	--	--	--	--	--	anhydrite
BC1-1445.5	--	--	--	--	--	x	x	x	--	--	--	--	--	--	--	--	--	x	--	anhydrite
BC1-1472	--	--	--	--	--	x	x	x	--	--	--	--	x	--	--	--	--	--	x	epidote
BC1-1474	--	--	--	--	--	--	x	x	--	--	--	--	--	--	--	--	--	x	--	--
BC1-1522	--	--	x	--	--	--	x	x	--	--	--	--	--	--	--	--	--	x	--	anhydrite
BC1-1566-1568	--	--	--	--	--	--	x	x	--	--	--	--	--	--	--	--	--	x	--	anhydrite, titanite
BC1-1568-1572	--	--	--	--	--	--	x	x	--	--	--	--	--	--	--	--	--	--	--	saponite, anhydrite, sphalerite
BC1-1572-1577	--	--	--	--	--	x	x	x	--	--	--	--	--	--	--	x	--	x	--	galena, sphalerite
BC1-1573	--	--	--	--	--	x	x	x	--	--	--	--	--	--	--	--	--	x	--	anhydrite, titanite
BC1-1647-1648	--	--	--	--	--	x	x	x	--	--	--	--	--	--	--	--	x	x	--	sphalerite

Appendix 11.3 (continued)

Sample no.	Clay	K	I/S	I	S	Chl	Q	Feld	Alu	Pyr	Jar	Hem	Calc	Dias	Gyp	Fluor	Ana	Py	Ep	Other
BC1-1753	--	--	--	--	?	?	x	x	--	--	--	--	--	--	--	--	--	--	--	--
BC1-1797	--	x	--	--	x	--	--	--	--	--	--	--	x	--	--	--	--	--	--	--
BC1-1826-1827	--	--	--	x	x	x	x	--	--	--	--	--	--	--	--	--	--	--	--	--
BC1-1989-1989.6	--	--	x	--	--	x	x	x	--	--	--	--	x	--	--	--	--	--	--	--
BC1-1996	--	--	--	--	--	--	x	x	--	--	--	--	x	--	--	--	--	x	--	--
BC1-1997	--	--	x	--	--	--	x	x	--	--	--	--	--	--	--	--	--	--	--	titanite
BC1-1997.8	--	x	--	--	--	--	x	x	--	--	--	--	--	--	--	--	--	--	--	anhydrite
BC1-2144	--	--	--	x	--	x	x	x	--	--	--	--	--	--	--	--	--	--	--	anhydrite
BC1-2198.6	--	x	--	x	--	--	x	x	--	--	--	--	--	--	--	--	--	x	--	anhydrite, pseudobrookite
BC1-2220	--	--	x	x	--	--	x	x	--	--	--	--	--	--	--	--	--	--	--	anhydrite, titanite
BC1-2250	--	--	--	x	--	x	--	x	--	--	--	--	--	--	--	--	--	x	--	--
BC1-2425	--	--	--	--	--	x	x	x	--	--	--	--	--	--	--	--	--	--	--	titanite
BC1-2426	--	--	--	--	--	x	x	x	--	--	--	--	--	--	--	--	--	x	--	--
Samples from Morenci pit, Arizona																				
Coronado	--	--	--	x	--	--	x	--	x	--	--	--	--	--	--	--	--	--	--	--
Marquin 5900	--	--	--	--	--	--	x	--	x	--	--	--	--	--	--	--	--	x	--	greigite
andesite 5950	--	--	--	--	--	--	--	--	x	--	--	--	--	--	--	--	--	--	--	--
Sample from Round Mountain Nevada																				
Round Mtn	--	--	--	--	--	--	--	--	x	--	--	--	--	--	--	--	--	--	--	greigite

Appendix 11.4—Chemical analyses of host rocks

Major and trace elements of host rocks and altered rocks from the Steeple Rock district are given in this appendix. Analyses are by XRF except for mercury which is analyzed by cold fusion AA. CIPW Norms are calculated using PETCAL (Bingler et al., 1976). Major oxides are in percent (%); trace elements are in parts per million (ppm). CIPW Norms are in percent. Alteration intensity (alt. int.) is described in Chapter 5. Rock Unit refers to formation (Fig. 2.1). XRD and TS refers to analyses by x-ray diffraction and thin section description (Appendix 11.2). Sample locations are on Map 2.

Appendix 11.4a—Chemical analyses of rhyolite intrusives (by XRF, NNMMR). Fe_2O_3 is total iron calculated as Fe_2O_3. * From Hedlund (1990b). @ From Wahl (1980). ^From Bornhorst (1986,1988). bd - below detection limit (Table 1.3).

	59	280	251	315	314	366	553	598	620	651	717	239B	936	977	988	1047	1048	1045	1046	1028	TVG*	SR42-83*	V23@	AB1@	A52@	Avg Rhyolite^	Avg HI-Si Rhyolite^	Avg Rhyodacite^
SiO_2	80.4	74.8	80.1	68.2	73.9	94.1	70.4	83.8	76.8	73.0	73.8	83.7	78.0	77.5	78.6	79.7	83.0	79.4	82.8	78.1	74.4	77.0	74.3	81.8	70.1	72.7	76.9	68.26
TiO_2	0.12	0.09	0.43	0.42	0.32	0.80	0.24	0.16	0.22	0.32	0.31	0.11	0.08	0.10	0.20	0.09	0.03	0.13	0.05	0.19	0.19	0.08	0.20	0.04	0.49	0.28	0.15	0.48
Al_2O_3	9.70	7.30	6.00	14.90	12.40	1.80	12.60	8.30	11.20	14.10	12.60	9.05	11.90	11.90	11.20	9.98	7.10	11.40	10.50	10.70	14.12	11.20	13.96	9.59	15.98	13.60	12.40	14.84
Fe_2O_3	0.71	2.50	5.52	3.72	2.78	0.63	1.65	1.27	1.64	1.97	0.02	0.73	0.92	0.96	0.56	0.91	0.50	0.81	0.81	1.43	1.49	0.74	1.67	1.00	2.34	1.62	1.06	2.83
MnO	0.03	0.03	0.01	0.06	0.06	0.01	0.07	0.02	0.04	0.06	0.03	0.02	0.06	0.06	0.04	0.06	0.03	0.06	0.04	0.06	0.04	--	0.02	0.01	0.00	0.05	0.05	0.05
MgO	0.37	0.27	0.29	1.40	0.76	0.22	0.34	0.44	0.60	0.69	0.57	0.16	0.23	0.25	0.43	0.42	0.95	0.58	0.58	0.47	0.46	0.13	0.20	0.16	0.31	0.59	0.37	1.14
CaO	0.13	6.49	0.16	1.00	0.72	0.07	1.98	0.15	0.12	0.98	1.37	0.00	0.10	0.42	0.01	0.19	0.05	0.16	0.14	0.11	1.54	0.15	0.55	0.10	0.64	0.99	0.49	2.66
Na_2O	0.55	1.05	0.07	4.20	2.29	0.14	0.73	0.53	0.79	3.76	2.31	0.05	3.28	3.77	0.28	3.12	0.36	1.33	0.31	0.75	3.99	0.70	5.16	0.33	5.48	3.26	3.07	3.58
K_2O	7.10	4.05	1.54	4.60	5.91	0.35	9.62	4.46	8.47	5.19	4.26	7.49	4.97	4.88	7.96	5.36	7.26	6.93	4.39	8.15	4.44	7.98	3.96	7.54	5.48	5.03	4.89	3.5
P_2O_5	0.03	0.02	0.10	0.13	0.11	0.04	0.06	0.06	0.06	0.07	0.06	0.03	0.03	0.05	0.04	0.03	0.03	0.03	0.03	0.07	0.05	--	0.09	0.11	0.01	0.08	0.04	0.14
LOI	0.19	2.63	4.60	1.14	1.56	0.51	1.79	1.10	0.26	0.60	2.22	0.67	0.68	0.38	1.02	0.66	0.35	1.36	2.12	0.76	--	0.84	0.43	0.73	0.66	--	--	--
TOTAL	99.33	99.23	98.82	99.77	100.81	98.67	99.48	100.29	100.20	100.74	97.55	102.01	100.25	100.27	100.34	100.52	99.66	102.19	101.77	100.79	100.73	98.82	100.57	101.45	101.46	98.20	99.42	97.48
Ba	260	--	bd	880	--	200	540	320	700	630	370	150	100	130	320	120	210	380	100	460	--	--	--	--	--	425	169	1015
V	26	--	bd	49	--	35	21	14	27	27	21	13	7	bd	12	12	bd	7	20	27	--	--	--	--	--	24	12	44
Cr	76	--	bd	74	--	278	294	321	487	241	52	297	60	49	85	63	65	60	159	88	--	--	--	--	--	8	6	12
Pb	15	31	63	19	12	28	22	15	16	22	20	33	17	20	25	24	35	23	9	22						27	31	--
Th	30	20	10	10	10	bd	30	20	20	30	30	20	40	30	30	30	30	40	30	30	--	--	--	--	--	23	26.2	12.2
Rb	279	237	96	141	238	6	249	186	430	186	179	37	74	235	340	293	501	393	257	373	--	--	--	--	--	225	255	116
U	bd	8	bd	bd	bd	4	5	5	5	7	3	6	5	5	5	5	7	7	bd	6	--	--	--	--	--	4.9	5.3	2.1
Sr	82	47	7	326	134	80	85	48	26	150	53	57	27	11	155	20	36	49	27	77	--	--	--	--	--	128	42	371
Y	27	45	11	28	26	4	27	11	24	31	32	29	47	31	21	44	58	35	34	29	--	--	--	--	--	48	52	30
Zr	72	64	96	168	152	239	152	97	124	184	160	82	99	95	130	103	166	107	85	136	--	--	--	--	--	245	153	221
Nb	10	17	5	12	9	13	25	18	23	24	23	27	39	25	27	32	109	28	36	27	--	--	--	--	--	37	46	--
Mo	23	--	31	bd	bd	--	--	--	--	--	--	5	bd	16	5	bd	bd	bd	7	bd	--	--	--	--	--	--	--	--
Ga	8	10	11	13	14	bd	16	7	11	16	14	--	18	14	14	15	17	14	14	11	--	--	--	--	--	--	--	--
Zn	8	14	15	42	44	bd	37	13	10	19	42	--	18	25	9	37	39	22	30	41	--	--	--	--	--	50	45	54
Cu	89	bd	20	18	8	10	bd	7	bd	6	bd	--	8	bd	bd	bd	bd	bd	bd	12	--	--	--	--	--	4	2	17
Ni	7	4	20	11	9	145	135	145	220	125	8	--	8	5	10	8	11	7	74	7	--	--	--	--	--	7	4	12
Hg	--	--	0.3	<0.1	--	--	--	--	--	--	--	--	--	--	<0.02	0.07	0.03	<0.02	<.02	--	--	--	--	--	--	--	--	--
CIPW NORM																												
Quartz	49.3	44.4	--	21.7	35.2	91.6	26.2	62.8	38.8	28.3	40.4	54.8	39.4	35.9	45.9	42.4	52.4	44.0	63.1	41.8	30.3	41.9	27.9	50.9	15.4	--	--	--
Corundum	0.9	--	--	1.5	1.2	1.2	--	2.5	0.7	0.7	1.8	1.1	1.0	--	2.2	0.3	--	1.5	5.1	0.6	0.1	1.1	0.4	1.0	32.4	--	--	--
Orthoclase	42.0	23.9	--	27.2	34.9	2.1	56.9	26.4	50.1	30.7	25.2	44.3	29.4	28.8	47.0	31.3	42.9	41.0	25.9	48.2	26.2	47.1	23.4	44.6	46.4	--	--	--
Albite	4.7	8.9	--	35.6	19.4	1.2	6.2	4.5	6.7	31.8	19.5	0.4	27.8	31.9	2.4	24.3	3.0	11.3	2.6	6.3	33.8	5.9	43.7	2.8	2.8	--	--	--
Anorthite	0.4	3.2	--	4.1	2.9	0.1	2.7	0.4	0.2	4.4	6.4	--	0.3	1.1	--	0.7	0.1	0.1	0.5	0.1	7.3	0.7	2.1	--	--	--	--	--
Hypersthene	0.9	--	--	4.8	2.7	0.5	--	1.1	1.5	1.7	1.4	0.4	0.6	0.4	1.1	1.3	2.4	1.4	1.4	1.2	1.1	0.3	0.5	0.4	0.7	--	--	--
Magnetite	--	1.5	--	2.5	2.0	--	1.2	1.1	1.4	1.4	--	0.3	0.2	0.2	--	0.3	0.2	--	0.2	1.2	0.7	--	1.0	0.7	1.3	--	--	--
Hematite	0.7	--	--	--	--	0.3	0.2	--	0.1	0.2	0.6	0.5	0.7	0.7	0.7	0.6	0.5	0.8	0.6	0.1	0.6	0.7	0.4	0.3	0.6	--	--	--

Appendix 11-4a (continued)

	59	280	251	315	314	366	553	598	620	651	717	239B	936	977	988	1047	1048	1045	1046	1028	TVG*	SR42-83*	V23@	AB1@	A52@	Avg Rhyolite^	Avg HI-Si Rhyolite^	Avg Rhyodacite^
Ilmenite	0.10	0.20	--	0.80	0.60	0.70	0.50	0.30	0.40	0.60	0.06	0.06	0.20	0.20	0.08	0.20	0.06	0.20	0.09	0.40	0.40	--	0.40	0.08	0.90	--	--	--
Rutile	0.05	--	--	--	--	0.40	--	--	--	--	0.30	--	--	--	0.20	--	--	0.04	--	--	--	0.08	--	0.30	--	--	--	--
Apatite	0.07	0.05	--	0.30	0.30	0.09	0.10	0.10	0.10	0.20	0.10	0.30	0.07	0.10	0.09	0.05	0.07	0.07	0.07	0.20	0.10	--	0.20	--	0.02	--	--	--
Wollastonite	--	9.90	--	--	--	--	--	--	1.80	--	--	--	--	--	--	--	--	--	--	--	--	--	--	--	--	--	--	--
Diopside	--	4.30	--	--	--	--	--	--	1.80	--	--	--	--	0.50	--	--	0.02	--	--	--	--	--	--	--	0.20	--	--	--
Alt. int.	8	25	45	25	35	60	46	48	--	25	38	49	49	43	41	20	56	48	28	29	--	--	--	--	--	--	--	--
Rock Unit	Tr	Tr	Tr	Tr	Tr	Tr	Twd	Tr	Tr	Tq	Tr	Tr	Tr	Tr	Tr	Tr	Tr	Tr	Tr	Tr	Tr	Tr	Tsr	Tsr	Tr	--	--	--
XRD	yes	--	--	yes	yes	yes	--	yes	--	--	yes	yes	yes	--	yes	yes	yes	yes	yes	yes	--	--	--	--	--	--	--	--
TS	yes	yes	yes	yes	yes	yes	yes	yes	--	yes	yes	yes	yes	yes	yes	yes	yes	yes	yes	yes	--	--	--	--	--	--	--	--

Appemdix 11–4b—Chemical analyses of ash-flow tuffs (by XRD, NMBMMR) Fe_2O_3 is total iron calculated as Fe_2O_3. * From White and Foster (1981). @ From Wahl (1980). ^ From Bornhorst (1986).

	281	240	293	732	1083	NM985	274
SiO_2	76.6	46.0	76.0	82.9	78.7	74.8	76.0
TiO_2	0.09	2.40	0.16	0.18	0.21	0.09	0.21
Al_2O_3	11.50	17.10	12.20	8.84	11.40	11.80	10.70
Fe_2O_3	0.61	11.10	1.10	1.27	1.67	1.22	1.32
MnO	0.02	0.16	0.03	0.05	0.04	0.07	0.02
MgO	0.19	6.12	1.10	0.50	0.47	0.37	0.21
CaO	0.01	9.43	0.28	0.26	0.04	0.66	0.09
Na_2O	0.80	4.01	2.18	2.32	0.74	4.06	2.80
K_2O	7.59	2.27	3.70	3.29	7.22	4.53	4.83
P_2O_5	0.01	0.69	0.03	0.03	0.04	0.03	0.04
LOI	0.88	1.20	3.33	1.07	1.05	4.61	0.87
TOTAL	98.30	100.48	100.11	100.71	101.58	102.24	97.09
Ba	90	190	330	310	240	--	130
V	5	6	21	15	20	--	32
Cr	134	185	35	136	358	--	87
Pb	16	bd	23	17	14	22	9
Th	20	30	40	20	30	30	30
Rb	405	118	280	111	363	263	199
U	3	5	bd	3	7	6	9
Sr	11	93	211	141	28	25	73
Y	36	27	51	27	92	35	43
Zr	91	84	155	121	196	101	140
Nb	28	27	36	21	33	31	30
Mo	--	--	--	--	8	11	--
Ga	13	12	17	11	17	15	12
Zn	17	17	64	22	64	33	25
Cu	bd	15	bd	bd	7	bd	bd
Ni	8	bd	bd	71	201	151	6
ALT INT	48	--	35	32	38	--	36
Formation	Tya	Ta	Ta	Ta	Ta	Ta	Tyal
XRD	--	--	yes	--	--	--	--
TS	yes	--	yes	yes	yes	--	yes
CIPW NORM							
Quartz	42.6	--	47.0	55.6	46.1	32.5	40.8
Corundum	2.0	--	4.2	1.1	2.4	--	0.8
Orthoclase	44.9	13.4	21.9	19.4	42.7	26.8	28.5
Albite	6.8	16.8	18.4	19.6	6.3	34.4	23.7
Anorthite	22.0	1.2	3.9	--	0.6	0.2	--
Hypersthene	0.5	--	2.7	1.2	1.2	0.0	0.5
Magnetite	--	5.6	0.2	1.1	1.4	0.9	0.7
Hematite	0.70	--	0.80	0.06	0.04	0.30	0.40
Ilmenite	0.06	4.60	0.30	0.30	0.40	0.20	0.40
Rutile	0.05	--	--	--	0.09	--	--
Apatite	0.02	1.60	0.07	0.07	--	0.07	0.09
Wollastonite	--	--	--	--	--	--	--
Diopside	--	16.3	--	--	--	--	1.9
Acmite	--	--	--	--	--	--	--
Olivine	--	9.2	--	--	--	--	--
Nepheline	--	9.3	--	--	--	--	--

Appendix 11.4b (continued)

	271	270	428	438	520	728	729	730	726b	727
SiO_2	75.8	78.7	80.1	75.5	76.7	76.8	76.3	77.7	76.7	76.3
TiO_2	0.20	0.15	0.16	0.22	0.21	0.18	0.19	0.16	0.17	0.18
Al_2O_3	12.40	11.20	10.30	11.70	11.90	12.40	12.30	12.00	12.20	12.20
Fe_2O_3	1.10	1.05	1.09	1.58	1.38	1.06	1.10	0.97	1.19	1.25
MnO	0.10	0.02	0.03	0.04	0.03	0.05	0.05	0.04	0.06	0.07
MgO	0.32	0.36	0.62	0.32	0.57	0.44	0.26	1.24	0.89	0.67
CaO	0.22	0.17	0.24	0.24	0.26	0.19	0.12	0.20	0.19	0.21
Na_2O	2.84	0.32	1.60	2.78	1.45	3.45	0.85	0.32	2.53	2.67
K_2O	5.03	6.86	5.27	5.14	6.01	5.16	6.98	6.82	5.31	5.37
P_2O_5	0.07	0.02	0.03	0.03	0.03	0.05	0.04	0.02	0.05	0.03
LOI	1.23	1.35	1.25	1.03	1.55	1.13	1.18	1.35	1.03	1.13
TOTAL	99.31	100.20	100.69	98.58	100.09	100.91	99.37	100.82	100.32	100.08
Ba	--	--	180	160	160	--	--	--	110	240
V	--	--	11	22	39	--	--	--	7	13
Cr	--	--	301	131	99	--	--	--	40	19
Pb	52	26	14	22	23	33	25	--	35	25
Th	30	30	30	30	30	40	40	--	40	40
Rb	216	372	229	230	266	227	363	--	290	310
U	7	5	7	6	4	9	4	--	6	4
Sr	75	4049	82	39	81	61	--	--	56	62
Y	38	33	35	38	95	41	49	--	48	49
Zr	149	149	140	165	201	179	170	--	170	160
Nb	31	29	28	29	23	32	32	--	32	33
Mo	bd	bd	--	--	--	--	--	--	--	bd
Ga	16	15	11	15	17	17	17	--	19	18
Zn	68	46	34	56	26	56	47	--	80	66
Cu	17	bd	13	10	bd	bd	bd	--	27	bd
Ni	24	40	135	65	53	35	9	--	28	6
ALT INT	--	39	28	29	36	37	46	36	31	29
Formation	Tya1	Tya1	Tya1	Tya1	Tya1	Tya1	Tya1	Tya1	Tya2	Tya2
XRD	--	yes	yes		yes	yes	yes	yes	yes	yes
TS	--	yes	yes	yes	yes	yes	yes	yes	yes	yes
CIPW NORM										
Quartz	39.2	49.7	49.3	38.7	43.9	36.1	44.1	47.5	40.1	38.8
Corundum	2.1	3.0	1.6	1.2	2.6	0.9	3.2	3.8	2.1	1.7
Orthoclase	29.7	40.5	31.1	30.3	35.5	30.5	41.3	40.3	31.3	31.7
Albite	24.0	2.7	13.5	23.5	12.3	29.2	7.2	2.7	21.4	22.5
Anorthite	0.6	0.7	1.0	1.0	1.1	0.6	0.3	0.9	0.6	0.8
Hypersthene	0.8	0.9	1.5	0.8	1.4	1.1	0.6	3.1	2.2	1.7
Magnetite	0.3	0.2	0.5	1.2	0.7	0.1	--	--	0.5	1.0
Hematite	0.70	0.70	0.50	0.20	0.50	0.80	0.90	0.90	0.60	0.30
Ilmenite	0.40	0.30	0.30	0.40	0.40	0.30	0.30	0.30	0.30	0.30
Rutile	--	--	--	--	--	--	0.02	0.03	--	--
Apatite	0.20	0.05	0.07	0.07	0.07	0.10	0.09	0.05	0.10	0.07
Wollastonite	--	--	--	--	--	--	--	--	--	--
Diopside	--	--	--	--	--	--	--	--	--	--
Acmite	--	--	--	--	--	--	--	--	--	--
Olivine	--	--	--	--	--	--	--	--	--	--
Nepheline	--	--	--	--	--	--	--	--	--	--

Appendix 11.4b (continued)

	733	1088	NM989a	NM989b	288	272	527	529	637	645
SiO_2	78.1	67.7	76.6	75.9	76.6	75.8	82.6	75.6	76.6	74.0
TiO_2	0.16	0.10	0.16	0.15	0.23	0.23	0.10	0.25	0.26	0.24
Al_2O_3	10.70	12.20	11.60	11.70	12.30	12.30	11.00	12.10	11.50	11.90
Fe_2O_3	1.12	1.06	1.21	1.23	1.35	1.35	0.95	1.45	1.52	1.54
MnO	0.04	0.04	0.09	0.10	0.04	0.05	0.02	0.07	0.02	0.03
MgO	0.71	1.65	0.44	0.52	0.28	0.27	0.48	0.63	0.64	0.65
CaO	0.24	0.96	0.15	0.19	0.03	0.02	0.13	0.85	0.18	0.17
Na_2O	1.13	0.48	1.09	1.14	1.80	2.34	0.11	2.00	1.10	0.45
K_2O	6.60	6.89	8.51	8.48	6.42	5.96	3.70	4.54	7.18	7.82
P_2O_5	0.05	0.02	0.10	0.15	0.02	0.03	0.02	0.03	0.03	0.04
LOI	1.27	9.76	0.83	0.84	1.23	0.94	1.88	2.05	0.98	1.30
TOTAL	100.12	100.86	100.78	100.40	100.30	99.29	100.99	99.57	100.01	98.14
Ba	170	100	210	200	90	--	120	250	210	170
V	18	bd	7	7	18	--	8	12	30	27
Cr	41	36	89	76	96	--	141	79	169	146
Pb	23	21	29	27	21	27	16	42	24	--
Th	30	30	40	40	20	30	30	30	30	--
Rb	266	348	482	485	282	269	173	143	301	--
U	3	6	6	5	7	5	4	4	6	--
Sr	59	436	56	78	40	30	8	88	66	--
Y	38	32	49	49	93	81	24	93	73	--
Zr	149	107	157	158	201	204	99	205	189	--
Nb	25	26	36	36	25	28	23	22	23	--
Mo	--	bd	bd	bd	--	bd	--	--	--	--
Ga	13	16	17	20	16	16	12	17	15	19
Zn	45	49	55	69	42	51	19	55	48	62
Cu	bd	5	5	39	bd	15	bd	116	5	5
Ni	12	30	60	72	5	40	63	45	79	78
Alt. int.	35	41	15	15	32	--	27	32	33	31
Formation	Tya2	Tya2	Tya2	Tya2	Tbg?	Tbg	Tbg?	Tbg	Tbg	Tbg?
XRD	yes	yes	--	--	--	--	--	--	--	--
TS	yes	yes	yes	yes	yes	--	yes	yes	yes	yes
CIPW NORM										
Quartz	44.8	34.1	37.0	36.0	41.1	39.0	67.0	43.9	41.4	40.2
Corundum	1.4	2.3	0.6	0.7	2.4	2.0	7.0	2.4	1.7	2.5
Orthoclase	39.0	40.7	50.3	50.1	37.9	35.2	22.0	26.8	42.4	46.2
Albite	9.6	4.1	9.2	9.6	15.2	19.8	0.9	16.9	9.3	3.8
Anorthite	0.9	4.6	0.1	--	0.0	--	0.5	4.0	0.7	0.6
Hypersthene	1.8	4.1	1.1	1.3	0.7	0.7	1.2	1.6	0.6	1.6
Magnetite	0.5	0.3	0.7	0.8	0.6	0.6	0.2	0.9	0.9	1.0
Hematite	0.50	0.70	0.40	0.30	0.60	0.60	0.60	0.40	0.40	0.30
Ilmenite	0.30	0.20	0.30	0.30	0.40	0.40	0.20	0.50	0.50	0.50
Rutile	--	--	--	--	--	--	--	--	--	--
Apatite	0.10	0.05	0.20	0.40	0.04	0.07	0.05	0.07	0.07	0.09
Wollastonite	--	--	--	--	--	--	--	--	--	--
Diopside	--	--	--	--	--	--	--	--	--	--
Acmite	--	--	--	--	--	--	--	--	--	--
Olivine	--	--	--	--	--	--	--	--	--	--
Nepheline	--	--	--	--	--	--	--	--	--	--

Appendix 11.4b (continued)

	725	739	916	1036	1031	1039	NM987	TF2@	AG7@	DC2@
SiO_2	77.1	80.0	75.4	78.8	78.7	78.4	76.9	78.2	75.9	75.7
TiO_2	0.24	0.21	0.19	0.20	0.21	0.22	0.23	0.14	0.30	0.14
Al_2O_3	12.30	10.50	10.90	11.60	9.97	11.40	12.30	13.24	13.34	11.79
Fe_2O_3	1.36	1.27	1.28	1.27	1.28	1.25	1.59	1.66	1.46	1.90
MnO	0.07	0.06	0.06	0.08	0.05	0.09	0.08	0.01	0.06	0.04
MgO	0.44	0.68	1.19	0.49	0.68	0.92	0.61	0.49	0.43	0.02
CaO	0.25	0.30	0.15	0.24	0.18	0.42	0.29	0.36	0.35	0.49
Na_2O	0.28	1.65	1.77	4.08	0.68	3.03	2.79	0.80	3.68	4.05
K_2O	6.95	4.97	7.02	3.89	6.78	5.34	5.13	7.34	5.39	4.98
P_2O_5	0.10	0.03	0.04	0.04	0.04	0.03	0.04	0.07	0.06	0.08
LOI	1.52	1.00	0.60	1.16	1.79	1.33	2.49	--	0.83	--
TOTAL	100.61	100.67	98.60	101.85	100.36	102.43	102.46	102.34	101.77	99.15
Ba	--	410	180	180	410	300	180	--	--	--
V	--	9	19	35	44	17	16	--	--	--
Cr	--	112	80	98	33	65	101	--	--	--
Pb	17	19	21	17	20	24	24	--	--	--
Th	30	20	30	30	30	30	40	--	--	--
Rb	388	154	368	155	321	245	267	--	--	--
U	5	3	7	4	4	6	6	--	--	--
Sr	26	157	21	111	45	53	53	--	--	--
Y	87	80	92	81	64	97	78	--	--	--
Zr	220	184	189	178	167	202	197	--	--	--
Nb	28	20	28	26	29	29	34	--	--	--
Mo	--	--	bd	bd	bd	bd	bd	--	--	--
Ga	--	14	16	16	13	18	20	--	--	--
Zn	--	22	26	32	53	73	59	--	--	--
Cu	--	5	17	bd	13	5	bd	--	--	--
Ni	--	61	13	59	7	12	54	--	--	--
Alt. int.	--	38	37	43	41	41	16	--	--	--
Formation	Tbg	Tbg	Tbg	Tbg?	Tbg	Tbg	Tbg	Tbg	Tbg	Tbg
XRD	--	--	--	--	yes	--	--	--	--	--
TS	--	yes	yes	yes	yes	yes	--	--	--	--
CIPW NORM										
Quartz	48.0	49.8	36.2	39.0	48.0	35.1	39.6	44.2	32.6	32.6
Corundum	4.0	1.9	0.2	0.3	2.0	1.0	1.7	3.5	1.0	--
Orthoclase	41.1	29.4	41.5	23.0	40.0	31.6	30.3	43.4	31.9	29.4
Albite	2.4	14.0	15.0	34.5	4.9	26.1	23.6	6.8	31.1	32.9
Anorthite	0.6	1.3	0.5	0.9	0.5	2.3	1.2	1.3	1.3	--
Hypersthene	1.1	1.7	3.0	1.2	1.9	6.4	1.5	1.2	1.1	--
Magnetite	0.7	0.8	0.8	0.7	0.9	0.8	1.2	1.3	0.5	1.0
Hematite	0.50	0.30	0.30	0.40	0.30	0.40	0.20	0.20	0.70	--
Ilmenite	0.50	0.40	0.40	0.40	0.40	0.40	0.40	0.30	0.60	0.30
Rutile	--	--	--	--	--	--	--	--	--	--
Apatite	0.20	0.07	0.09	0.09	0.09	0.07	0.09	0.20	0.10	0.20
Wollastonite	--	--	--	--	--	--	--	--	--	0.2
Diopside	--	--	--	--	--	--	--	--	--	1.3
Acmite	--	--	--	--	--	--	--	--	--	1.2
Olivine	--	--	--	--	--	--	--	--	--	--
Nepheline	--	--	--	--	--	--	--	--	--	--

Appendix 11.4b (continued)

	MLQ536*	MLQ538*	MLQ539*	MLQ542*	MLQ548*	MLQ55*	Average tuff
SiO_2	78.1	77.3	76.1	75.5	79.7	80.7	72.9
TiO_2	0.19	0.19	0.17	0.22	0.14	0.25	0.28
Al_2O_3	13.27	13.85	13.62	15.14	22.74	13.12	13.80
Fe_2O_3	0.90	0.60	0.90	1.01	0.62	0.87	1.68
MnO	0.04	0.05	0.06	0.04	0.04	0.06	0.05
MgO	0.32	0.39	0.28	0.24	0.12	0.16	0.66
CaO	0.41	0.88	0.37	0.24	0.11	0.33	1.00
Na_2O	3.47	3.87	3.26	3.19	3.87	3.87	3.51
K_2O	5.03	5.34	5.03	4.71	4.07	4.07	5.15
P_2O_5	--	--	--	--	--	--	--
LOI	--	--	--	--	--	--	--
TOTAL	101.71	102.45	99.81	100.32	111.45	103.38	99.11
Ba	--	--	--	--	--	--	452
V	--	--	--	--	--	--	22
Cr	--	--	--	--	--	--	7
Pb	--	--	--	--	--	--	27
Th	--	--	--	--	--	--	23
Rb	--	--	--	--	--	--	218
U	--	--	--	--	--	--	4.7
Sr	--	--	--	--	--	--	110
Y	--	--	--	--	--	--	51
Zr	--	--	--	--	--	--	244
Nb	--	--	--	--	--	--	37
Mo	--	--	--	--	--	--	--
Ga	--	--	--	--	--	--	--
Zn	--	--	--	--	--	--	50
Cu	--	--	--	--	--	--	4
Ni	--	--	--	--	--	--	6
Alt. int.	--	--	--	--	--	--	--
Formation	Tbg	Tbg	Tbg	Tbg	Tbg	Tbg	--
XRD	--	--	--	--	--	--	--
TS	--	--	--	--	--	--	--

Appendix 11.4c—Chemical analyses of andesites and dacites (by XRF, NMBMMR). Fe_2O_3 is total iron calculated as Fe_2O_3. * From Hedlund (1990b). @ From Wahl (1980). ^ From Bornhorst (1986, 1988).

	332	327	353	352	341	345	346
SiO_2	55.9	62.4	63.3	60.2	60.7	52.0	59.1
TiO_2	0.91	0.57	0.64	0.72	0.85	1.49	0.84
Al_2O_3	17.00	15.10	15.80	15.90	16.80	15.60	24.00
Fe_2O_3	13.30	5.34	6.25	5.82	6.42	8.80	3.41
MnO	0.24	0.08	0.04	0.08	0.05	0.09	0.07
MgO	2.99	1.12	1.32	3.74	2.41	3.90	0.27
CaO	0.54	3.95	2.56	2.24	2.33	5.28	0.10
Na_2O	0.00	3.61	3.08	0.64	2.80	4.00	0.03
K_2O	4.09	3.83	5.26	7.89	3.10	0.98	0.05
P_2O_5	0.23	0.15	0.16	0.18	0.23	0.37	0.29
LOI	5.52	4.21	2.60	3.12	4.94	6.77	10.48
TOTAL	100.72	100.36	101.01	100.53	100.63	99.28	98.64
Ba	830	900	690	730	860	300	290
V	193	107	103	139	160	174	212
Cr	40	87	63	73	110	59	588
Pb	10	30	10	---	10	10	90
Th	bd	17	18	---	19	bd	20
Rb	370	174	187	---	94	44	bd
U	bd	bd	5	---	7	bd	bd
Sr	26	692	235	---	335	471	965
Y	37	32	34	---	28	40	13
Zr	175	147	172	---	230	289	217
Nb	9	10	11	---	11	18	6
Mo	---	---	---	---	---	---	bd
Ga	18	15	13	39	18	22	19
Zn	246	55	64	1330	81	93	9
Cu	37	7	29	132	41	24	22
Ni	42	17	9	23	42	44	17
Hg	---	<0.1	---	<0.1	<0.2	<0.1	0.5
CIPW NORM							
Quartz	30.7	16.9	16.8	15.1	23.2	7.3	58.9
Corundum	12.1	0.8	2.7	13.3	---	24.4	---
Albite	---	30.5	26.1	5.4	23.7	33.8	0.3
Orthoclase	24.2	22.6	31.1	46.6	18.3	5.8	0.3
Anorthite	1.2	13.7	11.7	9.9	10.1	21.7	---
Hypersthene	17.5	3.4	6.6	12.1	9.0	13.5	0.7
Magnetite	6.4	3.2	3.6	3.4	3.8	4.6	1.6
Hematite	---	---	---	---	---	---	1.0
Ilmenite	1.7	1.1	1.2	1.4	1.6	2.8	1.6
Rutile	---	---	---	---	---	---	---
Apatite	0.5	0.4	0.4	0.4	0.5	0.9	0.7
Diopside	---	4.1	---	---	---	1.7	---
Alt. int.	81	68	84	95	30	70	90
Rock Unit	Tss	Tss	Tss	Tss	Tss	Tss	Tsed
XRD	yes	yes	yes	yes	yes	yes	yes
TS	yes	yes	yes	yes	yes	yes	yes

Appendix 11.4c (continued)

	369a	687	714	715	716a	736	882	907	914
SiO_2	66.2	68.1	60.4	54.5	64.2	62.7	61.3	63.2	62.9
TiO_2	1.24	0.60	0.49	0.91	0.78	0.59	0.61	0.61	0.61
Al_2O_3	11.20	15.90	16.40	17.60	17.40	15.90	15.50	16.00	15.30
Fe_2O_3	5.04	4.13	4.67	7.71	4.12	4.17	4.94	5.01	5.20
MnO	0.10	0.03	0.11	0.12	0.02	0.05	0.10	0.09	0.10
MgO	1.48	0.83	4.14	3.78	0.63	2.30	3.68	1.86	2.60
CaO	3.30	2.79	3.15	6.28	0.73	1.83	3.05	3.60	4.73
Na_2O	1.16	5.17	4.16	4.23	4.99	2.39	3.62	4.19	3.30
K_2O	6.60	1.54	3.38	2.16	2.66	6.82	2.67	3.42	1.72
P_2O_5	0.40	0.14	0.27	0.27	0.14	0.12	0.22	0.20	0.21
LOI	1.00	1.49	3.64	1.75	4.56	4.15	1.57	2.29	3.96
TOTAL	97.72	100.72	100.81	99.31	100.23	101.02	97.26	100.47	100.63
Ba	---	620	860	770	1070	880	940	870	1410
V	---	121	76	170	149	110	98	123	94
Cr	---	63	26	44	31	43	39	56	49
Pb	---	15	10	12	17	22	13	17	19
Th	---	10	bd	bd	bd	20	10	20	bd
Rb	---	46	109	50	75	338	64	131	53
U	---	bd	bd	bd	bd	bd	bd	bd	bd
Sr	---	763	358	757	347	178	582	444	1060
Y	---	19	21	23	10	26	20	24	21
Zr	---	157	254	232	241	226	176	211	151
Nb	---	6	6	5	7	7	5	7	4
Mo	---	---	---	---	---	---	---	---	---
Ga	---	15	18	21	18	18	19	20	18
Zn	---	69	91	93	36	59	73	80	88
Cu	---	12	bd	51	15	27	12	78	19
Ni	---	25	7	25	6	30	23	18	19
Hg	---	---	---	---	---	---	---	---	---
CIPW NORM									
Quartz	26.9	24.8	12.1	2.8	22.6	15.1	17.6	15.2	22.6
Corundum	1.0	1.8	---	---	5.3	1.5	1.6	---	---
Albite	9.8	43.7	35.2	35.8	42.2	20.2	30.6	35.5	27.9
Orthoclase	39.0	9.1	20.0	12.8	15.7	40.3	15.8	20.2	10.2
Anorthite	5.8	12.9	13.9	22.7	2.7	8.3	13.7	14.7	21.9
Hypersthene	2.4	3.3	12.2	11.0	2.3	7.0	11.3	6.1	8.8
Magnetite	2.8	2.8	3.1	4.3	2.9	2.8	3.0	3.1	3.1
Hematite	---	---	---	---	---	---	---	---	---
Ilmenite	2.4	1.1	0.9	1.7	1.5	1.1	1.1	1.2	1.2
Rutile	---	---	---	---	---	---	---	---	---
Apatite	0.9	0.3	0.6	0.6	0.3	0.3	0.5	0.5	0.5
Diopside	6.4	---	---	5.4	---	---	---	1.5	0.2
Alt. int.	83	75	95	87	--	77	77	70	63
Rock Unit	Tss	Tss-and	Tss-and	Tss-and	Tss-bx	Tss	Tss-and	Tss-and	Tss-dac
XRD	---	---	yes	yes	---	---	---	---	---
TS	yes	yes	yes	yes	---	yes	yes	yes	yes

Appendix 11.4c (continued)

	C369	913	1091	H7-33.8-34.4	H7-143.1-143.3	H7.213	H10-326-.5
SiO_2	58.4	60.4	56.7	59.0	60.6	57.8	56.0
TiO_2	0.89	0.63	0.64	0.64	0.88	0.75	0.88
Al_2O_3	15.70	15.20	14.80	17.00	15.80	17.70	16.80
Fe_2O_3	7.36	5.13	5.53	6.40	9.22	6.13	8.19
MnO	0.15	0.11	0.07	0.14	0.10	0.19	0.24
MgO	3.24	1.85	2.61	3.36	2.32	2.90	5.64
CaO	3.59	5.44	4.95	3.01	0.58	3.09	0.77
Na_2O	1.53	3.66	3.69	3.13	0.30	4.49	0.14
K_2O	3.59	3.26	2.94	5.65	4.22	2.24	3.86
P_2O_5	0.16	0.19	0.24	0.20	0.27	0.21	0.21
LOI	5.37	5.62	2.32	3.88	6.03	5.68	8.40
TOTAL	99.98	101.49	94.49	102.41	100.32	101.18	101.13
Ba	380	---	---	850	---	---	---
V	450	---	---	176	---	---	---
Cr	77	---	---	42	---	---	---
Pb	14	---	14	---	22	49	218
Th	10	10	---	---	20	10	200
Rb	158	122	---	---	240	110	201
U	bd	bd	---	---	bd	bd	121
Sr	348	585	---	---	25	262	109
Y	28	25	---	---	41	28	23
Zr	175	169	---	---	210	236	188
Nb	4	11	---	---	6	11	9
Mo	---	bd	---	---	---	---	---
Ga	---	17	20	16	20	16	17
Zn	---	78	84	92	108	127	262
Cu	---	14	23	25	33	7	20
Ni	---	22	146	23	86	6	45
Hg	---	---	---	---	---	---	---
CIPW NORM							
Quartz	21.8	13.9	---	6.7	36.1	11.4	28.6
Corundum	3.2	---	---	0.7	10.3	2.8	11.5
Albite	21.2	31.0	---	26.5	2.5	38.0	1.2
Orthoclase	12.9	19.3	---	33.4	24.9	13.2	22.8
Anorthite	16.8	15.4	---	13.6	1.1	14.0	2.4
Hypersthene	12.3	2.9	---	11.8	11.7	10.3	19.1
Magnetite	4.0	3.1	---	3.7	4.8	3.7	4.4
Hematite	---	---	---	---	---	---	---
Ilmenite	1.7	1.2	---	1.2	1.7	1.4	1.7
Rutile	---	---	---	---	---	---	---
Apatite	0.4	0.5	---	0.4	0.6	0.5	0.5
Diopside	---	8.4	---	---	---	---	---
Alt. int.	---	94	88	93	93	86	85
Rock Unit	Tss	Tss-and	Tss	Tss	Tss	Tss	Tss-and
XRD	---	yes	---	yes	---	---	---
TS	---	yes	yes	yes	yes	yes	yes

Appendix 11.4c (continued)

	H10-353.3-	H10-369-.4	H10-412-.6	H9-259.7-260.2	H9-295	H9-376-.8
SiO_2	61.5	62.3	58.9	63.0	68.5	62.6
TiO_2	0.99	0.86	0.67	0.61	0.68	0.71
Al_2O_3	19.10	17.10	15.90	15.20	17.10	17.00
Fe_2O_3	5.33	4.44	6.72	4.80	7.70	7.17
MnO	0.15	0.09	0.11	0.10	0.08	0.10
MgO	1.15	1.14	3.71	2.94	5.87	2.39
CaO	0.46	0.36	2.47	3.12	0.57	2.58
Na_2O	0.18	0.28	0.27	2.78	0.49	0.25
K_2O	5.59	8.17	3.44	4.05	4.03	4.06
P_2O_5	0.24	0.22	0.23	0.17	0.12	0.07
LOI	5.85	3.19	7.58	4.06	4.53	6.50
TOTAL	100.54	98.15	100.00	100.83	109.67	103.43
Ba	---	---	400	650	910	660
V	---	---	112	117	183	119
Cr	---	---	105	179	35	25
Pb	105	28	9	14	15	---
Th	20	10	10	20	20	---
Rb	233	348	165	151	207	---
U	3	bd	5	3	6	---
Sr	102	145	56	24	50	---
Y	36	37	39	159	77	---
Zr	233	204	193	9	162	---
Nb	10	10	8	---	6	---
Mo	---	---	---	---	---	---
Ga	21	17	18	15	15	---
Zn	262	118	151	66	167	---
Cu	52	43	14	22	63	---
Ni	16	16	22	101	48	---
Hg	---	<0.1	<0.1	---	---	---
CIPW NORM						
Quartz	36.3	27.1	32.2	19.8	38.5	34.9
Corundum	12.5	7.7	7.8	1.0	11.2	7.7
Albite	1.5	2.4	2.2	23.5	4.1	2.1
Orthoclase	33.0	48.3	20.3	23.9	23.8	24.0
Anorthite	0.7	0.4	10.8	14.4	2.0	12.3
Hypersthene	4.5	3.9	13.1	9.4	19.2	10.0
Magnetite	3.5	3.0	3.8	3.0	4.2	4.0
Hematite	---	---	---	---	---	---
Ilmenite	1.9	1.6	1.3	1.2	1.3	1.3
Rutile	---	---	---	---	---	---
Apatite	0.6	0.5	0.5	0.4	0.3	0.2
Diopside	---	---	---	---	---	---
Alt. int.	---	93	90	80	---	---
Rock Unit	Tss-and	Tss-and	Tss-and	Tss-and	Tss-and	Tss-and
XRD	---	---	---	---	---	---
TS	---	yes	yes	yes	---	---

Appendix 11.4c (continued)

	H9-379.6-388	H9-420-421	H9-472.9-473.2	H9-506.6-507.2	H14-269-270
SiO_2	59.2	59.0	66.4	56.8	67.3
TiO_2	0.79	0.65	0.51	0.83	0.96
Al_2O_3	19.10	15.20	12.70	17.00	22.00
Fe_2O_3	8.51	5.95	7.00	6.65	0.44
MnO	0.13	0.15	0.10	0.15	0.04
MgO	1.92	3.21	2.73	3.73	0.71
CaO	1.34	2.28	1.54	2.43	0.13
Na_2O	0.16	0.82	0.34	0.09	0.32
K_2O	3.60	8.08	5.35	5.13	5.37
P_2O_5	0.26	0.20	0.12	0.17	0.20
LOI	6.20	3.78	3.99	6.73	3.71
TOTAL	101.21	99.32	100.78	99.71	101.18
Ba	---	780	900	1350	160
V	---	116	133	198	245
Cr	---	220	146	90	65
Pb	227	15	16	20	55
Th	200	10	10	20	20
Rb	288	304	290	290	228
U	140	bd	bd	bd	5
Sr	40	299	117	123	948
Y	41	24	23	28	32
Zr	156	149	140	216	149
Nb	10	9	7	7	7
Mo	---	bd	---	---	--
Ga	18	16	14	20	26
Zn	148	126	182	187	35
Cu	25	36	13	20	9
Ni	76	136	91	67	7
Hg	---	---	---	---	---
CIPW NORM					
Quartz	37.2	12.7	34.8	18.9	44.1
Corundum	13.1	1.4	3.8	0.9	15.9
Albite	1.4	6.9	2.9	39.6	2.7
Orthoclase	21.3	47.8	31.6	30.3	31.7
Anorthite	5.0	10.0	6.9	10.9	1.8
Hypersthene	9.8	11.2	11.5	12.7	1.8
Magnetite	4.7	3.4	3.7	3.8	---
Hematite	---	---	---	---	1.2
Ilmenite	1.5	1.2	1.0	1.6	0.1
Rutile	---	---	---	---	0.9
Apatite	0.6	0.5	0.3	0.4	0.5
Diopside	---	---	---	---	---
Alt. int.	---	---	---	---	99
Rock Unit	Tss-and	Tss-and	Tss-and	Tss-and	Tss
XRD	---	---	---	---	---
TS	---	---	---	---	yes

Appendix 11.4c (continued)

	B91-17-18	B91-17-112	B91-17-651	M91-4-689-690	S85-5-463	SR41-83*
SiO_2	69.4	63.0	60.0	62.2	61.8	66.0
TiO_2	0.56	0.63	0.68	0.60	0.59	0.57
Al_2O_3	16.30	15.30	16.80	16.00	14.60	14.90
Fe_2O_3	0.65	4.85	5.81	4.48	4.23	3.49
MnO	0.02	0.08	0.10	0.14	0.09	0.05
MgO	0.58	2.53	2.78	3.75	2.29	1.46
CaO	0.09	2.57	1.26	1.33	2.81	2.71
Na_2O	0.32	2.95	0.68	4.22	1.44	3.42
K_2O	1.23	4.90	6.67	3.62	6.18	4.05
P_2O_5	0.19	0.13	0.19	0.16	0.11	0.20
LOI	10.70	3.78	5.41	3.58	4.89	1.71
TOTAL	100.04	100.72	100.38	100.08	99.03	98.56
Ba	530	700	960	---	---	---
V	131	137	165	---	---	---
Cr	171	154	53	---	---	---
Pb	44	14	21	10	14	---
Th	9	17	20	12	19	---
Rb	4	248	290	144	382	---
U	bd	4	4	bd	8	---
Sr	1020	230	242	210	74	---
Y	4	21	22	22	27	---
Zr	209	177	188	191	192	---
Nb	10	7	7	6	7	---
Mo	---	---	---	---	---	---
Ga	19	18	20	18	19	---
Zn	bd	62	99	149	60	---
Cu	9	23	21	32	30	---
Ni	105	93	29	20	30	---
Hg	---	---	---	---	---	---
CIPW NORM						
Quartz	62.3	17.2	22.9	15.0	19.9	22.8
Corundum	14.7	0.8	6.6	3.1	0.7	0.4
Albite	2.7	25.0	5.8	35.7	12.2	28.9
Orthoclase	7.3	29.0	39.4	21.4	36.5	23.9
Anorthite	---	12.0	5.0	5.6	13.2	12.1
Hypersthene	1.4	8.0	9.7	11.1	7.3	4.4
Magnetite	3.0	3.5	2.9	2.7	2.5	---
Hematite	1.0	---	---	---	---	---
Ilmenite	0.0	1.2	1.3	1.1	1.1	1.1
Rutile	0.5	---	---	---	---	---
Apatite	0.5	0.3	0.5	0.4	0.3	0.5
Diopside	---	---	---	---	---	---
Alt. int.	---	---	92	87	92	---
Rock Unit	Tss-alt	Tss-and	Tss-and	Tss-and	Tss-and	Tss
XRD	---	---	yes	yes	yes	---
TS	---	---	yes	yes	yes	---

Appendix 11.4c (continued)

	SR122-78*	YV44-83*	YV45-83*	YV46-83@	NM1@	VD@	A16@
SiO_2	59.7	60.0	54.1	62.1	60.9	56.7	55.9
TiO_2	0.61	0.63	1.30	0.64	0.78	0.86	1.08
Al_2O_3	16.70	16.80	15.10	15.60	16.69	17.51	17.60
Fe_2O_3	5.80	4.53	7.71	5.08	6.19	6.17	7.45
MnO	0.10	0.07	0.11	0.05	0.29	0.19	0.12
MgO	3.10	2.19	3.36	2.03	3.19	3.90	2.78
CaO	3.60	3.65	3.95	2.11	3.55	5.84	5.81
Na_2O	3.60	3.81	3.56	2.86	3.46	2.82	4.62
K_2O	3.30	3.49	3.42	4.07	2.88	2.52	2.85
P_2O_5	0.21	0.17	0.56	0.18	0.08	0.26	0.60
LOI	4.36	3.29	5.72	4.32	2.46	---	1.90
TOTAL	101.08	98.63	98.89	99.04	100.48	96.75	100.71
Ba	---	---	---	---	---	---	---
V	---	---	---	---	---	---	---
Cr	---	---	---	---	---	---	---
Pb	---	---	---	---	---	---	---
Th	---	---	---	---	---	---	---
Rb	---	---	---	---	---	---	---
U	---	---	---	---	---	---	---
Sr	---	---	---	---	---	---	---
Y	---	---	---	---	---	---	---
Zr	---	---	---	---	---	---	---
Nb	---	---	---	---	---	---	---
Mo	---	---	---	---	---	---	---
Ga	---	---	---	---	---	---	---
Zn	---	---	---	---	---	---	---
Cu	---	---	---	---	---	---	---
Ni	---	---	---	---	---	---	---
Hg	---	---	---	---	---	---	---
CIPW NORM							
Quartz	14.4	13.2	6.8	21.9	16.1	11.7	2.8
Corundum	1.2	0.5	---	3.1	1.6	0.1	---
Albite	30.5	32.2	30.1	24.2	29.3	23.9	39.1
Orthoclase	19.5	20.6	20.2	24.1	17.0	14.9	16.8
Anorthite	16.5	17.0	15.1	9.3	17.1	27.3	18.9
Hypersthene	7.7	7.0	11.9	7.2	11.3	12.6	8.2
Magnetite	1.5	3.0	4.1	3.1	3.6	3.7	4.2
Hematite	3.9	---	---	---	---	---	---
Ilmenite	1.2	1.2	2.5	1.2	1.5	1.6	2.1
Rutile	---	---	---	---	---	---	---
Apatite	0.5	0.4	1.3	0.4	0.2	0.6	1.4
Diopside	---	---	0.7	---	---	---	4.9
Alt. int.	---	---	---	---	---	---	---
Rock Unit	Tss	Tss	Tss	Tss	Tss	Tss	Tbd
XRD	---	---	---	---	---	---	---
TS	---	---	---	---	---	---	---

Appendix 11.4c (continued)

	217a	292	602	613	703	A1-19	A1-67-.5	A1-85	A1.93
SiO_2	65.3	67.8	46.0	60.6	54.3	42.4	46.7	49.0	59.6
TiO_2	1.28	0.53	1.89	0.85	1.76	1.75	1.78	1.96	1.78
Al_2O_3	12.00	15.00	14.70	16.70	15.80	15.70	16.60	18.20	16.10
Fe_2O_3	6.04	4.11	11.10	5.22	9.77	7.92	9.81	10.30	9.26
MnO	0.01	0.06	0.17	0.11	0.14	0.27	0.18	0.15	0.12
MgO	0.26	1.26	5.40	2.77	3.91	3.27	4.34	3.43	1.77
CaO	0.70	0.95	7.49	4.93	7.15	9.90	6.15	2.89	1.03
Na_2O	0.11	4.67	3.80	4.04	3.11	1.49	1.95	4.28	3.88
K_2O	8.90	4.58	2.60	3.13	2.54	2.05	3.17	3.89	4.95
P_2O_5	0.49	0.13	0.60	0.22	0.55	0.56	0.57	0.62	0.57
LOI	1.78	1.53	6.61	1.70	1.94	14.75	9.23	5.26	2.37
TOTAL	96.87	100.62	100.36	100.27	100.97	100.06	100.48	99.98	101.43
Ba	---	840	1410	930	830	---	---	950	---
V	---	73	199	139	245	---	---	251	---
Cr	---	86	171	243	156	---	---	71	---
Pb	bd	25	bd	17	13	38	15	17	35
Th	bd	20	bd	10	bd	bd	bd	bd	bd
Rb	529	155	50	94	71	91	154	168	201
U	bd	bd	bd	bd	bd	3	bd	bd	bd
Sr	163	254	698	518	618	291	395	161	149
Y	41	25	35	36	43	48	40	41	42
Zr	282	190	267	320	358	316	332	370	323
Nb	16	10	12	14	24	20	18	17	22
Mo	bd	---	---	---	bd	---	---	---	---
Ga	11	16	18	20	21	20	17	23	12
Zn	34	51	104	67	116	159	138	160	244
Cu	19	11	26	28	14	25	10	38	261
Ni	18	20	154	150	123	71	71	93	76
Hg	---	---	---	---	<.03	---	---	---	---
CIPW NORM									
Quartz	---	18.9	---	11.2	6.8	3.1	2.9	---	12.8
Corundum	---	0.9	---	---	---	---	0.1	3.2	3.8
Albite	---	39.6	23.5	34.2	26.3	12.6	16.5	36.2	32.8
Orthoclase	---	27.1	15.4	18.2	15.0	12.1	18.7	23.0	29.3
Anorthite	---	1.1	15.4	---	21.6	30.1	26.8	10.3	1.4
Hypersthene	---	4.6	---	7.0	10.8	5.7	15.9	3.9	8.9
Magnetite	---	2.7	5.4	3.2	5.0	4.2	5.0	5.4	4.8
Hematite	---	---	---	---	---	---	---	---	---
Ilmenite	---	1.00	3.6	1.6	3.3	3.3	3.4	3.7	3.4
Rutile	---	---	---	---	---	---	---	---	---
Apatite	---	0.30	1.4	0.5	1.3	1.3	1.3	1.5	1.4
Diopside	---	---	14.4	3.9	8.3	---	---	---	---
Olivine	---	---	9.3	---	---	---	---	7.0	---
Nepheline	---	---	4.7	---	---	---	---	---	---
Alt. int.	---	70	57	55	50	---	---	---	---
Rock Unit	Tbd	Tbd	Tbd	Tbd	Tbd	Tbd	Tbd	Tbd	Tbd
TS	---	yes	yes	yes	---	---	---	---	

Appendix 11.4c (continued)

	A1-105	A1.177	A2-19	A2-23.6-24	A2-35.2-3	N5F@	Avg Dacite^
SiO_2	59.7	53.7	45.0	50.2	55.0	55.5	63.8
TiO_2	1.61	1.17	1.69	1.93	1.57	1.46	0.75
Al_2O_3	14.40	17.00	15.30	17.20	13.90	17.40	16.23
Fe_2O_3	10.20	6.91	9.80	10.00	8.47	7.91	4.23
MnO	0.11	0.15	0.16	0.21	0.15	0.12	0.07
MgO	4.37	3.54	3.55	6.25	3.51	3.86	1.60
CaO	1.07	3.60	0.98	1.15	3.88	1.97	3.58
Na_2O	0.69	2.31	0.96	2.88	2.56	5.06	3.97
K_2O	8.49	6.31	9.34	4.68	4.64	2.60	3.33
P_2O_5	0.55	0.48	0.57	0.62	0.52	0.80	0.24
LOI	3.24	5.09	2.67	5.06	5.37	3.06	---
TOTAL	104.43	100.21	90.02	100.18	99.57	99.70	97.81
Ba	1620	1440	960	470	710	---	1090
V	343	213	421	305	292	---	57
Cr	78	79	75	74	88	---	17
Pb	171	32	13	14	13	---	22
Th	bd	bd	bd	bd	bd	---	20
Rb	381	281	423	193	219	---	139
U	bd	bd	bd	bd	bd	---	bd
Sr	153	460	118	122	178	---	461
Y	40	28	39	42	35	---	34
Zr	307	301	316	340	306	---	296
Nb	13	10	13	22	13	---	25
Mo	---	---	---	bd	---	---	---
Ga	26	19	19	29	19	---	---
Zn	1050	115	140	190	134	---	68
Cu	126	26	10	34	13	---	26
Ni	98	75	72	79	74	---	22
Hg	---	---	---	---	---	---	---
CIPW NORM							
Quartz	13.2	3.0	7.8	3.2	8.9	6.7	---
Corundum	3.4	1.0	3.2	6.8	---	4.6	---
Albite	5.8	19.5	8.1	24.4	21.7	42.8	---
Orthoclase	50.2	37.3	55.2	27.8	27.4	15.4	---
Anorthite	1.7	14.7	1.1	1.7	12.7	4.6	---
Hypersthene	16.8	11.9	14.2	20.6	11.9	13.1	---
Magnetite	5.0	3.9	4.9	5.1	4.3	4.4	---
Hematite	---	---	---	---	---	---	---
Ilmenite	3.1	2.2	3.2	3.7	3.0	2.8	---
Rutile	---	---	---	---	---	---	---
Apatite	1.3	1.1	1.4	1.5	1.2	1.9	---
Diopside	---	---	---	---	---	---	---
Alt. int.	---	---	---	---	---	---	---
Rock Unit	Tbd	Tbd	Tbd	Tbd	Tbd	Tbd	---
TS	---	---	---	---	---	---	---

Appendix 11.4c (continued)

	Avg Andesite^	Avg Bas. And.^
SiO_2	58.9	54.8
TiO_2	0.99	1.37
Al_2O_3	16.14	16.01
Fe_2O_3	5.98	7.57
MnO	0.09	0.12
MgO	2.88	4.37
CaO	5.16	6.46
Na_2O	3.67	3.52
K_2O	3.18	2.84
P_2O_5	0.42	0.61
LOI	---	---
TOTAL	97.45	97.66
Ba	1288	1191
V	96	135
Cr	49	77
Pb	---	---
Th	11.6	7.9
Rb	92	76
U	2.4	2.2
Sr	662	783
Y	31	31
Zr	284	328
Nb	---	---
Mo	---	---
Ga	---	---
Zn	---	---
Cu	37	45
Ni	47	87
Hg	---	---
CIPW NORM		
Quartz	---	---
Corundum	---	---
Albite	---	---
Orthoclase	---	---
Anorthite	---	---
Hypersthene	---	---
Magnetite	---	---
Hematite	---	---
Ilmenite	---	---
Rutile	---	---
Apatite	---	---
Diopside	---	---
Alt. int.	---	---
Rock Unit	---	---
TS	---	---

APPENDIX 11.4d - Chemical analyses of acid-sulfate altered rocks (by XRF, NMBMMR). Fe_2O_3 is total iron calculated as Fe_2O_3. Additional assays of some samples are in Appendix 11.6.

	792	793	868b	944b	944e	948a	948b	951	952
SiO_2	58.7	42.0	52.2	50.0	99.0	78.4	63.7	69.1	74.0
TiO_2	0.65	0.80	0.59	0.54	0.55	0.28	0.78	0.94	0.08
Al_2O_3	26.90	44.80	23.40	16.80	0.00	12.00	20.20	14.60	12.70
Fe_2O_3	0.33	0.19	0.65	1.57	0.35	0.15	1.21	5.44	0.18
MnO	0.03	0.03	0.04	0.03	0.03	0.03	0.04	0.05	0.04
MgO	0.51	0.47	1.15	0.00	0.67	0.63	0.37	0.98	0.25
CaO	0.11	0.26	0.14	0.00	0.06	0.16	0.28	0.17	0.06
Na_2O	0.40	0.27	0.77	1.20	0.25	2.76	4.97	0.40	0.36
K_2O	6.72	5.18	3.70	3.29	0.05	4.20	2.11	3.44	2.70
P_2O_5	0.08	0.38	0.34	0.18	0.03	0.05	0.12	0.09	0.02
LOI	11.00	8.95	2.22	20.95	0.52	2.67	7.26	5.18	9.85
TOTAL	105.43	103.33	85.20	94.56	101.51	101.33	101.04	100.39	100.24
Ba	280	230	---	---	---	---	---	---	110
V	457	499	---	---	---	---	---	---	bd
Cr	132	67	---	---	---	---	---	---	62
Pb	15	233	17	---	---	---	---	---	---
Th	14	20	13	---	---	---	---	---	---
Rb	321	276	bd	---	---	---	---	---	---
U	3	bd	3	---	---	---	---	---	---
Sr	90	790	707	---	---	---	---	---	---
Y	11	19	12	---	---	---	---	---	---
Zr	146	222	186	---	---	---	---	---	---
Nb	4	3	5	---	---	---	---	---	---
Mo	---	---	---	---	---	---	---	---	---
Ga	35	48	13	17	1	15	16	20	13
Zn	12	6	9	8	bd	13	36	14	25
Cu	bd	6	12	6	bd	5	37	30	4
Ni	7	3	5	6	8	5	14	bd	8
Hg	---	---	---	---	---	---	---	---	---
Alt. int.	100	---	95	99	93	98	---	99	100
Rock Unit	Tasc	Tasc	Tasc	Tass	Tassi	Tassi	Tassi	Tassi	Tassi
XRD	yes	yes	yes	yes	yes	yes‘	yes	yes	yes
TS	yes	yes	yes	yes	yes	yes	---	yes	yes
Location	TR	TR	EB	SB	SB	SB	SB	SB	SB

Appemdix 11.4d (continued)

	959	960	1001	1104	1102	71b	217a	338	339	337
SiO_2	56.8	69.5	44.2	75.0	77.4	67.0	65.3	66.0	61.4	67.2
TiO_2	1.35	0.60	0.07	0.16	0.20	0.63	1.28	0.83	0.73	0.68
Al_2O_3	18.10	9.48	41.00	13.20	11.40	17.10	12.00	22.20	14.70	21.90
Fe_2O_3	0.53	1.60	0.08	0.96	1.54	3.96	6.04	1.88	0.20	2.39
MnO	0.03	0.04	0.03	0.04	0.06	0.02	0.01	0.01	0.01	0.01
MgO	0.53	0.13	0.02	0.68	0.69	1.68	0.26	0.10	0.00	0.09
CaO	0.26	0.20	0.00	0.10	0.09	0.16	0.70	0.15	0.00	0.31
Na_2O	1.09	0.97	0.13	2.28	1.80	1.64	0.11	0.00	0.33	0.00
K_2O	3.23	2.00	0.12	4.71	5.09	3.91	8.90	0.00	3.11	0.02
P_2O_5	0.50	0.20	0.38	0.03	0.06	0.11	0.49	0.35	0.14	0.67
LOI	17.30	14.00	14.88	2.40	1.78	7.79	1.78	7.88	17.66	6.52
TOTAL	99.72	98.72	100.91	99.56	100.11	104.00	96.87	99.40	98.28	99.79
Ba	---	620	---	---	---	---	---	290	410	800
V	---	97	---	---	---	---	---	187	74	188
Cr	---	43	---	---	---	---	---	55	131	156
Pb	---	---	---	---	---	---	bd	18	35	22
Th	---	---	---	---	---	---	bd	20	10	30
Rb	---	---	---	---	---	---	529	bd	3	0
U	---	---	---	---	---	---	bd	11	9	3
Sr	---	---	---	---	---	---	163	648	486	1180
Y	---	---	---	---	---	---	41	24	6	21
Zr	---	---	---	---	---	---	282	176	137	151
Nb	---	---	---	---	---	---	16	5	3	5
Mo	---	---	---	---	---	---	bd	---	---	---
Ga	18	7	38	16	14	---	11	15	7	16
Zn	21	30	25	39	47	---	34	bd	26	bd
Cu	12	bd	6	5	12	---	19	16	25	34
Ni	9	5	7	76	117	---	18	0	14	3
Hg	---	---	---	---	---	---	---	0.4	<0.1	<0.1
Alt. int.	---	---	---	---	---	99	93	97	98	100
Rock Unit	Tassi	Tassi	Tasc	Tasc (Tsed)	Tasc (Tsed)	Tassi	Tasc (Tbd)	Tassi	Tassi	Tassi
XRD	---	---	---	---	---	---	---	yes	yes	yes
TS	yes	yes	yes	yes	yes	yes	yes	yes	yes	yes
Location	SB	SB	WB	EB	EB	TR	RH	TR	TR	TR

Appendix 11.4d (continued)

	336	335	334	333	331	329	326	343	342	344	101
SiO_2	61.8	35.3	66.5	55.9	59.0	58.0	78.4	68.7	73.3	55.8	91.2
TiO_2	0.86	0.53	0.75	0.59	0.82	0.87	0.60	0.51	0.61	0.91	0.83
Al_2O_3	26.10	23.50	24.00	15.80	32.64	28.90	14.00	10.00	16.60	17.20	7.05
Fe_2O_3	1.24	1.24	1.99	5.79	0.10	2.09	0.50	5.00	2.16	0.89	0.41
MnO	0.01	0.01	0.01	0.01	0.01	0.01	0.01	0.02	0.01	0.01	0.01
MgO	0.00	0.02	0.07	0.00	0.01	0.31	0.00	0.33	0.32	0.30	0.00
CaO	0.06	0.00	0.10	0.03	0.07	0.21	0.10	0.07	0.14	0.12	0.00
Na_2O	0.00	2.50	0.00	1.64	0.00	0.00	0.00	0.55	0.13	0.87	0.00
K_2O	0.00	2.70	0.03	0.72	0.01	0.02	3.55	1.78	0.19	2.72	0.00
P_2O_5	0.34	0.20	0.30	0.23	0.43	0.33	0.02	0.18	0.30	0.29	0.11
LOI	7.70	29.73	6.35	18.11	6.87	8.79	2.91	12.48	5.21	19.84	2.13
TOTAL	98.11	95.73	100.10	98.82	99.96	99.53	100.09	99.62	98.97	98.95	101.74
Ba	260	320	600	420	---	320	340	590	580	490	170
V	211	122	240	106	---	265	77	119	114	170	71
Cr	99	54	159	122	---	73	205	80	106	197	234
Pb	19	26	17	6	---	19	4	10	34	20	48
Th	20	10	20	bd	---	20	bd	bd	10	20	bd
Rb	bd	15	bd	19	---	bd	140	3	3	bd	bd
U	bd	bd	bd	bd	---	4	bd	bd	3	bd	6
Sr	1030	473	680	213	---	759	33	375	897	576	414
Y	17	10	17	9	---	14	12	11	18	14	7
Zr	203	141	150	104	---	181	116	179	147	176	163
Nb	7	5	5	5	---	6	5	6	6	7	5
Mo	---	---	---	---	---	---	---	---	---	---	---
Ga	25	5	12	11	---	18	34	11	16	14	11
Zn	7	bd	bd	bd	---	bd	bd	4	bd	bd	bd
Cu	bd	13	bd	bd	---	28	8	10	15	bd	bd
Ni	3	1	bd	bd	---	bd	bd	bd	110	bd	3
Hg	---	<0.2	---	---	---	0.1	---	<0.1	<0.2	0.4	<0.1
Alt. int.	99	92	95	100	100	95	100	95	100	100	100
Rock Unit	Tassi	Tassi	Tassi	Tassi	Tassi	Tassi	Tasc	Tassi	Tassi	Tassi	Tass
XRD	yes	yes	yes	yes	yes	yes	yes	yes	yes	yes	---
TS	yes	yes	yes	yes	yes	yes	yes	yes	yes	yes	yes
Location	Ont	Ont	Ont	Ont	Ont	Ont	Ont	TR	TR	TR	TR

Appendix 11.4d (continued)

	103	359	368	419f	534	541	582	601a	608c	628
SiO_2	90.9	79.4	73.3	52.4	65.9	57.1	78.0	67.7	73.3	61.7
TiO_2	1.12	0.72	0.87	1.92	0.77	0.49	0.50	0.88	0.58	0.47
Al_2O_3	2.21	14.10	16.10	17.10	17.40	15.60	14.20	16.40	12.80	20.90
Fe_2O_3	4.30	0.09	1.11	11.40	0.78	3.72	0.90	3.10	2.03	8.59
MnO	0.02	0.03	0.02	0.04	0.01	0.01	0.01	0.02	0.02	0.02
MgO	0.00	0.34	0.54	1.52	1.05	0.78	0.91	0.65	0.96	0.32
CaO	0.00	0.22	0.06	1.41	0.12	0.13	0.30	0.14	0.17	0.11
Na_2O	0.00	0.67	0.18	0.36	4.02	1.09	0.07	0.47	0.00	0.23
K_2O	0.08	0.07	4.08	5.67	2.48	2.49	0.34	3.66	6.29	0.32
P_2O_5	0.07	0.47	0.04	0.47	0.03	0.17	0.22	0.11	0.04	0.16
LOI	1.81	4.65	3.99	2.49	18.70	18.70	5.80	6.52	2.84	8.93
TOTAL	100.51	100.76	100.29	94.78	111.26	100.28	101.25	99.65	99.03	101.75
Ba	---	---	430	---	---	---	---	690	---	---
V	---	---	196	---	---	---	---	220	---	---
Cr	---	---	81	---	---	---	---	55	---	---
Pb	214	133	11	20	18	17	17	21	19	13
Th	10	20	20	bd	10	bd	bd	10	bd	10
Rb	7	bd	173	313	82	6	bd	86	307	bd
U	4	4	4	bd	bd	bd	bd	bd	bd	bd
Sr	133	1406	69	199	270	685	837	352	116	1217
Y	12	7	35	47	16	3	5	148	15	3
Zr	234	139	227	407	207	150	101	238	129	110
Nb	8	bd	7	17	6	7	3	4	5	3
Mo	25	---	---	---	---	---	---	---	---	---
Ga	6	13	15	29	17	13	12	22	16	22
Zn	30	9	11	151	24	8	10	9	25	bd
Cu	63	bd	bd	33	10	15	9	17	8	60
Ni	17	21	26	91	14	56	53	24	55	28
Hg	0.5	---	---	---	---	---	---	---	---	---
Alt. int.	---	---	100	93	94	99	99	99	85	99
Rock Unit	Tass	Tassi	Tasc	Tasc	Tasc	Tassi	Tasc	Tasc	Tassi	Tasc
XRD	yes	---	---	---	---	---	---	---	---	yes
TS	yes	yes	yes	yes	yes	yes	yes	yes	yes	yes
Location	TR	TR	TR	EC	GC	GC	GC	SB	SB	SB

Appendix 11.4d (continued)

	629	630	631	716b	716c	718	720	722	744	781	H9-558-559
SiO_2	59.3	59.1	47.8	64.5	62.3	42.7	56.5	67.9	97.6	65.2	76.8
TiO_2	0.94	0.76	0.34	0.52	0.52	0.58	0.64	0.69	0.83	0.69	0.19
Al_2O_3	14.00	13.10	18.50	17.80	17.80	9.26	17.10	17.90	0.22	23.80	11.40
Fe_2O_3	2.23	4.37	6.48	3.64	4.39	34.30	8.12	3.23	0.35	0.00	0.98
MnO	0.00	0.00	0.00	0.02	0.09	0.04	0.15	0.01	0.03	0.03	0.05
MgO	0.42	0.15	0.49	1.05	2.50	1.00	2.38	0.54	0.67	0.00	0.37
CaO	0.19	0.12	0.31	1.41	2.03	0.12	4.86	0.14	0.03	0.07	0.74
Na_2O	1.38	1.25	1.44	5.40	5.26	1.04	4.49	0.47	0.06	0.00	1.89
K_2O	2.13	1.84	3.13	2.96	2.83	2.21	1.73	2.22	0.02	0.05	5.77
P_2O_5	0.34	0.22	0.44	0.26	0.29	0.28	0.21	0.20	0.05	0.17	0.06
LOI	18.30	17.80	20.70	4.44	3.89	7.79	4.63	8.22	0.40	9.09	1.80
TOTAL	99.23	98.71	99.63	102.00	101.90	99.32	100.81	101.52	100.26	99.10	100.05
Ba	880	480	---	---	1110	---	---	970	---	---	1100
V	182	151	---	---	170	---	---	148	---	---	31
Cr	48	90	---	---	29	---	---	171	---	---	78
Pb	14	25	261	---	18	14	16	6	12	8	22
Th	bd	20	bd	---	bd	bd	bd	bd	bd	bd	20
Rb	4	7	82	---	78	67	93	42	48	1	192
U	bd	4	bd	---	bd	bd	bd	bd	bd	5	3
Sr	1130	573	1370	---	404	474	95	535	1140	36	100
Y	14	19	12	---	18	23	9	21	14	4	23
Zr	232	199	101	---	281	261	151	170	166	236	154
Nb	5	8	bd	---	7	7	4	9	4	9	9
Mo	---	---	---	---	---	---	---	bd	---	---	4
Ga	13	12	20	---	18	17	13	19	16	---	10
Zn	5	3	14	---	29	143	53	97	12	---	25
Cu	21	bd	14	---	4	5	bd	21	6	---	4
Ni	11	44	21	---	6	11	bd	117	6	---	8
Hg	---	---	---	---	---	---	---	---	---	---	
Alt. int.	99	99	99	---	---	---	---	---	---	---	100
Rock Unit	Tassi	Tassi	Tassi	Tasc	Tasc	Tasc	Tassi	Tassi	Tass	Tassi	Tss
XRD	---	---	---	---	---	---	---	---	---	---	---
TS	yes	yes	yes	yes	yes	---	---	yes	yes	yes	yes
Location	SB	SB	SB	GC	GC	GC	GC	EC	RH	TR	---

Appendix 11.4d (continued)

	H10.26.4-.5	H10.57.8-.9	H10.85.9-86	H10.90.6-91	H10.92-0.1
SiO_2	95.1	89.3	62.9	75.0	65.7
TiO_2	0.86	0.56	1.10	0.34	0.91
Al_2O_3	2.05	6.58	28.80	4.82	24.50
Fe_2O_3	0.98	0.25	0.21	4.05	0.55
MnO	0.02	0.01	0.01	0.20	0.04
MgO	0.43	0.31	0.80	1.76	0.15
CaO	0.16	0.19	0.27	2.57	0.07
Na_2O	0.00	0.04	0.07	0.00	0.01
K_2O	0.03	0.01	0.02	3.04	0.03
P_2O_5	0.05	0.14	0.29	0.19	0.25
LOI	0.80	2.54	6.19	4.52	8.62
TOTAL	100.48	99.93	100.66	96.49	100.83
Ba	34	1170	116	---	---
V	52	77	119	---	---
Cr	162	110	228	---	---
Pb	bd	20	29	---	76
Th	bd	10	10	---	70
Rb	3	bd	bd	---	4
U	6	3	3	---	38
Sr	108	762	2261	---	1227
Y	16	9	8	---	30
Zr	277	245	182	---	216
Nb	9	6	5	---	4
Mo	---	---	---	---	---
Ga	4	12	69	---	25
Zn	17	7	38	---	35
Cu	2	19	3	---	bd
Ni	6	bd	bd	---	bd
Hg	0.4	---	---	---	0.9
Alt. int.	98	95	95	100	100
Rock Unit	Tass	Tass	Tassi	Tassi	Tassi
XRD	---	---	---	---	---
TS	---	---	---	---	---
Depth (ft)	26	57	85	90	92

Appendix 11.4d (continued)

	H10.123.9-124	H10.134.2-134	H10.145.5-.8	H10.215.8-216	H10.219.9-220.7
SiO_2	65.2	62.8	54.2	75.8	41.9
TiO_2	0.98	0.78	0.79	0.65	1.59
Al_2O_3	18.20	20.60	20.00	16.10	34.20
Fe_2O_3	7.57	5.81	10.60	0.22	5.70
MnO	0.01	0.04	0.03	0.01	0.01
MgO	0.25	1.10	0.15	0.27	0.06
CaO	0.25	0.05	0.00	0.27	0.13
Na_2O	0.01	0.14	0.26	0.00	0.04
K_2O	0.04	0.02	0.05	0.07	0.12
P_2O_5	0.21	0.16	0.22	0.26	0.44
LOI	7.25	11.20	15.29	5.94	15.38
TOTAL	99.97	102.70	101.59	99.59	99.57
Ba	540	---	300	260	330
V	403	---	148	141	391
Cr	138	---	75	110	52
Pb	25	25	23	13	25
Th	10	20	10	10	20
Rb	bd	bd	bd	bd	5
U	3	10	3	3	10
Sr	1770	1240	1910	991	1820
Y	9	10	17	5	8
Zr	209	189	210	141	300
Nb	8	13	7	6	9
Mo	---	---	---	---	---
Ga	39	16	18	11	23
Zn	26	92	61	13	48
Cu	11	25	68	4	30
Ni	3	23	263	bd	69
Hg	---	---	0.5	<0.1	0.1
Alt. int.	100	100	99	---	---
Rock Unit	Tassi	Tasc	Tasc (Tss)	Tss (Tss)	Tasc (Tss)
XRD	yes	yes	yes	---	---
TS	---	---	---	---	---
Depth	123	134	145	215	219

Appendix 11.4d (continued)

	H10.253.6-255.9	H14.218.6-219	H4.228.4-229.6	Round Mtn	Morenci 5900	Morenci 4196
SiO_2	61.7	70.5	62.8	5.7	0.0	50.9
TiO_2	0.61	0.99	1.08	0.00	0.00	1.72
Al_2O_3	10.50	19.10	25.20	32.10	35.10	13.30
Fe_2O_3	11.30	0.74	0.93	1.34	0.04	9.05
MnO	0.01	0.02	0.02	0.01	0.01	0.16
MgO	0.12	1.07	0.90	0.43	0.11	3.94
CaO	1.79	0.27	0.20	0.11	0.02	5.63
Na_2O	0.22	0.17	0.19	0.00	0.00	4.20
K_2O	2.74	4.35	4.68	10.00	10.10	2.97
P_2O_5	0.15	0.19	0.20	3.64	5.34	1.96
LOI	10.30	0.29	5.55	38.66	41.50	6.12
TOTAL	99.44	97.69	101.75	92.01	92.22	99.95
Ba	90	560	720	---	---	---
V	144	408	436	---	---	---
Cr	134	112	102	---	---	---
Pb	10	10	30	---	---	---
Th	16	31	14	---	---	---
Rb	157	177	203	---	---	---
U	3	bd	3	---	---	---
Sr	36	1130	1120	---	---	---
Y	16	22	12	---	---	---
Zr	278	202	226	---	---	---
Nb	5	4	6	---	---	---
Mo	---	---	---	---	---	---
Ga	17	19	23	---	---	---
Zn	45	12	8	---	---	---
Cu	33	7	8	---	---	---
Ni	233	38	22	---	---	---
Hg	---	---	---	---	---	---
Alt. int.	---	---	99	---	---	---
Rock Unit	vein	Tassi (Tss)	Tassi (Tss)	---	---	---
XRD	---	---	---	---	---	---
TS	---	---	---	---	---	---
Depth (ft)	253	218	228	---	---	---

Appendix 11.5—Chemical analyses of quartz veins.

Major and trace elements of quartz veins from the Steeple Rock district are given in this Appendix. Analyses are by XRF, except for gold and silver (fire assay), copper, lead, zinc, and mercury (AA). Methods, detection limits, and errors are discussed in section 1.5.4. Alteration intensity (ALT) is described in section 5.1. Rock unit refers to formation (Fig. 2.1). XRD and TS refers to analyses by x-ray diffraction and thin section description (Appendix 11.2). FI indicates analyses by fluid inclusion (Appendix 11.7). Sample locations are on Map 2. Major oxides are in percent (%); trace elements are in parts per million (ppm).

Appendix 11.5a—Chemical analyses of quartz veins (by XRF, NMBMMR). Fe_2O_3 is total iron calculated as Fe_2O_3. Additional assays of some samples are in Appendix 11.6.

	47	148	201a	217c	230	231a	287	486	340c
SiO_2	91.0	82.0	97.5	90.9	80.2	58.7	93.5	65.3	64.8
TiO_2	0.16	0.27	0.04	0.15	0.36	0.39	0.07	0.15	0.83
Al_2O_3	3.32	7.00	0.47	2.26	8.16	13.00	1.66	3.89	21.80
Fe_2O_3	2.18	2.55	0.32	1.25	2.53	3.30	1.18	1.58	0.65
MnO	0.03	0.11	0.03	0.02	0.02	0.01	0.09	0.12	0.01
MgO	0.69	1.30	1.79	0.22	0.57	0.09	0.56	0.62	0.06
CaO	0.06	0.14	0.16	0.31	0.12	0.00	0.05	13.80	0.33
Na_2O	0.20	0.30	0.33	0.03	0.18	0.15	0.12	1.02	0.49
K_2O	1.69	4.72	0.07	1.12	5.31	10.30	1.24	1.07	5.90
P_2O_5	0.09	0.08	0.03	0.09	0.09	0.12	0.07	0.06	0.30
LOI	1.08	1.33	0.50	0.94	0.13	1.63	0.57	11.90	4.50
TOTAL	100.50	99.80	101.24	97.29	97.67	87.69	99.11	99.51	99.67
Ba	100	---	---	bd	---	bd	280	200	260
V	bd	---	---	bd	---	bd	37	42	188
Cr	bd	---	---	bd	---	bd	58	98	82
Pb	777	360	---	19	59	215	650	7	3
Th	bd	bd	---	bd	10	10	10	bd	20
Rb	77	181	---	77	206	460	53	66	252
U	bd	bd	---	bd	bd	bd	bd	bd	10
Sr	25	70	---	30	92	174	16	122	16
Y	10	13	---	8	11	16	11	13	32
Zr	39	79	---	52	92	126	29	53	163
Nb	bd	bd	---	bd	3	8	bd	5	4
Mo	5	bd	---	bd	5	145	3	3	---
Ga	13	11	---	8	7	11	11	5	12
Zn	334	494	26	36	54	739	29	22	---
Cu	2210	129	---	27	17	52	87	179	17
Ni	21	14	---	21	9	4	9	42	8
Hg	---	0.6	---	---	---	---	0.22	---	---
ALT	100	---	---	---	---	---	---	---	---
Rock	qv	qv	qv	qv	qv	qv	qv	qv	qv-clay
XRD	yes	---	---	---	---	---	---	---	yes
TS	yes	yes	---	---	yes	yes	---	---	yes
FI	yes	yes	---	---	---	yes	---	---	---

Appendix 11.5a (continued)

	ML4	CT1	CT2	367	419g	724a	724c	783	1064a	Ontario
SiO_2	69.1	58.9	69.1	52.8	54.4	71.8	59.4	70.3	41.1	82.1
TiO_2	0.52	0.88	0.67	1.59	1.67	0.76	0.62	0.69	0.52	0.45
Al_2O_3	12.90	16.90	15.20	15.80	14.90	10.20	15.00	16.20	22.90	10.80
Fe_2O_3	4.11	7.34	4.20	12.50	8.54	5.46	5.31	0.84	0.35	0.95
MnO	0.06	0.09	0.01	0.04	0.12	0.07	0.08	0.04	0.03	0.01
MgO	1.34	3.83	1.09	0.40	4.66	1.88	2.16	1.07	0.71	0.21
CaO	0.69	2.77	0.09	0.22	5.48	0.60	1.51	0.19	0.14	0.00
Na_2O	0.80	3.25	0.49	0.52	4.29	0.18	1.03	0.41	1.43	0.00
K_2O	8.22	3.84	6.21	8.85	2.92	6.24	7.18	3.81	4.63	2.85
P_2O_5	0.14	0.23	0.11	0.53	0.40	0.18	0.20	0.06	0.16	0.03
LOI	2.57	5.17	3.74	6.93	5.38	2.72	6.92	4.73	26.20	2.99
TOTAL	100.45	103.20	100.91	100.18	102.76	100.09	99.41	98.34	98.17	100.39
Ba	330	790	660	---	840	---	---	---	---	---
V	64	168	125	---	256	---	---	---	---	---
Cr	70	102	53	---	156	---	---	---	---	---
Pb	5	7	5	23	13	66	44	19	---	32000
Th	bd	30	30	bd	10	bd	10	10	---	50
Rb	390	233	332	500	125	292	348	163	---	bd
U	bd	4	6	bd	bd	bd	bd	bd	---	bd
Sr	136	201	52	257	262	80	178	84	---	20
Y	22	35	36	22	39	19	21	29	---	188
Zr	119	230	259	417	345	134	177	196	---	78
Nb	8	13	16	15	15	4	5	6	---	bd
Mo	---	---	---	---	---	---	---	---	---	4
Ga	13	22	18	21	20	12	15	16	15	322
Zn	45	126	15	39	110	173	166	16	5	4810
Cu	12	43	14	29	80	113	200	5	8	1450
Ni	29	45	bd	5	96	78	31	5	95	32
Hg	<0.1	0.2	<0.1	---	---	---	---	---	---	---
ALT	---	---	---	---	---	---	---	---	---	---
Rock	qv	qv	qv	qv	qv	qv-clay	qv-clay	qv	qv	qv
XRD	yes	yes	yes	---	---	---	---	---	---	---
TS	yes	yes	yes	---	---	yes	---	---	yes	---
FI	---	---	---	---	---	---	---	---	---	yes

Appendix 11.5a (continued)

	CENDUMP	Lot18759	Lot5-91	Lot26-91	Lot54-91	Lot93-91	H10.273.3-274.7
SiO_2	73.2	71.9	73.3	70.4	72.7	72.2	82.9
TiO_2	0.51	0.14	0.12	0.15	0.12	0.12	0.35
Al_2O_3	14.40	5.57	4.83	5.83	4.89	4.10	6.34
Fe_2O_3	3.89	5.17	5.35	5.76	5.48	5.71	2.44
MnO	0.04	0.17	0.15	0.18	0.17	0.17	0.05
MgO	1.73	2.21	1.97	2.36	2.38	2.26	0.17
CaO	0.21	1.29	1.15	1.18	1.15	1.16	0.58
Na_2O	0.28	1.13	1.10	0.89	1.19	1.12	0.00
K_2O	3.81	0.85	0.66	0.83	0.50	0.51	2.14
P_2O_5	0.08	0.04	0.05	0.05	0.05	0.04	0.08
LOI	4.12	3.70	3.51	4.16	3.74	3.83	2.89
TOTAL	102.27	92.17	92.19	91.79	92.37	91.22	97.94
Ba	---	27700	32000	28400	34800	35300	50
V	---	---	---	---	---	---	10
Cr	---	---	---	---	---	---	91
Pb	---	---	---	---	---	---	bd
Th	---	---	---	---	---	---	40
Rb	---	---	---	---	---	---	8
U	---	---	---	---	---	---	81
Sr	---	---	---	---	---	---	4
Y	---	---	---	---	---	---	---
Zr	68	---	---	---	---	---	---
Nb	94	40000	40900	35000	38000	37300	---
Mo	429	3800	3860	4390	3880	3890	---
Ga	16	---	---	---	---	---	---
Zn	---	---	---	---	---	---	---
Cu	---	bd	bd	bd	bd	bd	---
Ni	---	---	---	---	---	---	---
Hg	---	---	---	---	---	---	---
ALT	---	---	---	---	---	---	---
Rock	qv	prod	prod	prod	prod	prod	vein
XRD	---	---	---	---	---	---	---
TS	---	---	---	---	---	---	---
FI	---	---	---	---	---	---	---

APPENDIX 11.5b—Chemical analyses of selected samples collected along the Alabama vein (majors and trace analyzed by XRF, NMBMMR; Au, Ag, Hg, As, Sb, and F analyzed by Sky Labs). Samples located in Figure 4.27. Fe_2O_3 is total iron calculated as Fe_2O_3.

	15003	15009	15015	15019	15020	15022	15023	15024	15028
SiO_2	90.8	86.2	88.8	80.1	89.3	90.8	92.1	91.7	92.2
TiO_2	0.31	0.30	0.30	0.28	0.06	0.04	0.08	0.08	0.17
Al_2O_3	3.32	5.97	4.89	8.69	4.76	4.50	3.51	4.21	3.83
Fe_2O_3	1.97	2.29	2.02	2.94	1.85	0.79	2.16	1.27	1.27
MnO	0.04	0.01	0.04	0.02	0.04	0.02	0.03	0.01	0.01
MgO	0.35	0.61	0.52	0.47	0.50	0.04	0.20	0.16	0.13
CaO	0.31	0.35	0.24	0.39	0.14	0.18	0.16	0.18	0.05
Na_2O	0.00	0.05	0.15	0.33	0.11	0.06	0.01	0.00	0.19
K_2O	1.47	3.97	2.19	5.94	2.38	2.43	1.28	2.19	2.30
P_2O_5	0.17	0.09	0.09	0.11	0.06	0.03	0.07	0.06	0.05
LOI	1.30	0.84	1.30	1.33	0.86	0.52	0.70	0.63	0.47
TOTAL	100.04	100.68	100.54	100.60	100.06	99.41	100.30	100.49	100.67
Au ppm	0.06	1.00	0.09	0.04	2.30	0.16	1.50	0.69	7.10
Ag ppm	22	44	16	4.6	70	30	42	19	24
Hg	0.07	0.04	0.04	0.02	0.18	0.04	0.15	0.07	0.03
Sb	4	11	5	12	5	4	13	5	7
As	46	60	36	70	55	14	70	32	38
F%	0.052	0.050	0.031	0.042	0.041	0.030	0.042	0.031	0.035
Ba	380	270	530	334	190	310	160	160	220
V	54	36	53	66	96	115	80	55	29
Cr	108	104	85	75	50	55	70	41	56
Ga	6	8	6	11	13	15	12	8	6
Pb	106	54	131	47	810	346	968	572	58
Th	bd	10	bs	20	10	10	bd	10	bd
Rb	65	198	95	254	105	113	60	95	109
U	bd	3	bd	10	bd	4	bd	bd	3
Sr	66	58	54	59	35	42	30	29	32
Y	20	21	19	45	18	15	15	15	9
Zr	52	75	57	109	33	28	21	30	37
Nb	bd	11	8	22	10	9	6	8	8
Zn	164	59	106	127	264	528	157	131	28
Cu	54	10	43	23	131	328	118	80	8
Ni	14	4	7	5	5	10	5	bd	bd

Appendix 11.5b (continued)

	15033	15034	15036	15037	15038	15040	15044	15049	15050
SiO_2	85.7	91.7	89.5	83.4	78.2	79.7	87.5	81.2	90.2
TiO_2	0.07	0.04	0.04	0.52	0.45	0.49	0.41	0.68	0.32
Al_2O_3	7.73	3.80	4.84	6.27	10.00	8.40	4.73	6.62	3.86
Fe_2O_3	0.92	1.71	1.79	4.06	3.66	3.68	3.05	4.10	2.39
MnO	0.02	0.02	0.02	0.02	0.02	0.03	0.02	0.03	0.02
MgO	0.19	0.10	0.38	0.63	0.30	0.29	0.33	0.49	0.20
CaO	0.21	0.17	0.19	0.48	0.25	0.45	0.27	0.49	0.28
Na_2O	0.01	0.02	0.09	0.08	0.16	0.15	0.03	0.03	0.09
K_2O	4.92	1.94	2.77	4.23	7.06	5.81	2.57	4.01	1.66
P_2O_5	0.02	0.02	0.03	0.22	0.15	0.21	0.13	0.22	0.11
LOI	0.88	0.73	0.85	0.82	0.99	1.14	1.60	1.25	1.01
TOTAL	100.67	100.25	100.50	100.73	101.24	100.35	100.64	99.12	100.14
Au ppm	0.05	2.50	4.00	0.39	0.14	0.27	0.04	0.74	1.20
Ag ppm	7.5	40	38	6.8	4	26	1.7	60	70
Hg	0.04	0.07	0.31	0.14	0.10	0.19	0.07	0.08	0.06
Sb	4	18	19	20	16	11	4	14	6
As	24	44	46	80	80	65	42	140	42
F%	0.040	0.060	0.022	0.054	0.066	0.056	0.072	0.046	0.036
Ba	200	220	290	490	620	640	300	460	280
V	26	51	73	59	77	76	42	87	41
Cr	86	69	65	107	105	75	47	71	48
Ga	9	18	18	7	10	9	6	9	6
Pb	104	1555	1752	47	61	87	78	133	157
Th	20	20	20	bd	20	10	bd	bd	bd
Rb	247	91	124	197	351	282	115	195	75
U	bd	bd	bd	4	3	bd	9	bd	6
Sr	64	27	35	82	155	91	61	60	47
Y	21	9	18	26	35	31	16	25	14
Zr	65	27	35	137	143	150	80	137	61
Nb	22	8	11	11	22	19	5	8	3
Zn	47	540	441	29	33	98	33	82	136
Cu	22	307	274	19	20	34	9	29	35
Ni	7	5	bd	6	7	11	bd	5	3

APPENDIX 11.5c - Trace element analyses of additional selected quartz veins by XRF, NMBMMR; Au, Ag by fire assay, Cu, Pb, Zn, Sb, Hg by NMBMMR Chemical Laboratory). Au and Ag in oz/ton, others in ppm.

Sample	Pb	Th	Rb	U	Sr	Y	Zr	Nb	Mo	Ga	Zn	Cu	Ni	Au	Ag	Cu	Pb	Zn	Hg	Sb	Comments
15	478	bd	59	bd	25	8	37	3	20	--	--	--	--	tr	5.8	3400	480	400	--	--	East Camp vein
24	17	bd	280	bd	111	18	172	7	bd	10	41	11	35	0	0.06	13	18	44	--	--	East Camp vein
31	164	10	367	3	110	22	146	8	bd	13	129	24732	3	0	1	26200	1000	72	--	--	Blue Bell vein
32	8	bd	4	bd	419	bd	11	bd	bd	bd	6	bd	8	0	0	8	25	15	--	--	Blue Bell vein
47	777	bd	77	bd	25	10	39	bd	5	13	334	2214	21	0.03	4.94	3000	800	400	--	--	East Camp vein
60	330	bd	143	bd	74	14	70	3	bd	14	614	129	27	0	0	180	330	560	--	--	Blue Goose vein
61	60	bd	56	bd	235	27	173	11	bd	16	155	14488	62	0	0.68	16600	76	100	1.9	33	Blue Goose vein
103	214	10	7	4	133	12	234	8	30	6	30	63	17	0	0	50	200	44	0.5	--	Tass
148	360	bd	181	bd	70	13	79	bd	bd	11	494	129	14	0	0.54	734	654	482	0.6	<2.0	Blue Goose vein
183	18	10	379	3	195	69	144	8	bd	16	58	33	17	--	--	--	--	--	--	--	breccia
186	230	bd	75	3	35	8	39	bd	8	7	43	33	10	--	--	--	--	--	--	--	
210A	8	bd	4	3	11	bd	6	bd	bd	11	5	9	8	--	--	--	--	--	--	--	
217A	8	bd	529	bd	163	41	282	16	bd	11	34	19	18	--	--	--	--	--	--	--	Tbd
217C	19	bd	77	bd	30	8	52	bd	bd	8	26	27	21	--	--	--	--	--	--	--	
227	25	bd	200	bd	116	13	87	4	20	8	45	21	14	--	--	--	--	--	--	--	dacite
230	59	bd	206	bd	92	11	92	3	5	7	36	17	9	--	--	--	--	--	--	--	
231Q	215	10	460	3	174	16	126	8	150	11	54	52	4	--	--	--	--	--	--	--	breccia
233	56	bd	188	bd	203	23	129	5	bd	--	--	--	--	0	11.56	65000	79	113	0.18	--	
236	26420	50	bd	bd	48	193	52	0	bd	249	15313	13711	48	0	1.6	4720	10900	9050	2	30	Laura vein
244	684	10	80	bd	39	16	51	2	50	--	--	--	--	0.07	1.05	170	800	670	--	--	Laura vein
246	554	bd	21	bd	26	8	26	0	10	--	--	--	--	0.12	11.24	246	631	541	0.3	14	Laura vein
251	63	bd	96	bd	7	11	96	5	30	11	15	20	20	0	0	<70	631	541	0.3	<2.0	Alabama vein
254	155	bd	303	bd	114	19	101	7	5	13	154	94	52	0	0	75	210	120	--	--	New Year's Gift vein
257D	3750	20	217	bd	81	51	101	10	bd	42	3036	998	48	0	0.52	990	5340	2470	--	--	New Year's Gift vein
269	833	10	32	bd	33	13	24	1	80	--	--	--	--	0.02	1.1	230	950	770	2	7.3	Alabama vein
270	22	30	382	5	39	34	139	22	bd	16	45	13	29	--	--	--	--	--	--	--	tuff
273	3780	20	110	bd	30	19	36	15	--	35	1410	1240	84	0.3	2.4	1310	3960	1230	0.6	--	Alabama vein
287	650	bd	53	bd	16	11	29	0	3	11	739	87	9	--	--	--	--	--	0.22		
310	5740	60	48	bd	22	54	51	0	bd	--	--	--	--	0.03	0.7	1200	7000	7300	0.8	<2.0	Jim Crow vein
311	644	bd	7	bd	6	8	13	0	5	--	--	--	--	0.02	0.76	240	710	477	--	--	Jim Crow vein
312A	272	bd	59	bd	20	8	38	0	20	--	--	--	--	0.04	0.54	147	320	159	0.3	<2.0	Jim Crow vein
340c	bd	20	252	10	16	32	163	4	--	12	22	17	8	--	--	--	--	--	--	--	
348	52	bd	18	bd	46	15	110	3	4	--	--	--	--	tr	0.24	<10	85	88	--	--	Carlisle vein
367	23	bd	500	bd	257	22	417	15	--	21	39	29	5	--	--	--	--	--	--	--	
368B	974	10	138	bd	35	25	97	4	15	--	--	--	--	0.11	1.29	160	1220	1360	--	--	
369B	1400	20	121	bd	25	25	56	8	15	--	--	--	--	0.07	0.07	340	1780	1800	--	--	
369C	1990	30	171	bd	23	35	52	12	2	--	--	--	--	0	1.34	2660	2880	1140	--	--	

Appendix 11.5c (continued)

Sample	Pb	Th	Rb	U	Sr	Y	Zr	Nb	Mo	Ga	Zn	Cu	Ni	Au	Ag	Cu	Pb	Zn	Hg	Sb	Comments
372	40	10	139	5	99	38	230	21	bd	--	--	--	--	0.03	2.29	58180	60	240	--	--	Delmire vein
419	36	bd	205	bd	82	19	140	9	20	--	--	--	--	0	0.2	29	23	43	--	--	
426	44	bd	98	bd	55	15	113	3	15	--	--	--	--	tr	0.66	128	51	75	--	--	
434C	bd	bd	302	3	233	34	256	16	20	--	--	--	--	0	6.02	24000	40	34	--	--	
450	135	bd	134	bd	19	16	35	15	20	--	--	--	--	0.14	13.14	39	150	46	0.5	2.4	
451	712	10	70	bd	18	15	30	8	20	--	--	--	--	0.06	21.84	80	850	615	0.4	1	
469	153	bd	7	bd	18	4	12	bd	20	--	--	--	--	0	0.24	41	190	79	0.1	<1.0	
472	17	bd	13	bd	322	25	30	7	20	--	--	--	--	0	0.12	71	46	17	0.7	<1.0	
486	bd	bd	66	bd	122	13	53	5	3	5	29	179	42	--	--	--	--	--	--	--	
488	421	10	108	bd	64	19	86	13	330	--	--	--	--	0.01	3.74	39400	460	50	0.1	1.6	
491	526	10	88	bd	34	13	36	0	10	--	--	--	--	0	0	270	605	140	<0.1	<1.0	
510a	16	bd	50	bd	120	39	46	6	20	--	--	--	--	0	0	33	39	37	0.1	<1.0	
515	15	bd	bd	bd	599	9	237	7	5	--	--	--	--	0	0.12	120	14	12	0.2	<1.0	
516d	32	bd	30	bd	177	8	42	7	20	--	--	--	--	tr	0.34	1300	29	61	0.6	<1.0	
546	86	20	100	10	76	14	82	15	7	--	--	--	--	0	0.88	82800	70	20	0.3	<1.0	
584	13	bd	31	bd	370	18	95	5	10	--	--	--	--	0	0	3700	40	50	<0.1	<2.0	
586	67	bd	54	3	42	11	56	bd	20	--	--	--	--	0	0.12	161	711	51	0.2	5	
588	34	bd	199	bd	75	29	170	10	4	--	--	--	--	0	0.24	5000	51	79	<0.1	<2.0	
600	11	bd	9	4	89	5	188	8	20	--	--	--	--	0	0.08	25	16	6.4	0.9	<2.0	
701	264	bd	23	bd	105	6	24	bd	60	--	--	--	--	0.04	0.64	171	352	583	0.21	--	
710	16750	180	0	bd	30	136	48	bd	20	--	--	--	--	0.058	0.382	11000	18000	18000	--	--	
724a	66	bd	292	bd	80	19	134	4	--	12	173	113	78	--	--	--	--	--	--	--	
724c	44	10	348	bd	178	21	177	5	--	15	166	200	31	--	--	--	--	--	--	--	
783	19	10	163	bd	84	29	196	6	--	16	16	5	5	--	--	--	--	--	--	--	
1064a	--	--	--	--	--	--	--	--	--	15	5	8	95	--	--	--	--	--	--	--	
ML4	bd	bd	390	bd	136	22	119	8	--	13	45	12	29	--	--	--	--	--	--	<0.1	
CT1	bd	30	233	4	201	35	230	13	--	22	126	43	45	--	--	--	--	--	--	0.2	
CT2	bd	30	332	6	52	36	259	16	--	--	--	--	--	--	--	--	--	--	--	<0.1	Carlisle
Carl3	1950	10	87	bd	37	21	58	bd	7	26	5710	1740	11	0	0.12	2600	2700	5200	3.5	--	Carlisle
Carl3A	34	bd	184	7	41	42	131	5	10	14	443	329	122	0	0.02	300	46	200	--	--	Carlisle
Carl3B	185	bd	206	6	90	36	112	4	20	13	435	202	45	0	0.04	200	200	300	--	--	Carlisle
Carl3C	142	10	335	bd	67	47	179	8	30	--	--	--	--	0	0	70	100	500	3.5	--	Carlisle
CenterDump	--	--	--	--	--	--	--	--	--	68	94	429	16	--	--	--	--	--	--	--	--
Center6	34738	40	5	bd	24	208	96	bd	bd	19	282	368	68	0	0.28	600	500	300	--	--	Center
Center9	478	10	154	bd	34	24	115	5	9	385	12800	10730	97	0.018	3.04	10100	17600	77	--	--	Center
Gold Rod	4788	10	221	bd	118	50	98	2	bd	65	6560	897	33	0	0.22	1200	5600	5300	--	--	Golden Rod vein
Ontario	32025	50	bd	0	20	188	78	bd	4	322	4810	1450	32	0	0.3	4500	29200	3200	--	--	Ontario vein
H10.273.	51	10	91	bd	40	8	81	4	--	--	--	--	--	0	0	33	57	53	--	--	

APPENDIX 11.6

Chemical analyses of mineralized samples. Analyses in parts per million except for Au and Ag, which are in oz/ton and Fe, CaF_2 which are in percent (%). Sample locations are on Map 2. Analyses by Lynn Brandvold and associates or by Chris McKee (XRF), designated by *. Samples are selected grab samples, unless otherwise specified. See Table 1.3 for detection limits, methods of analyses, and % error.

Sample	Au	Ag	Cu	Pb	Zn	Hg	Sb	Mn*	Fe	CaF_2	Mo	Ga*	Ni*	Rock type	Comments
East Camp Area															
15	tr	5.8	3400	4800	400	--	--	--	--	--	23	--	--	EC vein	dump sample
20	0.038	11.442	149000	201	167	0.15	--	--	--	--	--	--	--	vein	dump sample
24	0	0.06	13	18	44	--	--	--	--	--	bd*	10	35	EC vein	3 m chip across vein
27B	tr	0.98	15	25	24	--	--	--	--	--	--	--	--	vein	1 m chip across breccia
27C	tr	1.32	31	84	85	--	--	--	--	--	--	--	--	vein	1 m chip across vein
31	0	1	26200	1000	72	--	--	--	--	--	bd*	13	3	BB vein	--
32	0	0	8	25	15	--	--	--	--	--	bd*	bd1	8	BB vein	--
47	0.03	4.94	3000	800	400	--	--	300	--	--	5*	13	21	EC vein	--
216A	0	0	<70	<59	<10	0.2	<2.0	--	--	--	--	--	--	EC vein	--
296	0	0	<70	199	32	0.3	3.6	--	--	--	--	--	--	BB vein	select outcrop
323	0	0	31	68	51	--	--	--	--	--	--	--	--	EC vein	1.4 m across vein
633	0	8.46	11700	810	37	0.5	30	--	--	--	--	--	--	EC vein	dump sample
634	0.094	29.31	480	940	740	<0.1	<2.0	--	--	--	--	--	--	EC vein	dump sample
724b	0	0	104	125	96	0.17	--	--	--	--	--	--	--	--	1.5 m chip across vein
917a	0.042	3.22	12000	147	20	0.11	--	--	--	--	--	--	--	--	--
917d	0.09	0.56	192	720	38	<0.02	--	--	--	--	--	--	--	clay	--
918	0	2.78	511	1400	1900	0.2	--	--	--	--	--	--	--	--	dump select
920	0	23.86	88000	242	34	0.29	--	--	--	--	--	--	--	--	--
1033a	0.024	1.532	46000	260	21	0.22	--	--	--	--	--	--	--	--	1 m chip across vein
ML1	tr	0.54	100	319	280	--	--	--	--	--	--	--	--	EC vein	--
ML2	tr	0.36	34	84	148	--	--	--	--	--	--	--	--	EC vein	--
ML3	tr	1	89	209	193	--	--	--	--	--	--	--	--	EC vein	--
EC dup	0.34	62.82	1110	1140	720	--	--	--	--	--	--	--	--	EC vein	dump sample
McDonUp	0.6	33.23	480	1460	700	--	--	--	--	--	--	--	--	EC vein	dump sample
M3	0.13	8.13	260	700	330	--	--	--	--	--	--	--	--	EC vein	--
M2	0	0.04	171	108	91	--	--	--	--	--	--	--	--	EC vein	--
M1	tr	13.42	214	326	391	--	--	--	--	--	--	--	--	EC vein	--
Blue Goose and Vicinity															
60	0	0	180	330	560	--	--	--	--	--	bd*	14	27	BG vein	6.1 m chip across back
61	0	0.68	16600	76	100	1.9	33	--	--	--	bd*	16	62	BG vein	

Appendix 11.6 (continued)

Sample	Au	Ag	Cu	Pb	Zn	Hg	Sb	Mn*	Fe	CaF_2	Mo	Ga*	Ni*	Rock type	Comments
148	0	0.54	734	654	482	0.6	<2.0	--	--	--	bd*	11	14	BG vein	0.3 m chip across vein
922	0.001	2.16	2800	45000	977	0.06	--	--	--	--	--	--	--	--	0.5 m chip across vein
923	0	3.18	14900	3700	1600	0.08	--	--	--	--	--	--	--	--	dump sample
927	0	1.94	7800	894	235	0.02	--	--	--	--	--	--	--	--	--
Blue Goose	0.018	0.4	27	240	18	0.04	--	--	--	--	--	--	--	--	dump sample
Gold Rod	0	0.22	1200	5600	5300	--	--	--	--	--	bd*	65	33	GR vein	1 m chip across back
Telephone Ridge Area															
85	0	0.1	15	41	14	0.06	--	--	--	--	<25	--	--	--	--
103	0	0	50	200	44	0.5	--	200	--	--	25*	6	17	Tele Rid	1.5 m chip across breccia
105	0	0.52	49	38	73	<0.4	--	--	--	--	30	--	--	--	dump sample
187	0	0	21	26	78	--	--	--	--	--	--	--	--	--	--
207	0	0.18	<70	59	23	0.1	<2.0	--	--	--	--	--	--	EC fault	--
357	0.05	2.13	57	99	20	--	--	--	--	--	--	--	--	Tele cap	massive silica zone- Tass
328A	0	0	<10	48	65	--	--	--	--	--	--	--	--	vein	silified zone- Tass
328C	0	0	<10	30	48	--	--	--	--	--	--	--	--	Ont	silicified zone- Tass
340A	0	0	<10	34	57	--	--	--	--	--	--	--	--	Ont	1.2 m chip across back
340B	0	0	35	54	18	--	--	--	--	--	--	--	--	Ont	1.5 m chip across back at entrance
569	0	0	11	8	4	0.3	<2.0	--	--	--	--	--	--	--	--
570	0	0.14	359	42	172	<0.3	--	--	--	--	--	--	--	--	--
769	0	0	20	17	16	0.03	--	--	--	--	--	--	--	--	Tassc
770	0	0	31	30	33	0.09	--	--	--	--	--	--	--	--	Tassc
771	0	0	42	51	29	0.13	22	--	17.2	--	--	--	--	--	Tassi
772	0	0	16	8	13	0.1	--	--	--	--	--	--	--	--	Tass
773	0	0	16	13	31	0.1	--	--	--	--	--	--	--	--	Tass
775	0	0	12	35	830	<0.2	0.14	--	19.2	--	--	--	--	--	dump sample - Tass
776	0	0	75	65	49	0.1	--	--	--	--	--	--	--	--	Tassi
777	--	--	6	8	8	0.02	--	--	--	--	--	--	--	--	Tassc
779	0	0	5	<5	7	0.05	--	--	--	--	--	--	--	--	Tassi
780	0	0	6	7	8	0.02	--	--	--	--	--	--	--	--	Tass
781	0	0	5	10	10	0.02	--	--	--	--	--	--	--	--	Tassi
785	0	0.02	16	5	10	0.03	--	300	--	--	--	--	--	--	Tassc
Ontario	0	0.3	4500	29200	3200	--	--	--	--	--	bd*	322	32	Ont	0.8 m chip across face end of adit

Appendix 11.6 (continued)

Sample	Au	Ag	Cu	Pb	Zn	Hg	Sb	Mn*	Fe	CaF_2	Mo	Ga*	Ni*	Rock type	Comments
O-1	0	0	12700	16700	46800	--	--	--	--	--	--	10	bd	Ont	1 m chip across back
Carlisle-Center Area															
231	0.09	5.90	--	--	--	--	--	--	--	--	--	--	--	Sec 2	1 m chip across breccia
348	tr	0.24	<10	85	88	--	--	--	--	--	4	--	--	Carl	dump sample
349	0	0	141	480	102	--	--	--	--	--	--	--	--	Carl	dump sample
350	0	0	10	20	47	--	--	--	--	--	--	--	--	Carl	7.6 m chip across breccia
351	0	0	63	78	56	--	--	--	--	--	--	--	--	P vein	
564	0	0	56	33	97	<0.1	<2.0	--	--	--	--	--	--	--	1.2 m chip across vein
632	0	0	63	36	8	0.2	<2.0	--	--	--	--	--	--	sandstone	--
652a	0	0	904	17	31	0.02	--	--	--	--	--	--	--	--	clay zone
652b	0	0	8.5	18	26	<0.2	--	--	--	--	--	--	--	--	silicified
679	0.082	0.278	90	165	245	0.1	--	--	--	--	--	--	--	--	dump sample
792b	0	0	20	15	10	<0.2	--	--	--	--	--	--	--	--	Tassi
797	0	0	14	37	14	<0.2	--	--	--	--	--	--	--	Carl	Tassi
798	0	0	29	96	93	0.04	--	--	--	--	--	--	--	--	Tassi
1075	Tr	1.58	13000	57000	85000	0.02	--	--	--	--	--	--	--	--	--
S1	0	0	46	67	85	--	--	--	--	--	--	--	--	Sec 2	--
S2	0	0	30	198	210	--	--	--	--	--	--	--	--	Sec 2	--
S3	0	0.62	239	994	1200	--	--	--	--	--	--	--	--	Sec 2	--
Carl3C	0	0	70	100	500	3.5	--	--	--	--	25	--	--	Carl	--
Carl1	0.34	1.16	--	--	--	--	--	--	--	--	--	--	--	Carl	--
Carl1PitW	0	0.06	310	760	50	--	--	--	--	--	--	--	--	Carl	--
Center9	0.018	3.04	10100	17600	7700	--	--	--	--	--	10*	385	97	Center	dump sample
Center6	0	0.28	600	500	300	--	--	--	--	--	bd*	19	68	Center	dump sample
Center	0	0	600	69400	25700	--	--	--	--	--	--	--	--	Center	dump sample
Center91	0.46	0.94	990	84000	80690	--	--	--	--	--	--	--	--	Center	dump sample
CenFac91	0	0.82	4070	28000	27280	--	--	--	--	--	--	--	--	Center	
Cen187Xfaul	0	0	21	26	78	0.1	--	--	--	--	--	--	--	--	--
Cen16B	0	0.26	400	990	1700	0.23	--	--	--	--	--	--	--	--	--
Cen16A	0	0	1900	26000	43000	1.05	--	--	--	--	--	--	--	--	--
Lot18759	0.6	5.14	3800	27700	40000	0.9	4	--	--	--	--	--	--	--	ore production
Lots5-91	0.21	3.38	3860	32000	40900	1.3	6.6	--	--	--	--	--	--	--	ore production
Lot26-91	0.23	5.3	4390	28400	35000	0.5	<2.0	--	--	--	--	--	--	--	ore production
Lot54-91	0.72	4.84	3880	34800	38000	0.5	2.7	--	--	--	--	--	--	--	ore production
Lot93-91	0.81	4.4	3890	35300	37300	0.5	4.4	--	--	--	--	--	--	--	ore production

Appendix 11.6 (continued)

Sample	Au	Ag	Cu	Pb	Zn	Hg	Sb	Mn*	Fe	CaF_2	Mo	Ga*	Ni*	Rock type	Comments
R&B80-82	0	0	157	775	596	0.09	--	--	--	--	--	--	--	--	drill core
R&B84-86	0	1.9	56	33	234	<0.02	--	--	--	--	--	--	--	--	drill core
R&B86-88	0.03	0.8	1600	2300	4200	0.05	--	--	--	--	--	--	--	--	drill core
R&B88-90	0	0	1900	7400	4100	<0.02	--	--	--	--	--	--	--	--	drill core
R&B90-92	0	3.26	1100	4000	8300	<0.02	--	--	--	--	--	--	--	--	drill core
R&B92-94	0	0	3000	1300	3200	0.21	--	--	--	--	--	--	--	--	drill core
R&B94-97.5	0.242	11.336	477	5500	2900	0.03	--	--	--	--	--	--	--	--	drill core
P1	0	0	<10	23	89	--	--	--	--	--	--	--	--	Penn	--
P2	0	0	1000	4400	4400	--	--	--	--	--	--	--	--	Penn	--
Carl3	0	0.12	2600	2700	5200	3.5	--	--	--	--	7*	26	11	Carl	--
Carl3A	0	0.02	300	46	200	--	--	--	--	--	11*	14	122	Carl	--
Carl3B	0	0.04	200	200	300	--	--	--	--	--	15*	13	45	Carl	--
C3-48	0.03	1.51	6810	13000	11000	0.47	--	--	--	--	--	--	--	--	--
C-124	0	1.48	7150	22000	50000	0.67	--	--	--	--	--	--	--	--	--
C6-7,181	--	--	<100	<100	161	<0.2	--	--	--	--	--	--	--	--	--
C9-16a	0	0	3800	36000	90400	1.64	--	--	--	--	--	--	--	--	--
C9-16b	0	0.26	558	2500	5000	0.2	--	--	--	--	--	--	--	--	--
Vanderbilt Peak-Alabama-Imperial Area															
233	0	11.56	65000	79	113	0.18	--	--	--	--	3	--	--	--	--
236	0	1.6	4720	10900	9050	2	30	--	--	--	bd*	249	48	L vein	dump sample
244	0.07	1.05	170	800	670	--	--	--	--	--	50	--	--	L vein	3 m chip across vein
246	0.12	11.24	246	631	541	0.3	14	--	--	--	12	--	--	L vein	--
251	0	0	<70	631	541	0.3	<2.0	100	--	--	31*	11	20	A vein	--
254	0	0	75	210	120	--	--	--	--	--	5*	13	52	NYG vein	1.5 m chip across vein
257D	0	0.52	990	5340	2470	--	--	--	--	--	bd*	42	48	NYG vein	1.5 m chip across vein
263	0	1.42	81000	239	1190	0.22	--	--	--	--	--	--	--	--	dump sample
268	0	0	9	19300	23	0.3	<2.0	--	--	--	--	--	--	L vein	1 m chip across vein
269	0.02	1.1	230	950	770	2	7.3	--	--	--	77	--	--	A vein	dump sample
273	0.3	2.4	1310	3960	1230	0.6	--	--	--	--	--	35	84	A vein	0.3 m chip across vein
284	0	0	<70	<50	17	0.3	17	--	--	--	--	--	--	L vein	1.2 m chip across vein
287	0.182	3.46	108	744	759	0.22	--	900	--	--	3*	11	9	--	dump sample
302	0.02	3.84	126	459	220	0.9	2.7	--	--	--	--	--	--	A vein	--
309	0.01	1.8	1500	5300	5100	1.4	<2.0	--	--	--	--	--	--	JC vein	dump sample
310	0.03	0.7	1200	7000	7300	0.8	<2.0	--	--	--	bd	--	--	JC vein	dump sample
311	0.02	0.76	240	710	477	--	--	--	--	--	5	--	--	JC vein	--
312A	0.04	0.54	147	320	159	0.3	<2.0	--	--	--	20	--	--	JC vein	--

Appendix 11.6 (continued)

Sample	Au	Ag	Cu	Pb	Zn	Hg	Sb	Mn*	Fe	CaF_2	Mo	Ga*	Ni*	Rock type	Comments
312B	0.01	1.46	183	1230	230	1.5	<2.0	--	--	--	--	--	--	JC vein	--
368A	0	0	13	122	34	--	--	--	--	--	--	--	--	vein	1 m chip across breccia zone
368B	0.11	1.29	160	1220	1360	--	--	--	--	--	15	--	--	vein	1 m chip across vein
369B	0.07	0.07	340	1780	1800	--	--	--	--	--	15	--	--	vein	breccia
369C	0	1.34	2660	2880	1140	--	--	--	--	--	2	--	--	vein	--
371	0	0	320	520	220	--	--	--	--	--	--	--	--	vein	dump sample
372	0.03	2.29	58180	60	240	--	--	--	--	--	bd	--	--	Delmire	--
373	0	0.18	28	40	40	--	--	--	--	--	--	--	--	A vein	--
401	0	0.3	95	15	62	--	--	--	--	--	--	--	--	vein	1.5 m chip across vein
411	0	0.12	12	12	12	--	--	--	--	--	--	--	--	vein	--
419	0	0.2	29	23	43	--	--	--	--	--	17	--	--	vein	1.2 m chip across back at entrance
419a	0	0	45	49	100	0.4	--	--	--	--	--	--	--	rhyolite	4.7 m chip across breccia zone
419b	0	0	35	57	65	0.7	--	--	--	--	--	--	--	--	0.3 m chip across vein
423	0	0.04	32	20	20	--	--	--	--	--	--	--	--	vein	--
424	0	0.56	40	34	36	--	--	--	--	--	--	--	--	vein	dump sample
426	tr	0.66	128	51	75	--	--	--	--	--	15	--	--	vein	--
427	0	0.32	61	285	201	--	--	--	--	--	--	--	--	NY vein	1.2 m chip across vein
429	0	0.34	24	127	97	--	--	--	--	--	--	--	--	vein	1 m chip across vein
431a	0	0	51	28	62	0.5	--	--	--	--	--	--	--	--	0.3 m chip across vein
434	0	0.3	171	106	35	--	--	--	--	--	--	--	--	vein	1.5 m chip across back
434C	0	6.02	24000	40	34	--	--	--	--	--	17	--	--	vein	dump sample
449	0.001	6.18	120	2400	205	0.2	1.3	--	--	--	--	--	--	--	dump sample
450	0.14	13.14	39	150	46	0.5	2.4	--	--	--	19	--	--	--	dump sample
451	0.06	21.84	80	850	615	0.4	1	--	--	--	18	--	--	--	dump sample
467	0	0	25	15	22	0.2	2.7	--	--	--	--	--	--	--	0.3 m chip across vein
469	0	0.24	41	190	79	0.1	<0.1	--	--	--	18	--	--	--	dump sample
605	0	0	2900	16	20	0.5	<2.0	--	--	--	--	--	--	--	dump sample
607	0	0	34	23	20	0.4	<2.0	--	--	--	--	--	--	--	--
608A	0	0	35	73	63	0.2	2.3	--	--	--	--	--	--	--	1.5 m chip across vein
608B	0	0	29	87	77	0.6	<2.0	--	--	--	--	--	--	--	dump sample
624	0	0.1	225	2000	290	0.3	<2.0	--	--	--	--	--	--	A vein	dump sample
625	0.096	4.32	1300	6400	4300	0.2	21	--	--	--	--	--	--	A vein	dump sample
695	1.248	75.152	459	1880	1280	0.1	--	--	--	--	--	--	--	--	dump sample
701	0.04	0.64	171	352	583	0.21	--	--	--	--	58	--	--	--	--

Appendix 11.6 (continued)

Sample	Au	Ag	Cu	Pb	Zn	Hg	Sb	Mn*	Fe	CaF_2	Mo	Ga*	Ni*	Rock type	Comments
703	0	0.26	23	30	126	<0.03	--	1400	--	--	bd*	21	123	--	dump sample
708	0.184	23.716	1200	3570	3720	0.72	--	--	--	--	--	--	--	--	--
710	0.058	0.382	11000	18000	18000	--	--	--	--	--	19	--	--	--	dump sample
941	0	1	38000	35	50	<0.2	--	--	--	--	--	--	--	--	dump sample
Imperial 200	0	13.18	678	1400	3570	0.73	--	--	--	--	31	--	--	--	--
Rattlesnake Mines															
472	0	0.12	71	46	17	0.7	<1.0	--	--	--	20	--	--	Rat vein	--
473	0	0	28	64	14	0.5	<1.0	--	--	--	--	--	--	Rat vein	--
Charlie Hill and Vicinity															
486	0	6.12	29	31	17	<0.1	<0.1	1200	--	--	--	5	42	--	dump sample
487	0	0.18	40	29	49	0.6	<1.0	--	--	--	--	--	--	--	--
488	0.01	3.74	39400	460	50	0.1	1.6	--	--	--	325	--	--	vein	--
491	0	0	270	605	140	<0.1	<0.1	--	--	--	9	--	--	--	--
Goat Camp Springs Area															
510a	0	0	33	39	37	0.1	<1.0	--	--	--	22	--	--	--	--
510b	0	0	30	54	37	0.5	<1.0	--	--	--	--	--	--	--	--
510c	0	0	195	34	46	1.5	<1.0	--	--	--	--	--	--	--	--
513	0	0	24	26	14	<0.1	<1.0	--	--	--	--	--	--	--	--
515	0	0.12	120	14	12	0.2	<1.0	--	--	--	5	--	--	vein	--
516d	tr	0.34	1300	29	61	0.6	<1.0	--	--	--	18	--	--	--	--
532	0	0	41	14	10	0.8	<1.0	--	--	--	--	--	--	--	--
533	0	0	17	14	12	0.3	<1.0	--	--	--	--	--	--	--	--
536d	0	0	16	12	20	0.2	<1.0	--	--	--	--	--	--	--	--
542	0	0	14	5	20	0.2	106	--	--	--	--	--	--	--	dump sample
543	0	0	28	10	20	0.2	<1.0	--	--	--	--	--	--	--	dump sample
545	0	0	48	10	30	<0.1	1.3	--	--	--	--	--	--	--	dump sample
546	0	0.88	82800	70	20	0.3	<1.0	--	--	--	7	--	--	--	--
581	0	0	15	9	3	0.8	<2.0	--	--	--	--	--	--	--	--
584	0	0	3700	40	50	<0.1	<2.0	--	--	--	12	--	--	--	--
718	0	0	21	32	37	0.02	--	400	14.7	--	--	13	0	--	Tassi
719	0	0	8	13	7	0.3	--	--	--	--	--	--	--	--	Tassi
723	0	0	19	13	11	0.18	--	--	--	--	--	--	--	--	clay zone
1041	9	9	86	52	20	0.03	--	--	--	7.47	--	--	--	Forbis	--
1042	0	0	46	27	50	0.02	--	96	--	0.3	--	--	--	--	dump sample

Appendix 11.6 (continued)

Sample	Au	Ag	Cu	Pb	Zn	Hg	Sb	Mn*	Fe	CaF_2	Mo	Ga*	Ni*	Rock type	Comments
1043	0.24	0.2	180	160	69	0.06	--	--	--	3	--	--	--	--	--
1050	0	0	8.6	25	35	0.06	--	--	--	--	--	--	--	--	--
1053	0.644	0.756	16000	62	30	0.08	--	31	--	0.05	--	--	--	--	dump sample
Foothills Fault Area															
548	0	0	14	5	20	0.3	<1.0	--	--	--	--	--	--	vein	--
549	0	0	90	8	20	<0.1	<1.0	--	--	--	--	--	--	--	dump sample
551	0	0	24	10	20	0.2	<1.0	--	--	--	--	--	--	vein	--
557	0	0	50	17	31	<0.1	<1.0	--	--	--	--	--	--	--	dump sample
559	0	0	43	80	60	0.6	3.9	--	--	--	--	--	--	--	dump sample
560	0	0	23	45	9	0.3	<2.0	--	--	--	--	--	--	--	--
574A	0	0	42	14	8	0.2	<2.0	--	--	--	--	--	--	--	--
574B	0	0	8	12	4	<0.1	<2.0	--	--	--	--	--	--	--	--
586	0	0.12	161	711	51	0.2	5	--	--	--	17	--	--	--	dump sample
587	0	0	38	23	32	0.2	<2.0	--	--	--	--	--	--	--	--
588	0	0.24	5000	51	79	<0.1	<2.0	--	--	--	4	--	--	--	dump sample
589	0	0	30	33	28	<0.1	2	--	--	--	--	--	--	--	dump sample
Black Cat	0	0	120	33	67	0.21	--	21.8	--	--	--	--	--	--	dump sample
Saddleback Mountain-Bitter Creek Areas															
594	0	0	17	25	11	<0.1	<2.0	--	--	--	--	--	--	--	--
600	0	0.08	25	16	6	0.9	<2.0	--	--	--	22	--	--	--	--
601A	0	0.12	35	820	13	0.09	--	200	--	--	<25	22	24	--	1.5 m chip across clay zone - Tass
601B	0	0	59	18	280	0.7	<2.0	--	--	--	--	--	--	--	1.5 m chip across breccia - Tassi
615	0	0	9	<5	4	0.1	<2.0	--	--	--	--	--	--	--	Tassi
621	0	0	11	49	9	0.2	<2.0	--	--	--	--	--	--	--	--
622	0	0	10	16	13	0.2	<2.0	--	--	--	--	--	--	--	--
932	0	0	18000	25	15	0.24	--	--	--	--	--	--	--	--	dump sample
949	0.592	79.94	196	20	15	0.16	--	--	--	--	--	--	--	--	Tassi
954	0	0	175	53	87	0.04	--	--	--	--	--	--	--	vein	--
984	0	0	110	41	18	0.25	--	14	--	0.09	--	--	--	--	--
988	0	0	71	47	44	0.04	--	400	--	7.13	5*	14	10	--	--
1068a	0	0	31000	6600	7200	0.13	--	--	--	0.08	--	--	--	--	0.5 m chip across vein
1068b	0	0.36	11000	16000	11000	0.17	--	--	--	0.04	--	--	--	--	1 m chip across vein
1071	0	7.24	75	45	24	0.02	--	--	--	--	--	--	--	--	dump sample

Appendix 11.6 (continued)

Sample	Au	Ag	Cu	Pb	Zn	Hg	Sb	Mn*	Fe	CaF_2	Mo	Ga*	Ni*	Rock type	Comments
Hext mines															
639	0.015	0.635	2085	72	25	<0.1	--	--	--	--	--	--	--	--	--
640	0.017	1.633	6145	192	27	<0.3	--	--	--	--	--	--	--	--	dump sample
641	0.014	5.176	37230	280	57	<0.1	--	--	--	--	--	--	--	--	dump sample
Raeburn Hills															
741	0	0	12	5	5	0.15	--	--	--	--	--	--	--	--	Tassi
742	0	0	6	57	5	0.12	--	--	--	--	--	--	--	--	Tassi
747	0	0.54	10	5	6	0.02	--	--	0.25	--	--	--	--	chert	Tass
748	0	0	10	15	6	0.09	--	--	--	--	--	--	--	--	Tassc
750	0	0	12	16	19	0.03	--	--	--	--	--	--	--	--	Tassi
754	0	0	20	17	12	0.03	--	--	--	--	--	--	--	--	Tassc
756	0	0	41	13	13	0.08	--	--	--	--	--	--	--	--	Tassi
760a	0	0	7	5	5	0.04	--	--	--	--	--	--	--	--	Tassc
761	0	0	14	63	27	0.06	--	--	--	--	--	--	--	--	Tass
Summit Area															
813a	0	0	59	17	20	0.45	--	--	--	--	--	--	--	--	vein
813b	0	0	19	14	25	1.6	--	--	--	--	--	--	--	vein	clay
817a	0	0	14	14	10	0.06	--	--	--	--	--	--	--	--	--
822d	0	0	7	44	27	0.05	--	--	--	--	--	--	--	--	--
837	0	0	25	20	10	0.02	--	--	--	--	--	--	--	--	--
850	0	0	30	20	40	<0.2	--	--	--	--	--	--	--	--	1.5 m chip across breccia
850a	0	0	15	27	40	0.11	--	--	--	--	--	--	--	--	--
872	0	0	29	38	10	0.04	--	--	--	--	--	--	--	--	dump sample
875b	0	0	15	15	20	0.05	--	--	--	--	--	--	--	--	clay
876	1.96	20.02	57	33	235	0.12	--	--	--	--	--	--	--	--	Tassi
878b	0	0	113	113	20	0.11	--	--	--	--	--	--	--	--	Tassc
886	0	0	29	10	15	0.13	--	--	--	--	--	--	--	--	Tassi
888-1	0	0	19	14	19	0.03	--	--	--	--	--	--	--	--	--
888-3	0	0	19	93	57	0.18	--	--	--	--	--	--	--	--	--
889-1	0	0.57	19	29	43	0.02	--	--	--	--	--	--	--	vein	clay
889-2	0	0.06	45	373	50	0.04	--	--	--	--	--	--	--	vein	clay
890-2	0	0.32	594	297	37	0.11	--	--	--	--	--	--	--	--	--
890-3	0	0	33	43	48	0.18	--	--	--	--	--	--	--	--	1 m chip across vein
903	0	11	15	44	20	0.08	--	--	--	--	--	--	--	--	dump sample

Appendix 11.6 (continued)

Sample	Au	Ag	Cu	Pb	Zn	Hg	Sb	Mn*	Fe	CaF_2	Mo	Ga*	Ni*	Rock type	Comments
909a	0	0	29	29	24	0.08	--	--	--	--	--	--	--	--	dump sample
1012	0	0	14	50	71	0.1	--	--	--	0.2	--	--	--	vein	--
BA	0.04	0.44	360	20	100	1.51	--	--	--	--	160	--	--	--	--
East Bitter Creek															
992	0	0	620	20	45	0.1	--	--	--	--	--	--	--	--	dump sample
1011	0	0	19	16	17	0.21	--	--	--	--	--	--	--	--	Tassc - dump sample
1045	0	0	<5	<15	15	0.06	--	600	--	0.3	bd*	14	7	rhyolite	--
1046	0	0	28	22	32	0.06	--	400	--	0.01	7*	14	74	rhyolite	--
1047	0	0	<5	<15	24	0.08	--	600	--	0.09	bd*	15	8	rhyolite	--
1048	0	0	5,7	38	51	0.09	--	300	--	--	bd*	17	11	rhyolite	--
1106	0	0.06	290	250	370	1.02	--	--	--	--	--	--	--	--	dump sample
Twin Peaks-Fraser Area															
1017	0	0	11000	29	17	0.16	--	--	--	--	--	--	--	--	dump sample
1026a	0	0	25000	52	88	0.17	--	--	--	--	--	--	--	--	dump sample
1086A	0.1	2.28	110	110	95	0.03	--	--	--	--	--	--	--	--	1 m chip across vein
1085	0	1.25	67000	<20	24	0.07	--	--	--	--	--	--	--	--	dump sample
Black Willow mines															
1130	0	0	30	42	84	0.75	--	--	--	--	--	--	--	--	dump sample
1131	0	0	16	25	9	<0.03	--	--	--	--	--	--	--	--	0.3 m chip across vein
1132f	0	0.42	11	25	9	0.04	--	--	--	32.4	--	--	--	--	2 m chip across vein
1132g	tr	0.22	22	30	13	0.88	--	--	--	--	--	--	--	--	1 m chip across vein

Appendix 11.7

Summary of fluid inclusion data

Over 1200 temperatures of homogenization and salinity measurements were made on samples from the Steeple Rock mining district. Methods are in section 1.5.6. These data are summarized in Tables 4.1, 4.2, and 4.3. This appendix includes graphical representation of temperatures of homogenization by mineral host, individual mines, and groups of mines. A number of samples were grouped together according to geographic location as follows:

Geographic location	–	Sample number
Carlisle fault (quartz)	–	400S, 404S, 182, Ontario, Center, 231
East Camp fault (quartz)	–	47, McDonald adit, 634
Alabama–Imperial	–	310, 434, Alabama DH1
Rattlesnake mines (fluorite)	–	472, 473
Goat Camp Springs (fluorite)	–	510, 516, 518, 536, 538, 545
Luckie Mines	–	559, Luckie No. 2
Forbis mines	–	1043, 1041

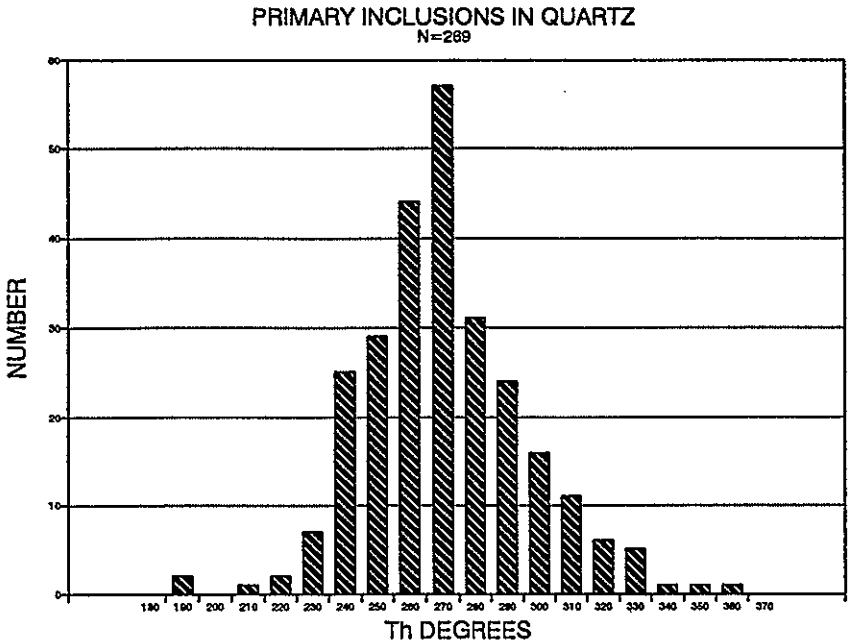

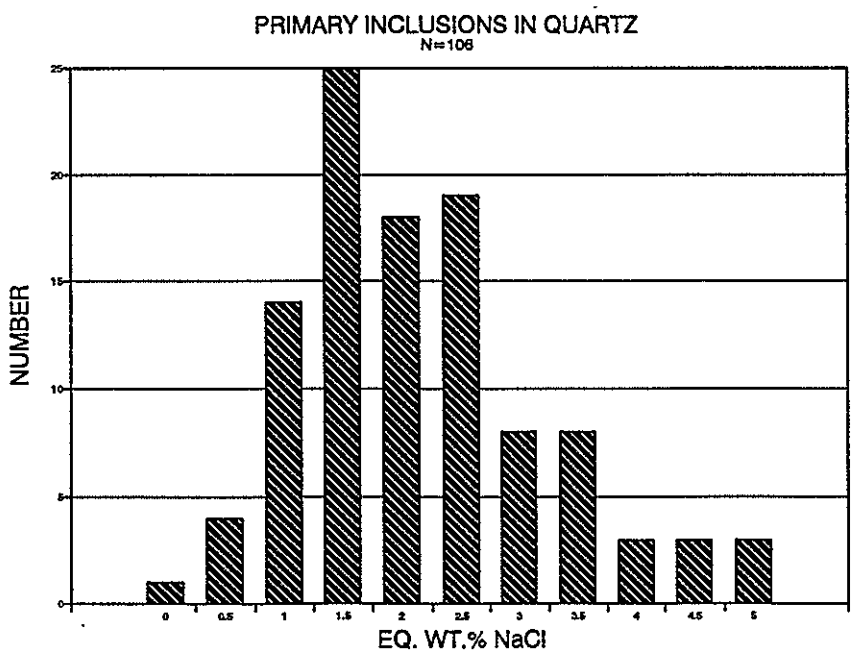

Plot of all primary inclusion data from all quartz samples.

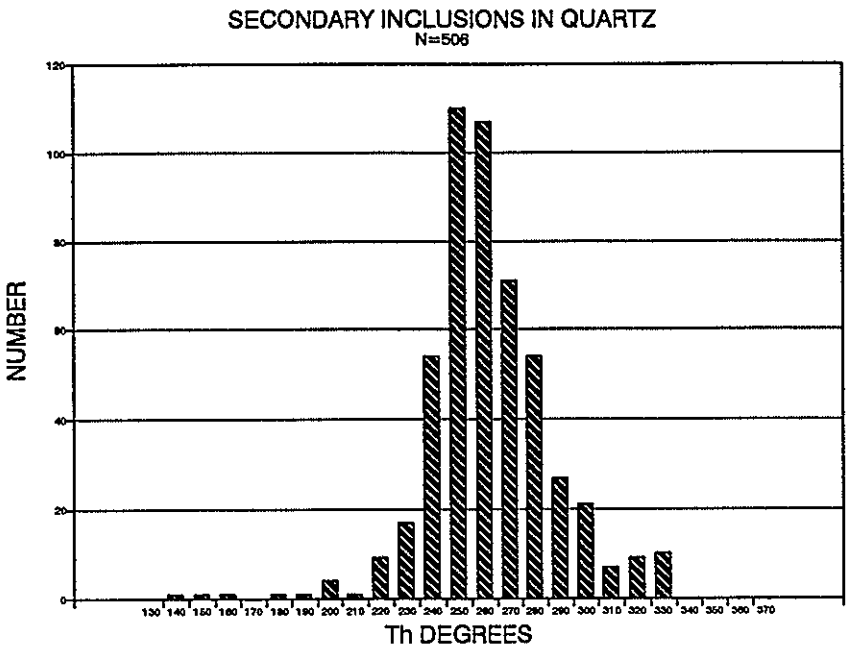

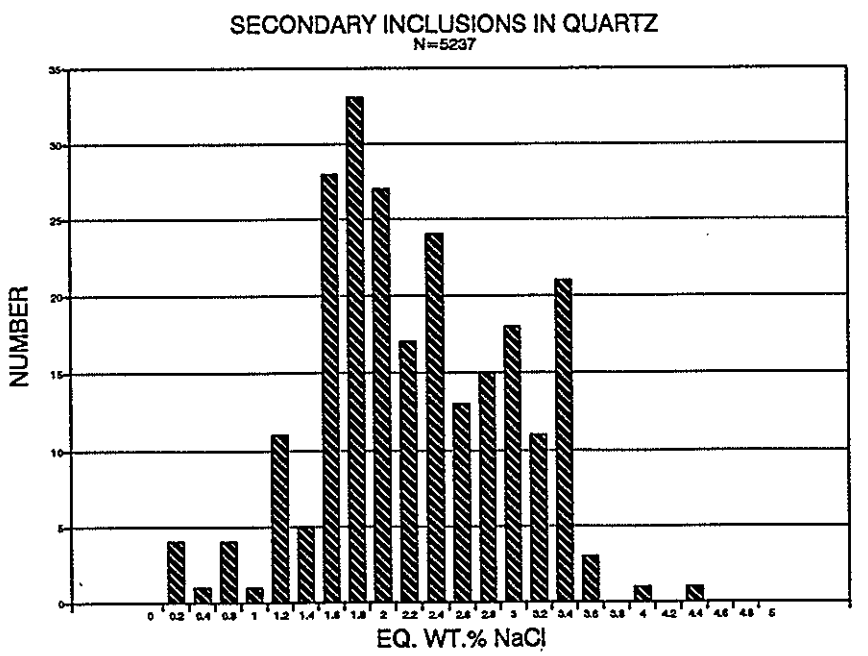

Plot of all secondary inclusion data from all quartz samples.

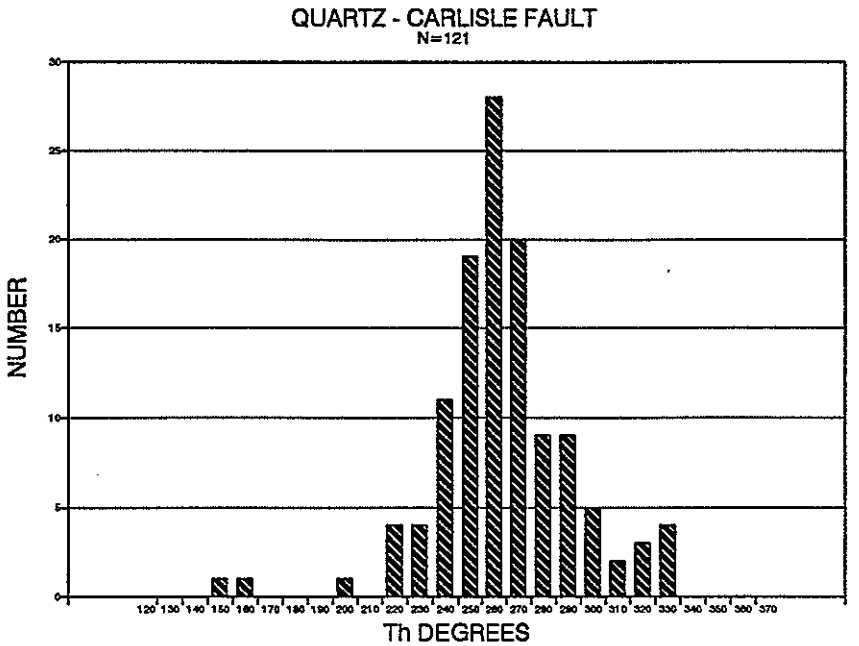

Base metals vein.

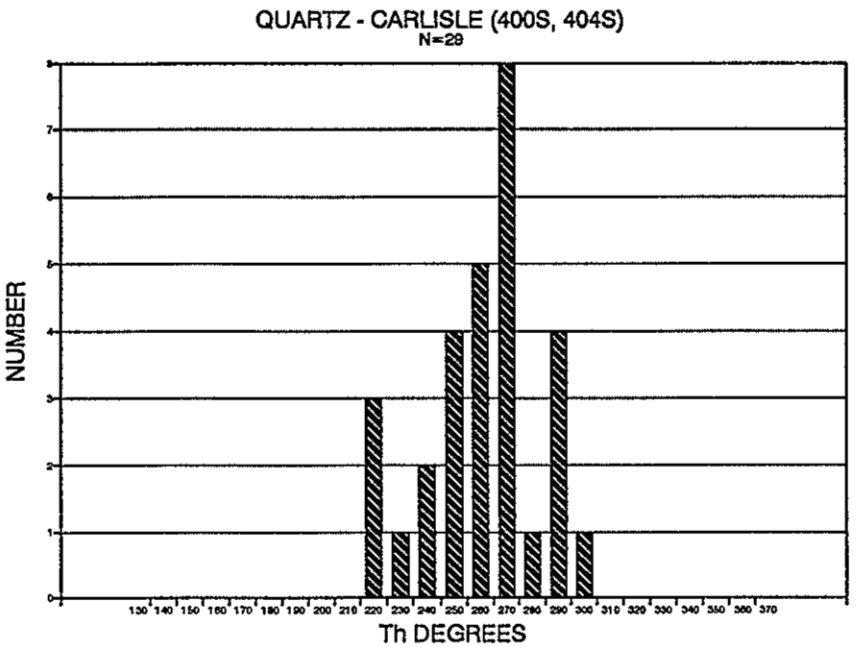

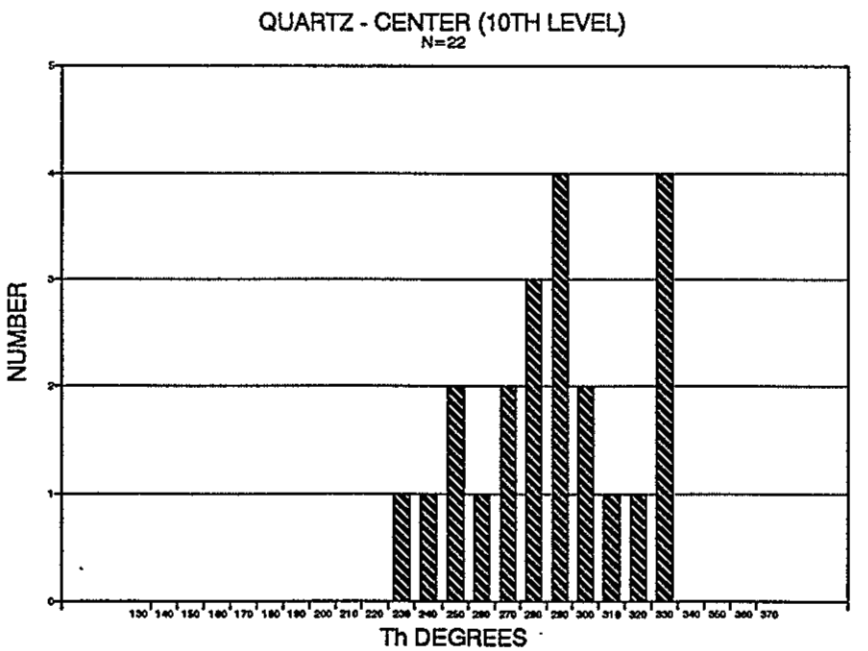

Base metals veins.

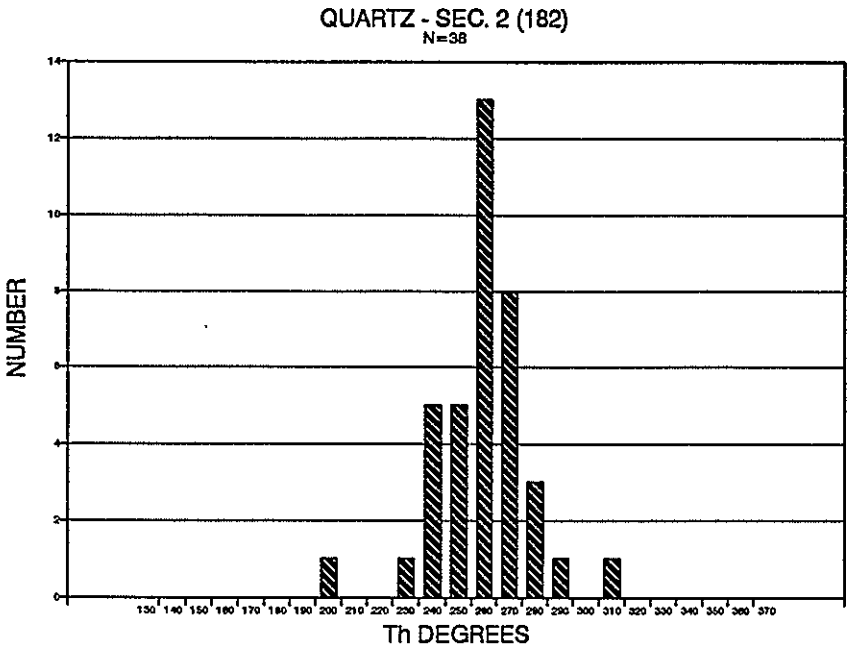

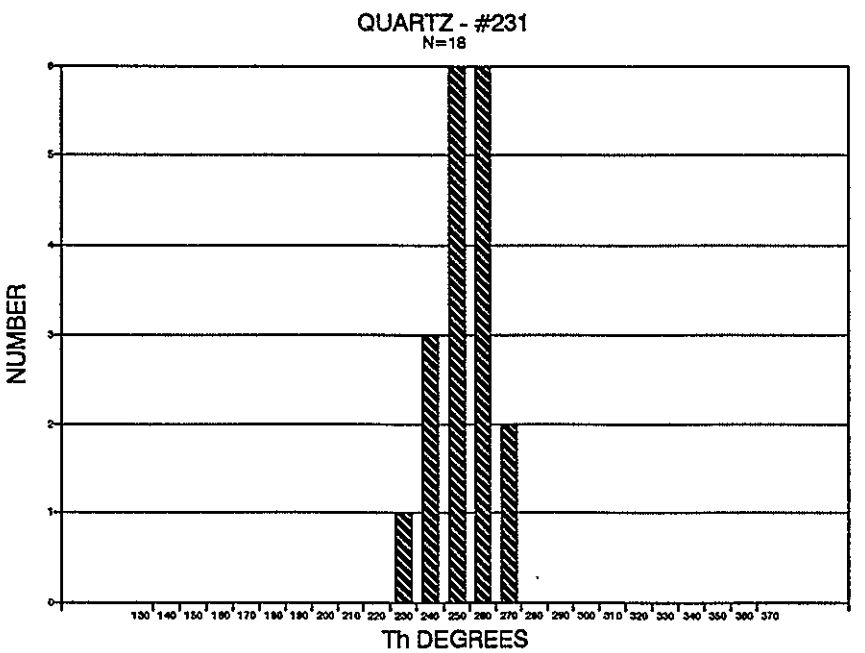

Base metals veins.

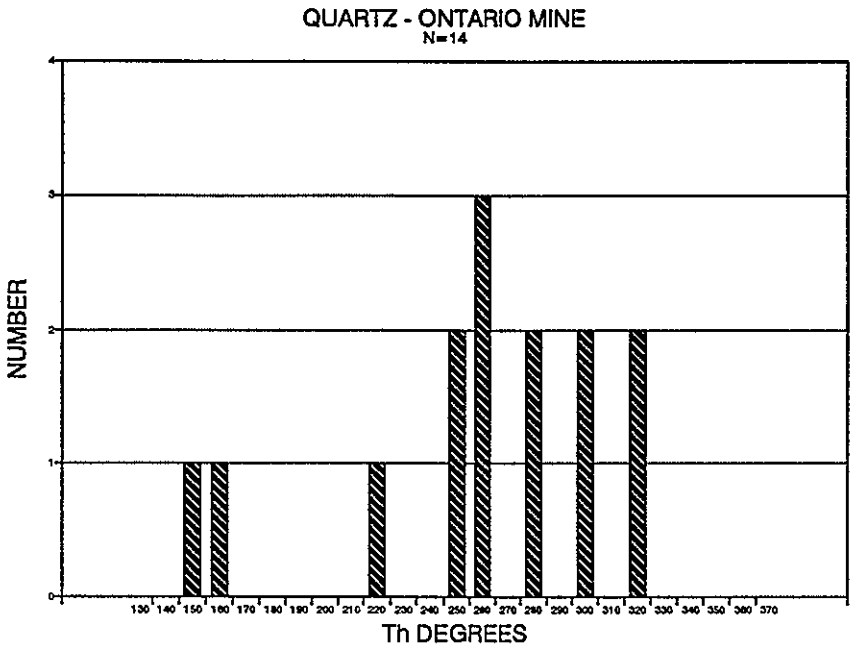

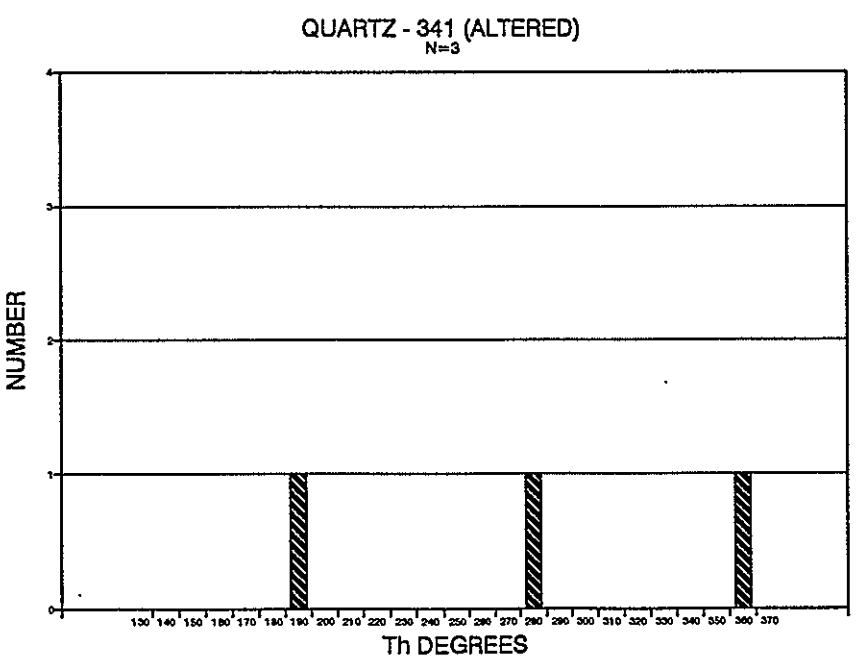

Base metals veins.

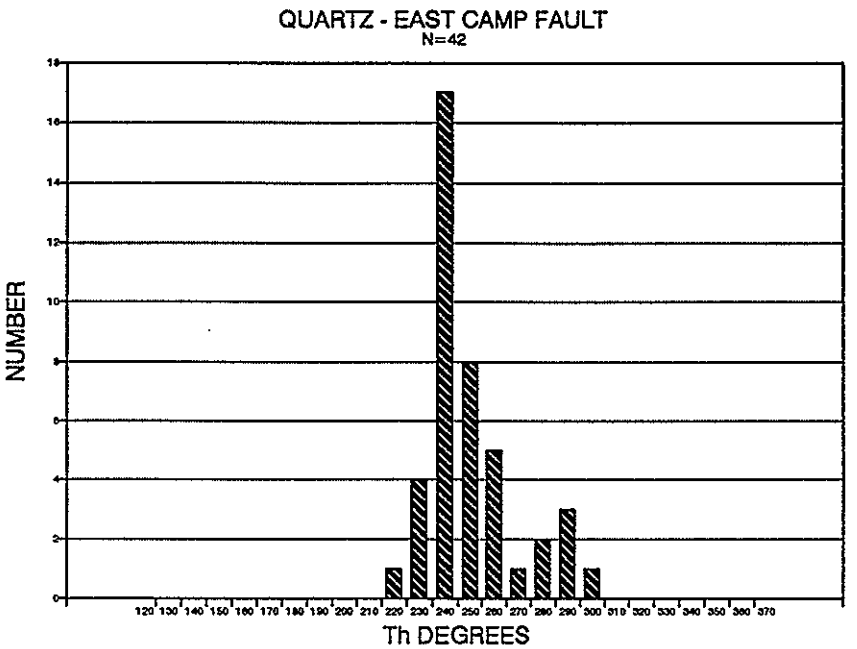

Gold-silver veins.

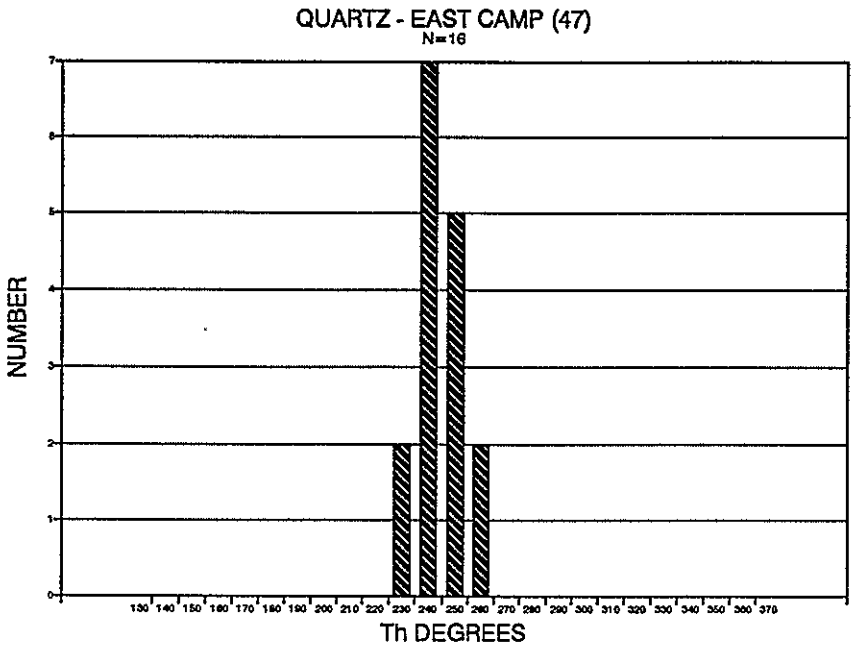
QUARTZ - EAST CAMP (47)
N=16
NUMBER
Th DEGREES

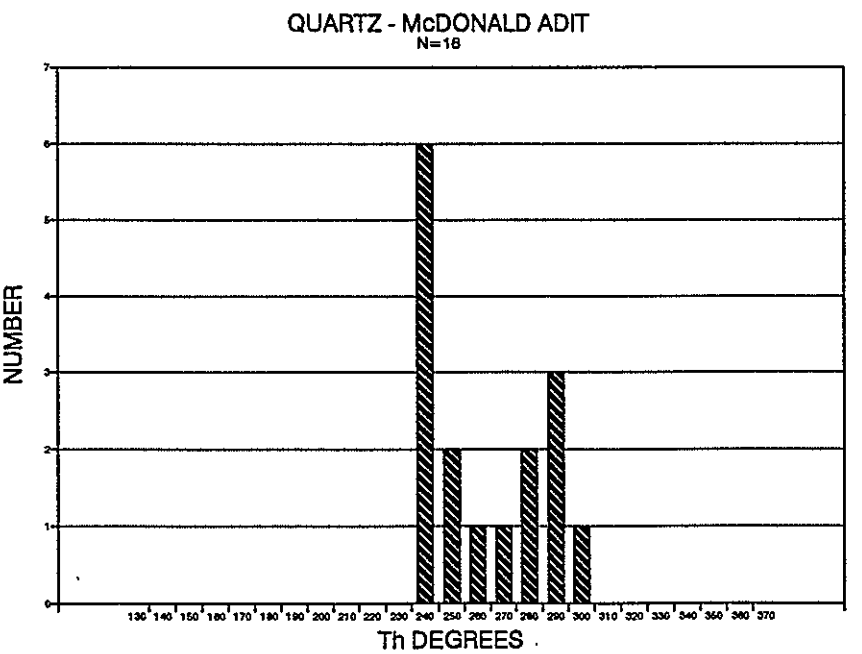
QUARTZ - McDONALD ADIT
N=18
NUMBER
Th DEGREES

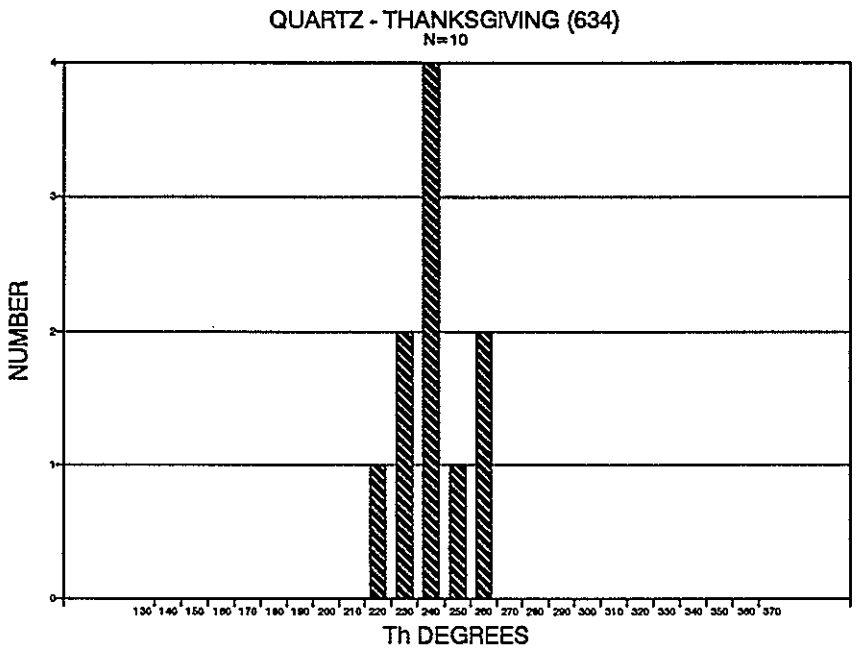

Gold-silver veins.

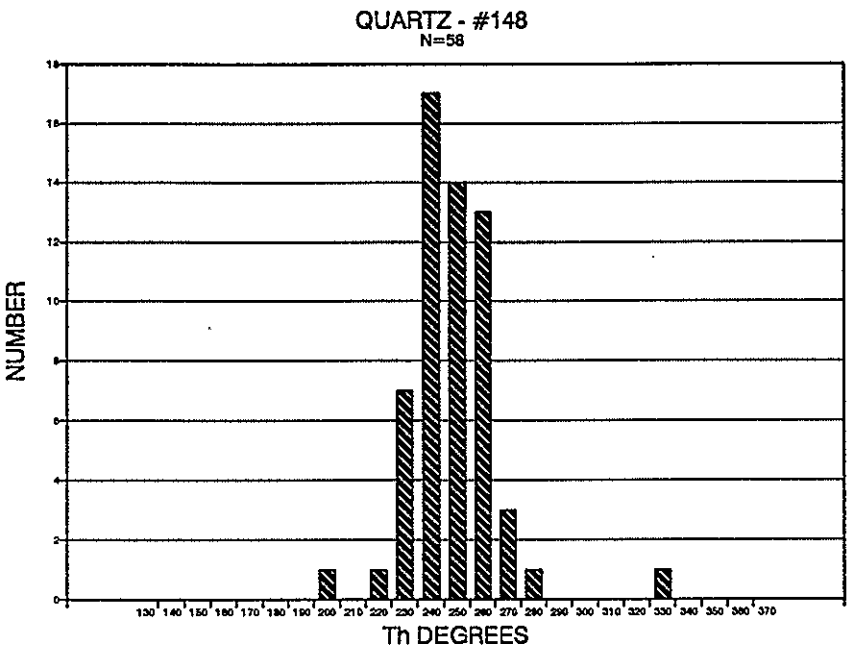

Gold- silver veins.

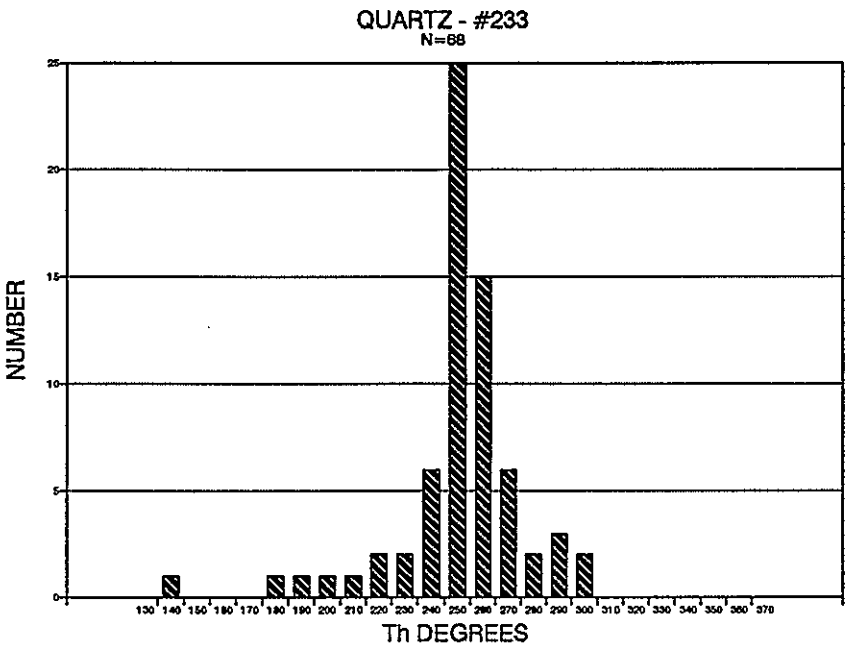

Gold-silver veins.

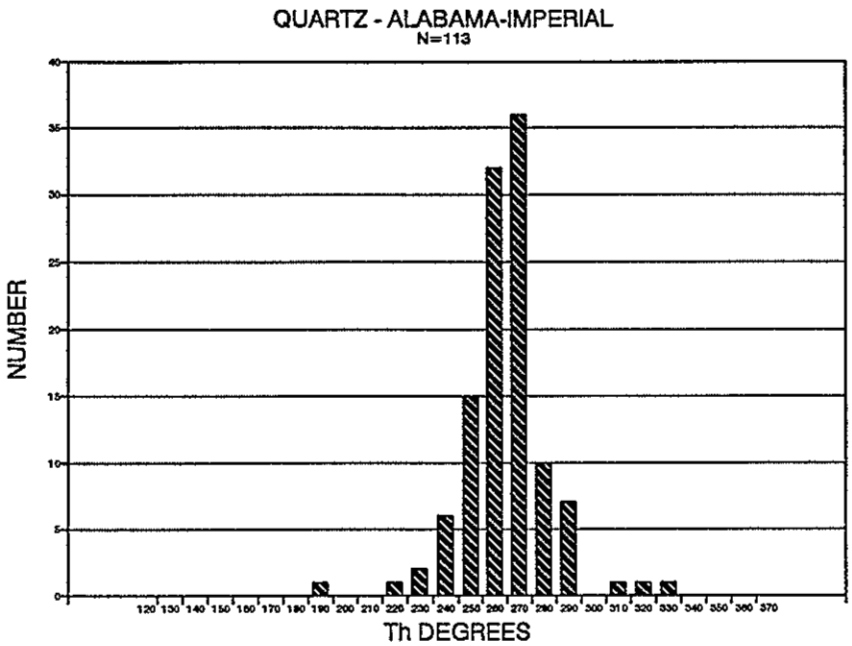

Gold-silver veins.

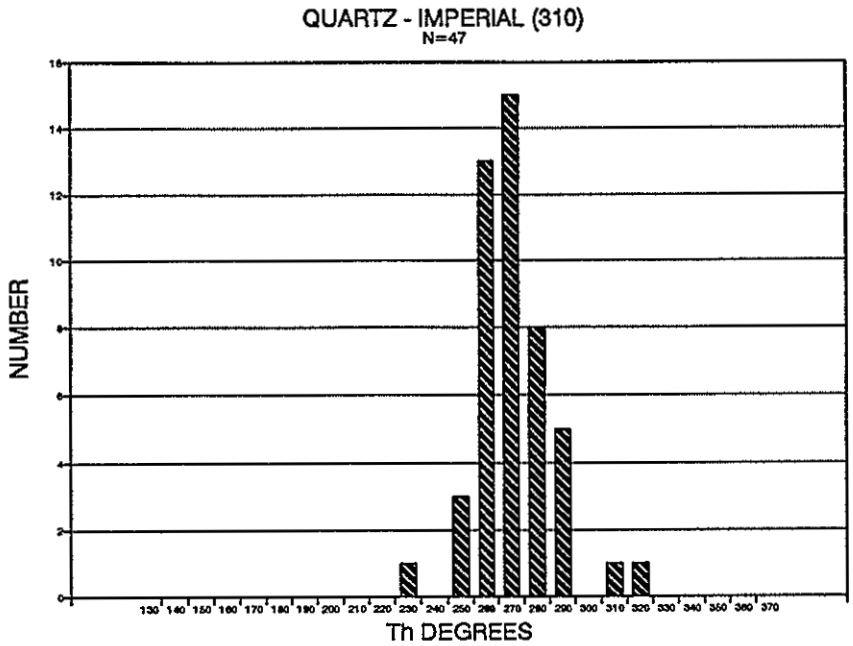

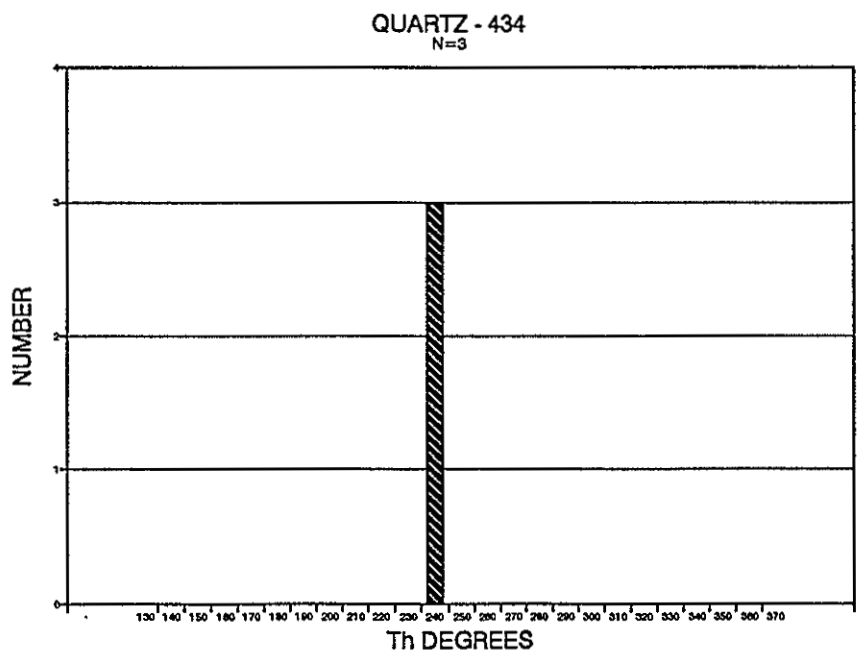

Gold- silver veins.

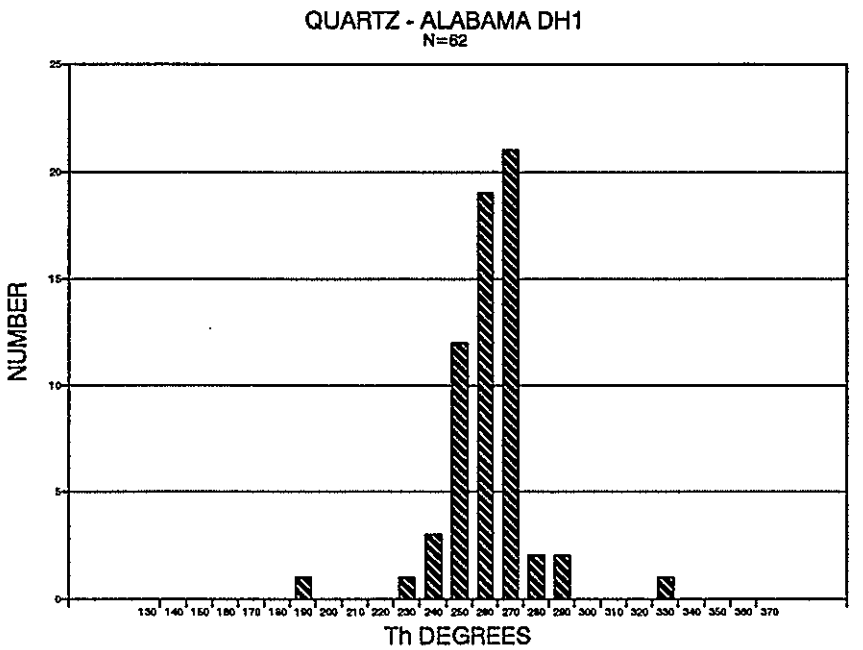

Gold-silver veins.

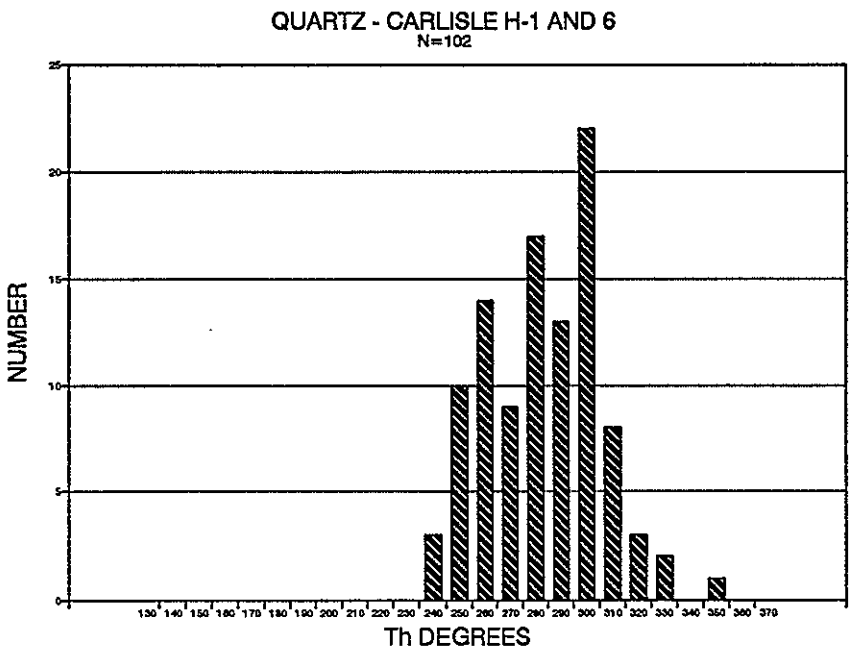

Base metals veins.

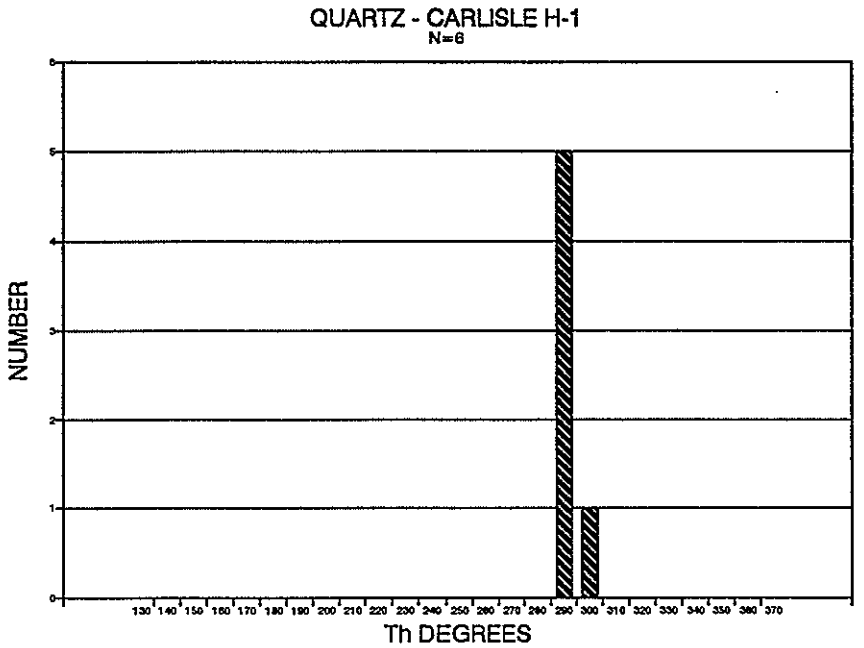

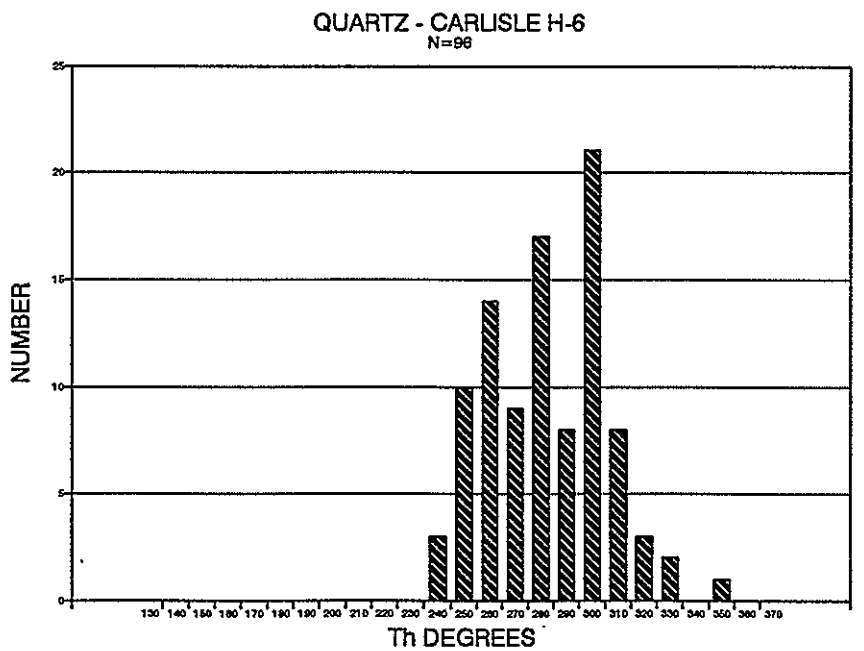

Base metals veins.

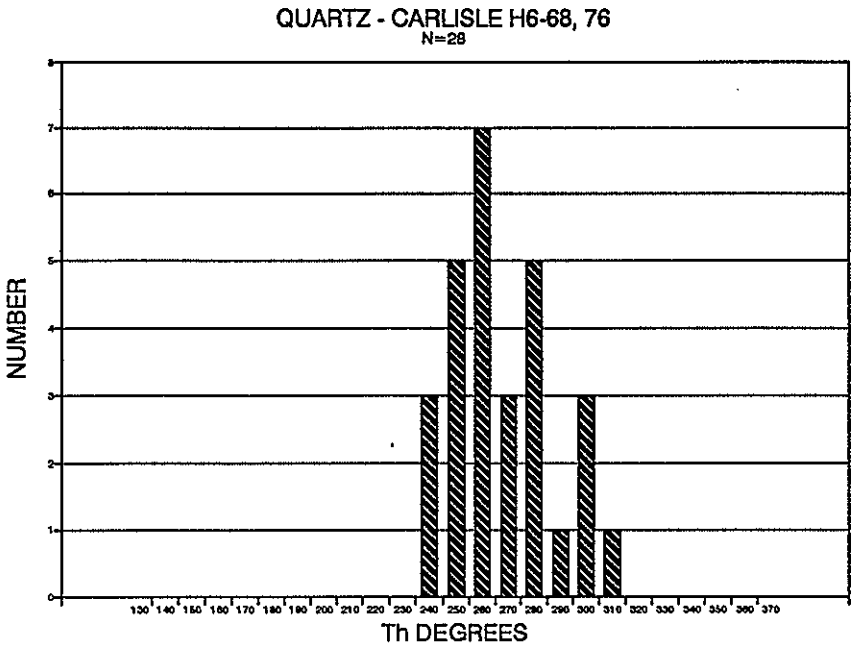

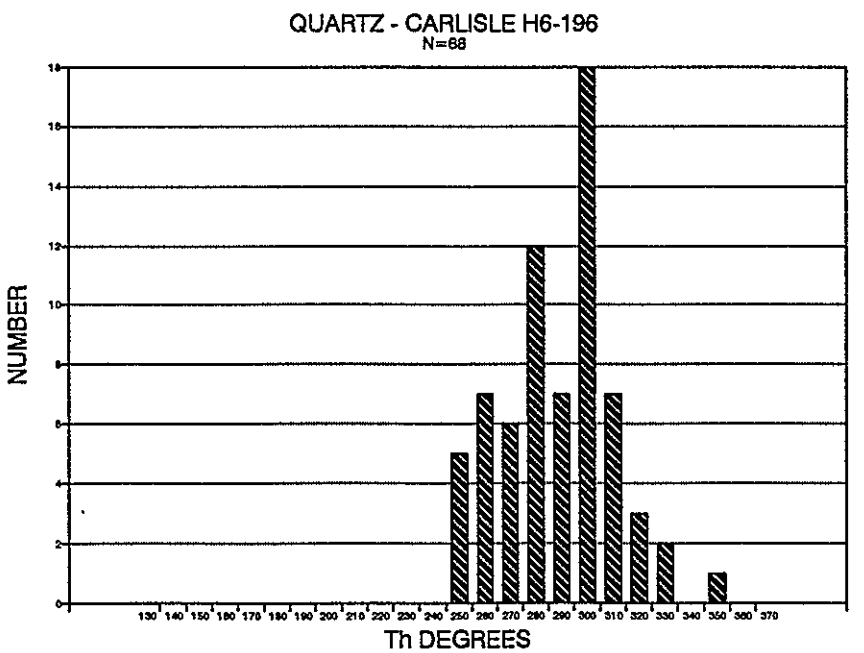

Base metals veins.

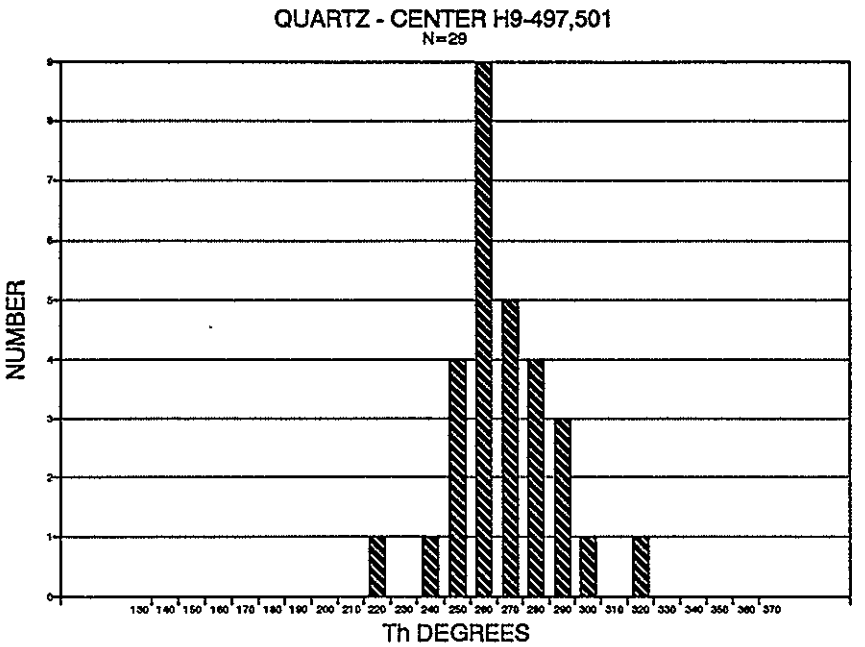

Base metals veins.

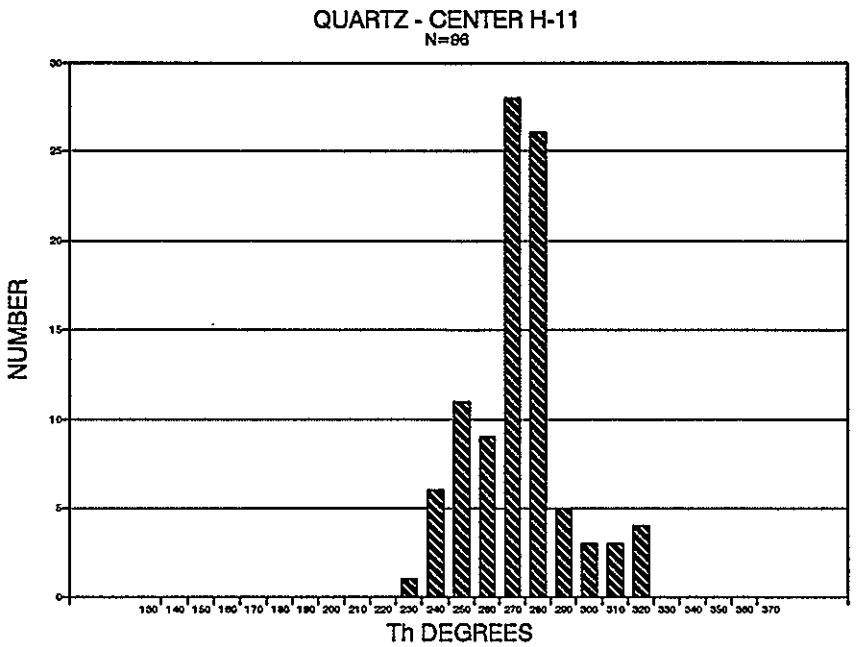

Base metals veins.

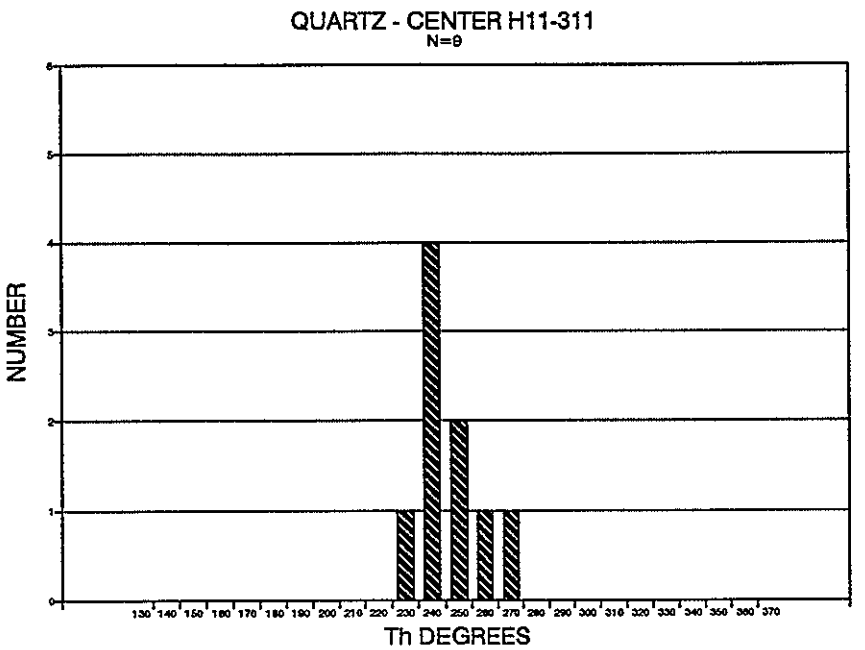

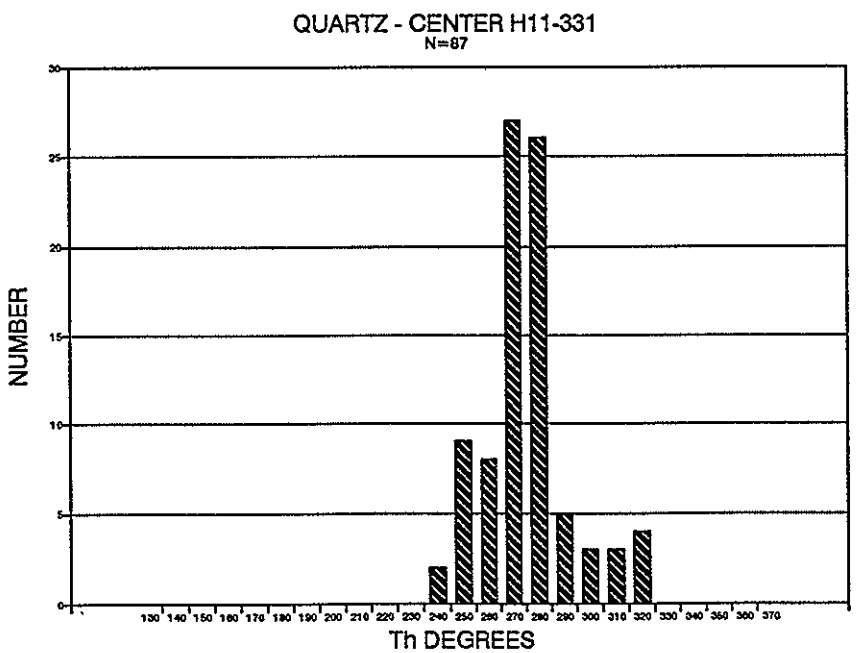

Base metals veins.

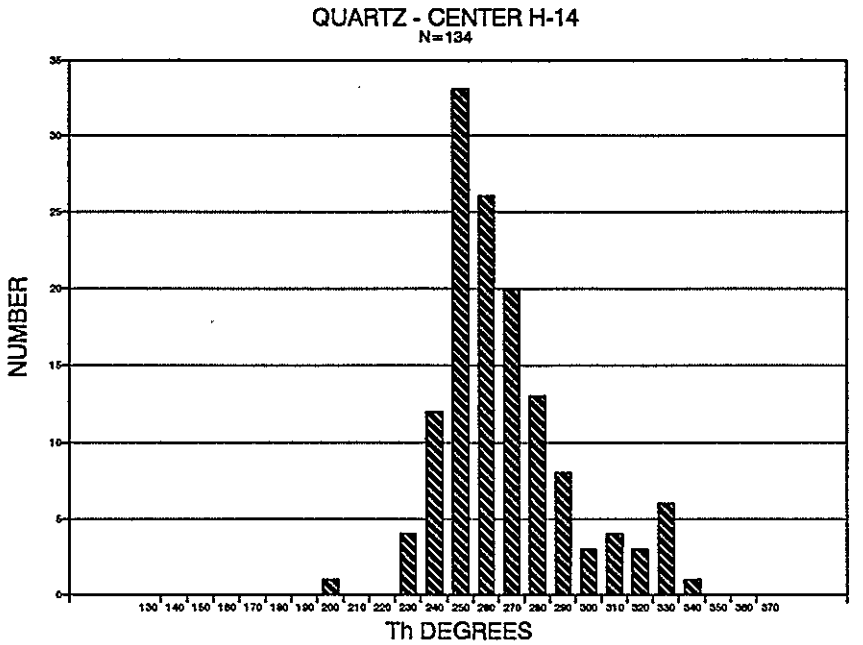

Base metals veins.

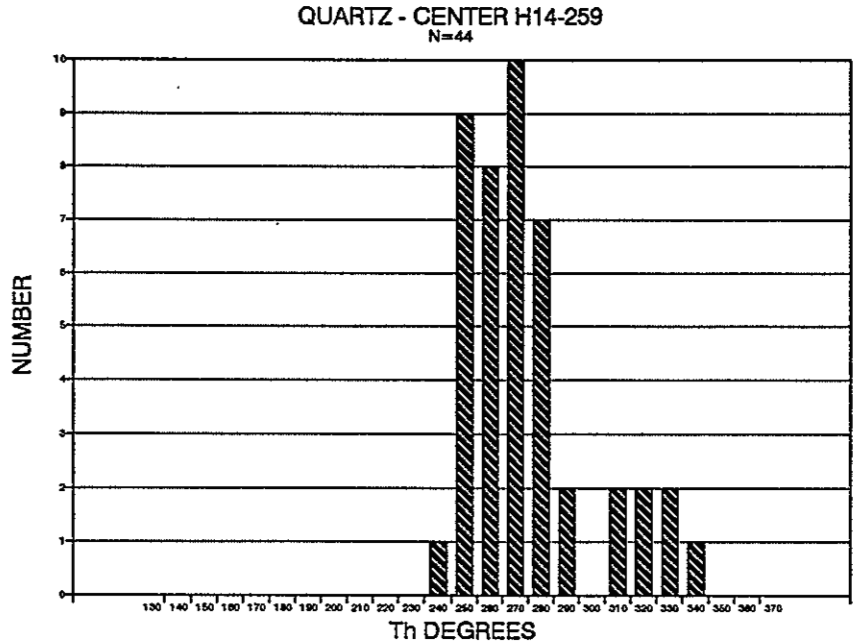

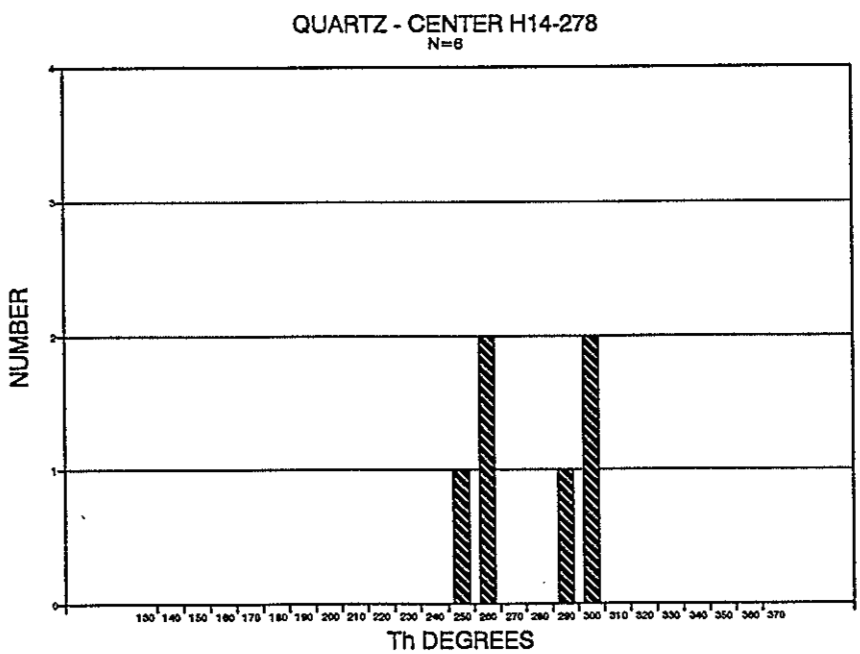

Base metals veins.

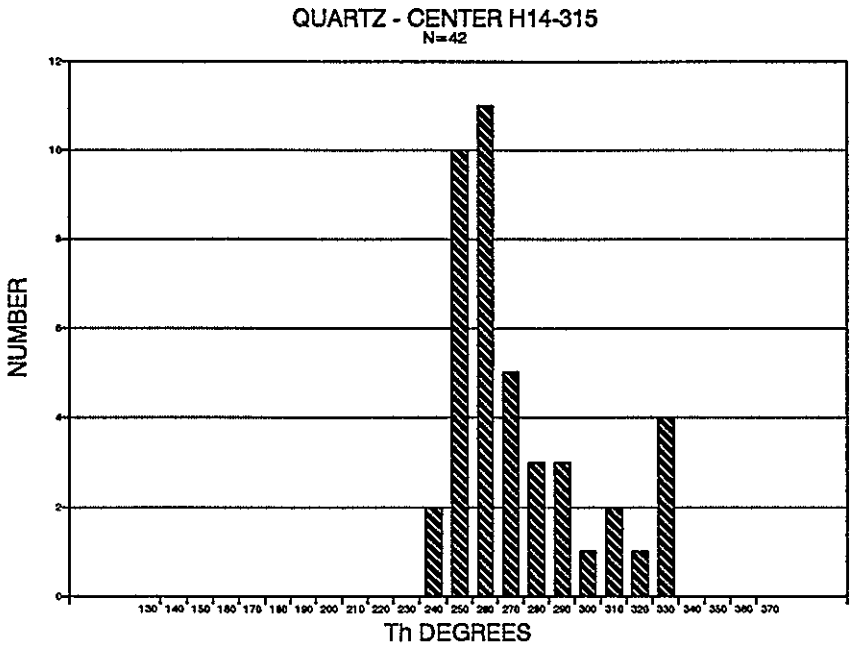

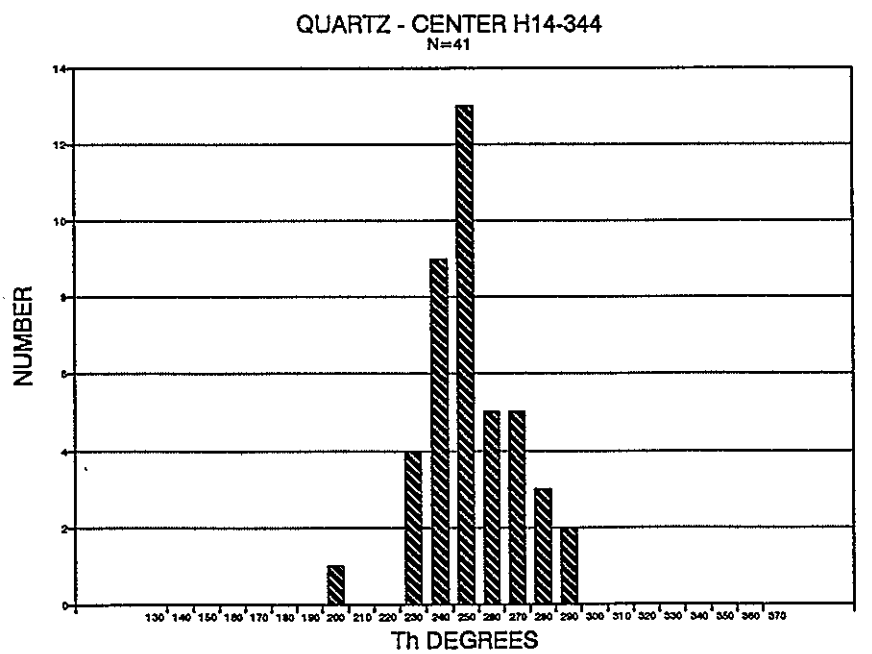

Base metals veins.

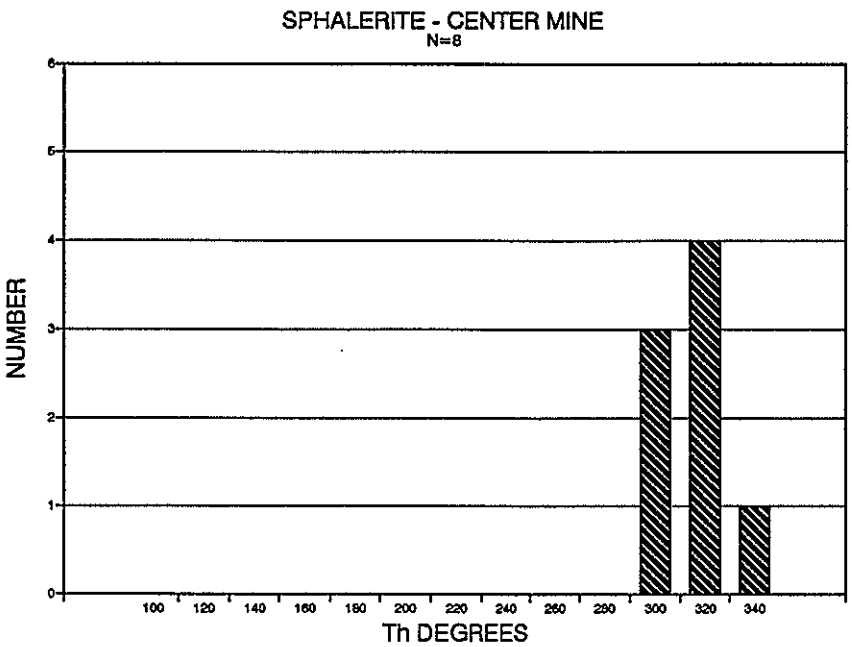

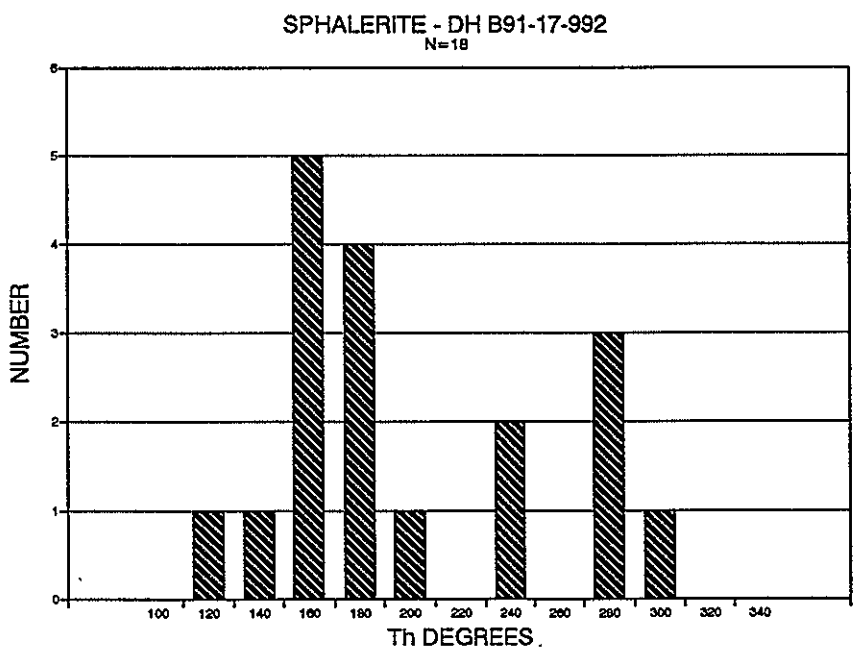

Base metals veins.

PRIMARY INCLUSIONS IN FLUORITE

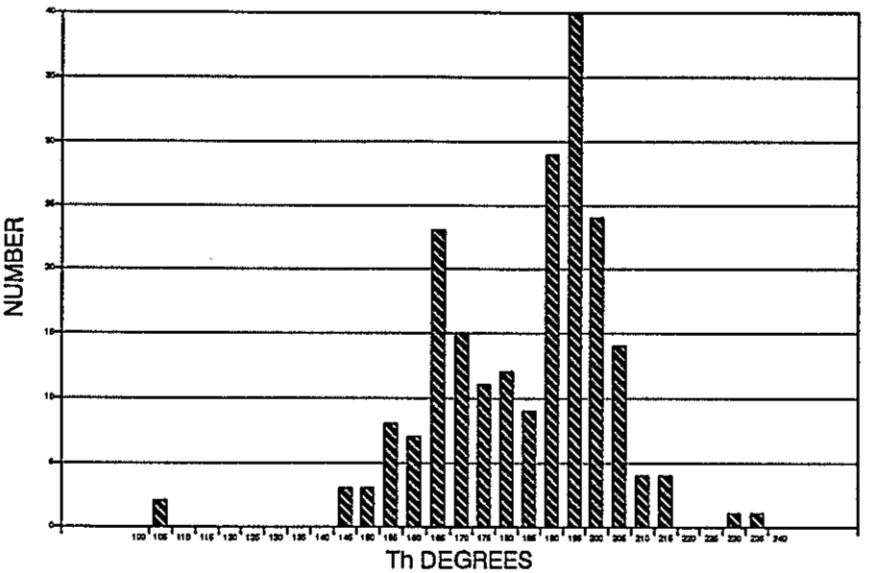

PRIMARY INCLUSIONS IN FLUORITE
N=141

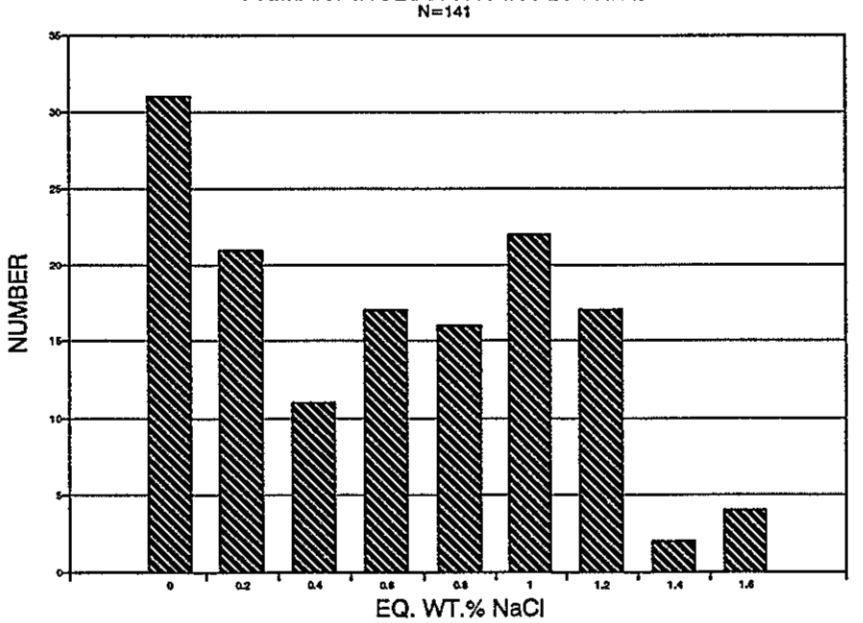

Plot of all primary inclusion data from all fluorite samples.

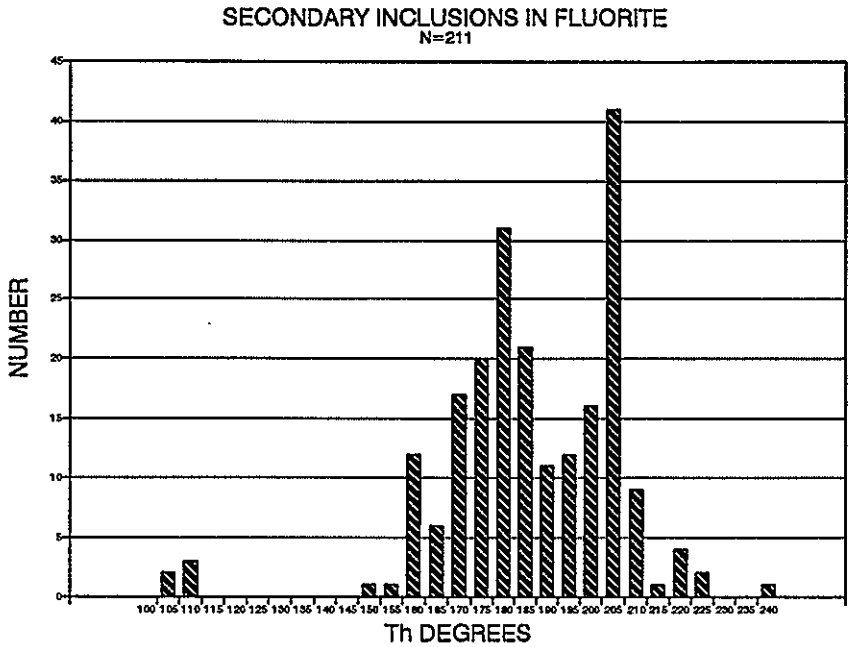

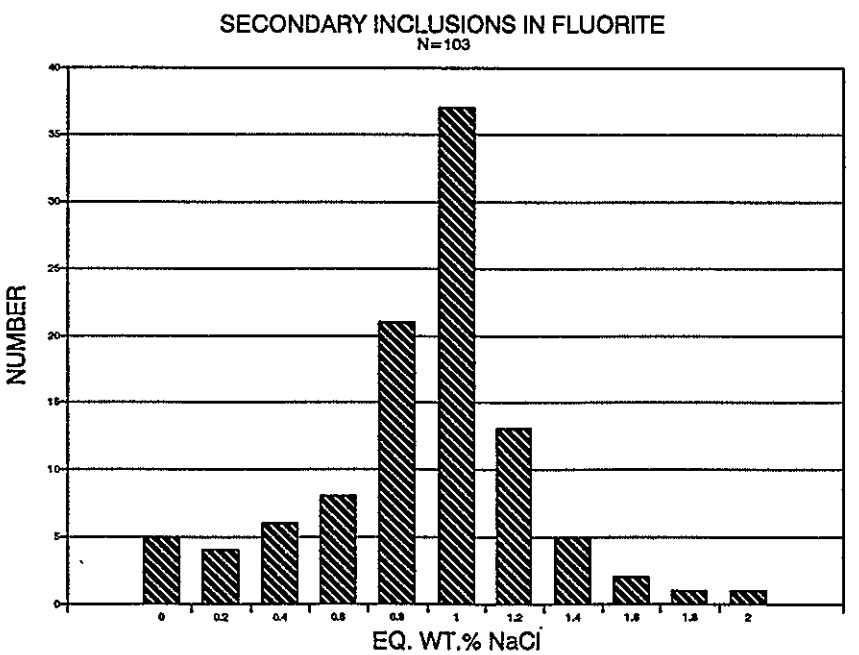

Plot of all secondary inclusion data from all fluorite samples.

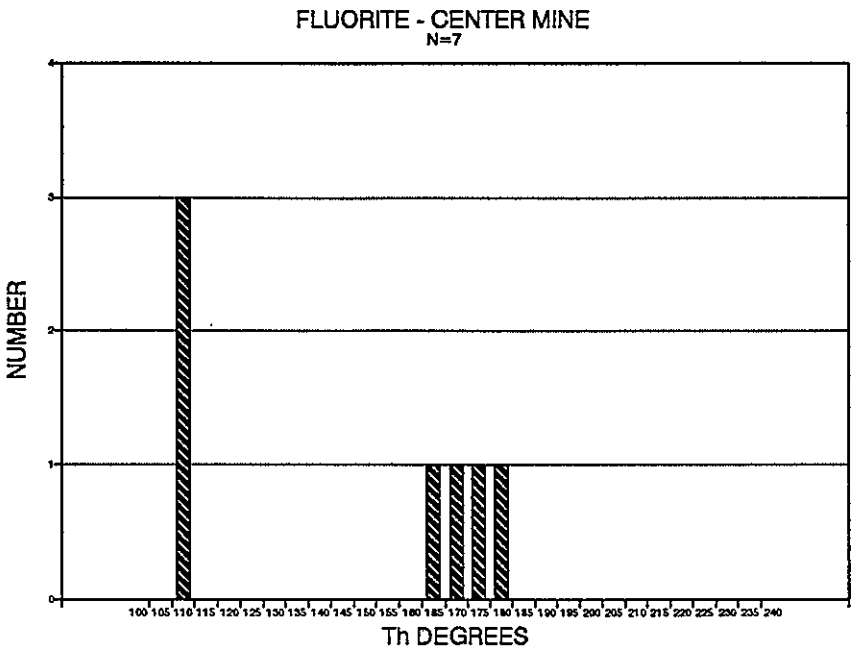

Base metals veins.

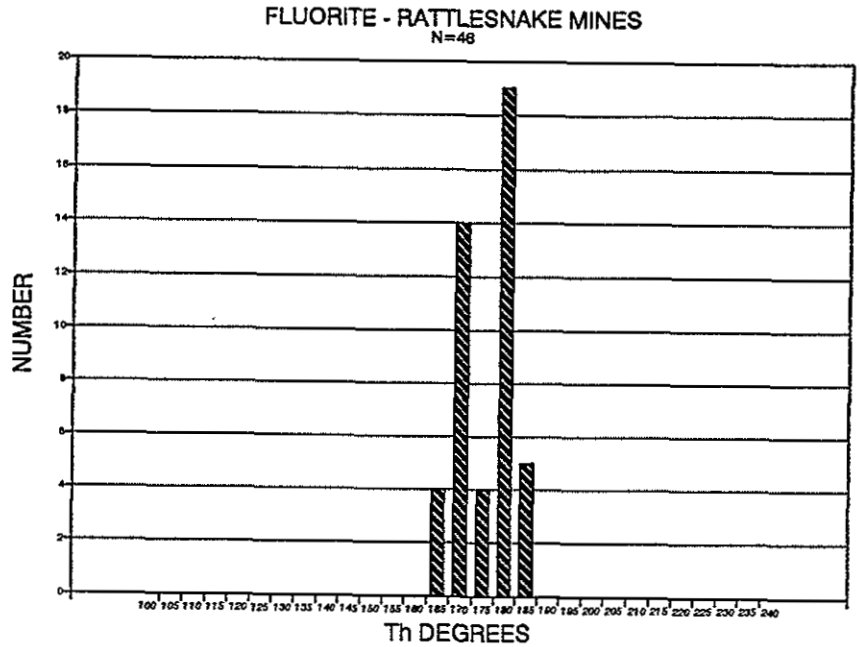
FLUORITE - RATTLESNAKE MINES
N=48
NUMBER
Th DEGREES

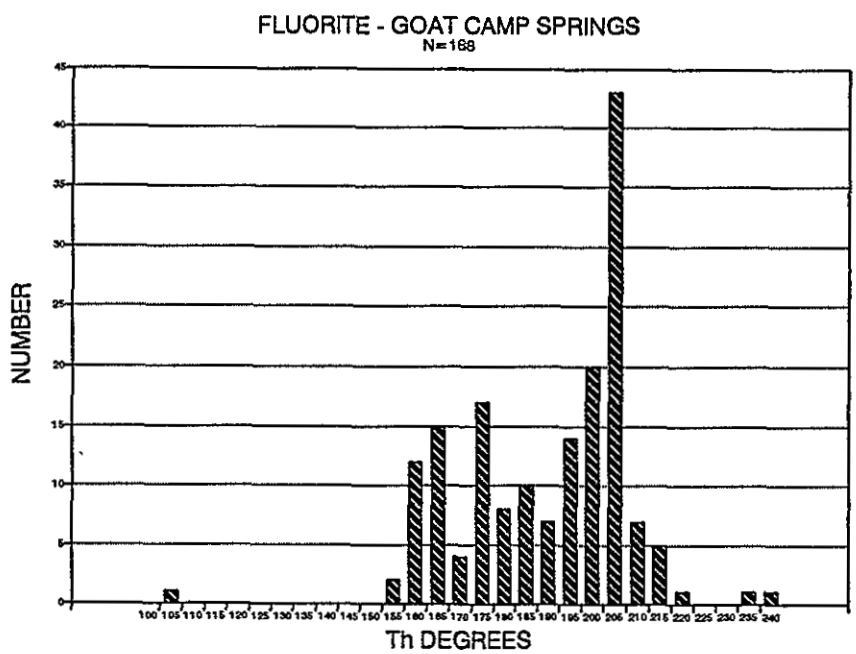
FLUORITE - GOAT CAMP SPRINGS
N=168
NUMBER
Th DEGREES

FLUORITE - LUCKIE MINES
N=21

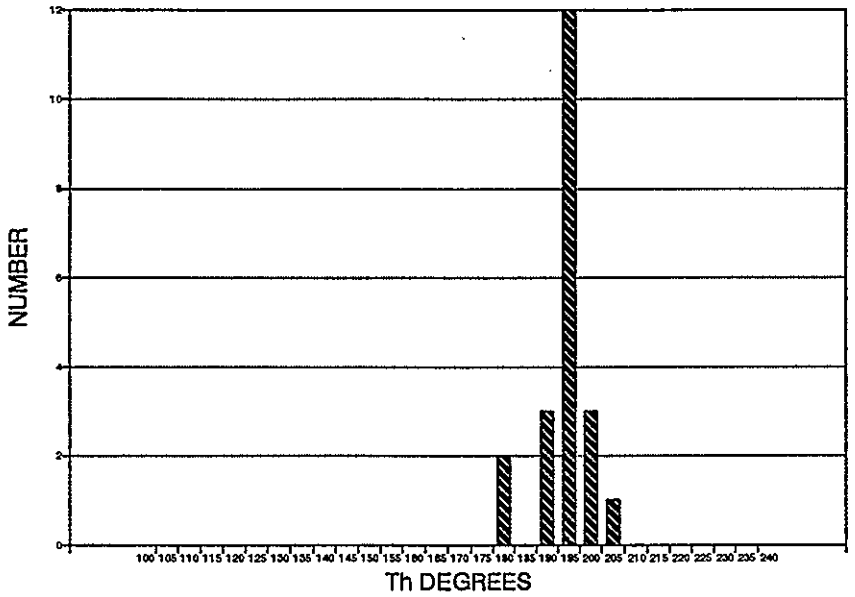

FLUORITE - FORBIS MINES
N=29

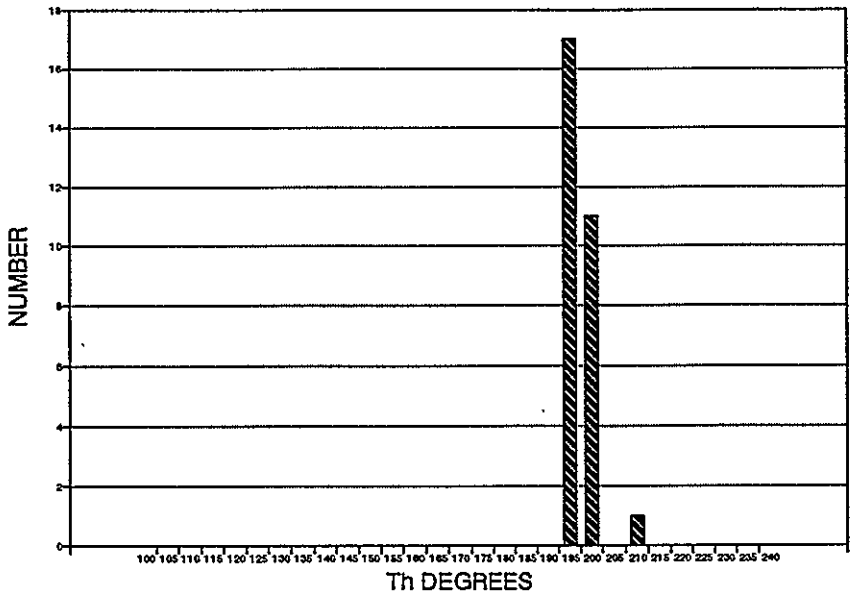

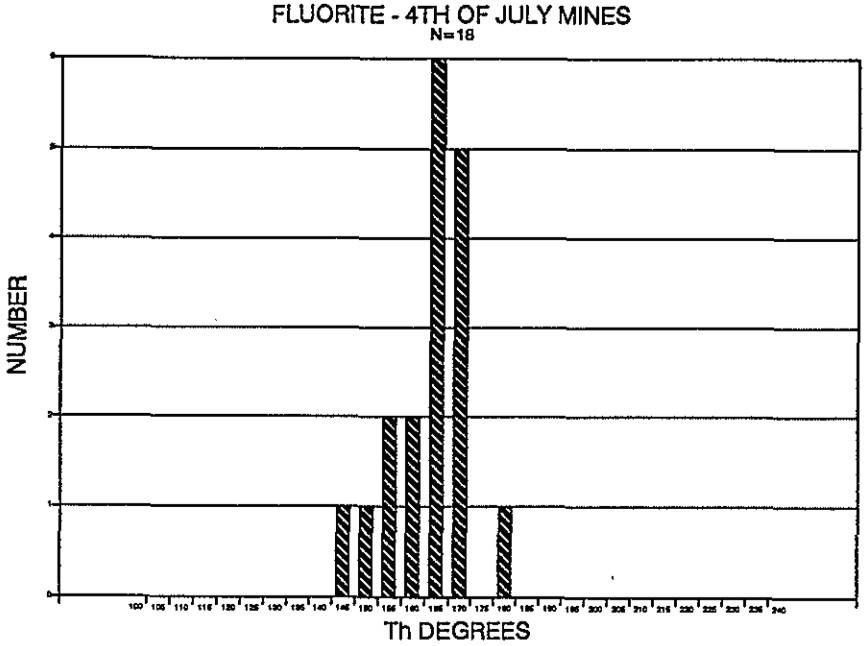
FLUORITE - 4TH OF JULY MINES
N=18
NUMBER
Th DEGREES

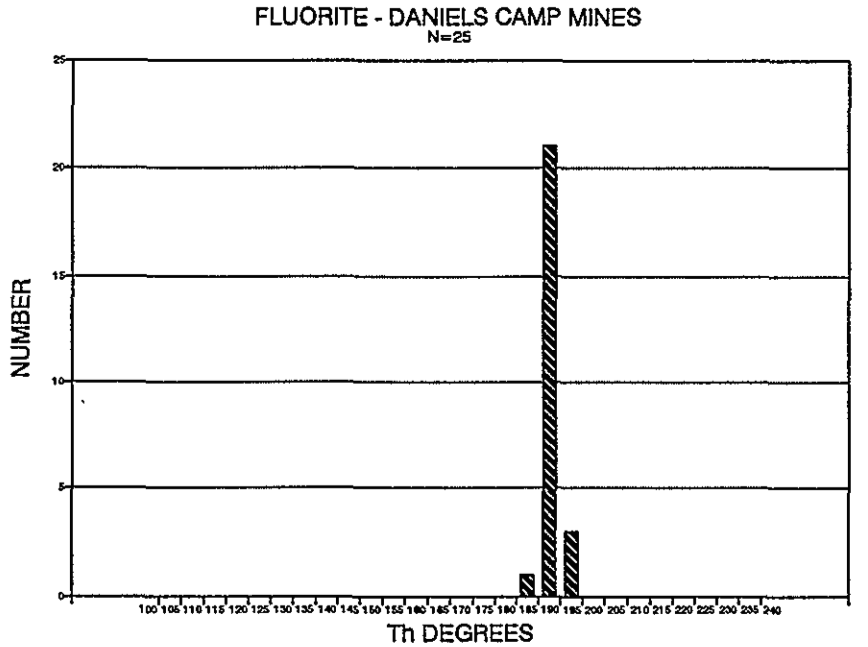
FLUORITE - DANIELS CAMP MINES
N=25
NUMBER
Th DEGREES

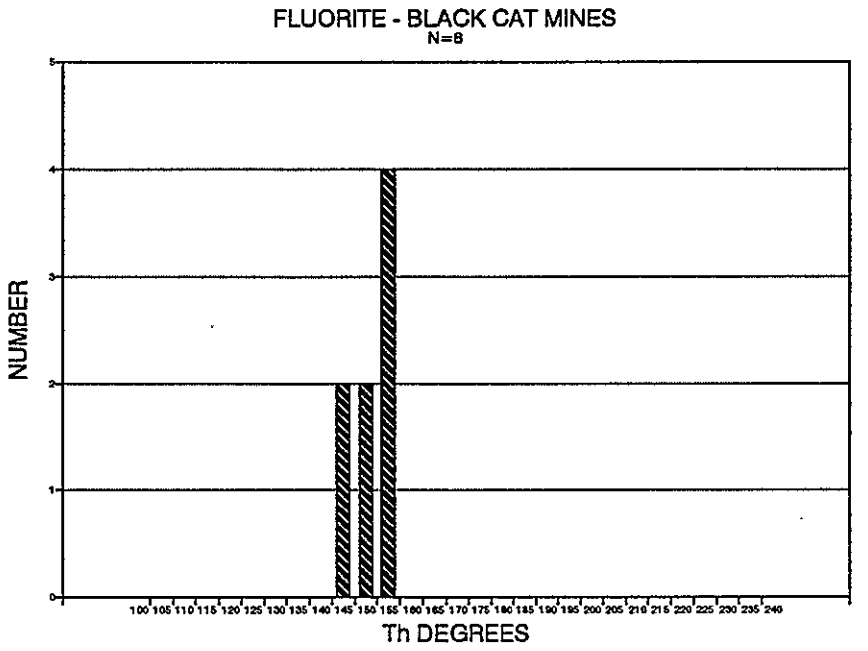
FLUORITE - BLACK CAT MINES
N=8
NUMBER
Th DEGREES

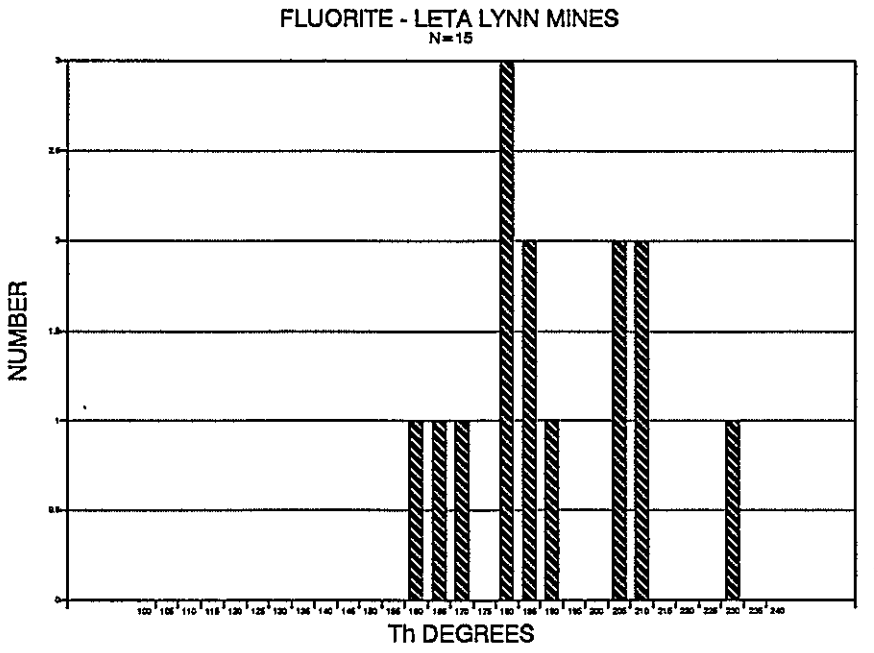
FLUORITE - LETA LYNN MINES
N=15
NUMBER
Th DEGREES

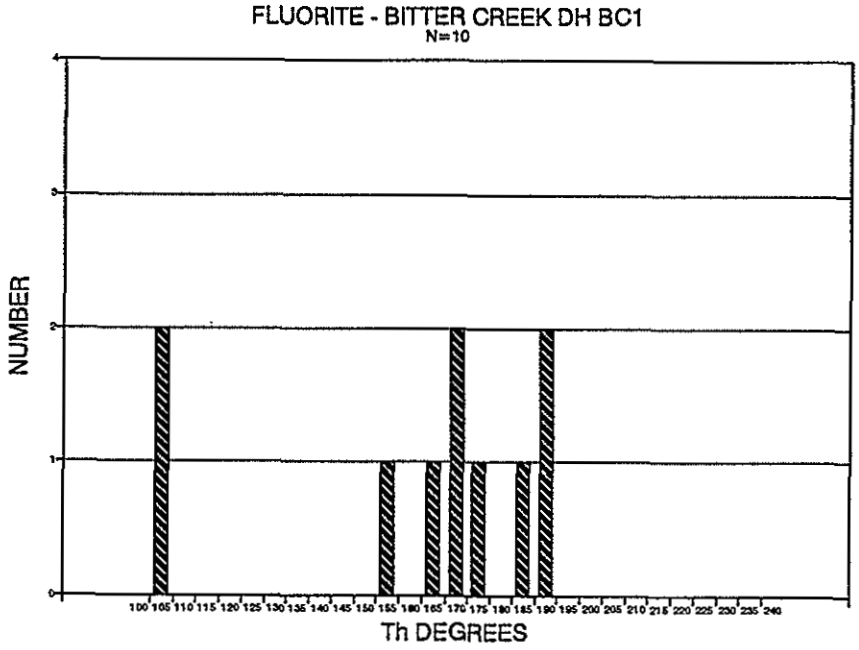

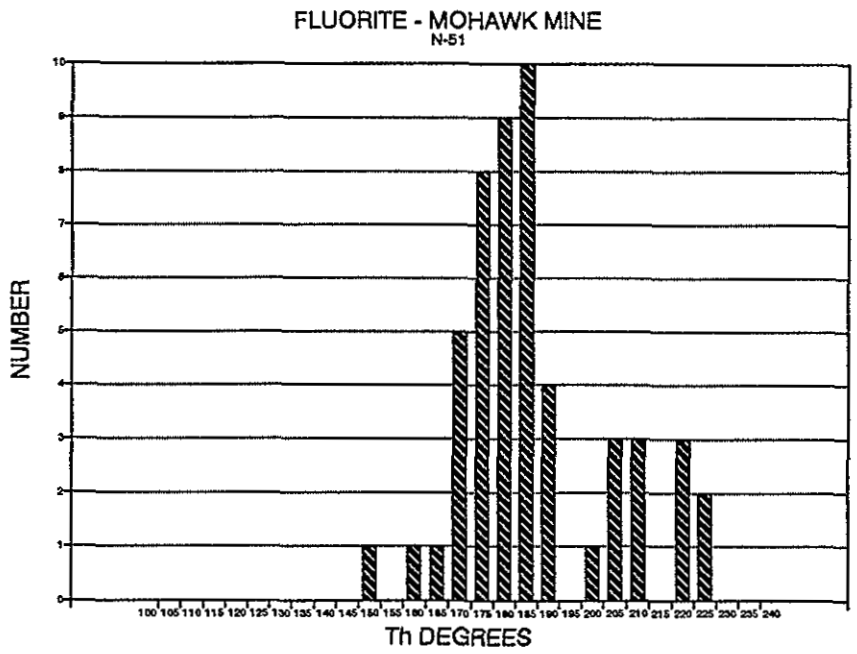

Gold-silver veins.

14. *CURRICULUM VITAE*

Virginia T. McLemore (maiden name Hill) was born on June 11, 1955, in Baltimore, Maryland. She graduated from Woodlawn Senior High School, Baltimore, MD in June 1973 and entered New Mexico Institute of Mining and Technology (NMIMT), Socorro, NM, in the fall, 1973. She worked as an exploration petroleum geologist with Natural Gas Pipeline Co. of America from June 1975 to September 1975. She married James V. McLemore on May 29, 1976. After graduating from NMIMT with a B.S. in Geology and a B.S. in Geophysics in May 1977, she was an assistant field geologist (uranium exploration) for Urangesellscheft, USA, Inc. from May 1977 to September 1977. In the fall, 1977, she entered graduate school at NMIMT. Daughter Jennifer G. McLemore was born September 17, 1978. Virginia graduated from NMIMT with a M.S. in Geology in May 1980 and her M.S. thesis was entitled Geology of the Precambrian rocks of the Lemitar Mountains, Socorro County, New Mexico. In June 1980 she became a Uranium Geologist for the New Mexico Bureau of Mines and Mineral Resources (NMBMMR), where she is currently employed as an Economic Geologist. On December 9, 1980, daughter Christine E. McLemore was born. Since employment with NMBMMR, she has written numerous articles on the geology of New Mexico and contributed to several books. In August 1988 she attended the Penrose Conference on Anorthosites in Laramie, WY. She is a member of several societies including AIME-SME (Society for Mining, Metallurgy, and Exploration), SEG (Society of Economic Geologists), AEG (Association of Exploration Geochemists), GSA (Geological Society of America), and NMGS (New Mexico Geological Society). She is serving on and has served on numerous committees, chaired sessions at local and national conferences, and chaired or assisted with local and national field conferences. In January 1990, she entered the Graduate School at the University of Texas at El Paso.

Permanent address: 701 Caine, Socorro, NM 87801.

This dissertation was typed by Lynne Hemenway.

MAP 1

R32E R21W

APACHE BOX

T6S T7S T16S T17S

32° 52' 30"

32° 50'

109°2'30"

109°00'

NOAH MESA

TWIN PEAKS

COPPER BASIN

COMMERCE-MAYFLOWER FAULT

WAMPOO WASH

CROOKSON FAULT

CROOKSON PEAK

UNMAPPED

TWIN PEAKS FAULT

BITTER CREEK SHEAR ZONE

SADDLEBACK MOUNTAIN

MOHAWK

NORMANDY RIDGE

BILLALI FAULT

BANK SHEAR ZONE

JUNIPER PEAK

SUMMIT MOUNTAINS

SUMMIT PEAK

EAST CAMP SUMMIT FAULT

RAEBURN HILLS

BLUE BELL FAULT

WILLOW CREEK

IRON CANYON

FOOTHILLS FAULT

DANIELS CAMP CREEK

TELEPHONE RIDGE

CARLISLE FAULT

LAURA CANYON

VANDERBILT PEAK

ROCKY TOP RIDGE

APACHE FAULT

GUADALUPE CANYON

GUADALUPE FAULT

NEW YEARS GIFT FAULT

ALABAMA FAULT

GOAT CAMP SPRINGS

CHARLIE HILL FAULT

PINON MOUNTAIN

NEW SEEP WINDMILL

BO HEXT WINDMILL

MT. ROYAL WINDMILL

STEEPLE ROCK

OLD MAN HEXT WINDMILL

IMPERIAL FAULT

ARIZONA NEW MEXICO

AZ NM

LOCATION

MN 11-1/2°

1/2 0 MILE

0.5 0 KILOMETER

SCALE 1:24,000

CONTOUR INTERVAL 20 or 40 FEET

R21W R20W

MAPPED BY V.T. McLEMORE (1990-1992). PORTIONS OF THIS MAP ARE MODIFIED FROM GRIGGS AND WAGNER (1966), BIGGERSTAFF (1976), AND HEDLUND (1991a,c, 1992).

MAP 1 OUTCROP GEOLOGIC MAP OF THE STEEPLE ROCK MINING DISTRICT, GRANT COUNTY, NEW MEXICO AND GREENLEE COUNTY, ARIZONA

VIRGINIA T. McLEMORE

1993

MAP 2

MAP 2 – GEOLOGIC MAP, STRUCTURE, AND MINES AND PROSPECTS, STEEPLE ROCK MINING DISTRICT, GRANT COUNTY, NEW MEXICO AND GREENLEE COUNTY, ARIZONA

VIRGINIA T. McLEMORE

1993

MAPPED BY V.T. McLEMORE (1990-1992). PORTIONS OF THIS MAP ARE MODIFIED FROM GRIGGS AND WAGNER (1966), BIGGERSTAFF (1976), AND HEDLUND (1991a,c, 1992).

THIS MAP IS AN INTERPRETATION OF THE OUTCROP GEOLOGIC MAP (MAP I). CHEMICAL ANALYSES ARE IN APPENDICES.

SCALE 1:24,000

CONTOUR INTERVAL 20 or 40 FEET

LOCATION

AZ NM

ARIZONA NEW MEXICO

GRANT CO HIDALGO CO GREENLEE CO

R2W R21W

T6S T7S T16S T17S

32°52'30" 32°50' 109°00'

NM 990 NM 989 NM 513 NM 512

MAP 3 - GEOLOGIC CROSS SECTIONS OF THE STEEPLE ROCK MINING DISTRICT

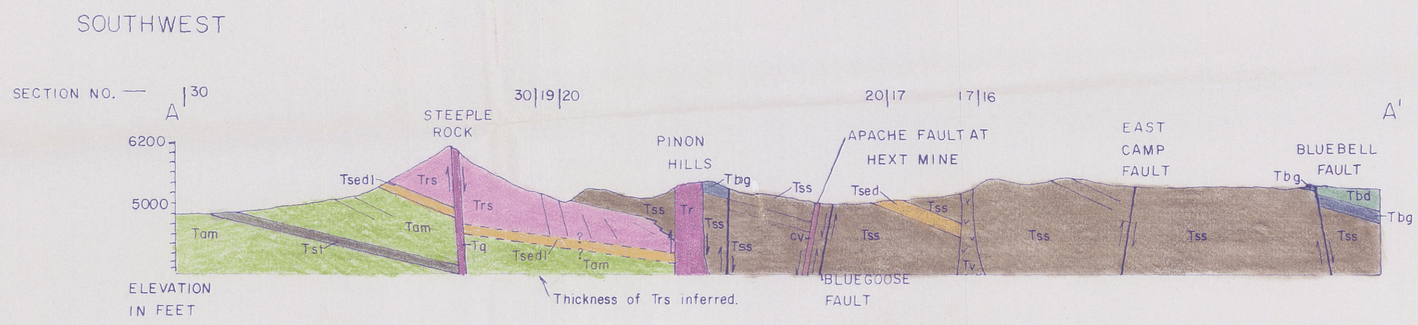

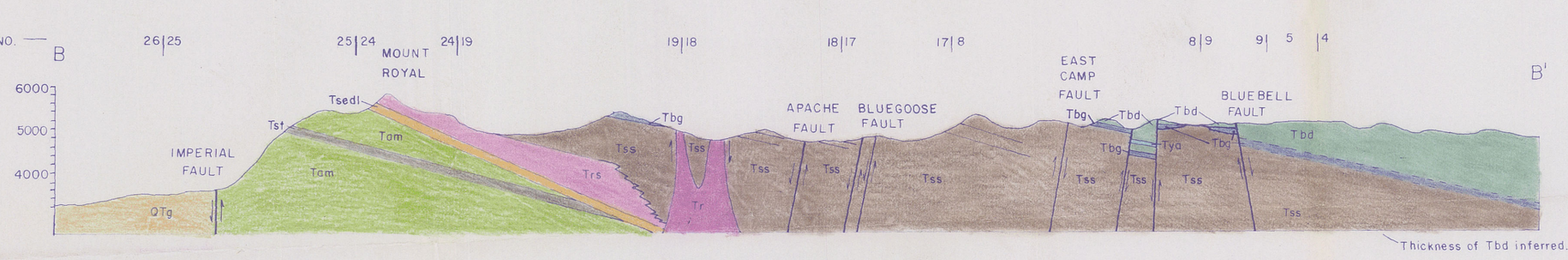

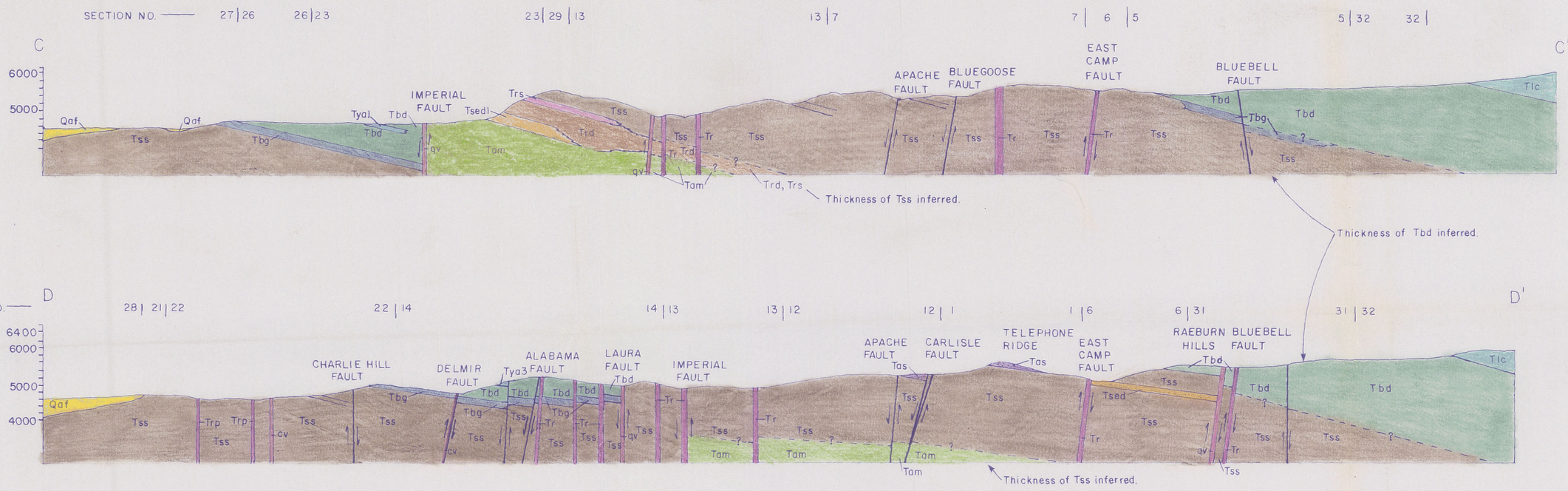

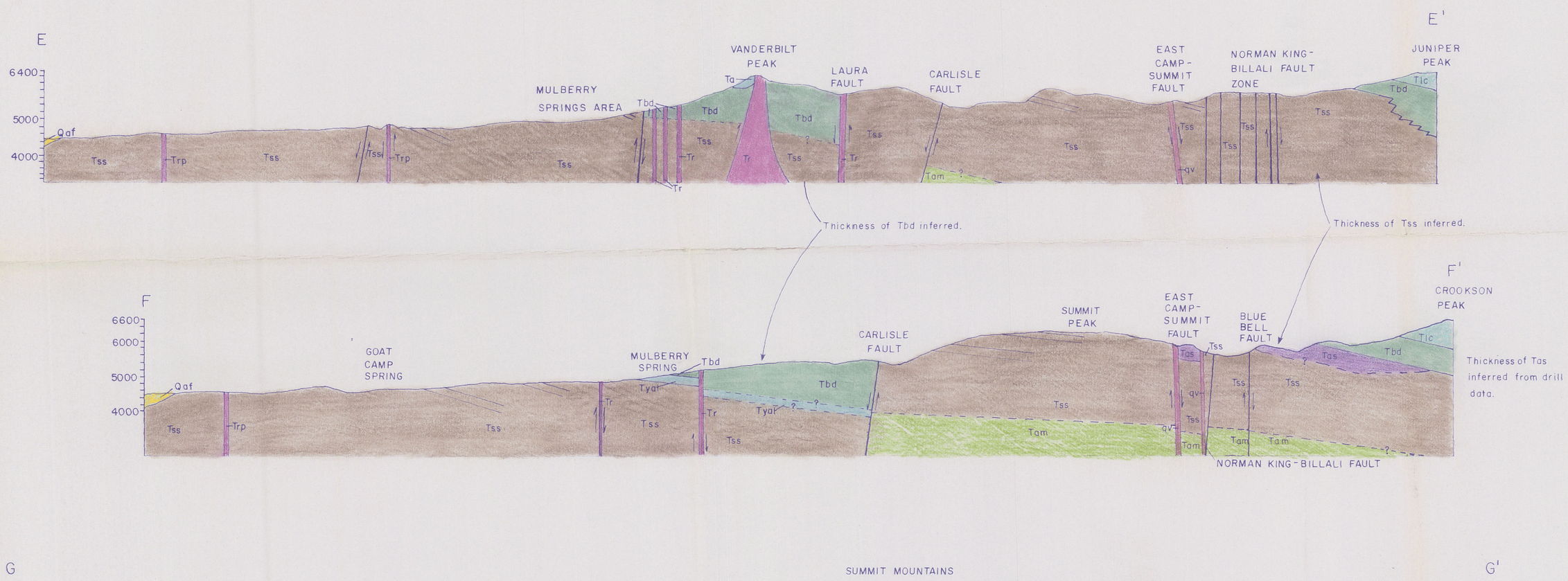

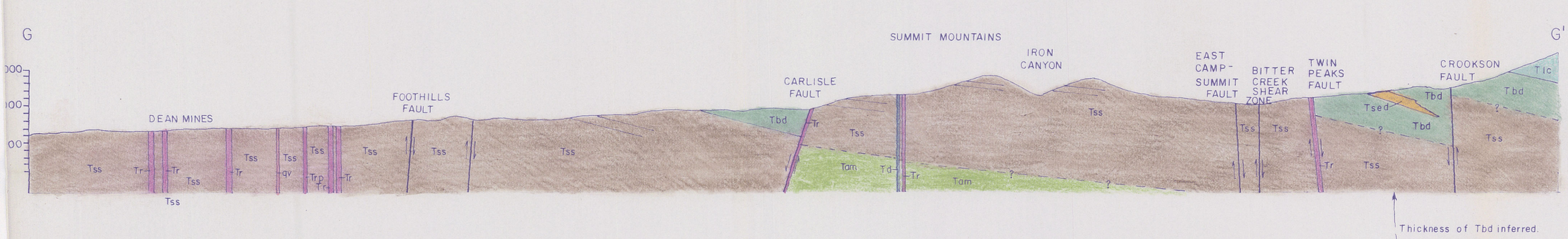

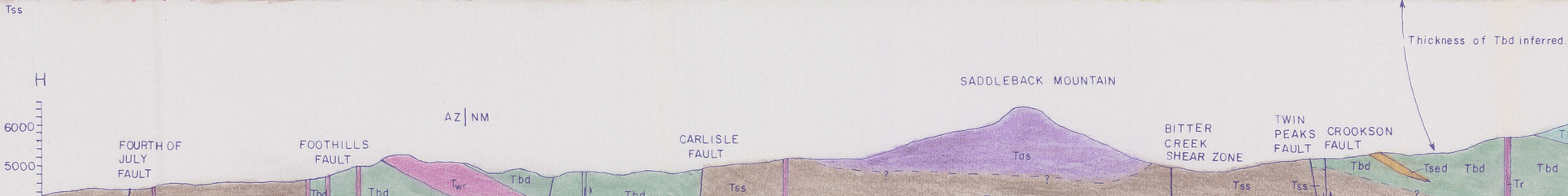

SCALE - HORIZONTAL = VERTICAL
1:24,000
0 1 MILE
0 1 KILOMETER

NOTE: THICKNESS OF SOME UNITS (qv, Tr, Trp, Ta, Tya, Tsed) MAY BE EXAGGERATED LOCALLY.

VIRGINIA T. McLEMORE - 1993

WEST

EAST

CENTER SHAFT (BILL CHUCK CLAIM)

MEXICANA SHAFT

PENNSYLVANIA SHAFT

vein pinched out in back

1st level (140 ft)

Underiser ore shoot

STOPED limits unknown

2nd level (250 ft)

DECLINE TO 2ND LEVEL

NEW 3rd LEVEL

DECLINE TO 3RD LEVEL

-WATER LEVEL-

CENTER FAULT (approximate dip)

BLUEGOOSE FAULT (approximate dip)

STOPED limits unknown

3rd level

sublevel

4th level

5th level

6th level

sump

7th level

8th level

9th level

10th level

END OF 5th LEVEL IN FOOTWALL

-5400

-5300

-5200

-5100

-5000

-4900

BC1 .06/1.35

BC2 no values

BC3 360-374 67/26 546-553 .3/81

BC4 313-315 4/2.7 418-420 3/1.9

BC5 373-377/.61/303 397-400/.58/3.24 403-406/.38/.4

BC6 - no values

BC7 407-408 64/16.6

BC8 338-387 low grade

BC9 459-463/.22/4.73 459-495/.01/.3 Cu- 5%, Pb-2.5%, Zn-3.9% 200 ft below

BC10 643-645 36 oz/ton Ag 200 ft below

BC11 546-576 .01/.94 160 ft below

USBM H11 285.7-289.5 03/.25

USBM H14 316.6-321.1 0.01/.54

PJ 317-320 .03/4.57

LONGITUDINAL SECTION

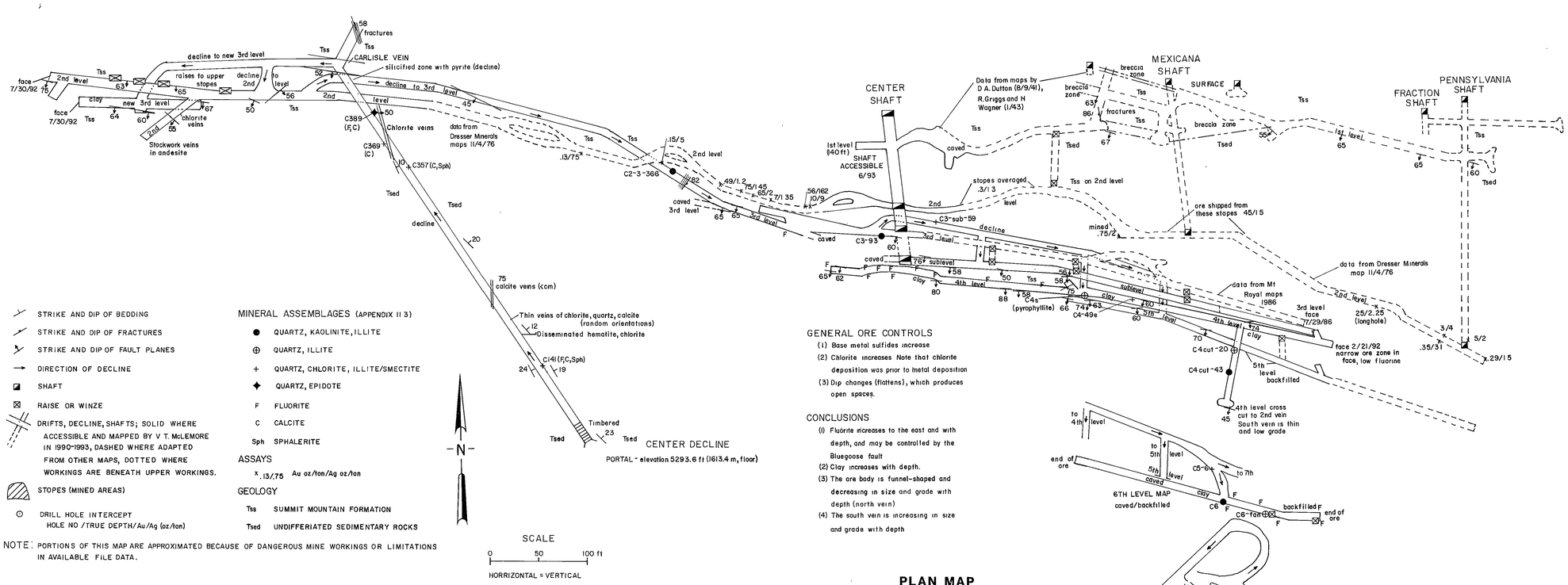

STRIKE AND DIP OF BEDDING

STRIKE AND DIP OF FRACTURES

STRIKE AND DIP OF FAULT PLANES

DIRECTION OF DECLINE

SHAFT

RAISE OR WINZE

DRIFTS, DECLINE, SHAFTS; SOLID WHERE ACCESSIBLE AND MAPPED BY V T. McLEMORE IN 1990-1993, DASHED WHERE ADAPTED FROM OTHER MAPS, DOTTED WHERE WORKINGS ARE BENEATH UPPER WORKINGS.

STOPES (MINED AREAS)

DRILL HOLE INTERCEPT HOLE NO /TRUE DEPTH/Au/Ag (oz/ton)

MINERAL ASSEMBLAGES (APPENDIX II 3)

- ● QUARTZ, KAOLINITE, ILLITE
- ⊕ QUARTZ, ILLITE
- \+ QUARTZ, CHLORITE, ILLITE/SMECTITE
- ✦ QUARTZ, EPIDOTE
- F FLUORITE
- C CALCITE
- Sph SPHALERITE

ASSAYS

x .13/.75 Au oz/ton/Ag oz/ton

GEOLOGY

- Tss SUMMIT MOUNTAIN FORMATION
- Tsed UNDIFFERIATED SEDIMENTARY ROCKS

NOTE: PORTIONS OF THIS MAP ARE APPROXIMATED BECAUSE OF DANGEROUS MINE WORKINGS OR LIMITATIONS IN AVAILABLE FILE DATA.

GENERAL ORE CONTROLS

(1) Base metal sulfides increase

(2) Chlorite increases Note that chlorite deposition was prior to metal deposition

(3) Dip changes (flattens), which produces open spaces.

CONCLUSIONS

(1) Fluorite increases to the east and with depth, and may be controlled by the Bluegoose fault

(2) Clay increases with depth.

(3) The ore body is funnel-shaped and decreasing in size and grade with depth (north vein)

(4) The south vein is increasing in size and grade with depth

PLAN MAP

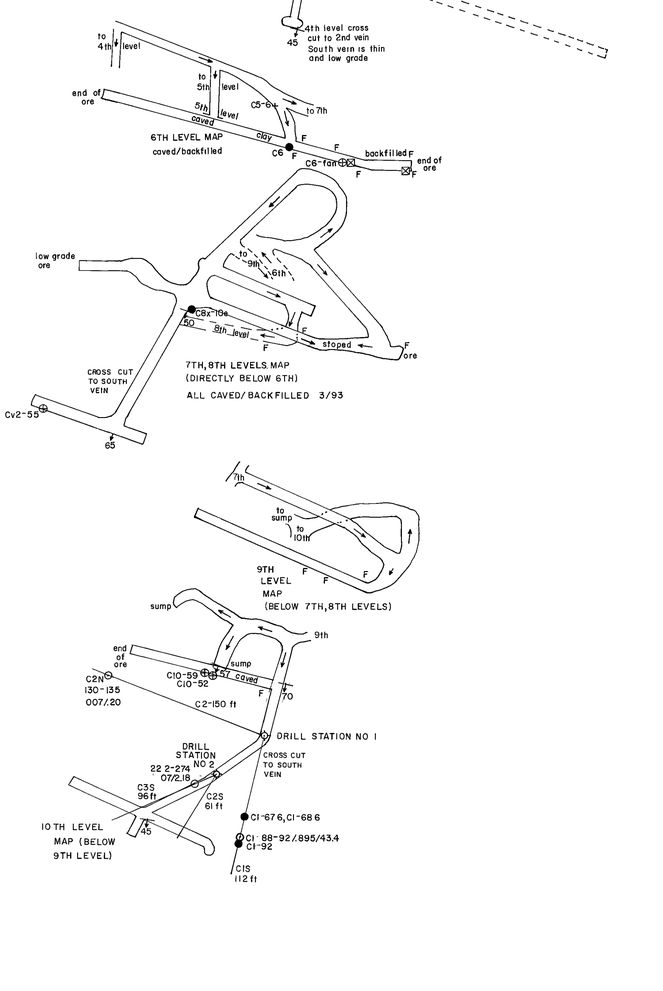

MAP 4 - GEOLOGIC MAP AND SECTION OF THE CENTER MINE

Virginia T. McLEMORE

1993

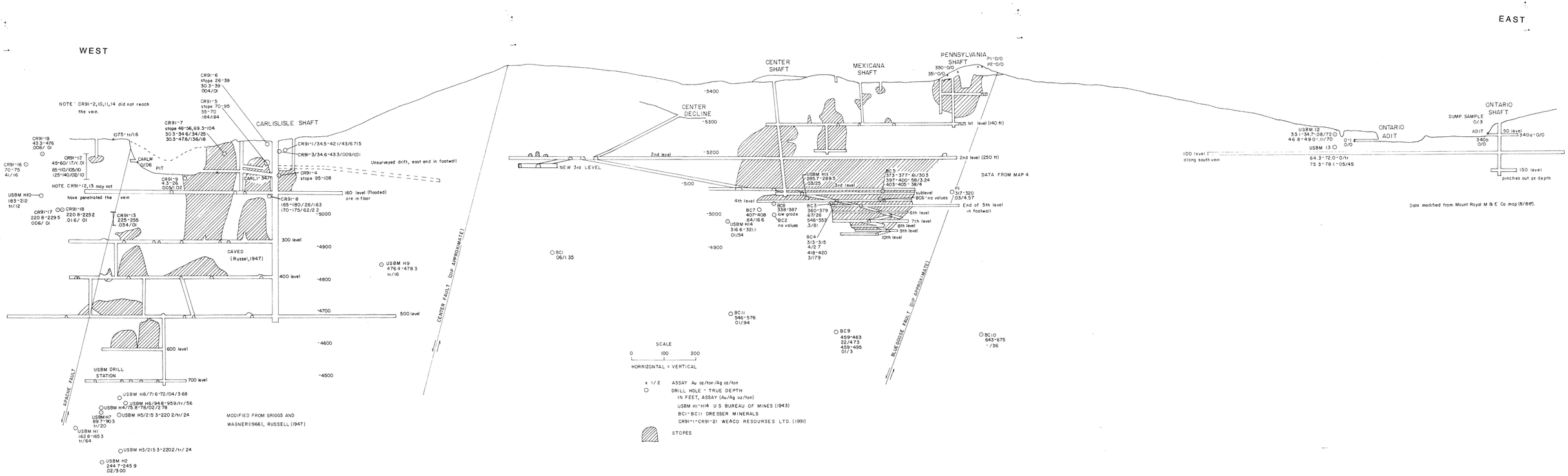

MAP 5 - LONGITUDINAL SECTION ALONG CARLISLE FAULT (CENTER-CARLISLE-ONTARIO MINES)

VIRGINIA T. McLEMORE

1993

STRATIGRAPHY

Darker shades represent exposure of outcrop.

QUATERNARY-PLIOCENE ROCKS

Qal — ALLUVIUM
Thickness 0-4 m

Qaf — ALLUVIAL FAN DEPOSITS
Thickness 0-85 m

Qs — SPRING DEPOSIT
Thickness 0-8 m

QTg — GILA GROUP
Thickness 0-300 m

OLIGOCENE-MIOCENE ROCKS

Tr — INTRUSIVE RHYOLITE DIKES AND PLUGS

Trp — INTRUSIVE PORPHYRITIC RHYODACITE/RHYOLITE DIKES

Tq — QUARTZ MONZONITE DIKE (21.4 Ma)

Td — DIABASE DIKE

Twr — RHYOLITE FLOWS AND/OR DOMES IN THE WILLOW CREEK AREA - Thickness 0-250 m

Twd — RHYODACITE OF WILLOW CREEK
Thickness 0-250 m

Tlc — LAVA FLOWS OF CROOKSON PEAK (27.6 Ma)
Thickness <460 m

Tbd — DARK THUNDER CANYON FORMATION
Thickness <800 m

Ta — UNDIFFERIENTIATED TUFFS
Thickness 0-30 m

Tya — YOUNGER ASH-FLOW TUFFS (27 Ma) (SEE FIG. 2.5) - Thickness 0-30 m

Tya1, Tya2 — YOUNGER ASH-FLOW TUFFS CORRELATED WITH ASH-FLOW TUFFS IN THE BOOTHEEL FIELD, HIDALGO COUNTY, NEW MEXICO

Tya3 — LOCAL DOME-RELATED ASH-FLOW TUFFS (?)

Tbg — BLOODGOOD CANYON TUFF (28.05 Ma)
Thickness 0-75 m

Tdc — DAVIS CANYON TUFF (29.01 Ma)
Thickness 0-30 m

Tas — ALTERED TUFFS, SEDIMENTS, AND ANDESITE UNDIFFERIENTIATED, AGE UNCERTAIN - Thickness 0-500m

Tss — SUMMIT MOUNTAIN FORMATION (31,32 Ma)
Thickness >760 m

Tsed — UNDIFFERIENTIATED SEDIMENTARY ROCKS
Thickness 0-213 m

Tv — INTRUSIVE ANDESITE

VOLCANIC ROCKS OF STEEPLE ROCK AND MT. ROYAL

Trd — RHYODACITE OF MT. ROYAL
Thickness 0-125 m

Trs — RHYOLITE OF STEEPLE ROCK (33.1 Ma)
Thickness 0-400 m

Tsed1 — UNDIFFERIENTIATED SEDIMENTARY ROCKS
Thickness <5 m

Tst — ASH-FLOW TUFF OF STEEPLE ROCK
Thickness <50 m

Tam — ANDESITE OF MT. ROYAL (34.3 Ma)
Thickness 125-900 m

MAP 6 - LEGEND

cv — COPPER VEIN
qv — QUARTZ VEIN
fv — FLUORITE VEIN
Mn — MANGANESE VEIN

ALTERED
BRECCIATION
LEISGANG BANDING

571-.2/4 — SAMPLE NO.-GOLD (oz/t)/SILVER (oz/t) - APPENDIX 11.6 (some samples have whole rock geochemistry in Appendix 11.4 and 5)

12 — STRIKE AND DIP OF BEDS
21 — STRIKE AND DIP OF FOLIATION
70 — DIP OF FAULTS, VEINS, DIKES

FAULT CONTACT, dashed where approximated
DEPOSITIONAL CONTACT, dashed where approximated
CONTACT OF EXPOSURE OF OUTCROP (Areas of greater than 80% bedrock exposed)

PROSPECT PIT, NO PRODUCTION
OPEN PIT WITH PRODUCTION
SHAFT
ADIT
DRILL HOLE
WINDMILL

LOCATION OF SAMPLE FOR PALEOMAGNETIC ANALYSES (TABLE 2.2, WHOLE ROCK CHEMICAL ANALYSES IN APPENDIX 11.4)
LOCATION OF SAMPLE FOR WHOLE ROCK CHEMICAL ANALYSES (APPENDIX 11.4 AND 5)
LOCATION OF SAMPLE FOR WATER ANALYSES (TABLE 2.4)